THE UNIVERSITY OF CHICAGO

C-N AND C-H BOND ACTIVATION VIA NEW REACTIVE INTERMEDIATES AND HYDROGEN ATOM TRANSFER PROCESSES

A DISSERTATION SUBMITTED TO

THE FACULTY OF THE DIVISION OF THE PHYSICAL SCIENCES

IN CANDIDACY FOR THE DEGREE OF

DOCTOR OF PHILOSOPHY

DEPARTMENT OF CHEMISTRY

BY

KATHLEEN JESSIE BERGER

CHICAGO, ILLINOIS

JUNE 2022

Nevertheless, she persisted

For Kristen

TABLE OF CONTENTS

Page

LIST OF FIGURES…… viii

LIST OF SCHEMES……xxviii

LIST OF EQUATIONS……...xxxvii

LIST OF TABLES…….xxxviii

ACKNOWLEDGEMENTS……xl

ABSTRACT……xliii

CHAPTER 1. Current Strategies for C-N Bond Activation and Associated Reactive Species… 1

1.1 Introduction……. 1

1.2 C-N Bond Activation of Secondary Aliphatic Amines……... 2

1.3 Activation and Substitution of Primary Aliphatic Amines……. 6

1.3.1 Deamination by a Polar Mechanism…….…. 6

1.3.2 Deamination by a Radical Mechanism……. 12

1.3.3 Other Transition Metal Catalyzed Deamination Reactions…….. 30

1.3.4 Oxidative Deamination……. 34

1.4 Conclusion……. 45

1.5 References ……. 46

CHAPTER 2. Skeletal Editing by Deletion of Secondary Amines from Molecular Scaffolds…58

2.1 Introduction…… 58

2.2 Results and Discussion……. 63

2.2.1 Reaction Scope and Limitations…… 63

2.2.2 Mechanistic Studies…… 68

2.3 Conclusion……. 74

2.4 Experimental…… 75

2.4.1 General Procedures……... 75

2.4.2 Synthesis of Anomeric Amide Derivatives for Mechanistic Studies…… 76

2.4.3 Hammett Plot Analysis……. 81

2.4.4 Crossover Experiment…….. 83

2.4.5 Radical Clock Experiments…….. 84

2.4.6 Synthesis of Secondary Amines……... 88

2.4.7 Isolation of Aprepitant Insertion Product……. 92

2.4.8. NMR Spectra of New Compounds…… 94

2.5. References…… 111

CHAPTER 3. Reductive Deamination of Primary Amines via Primary Isodiazene Intermediates……. 115

3.1 Introduction……. 115

3.2 Results and Discussion…… 118

3.2.1 Initial Investigation……. . 118

3.2.2 Reaction Optimization…… 120

3.2.3 Reaction Scope and Functional Group Tolerance…… 122

3.2.4 Additional Synthetic Applications……... 131

3.2.5 Mechanistic Investigation…… 135

3.3 Conclusion…… 140

3.4 Experimental……. 141

3.4.1 General Procedures…… 141

3.4.2 Isolation of Deaminated Substrates……. 143

3.4.3 Synthesis of Starting Materials…… 156

3.4.4 Diazene and Isodiazene Comparison…….. 157

3.4.5 Deuterium Labelling Studies…….. 159

3.4.6 TEMPO Trapping Experiments……. 160

3.4.7 Radical Clock Experiments……. 164

3.4.8 NMR Spectra of New Compounds……. 166

3.5 References…….. 182

CHAPTER 4. Development of New Anomeric Amide Derivatives and Optimization of a Large-Scale Synthesis of *N*-(benzyloxy)-*N*-(pivaloyloxy)-4-(trifluoromethyl)benzamide ……... 188

4.1 Introduction…..…….. 188

4.2 Results and Discussion for the Large Scale of Optimization of *N*-(benzyloxy)-N-(pivaloyloxy)-4-(trifluoromethyl)benzamide Synthesis…….. 193

4.3 Results and Discussion for the Synthesis of New Anomeric Amide Derivatives... 205

4.3.1 Anomeric Amides Containing New Leaving Groups…….. 207

4.3.2 Anomeric Amides Containing New Alkoxy and O-Benzyl Groups…… 211

4.3.3 Anomeric Amides Containing New Acyl Substituents…… 215

4.3.4 Exploration of Carbonyl Isosteres…… 229

4.4 Conclusion…….. 230

4.5 Experimental…….. 232

4.5.1 General Procedures…….. 232

4.5.2 Large Scale Synthesis of *N*-(benzyloxy)-*N*-(pivaloyloxy)-4-(trifluoromethyl)benzamide Synthesis…….…….. 233

4.5.3 Synthesis and Characterization of Anomeric Amides Derived from *N*-(benzyloxy)-*N*-(pivaloyloxy)-4-(trifluoromethyl)benzamide Containing New Leaving Groups ……. 239

4.5.4 Synthesis and Characterization of Anomeric Amides Containing New Alkoxy Groups…… 243

4.5.5 Synthesis and Characterization of Anomeric Amides Containing New Acyl Derivatives……. 249

4.5.6 NMR Spectra of New Compounds…… 259

4.6 References…… 300

CHAPTER 5. Mechanistic Studies of Tungsten-Alkylidyne Photoredox-Catalyzed C-H Arylation Reactions and the Synthesis of a Sterically Protected Tungsten-Alkylidyne Complex ……..…….304

5.1 Introduction……...304

5.2. Results and Discussion…….308

5.2.1 Synthesis and Characterization of [HW(CPh)(depe)$_2$Cl][BAr^{F24}]…….308

5.2.2. Production of [HW(CPh)(depe)$_2$Cl]$^+$ as a C-H Arylation Reaction Intermediate…….311

5.2.3. DFT Calculations of pK_as and Redox Potentials to Assess PCET Mechanistic Possibilities for the Production of [HW(CPh)(depe)$_2$Cl]$^+$……..315

5.2.4. Comparison of Reactions Under Catalytic Conditions that Generate Enyl Intermediates that are Thermodynamically Downhill or Uphill for Electron-Transfer to $W(CPh)(depe)_2Cl]^+$……...……...……..323

5.2.5. Stoichiometric Reactions with Benzene and 1,3,5-Triisopropylbenzene Acceptors……..……332

5.2.6. New Chromophore Development: Synthesis and Characterization of $W(CPh)(diBupe)_2Cl$…..……..….343

5.3 Conclusion……...……..348

5.4 Experimental……..……349

5.4.1 Synthesis and Characterization of New Metal Complexes…….……349

5.4.2 Single-Crystal X-ray Diffraction Studies……361

5.4.3 Photoredox C-H Arylation Reactions…….363

5.5 References……..377

LIST OF FIGURES

Figure **Page**

1.1 Examples of widely prescribed pharmaceuticals containing amine moieties……. 1

1.2 Proposed mechanism for secondary amine exchange *via* a metal allyl complex……3

1.3 Summary of the pre-functionalization strategies utilized for deamination by a polar mechanism……..… 7

1.4 Summary of deaminative functionalization enabled by a radical mechanism…….. 13

1.5 Proposed catalytic cycle for reductive deaminative cross-coupling……. 18

1.6 Proposed mechanism for cobalt catalyzed deaminative esterification……. 20

1.7 Proposed mechanism for deaminative C(sp^3)-C(sp) bond formation……... 22

1.8 Proposed mechanism for the deaminative synthesis of alkyl sulfones……. 23

1.9 Proposed mechanism for deaminative borylation *via* EDA complexation involving a) initiation and b) propagation……. 25

1.10 Proposed mechanism for deaminative synthesis of ketones *via* a Breslow intermediate. 28

1.11 Proposed mechanism for deaminative coupling of primary amines to form secondary amines……... 32

1.12 Scope of transformations enabled by oxidative deaminative……... 34

2.1 Late-stage C-H functionalization is an important drug discovery tool, but late-stage skeletal editing has not been developed to the same level……... 58

2.2 Anomeric amide derivatives prepared for Hammett plot study…… 69

2.3 Hammett plot analysis *versus* σ…… 69

2.4 Hammett plot analysis *versus* σ+…….. 69

2.5 Two mechanistic hypotheses for the rearrangement to produce an isodiazene intermediate……...…70

2.6 Example NMR spectrum of reaction aliquot for Hammett plot analysis…….... 82

2.7 GC-MS trace of crude crossover experiment reaction……83

2.8 NMR spectrum of crude reaction mixture from 4-bromo-*N*-(cyclopropylmethyl)-benzenemethanamine…… 85

2.9 NMR spectrum of crude reaction mixture from *trans*-1-([1,1'biphenyl]-4-yl)-*N*-((2-phenylcyclopropyl)methyl)methanamine……. 86

3.1 NMR spectrum of crude product mixture showing deuterium incorporation into the deletion product…….. 119

3.2 NMR spectrum of crude reaction products showing initial discovery that primary aliphatic amines undergo deletion……..……...… 120

3.3 Computational mechanism shows evidence for a radical chain pathway……...….. 139

3.4 NMR spectrum of Myers allene synthesis products……. 158

3.5 NMR spectrum of propargylic amine deletion products…….. 159

3.6 NMR spectrum of deuterium labelling experiment products...…… 160

3.7 NMR spectrum showing TEMPO trapping of aryl amine ……..……. 161

3.8 NMR spectrum showing TEMPO trapping of α-secondary primary amine …..... 162

3.9 NMR spectrum showing TEMPO trapping of α-primary primary amine …...……. 163

3.10 NMR spectrum from radical clock experiment with aryl amine substrate…… 164

3.11 NMR spectrum of aliphatic radical clock reaction…….…….. 165

3.12 ^{1}H NMR spectrum of *tert*-butyl 2-((*4R,6R*)-6-ethyl-2,2-dimethyl-1,3-dioxan-4-yl)acetate in $CDCl_3$, 400 MHz…… 166

3.13 $^{13}C\{^{1}H\}$ NMR spectrum of *tert*-butyl 2-((*4R,6R*)-6-ethyl-2,2-dimethyl-1,3-dioxan-4-yl)acetate (**12'**) in $CDCl_3$, 100 MHz……166

3.14 ^{1}H NMR spectrum of 4-[(4-fluorophenyl)methyl]-3-methylmorpholine in $CDCl_3$, 400 MHz…… 167

3.15 $^{13}C\{^{1}H\}$ NMR spectrum of 4-[(4-fluorophenyl)methyl]-3-methylmorpholine in $CDCl_3$, 100 MHz……..167

3.16 $^{19}F\{^{1}H\}$ NMR spectrum of 4-[(4-fluorophenyl)methyl]-3-methylmorpholine in $CDCl_3$, 376 MHz……..168

3.17 ^{1}H NMR spectrum of 6-methoxy-*N*-(pentan-2-yl)quinolin-8-amine in $CDCl_3$, 400 MHz…….168

3.18 $^{13}C\{^{1}H\}$ NMR spectrum of 6-methoxy-*N*-(pentan-2-yl)quinolin-8-amine in $CDCl_3$, 100 MHz…….169

3.19 ^{1}H NMR spectrum of ethyl (*3R,4R*)-4-acetamido-3-(pentan-3-yloxy)cyclohex-1-ene-1-carboxylate in $CDCl_3$, 400 MHz……..169

3.20 $^{13}C\{^{1}H\}$ NMR spectrum of ethyl (*3R,4R*)-4-acetamido-3-(pentan-3-yloxy)cyclohex-1-ene-1-carboxylate in $CDCl_3$, 100 MHz……170

3.21 ^{1}H NMR spectrum of 3-ethyl 5-methyl 4-(2-chlorophenyl)-2-(ethoxymethyl)-6-methyl-1,4-dihydropyridine-3,5-dicarboxylate in $CDCl_3$, 400 MHz……. 170

3.22 $^{13}C\{^{1}H\}$ NMR spectrum of 3-ethyl 5-methyl 4-(2-chlorophenyl)-2-(ethoxymethyl)-6-methyl-1,4-dihydropyridine-3,5-dicarboxylate in $CDCl_3$, 100 MHz…….. 171

3.23 ^{1}H NMR spectrum of 1-(3-(trifluoromethyl)-5,6-dihydro-[1,2,4]triazolo[4,3-*a*]pyrazin-7(8H)-yl-(4(2,4,5-trifluorophenyl)butan-1-one in $CDCl_3$, 400 MHz……. 171

3.24a. $^{13}C\{^{1}H\}$ NMR spectrum aromatic zoom 1 of 1-(3-(trifluoromethyl)-5,6-dihydro-[1,2,4]triazolo[4,3-*a*]pyrazin-7(8H)-yl-(4(2,4,5-trifluorophenyl)butan-1-one in CD_3CN, 100 MHz……. 172

3.24b. $^{13}C\{^{1}H\}$ NMR spectrum aromatic zoom 2 of 1-(3-(trifluoromethyl)-5,6-dihydro-[1,2,4]triazolo[4,3-*a*]pyrazin-7(8H)-yl-(4(2,4,5-trifluorophenyl)butan-1-one in CD_3CN, 100 MHz……. 172

3.24c. $^{13}C\{^{1}H\}$ NMR spectrum aliphatic zoom of 1-(3-(trifluoromethyl)-5,6-dihydro-[1,2,4]triazolo[4,3-*a*]pyrazin-7(8H)-yl-(4(2,4,5-trifluorophenyl)butan-1-one in CD_3CN, 100 MHz……. 173

3.24d $^{13}C\{^{1}H\}$ NMR full spectrum of 1-(3-(trifluoromethyl)-5,6-dihydro-[1,2,4]triazolo[4,3-*a*]pyrazin-7(8H)-yl-(4(2,4,5-trifluorophenyl)butan-1-one in CD_3CN, 100 MHz……173

3.25 $^{19}F\{^{1}H\}$ NMR spectrum of 1-(3-(trifluoromethyl)-5,6-dihydro-[1,2,4]triazolo[4,3-*a*]pyrazin-7(8H)-yl-(4(2,4,5-trifluorophenyl)butan-1-one in $CDCl_3$, 376 MHz……..174

3.26 ^{1}H NMR spectrum of 5-((*3R,6S*)-6-(2,5-difluorophenyl)tetrahydro-*2H*-pyran-3-yl)-2-(methylsulfonyl)-2,4,5,6-tetrahydropyrrolo[3,4-*c*]pyrazole in $CDCl_3$, 400 MHz…..… 174

3.27 $^{19}F\{^{1}H\}$ NMR spectrum of 5-((*3R,6S*)-6-(2,5-difluorophenyl)tetrahydro-*2H*-pyran-3-yl)-2-(methylsulfonyl)-2,4,5,6-tetrahydropyrrolo[3,4-*c*]pyrazole in $CDCl_3$, 376 MHz….. 175

3.28 $^{13}C\{^{1}H\}$ NMR spectrum of 5-((*3R,6S*)-6-(2,5-difluorophenyl)tetrahydro-*2H*-pyran-3-yl)-2-(methylsulfonyl)-2,4,5,6-tetrahydropyrrolo[3,4-*c*]pyrazole in $CDCl_3$, 100 MHz……175

3.29 ^{1}H NMR spectrum of 7-(but-2-yn-1-yl)-3-methyl-1-((4-methylquinazolin-2-yl)methyl)-8-(piperidin-1-yl)-3,7-dihydro-1*H*-purine-2,6-dione in $CDCl_3$, 400 MHz…….176

3.30 $^{13}C\{^{1}H\}$ NMR spectrum of 7-(but-2-yn-1-yl)-3-methyl-1-((4-methylquinazolin-2-yl)methyl)-8-(piperidin-1-yl)-3,7-dihydro-1*H*-purine-2,6-dione in $CDCl_3$, 100 MHz…176

3.31 ^{1}H NMR spectrum of benzyl (3-phenylpropanoyl)-*L*-leucinate in $CDCl_3$, 400 MHz… 177

3.32 $^{13}C\{^{1}H\}$ NMR spectrum of benzyl (3-phenylpropanoyl)-*L*-leucinate in $CDCl_3$, 100 MHz…… 177

3.33 ^{1}H NMR spectrum of 3-ethyl-3-phenylpiperidine-2,6-dione in $CDCl_3$, 400 MHz……. 178

3.34 $^{13}C\{^{1}H\}$ NMR spectrum of 3-ethyl-3-phenylpiperidine-2,6-dione in $CDCl_3$, 100 MHz…… 178

3.35 ^{1}H NMR spectrum of *tert*-butyl-3-methyl-8-oxo-5-thia-1-azabicyclo[4.2.0]oct-2-ene-2-carboxylate in $CDCl_3$, 400 MHz……. 179

3.36 $^{13}C\{^{1}H\}$ NMR spectrum of *tert*-butyl-3-methyl-8-oxo-5-thia-1-azabicyclo[4.2.0]oct-2-ene-2-carboxylate in $CDCl_3$, 100 MHz…….. 179

3.37 ^{1}H NMR spectrum of 4-(1-methylcycloheptyl)morpholine in $CDCl_3$, 400 MHz…….. 180

3.38 $^{13}C\{^{1}H\}$ NMR spectrum of 4-(1-methylcycloheptyl)morpholine in $CDCl_3$, 100 MHz..180

3.39 ^{1}H NMR spectrum of 1-(3-(1H-imidazol-1-yl)propoxy)-2,2,6,6-tetramethylpiperidine in $CDCl_3$, 400 MHz…… 181

3.40 $^{13}C\{^{1}H\}$ NMR spectrum of 1-(3-(1H-imidazol-1-yl)propoxy)-2,2,6,6-tetramethylpiperidine in $CDCl_3$, 100 MHz……. 181

4.1 Resonance typically observed in amides is impeded by two electronegative substituents (X, Y) at oxygen…….... 189

4.2 Four known classes of anomeric amide…… 189

4.3 a) Two potential anomeric interactions and b) molecular orbital diagram demonstrating an anomeric stabilization…….…….. 189

4.4 Optimized large scale synthesis of *N*-(benzyloxy)-4-(trifluoromethyl)benzamide…. 195

4.5 Product NMR spectrum of *N*-(benzyloxy)-4-(trifluoromethyl)benzamide……. 195

4.6 NMR spectrum of *N*-(benzyloxy)-4-(trifluoromethyl)benzamide in $CDCl_3$ demonstrating major and minor rotamers…… 196

4.7 Synthesis of *N*-chloramide intermediate using *tert*-butylhypochlorite as the limiting reagent……. 197

4.8 Product NMR Spectrum of *N*-chloramide intermediate……. 199

4.9 Synthesis of *N*-chloramide intermediate using TCICA…….. 199

4.10 NMR spectrum *N*-(benzyloxy)-*N*-(pivaloyloxy)-4-(trifluoromethyl)benzamide of demonstrating impurity peaks……. 201

4.11 Optimized synthesis of *N*-(benzyloxy)-*N*-(pivaloyloxy)-4-(trifluoromethyl)benzamide 203

4.12 NMR spectrum of *N*-(benzyloxy)-*N*-(pivaloyloxy)-4-(trifluoromethyl)benzamide showing 99% purity…….. 204

4.13 Modular approach for the development of new anomeric amide derivatives…… 205

4.14 Summary of anomeric amide derivatives studied……..…. 206

4.15 Substitution of *O*-benzyl moiety affects stabilization of HERON transition state…….. 212

4.16 NMR spectrum of demonstrating mixture of *ortho*-substituted amide and reductive elimination byproduct……. 217

4.17 Previous literature attempt at a bulky benzamide derivative is unsuccessful……. 217

4.18 Literature reports of alkyl derived anomeric amides…….. 223

4.19 ^{1}H NMR spectrum of *N*-(benzyloxy)-4-(trifluoromethyl)benzamide in DMSO-*d6*, 400 MHz…… 259

4.20 ^{19}F{^{1}H} NMR spectrum of *N*-(benzyloxy)-4-(trifluoromethyl)benzamide in DMSO-*d6*, 376 MHz……. 259

4.21 ^{13}C{^{1}H} NMR spectrum of *N*-(benzyloxy)-4-(trifluoromethyl)benzamide in DMSO-*d6*, 101 MHz……. 260

4.22 ^{1}H NMR spectrum of *N*-(benzyloxy)-*N*-(chloro)-4-(trifluoromethyl)benzamide in $CDCl_3$, 400 MHz…… 260

4.23 ^{13}C{^{1}H} NMR spectrum of *N*-(benzyloxy)-*N*-(chloro)-4-(trifluoromethyl)benzamide in $CDCl_3$, 100 MHz…… 261

4.24 $^{19}F\{^{1}H\}$ NMR spectrum of *N*-(benzyloxy)-*N*-(chloro)-4-(trifluoromethyl)benzamide in $CDCl_3$, 376 MHz……. 261

4.25 ^{1}H NMR spectrum of *N*-(benzyloxy)-*N*-(pivaloyloxy)-4-(trifluoromethyl)benzamide in $CDCl_3$, 400 MHz……. 262

4.26 $^{19}F\{^{1}H\}$ NMR spectrum of *N*-(benzyloxy)-*N*-(pivaloyloxy)-4-(trifluoromethyl)benzamide in $CDCl_3$, 376 MHz…… 262

4.27 $^{13}C\{^{1}H\}$ NMR spectrum of *N*-(benzyloxy)-*N*-(pivaloyloxy)-4-(trifluoromethyl)benzamide in $CDCl_3$, 101 MHz……..…….. 263

4.28 ^{1}H NMR spectrum of *N*-(benzyloxy)-*N*-(isobutyryloxy)-4-(trifluoromethyl)benzamide in $CDCl_3$, 400 MHz…….…… 263

4.29 $^{19}F\{^{1}H\}$ NMR spectrum of *N*-(benzyloxy)-*N*-(isobutyryloxy)-4-(trifluoromethyl)benzamide in $CDCl_3$, 376 MHz……..…….. 264

4.30 $^{13}C\{^{1}H\}$ NMR spectrum of *N*-(benzyloxy)-*N*-(isobutyryloxy)-4-(trifluoromethyl)benzamide in $CDCl_3$, 101 MHz……..……. 264

4.31 ^{1}H NMR spectrum of *N*-(benzyloxy)-*N*-((3-methylbutanoyl)oxy)-4-(trifluoromethyl)benzamide in $CDCl_3$, 400 MHz……..…….. 265

4.32 $^{19}F\{^{1}H\}$ NMR spectrum of *N*-(benzyloxy)-*N*-((3-methylbutanoyl)oxy)-4-(trifluoromethyl)benzamide in $CDCl_3$, 376 MHz……..…….. 265

4.33 $^{13}C\{^{1}H\}$ NMR spectrum of *N*-(benzyloxy)-*N*-((3-methylbutanoyl)oxy)-4-(trifluoromethyl)benzamide in $CDCl_3$, 101 MHz……..…….. 266

4.34 ^{1}H NMR spectrum of *N*-(benzyloxy)-*N*-((3,3,3-trifluoro-2,2-dimethylpropanoyl)oxy)-4-(trifluoromethyl)benzamide in $CDCl_3$, 400 MHz……..…….. 266

4.35 $^{19}F\{^{1}H\}$ NMR spectrum of *N*-(benzyloxy)-*N*-((3,3,3-trifluoro-2,2-dimethylpropanoyl)oxy)-4-(trifluoromethyl)benzamide in $CDCl_3$, 376 MHz…..…..… 267

4.36 $^{13}C\{^{1}H\}$ NMR spectrum of *N*-(benzyloxy)-*N*-((3,3,3-trifluoro-2,2-dimethylpropanoyl)oxy)-4-(trifluoromethyl)benzamide in $CDCl_3$, 101 MHz…….….. 267

4.37 ^{1}H NMR spectrum of *N*-(benzyloxy)-*N*-((2-fluoro-2-methylpropanoyl)oxy)-4-(trifluoromethyl)benzamide in $CDCl_3$, 400 MHz……..……. 268

4.38 ^{19}F NMR spectrum of *N*-(benzyloxy)-*N*-((2-fluoro-2-methylpropanoyl)oxy)-4-(trifluoromethyl)benzamide in $CDCl_3$, 376 MHz……..……. 268

4.39 $^{13}C\{^{1}H\}$ NMR spectrum of *N*-(benzyloxy)-*N*-((2-fluoro-2-methylpropanoyl)oxy)-4-(trifluoromethyl)benzamide in $CDCl_3$, 101 MHz……..…. 269

4.40 ^{1}H NMR spectrum of sodium 2-fluoro-2-methylpropanoate in D_2O, 400 MHz……..... 269

4.41 ^{19}F NMR spectrum of sodium 2-fluoro-2-methylpropanoate in D_2O, 376 MHz……... 270

4.42 $^{13}C\{^{1}H\}$ NMR spectrum of sodium 2-fluoro-2-methylpropanoate in D_2O, 101 MHz…… 270

4.43 ^{1}H NMR spectrum of sodium 3,3,3-trifluoro-2,2-dimethylpropanoate in D_2O, 400 MHz……..…….. 271

4.44 $^{19}F\{^{1}H\}$ NMR spectrum of *N*-(benzyloxy)-*N*-((2-fluoro-2-methylpropanoyl)oxy)-4-(trifluoromethyl)benzamide in D_2O, 376 MHz……...…… 271

4.45 $^{13}C\{^{1}H\}$ NMR spectrum of *N*-(benzyloxy)-*N*-((2-fluoro-2-methylpropanoyl)oxy)-4-(trifluoromethyl)benzamide in D_2O, 101 MHz…….. 272

4.46 ^{1}H NMR spectrum of 4-(trifluoromethyl)-*N*-((4-(trifluoromethyl)benzyl)oxy)benzamide in DMSO-*d6*, 400 MHz…….…..... 272

4.47 $^{19}F\{^{1}H\}$ NMR spectrum of 4-(trifluoromethyl)-*N*-((4-(trifluoromethyl)benzyl)oxy)benzamide in DMSO-*d6*, 376 MHz……..….... 273

4.48 $^{13}C\{^{1}H\}$ NMR spectrum of 4-(trifluoromethyl)-*N*-((4-(trifluoromethyl)benzyl)oxy)benzamide in DMSO-*d6*, 101 MHz…….. 273

4.49 ^{1}H NMR spectrum of *N*-((3,5-bis(trifluoromethyl)benzyl)oxy)-4-(trifluoromethyl)benzamide in DMSO-*d6*, 400 MHz……. 274

4.50 $^{19}F\{^{1}H\}$ NMR spectrum of *N*-((3,5-bis(trifluoromethyl)benzyl)oxy)-4-(trifluoromethyl)benzamide in DMSO-*d6*, 376 MHz……. 274

4.51 ^{1}H NMR spectrum of *N*-((perfluorophenyl)methoxy)-4-(trifluoromethyl)benzamide in DMSO-*d6*, 400 MHz…….. 275

4.52 $^{19}F\{^{1}H\}$ NMR spectrum of *N*-((perfluorophenyl)methoxy)-4-(trifluoromethyl)benzamide in DMSO-*d6*, 376 MHz……. 275

4.53 $^{13}C\{^{1}H\}$ NMR spectrum of *N*-((perfluorophenyl)methoxy)-4-(trifluoromethyl)benzamide in DMSO-*d6*, 101 MHz……. 276

4.54 ^{1}H NMR spectrum of N-(2,2,2-trifluoroethoxy)-4-(trifluoromethyl)benzamide in $CDCl_3$, 400 MHz……. 276

4.55 $^{19}F\{^{1}H\}$ NMR of N-(2,2,2-trifluoroethoxy)-4-(trifluoromethyl)benzamide in $CDCl_3$, 376 MHz…… 277

4.56 $^{13}C\{^{1}H\}$ NMR of N-(2,2,2-trifluoroethoxy)-4-(trifluoromethyl)benzamide in $CDCl_3$, 101 MHz…… 277

4.57 ^{1}H NMR of N-phenoxy-4-(trifluoromethyl)benzamide in DMSO-*d6*, 400 MHz..... 278

4.58 $^{19}F\{^{1}H\}$ NMR of N-phenoxy-4-(trifluoromethyl)benzamide in DMSO-*d6*, 376 MHz…….278

4.59 $^{13}C\{^{1}H\}$ NMR spectrum of N-phenoxy-4-(trifluoromethyl)benzamide in DMSO-*d6*, 101 MHz…… 279

4.60 ^{1}H NMR spectrum of *N*-(pivaloyloxy)-4-(trifluoromethyl)-*N*-((4-(trifluoromethyl)benzyl)oxy)benzamide in $CDCl_3$, 400 MHz…… 279

4.61 $^{19}F\{^{1}H\}$ NMR spectrum of *N*-(pivaloyloxy)-4-(trifluoromethyl)-*N*-((4-(trifluoromethyl)benzyl)oxy)benzamide in $CDCl_3$, 376 MHz…… 280

4.62 ^{1}H NMR spectrum of *N*-((3,5-bis(trifluoromethyl)benzyl)oxy)-*N*-(pivaloyloxy)-4-(trifluoromethyl)benzamide in $CDCl_3$, 400 MHz……... 280

4.63 ^{1}H NMR spectrum of *N*-(pivaloyloxy)-*N*-(2,2,2-trifluoroethoxy)-4-(trifluoromethyl)benzamide in $CDCl_3$, 400 MHz……... 281

4.64 ^{1}H NMR spectrum of quinoline-8-carbonyl chloride HCl in DMSO-*d6*, 400 MHz….. 281

4.65 $^{13}C\{^{1}H\}$ NMR spectrum of quinoline-8-carbonyl chloride HCl in DMSO-*d6*, 101 MHz…… 282

4.66 ^{1}H NMR spectrum of *N*-(benzyloxy)-2-fluoro-2-methylpropanamide in $CDCl_3$, 400 MHz…….282

4.67 ^{19}F NMR spectrum of *N*-(benzyloxy)-2-fluoro-2-methylpropanamide in $CDCl_3$, 376 MHz…….283

4.68 ^{19}F NMR spectrum expanded of *N*-(benzyloxy)-2-fluoro-2-methylpropanamide in $CDCl_3$, 376 MHz……..283

4.69 $^{13}C\{^{1}H\}$ NMR spectrum of *N*-(benzyloxy)-2-fluoro-2-methylpropanamide in $CDCl_3$, 101 MHz…… 284

4.70 ^{1}H NMR spectrum of *N*-(benzyloxy)-3,3,3-trifluoro-2,2-dimethylpropanamide in $CDCl_3$, 400 MHz……. 284

4.71 $^{19}F\{^{1}H\}$ NMR spectrum of *N*-(benzyloxy)-3,3,3-trifluoro-2,2-dimethylpropanamide in $CDCl_3$, 376 MHz……. 285

4.72 $^{13}C\{^{1}H\}$ NMR spectrum of *N*-(benzyloxy)-3,3,3-trifluoro-2,2-dimethylpropanamide in $CDCl_3$, 101 MHz……. 285

4.73 ^{1}H NMR spectrum of *N*-(benzyloxy)but-2-ynamide in $CDCl_3$, 400 MHz……. 286

4.74 $^{13}C\{^{1}H\}$ NMR spectrum of *N*-(benzyloxy)but-2-ynamide in $CDCl_3$, 101 MHz…… 286

4.75 ^{1}H NMR spectrum of *N*-(benzyloxy)cyclohex-1-ene-1-carboxamide in $CDCl_3$, 400 MHz…… 287

4.76 $^{13}C\{^{1}H\}$ NMR spectrum of *N*-(benzyloxy)cyclohex-1-ene-1-carboxamide in $CDCl_3$, 101 MHz…… 287

4.77 ^{1}H NMR spectrum of *N*-(benzyloxy)quinoline-8-carboxamide in $CDCl_3$, 400 MHz… 288

4.78 $^{13}C\{^{1}H\}$ NMR spectrum of *N*-(benzyloxy)quinoline-8-carboxamide in $CDCl_3$, 101 MHz…… 288

4.79 ^{1}H NMR spectrum of *N*-(benzyloxy)benzothioamide in $CDCl_3$, 400 MHz……... 289

4.80 $^{13}C\{^{1}H\}$ NMR spectrum of *N*-(benzyloxy)benzothioamide in $CDCl_3$, 101 MHz…….. 289

4.81 ^{1}H NMR spectrum of *N*-(benzyloxy)-2-methylbenzamide in $CDCl_3$, 400 MHz…… 290

4.82 $^{13}C\{^{1}H\}$ NMR spectrum of *N*-(benzyloxy)-2-methylbenzamide in $CDCl_3$, 100 MHz... 290

4.83 ^{1}H NMR spectrum of *N*-(benzyloxy)-2,6-dimethylbenzamide in $CDCl_3$, 400 MHz….. 291

4.84 $^{13}C\{^{1}H\}$ NMR spectrum of *N*-(benzyloxy)-2,6-dimethylbenzamide in $CDCl_3$, 100 MHz…… 291

4.85 ^{1}H NMR spectrum of *N*-(benzyloxy)-2,6-bis(trifluoromethyl)benzamide in $CDCl_3$, 400 MHz…… 292

4.86 ^{1}H NMR spectrum of *N*-(benzyloxy)-2-(trifluoromethyl)benzamide in $CDCl_3$, 400 MHz……... 292

4.87 $^{19}F\{^{1}H\}$ NMR spectrum of *N*-(benzyloxy)-2-(trifluoromethyl)benzamide in $CDCl_3$, 376 MHz…… 293

4.88 $^{13}C\{^{1}H\}$ NMR spectrum of *N*-(benzyloxy)-2-(trifluoromethyl)benzamide in $CDCl_3$, 101 MHz…… 293

4.89 ^{1}H NMR spectrum of *N*-(benzyloxy)-4-(trifluoromethyl)benzenesulfonamide in $CDCl_3$, 400 MHz…… 294

4.90 $^{19}F\{^{1}H\}$ NMR spectrum of *N*-(benzyloxy)-4-(trifluoromethyl)benzenesulfonamide in $CDCl_3$, 376 MHz……. 294

4.91 $^{13}C\{^{1}H\}$ NMR spectrum of *N*-(benzyloxy)-4-(trifluoromethyl)benzenesulfonamide in $CDCl_3$, 100 MHz……. 295

4.92 ^{1}H NMR spectrum of *N*-(benzyloxy)-*N*-(pivaloyloxy)-methylcarbamate in $CDCl_3$, 400 MHz…… 295

4.93 $^{13}C\{^{1}H\}$ NMR spectrum of *N*-(benzyloxy)-*N*-(pivaloyloxy)-methylcarbamate in $CDCl_3$, 100 MHz……. 296

4.94 ^{1}H NMR spectrum of *N*-(benzyloxy)-*N*-(pivaloyloxy)pivalamide in $CDCl_3$, 400 MHz. 296

4.95 $^{13}C\{^{1}H\}$ NMR spectrum of *N*-(benzyloxy)-*N*-(pivaloyloxy)pivalamide in $CDCl_3$, 100 MHz……. 297

4.96 ^{1}H NMR spectrum of *N*-(benzyloxy)-*N*-(pivaloyloxy)adamantane-1-carboxamide in $CDCl_3$, 400 MHz……. 297

4.97 $^{13}C\{^{1}H\}$ NMR spectrum of *N*-(benzyloxy)-*N*-(pivaloyloxy)adamantane-1-carboxamide in $CDCl_3$, 100 MHz……. 298

4.98 ^{1}H NMR spectrum of *N*-(benzyloxy)-*N*-(pivaloyloxy)thiophene-2-carboxamide in $CDCl_3$, 400 MHz…… 298

4.99 $^{13}C\{^{1}H\}$ NMR spectrum of *N*-(benzyloxy)-*N*-(pivaloyloxy)thiophene-2-carboxamide in $CDCl_3$, 101 MHz……. 299

5.1 Ground-state and excited-state redox potentials of photoredox chromophores…….. 304

5.2 a) W(CAr)L_4X chromophores with tunable HOMO and LUMO orbitals b) W(CPh)(depe)$_2$Cl c) proposed catalytic cycle for tungsten catalyzed C-H arylation…. 306

5.3 Potential multisite-proton-coupled electron-transfer mechanism……307

5.4 Potential proton-coupled electron-transfer mechanism……..…….…… 307

5.5 Molecular structure and DFT structure of $[HW(CPh)(depe)_2Cl]^+$ ……. 310

5.6 NMR spectrum of the stoichiometric reaction between 2-chlorobenzonitrile and W(CPh)(depe)$_2$Cl…… 312

5.7 NMR spectra of the aromatic region of the stoichiometric reaction between 2-chlorobenzonitrile and W(CPh)(depe)$_2$Cl……..……..313

5.8 Additional NMR spectra of the aromatic region of the stoichiometric reaction between 2-chlorobenzonitrile and W(CPh)(depe)$_2$Cl……313

5.9 NMR spectra of the aliphatic region of the stoichiometric reaction between 2-chlorobenzonitrile and W(CPh)(depe)$_2$Cl…….. 314

5.10 Additional NMR spectra of the aliphatic region of the stoichiometric reaction between 2-chlorobenzonitrile and W(CPh)(depe)$_2$Cl……...…..…….. 314

5.11 Step-wise outer-sphere electron-transfer followed by proton-transfer to generate C-H arylation product and a tungsten-hydride complex…….… 315

5.12 Step-wise proton transfer followed by outer-sphere electron-transfer to generate C-H product and a tungsten-hydride complex…….....316

5.13 Concerted hydrogen atom transfer (HAT) to generate C-H arylation product a tungsten-hydride complex…….. 316

5.14 Relationship between free energy values used to determine ΔG_T of deprotonation……317

5.15 Absorption spectra of a reaction mixture of $[HW(CPh)(depe)_2Cl]^+$ and TMG compared to $W(CPh)(depe)_2Cl$…….…….. 319

5.16 Bordwell diagrams illustrating BDFE calculation from pK_a and $E_{1/2}^{0/+}$ values……319

5.17 Relationship between free energy values used to determine ΔG_T of oxidation……...321

5.18 GC-MS trace of the reaction between 4-bromobenzenediazonium tetrafluoroborate and 2,5-dimethoxybenzene with $[Ru(bpy)_3]^{2+}$ chromophore…… 326

5.19 MS fragmentation at 9.22 min of the GC-MS trace of the reaction between 4-bromobenzenediazonium tetrafluoroborate and 2,5-dimethoxybenzene with $[Ru(bpy)_3]^{2+}$ chromophore…….…….. 327

5.20 GC-MS trace of the reaction between 1-bromo-4-iodobenzene and 2,5-dimethoxybenzene with $W(CPh)(depe)_2Cl$…….…….. 327

5.21 GC-MS trace of the reaction between 4-bromobenzenediazonium tetrafluoroborate and 1,3,5-triisopropylbenzene with $[Ru(bpy)_3]^{2+}$ chromophore……..... 329

5.22 MS fragmentation at 8.87 min of the GC-MS trace of the reaction between 4-bromobenzenediazonium tetrafluoroborate and 1,3,5-triisopropylbenzene with $[Ru(bpy)_3]^{2+}$ chromophore……..…... 330

5.23 GC-MS trace of the control reaction between 1-bromo-4-iodobenzene and 1,3,5-triisopropylbenzene with $W(CPh)(depe)_2Cl$ chromophore…… 330

5.24 NMR spectrum of the stoichiometric reaction between 2-chlorobenzonitrile and $W(CPh)(depe)_2Cl$ with 40 equivalents of benzene……. 334

5.25 Aromatic region of NMR spectrum of the stoichiometric reaction between 2-chlorobenzonitrile and W(CPh)(depe)$_2$Cl with 40 equivalents of benzene…… 335

5.26 NMR spectra stack showing the aromatic region of the stoichiometric reaction between 2-chlorobenzonitrile and W(CPh)(depe)$_2$Cl with 40 equivalents of benzene…… 335

5.27 NMR spectra stack showing the aliphatic region of the stoichiometric reaction between 2-chlorobenzonitrile and W(CPh)(depe)$_2$Cl with 40 equivalents of benzene……...…. 336

5.28 GC-MS trace of the stoichiometric reaction between 2-chlorobenzonitrile and W(CPh)(depe)$_2$Cl with 40 equivalents of benzene…….…… 336

5.29 HR-MS fragmentation of the GC-MS trace peak at 4.79 min corresponding to benzonitrile……..337

5.30 HR-MS fragmentation of the GC-MS trace peak at 4.79 min corresponding to benzonitrile shows proteo-benzonitrile…….…… 337

5.31 HR-MS fragmentation of the GC-MS trace peak at 4.79 min corresponding to benzonitrile shows d_1-benzonitrile…….. 338

5.32 NMR spectrum of the stoichiometric reaction between 2-chlorobenzonitrile and W(CPh)(depe)$_2$Cl with 10 equivalents of 1,3,5-triisopropylbenzene……...…….. 339

5.33 NMR spectra stack showing the aliphatic region of the stoichiometric reaction between 2-chlorobenzonitrile and W(CPh)(depe)$_2$Cl with 10 equivalents of 1,3,5-triisopropylbenzene……...…….. 340

5.34 NMR spectra stack showing the aromatic region of the stoichiometric reaction between 2-chlorobenzonitrile and W(CPh)(depe)$_2$Cl with 10 equivalents of 1,3,5-triisopropylbenzene…… 340

5.35 Additional NMR spectra stack showing the aromatic region of the stoichiometric reaction between 2-chlorobenzonitrile and W(CPh)(depe)$_2$Cl with 10 equivalents of 1,3,5-triisopropylbenzene…….. 341

5.36 Additional NMR spectra stack showing the aliphatic region of the stoichiometric reaction between 2-chlorobenzonitrile and W(CPh)(depe)$_2$Cl with 10 equivalents of 1,3,5-triisopropylbenzene……..341

5.37 GC-MS trace of the stoichiometric reaction between 2-chlorobenzonitrile and W(CPh)(depe)$_2$Cl with 10 equivalents of 1,3,5-triisopropylbenzene……. 342

5.38 HR-MS fragmentation of the GC-MS trace peak at 4.79 min corresponding to benzonitrile shows proteo-benzonitrile…… 342

5.39 Molecular structure and DFT structure of W(CPh)(diBupe)$_2$Cl……. 345

5.40 Space-filling models of the crystal structures of W(CPh)(dmpe)$_2$Cl, W(CPh)(depe)$_2$Cl and W(CPh)(diBupe)$_2$Cl…… 347

5.41 ^{1}H NMR spectrum of [HW(CPh)(depe)$_2$Cl][BAr^{F24}]……. 352

5.42 ^{13}C{^{1}H} NMR spectrum of [HW(CPh)(depe)$_2$Cl][BAr^{F24}]…… 352

5.43 Aromatic region of the ^{13}C{^{1}H} NMR spectrum of [HW(CPh)(depe)$_2$Cl][BAr^{F24}]……353

5.44 Aliphatic region of the ^{13}C{^{1}H} NMR spectrum of [HW(CPh)(depe)$_2$Cl][BAr^{F24}]….. 353

5.45 Alkylidyne resonance of $^{13}C\{^{1}H\}$ NMR spectrum of [HW(CPh)(depe)$_2$Cl][BAr^{F24}]… 354

5.46 HSQC spectrum (CD_3CN) of [HW(CPh)(depe)$_2$Cl][BAr^{F24}]…….. 354

5.47 $^{19}F\{^{1}H\}$ NMR spectrum of [HW(CPh)(depe)$_2$Cl][BAr^{F24}]……..…….355

5.48 Expanded $^{19}F\{^{1}H\}$ NMR spectrum of [HW(CPh)(depe)$_2$Cl][BAr^{F24}]…… 355

5.49 HR-MS of [HW(CPh)(depe)$_2$Cl][BAr^{F24}]……..……. 356

5.50 ^{1}H NMR spectrum of W(CPh)(diBupe)$_2$Cl……...…….. 356

5.51 Expanded aliphatic region of the ^{1}H NMR spectrum of W(CPh)(diBupe)$_2$Cl….…….. 357

5.52 Aliphatic region of COSY spectrum of W(CPh)(diBupe)$_2$Cl…….…… 357

5.53 $^{13}C\{^{1}H\}$ NMR spectrum of W(CPh)(diBupe)$_2$Cl…….…….. 358

5.54 Expanded aromatic region of $^{13}C\{^{1}H\}$ NMR spectrum of W(CPh)(diBupe)$_2$Cl…… 358

5.55 Expanded aliphatic region of $^{13}C\{^{1}H\}$ NMR spectrum of W(CPh)(diBupe)$_2$Cl…… 359

5.56 HSQC spectrum of W(CPh)(diBupe)$_2$Cl…… 359

5.57 $^{31}P\{^{1}H\}$ NMR spectrum of W(CPh)(diBupe)$_2$Cl…… 360

5.58 Expanded $^{31}P\{^{1}H\}$ NMR spectrum of W(CPh)(diBupe)$_2$Cl……... 360

5.59 HR-MS of W(CPh)(diBupe)$_2$Cl……..… 361

5.60 GC-MS trace of calibration for [1,1'-biphenyl]-2-carbonitrile……... 365

5.61 GC-MS trace of reaction producing [1,1'-biphenyl]-2-carbonitrile……...……. 365

5.62 GC-MS chromatogram and mass spectrum at 7.54 min of the reaction producing 2-(1-methyl-1H-pyrrol-2-yl)benzonitrile…….……..……. 366

5.63 GC-MS chromatogram and mass spectrum at 9.38 producing 2',4',6'-trimethoxy-[1,1'-biphenyl]-2-carbonitrile min of the reaction……. 367

5.64 GC-MS chromatogram and mass spectrum at 7.47 min of the reaction producing [1,1'-biphenyl]-2-carbonitrile……. 368

5.65 GC-MS chromatogram and mass spectrum at 8.83 min of the reaction producing 2',5'-dimethoxy-[1,1'-biphenyl]-2-carbonitrile……. 369

5.66 GC-MS chromatogram and mass spectrum at 7.96 min of the reaction producing 2',4',6'-trimethyl-[1,1'-biphenyl]-2-carbonitrile……. 370

5.67 GC-MS chromatogram and mass spectrum at 9.48 min of the reaction producing 2',4',6'-triisopropyl-[1,1'-biphenyl]-2-carbonitrile……..…….371

5.68 ^{1}H NMR spectrum of 2',4',6'-trimethoxy-[1,1'-biphenyl]-2-carbonitrile…… 374

5.69 ^{13}C{^{1}H} NMR spectrum of 2',4',6'-trimethoxy-[1,1'-biphenyl]-2-carbonitrile…...…… 374

5.70 ^{1}H NMR spectrum of 2-(1-methyl-1H-pyrrol-2-yl)benzonitrile……. 375

5.71 ^{13}C{^{1}H} NMR spectrum of 2-(1-methyl-1H-pyrrol-2-yl)benzonitrile…….…….. 375

5.72 ^{1}H NMR spectrum of 2',5'-dimethoxy-[1,1'-biphenyl]-2-carbonitrile…… 376

5.73 ^{13}C{^{1}H} NMR spectrum of 2',5'-dimethoxy-[1,1'-biphenyl]-2-carbonitrile……...…… 376

LIST OF SCHEMES

Scheme **Page**

1.1 Deaminative exchange of a secondary amine with a primary amine…….. 3

1.2 Deaminative exchange of two secondary amines……... 3

1.3 Deaminative synthesis of chiral α-allylated aldehydes using a palladium complex……. 4

1.4 Synthesis of pyrroles by C-N bond cleavage via a sigma bond metathesis…… 4

1.5 Oxidative deamination of secondary amines to ketone products via Friedel-Crafts alkylation……. 5

1.6 Deaminative redistribution of secondary amines to tertiary amines and ammonia…… 6

1.7 Deaminative substitution mediated by tosylation…….. 8

1.8 One-pot reductive deamination by *in-situ* silylation…….. 8

1.9 Enantioselective deaminative arylation of alkylated amines…….. 9

1.10 Enantioselective deamination of benzylic quaternary amines to silanes……. .10

1.11 Deaminative synthesis of alcohols via *N*-alkyl-*N*-nitrosamides……... 10

1.12 Pre-functionalization to primary amines to Katritzky salts…….. 11

1.13 Examples of Katritzky salt substitution chemistry including the nucleophiles a) piperidine; b) phenoxide and c) triphenylphosphine…… 11

1.14 Barton-Saegusa deamination of amines to alkanes……13

1.15 Radical deamination of Katritzky salts with a) nitronate and b) malonate……... 14

1.16 Reductive deamination of Katritzky salts including a) scope and b) mechanistic evidence for a radical mechanism…….15

1.17 Nickel catalyzed deaminate cross-coupling of Katritzky salts with a) aryl boronic acids and b) alkyl zinc halides……16

1.18 Deaminative hydroalkylation of a) unctivated alkenes and b) alkynes…….17

1.19 Reductive deaminative cross-coupling of Katritzky salts with aryl halides……..18

1.20 Conversion of amines to methyl esters using catalytic cobalt, methanol and carbon monoxide……....19

1.21 Conversion of primary amines to difluoromethane isosteres using catalytic cobalt and Vicic-Mikami reagent……20

1.22 Deaminative Minisci coupling enabled by photoredox catalysis……..21

1.23 Deaminative $C(sp^3)$-C(sp) bond formation using alkynyl sulfones…….. 22

1.24 Deaminative synthesis of alkyl sulfones…….….. 23

1.25 Deaminative borylation enabled by EDA complexation of Katritzky salts.……..…..… 24

1.26 EDA complex mediated deaminative conversion to a) alkyl thioesters and b) alkyl thioethers……..…. 26

1.27 Lewis base catalyzed deaminative borylation…….…….. 27

1.28 Proposed mechanism for Lewis base catalyzed deaminative borylation…….……. 27

1.29 NHC catalyzed deaminative synthesis of ketones…… 28

1.30 Deaminative $C(sp^3)$-$C(sp^3)$ bond formation by pre-functionalization to electron rich imines……...……. 29

1.31 Deaminative $C(sp^3)$-$C(sp^2)$ coupling by dual nickel – photoredox catalysis with pre-functionalized imines……... 30

1.32 Ruthenium catalyzed conversion of amines to alcohols using water……...…… 31

1.33 Ruthenium catalyzed deaminative coupling of primary amines to form symmetrical secondary amines……...31

1.34 Ruthenium catalyzed deaminative coupling of primary amines to form unsymmetrical secondary amines……...32

1.35 Deaminative coupling of allylic amines with aryl boronic acids……...……33

1.36 Deaminative synthesis of allylic sulfones……..33

1.37 Oxidative deamination enabled by a) CuAOs, b) ADH, and c) biomimetic strategies….35

1.38 Biomimetic oxidative deamination of primary amines using a) 3,5-di-*tert*-butyl-1,2-benzoquionone and b) mesitylglyoxyl derivatives……...…….37

1.39 Biomimetic oxidative deamination using ascorbic acid……37

1.40 Total synthesis of Chilocorine C enabled by biomimetic oxidative deamination…….38

1.41 Catalytic biomimetic oxidative deamination using a) a platinum electrode and b) catalytic copper and air…….38

1.42 Deaminative synthesis of unsymmetrical imines ……..……39

1.43 One-pot conversion of amines to ketones with a biomimetic catalyst……...40

1.44 Deaminative aza diels-alder synthesis of *N*-alkyl-4-pyridone……...…41

1.45 Deaminative oxidative trimerization of benzylic amines to produce an imidazolinone....41

1.46 Deaminative oxidative synthesis of a) carboxylic acids and b) lactones……...…42

1.47 Deaminative oxidative synthesis of thioamides……...……..42

1.48 One-pot oxidative deaminative four-component Ugi reaction with unsymmetrical disubstituted imines……...……43

1.49 Deaminative synthesis of benzimidazoles……...……..44

1.50 Oxidative olefination of 2-methylquinoline with NBS and *tert*-butylhydroperoxide…...44

1.51 Deaminative oxidative synthesis of 1,2-dihydropyridines……45

2.1. Examples of carbonyl dependent skeletal editing including a) the Wolff rearrangement b) the Favorskii rearrangement and c) deacetylation of ketones…….…….…… 59

2.2 Oxygen deletion of dibenzylic ethers…… 59

2.3 Desired nitrogen deletion of secondary amines……...……. 60

2.4 Synthesis of an isodiazene *via* reaction with nitrosyl chloride, followed by reduction with sodium metal and treatment with *tert*-butyl hypochlorite…….. 61

2.5 Isodiazene intermediate generated by mercury oxidation undergoes homolytic extrusion of dinitrogen……...……61

2.6 Sulfamoyl azide method for nitrogen deletion……..…… 61

2.7 Anomeric amide reagents convert secondary amines to isodiazene intermediates……62

2.8 Key hypothesis that anomeric amides can be applied for the direct deletion of amines...62

2.9 Sulfamoyl azide method for nitrogen deletion applied to ring contraction chemistry…..63

2.10 Ring contraction of pyrrolidines to cyclobutanes using ammonium carbonate and HTIB……..63

2.11. Application of nitrogen deletion towards the synthesis of a histone receptor modulator. 66

2.12. Application of nitrogen deletion towards the total synthesis of Polysiphenol…….……..66

2.13. Sterically bulky Norsertraline derivative is unreactive……..……67

2.14. Unsuccessful nitrogen deletion of α-tertiary secondary amines ……...……67

2.15. Aprepitant derivative undergoes nitrogen insertion chemistry……..68

2.16. Crossover experiment demonstrating an intramolecular rearrangement……...……71

2.17. [2,3]-Sigmatropic rearrangement to a diazene product suggests presence of isodiazene intermediate……71

2.18 Amine substrate containing a methylcyclopropyl radical clock moiety does not produce rearranged deletion product……...72

2.19. Synthesis of amine substrate containing the phenylcyclopropylmethyl radical clock.....72

2.20 Unsuccessful nitrogen deletion of substrate containing the phenylcyclopropylmethyl radical clock ……...…….. 72

2.21 Initial synthetic route to *trans*-1-([1,1'biphenyl]-4-yl)-*N*-((2-phenylcyclopropyl)methyl)methanamine is unsuccessful...……73

2.22. Alternative synthetic route to *trans*-1-([1,1'biphenyl]-4-yl)-*N*-((2-phenylcyclopropyl)methyl)methanamine by reductive amination.……73

2.23. Nitrogen deletion of *trans*-1-([1,1'biphenyl]-4-yl)-

N-((2-phenylcyclopropyl)methyl)methanamine gives approximately a 1:1 mixture of rearranged and unrearranged products……..……..……... 74

3.1 Reductive deamination of Katritzky salts using a) HAT with thiophenol and b) sodium borohydride followed by pyrolysis…….…… 116

3.2 State of the art for direct primary amine deletion including a) deamination with HOSA and b) Lewis acid catalyzed deamination with phenylsilane……..… 117

3.3 Proposed direct primary amine deletion using an anomeric amide reagent……..….. 117

3.4 Initial reaction screening with benzhydrylamine shows deaminated product……. 118

3.5 Rearrangement of a benzylic diazene to give an isotoluene product…….…... 126

3.6 Deamination of 1-naphthylamine gives isotoluene product…… 126

3.7 Comparison of HOSA deamination using Oseltamivir……..….. 126

3.8 Synthesis of caprolactam from lysine……..……..……. 128

3.9 Literature procedures for the synthesis of caprolactam…….……. 129

3.10 Selectivity of primary amine deletion using lysine methyl ester……. 129

3.11 Conversion of acetylated glucosamine to acetylated β-2-deoxyglucose…..……..… 130

3.12 Literature synthesis of β-2-deoxyglucose……...……. 130

3.13 Literature synthesis of (-)-Chamobtusin A from Leelamine……..….132

3.14 Conversion of Leelamine to Abietatriene in a single step…….…..….132

3.15 Literature deamination of β-lactam derivatives requires diazotization and reduction…133

3.16 Deamination of 7-β-amino-deacetoxy-cephalosporanic acid *tert*-butyl ester……..…...133

3.17 Deoxygenation of ketones in two steps……..…….…….134

3.18 Conversion of a nitrile to a methyl group in two steps……. 134

3.19 Traceless amine directed C-H arylation……..…… 135

3.20 Myers allene synthesis with propargylic alcohol and resulting ratio of products……. 136

3.21 Deamination of propargylic amine and resulting ratio of products…….……...….136

3.22 Aliphatic amine clock substrate rearranges suggesting radical intermediates……..... 137

3.23 Aromatic amine clock substrate rearranges suggesting radical intermediates…… 138

3.24 Unsuccessful Minisci coupling resulting in *N*-alkyl-4-(trifluoromethyl)benzamide product derivative……...……...……140

4.1 Elimination reaction of anomeric amides yields a nitrenium cation……..190

4.2 Radical homolysis of anomeric amides yields an alkoxyamidyl radical intermediate, which undergoes several decomposition pathways…….…….…… 190

4.3 Nucleophilic substitution of anomeric amides…….….. 191

4.4 Thermolysis of anomeric amides results in HERON migration and resulting decomposition products…….…….. 192

4.5 Initial synthetic route to *N*-(benzyloxy)-*N*-(pivaloyloxy)-4-(trifluoromethyl)benzamide…….……194

4.6 Synthesis of anomeric amides with new leaving groups including a) isopropyl and b) isobutyl derivatives……...……... 208

4.7 Anomeric amide with isopropyl derived leaving group is unreactive with an α-tertiary amine substrate…….…..……...….…….. 209

4.8 Generation of a captodatively stabilized radical species as a decomposition product…..212

4.9 Synthesis of anomeric amide bearing an alkoxy group with an α-trifluoromethyl group 215

4.10 Synthesis of an *O*-phenyl derived anomeric amide is unsuccessful…… 215

4.11 Dimerization observed during attempted synthesis of acetamide derived reagent……. 218

4.12 Literature synthesis of a dimerized hydrazine product……... 218

4.13 Synthesis of a methoxy derived reagent…….…… 219

4.14 Unsuccessful synthesis of a cyclohexyl derived anomeric amide reagent……. 220

4.15 Successful synthesis of a *tert*-butyl derived reagent…….…….. 220

4.16 Reactivity studies of *tert*-butyl derived amide……..……... 221

4.17 Successful synthesis of an adamantyl derived reagent…….……222

4.18 Reactivity studies of adamantyl derived reagent……. 222

4.19 Unsuccessful synthesis of a 2-fluoro-2-methylpropanoyl derived reagent……. 224

4.20 Unsuccessful synthesis of a 3,3,3-trifluoro-2,2-dimethyl derived reagent……... 224

4.21 Unsuccessful synthesis of an alkyne derived anomeric amide…… 226

4.22 Unsuccessful synthesis of an alkene derived anomeric amide……..…….. 226

4.23 Unsuccessful synthesis of a quinoline derived anomeric amide……... 227

4.24 Synthesis of thiophene derived anomeric amide…… 228

4.25 Reactivity of a thiophene derived reagent with secondary amine substrates……. 228

4.26 Attempted synthesis of an anomeric amide containing a thiocarbonyl isostere results in isolation of *N*-(benzyloxy)-*N*-(pivaloyloxy)benzamide……...229

4.27 Attempted synthesis of an anomeric amide containing a sulfonamide isostere……..…. 230

4.28 Literature report of *N*-chlorosulfonamide derivate is inert to substitution chemistry……230

5.1 Synthesis of [HW(CPh)(depe)$_2$Cl][BAr^{F24}]……. 308

5.2 Experimental deprotonation of [HW(CPh)(depe)$_2$Cl][BAr^{F24}] with TMG…….……..… 319

5.3 Possible reaction pathways for the aryl radical……...……. 333

5.4 Synthesis of W(CPh)(diBupe)$_2$Cl from W(CPh)(pic)$_2$(CO)$_2$Cl.....344

LIST OF EQUATIONS

Equation		Page
2.1	Ratio of initial amide integrations for Hammett plot analysis	82
2.2	Starting anomeric amide ratio for Hammett plot analysis	82
2.3	Hammett plot k value ratio calculation	83
2.4	Hammett plot σ value calculation	83
5.1	ΔG_T calculation of deprotonation	317
5.2	pK_α relationship to ΔG_T	317
5.3	pK_a^{calc} correction with experimental anchor for triethylamine	317
5.4	The equilibrium concentration of W(CPh)(depe)$_2$Cl using	319
5.5	pK_a calculation using TMG	319
5.6	Tungsten hydride BDFE calculation	320
5.7	ΔG_T from oxidized and neutral substrates	321
5.8	Nernst equation	321
5.9	GC-MS response factor calculation	365
5.10	GC-MS yield calculations	365

LIST OF TABLES

Table **Page**

2.1 Reagent optimization for secondary amine deletion…… 64

2.2 Select examples from the secondary amine substrate scope demonstrating functional group tolerance……..…… 65

2.3 NMR integration values used to determine Hammett plot values……... 82

3.1 Initial solvent screen for reaction optimization using GC…… 121

3.2 Screen for reaction optimization using NMR spectroscopy……. 121

3.3 Scope of small molecule deamination……123

3.4 Scope and limitations of late-stage deamination of pharmaceuticals…… 124

3.5 Scope of amino acid and peptide deamination……127

3.6 Scope of aniline deamination……. 131

3.7 Percent deuterium incorporation into deaminated product…….…… 137

4.1 Yield of nitrogen deletion product decreases with decreased leaving group sterics…...209

4.2 Synthesis of reagents containing new leaving groups……..…….. 210

4.3 Initial rate studies of reagents **30** and **39** by analyzing product yield after 1 hour…..…211

4.4 Initial rate studies of reagents **30** and **40** by analyzing product yield after 1 hour……..211

4.5 Synthesis of hydroxamates containing new *O*-benzyl groups……..……. 213

4.6 Synthesis of anomeric amides containing new *O*-benzyl groups……..……. 214

4.7 Synthesis of anomeric amide derivatives with *ortho*-benzamide substituents……216

4.8 Initial rate studies for comparison of secondary amine deletion between reagents **30** and **121**……228

5.1 Comparison of structural parameters between the crystal structures of $[HW(CPh)(dmpe)_2Cl]^+$ and $[HW(CPh)(depe)_2Cl]^+$ and the DFT structure of $[HW(CPh)(depe)_2Cl]^+$ ……..……..310

5.2 DFT computed pK_a values of select enyl intermediates……..……...317

5.3 DFT computed oxidation potentials of select enyl intermediates……..……....322

5.4 Catalytic reactions of 2-chlorobenzonitrile with different radical acceptors showing the oxidation potential of the enyl intermediate relative to $[HW(CPh)(depe)_2Cl]^+$, in comparison with GC yield……..…….324

5.5 Results of reactions under catalytic conditions where enyl intermediates have different steric effects and ET driving forces…….331

5.6 Comparison of geometric parameters for the crystal structure and DFT computed structure of $W(CPh)(diBupe)_2Cl$ with the crystal structures of $W(CPh)(depe)_2Cl$ and $W(CPh)(dmpe)_2Cl$ ……...……345

5.7 Crystal Data and Refinement Parameters for $[HW(CPh)(depe)_2Cl][BAr^{F24}]$ and $W(CPh)(diBupe)_2Cl$……..…….. 362

5.8 Calculated response factors for GC-MS calibrations with different product molecules…….364

ACKNOWLEDGEMENTS

Thank you Professor Mark Levin for your constant enthusiasm, encouragement, generation of ideas and passion for science. I am so grateful for all the opportunities you have given me during my time in the group. Thank you for your reliability and responsiveness, for your handling of all the pandemic constraints and for your commitment to creating a such positive working environment and group culture. Thank you Professor Mike Hopkins for your mentorship with the work presented in chapter 5. You have made me a better scientist and significantly fostered my independence. I was very fortunate to have been supported by two departmental fellowships, thank you both for your support in obtaining these. I also thank Professor Scott Snyder for giving his time and scientific guidance as my third committee member.

Thank you to all of the Levin group for making the lab a fun and supportive place to work. I have fond memories of our group socials and funday Mondays. Dr. Sean Kennedy, thank you so much for mentoring me and answering all of my synthesis and purification questions when I joined the group. Thank you for your friendliness and unwavering calmness. I am so fortunate to have collaborated on the nitrogen deletion project with you. Much of this thesis was built upon some of your key initial discoveries. Dr. Balu Dherange, thank you so much for all your support throughout the secondary amine deletion peer review process. I honestly don't know how I would have got through that time if I was alone. Thank you for your contributions to the primary amine deletion project, for fixing all my rotovap problems and for always having a good sense of humor. Patrick Kelly, thank you for being there from the very beginning, for always having a listening ear and for making work a supportive place. Julia Driscoll, I am so grateful for all of your brilliant contributions to the nitrogen deletion chemistry. Thank you for being wonderful to work with and

for all the effort you put into planning group socials. Megan Morales, you are a gem of a student. Thank you for all of your hard work, enthusiasm and willingness to teach me Gen Z pop culture. Working with you has significantly increased the confidence I have in my leadership and problem-solving capabilities. I would also like to thank Dr. Hunter Vibbert for all his mentorship and kindness during my time in the Hopkins lab. A big thanks to Dr. Josh Kurutz for being the best NMR facilities manager, as well as Dr. Alexander Filatov and Dr. Andrew McNeece for their assistance collecting and solving the X-ray crystal structures in this thesis. Adam Weiss and Dr. Thomas Speltz, thank you so much for your help with preparative HPLC.

For mentorship and support early on, I thank Dr. Rich Burford, Professor Mike Fryzuk, Professor Johanna Blaquiere, Dr. Peter Wallis and everyone who makes Canada-wide Science Fair such an amazing experience. Thank you for all so much for giving me a love for science and pushing me to pursue graduate school. I thank everyone from Women in Chemistry at UChicago for creating such a supportive network in the department. I will always cherish the coffee hours and arts and crafts nights, and in particular I want to thank Becca, Sarah, Julia, Tessa, Brooke, Nasim, Clare, Yuqing and Kathryn for all the work they have put into this organization. I also owe a huge thank you to everyone involved with GRIT for their efforts championing inclusivity in science. A big thank you to Dr. Erin Hurst for everything you have done for me.

Thank you to my parents and brother for always believing in me and encouraging me to pursue my dreams. I am so fortunate to have always had your support and love through all the ups and downs along the way. I would also like to thank the rest of my family for everything, especially the Ontario gang for welcoming me every time I wanted to escape Chicago. To all the forever friends I've made here - Steph Black, Leigh and Manish Singh, Jessy Morgan, Kaan Tarhan and Joshua Kirks – thanks for making Chicago feel like home. To my amazing fiancé Ben, I really

couldn’t imagine making this journey without you. Thank you for all your support along the way. I am so lucky you chose to stay in Chicago with me and I’m so excited for our next chapter together. This thesis was made possible by all of your cups of tea and Shepherd’s pies. Finally, I thank my little dog Jack for making graduate school so much cuddlier. I love you all.

ABSTRACT

This thesis explores new reactive intermediates and hydrogen atom transfer mechanisms that can be applied to C-N and C-H bond activation. Chapter 1 reviews the current strategies in the literature for C-N bond activation of both primary amine and secondary amines, with a particular emphasis on oxidative deamination, transition metal catalyzed deamination and radical mediated deaminative transformations. Chapter 2 demonstrates a conceptually distinct method for secondary amine activation using an anomeric amide reagent, which involves the conversion of the amine to an isodiazene. Subsequent extrusion of dinitrogen and recombination of the resulting carbon fragments facilitates the net deletion of secondary amines as new method for skeletal editing of organic molecules. Chapter 3 expands the scope of amine deletion using anomeric amides to include primary amines. This deamination proceeds with exquisite functional group tolerance under exceptionally mild conditions, and applications towards late-stage editing of biomolecules are demonstrated. Mechanistic studies demonstrate that this transformation proceeds by a previously unreported isodiazene intermediate which undergoes a novel hydrogen atom transfer chain mechanism. Chapter 4 presents the optimization of a reproducible large-scale synthesis for the anomeric amide reagent and also discusses the modular approach taken to the development of new anomeric amide derivatives. Chapter 5 explores the mechanism of a photoredox-catalyzed C-H arylation reaction using a super-reducing tungsten alkylidyne complex. Experimental studies and DFT calculations provide evidence for a unique proton coupled electron transfer event occurring between the oxidized chromophore and the enyl radical intermediate. A stepwise electron transfer followed by proton transfer and a concerted hydrogen atom transfer are both shown to be operative pathways depending on the reduction potential of the enyl intermediate.

CHAPTER 1

Current Strategies for C-N Bond Activation and Associated Reactive Species

Note: Portions of this work have been published in an alternate format in Berger, K. J.; Levin, M. D. Reframing Primary Alkyl Amines as Aliphatic Building Blocks. *Org. Biomol. Chem.* **2021**, *19*, 11-36.

1.1. Introduction.

Aliphatic amines are functional groups of high biological relevance, as evidenced by their abundance in natural products and pharmaceuticals. A recent survey of Pfizer's chemical database revealed over 47 000 primary amines alone.[1] Figure 1.1 depicts several widely prescribed pharmaceuticals containing either primary or secondary amines that have undoubtedly benefitted many people. However, despite their abundance, amines are known principally as challenging moieties to install during syntheses.[2-5] Perhaps unsurprisingly, less attention has been directed to strategies for removing amines from molecular scaffolds.

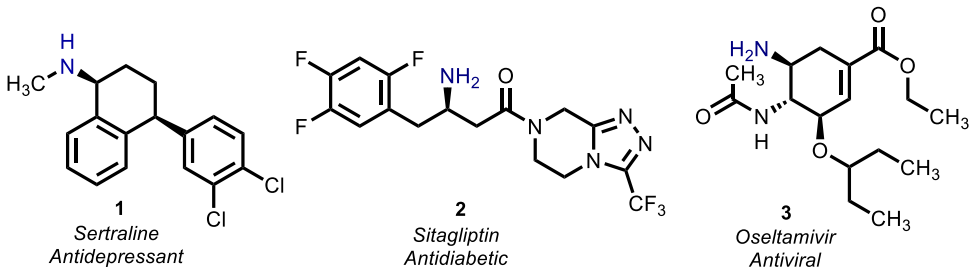

Figure 1.1. Examples of widely prescribed pharmaceuticals containing amine moieties.

One of the main frontiers of modern organic synthesis is the selective late-stage modification of molecules. The term late-stage functionalization is used throughout this thesis and refers to a chemoselective transformation which exhibits high functional group tolerance.[6] This

ability to make edits to complicated structures without having to re-synthesize new derivatives separately has the power to dramatically increase the efficiency of drug discovery. Late-stage functionalization has been most prominently demonstrated and explored in the field of C-H activation.[7-9] Less work has been directed towards carbon – heteroatom activation, however arguably commensurate potential would be afforded with such strategies.

In this vein, the following sections serve to summarize the classical and contemporary efforts that have been made towards aliphatic C-N bond activation. This introduction will provide context for the conversion of secondary amines to C-C bonds described in chapter 2, as well as the primary amine 'deletion' to alkanes presented in chapter 3. An emphasis is placed on the reactive intermediates employed to facilitate these transformations in the literature compared to the strategies described in this thesis.

1.2. C-N Bond Activation of Secondary Aliphatic Amines.

Transition metal catalysts have facilitated a wide range of C-N bond activation chemistry, including that of secondary aliphatic amines.[10, 11] One strategy for C-N activation of allylic secondary amines is *via* the formation of a palladium allyl intermediate. Trost first reported a palladium-catalyzed exchange of an allylic secondary amine (**4**) with a primary amine (**5**) in 1980 (Scheme 1.1).[12] This finding was expanded by the Hartwig group to include exchange between two secondary amines (**8** and **9**) using either catalytic nickel or palladium (Scheme 1.2).[13] The postulated mechanism involves the generation of a metal allyl complex *via* liberation of a primary amine (**11**) (Figure 1.2). Secondary allylic amines have also been harnessed by the deaminative generation of a palladium allyl complex in the presence of a chiral phosphoric acid co-catalyst (**14**) to yield chiral α-allylated aldehydes (**15**) (Scheme 1.3).[14]

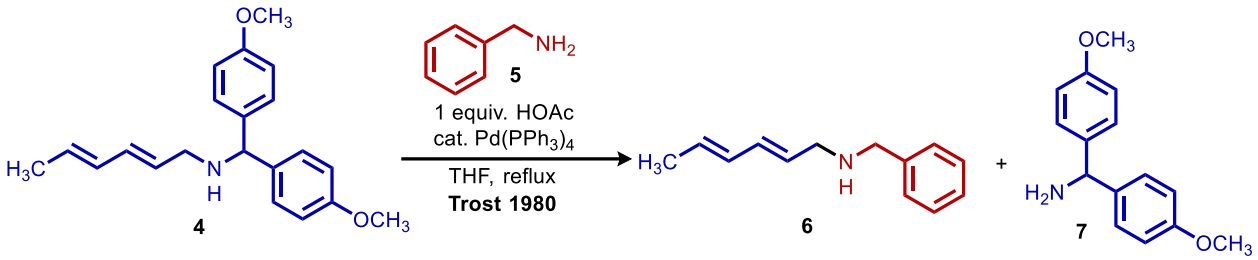

Scheme 1.1. Deaminative exchange of a secondary amine with a primary amine.

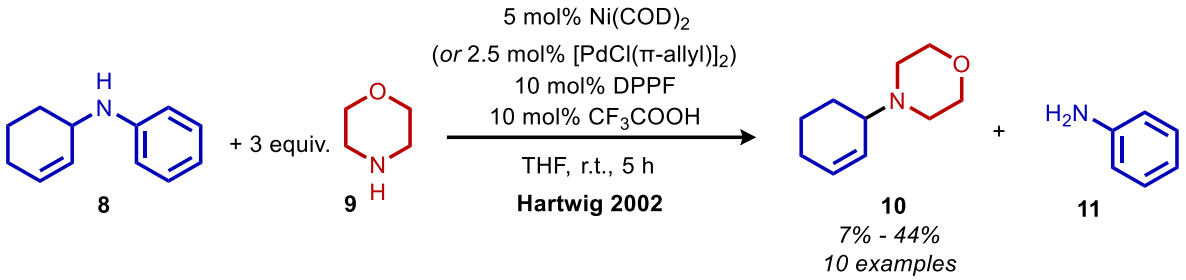

Scheme 1.2. Deaminative exchange of two secondary amines.

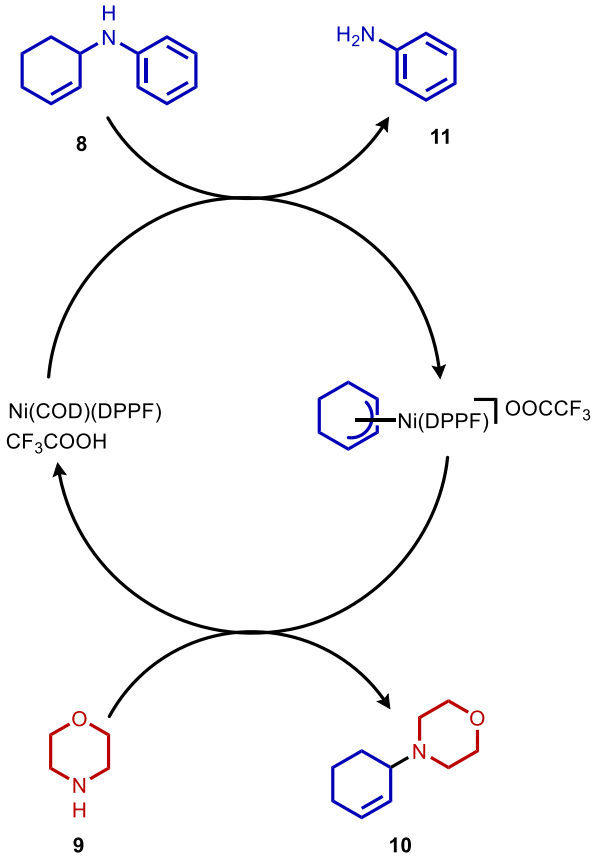

Figure 1.2. Proposed mechanism for secondary amine exchange *via* a metal allyl complex.

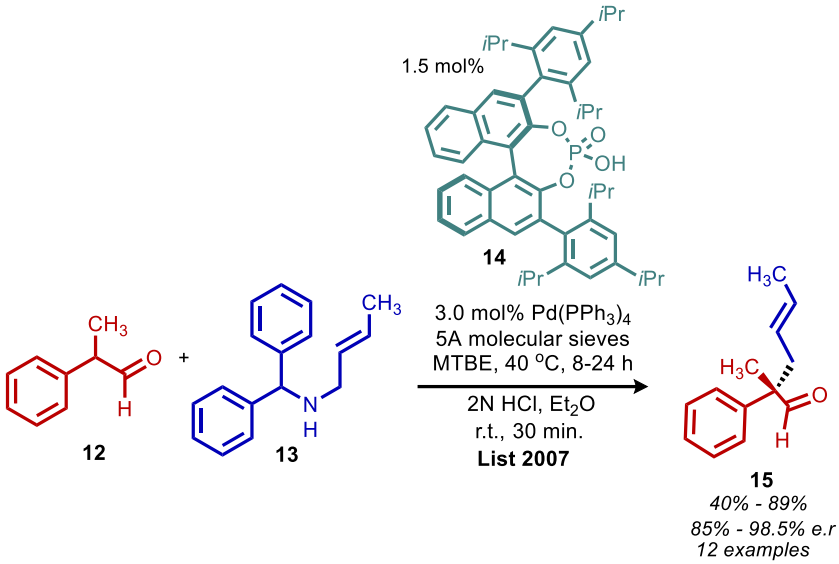

Scheme 1.3. Deaminative synthesis of chiral α-allylated aldehydes using a palladium complex.

The Xi group was able to achieve the deaminative synthesis of pyrroles (**17**) from secondary amines.[15] Catalytic palladium and cyclopentadiene-phosphine ligands facilitate this transformation *via* a proposed σ-bond metathesis with an alkyl dibromide moiety (**16**) (Scheme 1.4). This work was subsequently expanded to include the synthesis of indoles using an internal alkyne.[15]

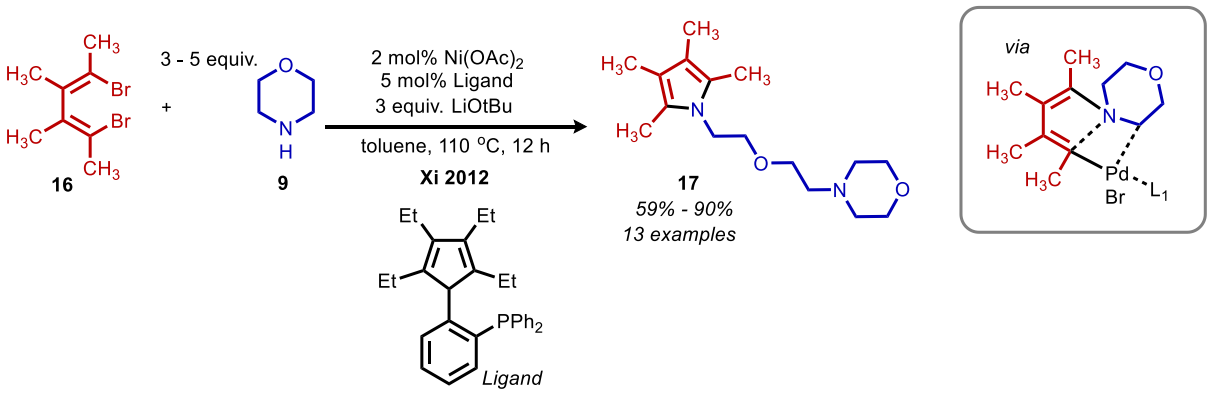

Scheme 1.4. Synthesis of pyrroles by C-N bond cleavage *via* a sigma bond metathesis.

Analogous to the deaminative oxidation of primary amines discussed in section 1.3.4, secondary amines can also be oxidized to imine species by α C-H abstraction and subsequent hydrolysis yields carbonyl compounds.[16] In the presence of catalytic copper and *tert*-butyl hydroperoxide, secondary amines (**18**) are oxidized to imine intermediates which can undergo Friedel-Crafts alkylation with indole moiety **19** (Scheme 1.5).[16] Subsequent oxidation and hydrolysis results in the ketone product (**20**). However, one drawback of this methodology is that dialkyl secondary amines could not be successfully reacted, hence the substrate scope is limited to monoalkyl aromatic secondary amines. This class of transformation has also been reported to proceed *via* oxidation with iron and ruthenium catalysts.[17]

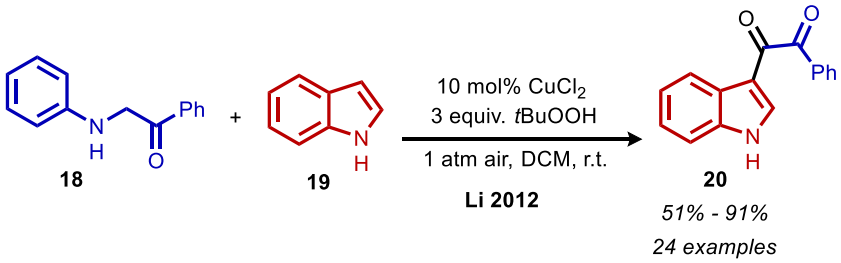

Scheme 1.5. Oxidative deamination of secondary amines to ketone products *via* Friedel-Crafts alkylation.

The conversion of a secondary amine to a primary amine and a ketone has been facilitated by a rhodium complex.[18] The secondary amine is oxidized to an imine by formation of a rhodium hydride complex and hydrolysis with water gives the ketone product. Another secondary amine activation which proceeds *via* an imine intermediate was reported by the Marciniec group. Using a ruthenium hydride complex, the re-distribution of secondary amines (**21**) to a tertiary amine (**22**) and ammonia (**23**) was demonstrated (Scheme 1.6).[19] This procedure was also used to facilitate the deaminative redistribution of primary amines to secondary amines and ammonia discussed in section 1.3.3.

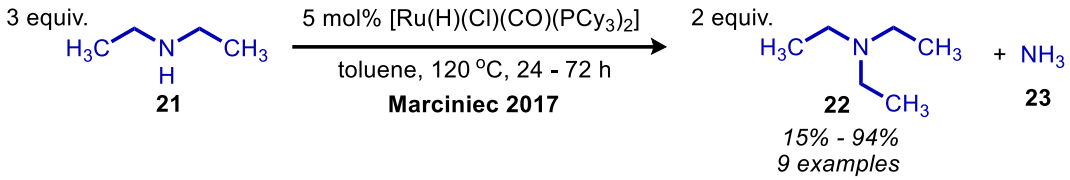

Scheme 1.6. Deaminative re-distribution of secondary amines to tertiary amines and ammonia.

1.3. Activation and Substitution of Primary Aliphatic Amines.

1.3.1. Deamination by a Polar Mechanism.

Primary amines exhibit poor nucleofugality, which renders a simple nucleophilic substitution highly challenging. Typically, primary amines must be converted to a better leaving group or "pre-functionalized' before they can participate in substitution and elimination chemistry. Figure 1.3 summarizes the different strategies for pre-functionalization of primary amines prior to substitution. While aromatic amines can be easily pre-functionalized by diazotization, this strategy is not usually employed with aliphatic amines due to the instability of such diazo intermediates and their associated propensity to eliminate.[20, 21] One notable exception from Wang has reported deaminative $C(sp^3)$-$C(sp^2)$ coupling of stabilized α-aminoesters *via in-situ* diazotization followed by coupling with aryl boronic acids.[22]

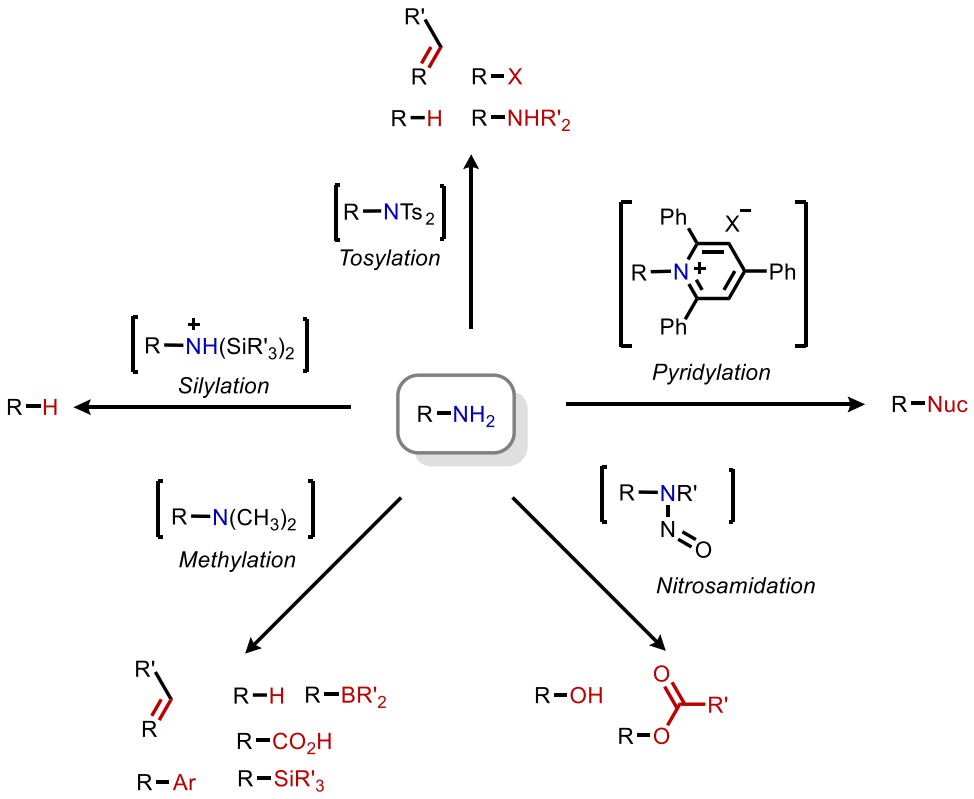

Figure 1.3. Summary of the pre-functionalization strategies utilized for deamination by a polar mechanism.

Given the ease with which alcohols undergo tosylation, pre-functionalization of primary amines was historically pursued in the same manner. DeChristopher reported installing two sulfonamide moieties on primary alkyl amines to yield *N*-alkyl-*N*,*N*-disulfonimides (**25**).[23] These moieties gave a mixture of elimination (**26**) and substitution products (**27**) upon reflux in DMF with aniline (**11**) as a nucleophile (Scheme 1.7). Subsequent work by Baumgarten showed that alkenes could be produced selectively when neat *N*-alkyl-*N*,*N*-disulfonimides were heated to high temperatures.[24] Selective substitution chemistry was also achieved using *N*-alkyl-*N*-sulfonimides. Treatment with potassium hydroxide and chloramine was shown to afford alkyl halides or alkanes, depending on the order of addition of reagents.[25] Inspired by these classical reports of tosylation, Oestreich has recently reported an *in-situ* pre-functionalization *via* silylation using phenylsilane

(Scheme 1.8).[26] The Lewis acid tris(pentafluorophenylborane) was used to abstract silylated amine **29**, resulting in a net reductive deamination. They propose two possible pathways, with one hypothesis involving reduction of the silylated amine (**32**) and the other invoking a dissociation to form a carbocation frustrated Lewis pair (**31**).

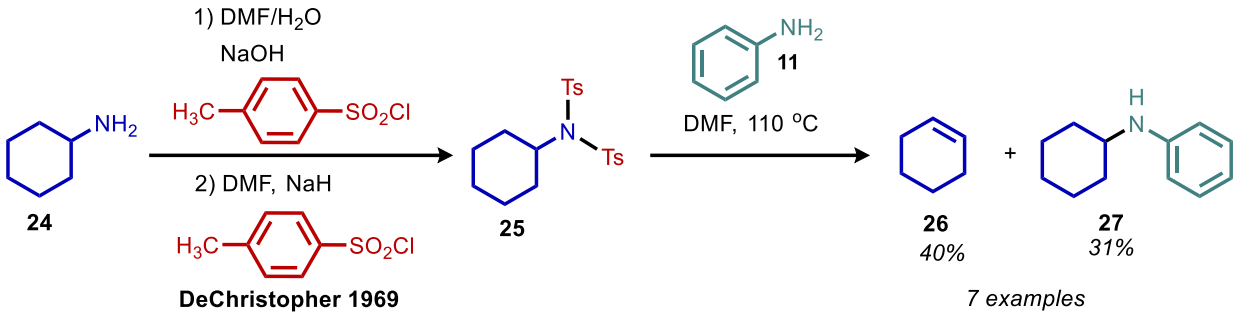

Scheme 1.7. Deaminative substitution mediated by tosylation.

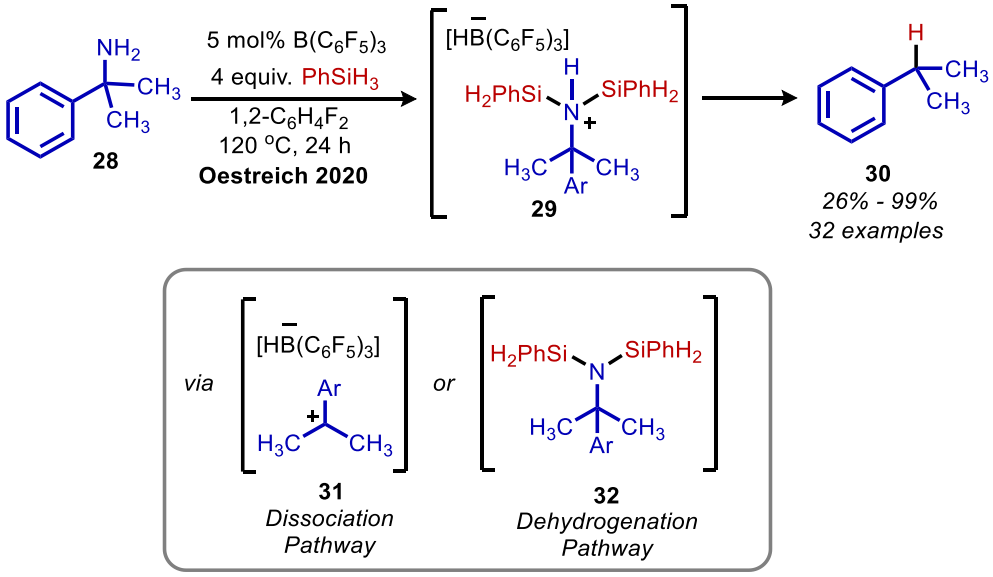

Scheme 1.8. One-pot reductive deamination by *in-situ* silylation.

Deamination *via* a polar mechanism can also be achieved by methylation. The classical Hoffman reaction involves facile methylation of primary amines with methyl iodide to yield a quaternary ammonium cation which undergoes subsequent *anti*-selective elimination.[27] An

analogous methylation of primary amines to tertiary amines and subsequent reaction with *m*-CPBA results in the production of an *N*-oxide intermediate which undergoes *syn*-selective elimination in the classical Cope reaction.[28] Recently, methylated quaternary ammonium salts have also been shown to participate in cross-coupling reactions. Watson and coworkers demonstrated deaminative cross-coupling with catalytic nickel and aryl boronic acids, resulting in enantiopure diarylethanes (**35**) (Scheme 1.9).[29] This enantioselectivity is thought to be from an inversion of configuration by S_N2 addition of the amine to the nickel catalyst, providing evidence for a polar mechanism. The Oestreich group has also demonstrated deaminative silylation of methylated quaternary ammonium salts (**36**) using catalytic copper with silyl boronic esters (Scheme 1.10).[30] There have also been several reports of metal catalyzed deaminative carbonylation of methylated quaternary amine salts.[31, 32]

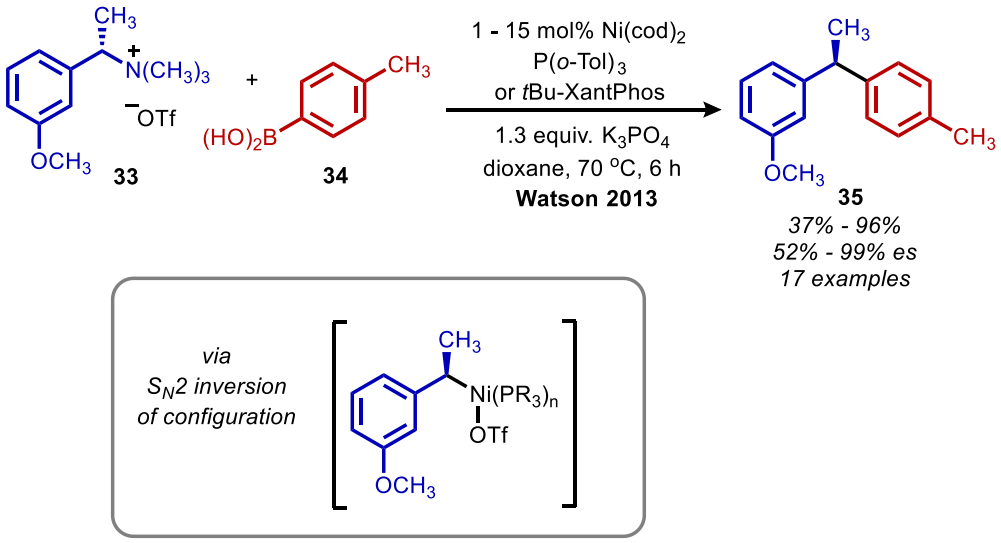

Scheme 1.9. Enantioselective deaminative arylation of alkylated amines.

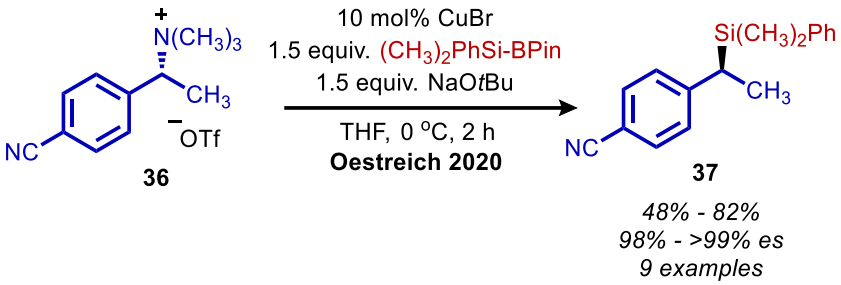

Scheme 1.10. Enantioselective deamination of benzylic quaternary amines to silanes.

Another strategy for the deamination of primary amines is by way of nitration to generate an *N*-nitroamide reactive intermediate. The Jakobsche group has demonstrated that following amidation with methyldichloroacetate (**39**), reaction with sodium nitrite yields the requisite intermediate **40** (Scheme 1.11).[33] A subsequent rearrangement liberates dinitrogen and an ester product (**41**), which is hydrolyzed to give the net amine **38** to alcohol **42** conversion.

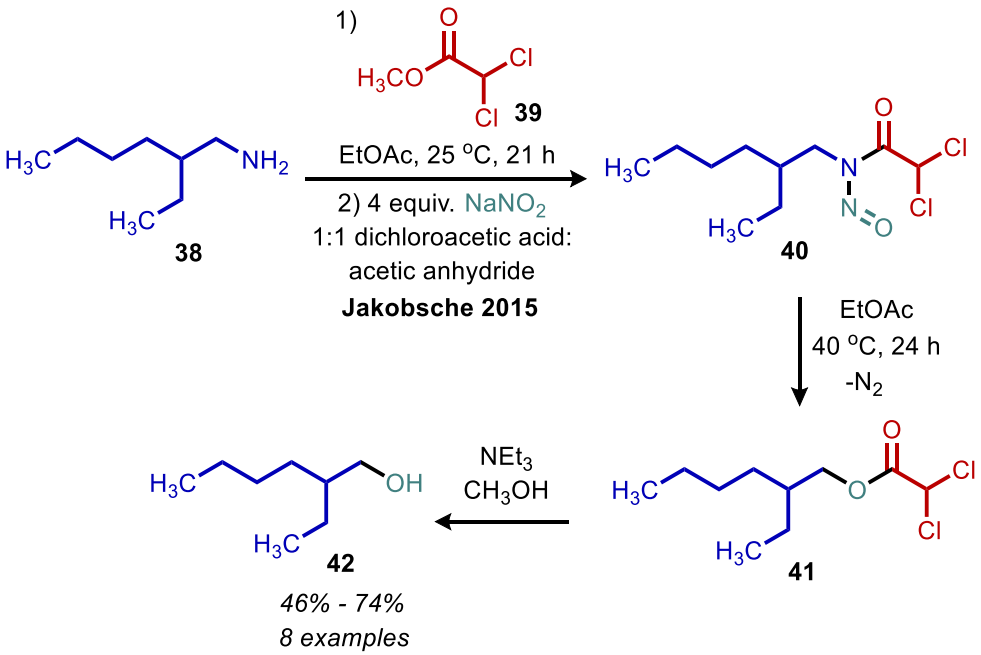

Scheme 1.11. Deaminative synthesis of alcohols *via* *N*-alkyl-*N*-nitrosamides.

The scope of deaminative substitution chemistry was vastly expanded by the work of the Katritzky laboratory. Primary amines were shown to undergo pre-functionalization by reaction

with pyrylium salts (**43**) to generate an *N*-alkylpyridium salt (subsequently named a "Katritzky salt"), which can undergo facile substitution with a variety of nucleophiles (Scheme 1.12).[34-40] Seminal work with *N*-benzyl 2,4,6-triphenylpyridinium perchlorate (**45**) showed that reflux with piperidine yielded tertiary amine product **47** (Scheme 1.13a).[34] Sodium phenoxide and aniline were also used as nucleophiles to generate ethers and secondary amine products, respectively (Scheme 1.13b).[34] The use of triphenylphosphine also produced phosphonium salt product **49** (Scheme 1.13c).[34] Substitution reactions of *N*-methyl, *N*-allyl and *N*-benzyl pyridinium salts demonstrated second order kinetics.[41, 42] However, substitution of secondary *N*-alkyl species such as *N*-isopropyl pyridinium salts exhibited S_N1 character, as the reaction rates were shown to be independent of the concentration of piperidine.[41, 42] As discussed in section 1.3.2, Katritzky salts are also capable of participating in radical chemistry.

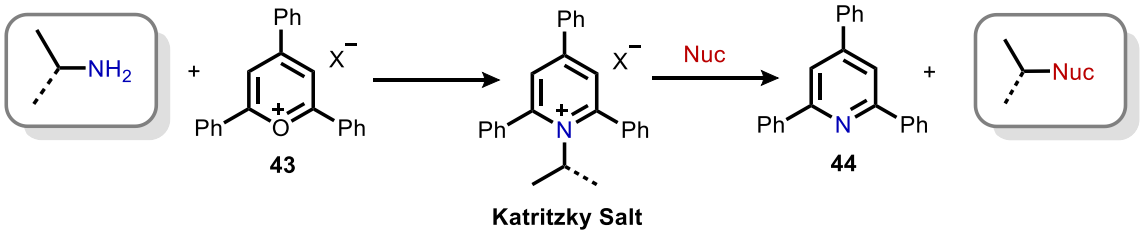

Scheme 1.12. Pre-functionalization of primary amines to Katritzky salts.

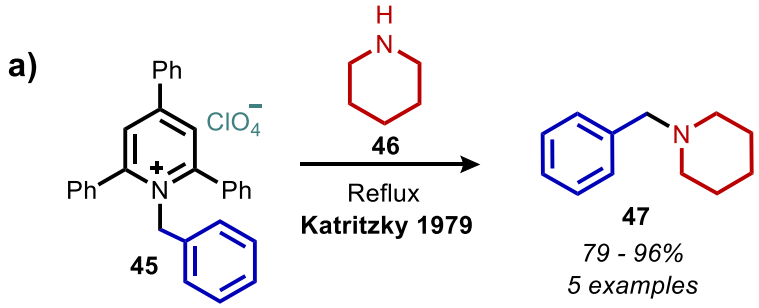

Scheme 1.13. Examples of Katritzky salt substitution chemistry including the nucleophiles a) piperidine; b) phenoxide and c) triphenylphosphine.

Scheme 1.13 continued. Examples of Katritzky salt substitution chemistry including the nucleophiles a) piperidine; b) phenoxide and c) triphenylphosphine.

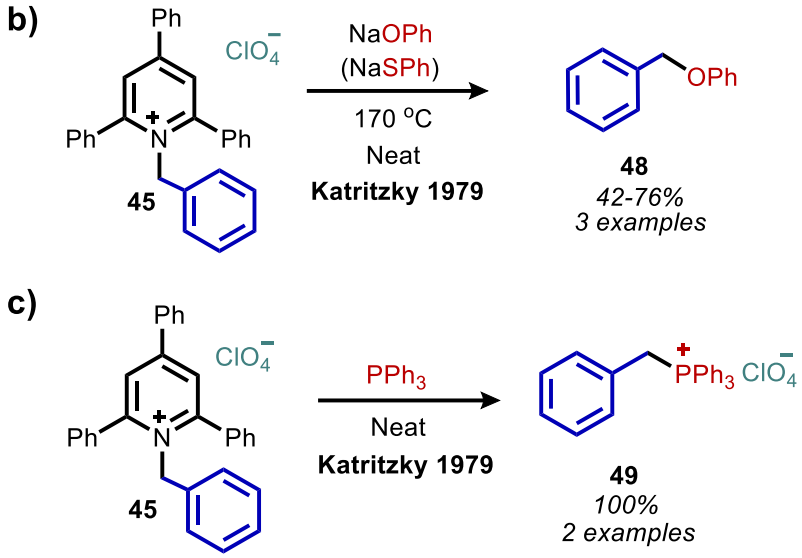

1.3.2. Deamination by a Radical Mechanism.

Radical intermediates have become increasingly important in modern organic synthesis due to the ease with which they can be accessed and transformed using photoredox and cross-coupling methods.[43, 44] This section highlights how primary amines have been harnessed as precursors to alkyl radical species which can be intercepted with photocatalytic and cross-coupling techniques (Figure 1.4). However, in a notable classical example, Barton and coworkers reported that primary amines (**50**) can be converted to isonitriles (**52**) by formylation and subsequent dehydration with either phosphorus oxychloride or *p*-toluenesulfonyl chloride.[45-48] This isonitrile species can then be converted to an alkane (**53**) by a radical mechanism using *n*$(Bu)_3$SnH and AIBN initiator (Scheme 1.14).

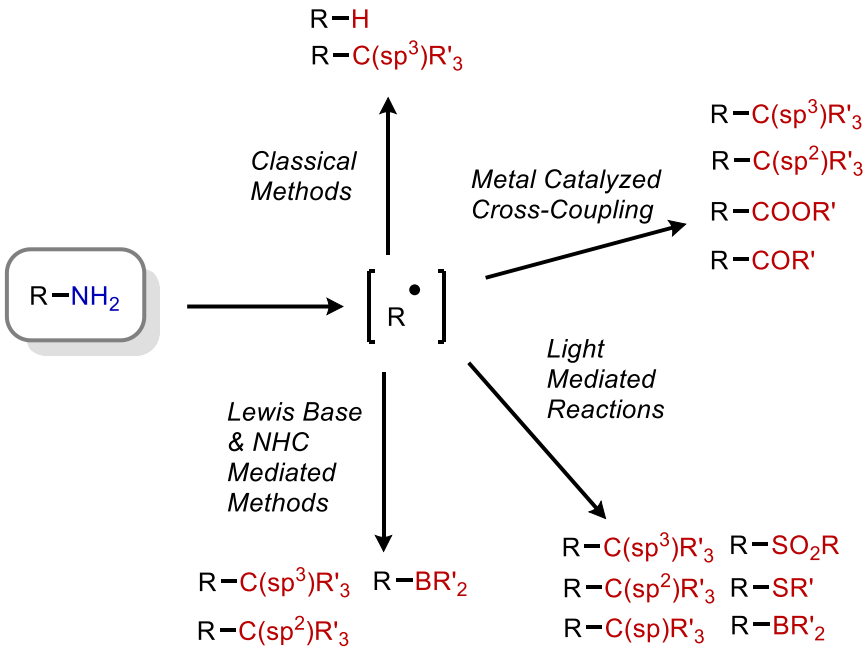

Figure 1.4. Summary of deaminative functionalization enabled by a radical mechanism.

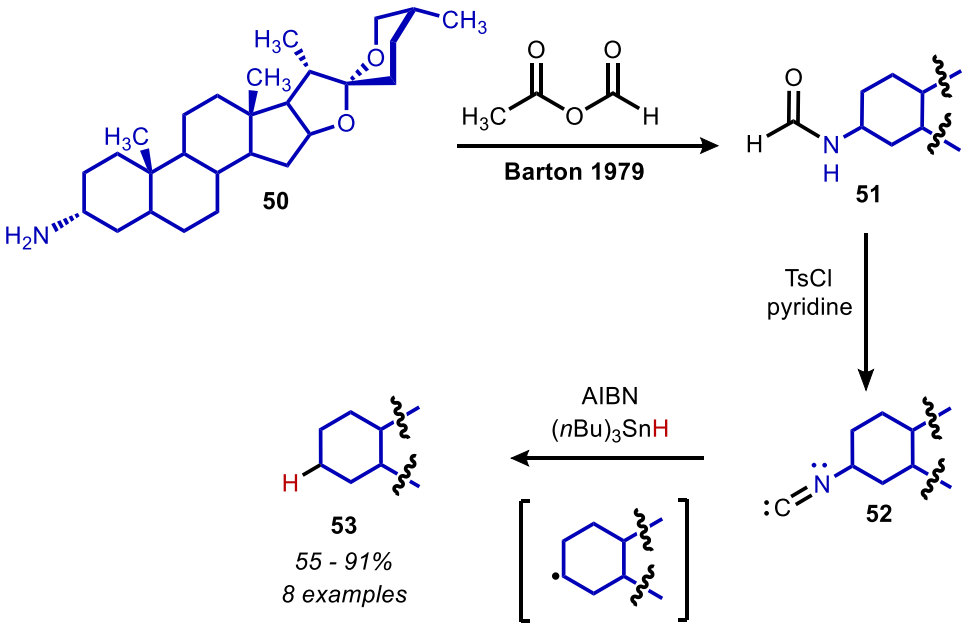

Scheme 1.14. Barton-Saegusa deamination of amines to alkanes.

In addition to their polar substitution chemistry, Katritzky salts can also be utilized for radical deamination reactions.[40] Deaminative alkylation of Katritzky salt **54** with nitronate (**55**)

and malonate (**57**) anions resulted in the formation of products **56** and **58** with C(sp^3)-C(sp^3) bonds (Scheme 1.15).[49, 50] Mechanistic evidence including bimolecular kinetics wherein secondary aliphatic substituents react at a faster rate than primary aliphatics, suggested the presence of a radical intermediate.[51] UV-vis spectroscopy demonstrated quenching of the Katritzky salt absorption upon addition of sodium nitromethanide solution, suggesting the reaction proceeds by a charge transfer complex (CTC).[41] Katritzky salts can also be reduced with sodium borohydride to form 1,2-dihydropyridines (**59**).[52, 53] Subsequent pyrolysis upon heating to 200 °C results in the production of alkane **60** (Scheme 1.16a). Deuterium labelling experiments with $NaBD_4$ were conducted to further elucidate the mechanism of reduction.[54] A concerted mechanism was expected to provide a mixture of both α-deutero-toluene (**60-*α*-D**) and *o*-deutero-toluene (**60-*o*-D**) products through formation of isotoluene intermediate **61**. However, **60-*o*-D** was the only product detected, providing evidence instead for a radical mechanism via intermediates **62** and **63** (Scheme 1.16b).[54]

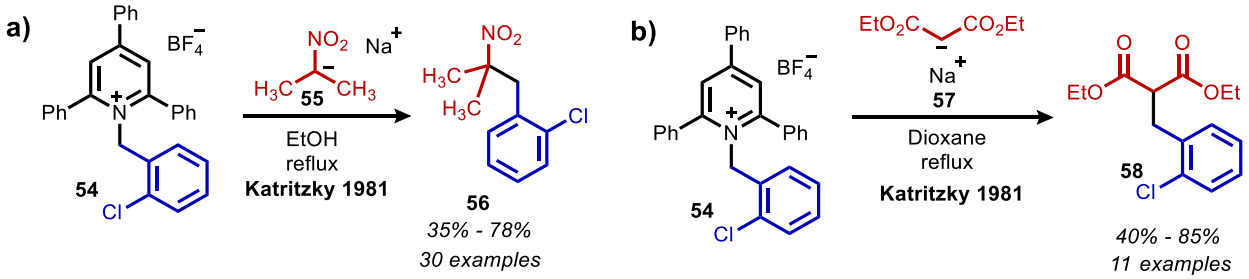

Scheme 1.15. Radical deamination of Katritzky salts with a) nitronate and b) malonate.

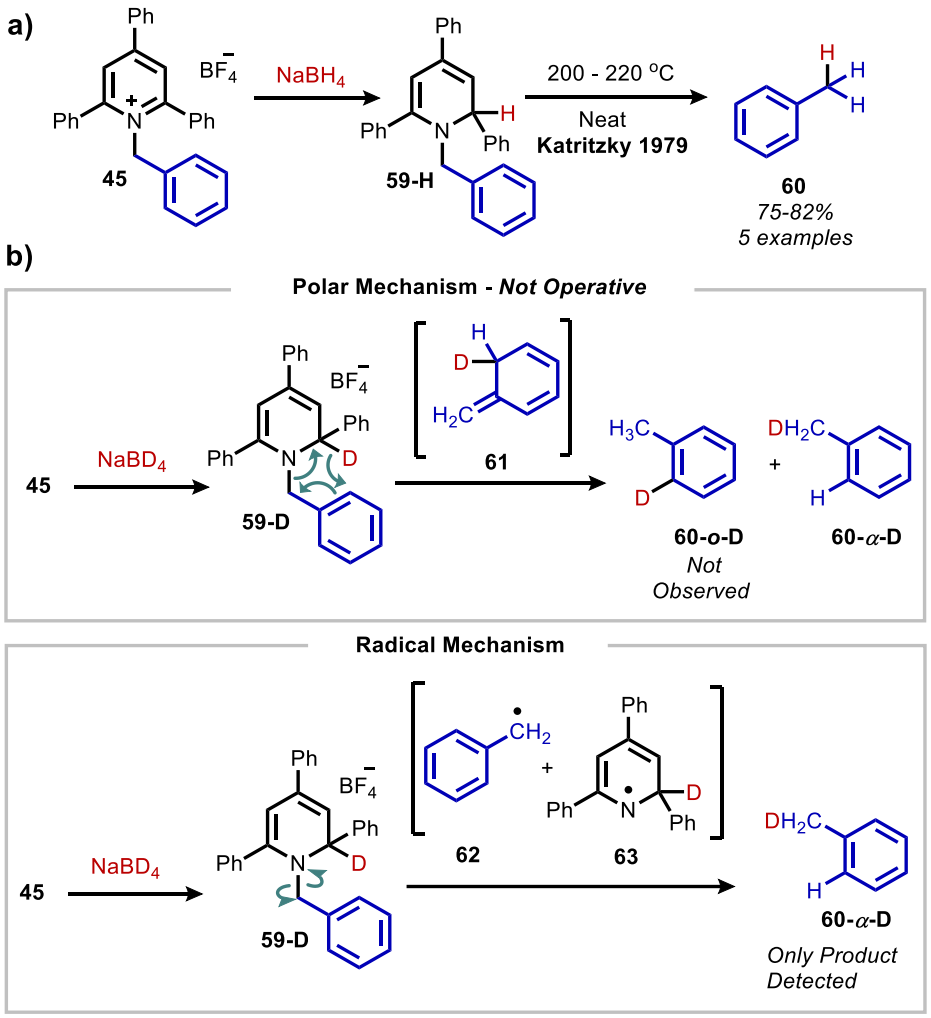

Scheme 1.16. Reductive deamination of Katritzky salts including a) scope and b) mechanistic evidence for a radical mechanism.

The Watson group cemented the modern use of Katritzky salts for aliphatic deaminative cross-coupling reactions. In their 2017 seminal report, catalytic nickel (II) acetate and bathophenanthroline (BPhen) ligand are employed for deaminative C(sp^3)-C(sp^2) coupling of *N*-alkylpyridinium tetrafluoroborate salts (**64**) with aryl boronic acids (**65**) (Scheme 1.17a).[55] A radical clock derived pyridinium salt produced a rearranged product and the addition of TEMPO produced trapped adducts, suggesting the presence of radical intermediates. Their postulated mechanism involves single electron reduction of the Katritzky salt by the nickel catalyst. The

reduced Katritzky salt intermediate then undergoes fragmentation to form 2,4,6-triphenylpyridine side product and an alkyl radical species which is intercepted by the nickel catalyst. The substrate scope of this procedure was further expanded to include Katritzky salts derived from benzylic amines and amino acid methyl esters, as well as vinyl boronic esters as cross-coupling partners.[56-58] 9-BBN has also been used for *in-situ* hydroboration with alkenes, which can subsequently undergo deaminative cross-coupling to result in $C(sp^3)$-$C(sp^3)$ products.[59] Deaminative $C(sp^3)$-$C(sp^3)$ bond formation (**68**) was also achieved using a Negishi-type coupling with alkyl zinc halides (Scheme 1.17b).[1]

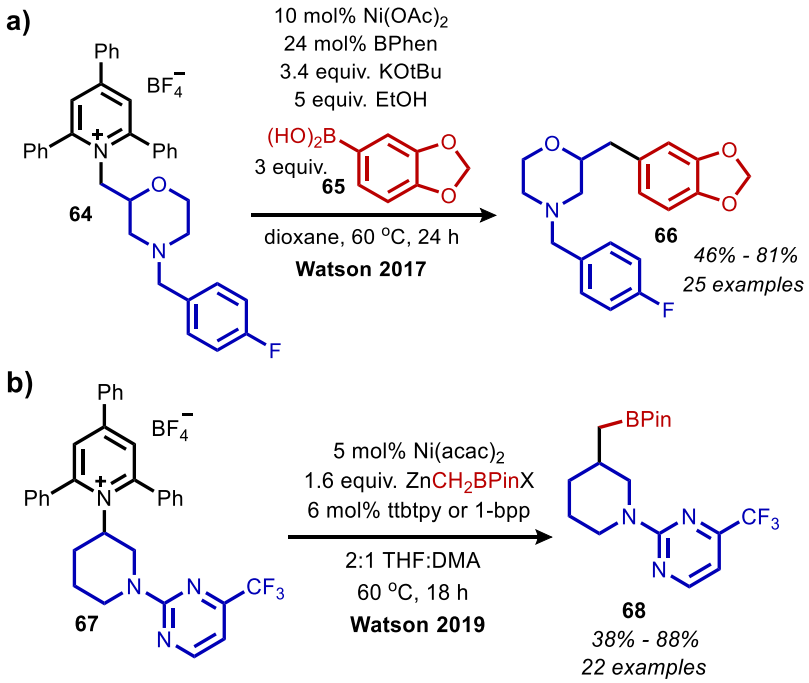

Scheme 1.17. Nickel catalyzed deaminative cross-coupling of Katritzky salts with a) aryl boronic acids and b) alkyl zinc halides.

An alternative method for $C(sp^3)$-$C(sp^3)$ coupling was disclosed by the Martin group using non-activated alkenes (**70**), $NiBr_2$·glyme and dtbpy (4,4′-di-*tert*-butyl-2,2′-bipyridine) ligand (Scheme 1.18a).[60] Terminal alkenes reacted with Katritzky salts to give anti-Markovnikov products (**71**) with $(EtO)_3SiH$ as the hydride source. The Liu group has also reported a deaminative

hydroalkylation using internal alkynes and $(Me_2SiH)_2O$ (Scheme 1.18b).[61] Using Katritzky salts derived from α-secondary amines (**72**) and aryl alkyl alkyne **73**, regioselectivity ratios of >20:1 were reported.

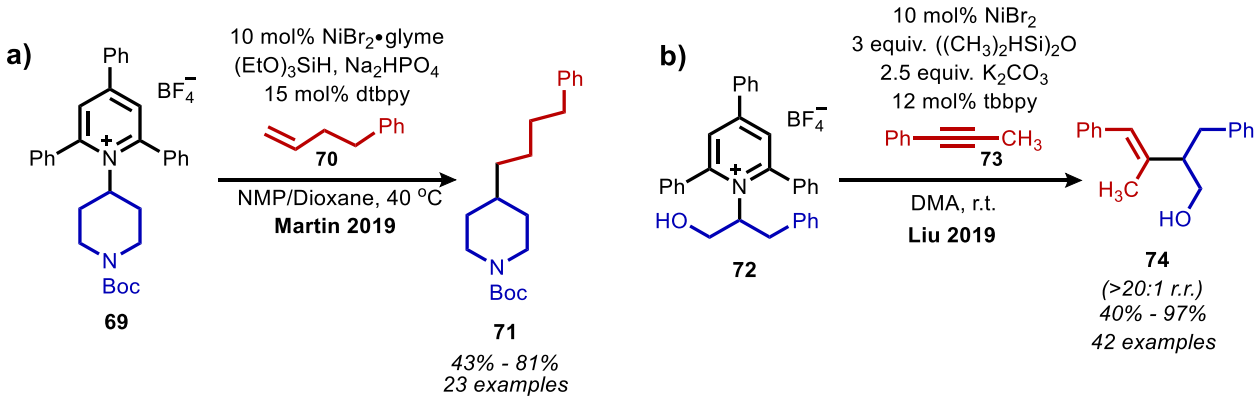

Scheme 1.18. a) Deaminative hydroalkylation of a) unctivated alkenes and b) alkynes.

Subsequent work on deaminative coupling reactions led to several reports of reductive cross-couplings. The Rueping group reported using Mn(0) for nickel catalyzed cross-coupling of Katritzky salts with aryl iodides and bromides (Scheme 1.19).[62-64] The proposed mechanism invokes initial oxidative addition of the aryl halide with nickel (0) (Figure 1.5). This nickel (II) intermediate is then reduced by Mn(0) to generate a nickel (I) aryl species, which subsequently reduces the Katritzky salt. A nickel (III) species bearing alkyl and aryl substituents is thus formed and undergoes reductive elimination to yield the $C(sp^2)$-$C(sp^3)$ product, and the nickel (0) catalyst is regenerated with Mn(0). The Han group has expanded reductive deamination to include $C(sp^3)$-$C(sp^3)$ coupling with the use of Zn(0).[65] Molander has also reported using the photoredox catalyst 4-CzIPN (1,2,3,5-tetrakis(carbazol-9-yl)-4,6-dicyanobenzene) and blue light for reductive deaminative cross-coupling, in place of Mn(0) or Zn(0) and with triethylamine as a sacrificial reductant.[66]

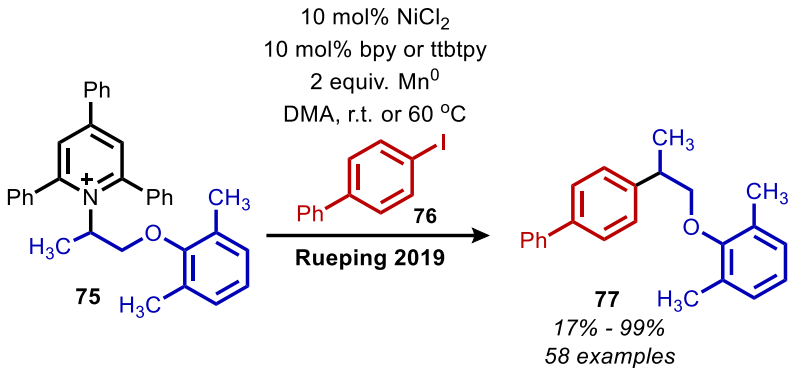

Scheme 1.19. Reductive deaminative cross-coupling of Katritzky salts with aryl halides.

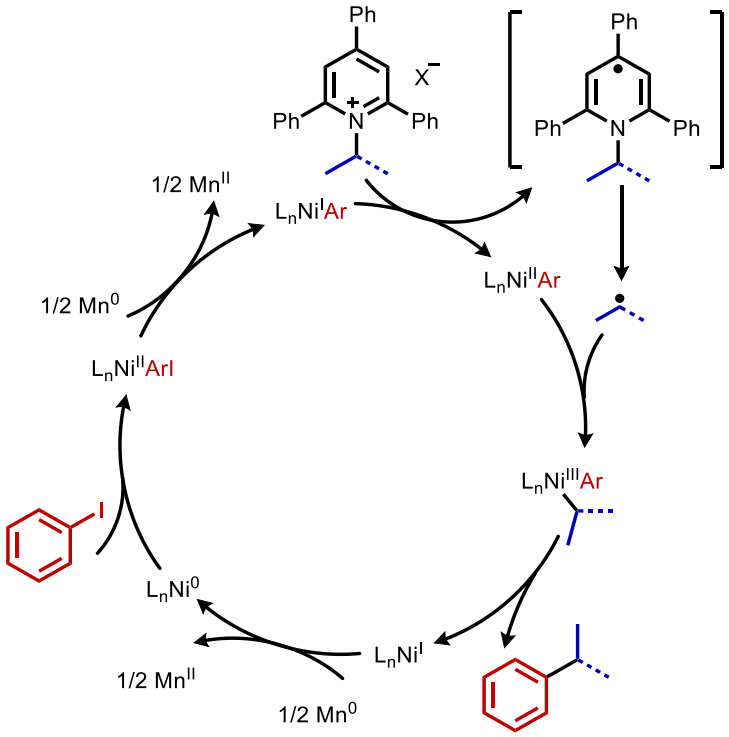

Figure 1.5. Proposed catalytic cycle for reductive deaminative cross-coupling.

The net conversion of a primary amine to a methyl ester (**79**) has also been enabled by deaminative cross-coupling methodology. Using $Co(acac)_2$ catalyst and 4,7-dihydroxy-1,10-phenanthroline (dhphen) ligand, Katritzky salts undergo deaminative coupling with carbon monoxide and methanol (Scheme 1.20).[67] The postulated mechanism invokes reduction of the Katritzky salt by cobalt (0) to generate a cobalt (II) alkyl species (Figure 1.6). This intermediate

participates in CO insertion and subsequently reacts with methanol to yield the ester product. A previously unreported conversion of primary amines to difluoromethane moieties (**81**) was recently disclosed by the Liu group.[68] Catalytic copper was used for cross-coupling of Katritzky salts with Vicic-Mikami reagent (Scheme 1.21). This reaction is a notable exception to previously reported deaminative cross-coupling reactions in that Katritzky salt derivatives containing additional electron-withdrawing substituents or ring fusions (**80**) were required to obtain high yields.

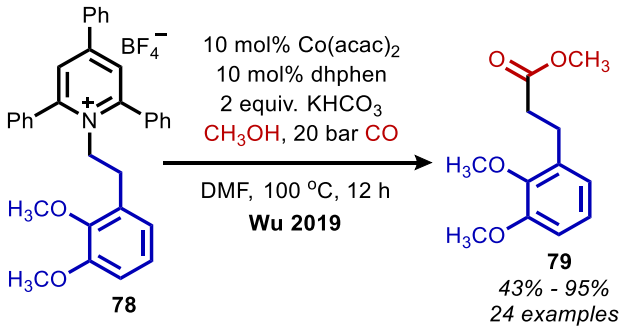

Scheme 1.20. Conversion of amines to methyl esters using catalytic cobalt, methanol and carbon monoxide.

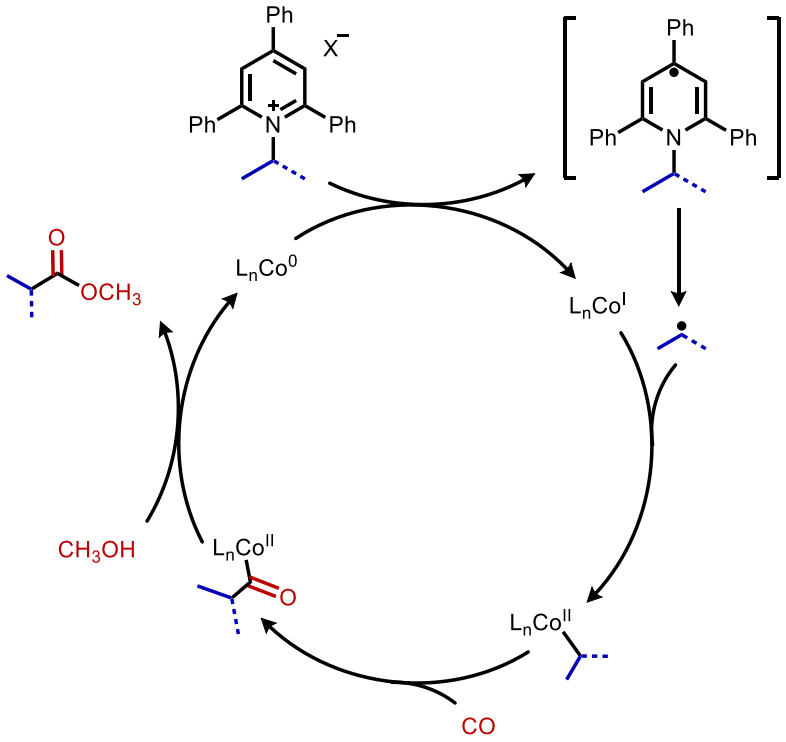

Figure 1.6. Proposed mechanism for cobalt catalyzed deaminative esterification.

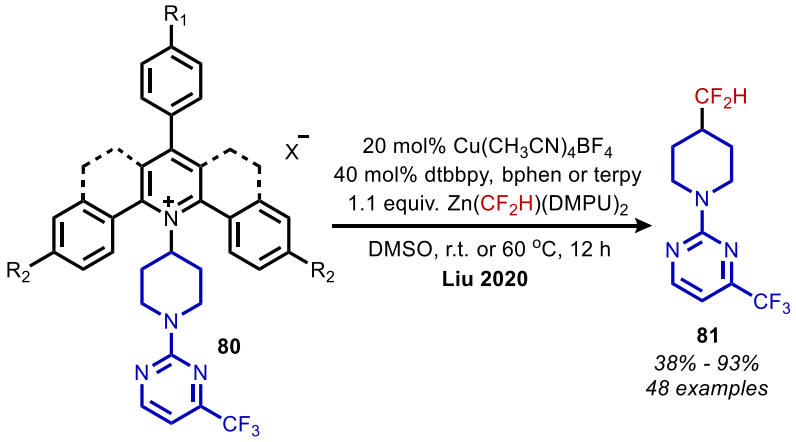

Scheme 1.21. Conversion of primary amines to difluoromethane isosteres using catalytic cobalt and Vicic-Mikami reagent.

In addition to metal catalyzed cross-coupling reactions, deaminative photocatalytic strategies have emerged as an equally useful tool. The Glorius group first demonstrated photoredox catalyzed deamination of Katritzky salts using $[Ir(ppy)_2(dtbbpy)]PF_6$ (Scheme 1.22). The resulting alkyl radical species were intercepted with electron rich arenes to yield Minisci

coupled products (**84**).[69] Subsequently, numerous groups reported photoredox catalyzed C(sp^3)–C(sp^3) and C(sp^3)–C(sp^2) coupling reactions *via* both Giese and Heck type syntheses.[70-77] Rather than comprehensively reviewing these methodologies for C-C bond formation, other deaminative transformations for C-heteroatom bond formation are highlighted here. Such transformations have not been achieved *via* metal catalyzed cross-coupling reactions and illustrate the merit of photocatalysis for radical chemistry. The breadth of deaminative functionalization illustrated here is intended to provide context for the reductive deamination presented in chapter 3.

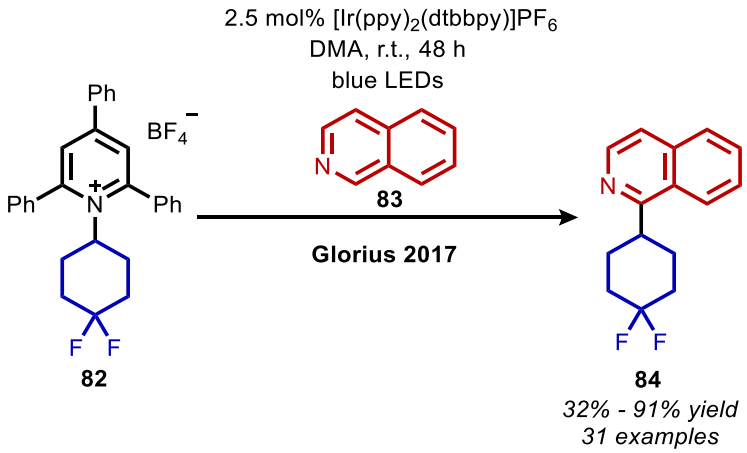

Scheme 1.22. Deaminative Minisci coupling enabled by photoredox catalysis.

Gryko reported the first deaminative C(sp^3)-C(sp) coupling of alkynyl sulfones (**86**) with Katritzky salts using eosin Y and green light (Scheme 1.23).[78] In the proposed mechanism, the liberation of a radical toluenesulfonyl species yields the requisite product (**87**) and DIPEA acts as a sacrificial reductant (Figure 1.7). The synthesis of alkyl sulfones (**90**) has also been achieved by deaminative coupling of potassium metabisulfite and silyl enol ethers (Scheme 1.24).[79] Initial radical addition to sulfur dioxide generates an alkylsulfonyl radical intermediate, which is trapped by the enol and is subsequently oxidized. Base-induced desilylation yields the desired ketone product (Figure 1.8).

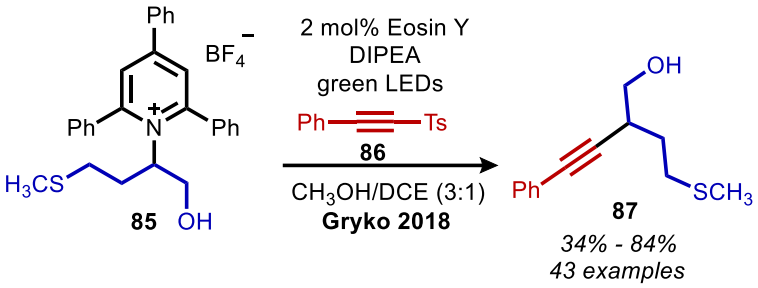

Scheme 1.23. Deaminative C(sp^3)-C(sp) bond formation using alkynyl sulfones.

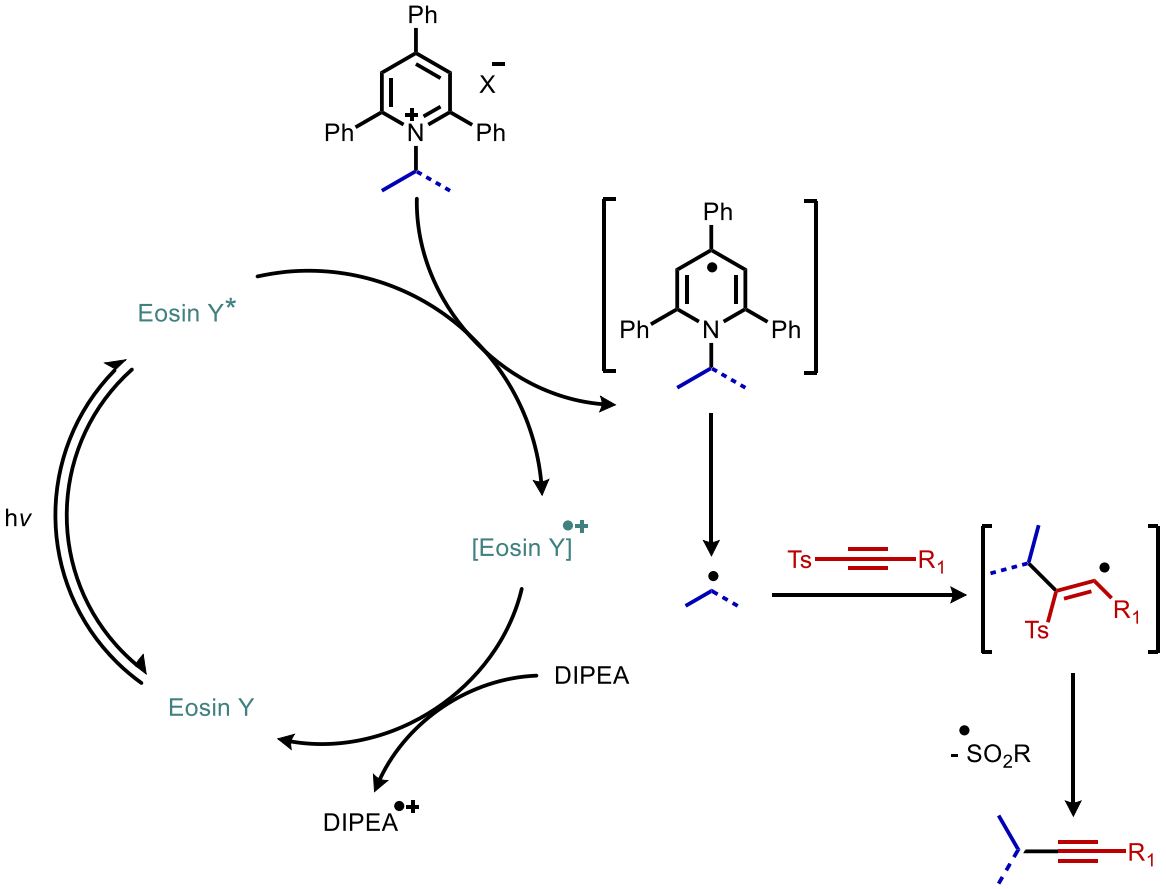

Figure 1.7. Proposed mechanism for deaminative C(sp^3)-C(sp) bond formation.

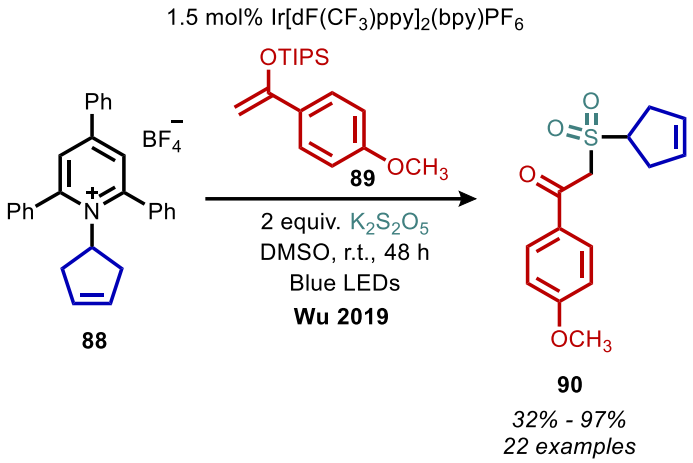

Scheme 1.24. Deaminative synthesis of alkyl sulfones.

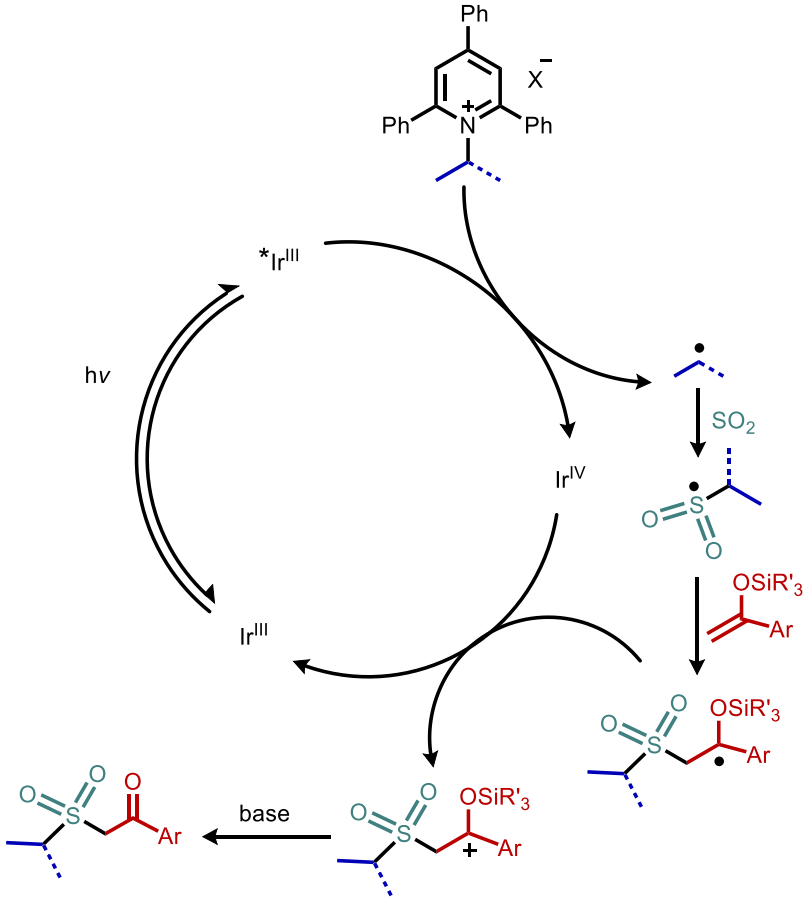

Figure 1.8. Proposed mechanism for the deaminative synthesis of alkyl sulfones.

Katrizky salts have also been shown to participate in visible light mediated electron-donor-acceptor (EDA) complexes. Such reactions involve two components in close intermolecular

association which are excited by a light source, causing one component (the donor) to transfer an electron to the other component (the acceptor).[80] An advantage of light induced EDA reactions is that they do not require the addition of a photoredox catalyst, which can be costly or time consuming to synthesize. Deaminative borylation enabled by EDA complexation was reported concurrently by the groups of Glorius and Aggarwal (Scheme 1.25).[81, 82] Alkyl boronic ester products (**92**) were achieved using blue LEDs, B_2cat_2 and Katritzky salts. Mechanistic studies including UV-vis spectroscopy demonstrated a bathochromic absorbance shift upon addition of B_2cat_2 with a solution of Katritzky salt in DMA, providing evidence for EDA complexation. A Job plot showed this EDA complex is formed in a 1:1 ratio and a reaction quantum yield of greater than 1 was obtained, suggesting a radical chain mechanism is occurring. They propose that a B_2cat_2·DMA adduct reduces the Katritzky salt during EDA complexation (Figure 1.9), which results in the formation of propagating radical species **94**. This mechanism is believed to be analogous to the reactions proceeding *via* a CTC originally reported by Katritzky (see Scheme 1.15).

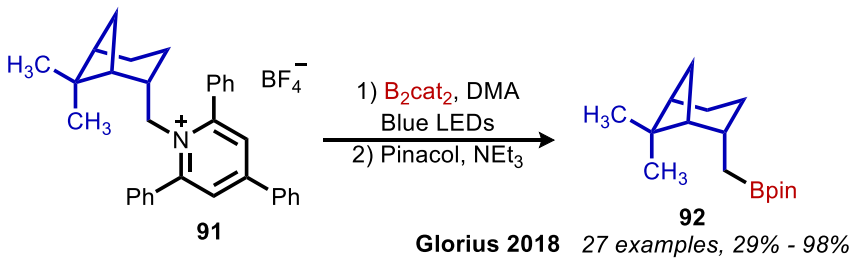

Scheme 1.25. Deaminative borylation enabled by EDA complexation of Katritzky salts.

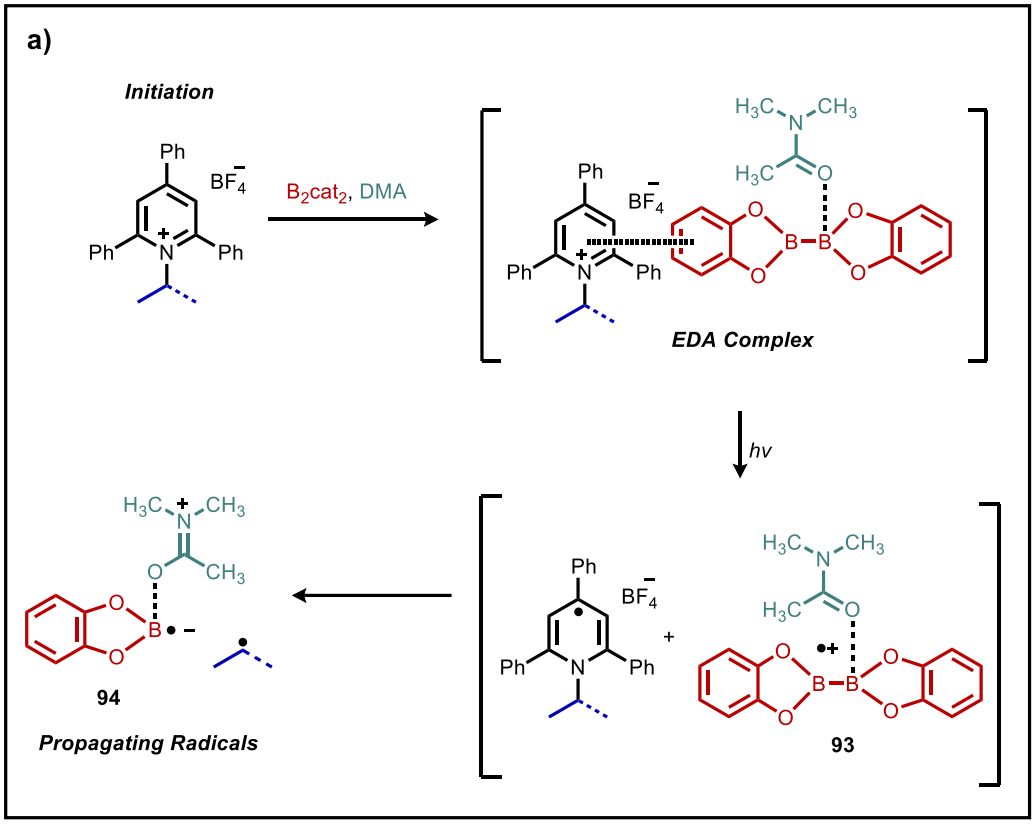

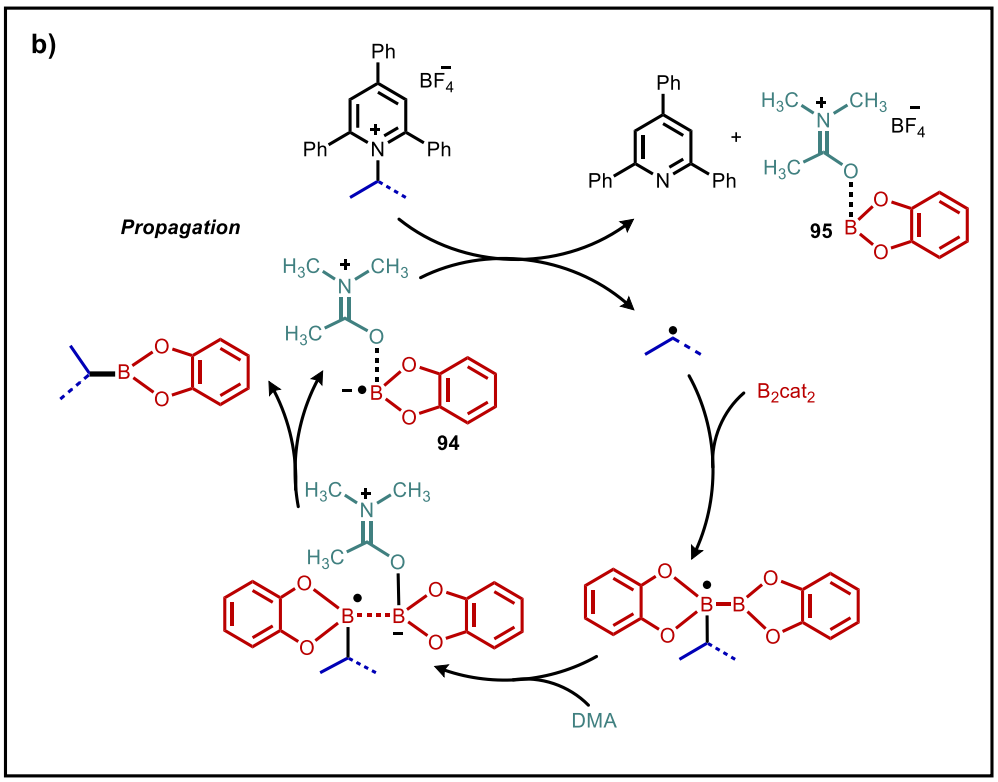

Figure 1.9. Proposed mechanism for deaminative borylation *via* EDA complexation involving a) initiation and b) propagation.

EDA complexation has also enabled the deaminative synthesis of alkyl thioesters (**97**) from amino acid derived Katritzky salts and thiobenzoic acid anions (Scheme 1.26a).[83] These thioester products can also undergo facile deprotection, resulting in the net conversion of amines to thiols. It was found that thiobenzoic acid could be replaced with alkyl and aromatic thiols, which also undergo EDA complexation to give thioether products (**99**) (Scheme 1.26b). There have additionally been reports of deaminative C(sp^3)–C(sp^3) and C(sp^3)–C(sp^2) bond formation enabled by EDA complexation.[82, 84, 85]

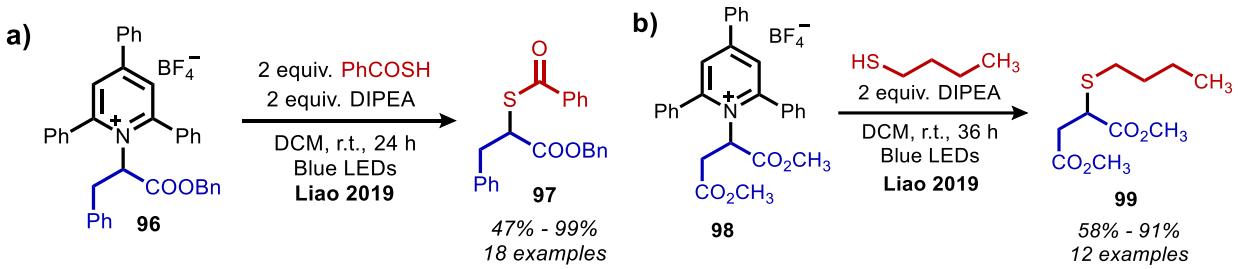

Scheme 1.26. EDA complex mediated deaminative conversion to a) alkyl thioesters and b) alkyl thioethers.

In addition to the wide range of deamination reactions involving Katritzky salts that are mediated by light, there have also been some reports of base catalyzed transformations. The Shi group first disclosed that deaminative borylation with B_2cat_2 can also be mediated with 10 mol% dtbpy ligand (Scheme 1.27).[86] Mechanistic studies demonstrated that the reaction proceeded in the dark, eliminating EDA complexation as a possible pathway. Boron NMR spectroscopy indicated that B_2cat_2 forms adduct **102** with dtbpy and enables the cleavage of the boron-boron bond (**103**) (Scheme 1.28). This moiety is proposed to form adduct **104** with the solvent DMAc, generating an intermediate with a sufficient reduction potential for single electron transfer to the

Katritzky salt. An alternative hypothesis is that this adduct may undergo homolysis to give a radical species with a similar reduction potential.

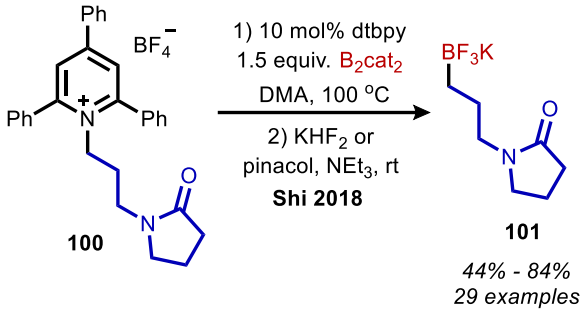

Scheme 1.27. Lewis base catalyzed deaminative borylation.

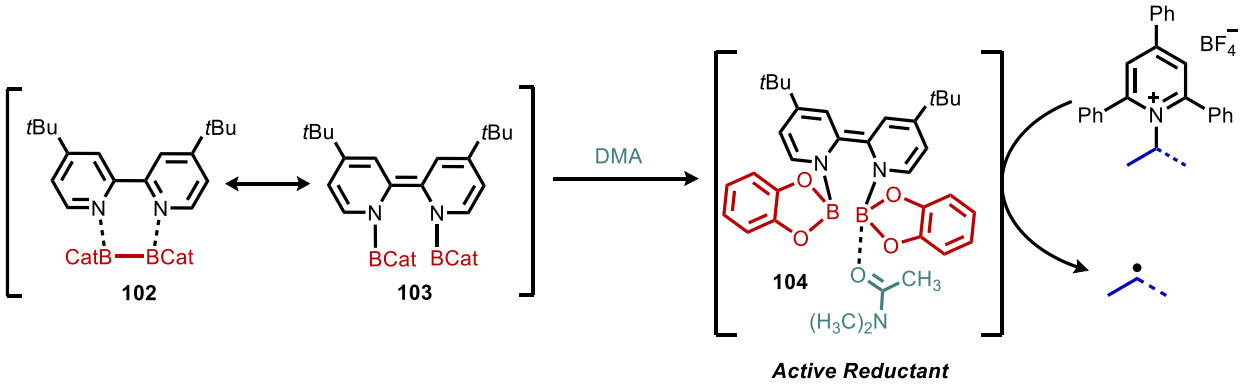

Scheme 1.28. Proposed mechanism for Lewis base catalyzed deaminative borylation.

The Hong group has subsequently disclosed using NHC **107** for base catalyzed deamination, resulting in the synthesis of ketone products (**108**) (Scheme 1.29).[87] The NHC reacts with aldehydes (**106**) to generate Breslow intermediate **111** capable of reducing Katritzky salts (Figure 1.10). DBU has also been used as a catalytic base for deaminative carbonylation with CO and styrene.[88, 89]

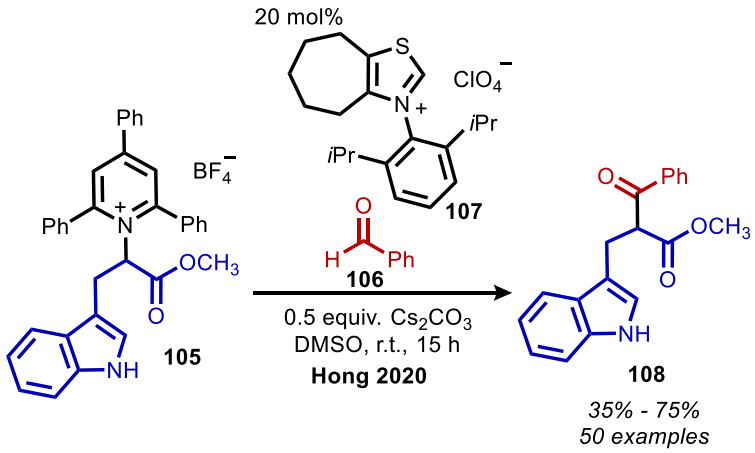

Scheme 1.29. NHC catalyzed deaminative synthesis of ketones.

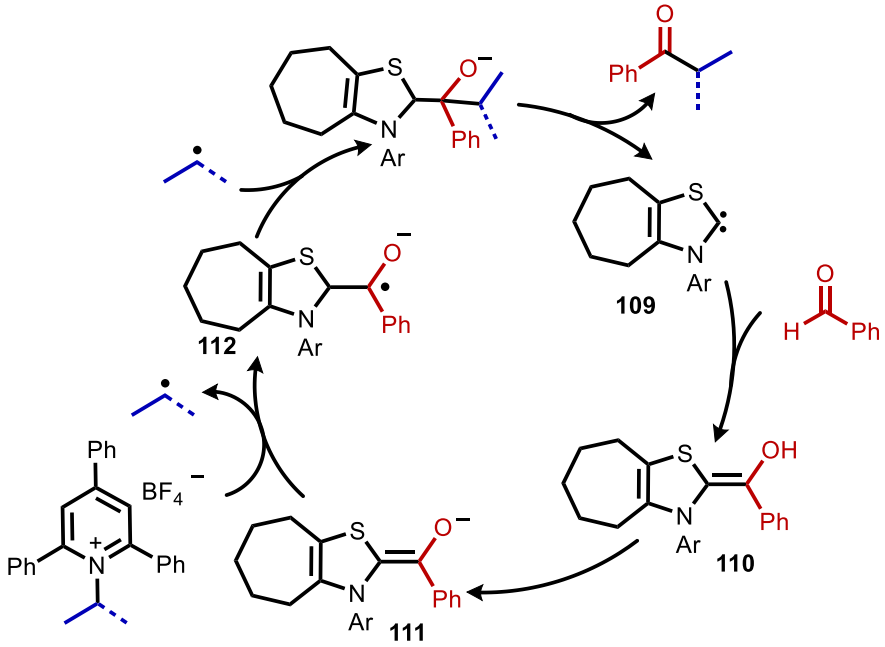

Figure 1.10. Proposed mechanism for deaminative synthesis of ketones *via* a Breslow intermediate.

While using Katritzky salts as a pre-functionalization strategy for the activation of primary amines has clearly facilitated a wide range of substitution reactions, a major drawback to this chemistry is α-tertiary primary amines cannot be utilized. Due to the steric bulk of 2,4,6-triphenylpyrylium salts, only α-primary and α-secondary amines can be converted to the requisite

Katritzky salt. Very recently, the Rovis group has demonstrated an alternative pre-functionalization strategy that address this limitation. α-Tertiary amines (**113**) undergo condensation with electron rich 2,4,6-trimethoxybenzaldehyde (**114**) to yield imine **115** which is then oxidized by the excited photoredox catalyst [Ir(dF-CF_3-ppy)$_2$(dtbbpy)]PF_6.[90] The resulting imidoyl radical species undergoes β-scission to give aryl nitrile byproduct, and the desired alkyl radical intermediate is trapped with an electron deficient olefin (**116**) (Scheme 1.30).

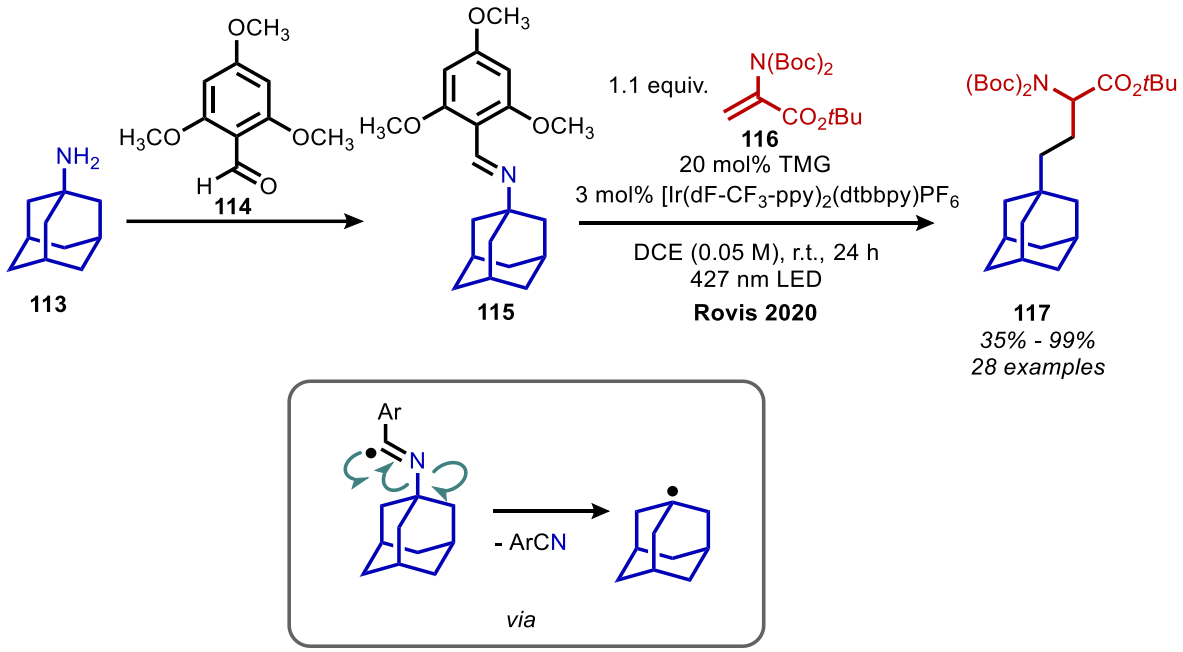

Scheme 1.30. Deaminative C(sp^3)-C(sp^3) bond formation by pre-functionalization to electron rich imines.

In a subsequent advance, Rovis has shown that α-tertiary radicals generated by photooxidation of pre-functionalized imine species **119** can be intercepted by a nickel catalyst. This dual catalysis reaction facilitates C(sp^3)-C(sp^2) cross-coupling with aryl bromides (**120**) to yield product **121** (Scheme 1.31).[91]

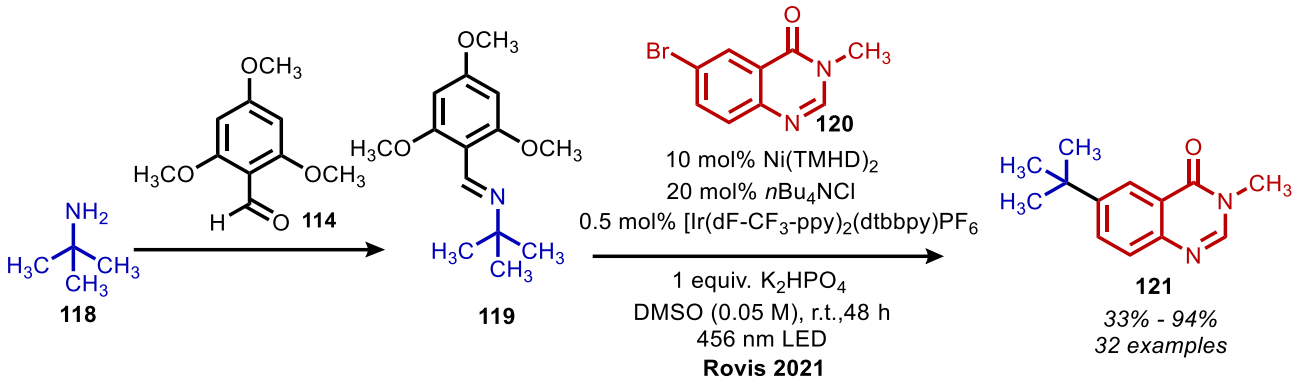

Scheme 1.31. Deaminative C(sp^3)-C(sp^2) coupling by dual nickel – photoredox catalysis with pre-functionalized imines.

1.3.3. Other Transition Metal Catalyzed Deamination Reactions.

In addition to the nickel catalyzed cross-coupling reactions described in chapter 1.3.2, there have been reports of ruthenium and palladium catalyzed deaminative transformations. Remarkably, these reactions activate primary amines without any pre-functionalization. Milstein has reported using water to convert primary amines (**123**) to alcohols (**125**) with ammonia as a byproduct, enabled ruthenium catalyst **124** (Scheme 1.32).[92] In the proposed mechanism, the catalyst facilitates dehydrogenation of amines to imines and dihydrogen. The imine moiety undergoes condensation with water to yield an aldehyde, which is subsequently reduced by the available dihydrogen to give the alcohol product. Recently, the Milstein group has been expanded this work to include the conversion of primary amines to carboxylic acids using ruthenium pincer complex **124**.[93]

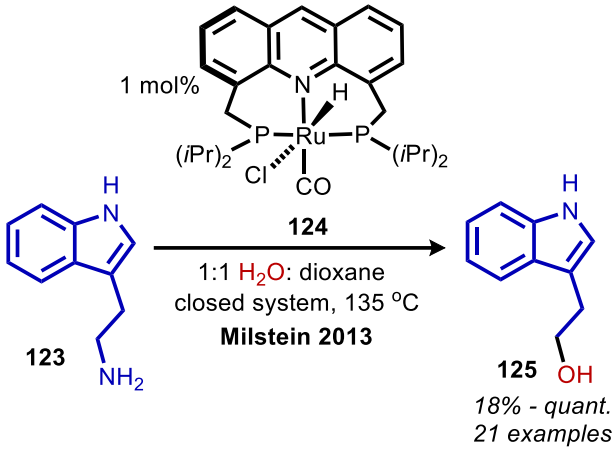

Scheme 1.32. Ruthenium catalyzed conversion of amines to alcohols using water.

Marciniec has reported a ruthenium catalyzed coupling of two primary alkyl amines (**126**) to form secondary amine **21** and liberate **23** (Scheme 1.33).[19] β-Hydride elimination is thought to produce a coordinated imine species which undergoes attack by the second amine moiety to give a dialkyl imine intermediate that is then reduced (Figure 1.11). The Yi group has further disclosed the selective synthesis of unsymmetrical secondary amines (**128**) from a mixture of two different primary amines (Scheme 1.34).[94] Quinazolinones were also synthesized from primary benzylic amines and 2-aminobenzamides.[95]

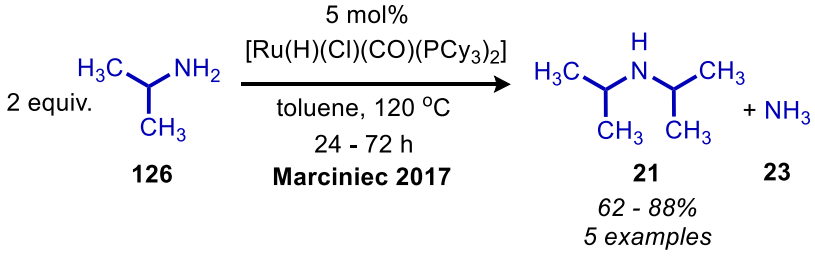

Scheme 1.33. Ruthenium catalyzed deaminative coupling of primary amines to form symmetrical secondary amines.

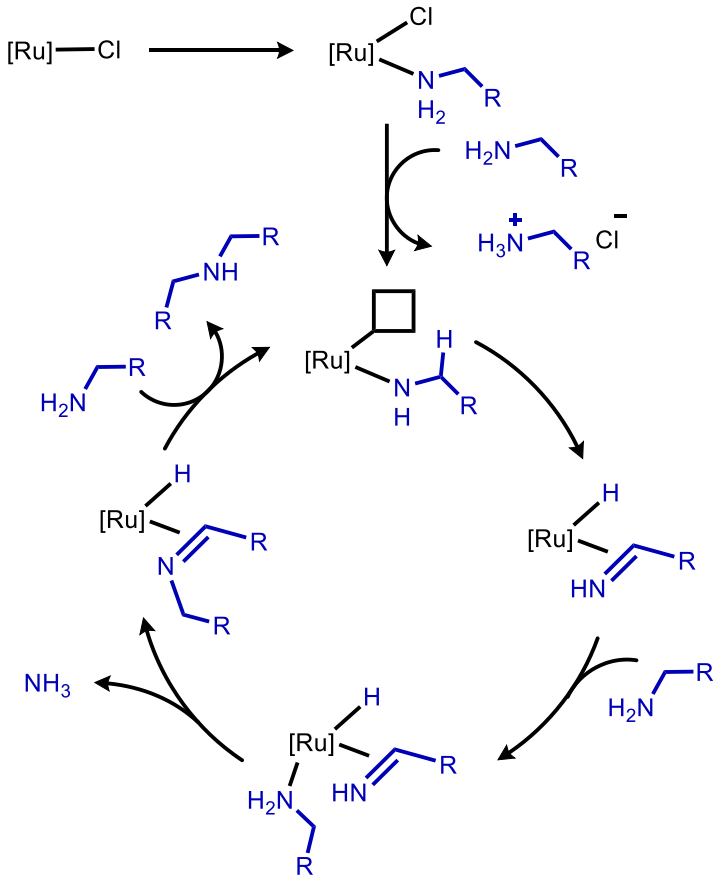

Figure 1.11. Proposed mechanism for deaminative coupling of primary amines to form secondary amines.

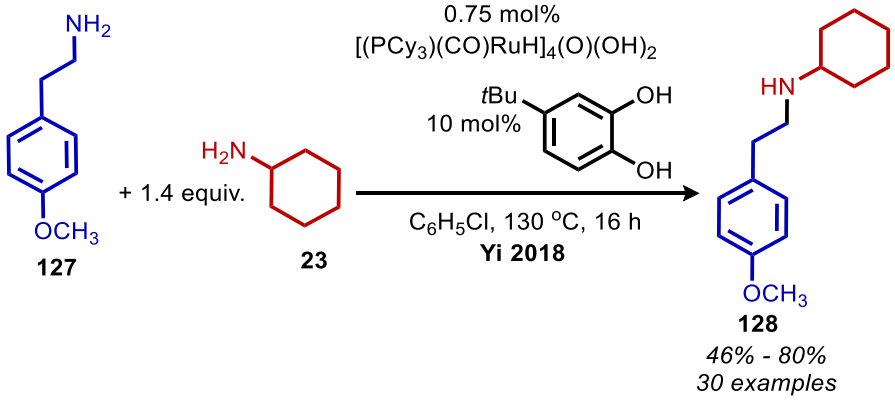

Scheme 1.34. Ruthenium catalyzed deaminative coupling of primary amines to form unsymmetrical secondary amines.

While the majority of deaminative cross-coupling reactions involve harnessing pre-functionalized amines for nickel catalysis as demonstrated in section 1.3.2, there have been several reports of cross-coupling reactions which do not require this pre-functionalization. The Tian group has demonstrated this with allylic primary amine **129** using palladium catalysis and aryl boronic acid **130** (Scheme 1.35).[96] The formation of a palladium allyl complex analogous to that of allylic secondary amine C-N functionalization (see section 1.2) is proposed. Product **131** exhibits inversion of configuration and retention of E-selectivity. The Tian group has also reported the deaminative conversion of allylic primary amines (**132**) to sulfones (**134**) with sodium sulfinates and catalytic palladium (Scheme 1.36).[97] The chiral ligand (*R*)-BINOL results in enantioselective products which exhibit retention of configuration.

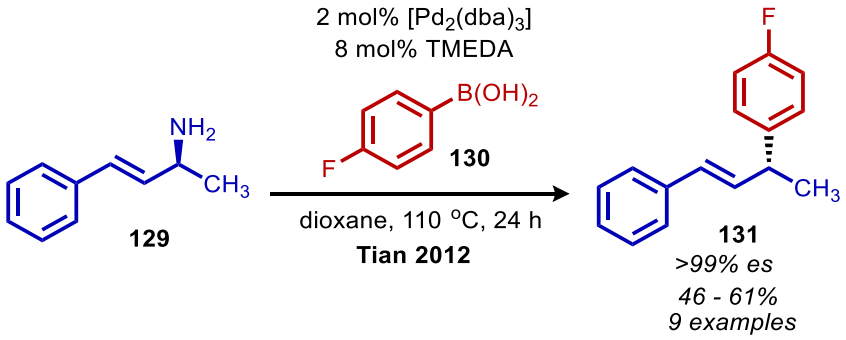

Scheme 1.35. Deaminative coupling of allylic amines with aryl boronic acids.

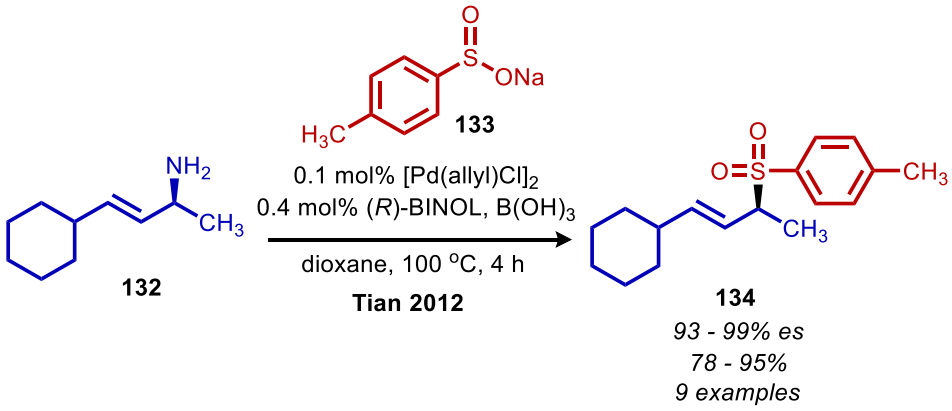

Scheme 1.36. Deaminative synthesis of allylic sulfones.

1.3.4. Oxidative Deamination.

Reductive amination is a powerhouse reaction used by the chemical industry for the conversion of ketones to amines.[98, 99] The reverse conversion of amines into ketones is also of interest, and a wide variety of reagents for this transformation has been disclosed. Figure 1.12 summarizes the scope of oxidative deamination and its applications towards the synthesis of heterocycles and multi-component reactions.

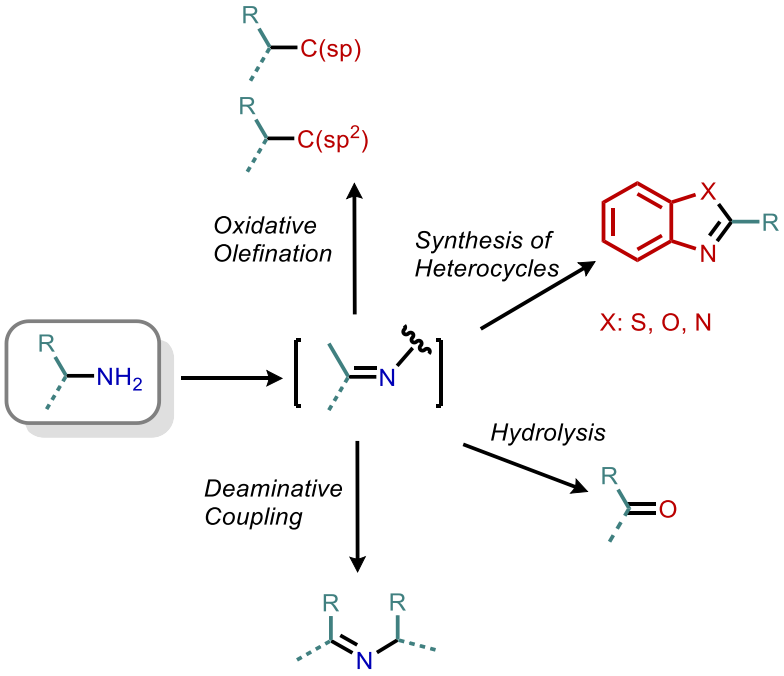

Figure 1.12. Scope of transformations enabled by oxidative deamination.

The oxidative deamination of amines is known to occur *in-vivo* by enzyme catalyzed processes.[100] Neurotransmitters and histamines are biological amines present in animals which are metabolized by a class of enzymes known as Copper-amine Oxidases (CuAOs).[100, 101] The co-factor of CuAOs has been identified by several groups as the quinone containing compound 2,4,5-trihydroxyphenylalaninequinone (TPQ).[102, 103] TPQ reacts with amines to form an imine, which

is then converted to an aldehyde product by reaction with water (Scheme 1.37a).[101, 103] This results in the reduced aminoquinol form of TPQ, which is then re-oxidized by the conversion of dioxygen to hydrogen peroxide. Another biological enzyme which catalyses the oxidative deamination of nitrogen containing compounds in prokaryotes is amine dehydrogenase (ADH). ADH contains a similar quinone derived co-factor tryptophan tryptophyquinone (TTQ) which also reacts *via* imine formation (Scheme 1.37b).[104] Instead of regeneration by reaction with dioxygen, the electrons gained by reduction are transferred to blue copper proteins including amicyanin or azurin.[105] Biomimetic strategies for oxidative deamination typically involve imine condensation and isomerization. Subsequent reaction with excess primary amine or hydrolysis results in either a dialkyl imine product or a carbonyl, respectively (Scheme 1.37c).

.

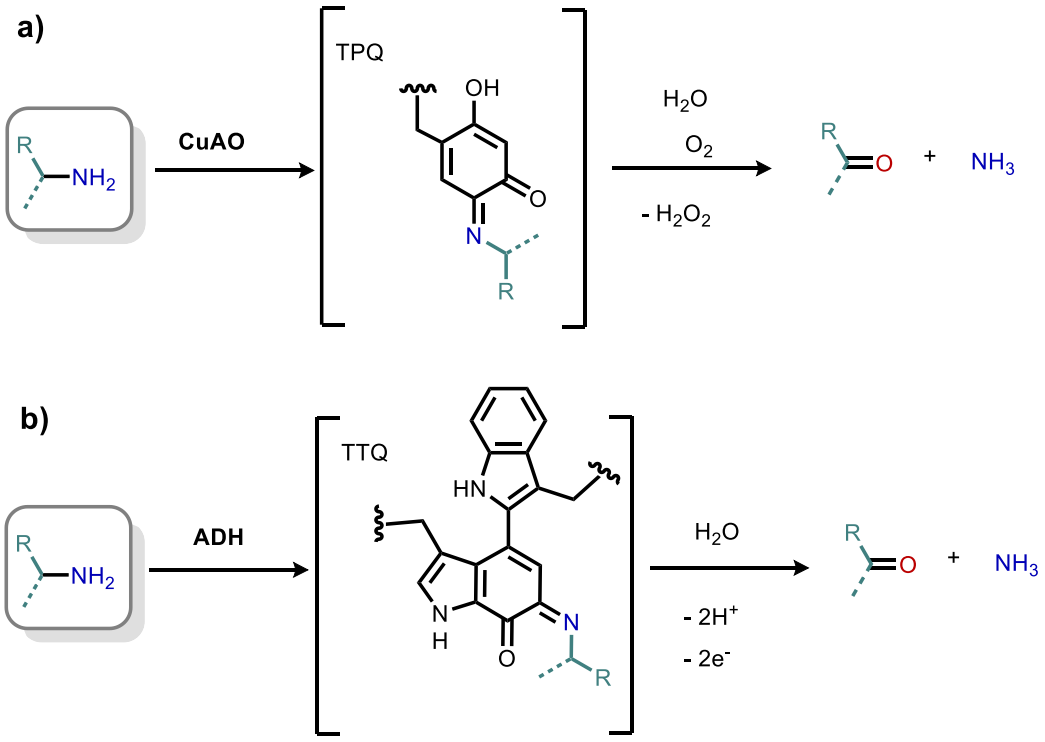

Scheme 1.37. Oxidative deamination enabled by a) CuAOs, b) ADH, and c) biomimetic strategies

Scheme 1.37 continued. Oxidative deamination enabled by a) CuAOs, b) ADH, and c) biomimetic strategies.

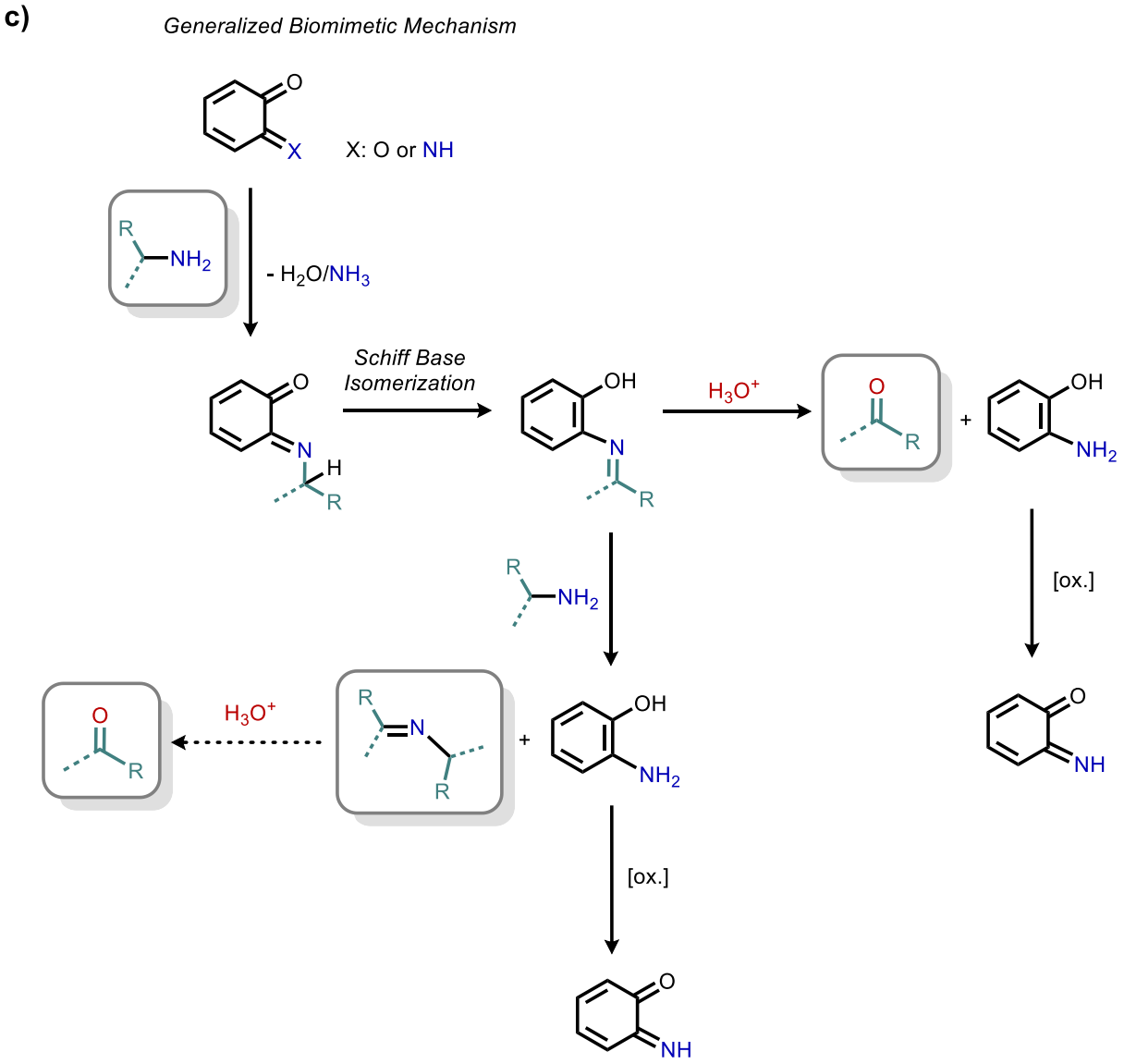

Corey first disclosed biomimetic deaminative oxidation in 1969 using 3,5-di-*tert*-butyl-1,2-benzoquionone (**135**) (Scheme 1.38a).[106] The steric hinderance of this quinone derived moiety favours imine condensation at only the C1 position in the presence of primary amines. Subsequent hydrolysis at low pH results in the production of ketone products (**138**). α-Primary amines (**5**) were also converted to aldehydes (**106**) using mesitylglyoxyl derivative **139** (Scheme 1.38b). This initial report inspired the use of readily available ascorbic acid (**142-red**) for deaminative

oxidation. Voltrova and Strogl report the *in-situ* oxidation of ascorbic acid (**142-red**) by air and catalytic copper to dehydroascorbic acid (**142-ox**), which facilitates the conversion of primary benzylic amines (**141**) to aldehydes (**143**) (Scheme 1.39).[107]

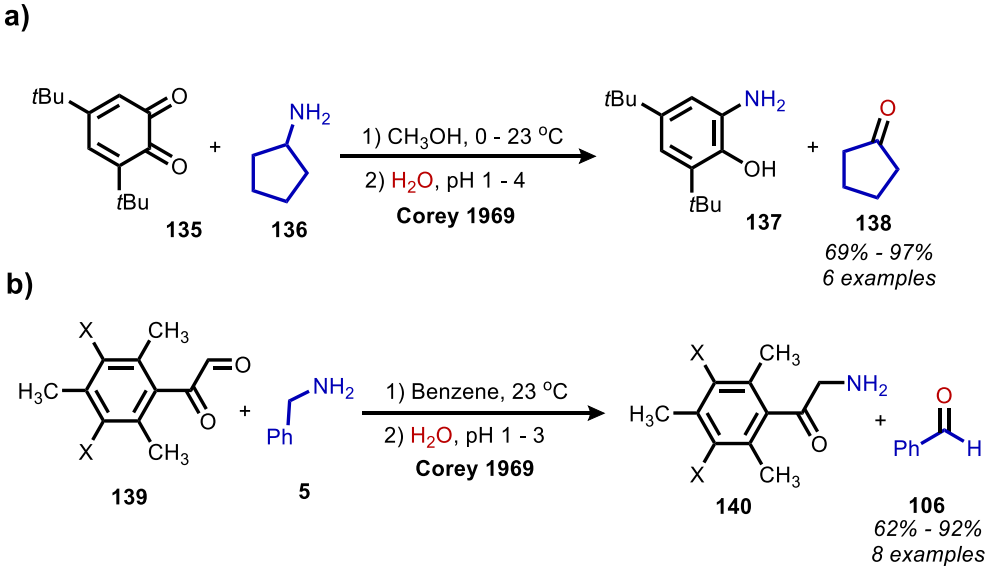

Scheme 1.38. Biomimetic oxidative deamination of primary amines using a) 3,5-di-*tert*-butyl-1,2-benzoquionone and b) mesitylglyoxyl derivatives.

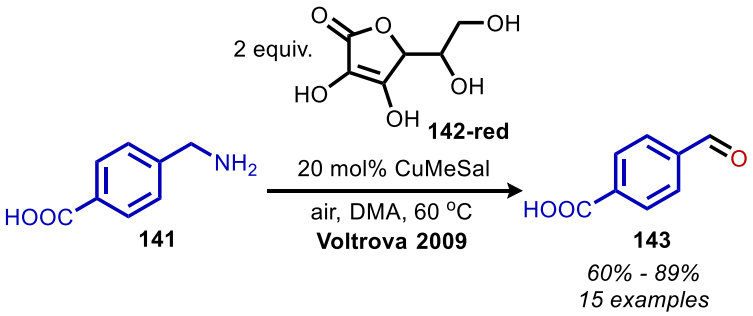

Scheme 1.39. Biomimetic oxidative deamination using ascorbic acid.

Lisnyak and Snyder have recently demonstrated the synthetic importance of oxidative deamination by applying this reaction as a key step in their total synthesis of Chilocorine C (**147**), a natural product isolated from ladybugs (Scheme 1.40).[108] Amine intermediate **144** was converted

to an aldehyde moiety (**145**) using the procedure reported by Voltrova and Strogl. Aldehyde **145** is then able to undergo an aldol cyclization sequence with **146** to yield the requisite natural product.

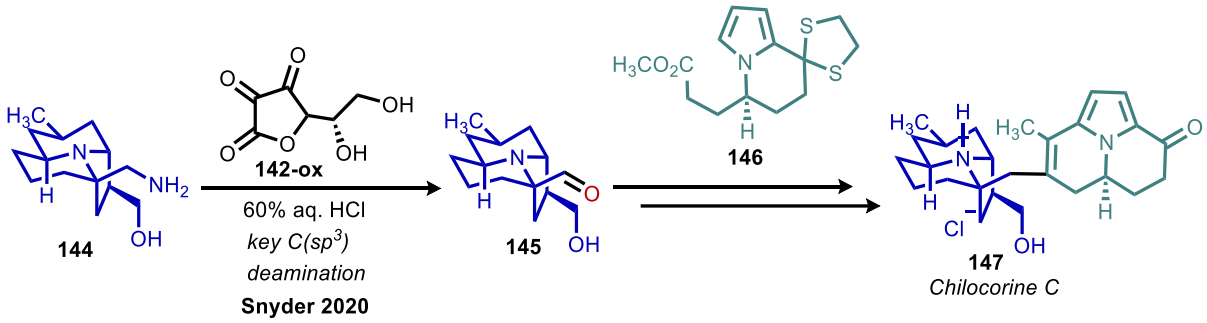

Scheme 1.40. Total synthesis of Chilocorine C enabled by biomimetic oxidative deamination.

Largeron and Fleury expanded biomimetic oxidative deamination to include a substrate scope containing mainly non-benzylic amines (**148**) using catalytic 3,4-iminoquinone (**149**).[109] Amines were coupled to afford unstable dialkyl imine species, which were subsequently hydrolyzed and isolated as aldehyde 2,4-dinitrophenylhydrazone adducts, capping the theoretical yield at 50% (Scheme 1.41a). The reduced aminoquinone species was re-oxidized using a platinum electrode, resulting in a catalytic turnover number of 23. Further work demonstrated that this electrode could be replaced with catalytic copper and an air atmosphere.[110] This procedure was used for the deaminative coupling of benzylic amines (**151**) to yield dibenzylic imine product **153** (Scheme 1.41b). Such imines are more stable than dialkyl imine species and can be isolated.

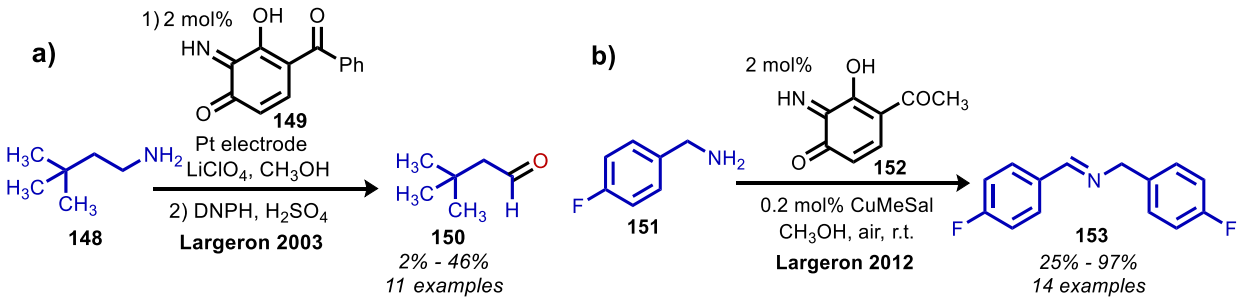

Scheme 1.41. Catalytic biomimetic oxidative deamination using a) a platinum electrode and b) catalytic copper and air.

Recent advances in the field of biomimetic oxidative deamination have been highlighted in a review by Largeron.[111] Select examples are highlighted here to demonstrate the scope and synthetic applications of this transformation. Stahl has reported deaminative cross-coupling of two different primary amine moieties to produce unsymmetrical imine products with the catalyst 4-*tert*-2-hydroxybenzoquinone (**155**) (Scheme 1.42).[112] Notably, α-tertiary primary amine substrates (**154**) were successfully engaged with this methodology. Mechanistic studies indicated that homo-coupled imines are initially formed and accumulate early in the reaction, but the reactivity of benzylic amines drives the equilibrium towards cross-coupled products (**156**) by trans-imination.[112, 113] In a more recent advance from Largeron, deaminative cross-coupled imines were synthesized by *in-situ* generation of the biomimetic catalyst purpurogallin from commercially available pre-catalyst pyrogallol.[114] This procedure eliminates the need for multi-step syntheses of biomimetic catalysts.

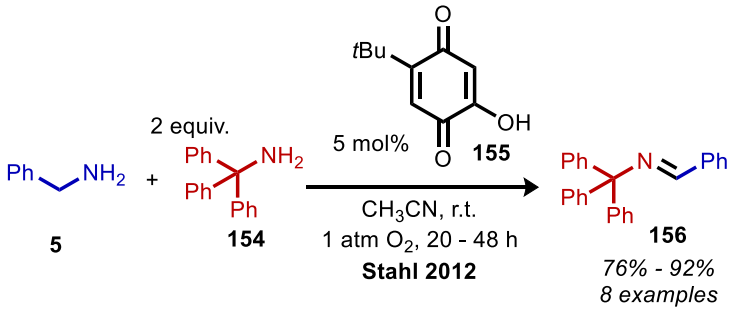

Scheme 1.42. Deaminative synthesis of unsymmetrical imines.

In the above procedures, the net conversion of amines to carbonyl compounds requires a second step involving hydrolysis of the imine products. Work from the Oh group has demonstrated a one-pot conversion of amines to ketones using the biomimetic compound *ortho*-naphthoquinone

(**158**).[115] The water produced from the initial condensation of amines with the catalyst is harnessed to hydrolyze the imine products under elevated temperature conditions (Scheme 1.43).

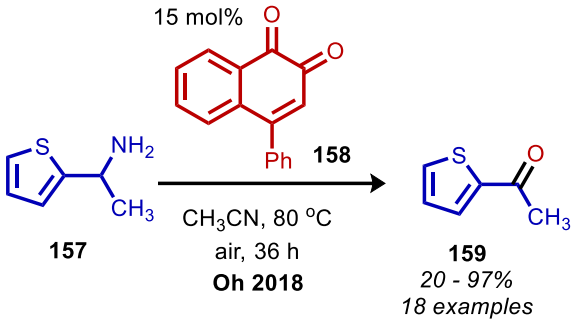

Scheme 1.43. One-pot conversion of amines to ketones with a biomimetic catalyst.

There are additional biomimetic strategies that have been reported for oxidative deamination, including procedures inspired by the monoamine oxidase (MAO) flavin co-factor[116, 117] and the cytochrome P450 (CYP) heme co-factor.[118, 119] There is also a very wide range of organic and inorganic non-biomimetic oxidants that can facilitate this transformation.[120-133] These methodologies are described in detail in *Org. Biomol. Chem.* **2021**, *19*, 11-36. The following oxidative deamination reactions are presented to show further synthetic applications and net deaminative conversions facilitated by this reaction.

A one-pot Wittig reaction was developed by Chandrasekhar in which amines undergo oxidative deamination and the carbonyl products are subsequently converted to α,β-unsaturated esters.[134] A subsequent hydrogenation reaction results in the production of C(sp^3) hybridized ester products. The Fu group has reported extracting dibenzylic imine product from oxidative deaminative homo-coupling of amines (**160**) and adding Danishefsky's diene (**161**).[135] This results in an aza Diels-Alder synthesis of *N*-alkyl-4-pyridone **162** (Scheme 1.44). Oxidative trimerization has also been reported by the Luo group, who demonstrated that dibenzylic imine moieties can

undergo an additional reaction with benzylic amine to yield imidazolinone **165** when the reaction is heated (Scheme 1.45).[136]

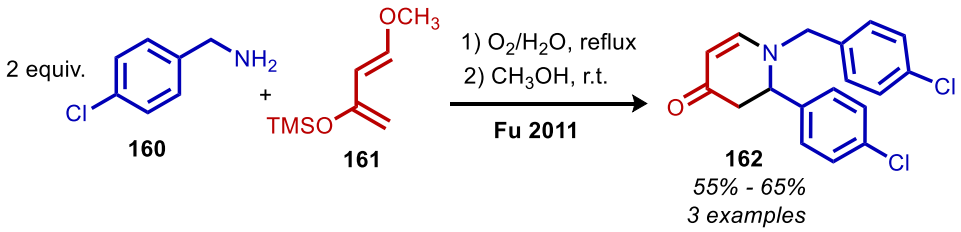

Scheme 1.44. Deaminative aza diels-alder synthesis of *N*-alkyl-4-pyridone.

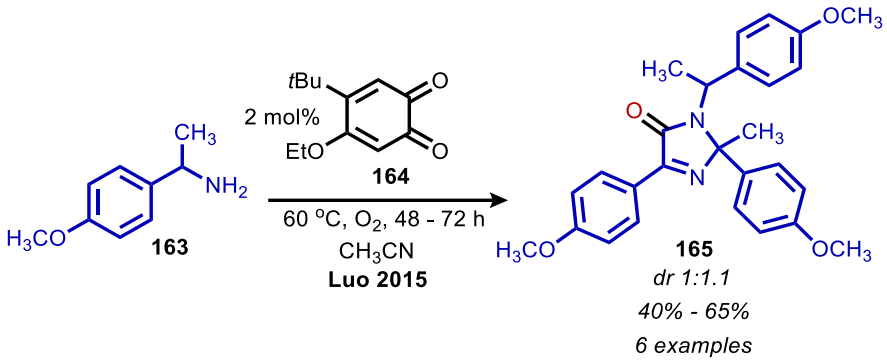

Scheme 1.45. Deaminative oxidative trimerization of benzylic amines to produce an imidazolinone.

The Lu group has reported photocatalyzed deaminative oxidation of 2-phenylcyclohexanamines (**166**). When dioxane and a compact fluorescent light were used, ring opened carboxylic acids (**167**) were obtained as products (Scheme 1.46a).[137] Interestingly, when the light source was switched to green LEDs, the production of lactones (**169**) occurred in DMF (Scheme 1.46b). They postulate that the change in solvent and light source results in the increased production of singlet oxygen *via* sensitization. The enolate tautomer of the carboxylate product is able to undergo another oxidation and cyclization to the requisite lactone upon release of hydrogen peroxide.

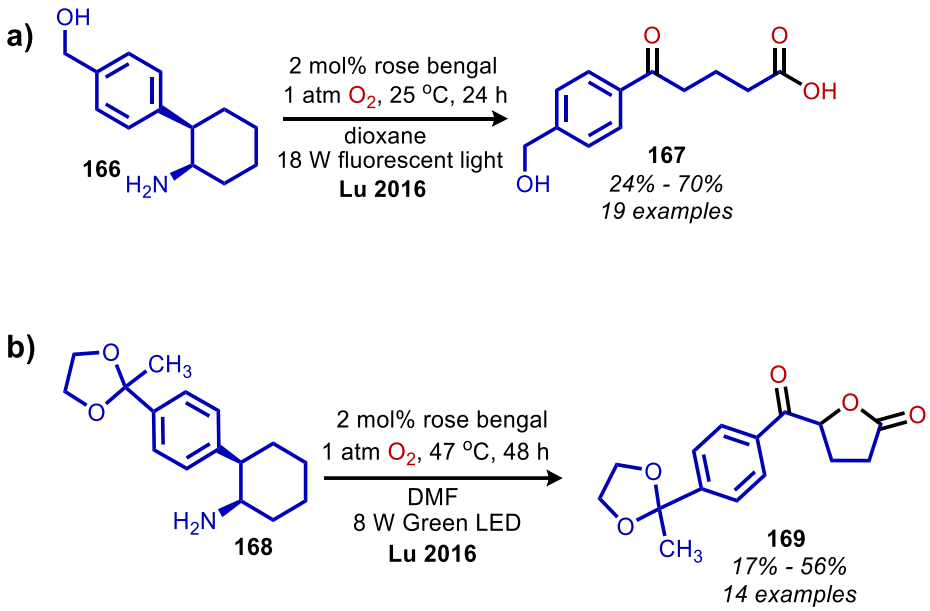

Scheme 1.46. Deaminative oxidative synthesis of a) carboxylic acids and b) lactones.

The deaminative synthesis of thioamides (**171**) has also been achieved by Nguyen and co-workers using elemental sulfur and two primary amines, one benzylic (**5**) and the other non-benzylic (**170**) (Scheme 1.47).[138] The benzylic amine is oxidized preferentially by sulfur to a benzylic imine moiety with release of hydrogen sulfide. Deaminative cross-coupling with the aliphatic amine subsequently occurs to produce a disubstituted imine, which reacts again with elemental sulfur to give thioamide **171**.

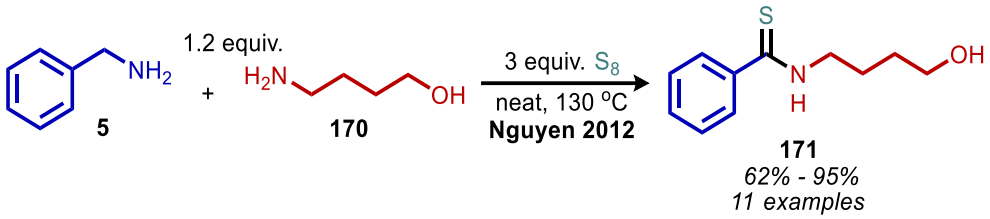

Scheme 1.47. Deaminative oxidative synthesis of thioamides.

Imine species produced by oxidative deamination can also be intercepted in four component Ugi reactions. The Sharma and Batra groups reported deaminative homo-coupling of benzylic

amines and subsequent reaction of the dibenzylic imine with isocyanide and carboxylic acid to form bis(amides).[139, 140] Unsymmetrical cross-coupled imine moieties were subsequently shown by the Ogawa group to undergo this reaction, resulting in the production of **176** (Scheme 1.48).[141]

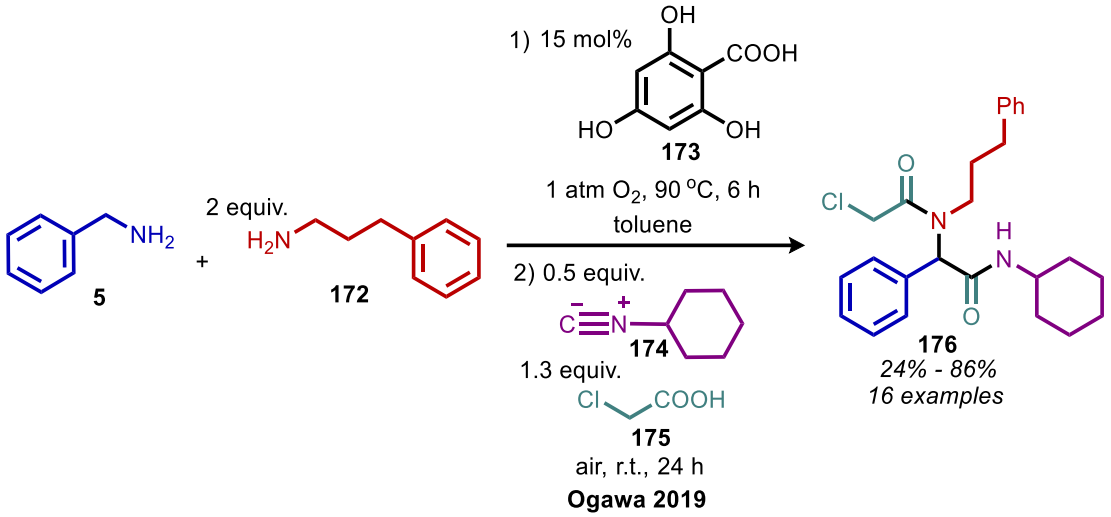

Scheme 1.48. One-pot oxidative deaminative four-component Ugi reaction with unsymmetrical disubstituted imines.

The use of oxidative deamination for the synthesis of heterocycles has gained a lot of interest in recent years. Benzimidazoles can be produced from the deaminative coupling of primary amines with *o*-phenylenediamines (**178**) (Scheme 1.49), a topic which has recently been reviewed by Largeron.[111] Similarly, benzoxazoles, benzothiazoles and quinazolinones have been synthesized *via* oxidative deamination and coupling with 2-aminophenol, 2-aminothiol and *o*-aminobenzamides, respectively.[142-144]

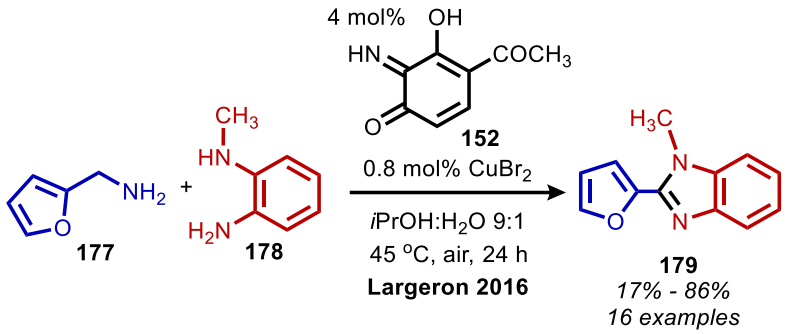

Scheme 1.49. Deaminative synthesis of benzimidazoles.

Amines can also be converted to alkenes *via* oxidative olefination. The Wang group has demonstrated oxidative olefination of 2-methylquinoline derivatives (**180**) using benzylic amines, catalytic NBS and *tert*-butylhydroperoxide as the oxidant (Scheme 1.50).[145] An aldol-type condensation is thought to occur between either an initially generated aldimine or its aldehyde hydrolysis product. In addition to quinolines, oxidative olefination has also been demonstrated with electron deficient olefins such as diethyl ethylidene malonate.[146] In the presence of ammonium acetate, alkyl acetoacetates (**183**) and primary amines were converted to dihydropyridines (**185**) (Scheme 1.51).[146]

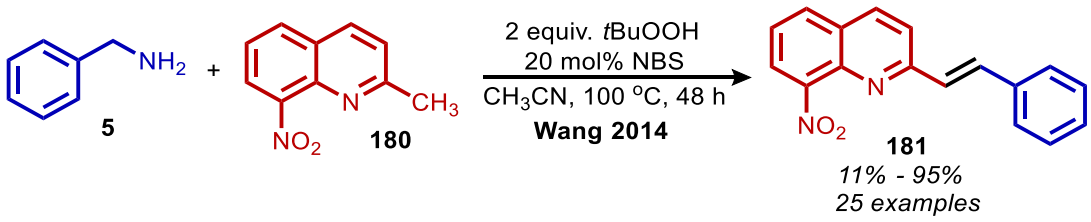

Scheme 1.50. Oxidative olefination of 2-methylquinoline with NBS and *tert*-butylhydroperoxide.

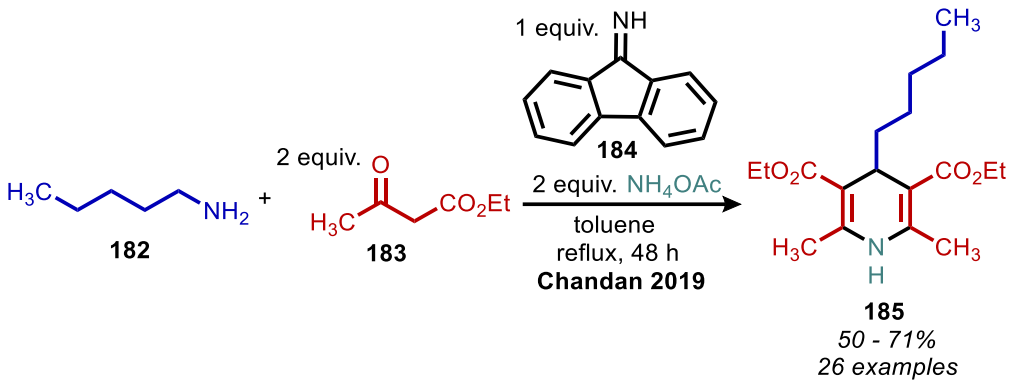

Scheme 1.51. Deaminative oxidative synthesis of 1,2-dihydropyridines.

1.4. Conclusion.

This chapter has surveyed the wide range of strategies for C-N activation of secondary and primary amines. While the activation of secondary aliphatic amines has facilitated carbonylation as well as amine 're-distribution' reactions, there are few existing reports in which the deaminated alkyl substituents are subsequently rejoined (see section 2.1). In chapter 2, a new methodology for this requisite secondary amine 'deletion' is presented using an anomeric amide reagent. Chapter 3 of this thesis describes the expansion of this methodology for the conversion of primary amines to alkane moieties. As demonstrated in this introduction, the majority of primary amine C-N activation chemistry has focused on C-C and C-heteroatom bond formation. Thus, there are few existing strategies for the conversion of a primary amine to a hydrogen atom. In contrast to oxidative deamination, these methods for reductive deamination require the use of harsh conditions and undesirable reagents. Chapter 3 presents a mild alternative to these chemistries by generation of a previously unreported isodiazene intermediate which engages in novel hydrogen atom transfer processes. While the majority of this thesis focuses on C-N bond activation, chapter 5 is a standalone chapter that also reports new hydrogen atom transfer processes but for a C-H bond activation reaction.

1.5. References.

1. Plunkett, S.; Basch, C. H.; Santana, S. O.; Watson, M. P. Harnessing Alkylpyridinium Salts as Electrophiles in Deaminative Alkyl–Alkyl Cross-Couplings. *J. Am. Chem. Soc.* **2019,** *141* (6), 2257-2262.

2. Bernardi, L.; Carlone, A.; Fini, F. Industrial Relevance of Asymmetric Organocatalysis in the Preparation of Chiral Amine Derivatives. In *Methodologies in Amine Synthesis: Challenges and Applications.* Ricci, A.; Bernardi, L. Eds.; John Wiley & Sons, Ltd.: Hoboken, New Jersey, 2021.

3. Cosgrove, S. C.; Ramsden, J. I.; Mangas-Sanchez, J.; Turner, N. J. Biocatalytic Synthesis of Chiral Amines Using Oxidoreductases. In *Methodologies in Amine Synthesis: Challenges and Applications.* Ricci, A.; Bernardi, L. Eds.; John Wiley & Sons, Ltd.: Hoboken, New Jersey, 2021.

4. Cunillera, A.; Claver, C.; Godard, C.; Urrutigoïty, M.; Kalck, P. Transition-Metal-Catalyzed Chiral Amines Synthesis. In *Methodologies in Amine Synthesis: Challenges and Applications.* Ricci, A.; Bernardi, L. Eds.; John Wiley & Sons, Ltd.: Hoboken, New Jersey, 2021.

5. Zhao, F.; Kim, S.-H.; Castagnolo, D. Propargylamines: Recent Advances in Asymmetric Synthesis and Use as Chemical Tools in Organic Chemistry. In *Methodologies in Amine Synthesis: Challenges and Applications.* Ricci, A.; Bernardi, L. Eds.; John Wiley & Sons, Ltd.: Hoboken, New Jersey, 2021.

6. Börgel, J.; Ritter, T. Late-Stage Functionalization. *Chem.* **2020,** *6* (8), 1877-1887.

7. Abrams, D. J.; Provencher, P. A.; Sorensen, E. J. Recent Applications of C–H Functionalization in Complex Natural Product Synthesis. *Chem. Soc. Rev.* **2018,** *47* (23), 8925-8967.

8. Godula, K.; Sames, D. C-H Bond Functionalization in Complex Organic Synthesis. *Science.* **2006,** *312* (5770), 67-72.

9. Cernak, T.; Dykstra, K. D.; Tyagarajan, S.; Vachal, P.; Krska, S. W. The Medicinal Chemist's Toolbox for Late Stage Functionalization of Drug-like Molecules. *Chem. Soc. Rev.* **2016,** *45* (3), 546-576.

10. Wang, Q.; Su, Y.; Li, L.; Huang, H. Transition-Metal Catalysed C–N Bond Activation. *Chem. Soc. Rev.* **2016,** *45* (5), 1257-1272.

11. Ouyang, K.; Hao, W.; Zhang, W.-X.; Xi, Z. Transition-Metal-Catalyzed Cleavage of C–N Single Bonds. *Chem. Rev.* **2015,** *115* (21), 12045-12090.

12. Trost, B. M.; Keinan, E. Pyrrole Annulation onto Aldehydes and Ketones *via* Palladium-Catalyzed Reactions. *J. Org. Chem.* **1980,** *45* (14), 2741-2746.

13. Pawlas, J.; Nakao, Y.; Kawatsura, M.; Hartwig, J. F. A General Nickel-Catalyzed Hydroamination of 1,3-Dienes by Alkylamines: Catalyst Selection, Scope, and Mechanism. *J. Am. Chem. Soc.* **2002,** *124* (14), 3669-3679.

14. Mukherjee, S.; List, B. Chiral Counteranions in Asymmetric Transition-Metal Catalysis: Highly Enantioselective Pd/Brønsted Acid-Catalyzed Direct α-Allylation of Aldehydes. *J. Am. Chem. Soc.* **2007,** *129* (37), 11336-11337.

15. Geng, W.; Zhang, W.-X.; Hao, W.; Xi, Z. Cyclopentadiene–Phosphine/Palladium-Catalyzed Cleavage of C–N Bonds in Secondary Amines: Synthesis of Pyrrole and Indole Derivatives from Secondary Amines and Alkenyl or Aryl Dibromides. *J. Am. Chem. Soc.* **2012,** *134* (50), 20230-20233.

16. Wu, J.-C.; Song, R.-J.; Wang, Z.-Q.; Huang, X.-C.; Xie, Y.-X.; Li, J.-H. Copper-Catalyzed C-H Oxidation/Cross-Coupling of α-Amino Carbonyl Compounds. *Angew. Chem. Int. Ed.* **2012,** *51* (14), 3453-3457.

17. Wu, W.; Su, W. Mild and Selective Ru-Catalyzed Formylation and Fe-Catalyzed Acylation of Free (N–H) Indoles Using Anilines as the Carbonyl Source. *J. Am. Chem. Soc.* **2011,** *133* (31), 11924-11927.

18. Yun, L.; Zhen, L.; Wang, Z.; Fu, X. Aerobic Oxidative *N*-dealkylation of Secondary Amines in Aqueous Solution Catalyzed by Rhodium Porphyrins. *J. Porphyr. Phthalocyanines.* **2014,** *18*, 937-943.

19. Kostera, S.; Wyrzykiewicz, B.; Pawluć, P.; Marciniec, B. Ruthenium-catalyzed Deaminative Redistribution of Primary and Secondary Amines. *Dalton Trans.* **2017,** *46* (35), 11552-11555.

20. Jurewicz, A. T.; Bayless, J. H.; Friedman, L. Reaction of Poorly Solvated Alkyl Cations with Arenes and Ethers. *J. Am. Chem. Soc.* **1965,** *87* (24), 5788-5790.

21. Bayless, J. H.; Mendicino, F. D.; Friedman, L. Aprotic Diazotization of Aliphatic Amines. Intra- and Intermolecular Reactions of Poorly Solvated Cations. *J. Am. Chem. Soc.* **1965,** *87* (24), 5790-5791.

22. Wu, G.; Deng, Y.; Wu, C.; Zhang, Y.; Wang, J. Synthesis of α-Aryl Esters and Nitriles: Deaminative Coupling of α-Aminoesters and α-Aminoacetonitriles with Arylboronic Acids. *Angew. Chem. Int. Ed.* **2014,** *53* (39), 10510-10514.

23. DeChristopher, P. J.; Adamek, J. P.; Lyon, G. D.; Galante, J. J.; Haffner, H. E.; Boggio, R. J.; Baumgarten, R. J. Approach to deamination. III. High-yield Conversion of Primary Aliphatic Amines into Alkyl Halides and Alkenes *via* the use of Sulfonimide Leaving Groups. *J. Am. Chem. Soc.* **1969,** *91* (9), 2384-2385.

24. Baumgarten, R. J. Aliphatic Deaminations in Organic Synthesis. *J. Chem. Ed.* **1966,** *43* (8), 398.

25. Guziec, F. S.; Wei, D. Convenient Halodeamination and Hydrodeamination of Primary Amines. *J. Org. Chem.* **1992,** *57* (14), 3772-3776.

26. Fang, H.; Oestreich, M. Reductive Deamination with Hydrosilanes Catalyzed by $B(C_6F_5)_3$. *Angew. Chem. Int. Ed.* **2020,** *59* (28), 11394-11398.

27. Clark, J.; Hoffman, A. W. V. XIV. Researches into the Molecular Constitution of the Organic Bases. *J. Philos. Trans R. Soc. Lond* **1851,** *141*, 357-398.

28. Cope, A. C.; Trumbull, E. R. Olefins from Amines: The Hofmann Elimination Reaction and Amine Oxide Pyrolysis. In *Organic Reactions* Eds. John Wiley & Sons, Ltd.: Hoboken, New Jersey, 2011.

29. Maity, P.; Shacklady-McAtee, D. M.; Yap, G. P. A.; Sirianni, E. R.; Watson, M. P. Nickel-Catalyzed Cross Couplings of Benzylic Ammonium Salts and Boronic Acids: Stereospecific Formation of Diarylethanes *via* C–N Bond Activation. *J. Am. Chem. Soc.* **2013,** *135* (1), 280-285.

30. Scharfbier, J.; Gross, B. M.; Oestreich, M. Stereospecific and Chemoselective Copper-Catalyzed Deaminative Silylation of Benzylic Ammonium Triflates. *Angew. Chem. Int. Ed.* **2020,** *59* (4), 1577-1580.

31. Moragas, T.; Gaydou, M.; Martin, R. Nickel-Catalyzed Carboxylation of Benzylic C−N Bonds with *CO2*. *Angew. Chem. Int. Ed.* **2016,** *55* (16), 5053-5057.

32. Yu, W.; Yang, S.; Xiong, F.; Fan, T.; Feng, Y.; Huang, Y.; Fu, J.; Wang, T. Palladium-catalyzed Carbonylation of Benzylic Ammonium Salts to Amides and Esters *via* C–N Bond Activation. *Org. Biomol. Chem.* **2018,** *16* (17), 3099-3103.

33. MacArthur, N. S.; Wang, L.; McCarthy, B. G.; Jakobsche, C. E. Using *N*-Nitrosodichloroacetamides to Conveniently Convert Linear Primary Amines into Alcohols. *Synth. Commun.* **2015,** *45* (17), 2014-2021.

34. Katritzky, A. R.; Bapat, J. B.; Blade, R. J.; Leddy, B. P.; Nie, P.-L.; Ramsden, C. A.; Thind, S. S. Heterocycles in Organic Synthesis. Part 6. Nucleophilic Displacements of Primary Amino-groups *via* 2,4,6-Triphenylpyridinium Salts. *J. Chem. Soc. Perkin Trans. I.* **1979,** *0*, 418-425.

35. Katritzky, A. R.; Chermprapai, A.; Patel, R. C. Preparation of Alkyl and Benzyl Fluorides from the Corresponding Primary Amines. *J. Chem. Soc. Chem. Commun.* **1979,** *5*, 238a.

36. Katritzky, A. R.; Eweiss, N. F.; Nie, P.-L. Heterocycles in Organic Synthesis. Part 16. The Conversion of Aliphatic, Aromatic, and Heteroaromatic Primary Amines into Iodides. *J. Chem. Soc. Perkin Trans. I.* **1979,** *0*, 433-435.

37. Katritzky, A. R.; Gruntz, U.; Ikizler, A. A.; Kenny, D. H.; Leddy, B. P. Heterocycles in Organic Synthesis. Part 17. Conversion of Primary Amines into Bromides and Chlorides. *J. Chem. Soc. Perkin Trans. I.* **1979,** *0*, 436-441.

38. Katritzky, A. R.; Al-Omran, F.; Patel, R. C.; Thind, S. S. Improved Methods for Conversion of Primary Amines into Bromides. *J. Chem. Soc. Perkin Trans. I.* **1980,** *0*, 1890-1894.

39. Katritzky, A. R.; Liso, G.; Lunt, E.; Patel, R. C.; Thind, S. S.; Zia, A. Heterocycles in Organic Synthesis. Part 42. Preparation of Azides, Phthalimides, and Sulphonamides from Primary Amines. *J. Chem. Soc. Perkin Trans. I.* **1980,** *0*, 849-851.

40. Katritzky, A. R.; Marson, C. M. Pyrylium Mediated Transformations of Primary Amino Groups into Other Functional Groups. New Synthetic Methods (41). *Angew. Chem. Int. Ed.* **1984,** *23* (6), 420-429.

41. Katritzky, A. R.; Musumarra, G. New Insights into Aliphatic Nucleophilic Substitution Reactions from the use of Pyridines as Leaving Groups. *Chem. Soc. Rev.* **1984,** *13* (1), 47-68.

42. Katritzky, A. R.; Musumarra, G.; Sakizadeh, K.; El-Shafie, S. M. M.; Jovanovic, B. Unimolecular and Bimolecular Transfer of *N*-substituents from Pyridinium Cations: Evidence for a Clear Mechanistic Changeover. *Tet. Lett.* **1980,** *21* (28), 2697-2699.

43. Shaw, M. H.; Twilton, J.; MacMillan, D. W. C. Photoredox Catalysis in Organic Chemistry. *J. Org. Chem.* **2016,** *81* (16), 6898-6926.

44. Yi, H.; Zhang, G.; Wang, H.; Huang, Z.; Wang, J.; Singh, A. K.; Lei, A. Recent Advances in Radical C–H Activation/Radical Cross-Coupling. *Chem. Rev.* **2017,** *117* (13), 9016-9085.

45. Barton, D. H. R.; Ok Jang, D.; Jaszberenyi, J. C. Hypophosphorous Acid and its Salts: New Reagents for Radical Chain Deoxygenation, Dehalogenation and Deamination. *Tet. Lett.* **1992,** *33* (39), 5709-5712.

46. Barton, D. H. R.; Bringman, G.; Lamotte, G.; Hay Motherwell, R. S.; Motherwell, W. B. Radical Deamination Reactions of Relevance to Aminoglycoside Chemistry. *Tet. Lett.* **1979,** *20* (24), 2291-2294.

47. Barton, D. H. R.; Bringmann, G.; Motherwell, W. B. Radical-Induced Reductive Deamination of Amino Acid Esters. *Synthesis.* **1980,** *1980* (01), 68-70.

48. Barton, D. H. R.; Bringmann, G.; Motherwell, W. B. Reactions of Relevance to the Chemistry of Aminoglycoside Antibiotics. Part 15. The Selective Modification of Neamine by Radical-induced Deamination. *J. Chem. Soc. Perkin Trans. I.* **1980,** *0*, 2665-2669.

49. Katritzky, A. R.; De Ville, G.; Patel, R. C. Carbon-alkylation of Simple Nitronate Anions by *N*-substituted Pyridiniums. *Tetrahedron.* **1981,** *37*, 25-30.

50. Katritzky, A. R.; Aurrecoechea, J. M. Alkylation of Monosubstituted Malonate Anions With Pyridinium and Quinolinium Salts. *Synthesis.* **1987,** *1987* (04), 342-345.

51. Katritzky, A. R.; Chen, J.-l.; Marson, C. M.; Maia, A.; Kashmiri, M. A. The Non-chain Radicaloid *C*-alkylation of Nitronate Anions: Further Evidence for the Mechanism. *Tetrahedron.* **1986,** *42* (1), 101-108.

52. Katritzky, A. R.; Horvath, K.; Plau, B. Reductive Deamination of Alkyl and Aryl Primary Amines *via* 1,4-Dihydropyridines and a Note on the Mechanism of Reductive Deamination of Benzylamine *via* a 1,2-Dihydropyridine. *J. Chem. Soc. Chem. Commun.* **1979,** *6*, 300-301.

53. Katritzky, A. R.; Lewis, J.; Nie, P.-L. Heterocycles in Organic Synthesis. Part 18. The Replacement of an Amino-group by Hydrogen *via* Dihydropyridines. *J. Chem. Soc. Perkin Trans. I.* **1979,** *0*, 442-445.

54. Katritzky, A. R.; Horvath, K.; Plau, B. Reductive Deamination of Primary Amines. *J. Chem. Soc. Perkin Trans. I.* **1980,** *0*, 2554-2560.

55. Basch, C. H.; Liao, J.; Xu, J.; Piane, J. J.; Watson, M. P. Harnessing Alkyl Amines as Electrophiles for Nickel-Catalyzed Cross Couplings *via* C–N Bond Activation. *J. Am. Chem. Soc.* **2017,** *139* (15), 5313-5316.

56. Guan, W.; Liao, J.; Watson, M. P. Vinylation of Benzylic Amines *via* C–N Bond Functionalization of Benzylic Pyridinium Salts. *Synthesis.* **2018,** *50* (16), 3231-3237.

57. Liao, J.; Guan, W.; Boscoe, B. P.; Tucker, J. W.; Tomlin, J. W.; Garnsey, M. R.; Watson, M. P. Transforming Benzylic Amines into Diarylmethanes: Cross-Couplings of Benzylic Pyridinium Salts *via* C–N Bond Activation. *Org. Lett.* **2018,** *20* (10), 3030-3033.

58. Hoerrner, M. E.; Baker, K. M.; Basch, C. H.; Bampo, E. M.; Watson, M. P. Deaminative Arylation of Amino Acid-derived Pyridinium Salts. *Org. Lett.* **2019,** *21* (18), 7356-7360.

59. Baker, K. M.; Lucas Baca, D.; Plunkett, S.; Daneker, M. E.; Watson, M. P. Engaging Alkenes and Alkynes in Deaminative Alkyl–Alkyl and Alkyl–Vinyl Cross-Couplings of Alkylpyridinium Salts. *Org. Lett.* **2019,** *21* (23), 9738-9741.

60. Sun, S.-Z.; Romano, C.; Martin, R. Site-Selective Catalytic Deaminative Alkylation of Unactivated Olefins. *J. Am. Chem. Soc.* **2019,** *141* (41), 16197-16201.

61. Zhu, Z.-F.; Tu, J.-L.; Liu, F. Ni-Catalyzed Deaminative Hydroalkylation of Internal Alkynes. *Chem. Commun.* **2019,** *55* (76), 11478-11481.

62. Liao, J.; Basch, C. H.; Hoerrner, M. E.; Talley, M. R.; Boscoe, B. P.; Tucker, J. W.; Garnsey, M. R.; Watson, M. P. Deaminative Reductive Cross-Electrophile Couplings of Alkylpyridinium Salts and Aryl Bromides. *Org. Lett.* **2019,** *21* (8), 2941-2946.

63. Yue, H.; Zhu, C.; Shen, L.; Geng, Q.; Hock, K. J.; Yuan, T.; Cavallo, L.; Rueping, M. Nickel-catalyzed C–N Bond Activation: Activated Primary Amines as Alkylating Reagents in Reductive Cross-coupling. *Chem. Sci.* **2019,** *10* (16), 4430-4435.

64. Martin-Montero, R.; Yatham, V. R.; Yin, H.; Davies, J.; Martin, R. Ni-catalyzed Reductive Deaminative Arylation at sp^3 Carbon Centers. *Org. Lett.* **2019,** *21* (8), 2947-2951.

65. Ni, S.; Li, C.-X.; Mao, Y.; Han, J.; Wang, Y.; Yan, H.; Pan, Y. Ni-catalyzed Deaminative Cross-electrophile Coupling of Katritzky salts with Halides *via* C─N Bond Activation. *Sci. Adv.* **2019,** *5* (6), eaaw9516.

66. Yi, J.; Badir, S. O.; Kammer, L. M.; Ribagorda, M.; Molander, G. A. Deaminative Reductive Arylation Enabled by Nickel/Photoredox Dual Catalysis. *Org. Lett.* **2019,** *21* (9), 3346-3351.

67. Li, C.-L.; Jiang, X.; Lu, L.-Q.; Xiao, W.-J.; Wu, X.-F. Cobalt(II)-Catalyzed Alkoxycarbonylation of Aliphatic Amines *via* C–N Bond Activation. *Org. Lett.* **2019,** *21* (17), 6919-6923.

68. Zeng, X.; Yan, W.; Zacate, S. B.; Cai, A.; Wang, Y.; Yang, D.; Yang, K.; Liu, W. Copper-Catalyzed Deaminative Difluoromethylation. *Angew. Chem. Int. Ed.* **2020,** *59* (38), 16398-16403.

69. Klauck, F. J. R.; James, M. J.; Glorius, F. Deaminative Strategy for the Visible-Light-Mediated Generation of Alkyl Radicals. *Angew. Chem. Int. Ed.* **2017,** *56* (40), 12336-12339.

70. Pang, Y.; Moser, D.; Cornella, J. Pyrylium Salts: Selective Reagents for the Activation of Primary Amino Groups in Organic Synthesis. *Synthesis* **2020,** *52* (04), 489-503.

71. M. Correia, J. T.; A. Fernandes, V.; Matsuo, B. T.; C. Delgado, J. A.; de Souza, W. C.; Paixão, M. W. Photoinduced Deaminative Strategies: Katritzky Salts as Alkyl Radical Precursors. *Chem. Commun.* **2020,** *56* (4), 503-514.

72. Jiang, X.; Zhang, M.-M.; Xiong, W.; Lu, L.-Q.; Xiao, W.-J. Deaminative (Carbonylative) Alkyl-Heck-type Reactions Enabled by Photocatalytic C−N Bond Activation. *Angew. Chem. Int. Ed.* **2019,** *58* (8), 2402-2406.

73. Yang, Z.-K.; Xu, N.-X.; Wang, C.; Uchiyama, M. Photoinduced $C(sp^3)$−N Bond Cleavage Leading to the Stereoselective Syntheses of Alkenes. *Chem. Eur. J.* **2019,** *25* (21), 5433-5439.

74. Zhu, Z.-F.; Zhang, M.-M.; Liu, F. Radical Alkylation of Isocyanides with Amino Acid-/Peptide-derived Katritzky Salts *via* Photoredox Catalysis. *Org. Biomol. Chem.* **2019,** *17* (6), 1531-1534.

75. Zhang, M.-M.; Liu, F. Visible-light-mediated Allylation of Alkyl Radicals with Allylic Sulfones *via* a Deaminative Strategy. *Org. Chem. Front.* **2018,** *5* (23), 3443-3446.

76. Xu, Y.; Xu, Z.-J.; Liu, Z.-P.; Lou, H. Visible-light-mediated Deaminative Alkylation of *N*-arylamines with Alkyl Katritzky Salts. *Org. Chem. Front.* **2019,** *6* (23), 3902-3905.

77. Klauck, F. J. R.; Yoon, H.; James, M. J.; Lautens, M.; Glorius, F. Visible-Light-Mediated Deaminative Three-Component Dicarbofunctionalization of Styrenes with Benzylic Radicals. *ACS Catal.* **2019,** *9* (1), 236-241.

78. Ociepa, M.; Turkowska, J.; Gryko, D. Redox-Activated Amines in $C(sp^3)$–C(sp) and $C(sp^3)$–$C(sp^2)$ Bond Formation Enabled by Metal-Free Photoredox Catalysis. *ACS Catal.* **2018,** *8* (12), 11362-11367.

79. Wang, X.; Kuang, Y.; Ye, S.; Wu, J. Photoredox-catalyzed Synthesis of Sulfones Through Deaminative Insertion of Sulfur Dioxide. *Chem. Commun.* **2019,** *55* (99), 14962-14964.

80. Crisenza, G. E. M.; Mazzarella, D.; Melchiorre, P. Synthetic Methods Driven by the Photoactivity of Electron Donor–Acceptor Complexes. *J. Am. Chem. Soc.* **2020,** *142* (12), 5461-5476.

81. Sandfort, F.; Strieth-Kalthoff, F.; Klauck, F. J. R.; James, M. J.; Glorius, F. Deaminative Borylation of Aliphatic Amines Enabled by Visible Light Excitation of an Electron Donor–Acceptor Complex. *Chem. Eur. J.* **2018,** *24* (65), 17210-17214.

82. Wu, J.; Grant, P. S.; Li, X.; Noble, A.; Aggarwal, V. K. Catalyst-Free Deaminative Functionalizations of Primary Amines by Photoinduced Single-Electron Transfer. *Angew. Chem. Int. Ed.* **2019,** *58* (17), 5697-5701.

83. Yang, M.; Cao, T.; Xu, T.; Liao, S. Visible-Light-Induced Deaminative Thioesterification of Amino Acid Derived Katritzky Salts *via* Electron Donor–Acceptor Complex Formation. *Org. Lett.* **2019,** *21* (21), 8673-8678.

84. Fu, M.-C.; Shang, R.; Zhao, B.; Wang, B.; Fu, Y. Photocatalytic Decarboxylative Alkylations Mediated by Triphenylphosphine and Sodium Iodide. *Science* **2019,** *363* (6434), 1429.

85. Wang, C.; Qi, R.; Xue, H.; Shen, Y.; Chang, M.; Chen, Y.; Wang, R.; Xu, Z. Visible-Light-Promoted $C(sp^3)$−H Alkylation by Intermolecular Charge Transfer: Preparation of Unnatural α-Amino Acids and Late-Stage Modification of Peptides. *Angew. Chem. Int. Ed.* **2020,** *59* (19), 7461-7466.

86. Hu, J.; Wang, G.; Li, S.; Shi, Z. Selective C−N Borylation of Alkyl Amines Promoted by Lewis Base. *Angew. Chem. Int. Ed.* **2018,** *57* (46), 15227-15231.

87. Kim, I.; Im, H.; Lee, H.; Hong, S. *N*-Heterocyclic Carbene-catalyzed Deaminative Cross-coupling of Aldehydes with Katritzky Pyridinium Salts. *Chem. Sci.* **2020,** *11* (12), 3192-3197.

88. Zhao, F.; Li, C.-L.; Wu, X.-F. Deaminative Carbonylative Coupling of Alkylamines with Styrenes Under Transition-metal-free Conditions. *Chem. Commun.* **2020,** *56* (64), 9182-9185.

89. Hu, J.; Cheng, B.; Yang, X.; Loh, T.-P. Transition-Metal-Free Deaminative Vinylation of Alkylamines. *Adv. Synth. Catal.* **2019,** *361* (21), 4902-4908.

90. Ashley, M. A.; Rovis, T. Photoredox-Catalyzed Deaminative Alkylation *via* C–N Bond Activation of Primary Amines. *J. Am. Chem. Soc.* **2020,** *142* (43), 18310-18316.

91. Dorsheimer, J. R.; Ashley, M. A.; Rovis, T. Dual Nickel/Photoredox-Catalyzed Deaminative Cross-Coupling of Sterically Hindered Primary Amines. *J. Am. Chem. Soc.* **2021,** *143* (46), 19294-19299.

92. Khusnutdinova, J. R.; Ben-David, Y.; Milstein, D. Direct Deamination of Primary Amines by Water To Produce Alcohols. *Angew. Chem. Int. Ed.* **2013,** *52* (24), 6269-6272.

93. Tang, S.; Rauch, M.; Montag, M.; Diskin-Posner, Y.; Ben-David, Y.; Milstein, D. Catalytic Oxidative Deamination by Water with H_2 Liberation. *J. Am. Chem. Soc.* **2020,** *142* (49), 20875-20882.

94. Arachchige, P. T. K.; Lee, H.; Yi, C. S. Synthesis of Symmetric and Unsymmetric Secondary Amines from the Ligand-Promoted Ruthenium-Catalyzed Deaminative Coupling Reaction of Primary Amines. *J. Org. Chem.* **2018,** *83* (9), 4932-4947.

95. Kirinde Arachchige, P. T.; Yi, C. S. Synthesis of Quinazoline and Quinazolinone Derivatives *via* Ligand-Promoted Ruthenium-Catalyzed Dehydrogenative and Deaminative Coupling Reaction of 2-Aminophenyl Ketones and 2-Aminobenzamides with Amines. *Org. Lett.* **2019,** *21* (9), 3337-3341.

96. Li, M.-B.; Wang, Y.; Tian, S.-K. Regioselective and Stereospecific Cross-Coupling of Primary Allylic Amines with Boronic Acids and Boronates through Palladium-Catalyzed C-N Bond Cleavage. *Angew. Chem. Int. Ed.* **2012,** *51* (12), 2968-2971.

97. Wu, X.-S.; Chen, Y.; Li, M.-B.; Zhou, M.-G.; Tian, S.-K. Direct Substitution of Primary Allylic Amines with Sulfinate Salts. *J. Am. Chem. Soc.* **2012,** *134* (36), 14694-14697.

98. Abdel-Magid, A. F.; Carson, K. G.; Harris, B. D.; Maryanoff, C. A.; Shah, R. D. Reductive Amination of Aldehydes and Ketones with Sodium Triacetoxyborohydride. Studies on Direct and Indirect Reductive Amination Procedures1. *J. Org. Chem.* **1996,** *61* (11), 3849-3862.

99. Afanasyev, O. I.; Kuchuk, E.; Usanov, D. L.; Chusov, D. Reductive Amination in the Synthesis of Pharmaceuticals. *Chem. Rev.* **2019,** *119* (23), 11857-11911.

100. Largeron, M. Aerobic Catalytic Systems Inspired by Copper Amine Oxidases: Recent Developments and Synthetic Applications. *Org. Biomol. Chem.* **2017,** *15* (22), 4722-4730.

101. Klinman, J. P. Mechanisms Whereby Mononuclear Copper Proteins Functionalize Organic Substrates. *Chem. Rev.* **1996,** *96* (7), 2541-2562.

102. Janes, S. M.; Mu, D.; Wemmer, D.; Smith, A. J.; Kaur, S.; Maltby, D.; Burlingame, A. L.; Klinman, J. P. A New Redox Cofactor in Eukaryotic Enzymes: 6-Hydroxydopa at the Active Site of Bovine Serum Amine Oxidase. *Science.* **1990,** *248* (4958), 981.

103. Lee, Y.; Sayre, L. M. Model Studies on the Quinone-containing Copper Amine Oxidases. Unambiguous Demonstration of a Transamination Mechanism. *J. Am. Chem. Soc.* **1995,** *117* (48), 11823-11828.

104. Hyun, Y.-L.; Davidson, V. L. Mechanistic Studies of Aromatic Amine Dehydrogenase, a Tryptophan Tryptophylquinone Enzyme. *Biochem.* **1995,** *34* (3), 816-823.

105. Roujeinikova, A.; Hothi, P.; Masgrau, L.; Sutcliffe, M. J.; Scrutton, N. S.; Leys, D. New Insights into the Reductive Half-reaction Mechanism of Aromatic Amine Dehydrogenase Revealed by Reaction with Carbinolamine Substrates. *J. Biol. Chem.* **2007,** *282* (33), 23766-23777.

106. Corey, E. J.; Achiwa, K. Oxidation of Primary Amines to Ketones. *J. Am. Chem. Soc.* **1969,** *91* (6), 1429-1432.

107. Srogl, J.; Voltrova, S. Copper/Ascorbic Acid Dyad as a Catalytic System for Selective Aerobic Oxidation of Amines. *Org. Lett.* **2009,** *11* (4), 843-845.

108. Lisnyak, V. G.; Snyder, S. A. A Concise, Enantiospecific Total Synthesis of Chilocorine C Fueled by a Reductive Cyclization/Mannich Reaction Cascade. *J. Am. Chem. Soc.* **2020,** *142* (28), 12027-12033.

109. Largeron, M.; Neudorffer, A.; Fleury, M.-B. Oxidation of Unactivated Primary Aliphatic Amines Catalyzed by an Electrogenerated 3,4-Azaquinone Species: A Small-Molecule Mimic of Amine Oxidases. *Angew. Chem. Int. Ed.* **2003,** *42* (9), 1026-1029.

110. Largeron, M.; Fleury, M.-B. A Biologically Inspired CuI/Topaquinone-Like Co-Catalytic System for the Highly Atom-Economical Aerobic Oxidation of Primary Amines to Imines. *Angew. Chem. Int. Ed.* **2012,** *51* (22), 5409-5412.

111. Largeron, M.; Nguyen, K. M. H. Recent Advances in the Synthesis of Benzimidazole Derivatives from the Oxidative Coupling of Primary Amines. *Synthesis* **2018,** *50* (02), 241-253.

112. Wendlandt, A. E.; Stahl, S. S. Chemoselective Organocatalytic Aerobic Oxidation of Primary Amines to Secondary Imines. *Org. Lett.* **2012,** *14* (11), 2850-2853.

113. Largeron, M.; Fleury, M.-B. A Metalloenzyme-Like Catalytic System for the Chemoselective Oxidative Cross-Coupling of Primary Amines to Imines under Ambient Conditions. *Chem. Eur. J.* **2015,** *21* (9), 3815-3820.

114. Largeron, M.; Deschamps, P.; Hammad, K.; Fleury, M.-B. A Dual Biomimetic Process for the Selective Aerobic Oxidative Coupling of Primary Amines using Pyrogallol as a Precatalyst. Isolation of the [5 + 2] Cycloaddition Redox Intermediates. *Green Chem.* **2020,** *22* (6), 1894-1905.

115. Golime, G.; Bogonda, G.; Kim, H. Y.; Oh, K. Biomimetic Oxidative Deamination Catalysis *via* ortho-Naphthoquinone-Catalyzed Aerobic Oxidation Strategy. *ACS Catal.* **2018,** *8* (6), 4986-4990.

116. Murray, A. T.; Dowley, M. J. H.; Pradaux-Caggiano, F.; Baldansuren, A.; Fielding, A. J.; Tuna, F.; Hendon, C. H.; Walsh, A.; Lloyd-Jones, G. C.; John, M. P.; Carbery, D. R. Catalytic Amine Oxidation under Ambient Aerobic Conditions: Mimicry of Monoamine Oxidase B. *Angew. Chem. Int. Ed.* **2015,** *54* (31), 8997-9000.

117. Murray, A. T.; King, R.; Donnelly, J. V. G.; Dowley, M. J. H.; Tuna, F.; Sells, D.; John, M. P.; Carbery, D. R. Symbiotic Transition-Metal and Organocatalysis for Catalytic Ambient Amine Oxidation and Alkene Reduction Reactions. *ChemCatChem.* **2016,** *8* (3), 510-514.

118. Yuan, Q.-L.; Zhou, X.-T.; Ji, H.-B. Efficient Oxidative Coupling of Amines to Imines Catalyzed by Manganese(III) Meso-tetraphenylporphyrin Chloride under Ambient Conditions. *Catal. Commun.* **2010,** *12* (3), 202-206.

119. Zhao, S.; Liu, C.; Guo, Y.; Xiao, J.-C.; Chen, Q.-Y. Oxidative Coupling of Benzylamines to Imines by Molecular Oxygen Catalyzed by Cobalt(II) β-Tetrakis(trifluoromethyl)-meso-tetraphenylporphyrin. *J. Org. Chem.* **2014,** *79* (18), 8926-8931.

120. Nicolaou, K. C.; Mathison, C. J. N.; Montagnon, T. *o*-Iodoxybenzoic Acid (IBX) as a Viable Reagent in the Manipulation of Nitrogen- and Sulfur-Containing Substrates: Scope, Generality, and Mechanism of IBX-Mediated Amine Oxidations and Dithiane Deprotections. *J. Am. Chem. Soc.* **2004,** *126* (16), 5192-5201.

121. Matsuo, J.-i.; Kawana, A.; Fukuda, Y.; Mukaiyama, T. Oxidative Deamination of Various Primary Amines to the Corresponding Carbonyl Compounds by Using *N*-tert-Butylphenylsulfinimidoyl Chloride. *Chem. Lett.* **2001,** *30* (7), 712-713.

122. Brisar, R.; Hollmann, D.; Mejia, E. Pyrazine Radical Cations as a Catalyst for the Aerobic Oxidation of Amines. *Eur. J. Org. Chem.* **2017,** *2017* (36), 5391-5398.

123. Dong, C.-p.; Uematsu, A.; Kumazawa, S.; Yamamoto, Y.; Kodama, S.; Nomoto, A.; Ueshima, M.; Ogawa, A. 2,4,6-Trihydroxybenzoic Acid-Catalyzed Oxidative Ugi Reactions with Molecular Oxygen *via* Homo- and Cross-Coupling of Amines. *J. Org. Chem.* **2019,** *84* (18), 11562-11571.

124. Chen, B.; Wang, L.; Gao, S. Recent Advances in Aerobic Oxidation of Alcohols and Amines to Imines. *ACS Catal.* **2015,** *5* (10), 5851-5876.

125. Ryland, B. L.; Stahl, S. S. Practical Aerobic Oxidations of Alcohols and Amines with Homogeneous Copper/TEMPO and Related Catalyst Systems. *Angew. Chem. Int. Ed.* **2014,** *53* (34), 8824-8838.

126. Hu, Z.; Kerton, F. M. Simple Copper/TEMPO Catalyzed Aerobic Dehydrogenation of Benzylic Amines and Anilines. *Org. Biomol. Chem.* **2012,** *10* (8), 1618-1624.

127. Sonobe, T.; Oisaki, K.; Kanai, M. Catalytic Aerobic Production of Imines en route to Mild, Green, and Concise Derivatizations of Amines. *Chem. Sci.* **2012,** *3* (11), 3249-3255.

128. Xu, B.; Hartigan, E. M.; Feula, G.; Huang, Z.; Lumb, J.-P.; Arndtsen, B. A. Simple Copper Catalysts for the Aerobic Oxidation of Amines: Selectivity Control by the Counterion. *Angew. Chem. Int. Ed.* **2016,** *55* (51), 15802-15806.

129. Gopalaiah, K.; Saini, A. A Solvent-Free Process for Synthesis of Imines by Iron-Catalyzed Oxidative Self- or Cross-Condensation of Primary Amines Using Molecular Oxygen as Sole Oxidant. *Catal. Letters* **2016,** *146* (9), 1648-1654.

130. Park, J. H.; Ko, K. C.; Kim, E.; Park, N.; Ko, J. H.; Ryu, D. H.; Ahn, T. K.; Lee, J. Y.; Son, S. U. Photocatalysis by Phenothiazine Dyes: Visible-Light-Driven Oxidative Coupling of Primary Amines at Ambient Temperature. *Org. Lett.* **2012,** *14* (21), 5502-5505.

131. Berlicka, A.; König, B. Porphycene-mediated Photooxidation of Benzylamines by Visible Light. *Photochem. Photobiol.* **2010,** *9* (10), 1359-1366.

132. Li, N.; Lang, X.; Ma, W.; Ji, H.; Chen, C.; Zhao, J. Selective Aerobic Oxidation of Amines to Imines by TiO_2 Photocatalysis in Water. *Chem. Commun.* **2013,** *49* (44), 5034-5036.

133. Monopoli, A.; Cotugno, P.; Iannone, F.; Ciminale, F.; Dell'Anna, M. M.; Mastrorilli, P.; Nacci, A. Ionic-Liquid-Assisted Metal-Free Oxidative Coupling of Amines To Give Imines. *Eur. J. Org. Chem.* **2014,** *2014* (27), 5925-5931.

134. Chandrasekhar, S.; Pavan Kumar Reddy, G.; Nagesh, C.; Raji Reddy, C. A Novel One-pot Conversion of Amines to Homologated Esters in Poly(ethylene glycol). *Tet. Lett.* **2007,** *48* (7), 1269-1271.

135. Liu, L.; Zhang, S.; Fu, X.; Yan, C.-H. Metal-free Aerobic Oxidative Coupling of Amines to Imines. *Chem. Commun.* **2011,** *47* (36), 10148-10150.

136. Qin, Y.; Zhang, L.; Lv, J.; Luo, S.; Cheng, J.-P. Bioinspired Organocatalytic Aerobic C–H Oxidation of Amines with an ortho-Quinone Catalyst. *Org. Lett.* **2015,** *17* (6), 1469-1472.

137. Cheng, X.; Yang, B.; Hu, X.; Xu, Q.; Lu, Z. Visible-Light-Promoted Metal-Free Aerobic Oxidation of Primary Amines to Acids and Lactones. *Chem. Eur. J.* **2016,** *22* (49), 17566-17570.

138. Nguyen, T. B.; Ermolenko, L.; Al-Mourabit, A. Efficient and Selective Multicomponent Oxidative Coupling of Two Different Aliphatic Primary Amines into Thioamides by Elemental Sulfur. *Org. Lett.* **2012,** *14* (16), 4274-4277.

139. Singh, K.; Kaur, A.; Mithu, V. S.; Sharma, S. Metal-Free Organocatalytic Oxidative Ugi Reaction Promoted by Hypervalent Iodine. *J. Org. Chem.* **2017,** *82* (10), 5285-5293.

140. Dighe, S. U.; Kolle, S.; Batra, S. Iron-Catalysed Oxidative Ugi-Type Multicomponent Reaction Using (Arylmethyl)amines as Imine Precursors. *Eur. J. Org. Chem.* **2015,** *2015* (19), 4238-4245.

141. Dong, C.-P.; Higashiura, Y.; Marui, K.; Kumazawa, S.; Nomoto, A.; Ueshima, M.; Ogawa, A. Metal-Free Oxidative Coupling of Benzylamines to Imines under an Oxygen Atmosphere Promoted Using Salicylic Acid Derivatives as Organocatalysts. *ACS Omega.* **2016,** *1 (5),* 799 - 807.

142. Zhang, R.; Qin, Y.; Zhang, L.; Luo, S. Oxidative Synthesis of Benzimidazoles, Quinoxalines, and Benzoxazoles from Primary Amines by ortho-Quinone Catalysis. *Org. Lett.* **2017,** *19* (20), 5629-5632.

143. Hudwekar, A. D.; Verma, P. K.; Kour, J.; Balgotra, S.; Sawant, S. D. Transition Metal-Free Oxidative Coupling of Primary Amines in Polyethylene Glycol at Room Temperature: Synthesis of Imines, Azobenzenes, Benzothiazoles, and Disulfides. *Eur. J. Org. Chem.* **2019,** *2019* (6), 1242-1250.

144. Mao, D.; Zhu, X.; Hong, G.; Wu, S.; Wang, L. Lanthanum Pentafluorobenzoate-Catalyzed Aerobic Oxidative Olefination of Benzylamines with 2-Methylquinoline through Deamination and C–H Bond Functionalization. *Synlett* **2016,** *27* (17), 2481-2484.

145. Gong, L.; Xing, L.-J.; Xu, T.; Zhu, X.-P.; Zhou, W.; Kang, N.; Wang, B. Metal-free Oxidative Olefination of Primary Amines with Benzylic C–H Bonds Through Direct Deamination and C–H Bond Activation. *Org. Biomol. Chem.* **2014,** *12* (34), 6557-6560.

146. Ghosh, S.; Jana, C. K. Metal Free Biomimetic Deaminative Direct C–C Coupling of Unprotected Primary Amines with Active Methylene Compounds. *Org. Biomol. Chem.* **2019,** *17* (48), 10153-10157.

CHAPTER 2

Skeletal Editing by Deletion of Secondary Amines from Molecular Scaffolds

Note: Portions of this work have been published in an alternate format in Kennedy, S. H.; Dherange, B. D.*; Berger, K. J.*; Levin, M. D. Skeletal Editing through Direct Nitrogen Deletion of Secondary Amines. *Nature*, **2021**, *593*, 223-227.

2.1. Introduction.

The ability to make late-stage edits to an existing pharmacophore is key for the development of new drug derivatives.[1] As highlighted in chapter 1, the field of late-stage functionalization has been typically limited to peripheral modifications such as C-H activation reactions.[2, 3] However, there is a commensurate potential to be gained from the ability to make changes to the molecular skeleton itself by 'insertion' or 'deletion' reactions.[4-6] Figure 2.1 shows an illustrative example with the antiemetic Aprepitant (**2**), in which peripheral derivatization of a lead target (**1**) led to the breakthrough compound.[7] In contrast, late-stage changes to the core heterocyclic moiety itself are not currently feasible using existing chemical technologies, limiting the chemical space a discovery program can rapidly explore.

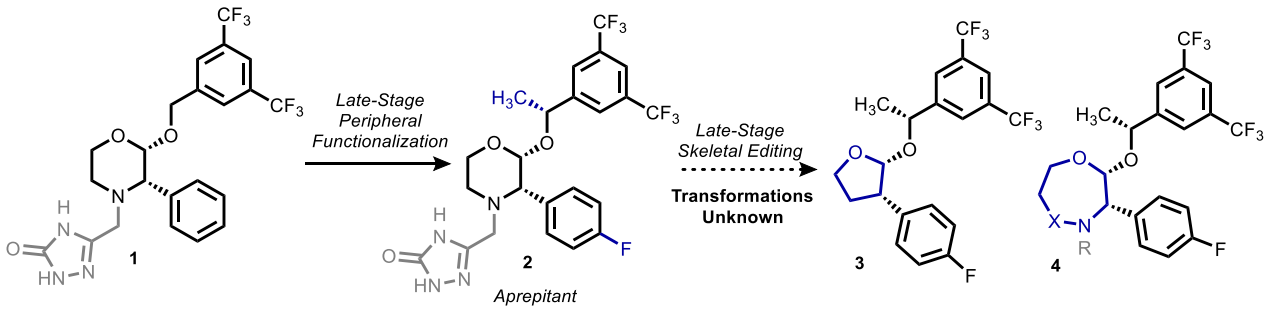

Figure 2.1. Late-stage C-H functionalization is an important drug discovery tool, but late-stage skeletal editing has not been developed to the same level.

The current state of the art for skeletal editing is largely limited to ring re-sizing reactions that are carbonyl driven, which severely restricts the scope of scaffolds that may be edited (Scheme 2.1).[8] Classical examples include Wolff and Favorskii Rearrangements, in which cyclohexanone derived moieties may undergo ring contraction.[9, 10] A more recent example from the Dong group demonstrates C-C bond cleavage to edit ketones from structures.[11] The 'deletion' of ethers from dibenzylic structures has also been reported, though its free-radical mechanism limits it to symmetric systems (Scheme 2.2).[12] In contrast to these transformations, the 'deletion' of a secondary amine from a molecular scaffold has not been as thoroughly studied (Scheme 2.3). As discussed in chapter 1.2, the field of C-N bond activation has mainly focused on oxidative deamination and amine 're-distribution' reactions.[13]

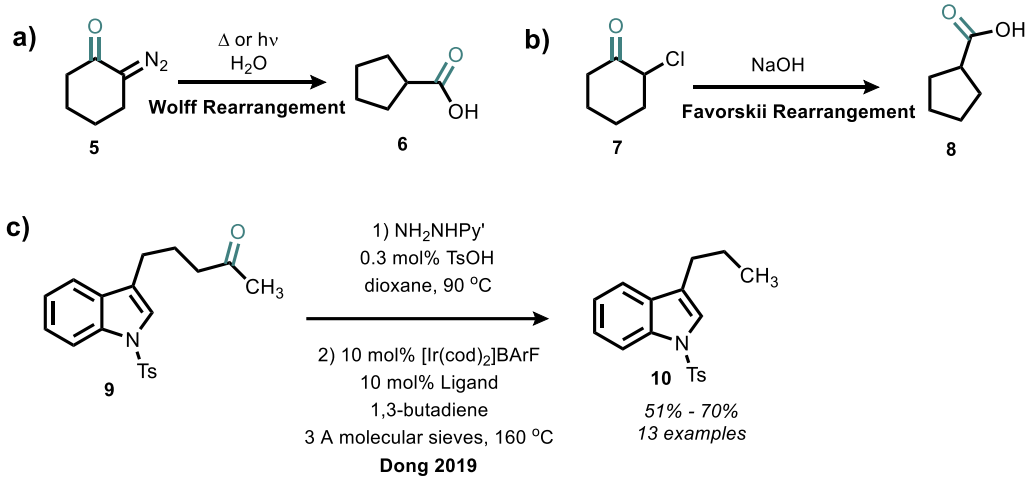

Scheme 2.1. Examples of carbonyl dependent skeletal editing including a) the Wolff rearrangement b) the Favorskii rearrangement and c) deacetylation of ketones.

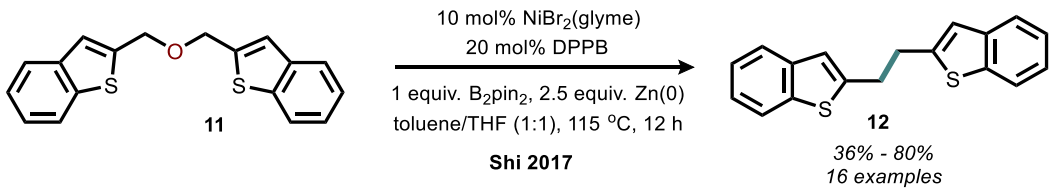

Scheme 2.2 Oxygen deletion of dibenzylic ethers.

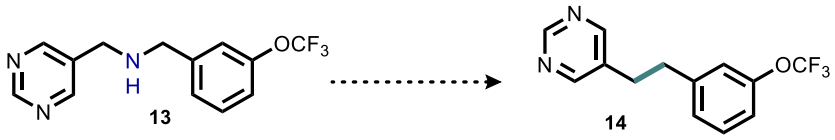

Scheme 2.3 Desired nitrogen deletion of secondary amines.

A retrosynthetic analysis of this desired transformation suggests that conversion of a secondary amine into a more reactive intermediate may facilitate the extrusion of nitrogen. One intermediate of interest is a secondary isodiazene or 1,1-diazene moiety, which has been shown to liberate dinitrogen with recombination of alkyl fragments.[14] However, existing methods for generating such intermediates involve the use of harsh reagents, and conditions that are inappropriate for the desired late-stage editing of complicated molecular scaffolds.[14, 15] Indeed, Dervan has reported the conversion of a secondary amine to a hydrazine moiety (**17**) by treatment with nitrosyl chloride followed by reduction with sodium metal. The requisite hydrazine is converted to an isodiazene (**18**) by treatment with *tert*-butyl hypochlorite (Scheme 2.4).[15] Isodiazene intermediates generated by mercuric oxide oxidation of benzylic hydrazine precursors were also shown to rearrange *via* loss of dinitrogen and formation of a C-C bond (**20**) (Scheme 2.5).[16] The observation that this rearrangement was limited to benzylic substrates is suggestive of a radical mechanism due to the stability of benzylic radical intermediates. This transformation is also known with isodiazene intermediates generated from amines using Angeli's salt (Na_2ONNO_2).[17, 18] More recently, Lu disclosed a two-step nitrogen deletion of secondary amines by pre-functionalization to sulfamoyl azides using sulfuryl diazide (Scheme 2.6).[19] These moieties subsequently liberate dinitrogen and sulfur dioxide upon heating to generate isodiazene intermediates. However, one drawback of this methodology is that sulfuryl diazide is a very hazardous reagent with toxicity and stability concerns.[20]

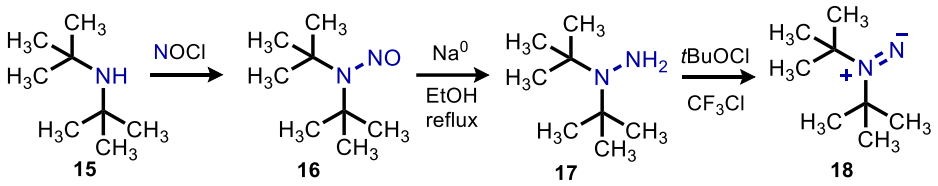

Scheme 2.4. Synthesis of an isodiazene *via* reaction with nitrosyl chloride, followed by reduction with sodium metal and treatment with *tert*-butyl hypochlorite.

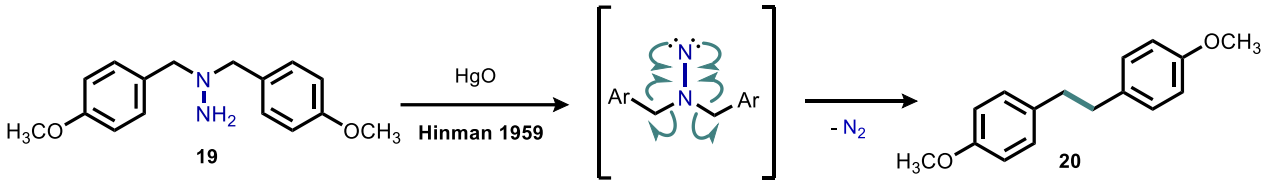

Scheme 2.5. Isodiazene intermediate generated by mercury oxidation undergoes homolytic extrusion of dinitrogen.

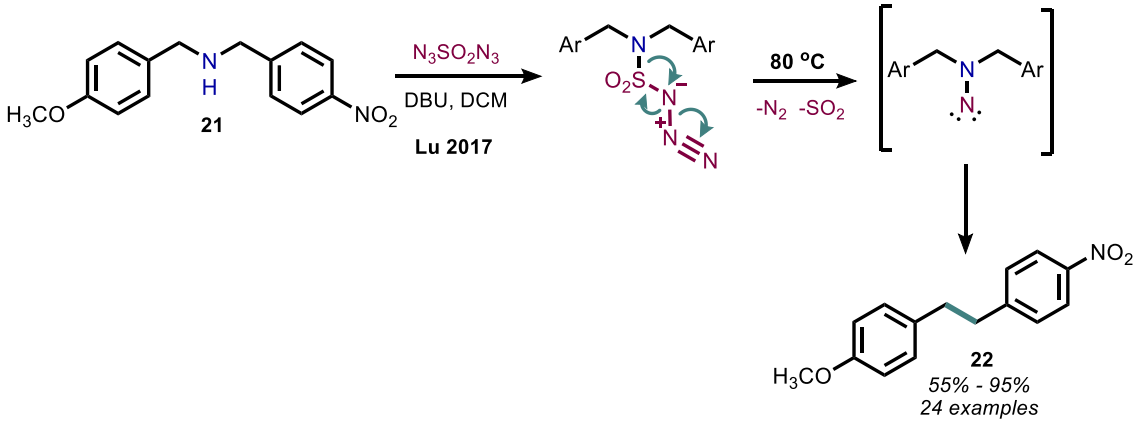

Scheme 2.6. Sulfamoyl azide method for nitrogen deletion.

We were interested in pursuing a milder route to generate isodiazene intermediates which could then be applied for facile skeletal editing. Glover has reported the reaction of *N*-methylaniline (**24**) with a reagent known as an anomeric amide (**23**).[21] Such amides consist of two electronegative oxygen substituents bonded to the amide nitrogen atom, rendering it electrophilic.[22] A more detailed overview of anomeric amides can be found in chapter 4.1. *N*-methylaniline was shown to undergo nucleophilic substitution at the electrophilic amide nitrogen (Scheme 2.7). The corresponding intermediate (**25**) undergoes a rearrangement, resulting in the

reductive elimination of an ester (**26**) and what was thought to be the requisite isodiazene moiety, as evidenced by the formation of a dimerized tetrazene product (**28**).[21] We hypothesized that secondary amines from which the resulting alkyl fragments can stabilize a radical intermediate would undergo homolytic extrusion preferentially over dimerization to yield the desired nitrogen deletion product (**30**) (Scheme 2.8).

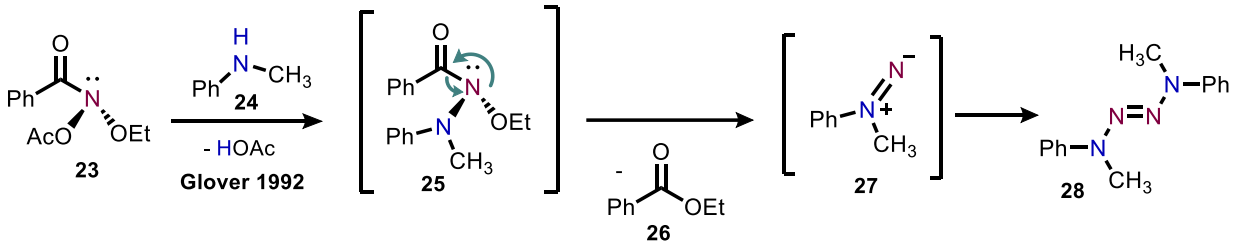

Scheme 2.7. Anomeric amide reagents convert secondary amines to isodiazene intermediates.

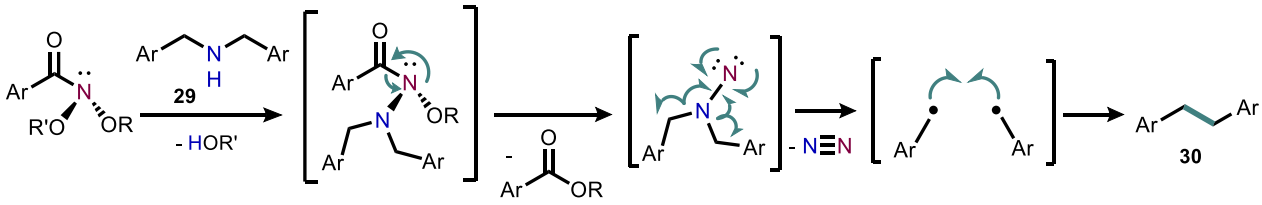

Scheme 2.8. Key hypothesis that anomeric amides can be applied for the direct deletion of amines.

It is also important to note that since the work presented in this chapter was published, two other strategies for nitrogen deletion have been disclosed. The sulfamoyl azide method for converting a secondary amine to an isodiazene was expanded to include a substrate scope of cyclic amines (**31**) which undergo ring contraction chemistry (Scheme 2.9).[23] Antonchick has also reported ring contraction of pyrrolidines (**33**) to give cyclobutanes (**34**) (Scheme 2.10). The requisite isodiazene intermediate in this latter example is generated by nitrene transfer from an iodonitrene intermediate (**35**) formed *in-situ* using ammonium carbonate and the oxidant HTIB at 80 °C.[24]

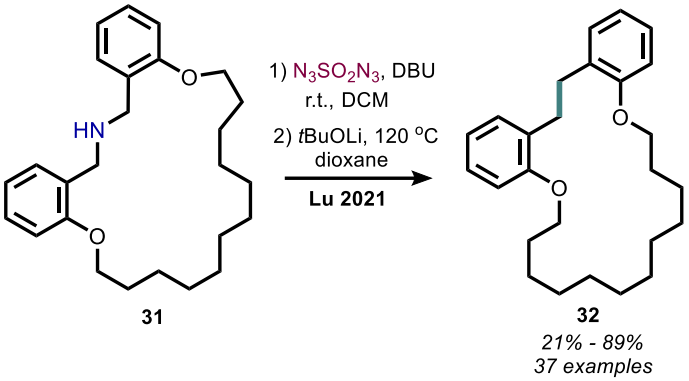

Scheme 2.9. Sulfamoyl azide method for nitrogen deletion applied to ring contraction chemistry.

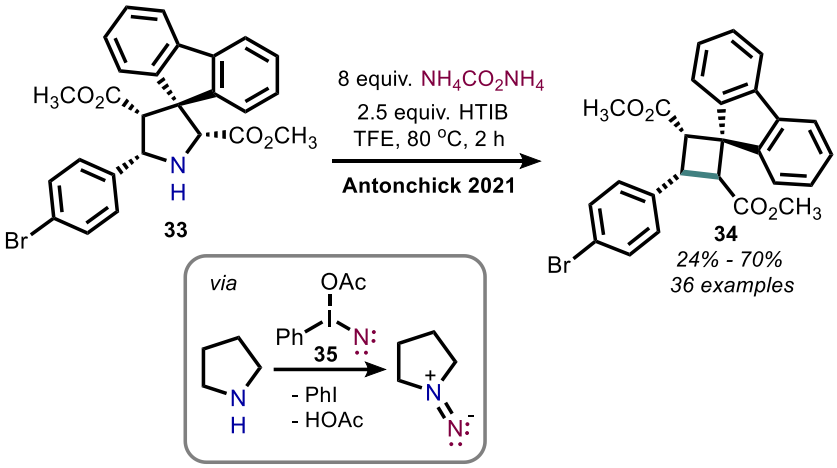

Scheme 2.10. Ring contraction of pyrrolidines to cyclobutanes using ammonium carbonate and HTIB.

2.2. Results and Discussion.

2.2.1. Reaction Scope and Limitations.

Anomeric amides were demonstrated to be effective reagents for nitrogen deletion of secondary amines by Dr. Sean Kennedy, a former post-doctoral scholar in our group who conducted the initial reaction optimization. Preliminary studies with the model secondary amine bis(4-bromobenzyl)amine (**36**) and anomeric amide **38** demonstrated that the desired deletion product **37** was produced in 35% yield (Table 2.1). However, unwanted *N*-acetylation of the amine

starting material was observed as a side product. In order to mitigate this, a more bulky pivalate derived reagent (**39**) was developed that increased the yield of **37** to 57%. Subsequent work demonstrated that the addition of an electron-withdrawing trifluoromethyl group to the benzamide ring (**40**) further increased the yield of **37** to 74%, and this anomeric amide was taken forward as the optimized reagent. Routine screening of reaction conditions demonstrated THF was the optimal solvent. Heating was shown to increase reaction rate, but unfortunately the reaction could not be heated above 45 °C due to the thermal instability of the reagent.

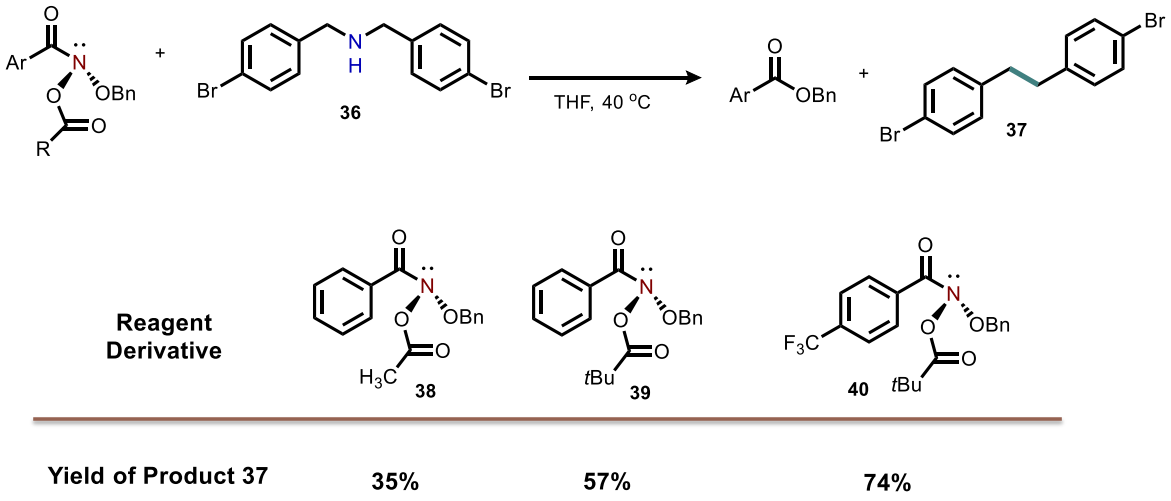

Table 2.1. Reagent optimization for secondary amine deletion conducted by Dr. Sean Kennedy.

The substrate scope (Table 2.2) was primarily conducted by Dr. Sean Kennedy, who demonstrated skeletal editing on a wide variety of dibenzylic amines. Tolerance was demonstrated for a number of potentially challenging functional groups that are typically present during late-stage editing of complicated molecules, including phosphates, sulfones and nitrogen-containing heterocycles (**41**-**51**). The benzylic nature of these amines was necessary to stabilize the homolytic extrusion of dinitrogen, and purely aliphatic secondary amines were unreactive. The monobenzylic secondary amine **57** yielded deletion product but in a lower yield of 34%.

Excitingly, a number of cyclic secondary amines (**52-56**) underwent ring contraction chemistry. Dr. Balu Dherange was able to demonstrate several synthetic applications of this methodology including the total synthesis of the marine metabolite Polysiphenol (**63**) (Scheme 2.12),[25] as well as a new synthesis of the histone receptor modulator drug target **60** (Scheme 2.11).[26]

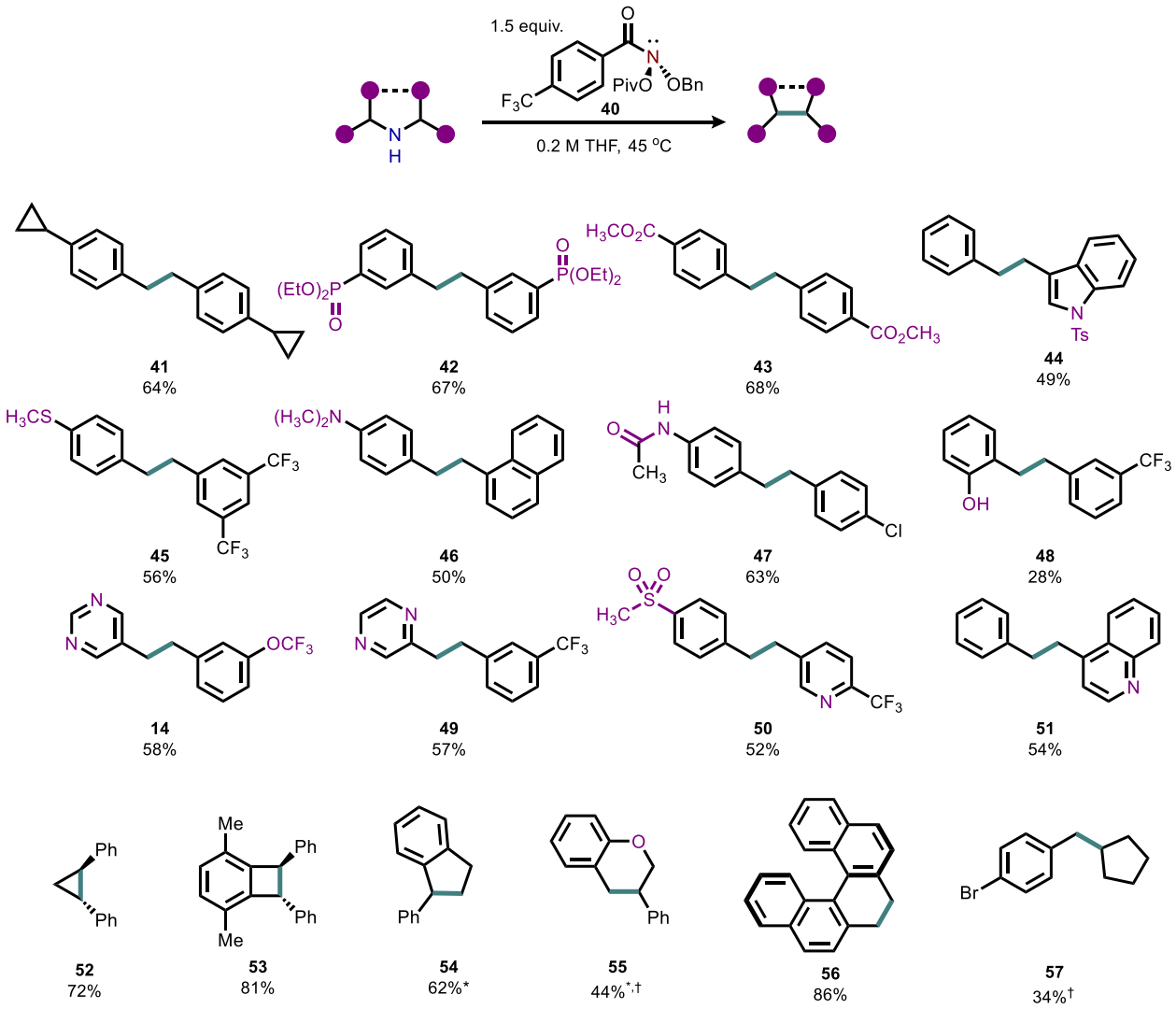

Table 2.2. Select examples from the secondary amine substrate scope demonstrating functional group tolerance. *2 equiv. triethylamine added; †2 equiv. reagent **40** added.

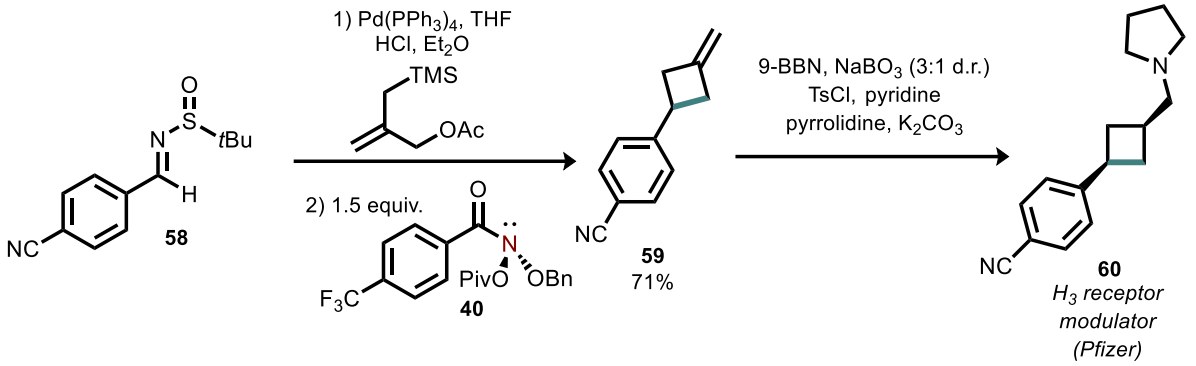

Scheme 2.11. Application of nitrogen deletion towards the synthesis of a histone receptor modulator.

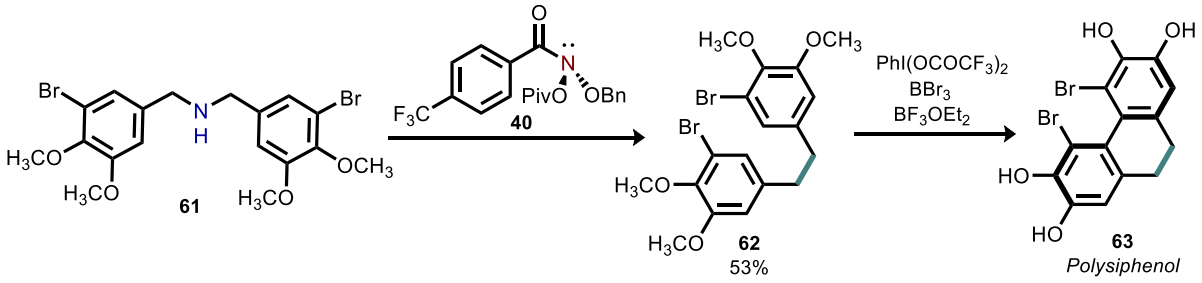

Scheme 2.12. Application of nitrogen deletion towards the total synthesis of Polysiphenol.

In addition to the stipulation that amines contain some degree of benzylic stabilization, there were several other limitations in scope. Steric hinderance of certain secondary amine substrates, coupled with the inability to force difficult transformations by heating the reaction higher than 45 °C, was a drawback of this methodology. For example, derivative **64** of the antidepressant Norsertraline was found to be unreactive despite the dibenzylic nature of the secondary amine moiety, possibly due to the bulky nature of the substituted tetralin core (Scheme 2.13). Additionally, α-tertiary secondary amines (**66** and **68**) were explored and found to be largely unreactive (Scheme 2.14). We postulate this is also due to steric constraints, as steric hinderance is known to be exacerbated at a nitrogen relative to carbon.[27]

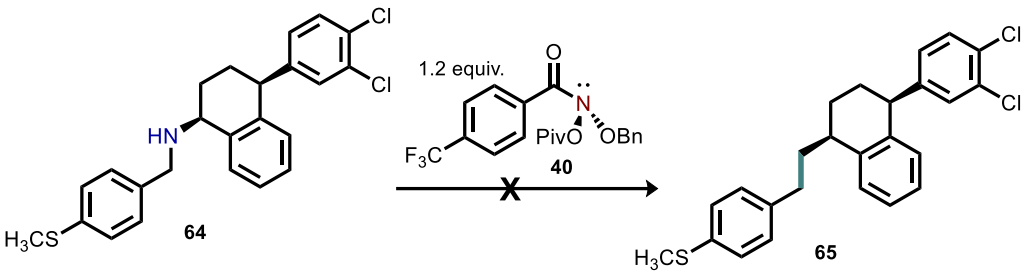

Scheme 2.13. Sterically bulky Norsertraline derivative is unreactive.

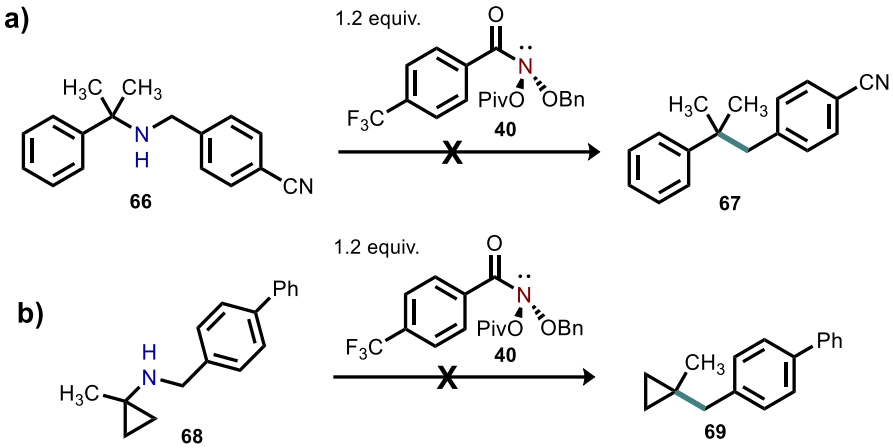

Scheme 2.14. Unsuccessful nitrogen deletion of α-tertiary secondary amines including a) dibenylic and b) monobenzylic substrates.

While homolytic extrusion of dinitrogen is the predominant pathway for acyclic substrates containing benzylic substitution, some cyclic compounds were shown to require either dibenzylic stabilization or a benzhydryl substituent if monobenzylic. This stipulation was demonstrated with the N-H derivative of Aprepitant (**2**), which is monobenzylic. Instead of liberating dinitrogen to yield the nitrogen deletion product, a rearrangement occurred to give hydrazone product **4** (Scheme 2.15). While this was not the desired product, it is of interest because it serves to demonstrate an example of skeletal editing *via* insertion chemistry. Heating **4** was not sufficient to liberate dinitrogen.

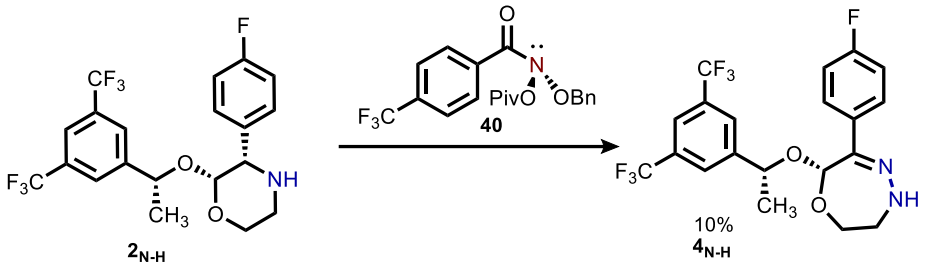

Scheme 2.15. Aprepitant derivative undergoes nitrogen insertion chemistry.

2.2.2. Mechanistic Studies.

With the substrate scope thoroughly investigated, the mechanism of the transformation was studied. The observation that substitution of the benzamide ring with a *p*-trifluoromethyl group increased the reaction rate prompted us to conduct a Hammett plot analysis. Anomeric amides bearing other substituents at the benzamide moiety - both electron-donating and electron-withdrawing - were synthesized in order to pursue this study (Figure 2.2). A one-pot Hammett competition study was conducted. When log(kx/kh) was plotted *versus* σ, and R^2 value of 0.9094 was obtained (Figure 2.3).[28] In contrast, a higher R^2 value of 0.9399 was obtained when the data was plotted against σ^+ and the intercept was closer to zero (Figure 2.4).[28, 29] This finding suggests that the transition state is stabilized by both resonance and inductive effects.[28] A rho value of 0.60 *versus* σ^+ was obtained, indicating a negative charge is built during the reaction and stabilized by the trifluoromethyl group.[28] However, the nature of the resonance stabilization in this system is less clear given that the site of nucleophilic attack is not directly conjugated to the arene ring. One possibility is that the initial substitution is not rate-limiting. Alternatively, related twisted amides have been shown to exhibit a similar dependence on σ^+, which was rationalized through competitive resonance between the arene and the amide.[30-33] Another possibility is that the Hammett plot *versus* σ is indicative of a change in rate-determining step. At this time, we cannot discount any of these possibilities.

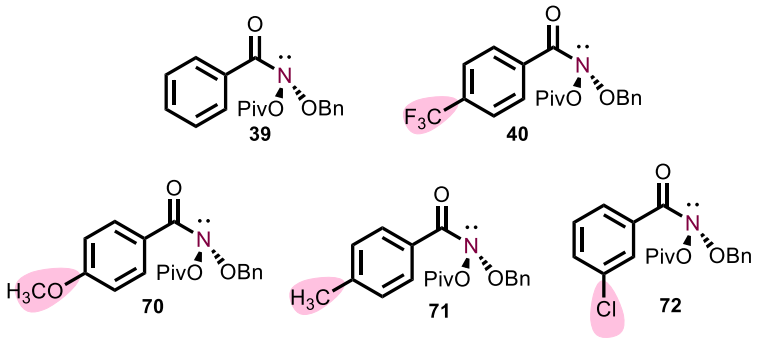

Figure 2.2. Anomeric amide derivatives prepared for Hammett plot study.

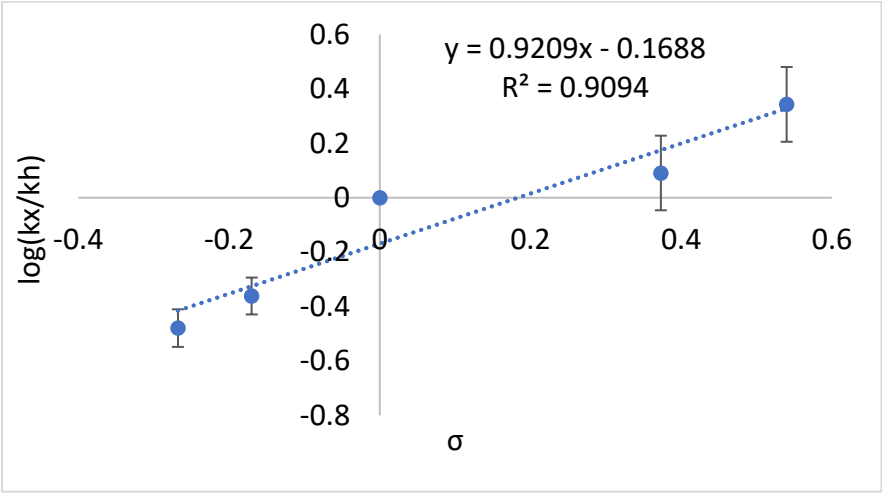

Figure 2.3. Hammett plot analysis *versus* σ.

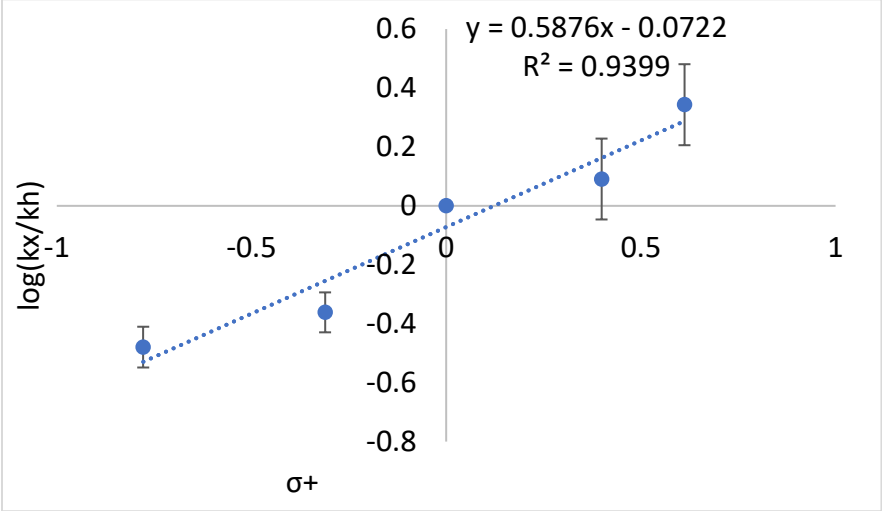

Figure 2.4. Hammett plot analysis *versus* σ+.

Following the initial substitution of the anomeric amide reagent **40**, it was hypothesized that a reductive elimination occurs to liberate the postulated isodiazene intermediate in addition to the ester byproduct. This rearrangement could occur *via* an intramolecular mechanism or an intermolecular mechanism by dissociation of a benzyloxy anion (Figure 2.5). In order to probe this, a cross-over experiment was performed using two anomeric amides which contain distinguishable benzamide and alkyoxy moieties (**72** and **73**) (Scheme 2.16). The nitrogen deletion reaction was conducted using both anomeric amides in a single pot. The ester by-products observed (**74** and **75**) corresponded to an intramolecular rearrangement and the crossover esters (**76** and **77**) which would be formed by a dissociative mechanism were not detected. This provided evidence for a concerted reductive elimination, which has been further supported by previous computational studies.[34, 35] The presence of an isodiazene intermediate following this rearrangement was further verified by Dr. Sean Kennedy using allylic amine **78** (Scheme 2.17). A [2,3]-sigmatropic rearrangement between the isodiazene and alkene occurred, resulting in 1,2-diazene product (**80**).[36]

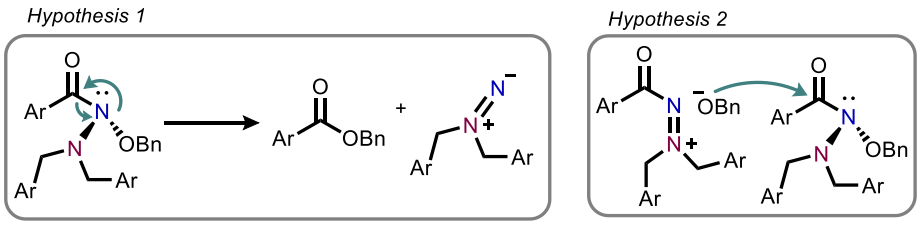

Figure 2.5. Two mechanistic hypotheses for the rearrangement to produce the isodiazene.

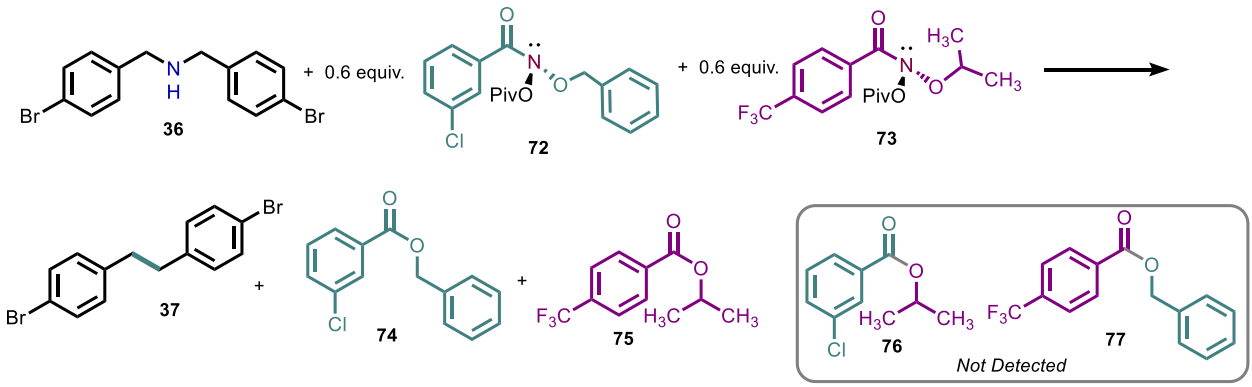

Scheme 2.16. Crossover experiment demonstrating an intramolecular rearrangement.

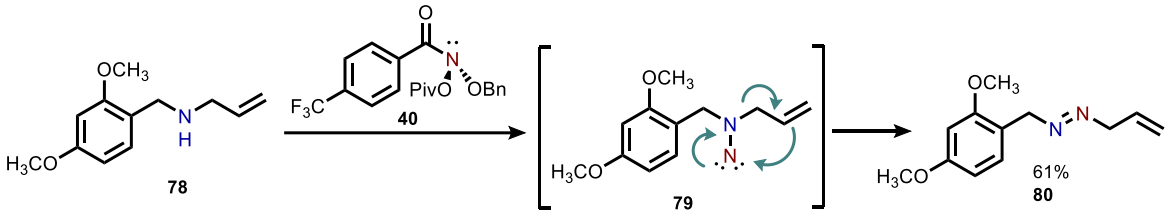

Scheme 2.17. [2,3]-Sigmatropic rearrangement to a diazene product suggests presence of isodiazene intermediate.

The observation that amines require benzylic substituents to produce deletion products suggested that the isodiazene intermediate liberates dinitrogen *via* a radical recombination. In order to verify this mechanism, we sought to use a secondary amine substrate which contained a radical clock (Scheme 2.18). Amine **81** containing a methylcyclopropyl moiety generates a radical species (**82**) which rearranges with a rate of 10^8 s^{-1}.[37] To our surprise, the rearranged product **84** was not detected and the unrearranged product **83** was observed in 30% yield. Because the rate that the methylcyclopropyl moiety rearranges is slower than the rate at which a free radical species diffuses from the solvent cage,[38] it was hypothesized that an in-cage radical mechanism was operative.

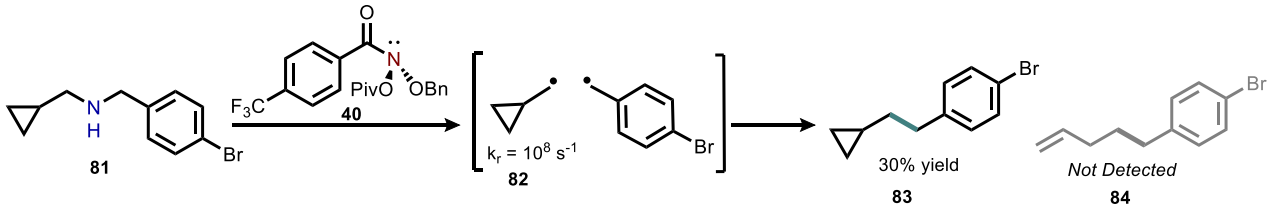

Scheme 2.18. Amine substrate containing a methylcyclopropyl radical clock moiety does not produce rearranged deletion product.

Thus, a secondary amine containing a faster radical clock moiety was subsequently pursued. The phenylcyclopropylmethyl radical clock (**89**) rearranges with a rate constant of 10^{11} s^{-1},[37] which is faster than the rate at which free radical species can diffuse from the solvent cage. *trans*-2-Phenylcyclopropane-1-carboxylic acid (**85**) is a commercially available compound that we sought to use as a precursor to a secondary amine containing the phenylcyclopropylmethyl radical clock (**88**). Amidation with benzylamine (**86**) was performed, followed by reduction to give the requisite amine (Scheme 2.19). However, this amine failed to produce deletion products (with or without rearrangement) in any appreciable yield when treated with **40** (Scheme 2.20).

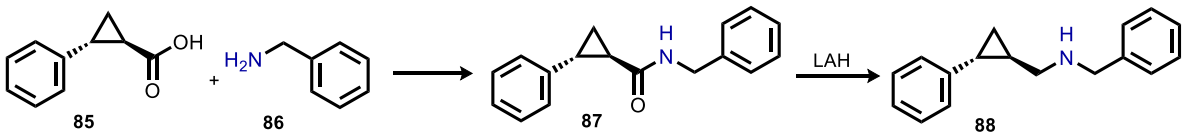

Scheme 2.19. Synthesis of amine substrate **88** containing the phenylcyclopropylmethyl radical clock.

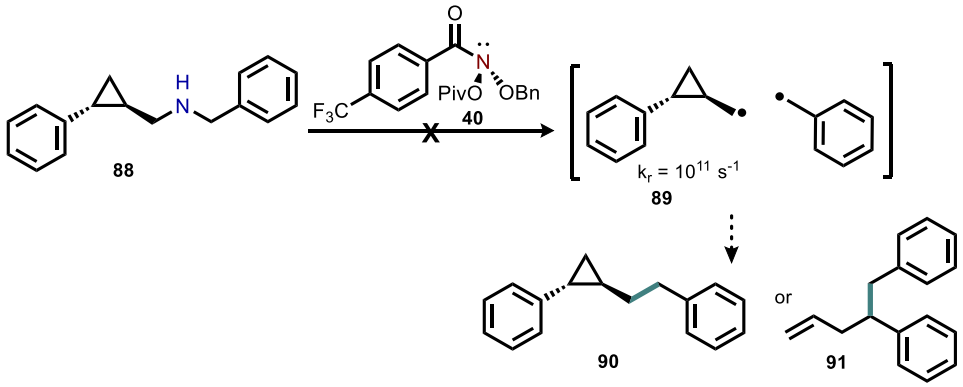

Scheme 2.20. Unsuccessful nitrogen deletion of amine substrate **88**.

It was hypothesized that increasing the stability of the benzylic radical generated upon nitrogen deletion might increase the yield of product. Consequently, an extra phenyl group was added to the benzylic moiety at the *para* position (a 4-phenyl substituent has a σ radical value of 0.46 relative to 0.0 for a 4-hydrogen substituent).[39] Coupling of *trans*-2-phenylcyclopropane-1-carboxylic acid (**85**) with 4-phenylbenzylamine (**92**) resulted in the desired amide precursor **93**, however a variety of reductants were screened and found to be ineffective at producing amine **94** (Scheme 2.21). Consequently, an alternative synthetic route was pursued in which the carboxylic acid precursor was converted to an aldehyde (**95**) in two steps (Scheme 2.22). A subsequent reductive amination with **92** successfully produced the requisite amine.

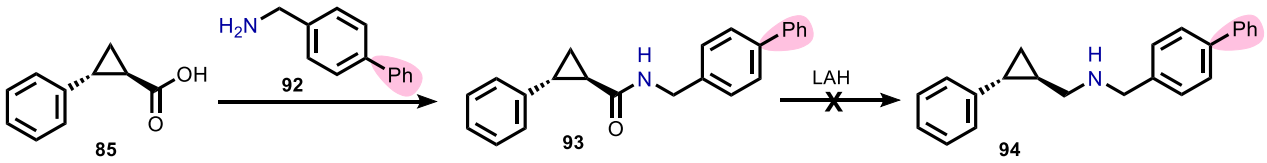

Scheme 2.21. Initial synthetic route to amine **94** is unsuccessful.

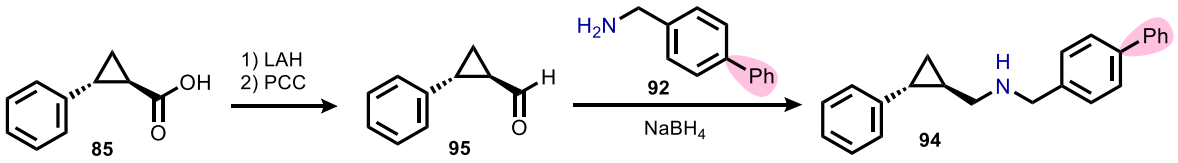

Scheme 2.22. Alternative synthetic route to amine **94** by conversion of **85** to an aldehyde followed by reductive amination.

With secondary amine **94** in hand, nitrogen deletion was performed. Fascinatingly, the rearranged (**97**) and unrearranged (**96**) deletion products were both produced in approximately a 1:1 ratio (Scheme 2.23). This finding suggests that the rate of radical recombination is

approximately equal to the rate of rearrangement of the phenylcyclopropylmethyl clock, which provides evidence for an in-cage radical process. However, it is also possible that product **96** is the result of a competing non-radical mechanism. Trace amounts of the homo-coupled product **98** were detected by GC-MS, further suggesting the fraction of alkyl radical species which escape the solvent cage is very low. Additionally, Dr. Sean Kennedy was able to detect radical trapped TEMPO adducts of alkyl radical species in low yield (between 1-10%), corroborating the above findings. In contrast, the recent report of ether deoxygenation (see scheme 2.2) proceeds *via* free radical diffusion and unsymmetrical ethers give a statistical mixture of products in approximately a 1:2:1 ratio.[12] Such levels of homo-coupled products were not observed in this system with unsymmetrical amines were used.

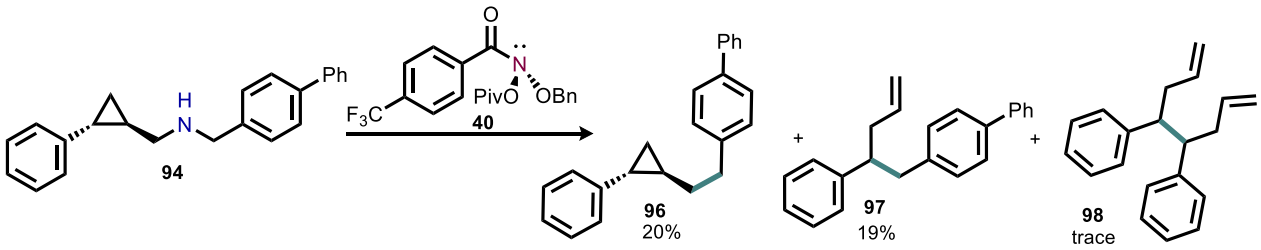

Scheme 2.23. Nitrogen deletion of radical clock substrate **94** gives approximately a 1:1 mixture of rearranged and unrearranged products.

2.3. Conclusion.

This chapter has presented a new strategy for skeletal editing *via* deletion of secondary amines from molecular scaffolds using an anomeric amide reagent. This methodology was shown to tolerate a number of potentially challenging functional groups that may be present during the late-stage editing of pharmaceuticals. Ring contraction chemistry of cyclic secondary amines was also demonstrated. New synthetic routes to the natural product polysiphenol, as well as a histone receptor modulator drug target were also demonstrated. However, one limitation of this

methodology is the requirement that amines are benzylic. The inability to heat the reaction above 45 ^{o}C may be responsible for such scope limitations and the development of more thermally stable anomeric amides is addressed in chapter 4.

Mechanistic studies demonstrated that following initial substitution by a secondary amine moiety, the requisite intermediate undergoes an intramolecular rearrangement to liberate an ester and an isodiazene species. The isodiazene intermediate rearranges by a radical mechanism to liberate dinitrogen, and the resulting alkyl fragments undergo in-cage radical recombination. This work represents a milder method for the generation of isodiazene intermediates compared to previous reports in the literature.

2.4. Experimental.

2.4.1. General Procedures.

Unless noted otherwise, all reactions were performed in oven-dried or flame-dried glassware under an atmosphere of dry N_2. THF, Et_2O, DCM, Toluene, ACN, Et_3N, and Pentane were dried by passing these previously degassed solvents through a PPT Solvent Purificatiton System, and all other solvents were dried over molecular sieves (4 Å) and degassed prior to use or purchased anhydrous and sealed under N_2 (e.g. VWR Dri-solv or equivalent). Reaction temperatures were reported as the temperatures of the bath surrounding the flasks or vials. Sensitive reagents and solvents were transferred under nitrogen into a nitrogen-filled glovebox with standard techniques. Unless otherwise noted, all reagents were used as received. Analytical thin-layer chromatography (TLC) was carried out using 0.2 mm commercial silica gel plates (silica gel 60, F254) and visualized by UV irradiation or staining as indicated.

Low resolution mass spectra were recorded on either an Agilent 6530 LC Q-TOF mass spectrometer using electrospray ionization with fragmentation voltage set at 115 V or an Agilent SQ GC-MMS with a 7890B GC using an Agilent HP-5MS column with a temperature gradient of 50 ^{o}C to 200 ^{o}C over 15 minutes and a 5977A single quad MS using electron ionization. High resolution mass spectra were recorded on either an Agilent 6224 TOF High Resolution Accurate MS with electrospray ionization or an Agilent 7200B QTOF High Resolution Accurate Mass GCMS using an Agilent HP-5MS column with a temperature gradient of 50 ^{o}C to 200 ^{o}C over 15 minutes and electron ionization. All mass spectra were processed with an Agilent MassHunter Operating System. Nuclear magnetic resonance spectra (^{1}H-NMR, ^{13}C-NMR and ^{19}F-NMR) were recorded with Bruker spectrometers operating at 400 or 500 MHz for ^{1}H. Chemical shifts are reported in parts per million (ppm, δ), downfield from tetramethylsilane (TMS, δ=0.00 ppm) and are referenced to residual solvent ($CDCl_3$, δ=7.26 ppm (^{1}H) and 77.160 ppm (^{13}C)). Coupling constants were reported in Hertz (Hz). Data for ^{1}H-NMR spectra were reported as follows: chemical shift (ppm, s = singlet, d = doublet, t = triplet, q = quartet, quin = quintet, dd = doublet of doublets, td = triplet of doublets, ddd = doublet of doublet of doublets, m = multiplet, coupling constant (Hz), and integration). *N*-(benzyloxy)-*N*-(pivaloyloxy)-4-(trifluoromethyl)benzamide) (**40**) was prepared according to the optimized procedure in chapter 4. *N*-acetoxy-*N*-(benzyloxy)benzamide (**38**) was synthesized according to the reported literature procedure.[40] Characterization data for the substrate scope conducted by Dr. Sean Kennedy and Dr. Balu Dherange can be found in the supporting information for *Nature*, **2021**, *593*, 223-227.

2.4.2. Synthesis of Anomeric Amide Derivatives for Mechanistic Studies.

General procedure for the synthesis of hydroxamate O-alkyl esters: A 500 ml round bottom flask equipped with a stir bar was charged with an *O*-alkyl hydroxylamine hydrochloride (29.3

mmol, 1 equiv), 100 ml DCM, 25 ml water and K_2CO_3 (58.6 mmol, 2 equiv) and cooled to 0 ^oC with an ice bath. After 20 min of stirring, the benzoyl chloride derivate (29.3 mmol, 1 equiv.) was added dropwise by syringe. The reaction was warmed to room temperature and overnight. The water phase was removed using a separatory funnel and the DCM was dried with magnesium sulfate, filtered and concentrated to a minimum volume by rotary evaporation until the product crystallized out of solution. The crystalline product was filtered, washed with ether and dried under vacuum to afford the hydroxamate *O*-alkyl ester.

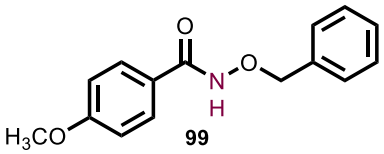

99

***N*-benzyloxy-4-methoxybenzamide (99):** Synthesized according to the general procedure from *O*-benzylhydroxylamine hydrochloride (4.78 g, 29.3 mmol) and *p*-methoxybenzoyl chloride (5 g, 29.3 mmol), with the exception that *p*-methoxybenzoyl chloride is a solid at room temperature and was added to the reaction in small portions using a spatula. The white crystalline product was obtained in 66% yield. ^{1}H NMR (400 MHz, $CDCl_3$): δ 8.35 (br s, 1 H), 7.63 (d, J = 9.1 Hz, 2 H), 7.46 – 7.42 (m, 2H), 7.41 – 7.35 (m, 3 H), 6.89 (d, J = 8.9 Hz, 2 H), 5.02 (s, 2 H), 3.83 (s, 3 H). Spectroscopic data were in agreement with the literature.[41]

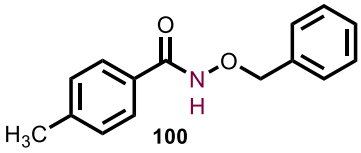

100

***N*-benzyloxy-4-methylbenzamide (100)**: Synthesized according to the general procedure from *O*-benzylhydroxylamine hydrochloride (5.16 g, 32.3 mmol) and *p*-methylbenzoyl chloride (5 g, 32.3 mmol). The white crystalline product was obtained in 33% yield. **^{1}H NMR** (400 MHz, $CDCl_3$): δ 8.34 (br s, 1 H), 7.56 (d, J = 7.0 Hz, 2 H), 7.47 – 7.43 (m, 2 H), 7.42 – 7.36 (m, 3 H), 7.21 (d, J = 7.7 Hz, 2 H), 5.05 (s, 2 H), 2.38 (s, 3H). Spectroscopic data are in agreement with those in the literature.[42]

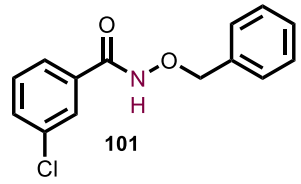

101

***N*-benzyloxy-3-chlorobenzamide (101)**: Synthesized according to the general procedure from *O*-benzylhydroxylamine hydrochloride (4.6 g, 28.5 mmol) and *m*-chlorobenzoyl chloride (5 g, 28.6 mmol). The white crystalline product was obtained in 53% yield. **^{1}H NMR** (400 MHz, $CDCl_3$): δ 8.38 (br s, 1 H), 7.64 (s, 1 H), 7.53 – 7.31 (m, 9 H), 5.03 (s, 2 H). Spectroscopic data are in agreement with those in the literature.[43]

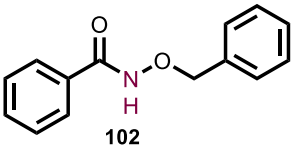

102

***N*-benzyloxybenzamide (102)**: Synthesized according to the general procedure from *O*-benzylhydroxylamine hydrochloride (3.8 g, 24 mmol) and benzoyl chloride (5 g, 24 mmol). The white crystalline product was obtained in 37% yield. **^{1}H NMR** (400 MHz, $CDCl_3$): δ 8.47 (br s, 1 H), 7.67 (d, J = 7.7 Hz, 2 H), 7.53 – 7.48 (m, 1 H), 7.47 – 7.38 (m, 7 H), 5.05 (s, 2 H). Spectroscopic data are in agreement with the literature.[44]

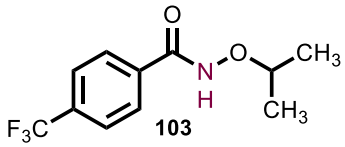

103

***N*-isopropyloxyl-4-(trifluoromethyl)benzamide (103)**: Synthesized according to the general procedure from *O*-isopropylhydroxylamine hydrochloride (1 g, 8.96 mmol, 1 equiv.) and *p*-trifluoromethyl benzoyl chloride (1.87 g, 8.96 mmol, 1 equiv.). The white crystalline product was obtained in 16% yield. **^{1}H NMR** (400 MHz, DMSO-*d*6): δ 11.67 (s, 1 H), 7.96 (d, J = 5.6 Hz, 2 H), 7.86 (d, J = 4.2 Hz, 2 H), 4.19 – 4.12 (m, 1 H), 1.22 (d, J = 3.1 Hz, 6 H). **^{19}F{^{1}H NMR** (376 MHz, DMSO-*d6*): δ -63.08. **^{13}C{^{1}H} NMR** (101 MHz, DMSO-*d6*): δ 163.3, 136.5, 131.5, 131.5 (q, J = 32 Hz), 128.1, 125.4 (m), 125.3, 122.6, 119.9, 76.8, 20.6. **HR-MS** (EI) calculated 247.0820 for $C_{11}H_{12}F_3NO_2$, found 247.0809.

General procedure for the synthesis of anomeric amides from hydroxamate O-alkyl esters:

To a stirred suspension of the hydroxamate *O*-alkyl ester (3.89 mmol, 1 equivalent) in CH_2Cl_2 (12 mL) was added freshly prepared *t*BuOCl (5.05 mmol, 1.3 equiv) in a single portion. The reaction was shielded from ambient light and stirred under nitrogen at room temperature for 2 hours (consumption of starting material by TLC). The solution was concentrated *in vacuo* to afford the *N*-chloroamide product as a yellow liquid, which was of sufficient purity and immediately used in the next step.

To a suspension of sodium pivalate (5.84 mmol, 1.5 equiv) in ACN (8 mL) under nitrogen was added a solution of *N*-chloroamide in ACN (8 mL). The reaction was shielded from light and vigorously stirred for 2 hours at ambient temperature. Upon consumption of the *N*-chloroamide (monitored by TLC), the reaction mixture was diluted with 20 ml ether and filtered over a small silica plug. The plug was rinsed with additional diethyl ether and solvent was removed under reduced pressure to afford the anomeric amide. Storage of the anomeric at 0 °C for 24-48 hours typically leads to a low-melting solid.

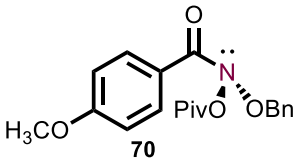

70

***N*-(benzyloxyl)-4-methoxy-*N*-(pivaloyloxy)benzamide (70)**: Synthesized according to the general procedure from *N*-benzyloxy-4-methoxybenzamide (1 g, 3.89 mmol). The title compound was isolated as a yellow liquid in 98% yield. **^{1}H NMR** (400 MHz, $CDCl_3$): δ 7.73 (d, J = 8.2 Hz, 2 H), 7.43 – 7.39 (m, 2 H), 7.37 – 7.31 (m, 3 H), 6.87 (d, J = 8.9 Hz, 2 H), 5.17 (s, 2 H), 3.85 (s, 3 H), 1.12 (s, 9 H). **^{13}C{^{1}H} NMR** (101 MHz, $CDCl_3$) δ 175.5, 173.8, 163.3, 135.3, 131.5, 129.1, 129.0, 128.6, 128.5, 123.7, 77.4, 55.5, 38.5, 26.8. **HR-MS** (ESI) calculated 357.1576 for $C_{20}H_{23}NO_5$, found 357.1549.

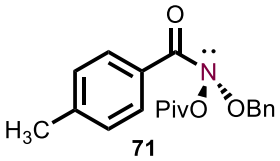

71

***N*-(benzyloxyl)-4-methyl-*N*-(pivaloyloxy)benzamide (71)**: Synthesized according to the general procedure from *N*-benzyloxy-4-methylbenzamide (1 g, 4.14 mmol). The title compound was isolated as a yellow liquid in 77% yield. **^{1}H NMR** (400 MHz, $CDCl_3$): δ 7.63 (d, J = 9.0 Hz, 2 H), 7.45 – 7. 41 (m, 2 H), 7.40 – 7.34 (m, 3 H), 7.21 (d, J = 8.0 Hz, 2 H), 5.19 (s, 2 H), 2.43 (s, 3 H), 1.13 (s, 9 H). **^{13}C{^{1}H} NMR** (101 MHz, $CDCl_3$) δ 175.4, 174.5, 143.5, 135.2, 129.2, 129.2, 128.9, 128.9, 128.6, 128.5, 77.6, 38.4, 26.7, 21.7. **HR-MS** (ESI) calculated 341.1627 for $C_{20}H_{23}NO_4$ found 341.1604.

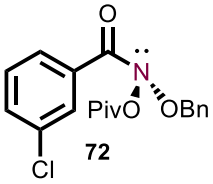

72

***N*-(benzyloxyl)-3-chloro-*N*-(pivaloyloxy)benzamide (72)**: Synthesized according to the general procedure from *N*-benzyloxy-3-chlorobenzamide (1 g, 3.82 mmol). The title compound was isolated as a yellow liquid in 94% yield. **^{1}H NMR** (400 MHz, $CDCl_3$): δ 7.64 (s, 1 H), 7.57 (d, J = 7.56 Hz, 1 H), 7.48 (d, J = 7.8 Hz, 1 H), 7.42 – 7.38 (m, 2 H), 7.38 – 7.32 (m, 4 H), 5.15 (s, 2 H), 1.11 (s, 9 H). **^{13}C{^{1}H} NMR** (101 MHz, $CDCl_3$) δ 175.3, 173.1, 134.8, 134.2, 133.5, 132.5, 129.5, 129.3, 128.9, 128.8, 128.5, 127.1, 77.8, 38.4, 26.6. **HR-MS** (ESI) calculated 361.1081 for $C_{19}H_{20}NO_4Cl$, found 361.1057.

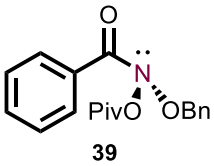

39

***N*-(benzyloxyl)-*N*-(pivaloyloxy)benzamide**: Synthesized according to the general procedure from *N*-benzyloxybenzamide (1 g, 4.40 mmol). The title compound was isolated as a yellow liquid in 46% yield. **^{1}H NMR** (400 MHz, $CDCl_3$): δ 7.70 (d, J = 8.0 Hz, 2 H), 7.50 (t, J = 7.2 Hz, 1 H), 7.42 – 7.38 (m, 4 H), 7.37 – 7.31 (m, 3 H), 5.17 (s, 2 H), 1.08 (s, 9 H). **^{13}C{^{1}H} NMR** (101 MHz, $CDCl_3$) δ 175.4, 174.6, 135.1, 132.5, 131.9, 129.2, 129.0, 128.6, 128.5, 128.2, 77.7, 38.4, 26.7. **HR-MS** (ESI) calculated 327.1471 for $C_{19}H_{21}NO_4$, found 327.1467.

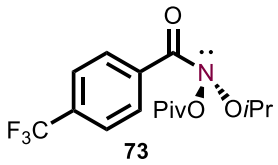

73

***N*-(isopropoxy)-*N*-(pivaloyloxy)-4-(trifluoromethyl)benzamide (73)**: Synthesized according to the general procedure from *N*-isopropyloxy-4-trifluoromethylbenzamide (310 mg, 1.25 mmol, 1 equiv.). The title compound was isolated as a yellow liquid in 94% yield. **^{1}H NMR** (400 MHz, $CDCl_3$): δ 7.83 (d, J = 7.69 Hz, 2 H), 7.66 (d, J = 8.1 Hz, 2 H), 4.43 (sept., J = 5.8 Hz, 1 H), 1.31 (d, J = 7.5 Hz, 6 H), 1.09 (s, 9 H). **^{13}C{^{1}H} NMR** (101 MHz, $CDCl_3$) δ 175.4, 129.3, 125.0, 125.0, 78.8, 38.2, 26.5, 21.0. **^{19}F{^{1}H} NMR** (376 MHz, $CDCl_3$): δ -63.13. **HR-MS** (ESI) calculated 347.1344 for $C_{16}H_{20}F_3NO_4$, found 347.1304.

2.4.3. Hammett Plot Analysis.

Two anomeric amides (each 0.14 mmol, 10 equiv.) were weighed, combined into a 20 ml vial and dissolved in minimal DCM. The DCM was removed by rotary evaporation and a small sample of the mixture (~3 mg) was taken for NMR spectroscopy. In the glovebox, a 20 ml bomb equipped with a stir bar was charged with 3 ml THF, the remaining mixture of the two anomeric amides and bis(*p*-bromobenzyl)amine (0.014 mmol, 1 equiv.). The bomb was sealed, removed from the glovebox and heated to 40 ^{o}C while stirring. The reaction was monitored hourly by NMR and after 3 hours the reaction with bis(*p*-bromobenzyl)amine was determined to be complete. A 0.3 ml aliquot of the completed reaction mixture was taken, the solvent was removed by rotary evaporation and the remaining residue was use for NMR spectroscopy. The NMR samples were prepared using C_6D_6 and integrated relative to the internal standard dodecane (Figure 2.6) to determine the values in Table 2.3. Calculations for the Hammett plot analysis were performed according to equations 2.1 – 2.4.

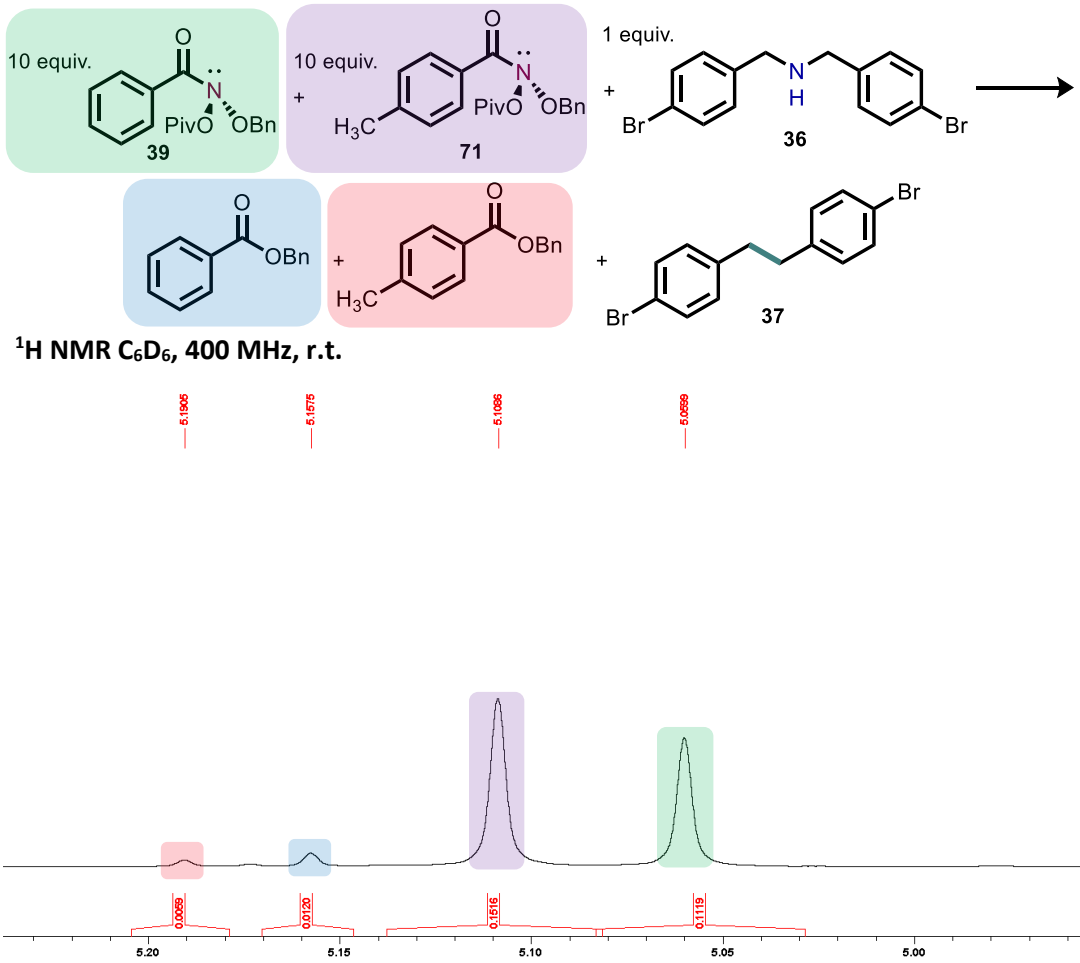

Figure 2.6. Example ^{1}H NMR spectrum of reaction aliquot after three hours for Hammett plot analysis.

Integrated Entity (I)	***p*-CH3**	**Ph**
Final amide (I-f1)	0.1516	0.1119
Final ester (I-f2)	0.0059	0.0120
Initial amide (I-intial)	0.1575	0.1239
Starting ratio sample (I-SM)	0.0642	0.0495

Table 2.3. NMR integration values used to determine Hammett plot values.

$$\text{Ratio of Initial Amide Integrations} = \frac{I\text{-}inital_{pCH3}}{I\text{-}initial_{Ph}} = \frac{1.575}{0.1239} = 1.271 \quad (2.1)$$

$$\text{Starting Anomeric Amide Ratio} = \frac{I\text{-}SM_{pCH3}}{I\text{-}SM_{Ph}} = \frac{0.0642}{0.0495} = 1.297 \quad (2.2)$$

$$\frac{k_{pCH3}}{k_{Ph}} = \frac{\ln\left(\frac{I-fl}{I-initial}\right)p-CH3}{\ln\left(\frac{I-fl}{I-initial}\right)Ph} = \frac{\ln\left(\frac{0.1516}{0.1575}\right)p-CH3}{\ln\left(\frac{0.1119}{0.1239}\right)Ph} = 0.3748 \quad (2.3)$$

$$\log\left(\frac{k_{pCH3}}{k_{Ph}}\right) = \log(0.3748) = -0.426 \quad \textit{Average of three replicates} = \textit{-0.365 +/- 0.066} \quad (2.4)$$

2.4.4. Crossover Experiment.

In the glovebox, a 1-dram vial with a screw cap and stir bar was charged with bis(4-bromophenylbenzyl)amine (10 mg, 0.0282 mmol, 1 equiv.), 4 ml THF, *N*-(benzyloxyl)-3-chloro-*N*-(pivaloyloxy)benzamide (6.1 mg, 0.0169 mmol, 0.6 equiv.) and *N*-(isopropoxy)-*N*-(pivaloyloxy)-4-(trifluoromethyl)benzamide (5.8 mg, 0.0169 mmol, 0.6 equiv.). The vial was sealed, removed from the glovebox and heated at 40 °C for 18 hours. The reaction was filtered with a 0.2 µm syringe filter and a 1 ml aliquot was analyzed by GC-MS (Figure 2.7). *Note*: This reaction does not go to full conversion because the anomeric amides utilized are non-optimal.

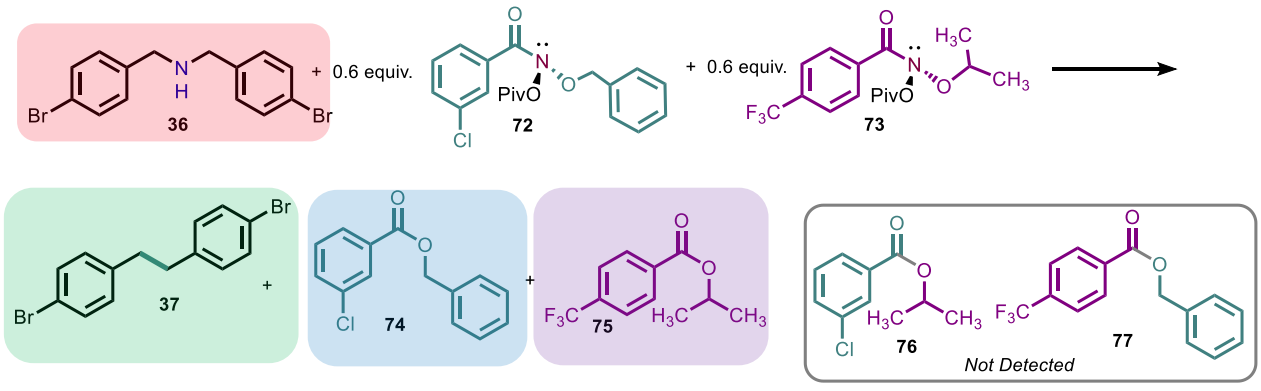

Figure 2.7. GC-MS trace of crude crossover experiment reaction. *Peak corresponds to a mass which could not be identified.

Figure 2.7 continued. GC-MS trace of crude crossover experiment reaction. *Peak corresponds to a mass which could not be identified.

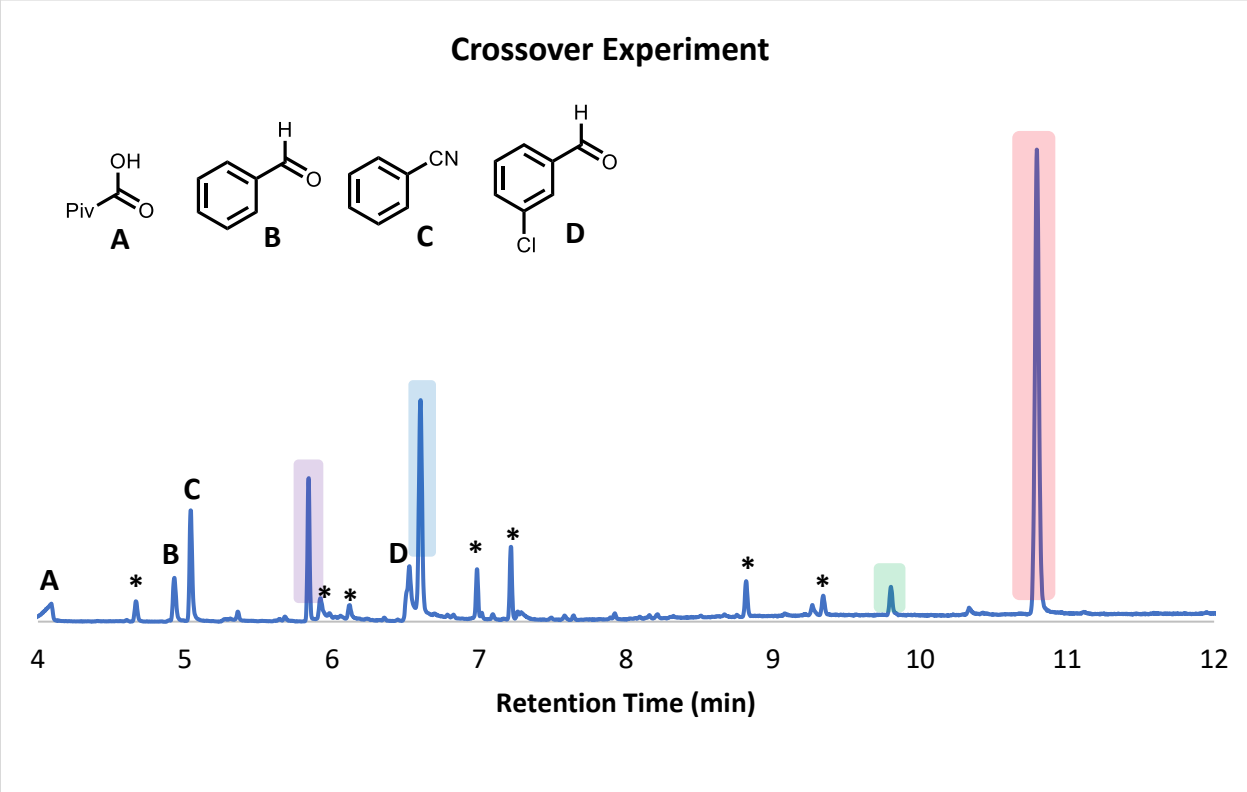

2.4.5. Radical Clock Experiments.

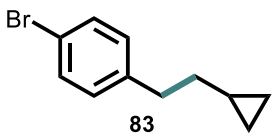

1-bromo-4-(2-cyclopropylethyl)benzene (83): In the glovebox, a 20 ml bomb with a stir bar was charged sequentially with 4-bromo-*N*-(cyclopropylmethyl)-benzenemethanamine (50 mg, 0.208 mmol, 1 equiv), 5 ml THF and the anomeric amide (99 mg, 0.249 mmol,1.2 equiv). The bomb was sealed, removed from the glovebox and heated at 40 ^{o}C while stirring for 18 hours. The reaction was cooled to room temperature and the solvent was removed *in vacuo*. The crude mixture was dissolved in 1 ml $CDCl_3$ and a 0.1 ml aliquot was taken, diluted with an additional 0.5 ml $CDCl_3$ and used to determine an NMR yield of 30% for the title compound relative to internal standard (Figure 2.8). The ring opened radical clock product 1-bromo-4-(4-penten-1-yl)-benzene was not

detected by NMR. The remaining $CDCl_3$ solution was concentrated in vacuo and the crude mixture was isolated by silica gel chromatography using the eluent 3:1 hexanes: ethyl acetate. *Note:* The ring opened alternative product 1-bromo-4-(pent-4-en-1-yl)benzene has olefinic peaks 5.88 – 5.75 (m, 1H), 5.06 – 4.94 (m, 2H) and is not detected.[45] **^{1}H NMR** (400 MHz, $CDCl_3$): δ 7.38 (d, J = 8.4 Hz, 2H), 7.06 (d, J = 8.9 Hz, 2H), 2.66 (t, J = 8.1 Hz, 2H), 1.48 (q, J= 7.4 Hz, 2H), 0.68 – 0.59 (m, 1H), 0.41 – 0.36 (m, 2H), 0.02 – 0.00 (m, 2H). **^{13}C{^{1}H} NMR** (100 MHz, $CDCl_3$) δ 141.6, 131.2, 130.3, 36.5, 35.4, 10.6, 4.5. **HR-MS** (ESI) calculated 224.0201 for $C_{11}H_{13}Br$, found 224.0188.

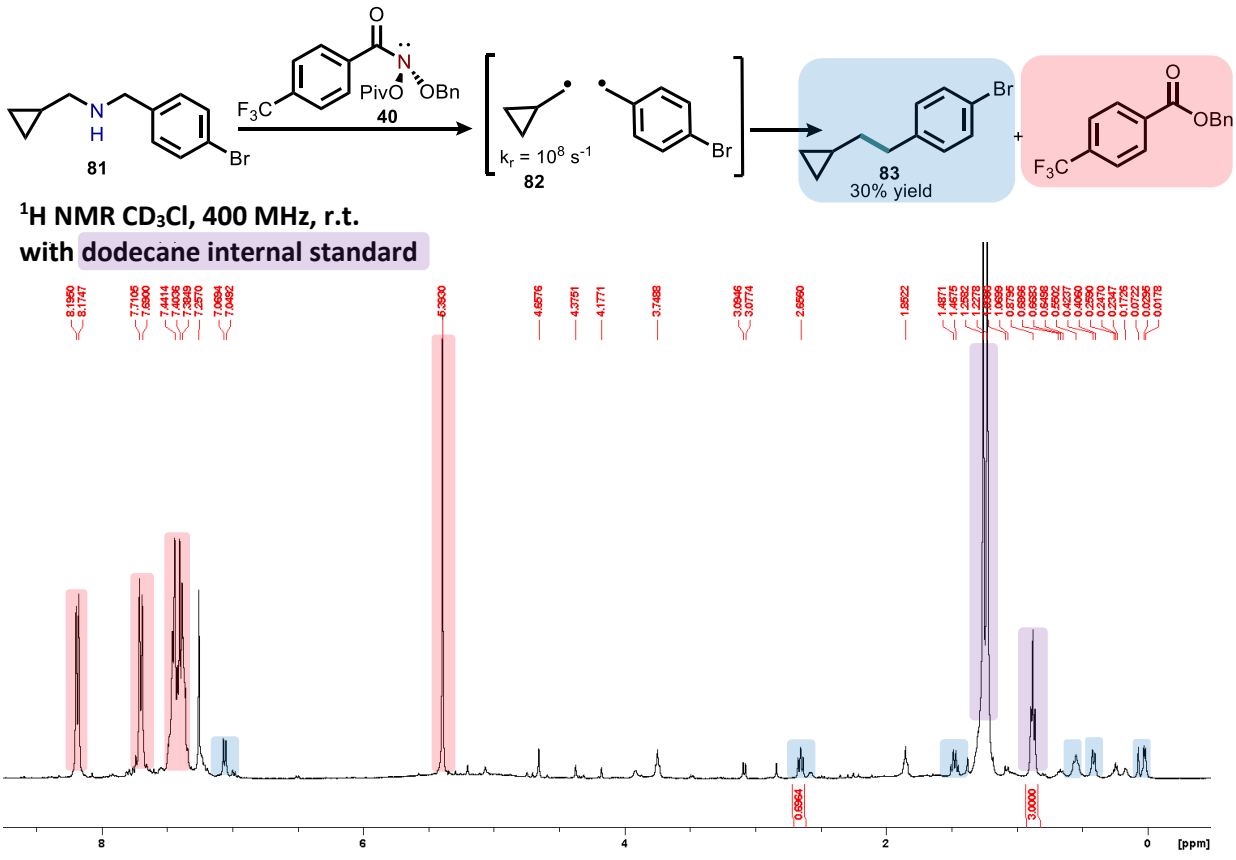

Figure. 2.8. NMR spectrum of crude reaction mixture from 4-bromo-*N*-(cyclopropylmethyl)-benzenemethanamine (**81**).

In the glovebox, a 20 ml vial with a stir bar was charged sequentially with *trans*-1-([1,1'biphenyl]-4-yl)-*N*-((2-phenylcyclopropyl)methyl)methanamine (15 mg, 0.0479 mmol, 1 equiv), 1 ml THF and the anomeric amide (23 mg, 0.0575 mmol,1.2 equiv). The vial was sealed, removed from the glovebox and heated at 40 ^{o}C while stirring for 18 hours. The reaction was cooled to room temperature and the solvent was removed *in vacuo*. The crude mixture was dissolved in $CDCl_3$ and the yield of products was determined relative to internal standard (Figure 2.9). The ring opened product was determined to be produced in 19% yield and the ring closed product was determined to produced in 20% yield.

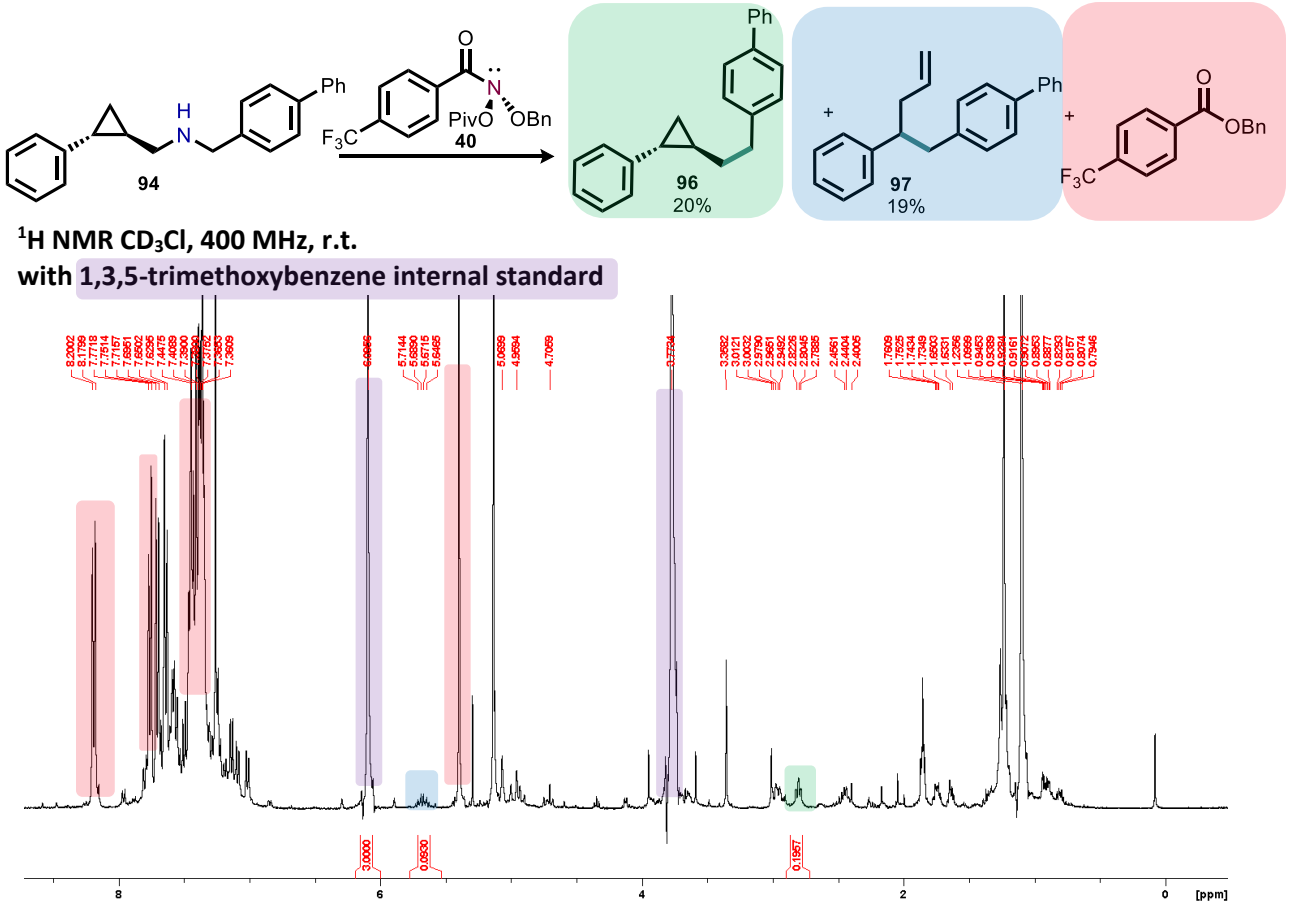

Figure 2.9. NMR spectrum of crude reaction mixture from *trans*-1-([1,1'biphenyl]-4-yl)-*N*-((2-phenylcyclopropyl)methyl)methanamine (**94**).

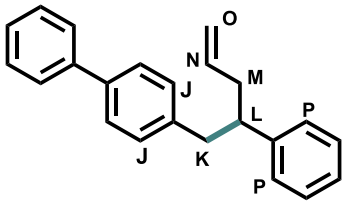

97

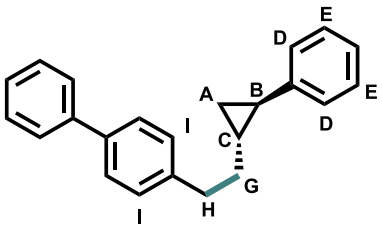

96

***trans*-4-(2-phenylcyclopropyl)ethyl)-1,1'-biphenyl (96) and 4-(2-phenylpent-4-en-1-yl)-1,1'-biphenyl (97):** In the glovebox, a 100 ml bomb with a stir bar was charged sequentially with *trans*-1-([1,1'biphenyl]-4-yl)-*N*-((2-phenylcyclopropyl)methyl)methanamine (590.1 mg, 1.89 mmol, 1 equiv), 20 ml THF and the anomeric amide (894 mg, 2.26 mmol,1.2 equiv). The bomb was sealed, removed from the glovebox and heated at 40 ^{o}C while stirring for 18 hours. The reaction was cooled to room temperature and the solvent was removed *in vacuo*. The crude mixture was purified by silica gel chromatography using the eluent 49:1 hexanes: diethyl ether. The two nitrogen deletion products are isolated from chromatography as a mixture of inseparable isomers. **^{1}H NMR** (400 MHz, $CDCl_3$): δ 7.61 – 7.55 (m, 4 H), 7.52 – 7.48 (m, 2 H), 7.46 – 7.38 (m, 6 H), 7.35 – 7.29 (m, 3 H), 7.25 – 7.22 (m, 4 H, H_I, H_E), 7.21 – 7.17 (m, 2 H), 7.16 – 7.12 (m, 3 H), 7.11 – 7.06 (m, 2 H, H_P or H_J), 7.04 – 6.99 (m, 2 H, H_D), 5.73 – 5.63 (m, 1 H, H_N), 5.06 – 4.92 (m, 2 H, H_O), 3.02 – 2.91 (m, 3 H, H_L and H_K), 2.80 (t, J = 7.5, 2 H, H_H), 2.50 – 2.39 (m, 2 H, H_M), 1.78 – 1.72 (m, 2 H, H_G), 1.67 – 1.60 (m, 1 H, H_B), 1.13 – 1.06 (m, 1H, H_C), 0.94 – 0.87 (m, 1H, H_A), 0.83 – 0.78 (m, 1 H, H_A). **^{13}C{^{1}H} NMR** (101 MHz, $CDCl_3$): δ 141.4, 141.2, 139.8, 138.7, 136.7 (C_N), 129.6, 128.9, 128.7, 128.7, 128.7, 128.2, 128.2, 127.9, 127.0, 127.0, 126.9, 126.2, 125.6, 125.2, 136.8, 116.4 (C_O), 47.7 (C_L or C_K), 42.4 (C_L or C_K), 39.9 (C_M), 36.4 (C_G), 35.4 (C_H), 30.9, 23.5 (C_C), 23.4 (C_B), 16.18 (C_A) **HR-MS** (EI) calculated 298.1722 for $C_{23}H_{22}$, found both 298.1731 and 298.1725 in the mixture of isomers. Maintenance of the *trans* geometry assigned by comparison to a related example.[46]

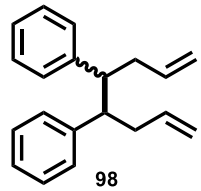

Octa-1,7-diene-4,5-diyldibenzene (98): A small portion of the ring opened cyclopropyl radical from *trans*-1-([1,1'biphenyl]-4-yl)-*N*-((2-phenylcyclopropyl)methyl)methanamine diffuses from the solvent cage to from the dimerized product octa-1,7-diene-4,5-diyldibenzene in a mixture of diastereomers. This compound was not produced in appreciable quantities to get an NMR yield from the NMR scale experiment, but in the preparative scale reaction it was detected in one of the column fractions and isolated. **^{1}H NMR** (400 MHz, $CDCl_3$): δ 7.34 – 7.29 (m, 10 H, 2 dias.), 7.22 – 7.09 (m, 10 H, 2 dias.), 5.72 – 5.56 (m, 1H), 5.47 – 5.36 (m, 1 H), 5.01 – 4.89 (m, 2H), 4.74 – 4.68 (m, 2H), 3.05 – 2.97 (m, 2H, 2 diast.), 2.85 – 2.80 (m, 2H, 2 diastereomers), 2.69 – 2.51 (m, 2H, 2 diast.), 2.40 – 2.30 (m, 2H, 2 diast.), 2.16 – 2.10 (m, 2 H, 2 diast.). Spectroscopic data are in agreement with those in the literature.[47]

2.4.6. Synthesis of Secondary Amines.

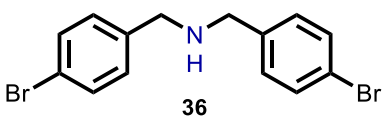

bis(4-bromobenzyl)amine (36): To a solution of 4-bromobenzylamine (932 mg, 5 mmol 1equiv.) in absolute EtOH (0.2 M) in a round-bottom flask was added 4-bromobenzaldehyde (925 mg, 5 mmol, 1 equiv.). The solution was stirred for 2 h at 70 °C and cooled to room temperature. $NaBH_4$ (15 mmol, 3 equiv.) was added and the reaction was stirred at room temperature. Upon completion, the mixture was concentrated *in vacuo* and diluted with EtOAc. 1 M NaOH was added and the aqueous was extracted twice with EtOAc. The combined extracts were washed with brine, dried over Na_2SO_4, and concentrated *in vacuo* to afford the desired product as a white solid (1.402 g, 3.95 mmol, 79%). **^{1}H NMR** (400 MHz, $CDCl_3$) δ 7.45 (d, J = 8.4 Hz, 4H), 7.21 (d, J = 8.3 Hz, 4H), 3.74 (s, 4H), 1.67 (s, 1H). Spectroscopic data were in agreement with the literature.[48]

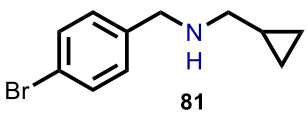

81

4-bromo-*N*-(cyclopropylmethyl)-benzenemethanamine (81): A round bottom flask fitted with septa and stir bar was sequentially charged with cyclopropylmethanamine (592 mg, 8.32 mmol,1.8 equiv), 10 ml methanol and *p*-bromobenzaldehyde (823 mg, 4.45 mmol,1 equiv) while stirring under N_2 atmosphere. $NaBH(OAc)_3$ (924 mg, 4.36 mmol, 1 equiv) was added in a single portion and the reaction was stirred overnight at room temperature. The reaction was monitored by TLC and upon completion was quenched with 1 M NaOH and extracted three times with DCM. The combined extracts were dried over $MgSO_4$, and concentrated *in vacuo*. The crude residue was purified *via* silica gel chromatography with the eluent 19:1 DCM: methanol. The product was isolated in 59% yield following chromatography. **^{1}H NMR** (400 MHz, $CDCl_3$): δ 7.44 (d, J = 8.4 Hz, 2 H), 7.21 (d, J= 8.4 Hz, 2 H), 3.77 (s, 2 H), 2.47 (d, J = 6.7 Hz, 2 H), 1.55 (br s, 1H), 0.97 (m, 1 H), 0.48 (m, 2H), 0.095 (m, 2 H). **^{13}C{^{1}H} NMR** (101 MHz, $CDCl_3$): δ 139.5, 131.4, 129.8, 120.6, 54.4, 53.1, 11.2, 3.4. **HR-MS** (EI) calculated 160.1126 for $[M-Br]^+$ found 160.1126.

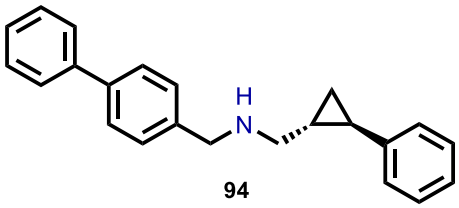

94

***trans*-1-([1,1'biphenyl]-4-yl)-N-((2-phenylcyclopropyl)methyl)methanamine (94):** *trans*-2-phenyl-cyclopropanecarboxaldehyde was prepared from *trans*-2-phenyl-cyclopropanecarboxylic acid according to the literature procedure.[49] A round bottom flask fitted with septa and stir bar was sequentially charged with 4-phenylbenzylamine (105 mg, 0.575 mmol,1.2 equiv), 5 ml methanol and *trans*-2-phenyl-cyclopropanecarboxaldehyde (70 mg, 0.479 mmol,1 equiv) while stirring under N_2 atmosphere. The reaction was refluxed for 4 hours and then cooled to room temperature. $NaBH(OAc)_3$ (406 mg, 1.916 mmol, 4 equiv.) was added in a single portion and the reaction was stirred at room temperature overnight. The reaction was monitored by TLC and upon completion

the reaction was quenched with water, diluted to 50 ml with ether and acidified with 1.5 equivalents of 4 M HCl in dioxane solution. The organic layer was extracted five times using 15 ml water and the combined aqueous layers were basified with 1 M NaOH solution. The water layer was extracted six times using 20 ml ether. The combined organic layers were dried with magnesium sulfate, filtered and concentrated *in vacuo*. The residue was purified by *via* silica gel chromatography using the eluent 19:1 DCM:methanol. The product was isolated in 33% yield. **^{1}H NMR** (400 MHz, $CDCl_3$): δ 7.60 – 7.55 (m 4 H), 7.46 – 7.39 (m, 4 H), 7.36 (t, J = 7.7 Hz, t), 7.27 – 7.23 (m, 2 H), 7.14 (t, J = 7.1 Hz, 1 H), 7.07 (d, J = 7.8 Hz, 2 H), 3.89 (s, 2H), 2.76 – 2.67 (m, 2 H), 1.76 – 1.71 (m, 1 H), 1.67 (br s, 1 H), 1.42 – 1.35 (m, 1 H), 0.97 – 0.92 (m, 1 H), 0.88 – 0.84 (m, 1 H). **^{13}C{^{1}H} NMR** (101 MHz, $CDCl_3$): δ 143.0, 141.0, 140.0, 128.8, 128.6, 128.31, 127.2, 127.1, 125.8, 125.5, 53.6, 53.3, 23.4, 22.2, 14.9. **HR-MS** (ESI) calculated 313.1830 for $C_{23}H_{23}N$ found 313.1815.

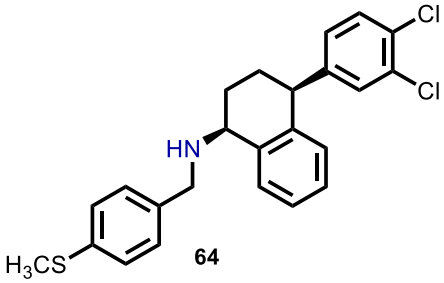

64

(1*S*,4*S*)-4-(3,4-dichlorophenyl)-*N*-(4-(methylthio)benzyl)-1,2,3,4-tetrahydronaphthalen-1-amine (64): (1*S*,4*S*)-4-(3,4-dichlorophenyl)-1,2,3,4-tetrahydronaphthalen-1-amine was prepared according to the literature.[50] To a round bottom flask equipped with a stirbar was added (1*S*,4*S*)-4-(3,4-dichlorophenyl)-1,2,3,4-tetrahydronaphthalen-1-amine (167 mg, 0.572 mmol, 1 equiv.), ethanol, several drops of acetic acid and 4-(methylthio)benzaldehyde (104 mg, 0.685 mmol, 1.2 equiv.). The flask was stirred at room temperature for 12 hours. The flask was cooled to zero degrees and sodium borohydride (86.4 mg, 2.28 mmol, 3.3 equiv.) were added to the flask in a single portion. The flask was stirred at room temperature for 3 hours and then the reaction was quenched by addition of 1 M NaOH solution. The product was extracted three times with DCM. The combined extracts were dried

over $MgSO_4$ and concentrated *in vacuo* to afford the title compound as a clear oil (114 mg, 0.266 mmol, 47% yield). **^{1}H NMR** (400 MHz, $CDCl_3$): δ 7.36 – 7.31 (m, 4 H), 7.28 – 7.24 (m, 3H), 7.19 (t, J = 7.6 Hz, 1H), 7.10 (td, J = 7.6 Hz, 1.1 Hz, 1H), 6.99 (dd, J = 8.2 Hz, 2.0 Hz), 4.20 – 3.96 (m, 1H), 3.96 – 3.90 (m, 1H), 3.87 – 3.80 (m, 2H), 2.49 (s, 3H), 2.21 – 2.10 (m, 1H), 2.06 – 1.95 (m, 2H), 1.90 – 1.79 (m, 1H), 1.47 (br. s, 1H). **^{13}C{^{1}H} NMR** (101 MHz, $CDCl_3$): δ 147.7, 139.8, 138.8, 137.9, 136.8, 132.3, 130.8, 130.4, 130.1, 129.9, 129.2, 128.8, 128.3, 127.3, 127.0, 126.6, 54.7, 51.0, 45.3, 28.6, 26.3, 16.2. **HR-MS:** (ESI) calculated 427.0928 for $C_{24}H_{23}NCl_2S$ found 427.0951.

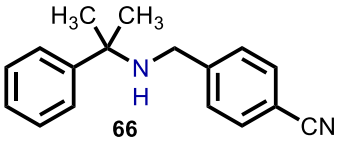

66

4-(((2-phenylpropan-2-yl)amino)methyl)benzonitrile (66): A 50 ml round bottom flask equipped with a stirrer was charged with 10 ml toluene, 4 Å molecular sieves, α,α-dimethylbenzylamine (100 mg, 0.740 mmol, 1 equiv.), and 4-cyanobenzaldehyde (97 mg, 0.740 mmol, 1 equiv.). A reflux condenser was affixed to the flask and the reaction was heated to 100 ^{o}C for 18 hours. The reaction was cooled to room temperature and the solvent was removed *in vacuo*. The crude residue was dissolved in 10 ml methanol and sodium borohydride (84 mg, 2.22 mmol, 3 equiv.) was added in a single portion. The reaction was monitored by TLC and upon completion, the volatiles were removed *in vacuo*. The crude residue was quenched by addition of 1 M NaOH solution and extracted three times into DCM. The organic fractions were washed with brine, dried over sodium sulfate and filtered. The filtrate was concentrated *in vacuo* to yield the title compound as a yellow solid (170.4 mg, 0.681 mmol, 92% yield). **^{1}H NMR** (400 MHz, $CDCl_3$): δ 7.59 (d, J = 8.4 Hz, 2H), 7.53 (d, J = 8.4 Hz, 2H), 7.45 (d, J = 8.6 Hz, 2H), 7.38 (t, J = 7.7 Hz, 2H), 7.26 (t, J = 7.6 Hz, 1H), 3.56 (s, 2H), 1.55 (s, 7H). **^{13}C{^{1}H} NMR** (101 MHz, $CDCl_3$): δ 147.3, 147.2, 132.1, 128.7,

128.4, 126.5, 125.9, 119.1, 110.4, 56.3, 47.3, 29.8. **HR-MS:** Calculated 250.1468 for $C_{17}H_{18}N_2$, found 250.1470.

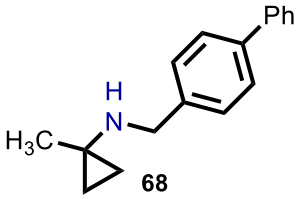

68

***N*-([1,1'-biphenyl]-4-ylmethyl)-1-methylcyclopropan-1-amine (68):** A 100 ml round bottom flask equipped with a stirrer was charged with 20 ml ethanol, (1-methylcyclopropyl)amine (250 mg, 2.32 mmol, 1 equiv.), 4-phenylbenzaldehyde (466 mg, 2.56 mmol, 1.1 equiv.) and sodium borohydride (263 mg, 6.96 mmol, 3 equiv.). The reaction was stirred at room temperature overnight. The volatiles were removed *in vacuo* and the reaction was quenched by addition of 1 M NaOH solution. The product was extracted three times with DCM and the organic layers were combined, washed with brine, dried over sodium sulfate and filtered. The volatiles were removed from the filtrate *in vacuo* and the crude material was recrystallized from diethyl ether to yield the title compound as a white crystalline solid (325 mg, 1.37 mmol, 60% yield). **^{1}H NMR** (400 MHz, $CDCl_3$): δ 7.63 (d, J = 7.6 Hz, 2H), 7.58 (d, J = 8.0 Hz, 2H), 7.45 (t, J = 7.6 Hz, 2H), 7.43 (d, J = 7.6 Hz, 2H), 7.37 (t, J = 7.1 Hz, 1H), 3.92 (s, 2H), 1.39 (s, 3H), 0.68 (m, 2H), 0.46 (m, 2H). **^{13}C{^{1}H} NMR** (101 MHz, $CDCl_3$): δ 141.1, 140.3, 140.0, 128.8, 128.6, 127.2, 127.1, 127.1, 50.1, 35.3, 22.3, 14.9. **HR-MS:** Calculated 237.1521 for $C_{17}H_{19}N$, found 237.1517.

2.4.7. Isolation of Aprepitant Insertion Product.

General procedure for nitrogen deletion of secondary amines: To a 1-dram screw cap vial equipped with a stir bar and PTFE/white silicone septum is added the amine. The anomeric amide (1.5 equiv) is added to a second vial and both vials are evacuated and backfilled with nitrogen twice. THF (degassed by sparging with N_2 for 30 minutes) is added to the second vial *via* syringe such that the concentration of anomeric amide is 0.3 M. This solution is then transferred *via* syringe

under N_2 to the amine-containing vial which is stirred at 45 °C for 12-16 hours. Upon cooling to room temperature, saturated $NaHCO_3$ (2 mL) is added and the reaction mixture is diluted with Et_2O (4 mL). The aqueous is extracted with Et_2O (4 mL) and the combined organic extracts are washed with brine (2 mL) and dried over Na_2SO_4. Solvent was concentrated under reduced pressure and the crude mixture adsorbed onto silica gel and purified by silica gel chromatography.

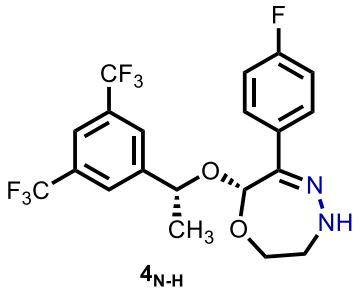

$\mathbf{4_{N\text{-}H}}$

(*R*)-7-((*R*)-1-(3,5-bis(trifluoromethyl)phenyl)ethoxy)-6-(4-fluorophenyl)-2,3,4,7-tetrahydro-1,4,5-oxadiazepine ($\mathbf{4_{N\text{-}H}}$): Synthesized according to the general procedure for nitrogen deletion from *cis*-(2*R*,3*S*)-2-({(1*R*)-1-[3,5-bis(trifluoromethyl)phenyl]ethyl}oxy)-3-(4-fluorophenyl)morpholine (50 mg, 0.1143 mmol). The title compound was obtained as an off-white solid in 10 % yield (5.3 mg, 0.012 mmol) after purification by preparative TLC using a silica plate pre-treated with triethylamine and an eluent of 4:1 hexanes: ethyl acetate ($\mathbf{R_f}$ = 0.18). **^{1}H NMR** (400 MHz, $CDCl_3$): δ 8.03 – 7.99 (m, 1H), 7.67 – 7.64 (m, 1H), 7.21 (s, 2H), 7.11 (t, *J* = 8.6 Hz, 1H), 7.01 (t, *J* = 8.8 Hz, 2 H), 4.90 (q, *J* = 6.6 Hz, 1H), 4.43 (m, 1H), 4.17 (td, *J* = 12.0 Hz, 3.3 Hz, 1 H), 4.04 – 4.01 (m, 1H), 3.64 (dd, *J* = 5.1 Hz, 2.8 Hz, 1H), 3.27 – 3.13 (m, 2H), 1.48 (d, *J* = 6.8 Hz, 3H). **^{19}F NMR** (376 MHz, $CDCl_3$): δ -62.9, -108.7. **^{13}C{^{1}H} NMR** (101 MHz, $CDCl_3$): δ 162.6, 160.2, 144.4, 131.1, 130.8, 130.5, 130.0, 129.9, 127.6, 127.5, 125.2, 120.5, 114.4, 114.2, 94.1, 71.5, 65.2, 60.8, 57.9, 57.5, 46.9, 45.1, 23.4. **HR-MS** (ESI) calculated 450.1182 for $C_{20}H_{17}F_7N_2O_2$, found 450.1178.

2.4.8. NMR Spectra of New Compounds.

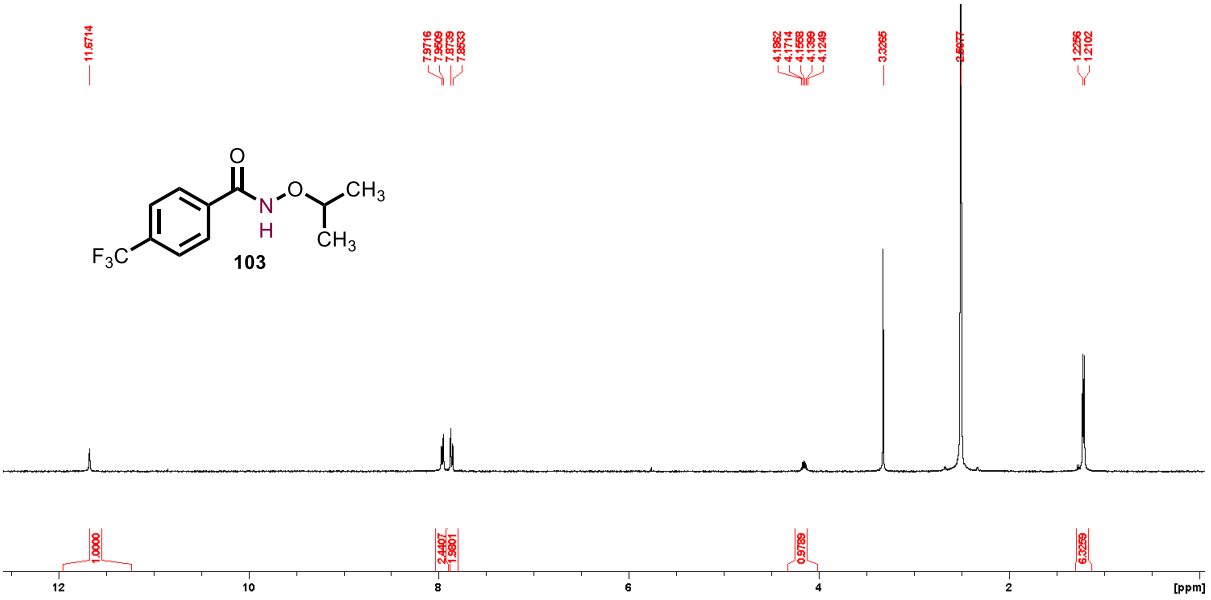

Figure 2.10. ^{1}H NMR spectrum of *N*-isopropyloxybenzamide (**103**) in DMSO-*d6*, 400 MHz.

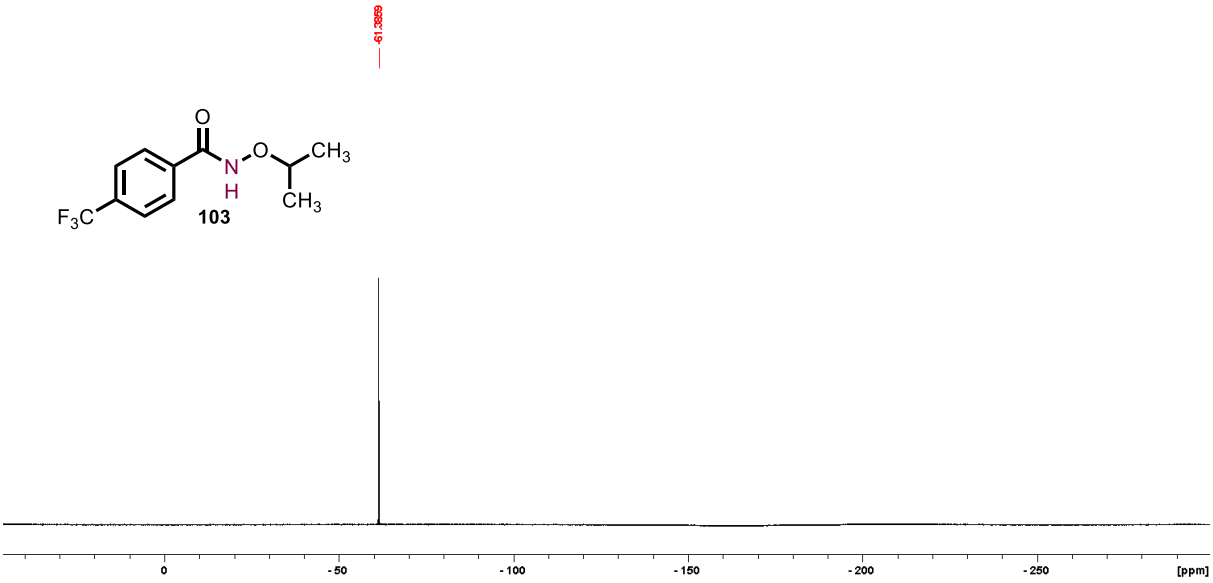

Figure 2.11. ^{19}F{^{1}H} NMR spectrum of *N*-isopropyloxybenzamide (**103**) in DMSO-*d6*, 376 MHz.

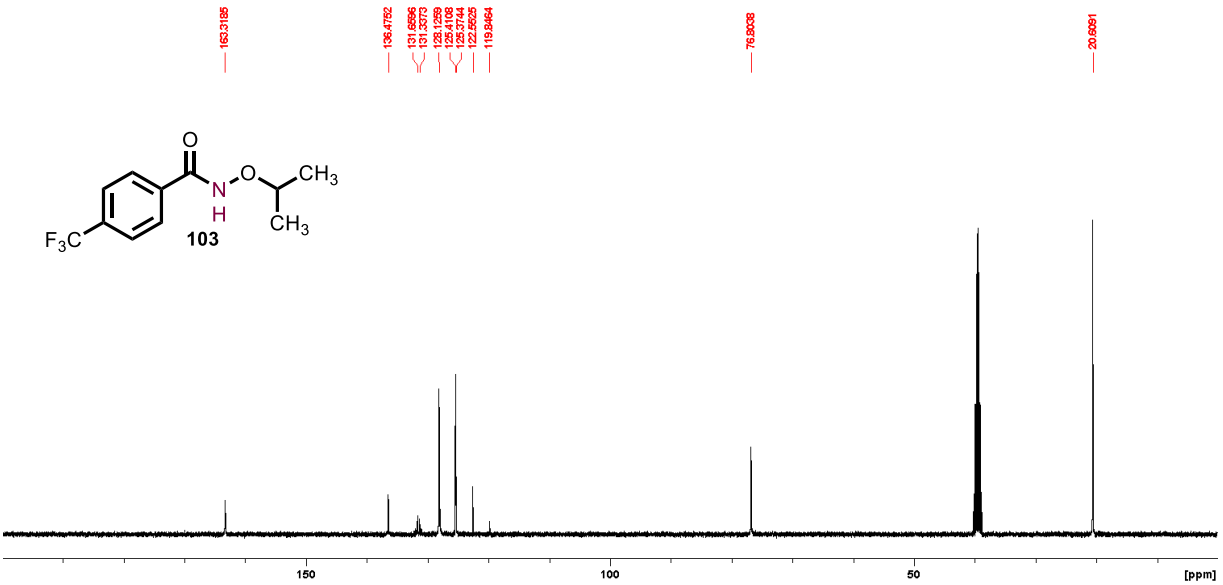

Figure 2.12. $^{13}C\{^{1}H\}$ NMR spectrum of *N*-isopropyloxybenzamide (**103**) in DMSO-*d6*, 101 MHz.

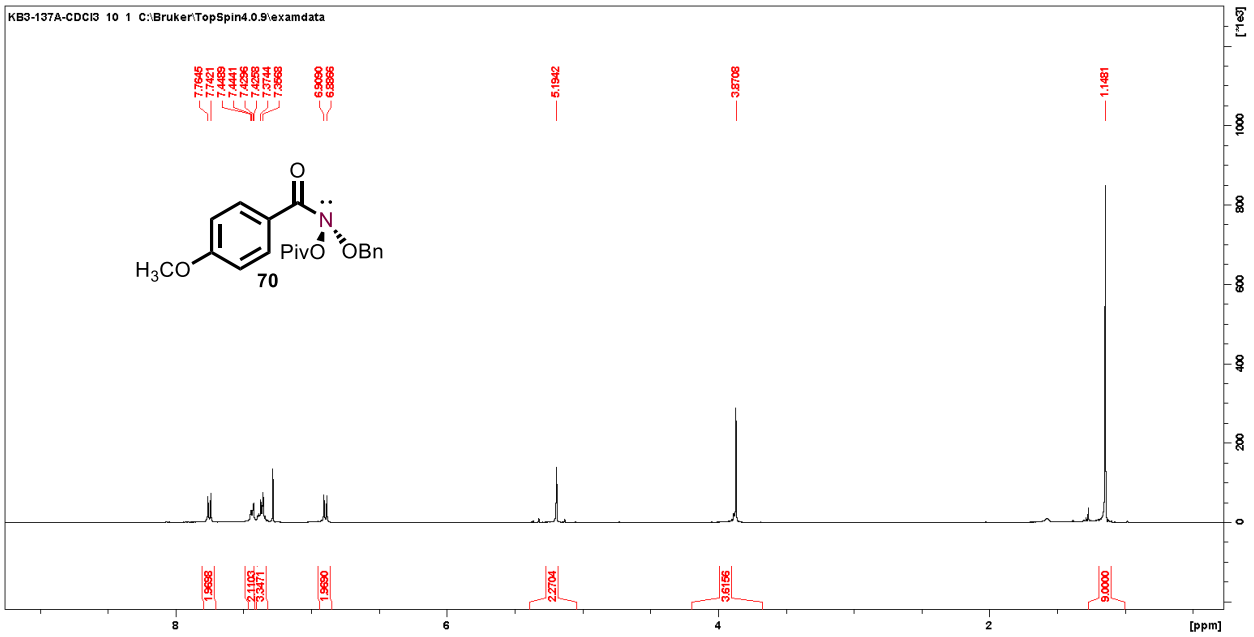

Figure 2.13. ^{1}H NMR spectrum of *N*-(benzyloxyl)-4-methoxy-*N*-(pivaloyloxy)benzamide (**70**) in $CDCl_3$, 400 MHz.

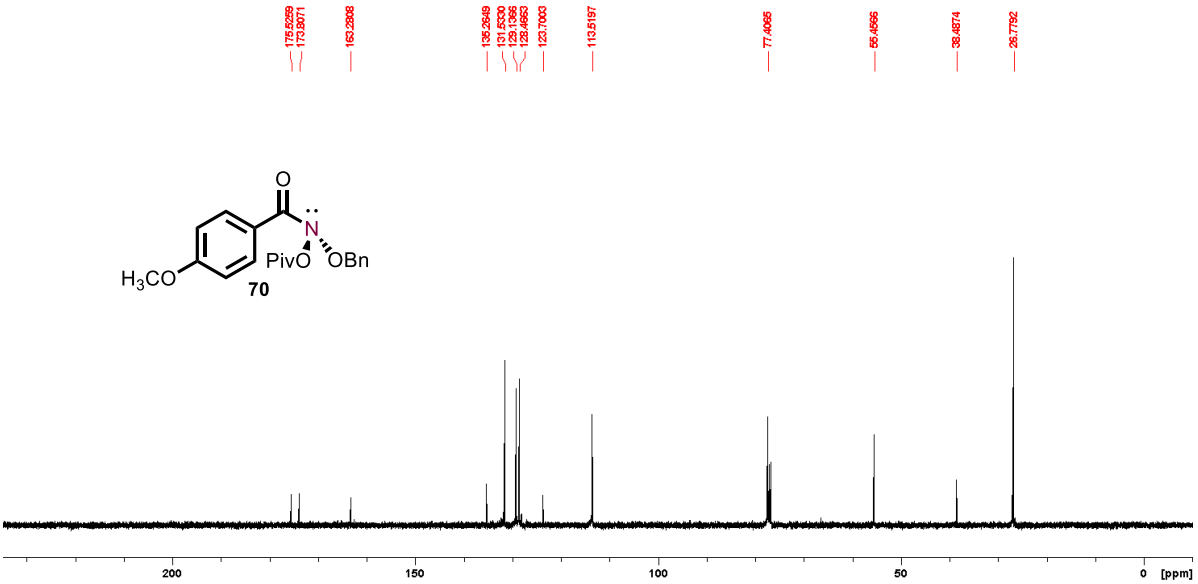

Figure 2.14. $^{13}C\{^{1}H\}$ NMR spectrum of *N*-(benzyloxyl)-4-methoxy-*N*-(pivaloyloxy)benzamide (**70**) in $CDCl_3$, 101 MHz.

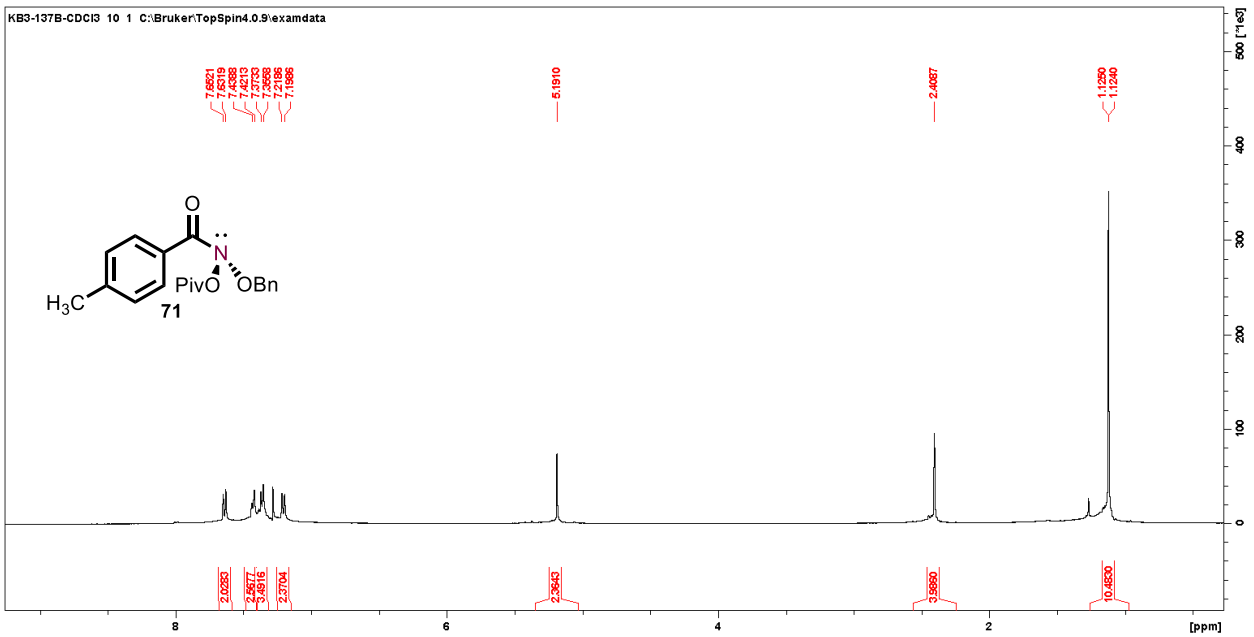

Figure 2.15. ^{1}H NMR spectrum of *N*-(benzyloxyl)-4-methyl-*N*-(pivaloyloxy)benzamide (**71**) in $CDCl_3$, 400 MHz.

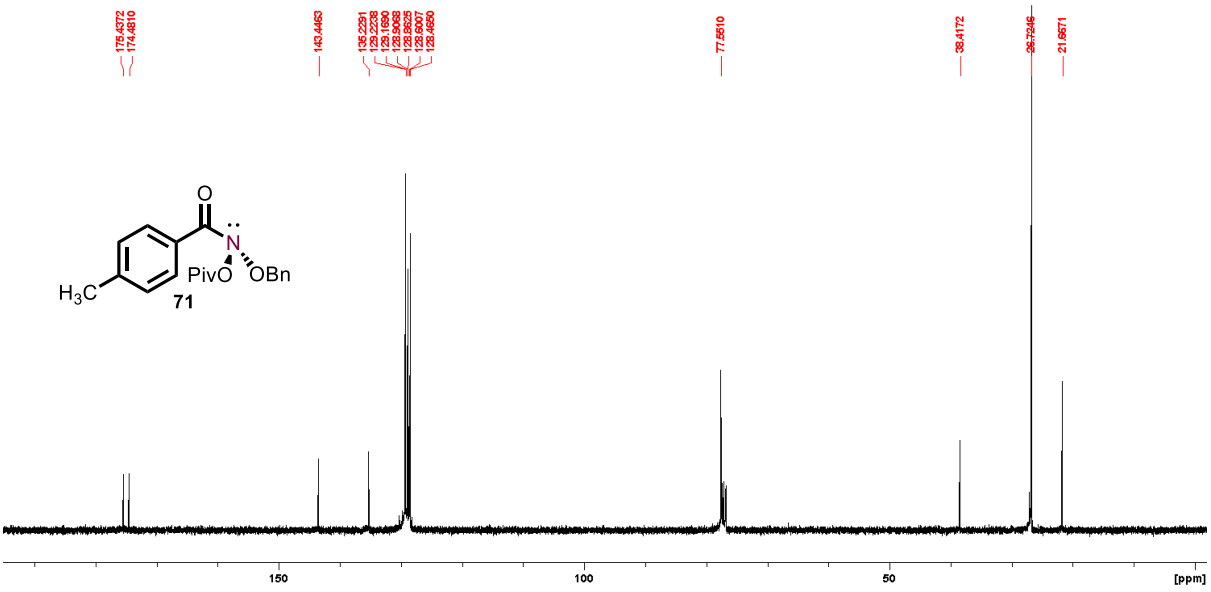

Figure 2.16. $^{13}C\{^{1}H\}$ NMR spectrum of *N*-(benzyloxyl)-4-methyl-*N*-(pivaloyloxy)benzamide (**71**) in $CDCl_3$, 101 MHz.

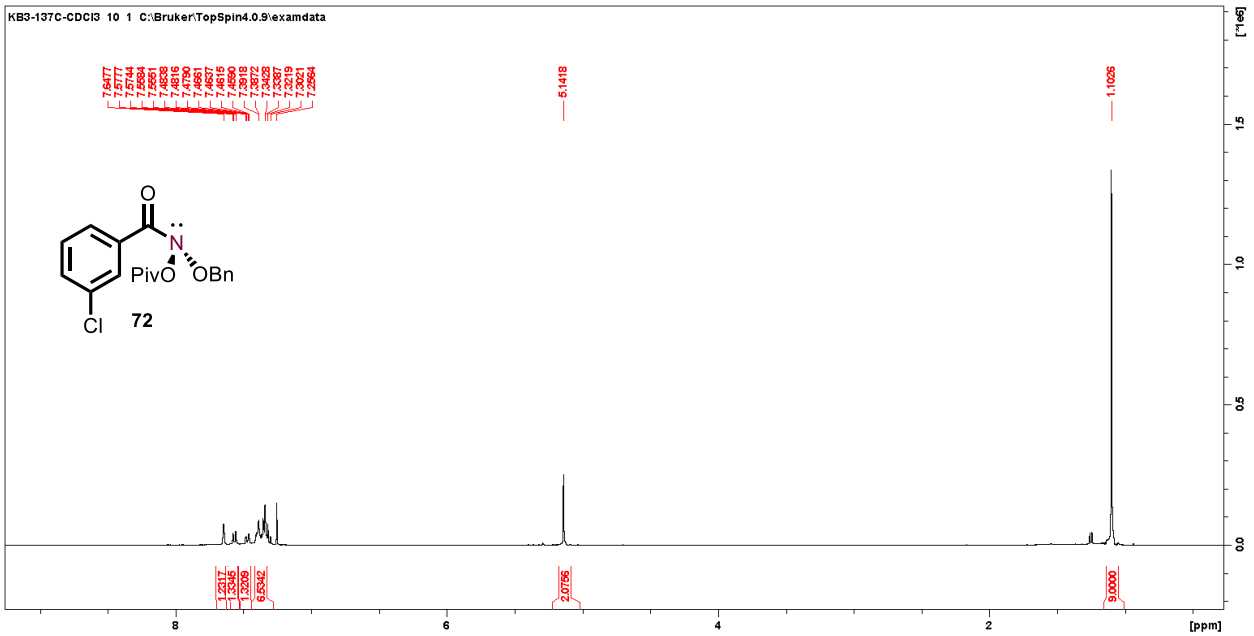

Figure 2.17. ^{1}H NMR spectrum of *N*-(benzyloxyl)-3-chloro-*N*-(pivaloyloxy)benzamide (**72**) in $CDCl_3$, 400 MHz.

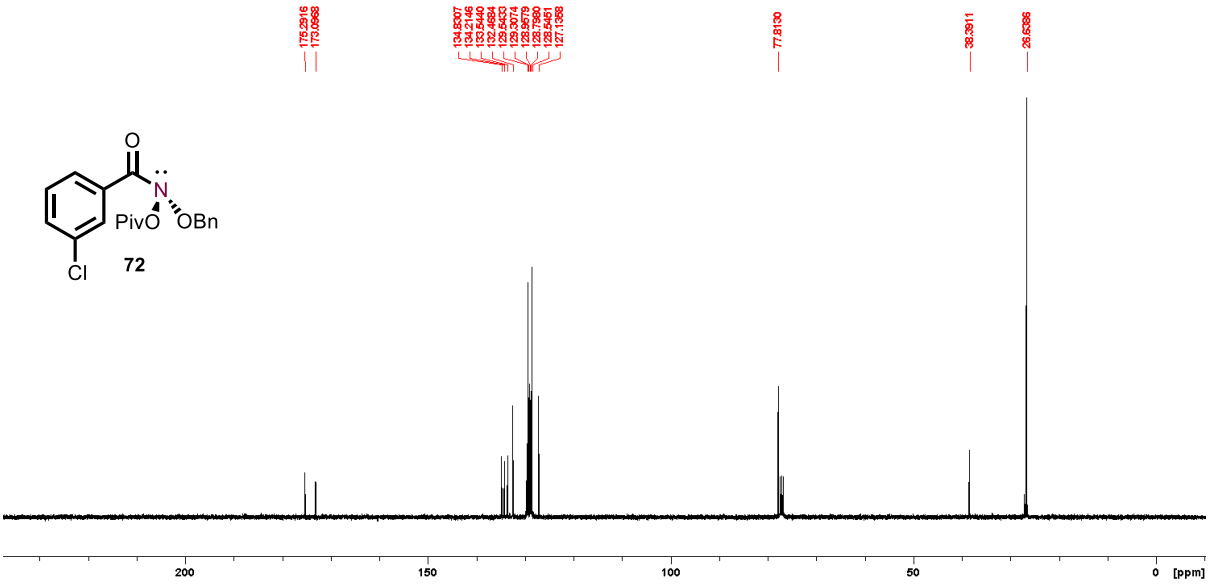

Figure 2.18. $^{13}C\{^{1}H\}$ NMR spectrum of *N*-(benzyloxyl)-3-chloro-*N*-(pivaloyloxy)benzamide (**72**) in $CDCl_3$, 101 MHz.

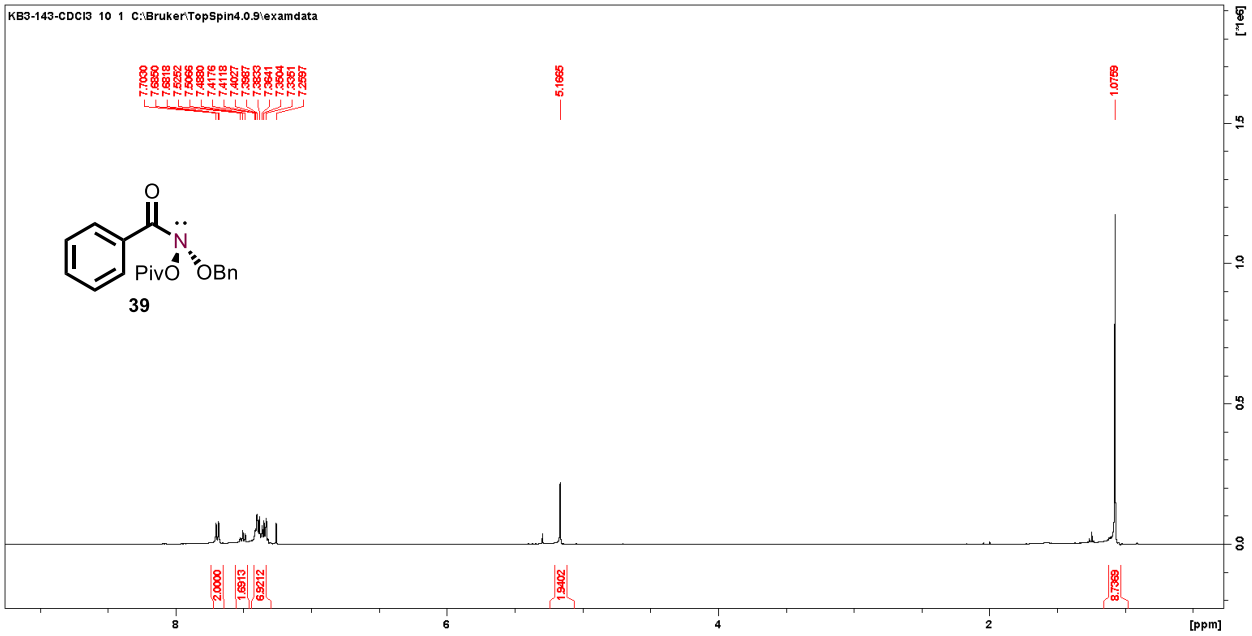

Figure 2.19. ^{1}H NMR spectrum of *N*-(benzyloxyl)-*N*-(pivaloyloxy)benzamide (**39**) in $CDCl_3$, 400 MHz.

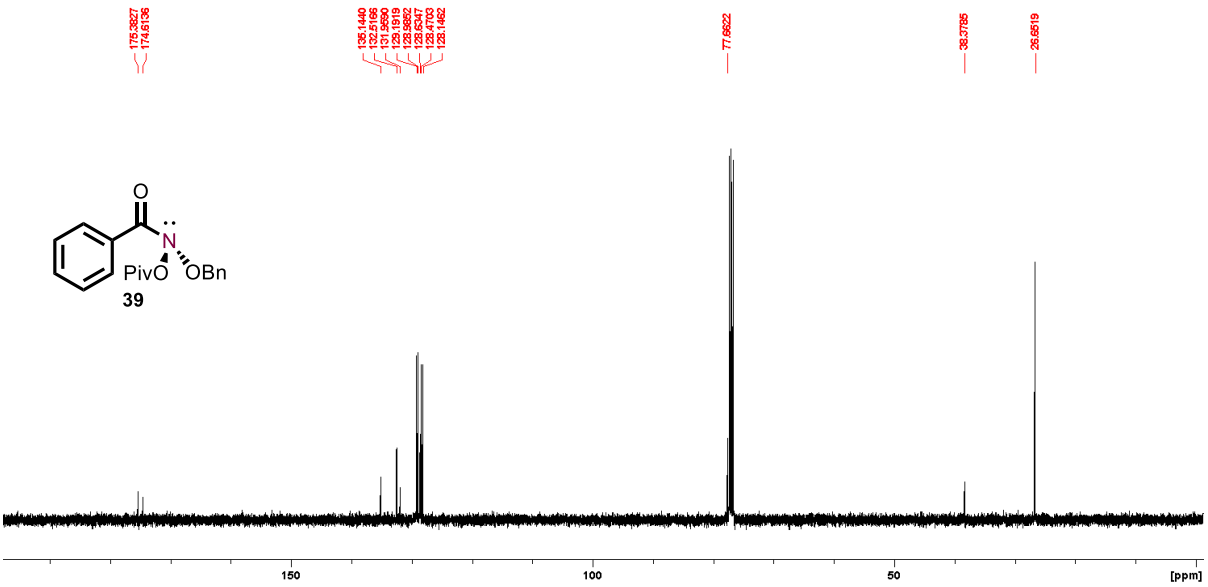

Figure 2.20. $^{13}C\{^{1}H\}$ NMR spectrum of *N*-(benzyloxyl)-*N*-(pivaloyloxy)benzamide (**39**) in $CDCl_3$, 101 MHz.

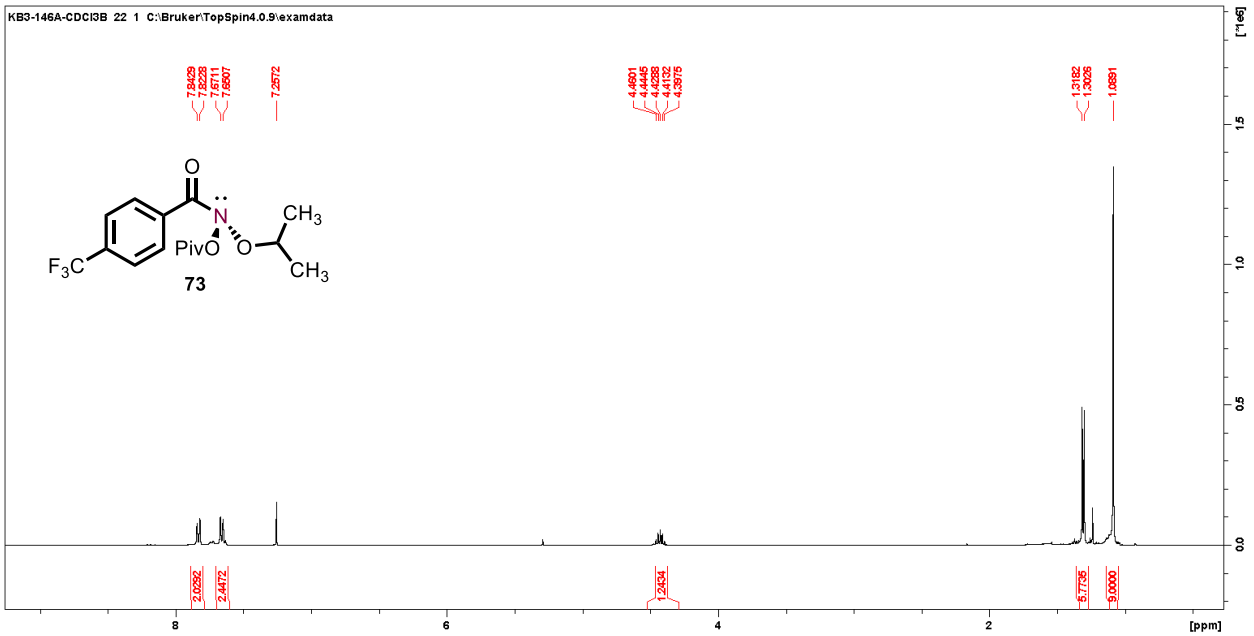

Figure 2.21. ^{1}H NMR spectrum of *N*-(isopropoxy)-*N*-(pivaloyloxy)-4-(trifluoromethyl)benzamide (**73**) in $CDCl_3$, 400 MHz.

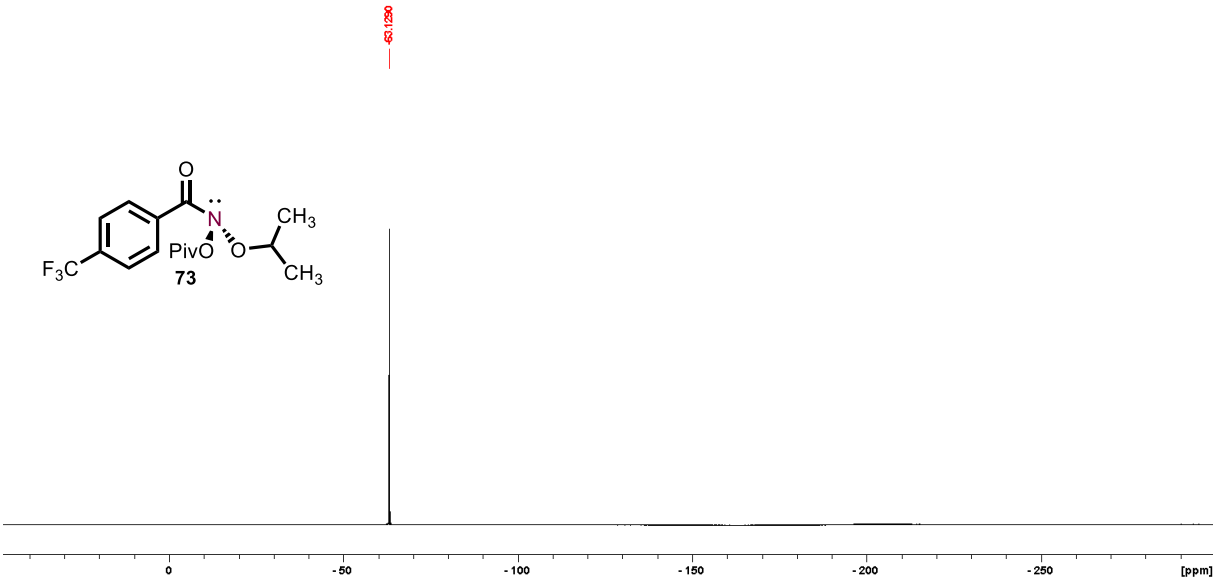

Figure 2.22. $^{19}F\{^{1}H\}$ NMR spectrum of *N*-(isopropoxy)-*N*-(pivaloyloxy)-4-(trifluoromethyl)benzamide (**73**) in $CDCl_3$, 376 MHz.

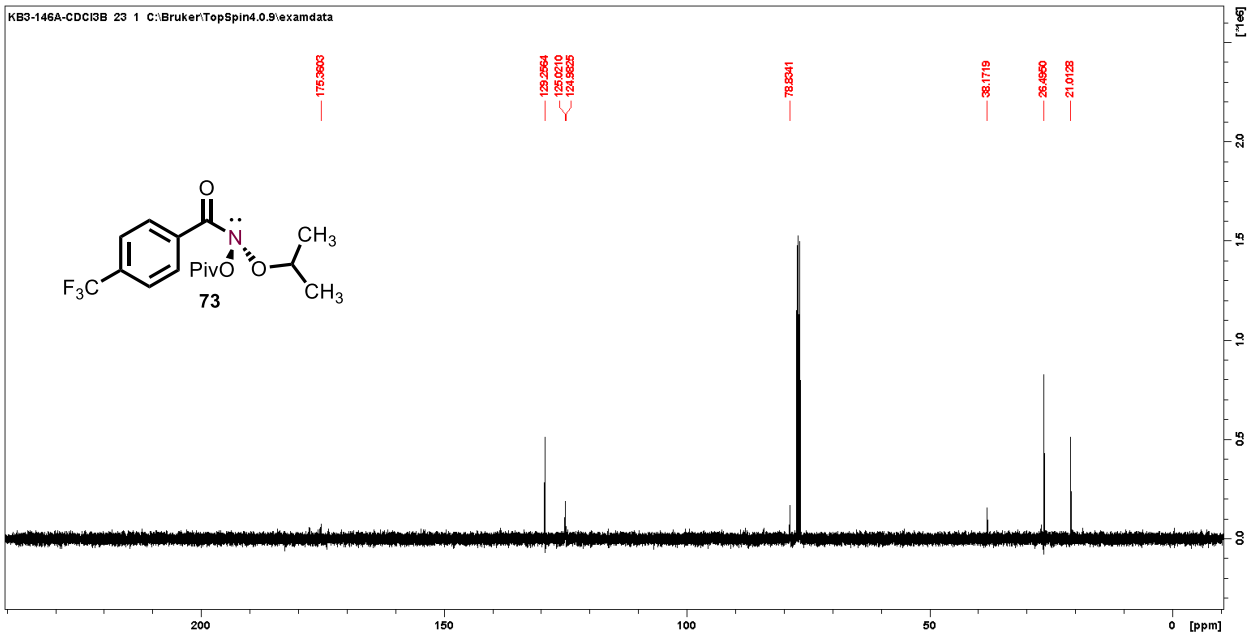

Figure 2.23. $^{13}C\{^{1}H\}$ NMR spectrum of *N*-(isopropoxy)-*N*-(pivaloyloxy)-4-(trifluoromethyl)benzamide (**73**) in $CDCl_3$, 101 MHz.

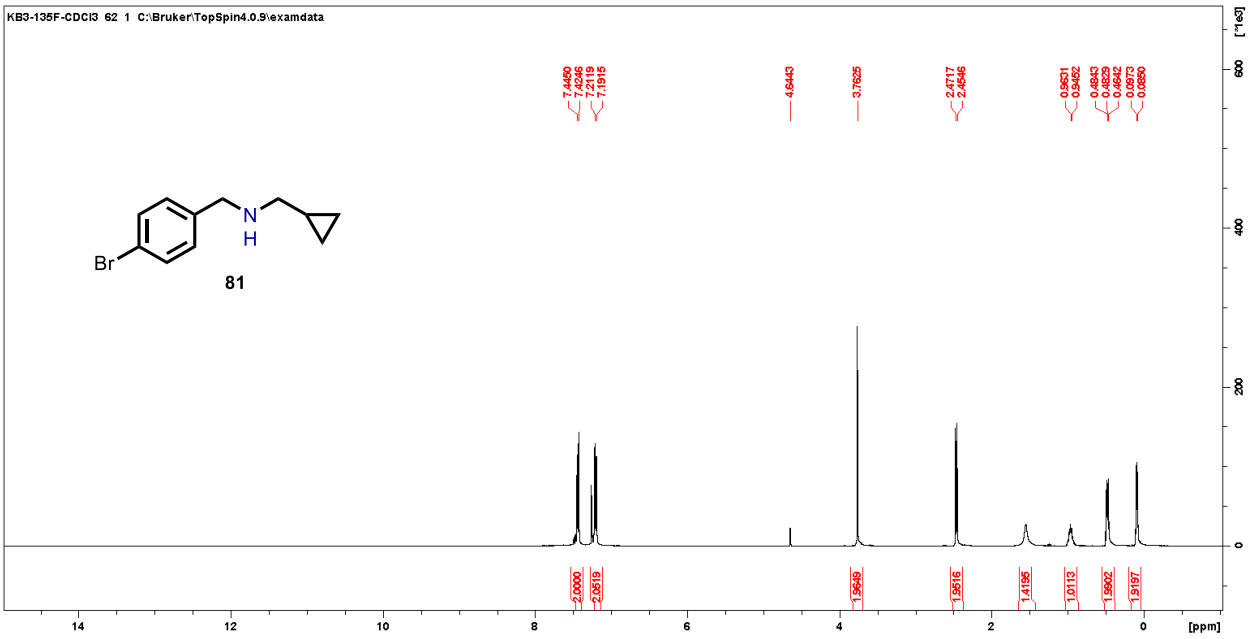

Figure 2.24. ^{1}H NMR spectrum of 4-bromo-*N*-(cyclopropylmethyl)-benzenemethanamine (**81**) in $CDCl_3$, 400 MHz.

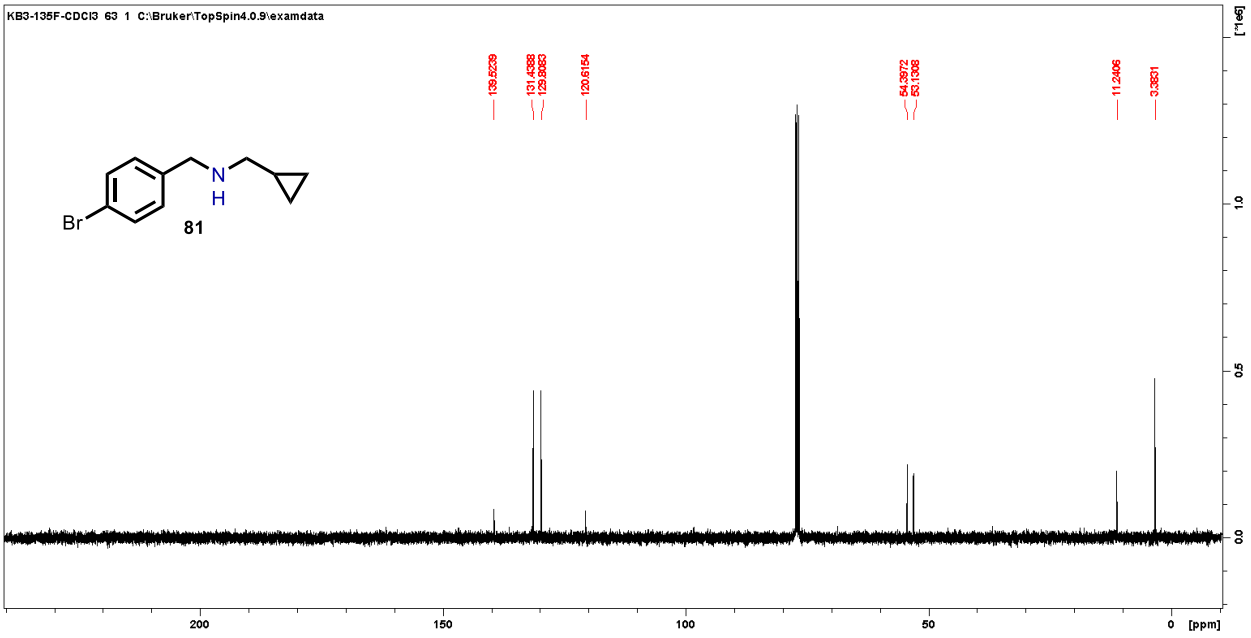

Figure 2.25. ^{13}C{^{1}H} NMR spectrum of 4-bromo-*N*-(cyclopropylmethyl)-benzenemethanamine (**81**) in $CDCl_3$, 101 MHz.

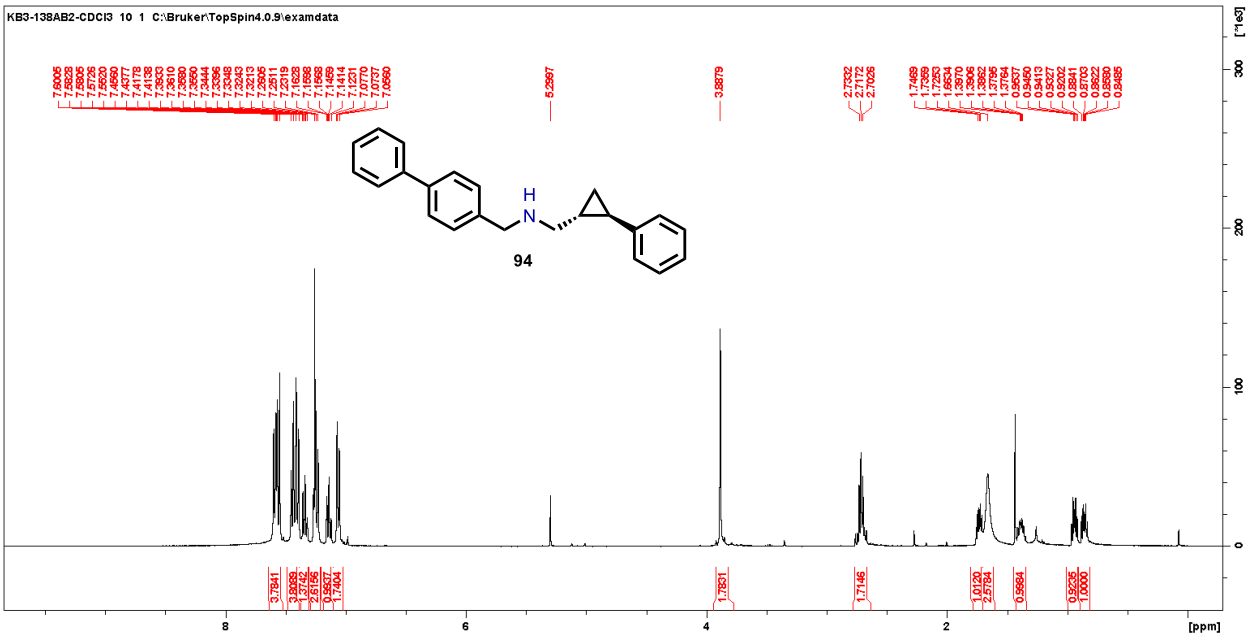

Figure 2.26. ^{1}H NMR spectrum of *trans*-1-([1,1'biphenyl]-4-yl)-*N*-((2-phenylcyclopropyl)methyl)methanamine (**94**) in $CDCl_3$, 400 MHz.

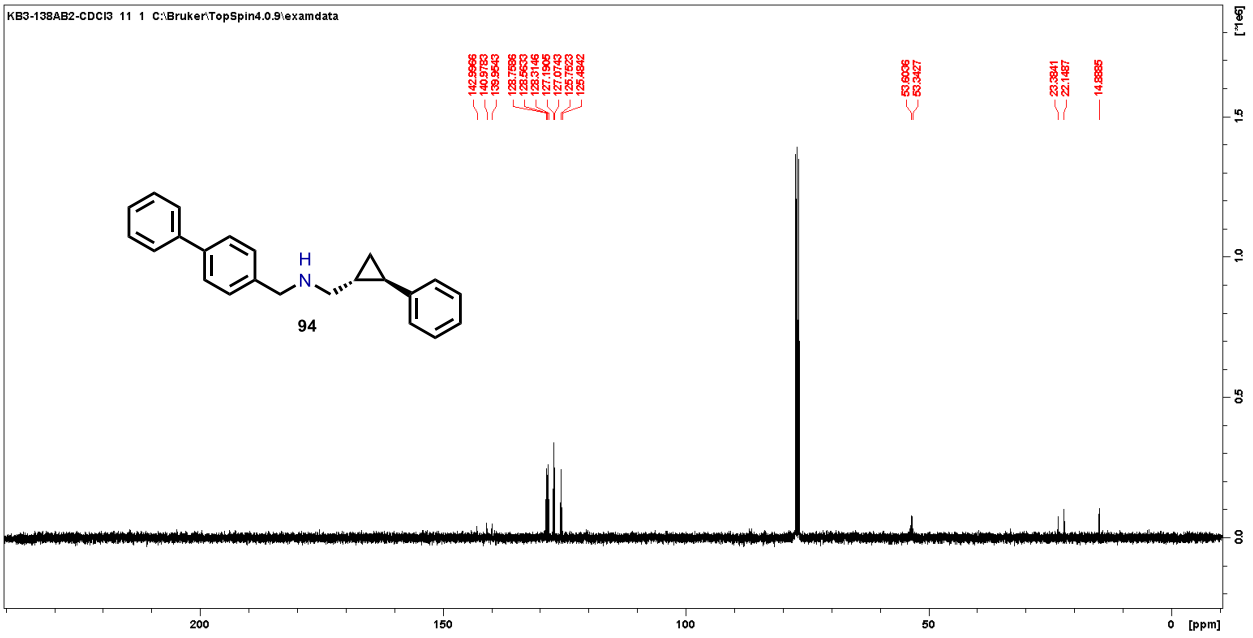

Figure 2.27. $^{13}C\{^{1}H\}$ NMR spectrum of *trans*-1-([1,1'biphenyl]-4-yl)-*N*-((2-phenylcyclopropyl)methyl)methanamine (**94**) in $CDCl_3$, 101 MHz.

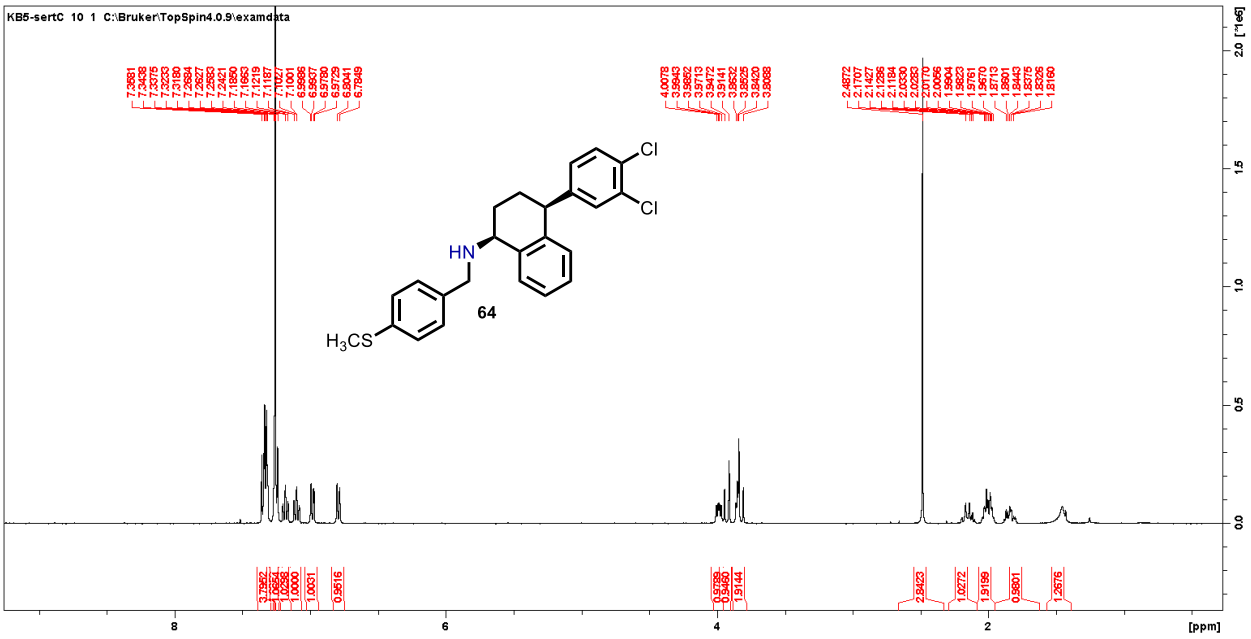

Figure 2.28. ^{1}H NMR spectrum of (1*S*,4*S*)-4-(3,4-dichlorophenyl)-*N*-(4-(methylthio)benzyl)-1,2,3,4-tetrahydronaphthalen-1-amine (**64**) in $CDCl_3$, 400 MHz.

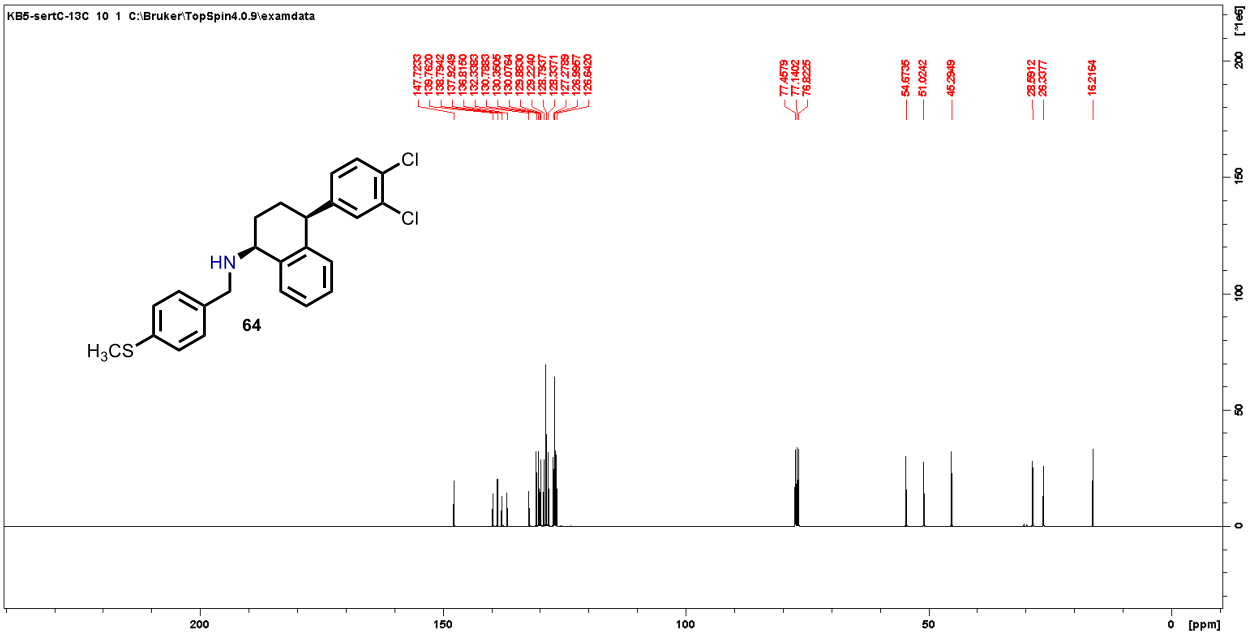

Figure 2.29. ^{13}C{^{1}H} NMR spectrum of (1*S*,4*S*)-4-(3,4-dichlorophenyl)-*N*-(4-(methylthio)benzyl)-1,2,3,4-tetrahydronaphthalen-1-amine (**64**) in $CDCl_3$, 101 MHz.

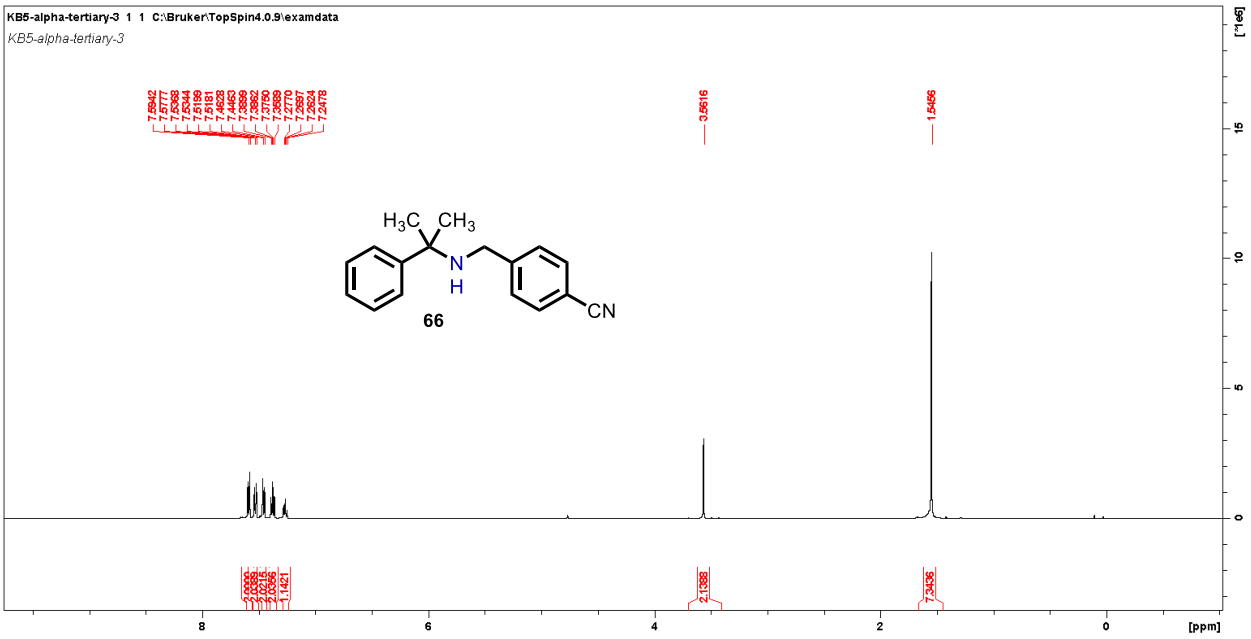

Figure 2.30. ^{1}H NMR spectrum of 4-(((2-phenylpropan-2-yl)amino)methyl)benzonitrile (**66**) in $CDCl_3$, 400 MHz.

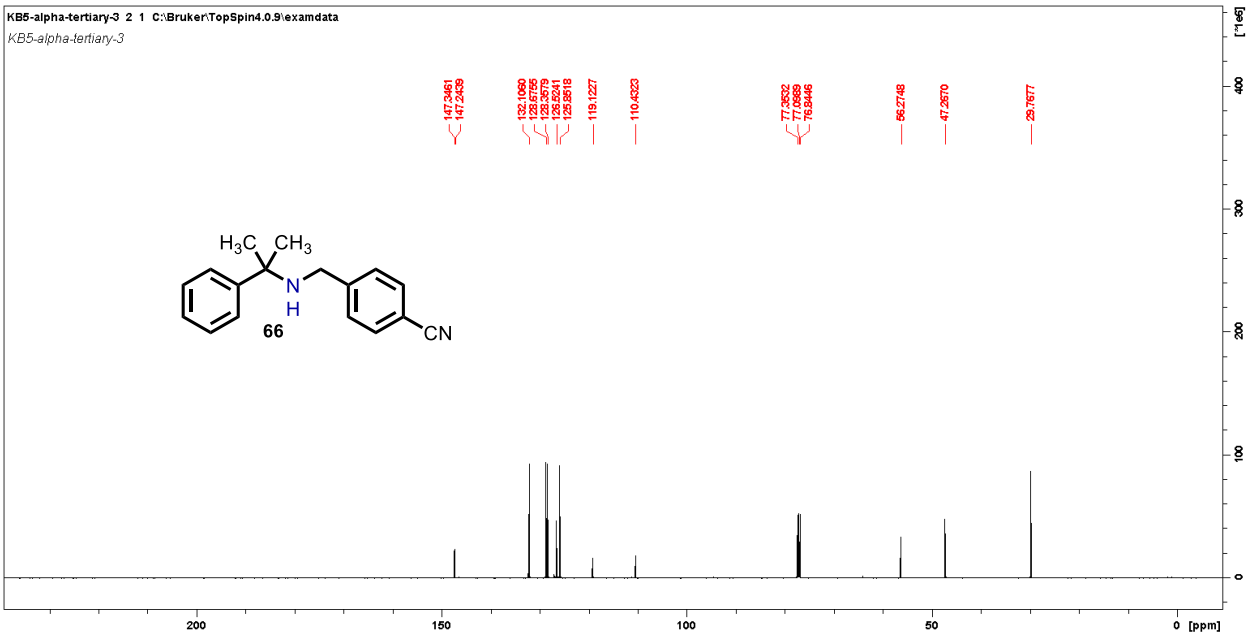

Figure 2.31. ^{13}C{^{1}H} NMR spectrum of 4-(((2-phenylpropan-2-yl)amino)methyl)benzonitrile (**66**) in $CDCl_3$, 101 MHz.

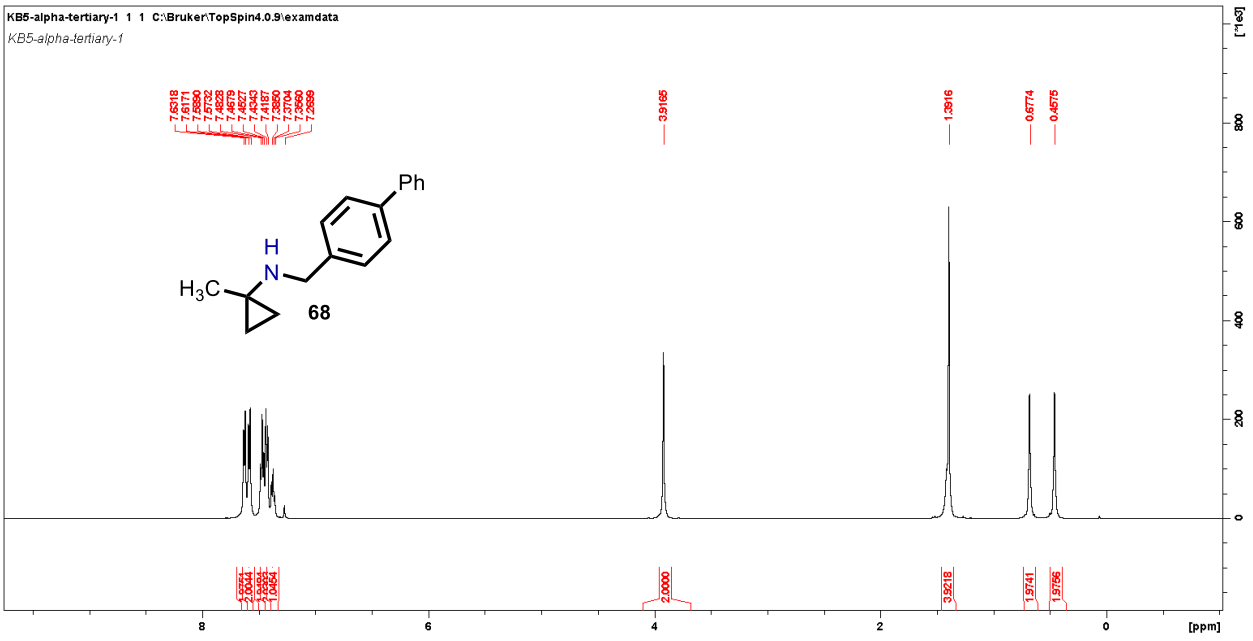

Figure 2.32. ^{1}H NMR spectrum of *N*-([1,1'-biphenyl]-4-ylmethyl)-1-methylcyclopropan-1-amine (**68**) in $CDCl_3$, 400 MHz.

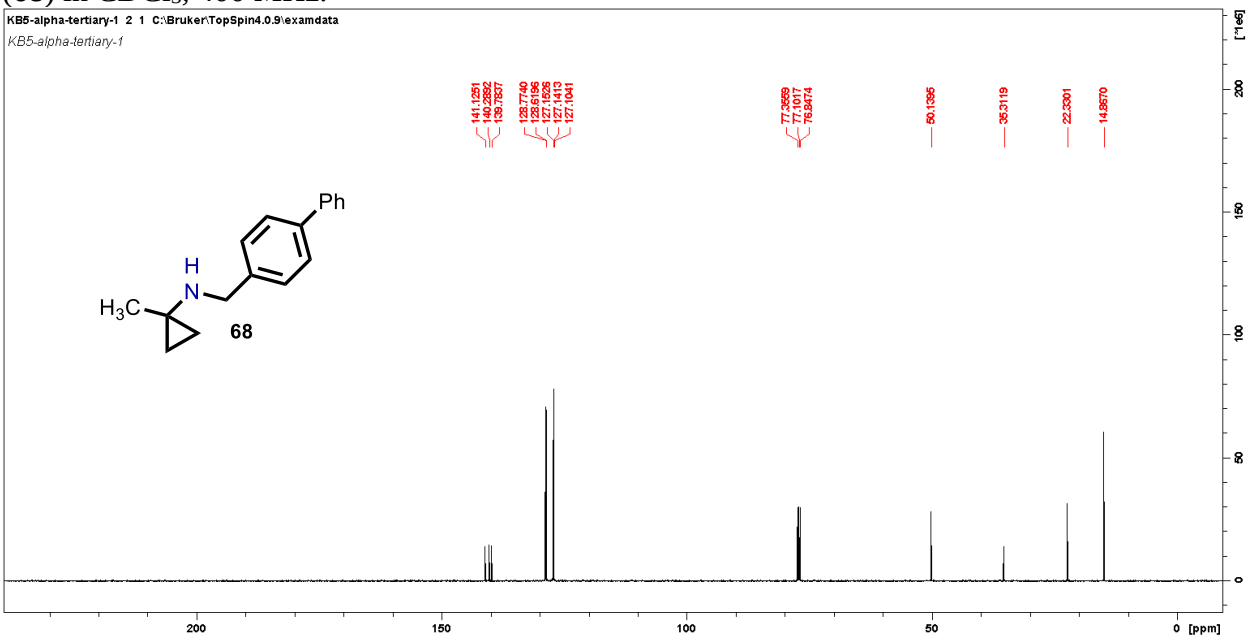

Figure 2.33. ^{13}C{^{1}H} NMR spectrum of *N*-([1,1'-biphenyl]-4-ylmethyl)-1-methylcyclopropan-1-amine (**68**) in $CDCl_3$, 101 MHz.

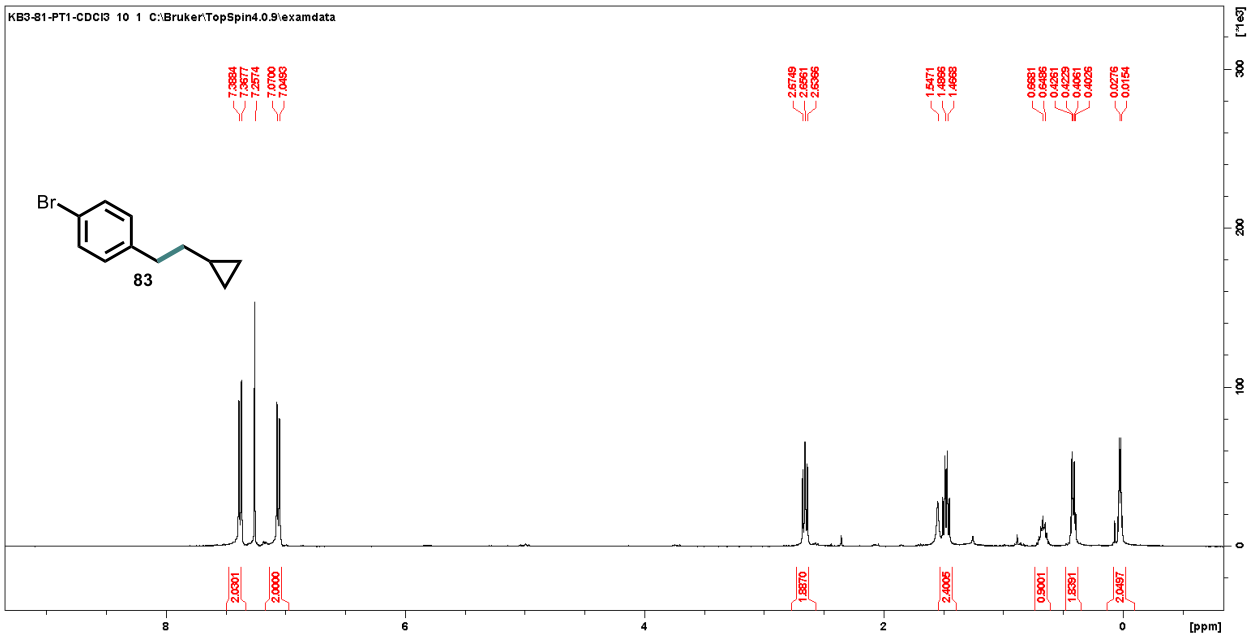

Figure 2.34. ^{1}H NMR spectrum of 1-bromo-4-(2-cyclopropylethyl)benzene (**83**) in $CDCl_3$, 400 MHz.

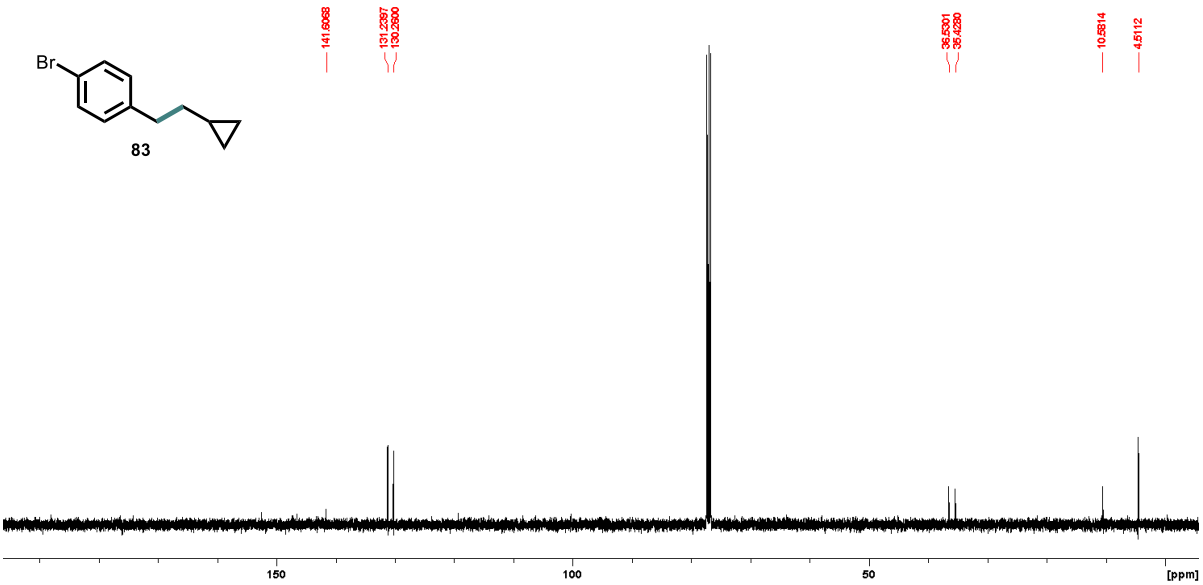

Figure 2.35. $^{13}C\{^{1}H\}$ NMR spectrum of 1-bromo-4-(2-cyclopropylethyl)benzene (**83**) in $CDCl_3$, 400 MHz.

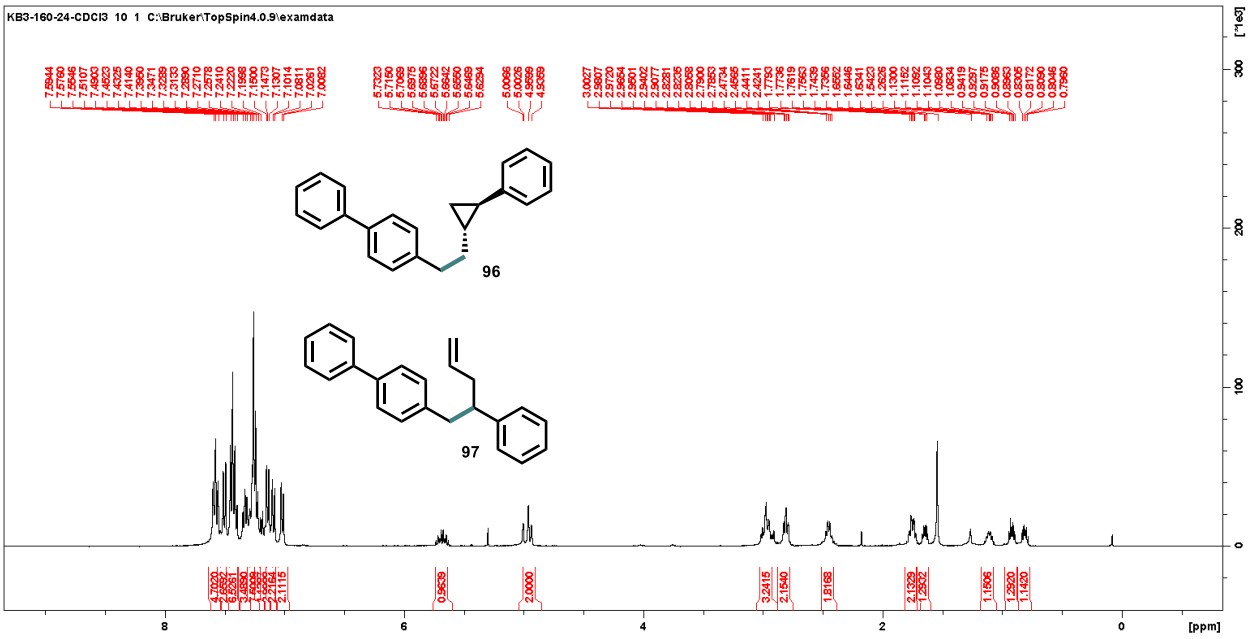

Figure 2.36. ^{1}H NMR spectrum of 4-(2-phenylpent-4-en-1-yl)-1,1'-biphenyl (**97**) and *trans*-4-(2-phenylcyclopropyl)ethyl)-1,1'-biphenyl (**96**) in $CDCl_3$, 400 MHz.

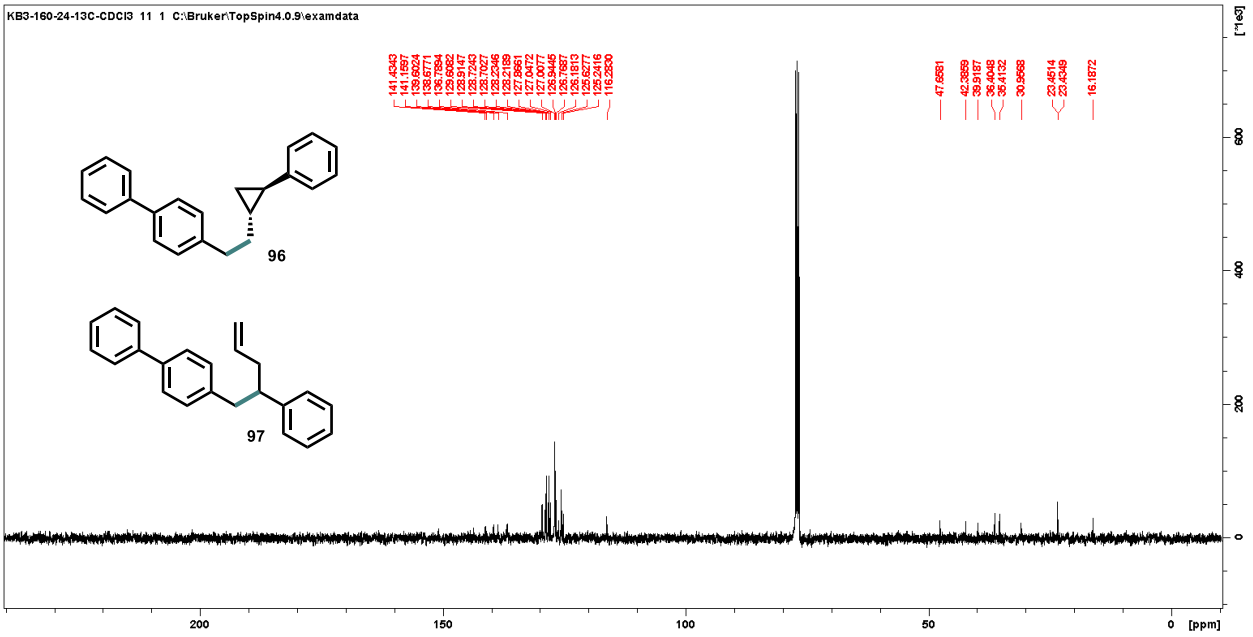

Figure 2.37. $^{13}C\{^{1}H\}$ NMR spectrum of 4-(2-phenylpent-4-en-1-yl)-1,1'-biphenyl (**97**) and *trans*-4-(2-phenylcyclopropyl)ethyl)-1,1'-biphenyl (**96**) in $CDCl_3$, 101 MHz.

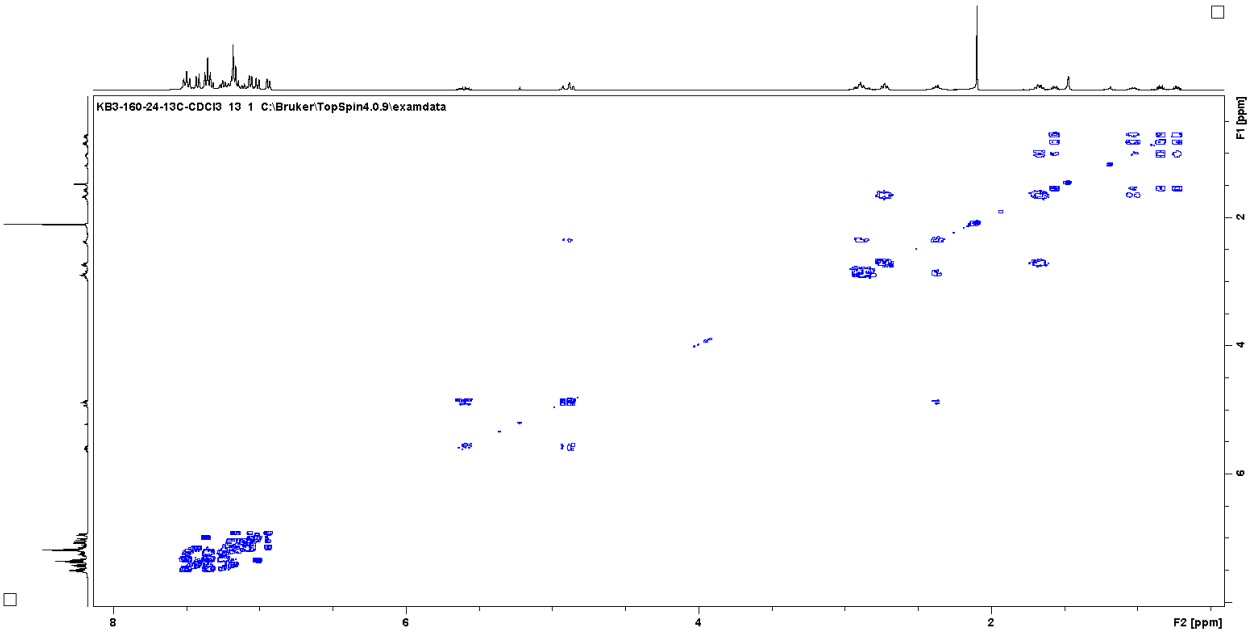

Figure 2.38. ^{1}H - ^{1}H COSY NMR spectrum of 4-(2-phenylpent-4-en-1-yl)-1,1'-biphenyl (**97**) and *trans*-4-(2-phenylcyclopropyl)ethyl)-1,1'-biphenyl (**96**) in $CDCl_3$.

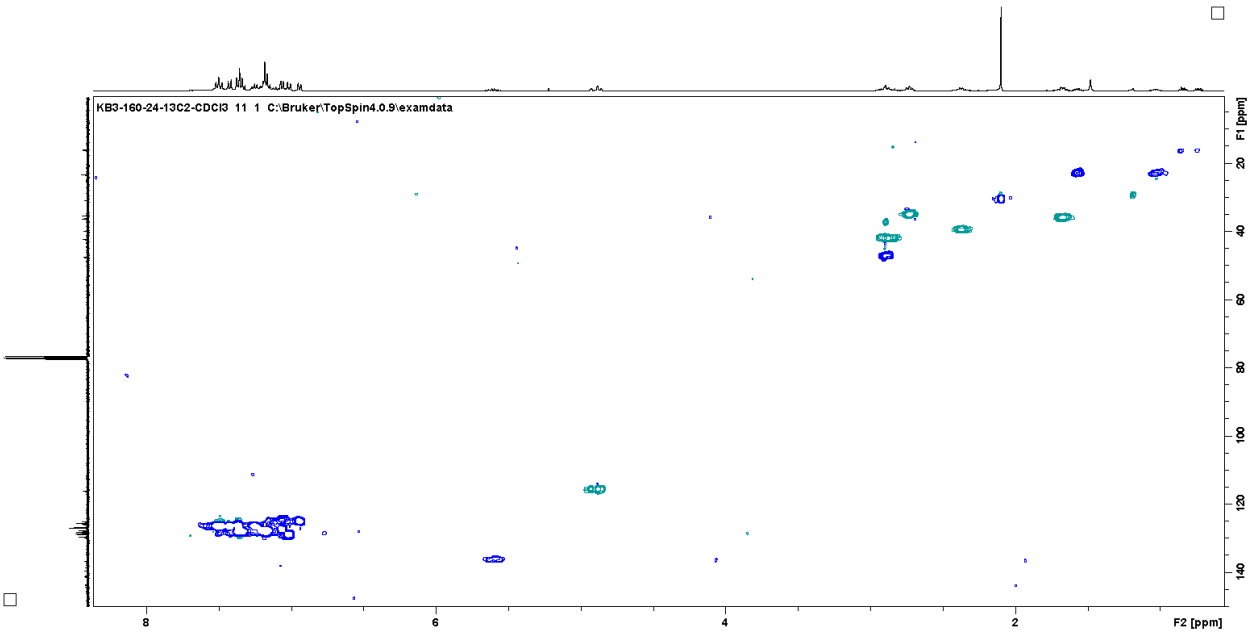

Figure 2.39. ^{1}H -^{13}C HSQC NMR spectrum of 4-(2-phenylpent-4-en-1-yl)-1,1'-biphenyl (**97**) and *trans*-4-(2-phenylcyclopropyl)ethyl)-1,1'-biphenyl (**96**) in $CDCl_3$.

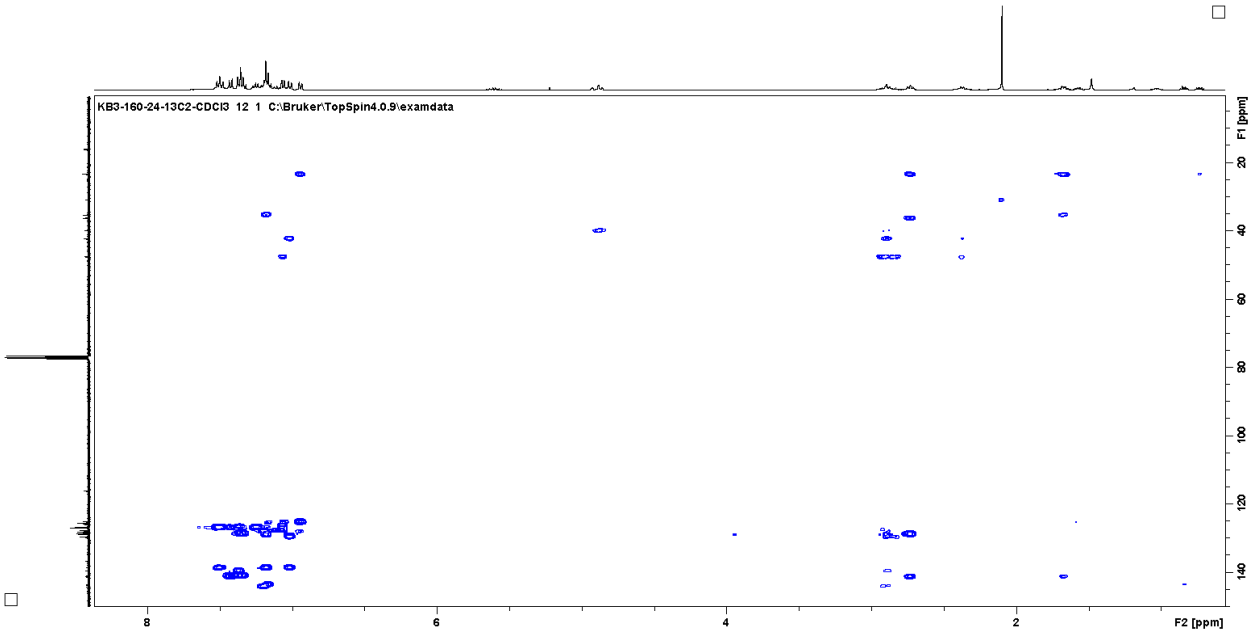

Figure 2.40. ^{1}H -^{13}C HMBC NMR spectrum of 4-(2-phenylpent-4-en-1-yl)-1,1'-biphenyl (**97**) and *trans*-4-(2-phenylcyclopropyl)ethyl)-1,1'-biphenyl (**96**) in $CDCl_3$.

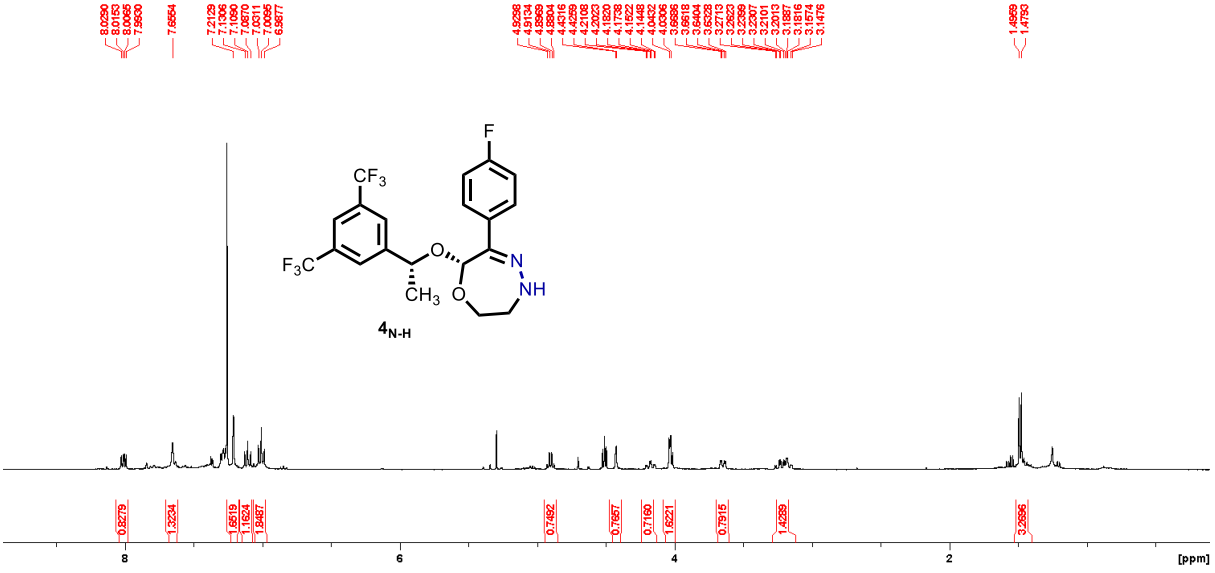

Figure 2.41. ^{1}H NMR spectrum of (*R*)-7-((*R*)-1-(3,5-bis(trifluoromethyl)phenyl)ethoxy)-6-(4-fluorophenyl)-2,3,4,7-tetrahydro-1,4,5-oxadiazepine (**4**$_{N\text{-}H}$) in $CDCl_3$, 400 MHz.

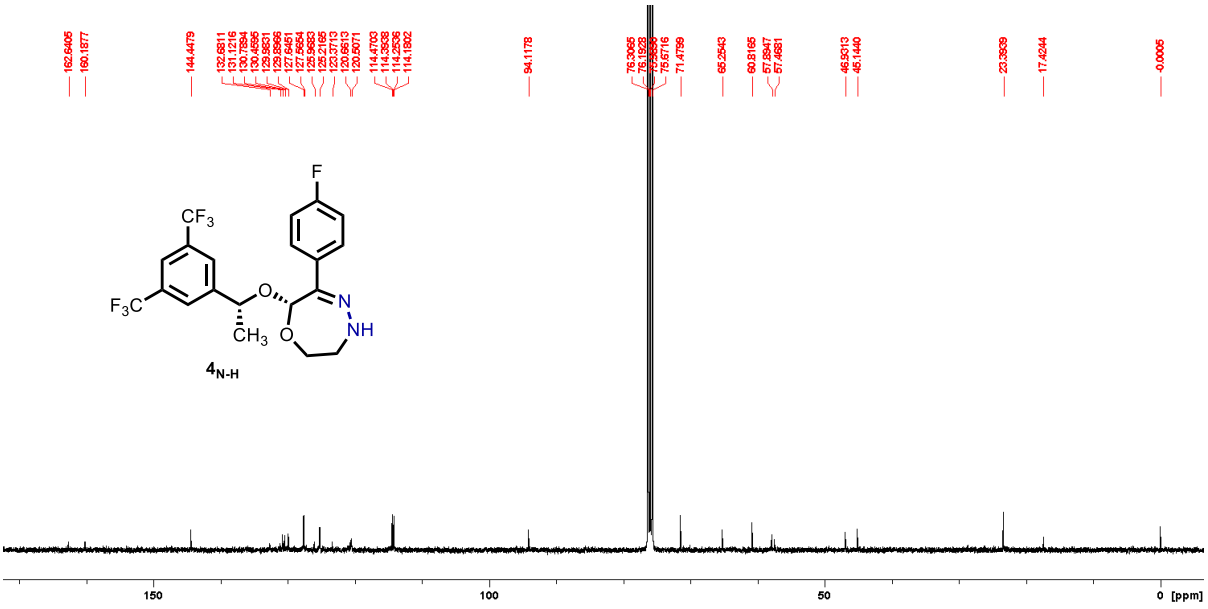

Figure 2.42. $^{13}C\{^{1}H\}$ NMR spectrum of (*R*)-7-((*R*)-1-(3,5-bis(trifluoromethyl)phenyl)ethoxy)-6-(4-fluorophenyl)-2,3,4,7-tetrahydro-1,4,5-oxadiazepine (**4**$_{\mathbf{N\text{-}H}}$) in $CDCl_3$, 101 MHz.

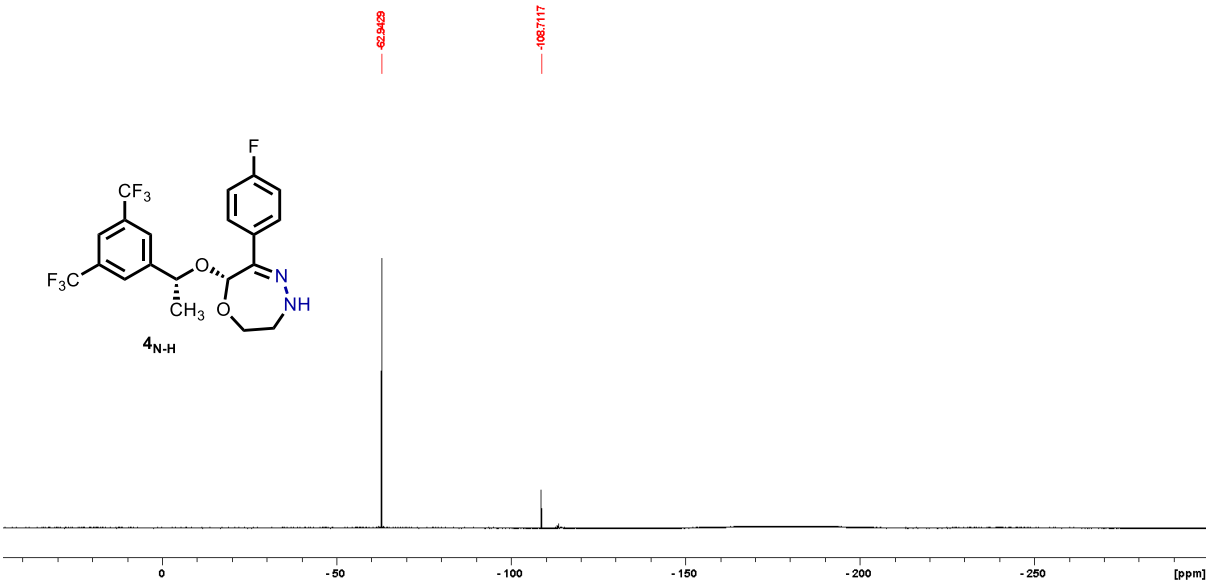

Figure 2.43 $^{19}F\{^{1}H\}$ NMR spectrum of (*R*)-7-((*R*)-1-(3,5-bis(trifluoromethyl)phenyl)ethoxy)-6-(4-fluorophenyl)-2,3,4,7-tetrahydro-1,4,5-oxadiazepine (**4**$_{\mathbf{N\text{-}H}}$) in $CDCl_3$, 376 MHz.

2.5. References.

1. Blakemore, D. C.; Castro, L.; Churcher, I.; Rees, D. C.; Thomas, A. W.; Wilson, D. M.; Wood, A. Organic Synthesis Provides Opportunities to Transform Drug Discovery. *Nat. Chem.* **2018,** *10* (4), 383-394.

2. Yamaguchi, J.; Yamaguchi, A. D.; Itami, K. C–H Bond Functionalization: Emerging Synthetic Tools for Natural Products and Pharmaceuticals. *Angew. Chem. Int. Ed.* **2012,** *51* (36), 8960-9009.

3. Abrams, D. J.; Provencher, P. A.; Sorensen, E. J. Recent Applications of C–H Functionalization in Complex Natural Product Synthesis. *Chem. Soc. Rev.* **2018,** *47* (23), 8925-8967.

4. Huigens III, R. W.; Morrison, K. C.; Hicklin, R. W.; Flood Jr, T. A.; Richter, M. F.; Hergenrother, P. J. A Ring-distortion Strategy to Construct Stereochemically Complex and Structurally Diverse Compounds from Natural Products. *Nat. Chem.* **2013,** *5* (3), 195-202.

5. Szpilman, A. M.; Carreira, E. M. Probing the Biology of Natural Products: Molecular Editing by Diverted Total Synthesis. *Angew. Chem. Int. Ed.* **2010,** *49* (50), 9592-9628.

6. Hu, Y.; Stumpfe, D.; Bajorath, J. Recent Advances in Scaffold Hopping. *J. Med. Chem.* **2017,** *60* (4), 1238-1246.

7. Cernak, T.; Dykstra, K. D.; Tyagarajan, S.; Vachal, P.; Krska, S. W. The Medicinal Chemist's Toolbox for Late Stage Functionalization of Drug-like Molecules. *Chem. Soc. Rev.* **2016,** *45* (3), 546-576.

8. Donald, J. R.; Unsworth, W. P., Ring-Expansion Reactions in the Synthesis of Macrocycles and Medium-Sized Rings. *Chem. Eur. J.* **2017,** *23* (37), 8780-8799.

9. Candeias, N. R.; Trindade, A. F.; Gois, P. M. P.; Afonso, C. A. M. 3.19 The Wolff Rearrangement. In *Comprehensive Organic Synthesis (Second Edition)*, Knochel, P., Ed. Elsevier: Amsterdam, 2014; pp 944-991.

10. Ross, A. G.; Townsend, S. D.; Danishefsky, S. J. Halocycloalkenones as Diels–Alder Dienophiles. Applications to Generating Useful Structural Patterns. *J. Org. Chem.* **2013,** *78* (1), 204-210.

11. Xu, Y.; Qi, X.; Zheng, P.; Berti, C. C.; Liu, P.; Dong, G. Deacylative Transformations of Ketones via Aromatization-promoted C–C Bond Activation. *Nature* **2019,** *567* (7748), 373-378.

12. Cao, Z.-C.; Shi, Z.-J. Deoxygenation of Ethers To Form Carbon–Carbon Bonds via Nickel Catalysis. *J. Am. Chem. Soc.* **2017,** *139* (19), 6546-6549.

13. Ouyang, K.; Hao, W.; Zhang, W.-X.; Xi, Z. Transition-Metal-Catalyzed Cleavage of C–N Single Bonds. *Chem. Rev.* **2015,** *115* (21), 12045-12090.

14. Hinsberg, W. D.; Dervan, P. B. Synthesis and Direct Spectroscopic Observation of a 1,1-Dialkyldiazene. Infrared and Electronic Spectrum of *N*-(2,2,6,6-tetramethylpiperidyl)nitrene. *J. Am. Chem. Soc.* **1978,** *100* (5), 1608-1610.

15. McIntyre, D. K.; Dervan, P. B. 1,1-Di-tert-butyldiazene. *J. Am. Chem. Soc.* **1982,** *104* (23), 6466-6468.

16. Hinman, R. L.; Hamm, K. L. The Oxidation of 1,1-Dibenzylhydrazines. *J. Am. Chem. Soc.* **1959,** *81* (13), 3294-3297.

17. Carpino, L. A. Oxidative Reactions of Hydrazines. IV. Elimination of Nitrogen from 1,1-Disubstituted-2-arenesulfonhydrazides1-4. *J. Am. Chem. Soc.* **1957,** *79* (16), 4427-4431.

18. Lemal, D. M.; Rave, T. W. Diazenes from Angeli's Salt. *J. Am. Chem. Soc.* **1965,** *87* (2), 393-394.

19. Zou, X.; Zou, J.; Yang, L.; Li, G.; Lu, H. Thermal Rearrangement of Sulfamoyl Azides: Reactivity and Mechanistic Study. *J. Org. Chem.* **2017,** *82* (9), 4677-4688.

20. Zeng, X.; Beckers, H.; Bernhardt, E.; Willner, H. Synthesis and Characterization of Sulfuryl Diazide, $O_2S(N_3)_2$. *Inorg. Chem.* **2011,** *50* (17), 8679-8684.

21. Campbell, J. J.; Glover, S. A. Bimolecular Reactions of Mutagenic *N*-acetoxy-N-alkoxybenzamides and *N*-methylaniline. *J. Chem. Soc. Perkin Trans. 2* **1992,** (10), 1661-1663.

22. Glover, S. A. Anomeric Amides - Structure, Properties and Reactivity. *Tetrahedron* **1998,** *54* (26), 7229-7271.

23. Qin, H.; Cai, W.; Wang, S.; Guo, T.; Li, G.; Lu, H. *N*-Atom Deletion in Nitrogen Heterocycles. *Angew. Chem. Int. Ed.* **2021,** *60* (38), 20678-20683.

24. Hui, C.; Brieger, L.; Strohmann, C.; Antonchick, A. P. Stereoselective Synthesis of Cyclobutanes by Contraction of Pyrrolidines. *J. Am. Chem. Soc.* **2021,** *143* (45), 18864-18870.

25. Barrett, T. N.; Braddock, D. C.; Monta, A.; Webb, M. R.; White, A. J. P. Total Synthesis of the Marine Metabolite (±)-Polysiphenol via Highly Regioselective Intramolecular Oxidative Coupling. *J. Nat. Prod.* **2011,** *74* (9), 1980-1984.

26. Wager, T. T.; Pettersen, B. A.; Schmidt, A. W.; Spracklin, D. K.; Mente, S.; Butler, T. W.; Howard, H.; Lettiere, D. J.; Rubitski, D. M.; Wong, D. F.; Nedza, F. M.; Nelson, F. R.; Rollema, H.; Raggon, J. W.; Aubrecht, J.; Freeman, J. K.; Marcek, J. M.; Cianfrogna, J.; Cook, K. W.; James, L. C.; Chatman, L. A.; Iredale, P. A.; Banker, M. J.; Homiski, M. L.; Munzner, J. B.; Chandrasekaran, R. Y. Discovery of Two Clinical Histamine H3 Receptor Antagonists: *trans*-*N*-Ethyl-3-fluoro-3-[3-fluoro-4-(pyrrolidinylmethyl)phenyl]cyclobutanecarboxamide (PF-03654746) and *trans*-3-Fluoro-3-[3-

fluoro-4-(pyrrolidin-1-ylmethyl)phenyl]-*N*-(2-methylpropyl)cyclobutanecarboxamide (PF-03654764). *J. Med. Chem.* **2011,** *54* (21), 7602-7620.

27. Banert, K.; Heck, M.; Ihle, A.; Kronawitt, J.; Pester, T.; Shoker, T. Steric Hindrance Underestimated: It is a Long, Long Way to Tri-*tert*-alkylamines. *J. Org. Chem.* **2018,** *83* (9), 5138-5148.

28. Hansch, C.; Leo, A.; Taft, R. W. A Survey of Hammett Substituent Constants and Resonance and Field Parameters. *Chem. Rev.* **1991,** *91* (2), 165-195.

29. Brown, H. C.; Okamoto, Y. Electrophilic Substituent Constants. *J. Am. Chem. Soc.* **1958,** *80* (18), 4979-4987.

30. Meng, G.; Zhang, J.; Szostak, M. Acyclic Twisted Amides. *Chem. Rev.* **2021,** *121* (20), 12746-12783.

31. Liu, C.; Szostak, M. Twisted Amides: From Obscurity to Broadly Useful Transition-Metal-Catalyzed Reactions by N−C Amide Bond Activation. *Chem. Eur. J.* **2017,** *23* (30), 7157-7173.

32. Liu, C.; Shi, S.; Liu, Y.; Liu, R.; Lalancette, R.; Szostak, R.; Szostak, M. The Most Twisted Acyclic Amides: Structures and Reactivity. *Org. Lett.* **2018,** *20* (24), 7771-7774.

33. Xu, M.; Paul, M. K.; Bullard, K. K.; DuPre, C.; Gutekunst, W. R. Modulating Twisted Amide Geometry and Reactivity Through Remote Substituent Effects. *J. Am. Chem. Soc.* **2021,** *143* (36), 14657-14666.

34. Glover, S. A.; Rauk, A.; Buccigross, J. M.; Campbell, J. J.; Hammond, G. P.; Mo, G.; Andrews, L. E.; Gillson, A.-M. E. The HERON Reaction - Origin, Theoretical Background, and Prevalence. *Can. J. Chem.* **2005,** *83* (9), 1492-1509.

35. De Almeida, M. V.; Barton, D. H. R.; Bytheway, I.; Ferreira, J. A.; Hall, M. B.; Liu, W.; Taylor, D. K.; Thomson, L. Preparation and Thermal Decomposition of *N,N'*-Diacyl-*N,N'*-Dialkoxyhydrazines: Synthetic Applications and Mechanistic Insights. *J. Am. Chem. Soc.* **1995,** *117* (17), 4870-4874.

36. Strick, B. F.; Mundal, D. A.; Thomson, R. J. An Oxidative [2,3]-Sigmatropic Rearrangement of Allylic Hydrazides. *J. Am. Chem. Soc.* **2011,** *133* (36), 14252-14255.

37. Newcomb, M. Radical Kinetics and Clocks. In *Encyclopedia of Radicals in Chemistry, Biology and Materials*. Chatgilialoglu, C.; Studer, A. Eds.; John Wiley & Sons, Ltd.: Hoboken, New Jersey, 2012; 1-18.

38. Herk, L.; Feld, M.; Szwarc, M. Studies of "Cage" Reactions. *J. Am. Chem. Soc.* **1961,** *83* (14), 2998-3005.

39. Creary, X. Super Radical Stabilizers. *Acc. Chem. Res.* **2006,** *39* (10), 761-771.

40. Gerdes, R. G.; Glover, S. A.; ten Have, J. F.; Rowbottom, C. A.. *N*-acetoxy-*N*-alkoxyamides - A New Class of Nitrenium Ion Precursors which are Mutagenic. *Tet. Lett.* **1989,** *30* (20), 2649-2652.

41. Gissot, A.; Volonterio, A.; Zanda, M. One-Step Synthesis of *O*-Benzyl Hydroxamates from Unactivated Aliphatic and Aromatic Esters. *J. Org. Chem.* **2005,** *70* (17), 6925-6928.

42. Ghosh, S.; Banerjee, J.; Ghosh, R.; Chattopadhyay, S. K. A Metal-free Iodine-mediated Conversion of Hydroxamates to Esters. *Synth. Commun.* **2020,** *50* (9), 1353-1360.

43. Palakurthy, N. B.; Dev, D.; Paikaray, S.; Chaudhury, S.; Mandal, B. Synthesis of *O*-Benzyl Hydroxamates Employing the Sulfonate Esters of *N*-hydroxybenzotriazole. *RSC Adv.* **2014,** *4* (16), 7952-7958.

44. Kurz, T.; Pein, M. K.; Marek, L.; Behrendt, C. T.; Spanier, L.; Kuna, K.; Brücher, K. Microwave-Assisted Conversion of 4-Nitrophenyl Esters into *O*-Protected Hydroxamic Acids. *Eur. J. Org. Chem.* **2009,** *2009* (18), 2939-2942.

45. Nouaille, A.; Pannecoucke, X.; Poisson, T.; Couve-Bonnaire, S. Access to Trisubstituted Fluoroalkenes by Ruthenium-Catalyzed Cross-Metathesis. *Adv. Synth. Catal.* **2021,** *363* (8), 2140-2147.

46. Lorenz, J. C.; Long, J.; Yang, Z.; Xue, S.; Xie, Y.; Shi, Y. A Novel Class of Tunable Zinc Reagents ($RXZnCH_2Y$) for Efficient Cyclopropanation of Olefins. *J. Org. Chem.* **2004,** *69* (2), 327-334.

47. Pozzi, D.; Scanlan, E. M.; Renaud, P. A Mild Radical Procedure for the Reduction of B-Alkylcatecholboranes to Alkanes. *J. Am. Chem. Soc.* **2005,** *127* (41), 14204-14205.

48. Ezawa, M.; Moriyama, K.; Togo, H. Transformation of *N*,*N*-Diisopropylarylmethylamines into *N*-Isopropylarylmethylamines with Molecular Iodine. *Tet. Lett.* **2015,** *56* (48), 6689-6692.

49. Malek, B.; Fang, W.; Abramova, I.; Walalawela, N.; Ghogare, A. A.; Greer, A. "Ene" Reactions of Singlet Oxygen at the Air–Water Interface. *J. Org. Chem.* **2016,** *81* (15), 6395-6401.

50. Balavoine, F.; Batch, A.; Rolland, C. Processes for Preparing Desmethylsertraline or a Pharmaceutically Acceptable Salt Thereof. WO2008065177A1, Nov. 30, 2006.

CHAPTER 3

Reductive Deamination of Primary Amines *via* Primary Isodiazene Intermediates

Note: Portions of this work have been published in an alternate format in Berger, K. J.; Driscoll, J. L.; Yuan, M.; Dherange, B. D.; Gutierrez, O.; Levin, M. D. Direct Deamination of Primary Amines *via* Isodiazene Intermediates. *J. Am. Chem. Soc.* **2021**, *143*, 17366 – 17373.

3.1. Introduction.

The "deletion" of a primary amine to an alkane is an exceptionally challenging transformation.[1, 2] As illustrated in chapter 1, primary amines that are pre-functionalized can undergo deaminative conversion to a range of functionalities. This has been most prominently demonstrated with Katritzky salts and modern photocatalytic or metal catalyzed cross-coupling techniques, which have provided facile routes for C-C and C-heteroatom bond formation.[1, 3-8] In contrast, the conversion of a primary amine to a C-H bond or "reductive deamination" has not been widely realized using Katritzky salts. Aggarwal has reported one example in which an alkyl radical generated by photocatalyzed EDA complexation of a Katritzky salt undergoes HAT with thiophenol (Scheme 3.1a), however a substrate scope of the reaction was not further investigated.[9] Earlier work by Katritzky showed that *N*-benzyl pyridinium salts can be reduced with sodium borohydride to generate 1,2-dihydripyridines (Scheme 3.1b).[10, 11] These species were able to generate the reductive deamination product, but the harsh pyrolysis conditions required severely limits the utility of this methodology.

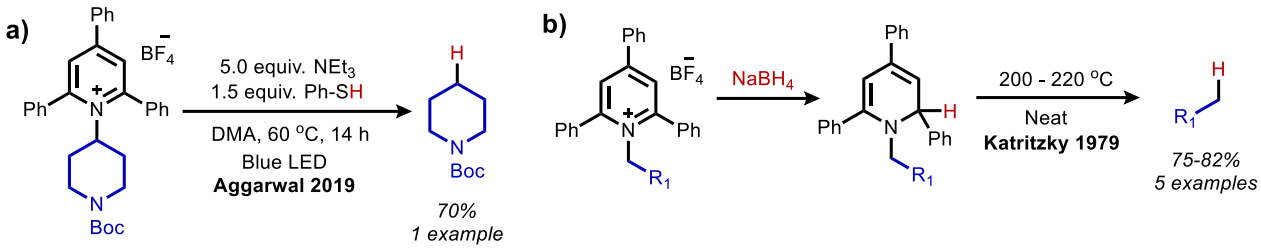

Scheme 3.1. Reductive deamination of Katritzky salts using a) HAT with thiophenol and b) sodium borohydride followed by pyrolysis.

Other pre-functionalization strategies for reductive deamination are discussed in chapter 1, including a formylation followed by dehydration to an isonitrile moiety, which may be reduced by tin hydride to give alkane product (see Scheme 1.14).[12, 13] Pre-functionalization by a two step tosylation, followed by reduction with sodium borohydride has also been reported (see Scheme 1.7).[14] Pre-functionalization with a single tosyl group, followed by treatment with potassium hydroxide and chloramine has been demonstrated to give the requisite alkane product.[15]

The multi-step nature of the above syntheses is less desirable compared to a one-pot transformation. There has been considerable effort dedicated to developing a set of reaction conditions for primary amine cleavage in a single step or "direct" deamination. Unfortunately, these reactions require very harsh conditions and the use of unappealing reagents such as difluoramine, hydrogenolysis with 40% platinum on silica, or diazotization with 1,3-propanedinitrite.[16-19] Doldouras has reported the use of *o*-hydroxylamine sulfonic acid for the direct deamination of primary amines under more mild conditions,[20] however this reaction still suffers from low functional group tolerance (Scheme 3.2a). Prior to our work, the current state of the art methodology was reported by Oestreich in 2020, in which deamination is facilitated in a single step *via in-situ* silylation (Scheme 3.2b).[2] This silylated intermediate is then reduced by phenylsilane to give the alkane product, as discussed more in depth in chapter 1. However, this

reaction still requires high temperature conditions, and the substrate scope is limited to benzylic, α-branched primary amines.

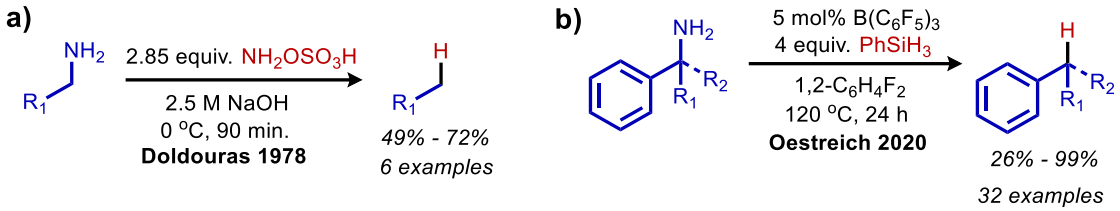

Scheme 3.2. State of the art for direct primary amine deletion including a) deamination with HOSA and b) Lewis acid catalyzed deamination with phenylsilane.

We were inspired by the nucleophilic substitution of secondary amines with the optimized anomeric amide reagent as described in chapter 2. We rationalized that primary amines would also undergo substitution with the electrophilic nitrogen moiety, thus mitigating the need for any pre-functionalization (Scheme 3.3). If an analogous mechanism is operative, a primary isodiazene intermediate would be generated during the reductive elimination step. Unlike secondary isodiazene moieties, which are well studied in the literature (see chapter 2.1), mono-alkyl substituted primary isodiazene species have never been reported. Only the unsubstituted analogue ($H_2N{=}N$) has been detected by Dervan,[21] and we were excited to pursue this elusive intermediate.

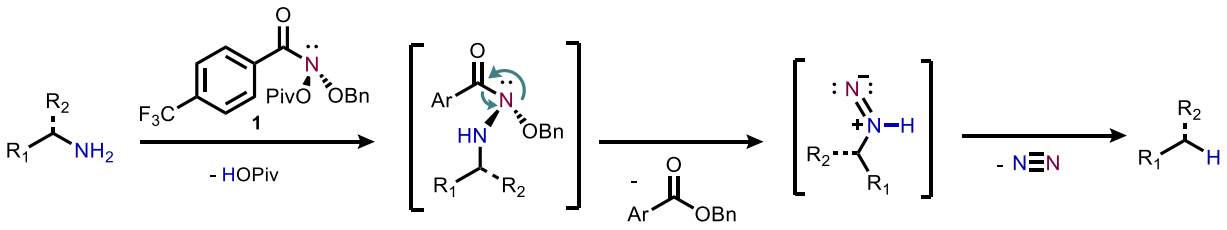

Scheme 3.3. Proposed direct primary amine deletion using an anomeric amide reagent.

3.2. Results and Discussion.

3.2.1. Initial Investigation.

Previous studies with secondary amines demonstrated that benzylic amines underwent deletion preferentially due to the stabilization of the radical intermediate. Using this knowledge, benzylic primary amines were selected as model substrates to probe the present reaction. Initial work with benzhydrylamine (**2-H$_2$**) showed adding one equivalent of previously optimized anomeric amide reagent (**1**) gave diphenylmethane in 59% yield at 45 ^{o}C in THF (Scheme 3.4). While this result was encouraging, the yield was never successfully optimized higher despite screening a wide range of conditions including solvent, temperature, and base and HAT reagent additives. More curiously, monobenzylic substrates such as 1-phenylcyclohexylamine and 1,1-diphenylethylamine gave a low yield of desired deletion product and elimination products, as evidenced by olefinic peaks in the product NMR spectra. α-Tertiary aliphatic primary amines were also explored, as it was thought they may also stabilize a hypothetical radical intermediate. However, adamantylamine mainly gave unreacted starting material, likely due to steric constraints for attack at the anomeric amide reagent.

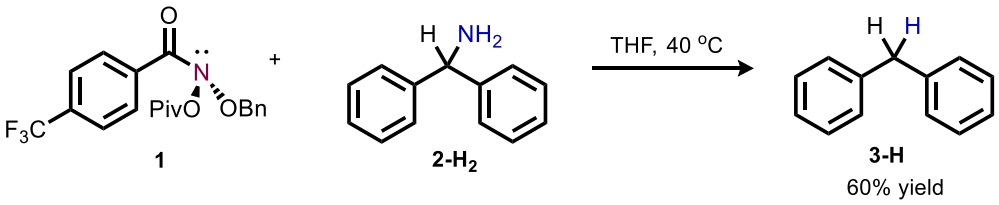

Scheme 3.4. Initial reaction screening with benzhydrylamine shows deaminated product.

Nevertheless, the conversion of benzhydrylamine to diphenylmethane was a promising result and we were eager to probe the source of the hydrogen atom which is incorporated in the product. The starting material amine was deuterated by heating the substrate in deuterated

methanol followed by subsequent removal of solvent *in vacuo*. When **2-D$_2$** was treated with anomeric amide **1**, deuterium incorporation into diphenylmethane was detected by NMR spectroscopy (Figure 3.1).[22] Indeed, 58% of the nitrogen deletion product obtained corresponded to **3-D**. The use of deuterated solvent and proteo-amine substrate did not produce any deuterium incorporated product. These results suggest that the source of the hydrogen atom in the reductive deamination product is from the amine -NH$_2$.

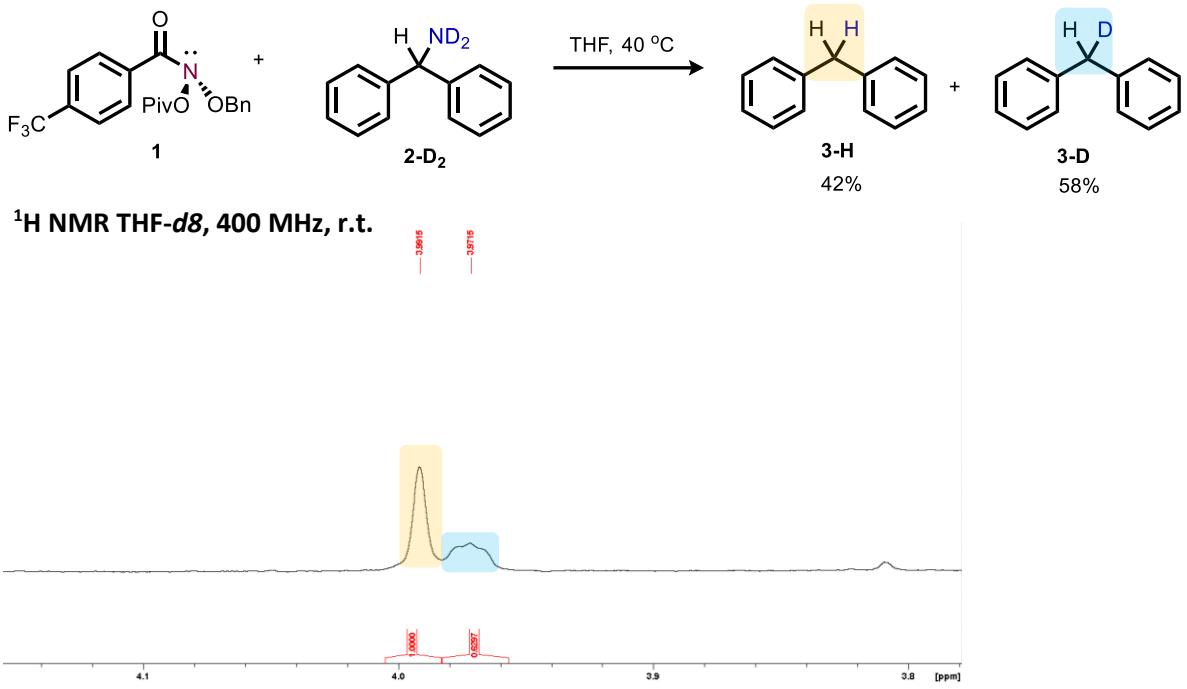

Figure 3.1. ^{1}H NMR spectrum (THF-*d8*) of crude product mixture showing **3-H** and **3-D**. Treatment of 2-D$_2$ with anomeric amide shows deuterium incorporation into deletion product.

We hypothesized that in analogy to the mechanistic studies of secondary amine deletion, a primary amine radical clock substrate might help elucidate the nature of deaminated alkyl intermediates in the reaction. However, as known primary amine radical clock structures do not contain any benzylic stabilization, it was unclear if these substrates would react productively. Thus, we first examined a simple unstabilized aliphatic primary amine. A solution of 4-tetrahydropyranmethylamine (**4**) was added to a solution of **1** and a rapid bubbling of gas was

observed at room temperature. To our excitement, this unstabilized aliphatic primary amine reacted rapidly under exceedingly mild conditions. The reductive deamination product 4-methyltetrahydropyran (**5**) was cleanly produced, as detected by NMR spectroscopy (Figure 3.2).[23]

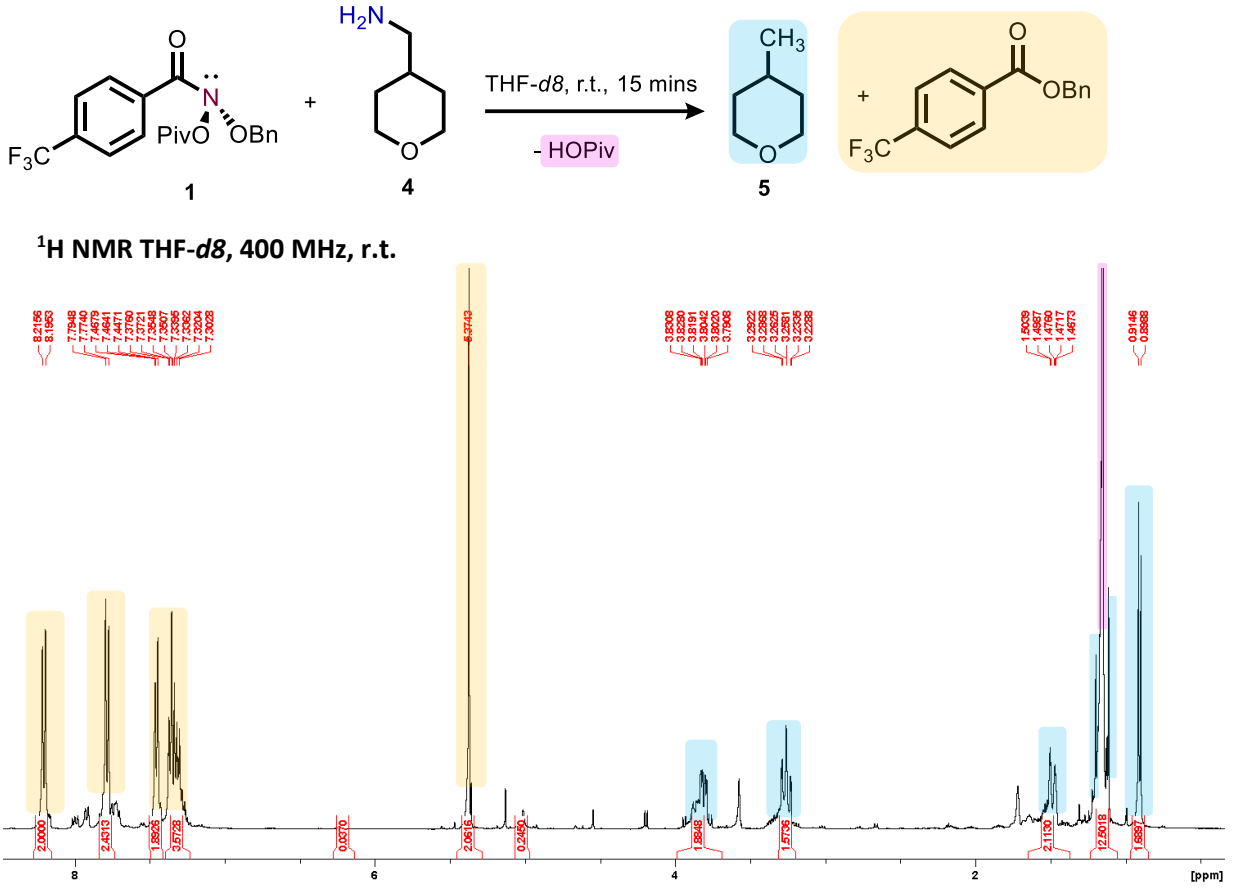

Figure 3.2. NMR spectrum (THF-*d8*) of crude reaction products showing initial discovery that primary aliphatic amines undergo deletion.

3.2.2. Reaction Optimization.

With this exciting initial result at hand, optimization of reaction conditions was pursued. Using the model primary amine substrate 1-methyl-3-phenylpropanamine (**6**), a solvent screen was conducted. The yield of deaminated product (**7**) was determined by GC using a calibration curve of authentic product relative to dodecane internal standard (Table 3.1). Acetonitrile, THF and

dioxane were shown to be similarly effective, with yields in the range of 74% – 88%. These solvents were further tested in three replicates with yields determined by NMR spectroscopy relative to internal standard (Table 3.2). Acetonitrile was shown to give the highest yield of product (88% +/- 7.2%). Addition of the base triethylamine was also explored because pivalic acid is produced in the reaction. However, this did not increase the yield of product. Cooling the reaction was also ineffective at increasing yield.

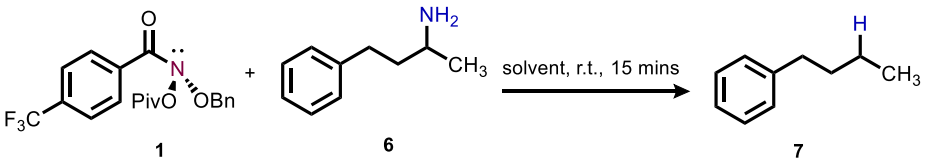

Solvent	**Yield of Product 7** (+/-5% error from calibration curve)
THF	74%
Dioxane	78%
Ether	46%
DCM	43%
DMF	68%
ACN	88%

Table 3.1. Initial solvent screen for reaction optimization using GC with a calibration curve of authentic product relative to dodecane internal standard.

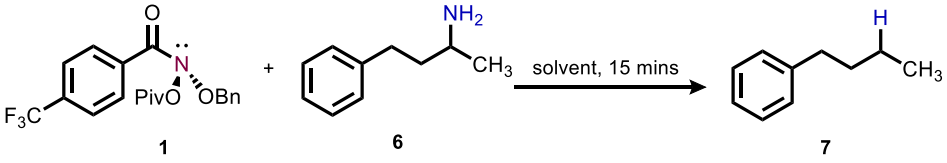

Conditions	**Yield of Product 7**
THF, r.t.	66.8% +/- 4.8%
Dioxane, r.t.	71.9% +/- 1.6%
ACN, r.t.	**88.0% +/- 7.2%**
ACN, r.t. with 1 equiv. NEt_3	73.7% +/- 0.2%
ACN, -15 ^{o}C – r.t.	80.6% +/- 3.1%

Table 3.2. Screen for reaction optimization using NMR spectroscopy relative to 1,3,5-trimethoxybenzene internal standard. Error bars represent standard deviation of three replicates.

3.2.3. Reaction Scope and Functional Group Tolerance.

With the optimized solvent conditions in hand, the functional group tolerance of the reaction was probed by obtaining isolated yields of deaminated derivatives of small molecules (Table 3.3). The biological metabolite tryptamine (**8**) was deaminated in 65% yield, which was an exciting result because unprotected indole moieties were not tolerated during the secondary amine deletion studies. Working in collaboration with Julia Driscoll, she was able to show functional group tolerance for nitro, imidazole, and unprotected alcohol moieties with substrates **9** – **11**. Lipitor precursor **12** was successfully deaminated, demonstrating tolerance for both ester and acetal moieties. However, this product was challenging to purify from the ester side product by column chromatography. An alternate purification procedure was developed in which sodium hydroxide was added to the crude product mixture. The ester was saponified and the mixture was subsequently filtered to give the deaminated derivative of **12** in 63% isolated yield. We were also interested in compound **13**, which is a precursor to the pharmaceutical Mosapride. Compound **13** was deaminated in 94% yield, showing tolerance for a substituted morpholine ring.

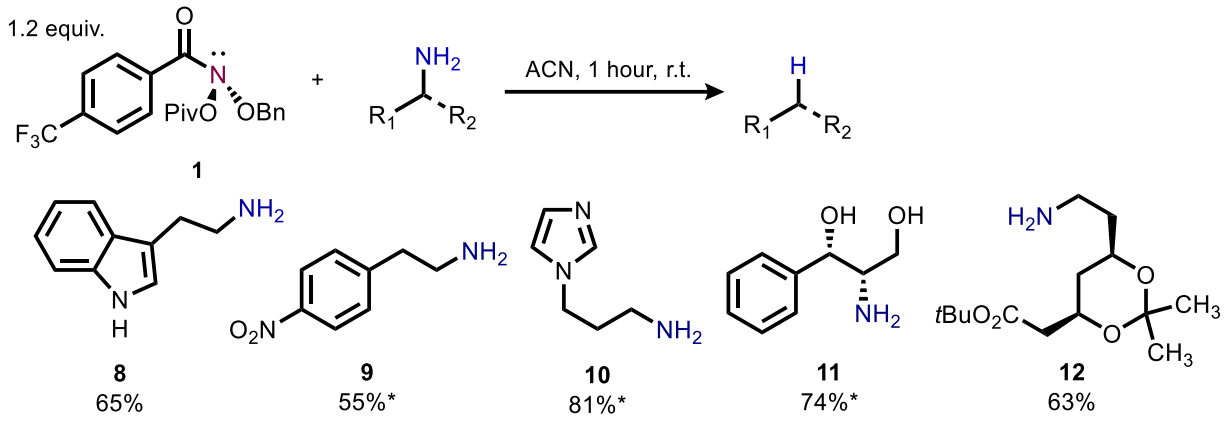

Table 3.3. Scope of small molecule deamination. *Isolated yields obtained by Julia Driscoll.

After obtaining the small molecule substrate scope, we wished to demonstrate the late-stage deamination of more complicated pharmaceuticals. Starting with the anti-malarial drug Primaquine (**14**), the deaminated derivative was isolated in 53% yield (Table 3.4). This product has been detected by mass spectrometry in biological samples as a known metabolite of Primaquine,[24] but until this work it had not been previously produced synthetically. The anti-vial Oseltamivir (**15**) was deaminated in 53% yield and the anti-arrhythmic Amlodipine (**16**) was deaminated in 71% yield, with its redox active dihydropyridine core retained during the reaction. Anti-viral Rimantadine (**17**) was deaminated in 77% yield by NMR, however attempts to quantitatively isolated the deaminated product were not successful due to the volatility of the alkane product. Nevertheless, the deamination of a bulky neopentylic amine demonstrates tolerance for β-branched sterics. We were also able to deaminate anti-diabetic compounds which contain complicated heterocyclic moieties including Sitagliptin (**18**) and Omarigliptin (**19**) in 52% and 77% yield, respectively. Linagliptin (**20**) was subsequently explored, which contains multiple potentially challenging heterocycles. However, this compound was not soluble in acetonitrile. Deamination was successful in a mixture of 1:1 acetonitrile: DMSO, and the deaminated derivative of **20** was isolated in 65% yield. It was necessary that the DMSO was anhydrous, and wet solvent

dramatically decreased the yield of isolated product. Additionally, several pharmaceuticals were found to be unsuccessful. The anti-arrhythmic drug Mexiletine (**21**) was deaminated in only 14% yield. The major side product of the reaction was the corresponding phenol compound, resulting from unwanted cleavage of the ether moiety. The anti-cancer drug Doxorubicin (**22**) did not yield any detectable deamination product, possible due to the reducing hydroquinone core.

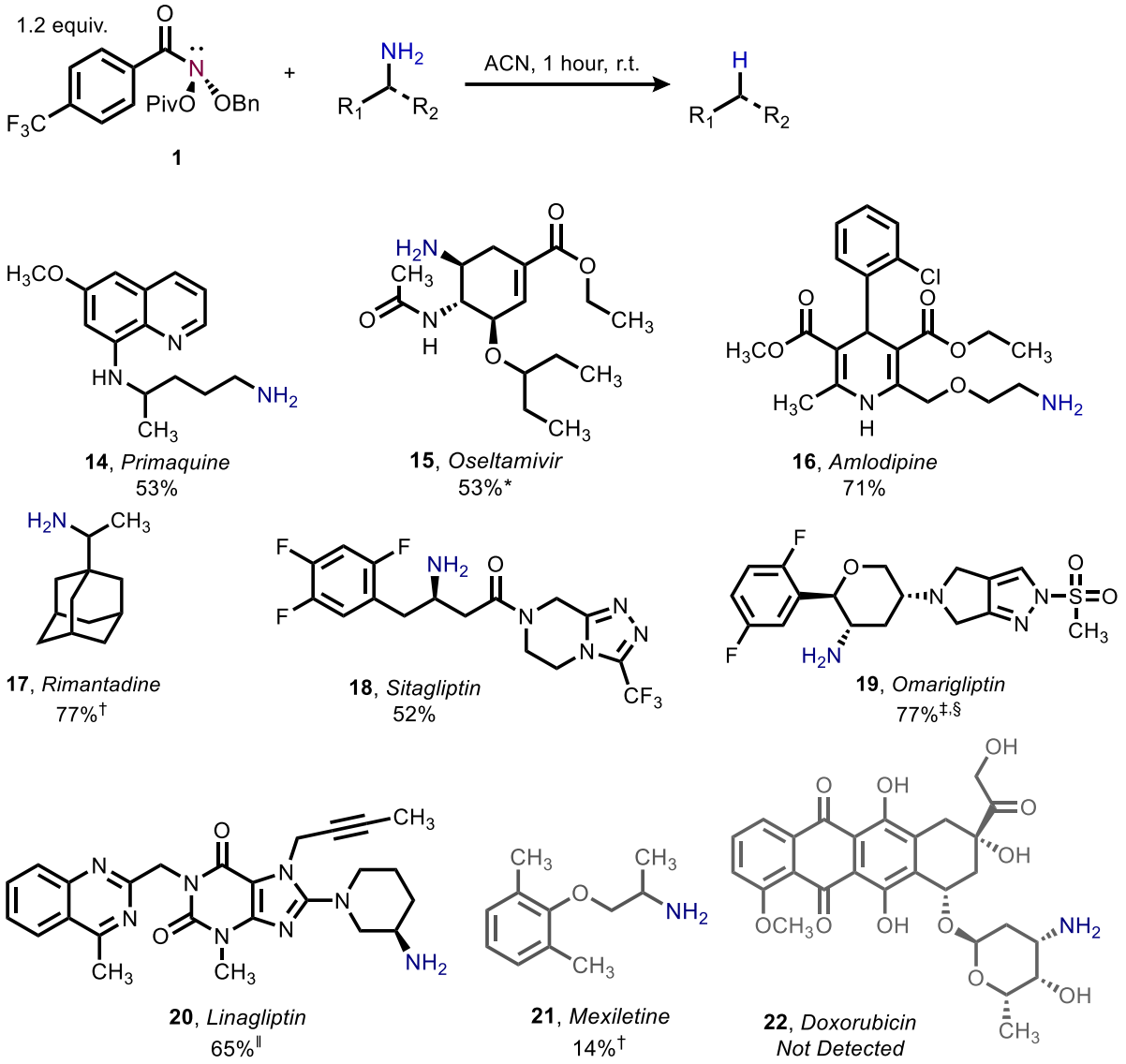

Table 3.4. Scope and limitations of late-stage deamination of pharmaceuticals. *reaction time 5 hours; †NMR yield; ‡isolated yield obtained by Julia Driscoll; §1.5 equiv. of **1**; ‖reaction time 16 hours and solvent mixture 1:1 DMSO: ACN.

There were several other limitations in scope that are worth noting. Early studies with adamantylamine demonstrated that α-tertiary amines were too encumbered to react and gave largely unreacted starting material. Indeed, sterics appears to play an important role in this reaction. Cyclic α-secondary primary amines were found to give lower yields and require longer reaction times (for example, Oseltamivir and Linagliptin) than unhindered α-primary primary amines throughout the substrates studied in this chapter. Additionally, sterically hindered α-secondary primary amines sometimes exhibit an unwanted attack at the amide carbonyl of **1**, resulting in the corresponding *N*-alkyl-4-(trifluoromethyl)benzamide derivative as a side product. This observation was found to be concentration dependent (see Scheme 3.24) and carefully dropwise addition of the solution of **1** to the solution of amine was helpful in mitigating side product formation.

Benzylic amines, as briefly discussed in section 3.2.1, did not react productively. We were inspired by a report by Myers in which a primary diazene intermediate – the isomer to our postulated primary isodiazene intermediate – is generated from **23** and undergoes a [2,3]-rearrangement with a benzylic system (Scheme 3.5).[25] When this rearrangement occurs with a 1-napthyl moiety, the resulting dearomatized alkene benzo-*p*-isotoluene (**24**) is stable and can be isolated. In contrast, other benzylic moieties form metastable alkenes that cannot be isolated. It was hypothesized that this rearrangement might be occurring in our reaction with benzylic amines, resulting in unsuccessful isolation of the deaminated product. In order to test this, 1-naphthylmethylamine (**25**) was treated with **1** and **24** was detected by NMR spectroscopy in 57% yield (Scheme 3.6). The unrearranged product **24'** was not detected.

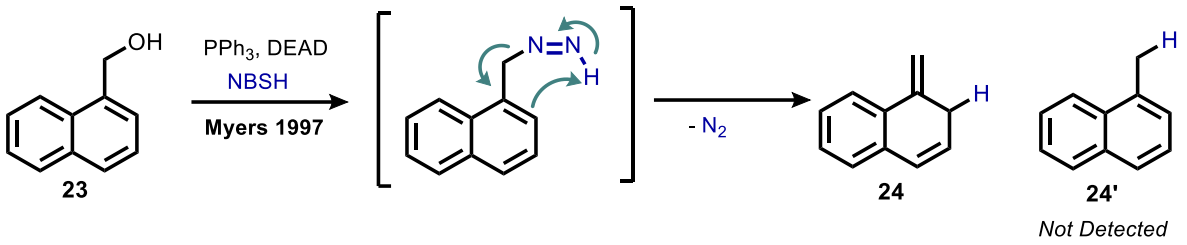

Scheme 3.5. Rearrangement of a benzylic diazene to give an isotoluene product.

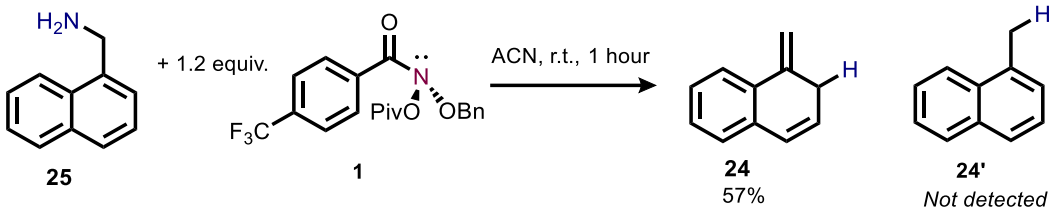

Scheme 3.6. Treatment of 1-naphthylamine with **1** gives isotoluene product.

We were also interested in comparing our methodology with the current state of the art for aliphatic deamination. Using the method reported by Doldouras, Oseltamivir (**15**) was treated with hydroxylamine *o*-sulfonic acid (Scheme 3.7).[20] No trace of deaminated product was detected. Similarly, Sitagliptin (**18**) was also subjected to these conditions and no deaminated product was detected.

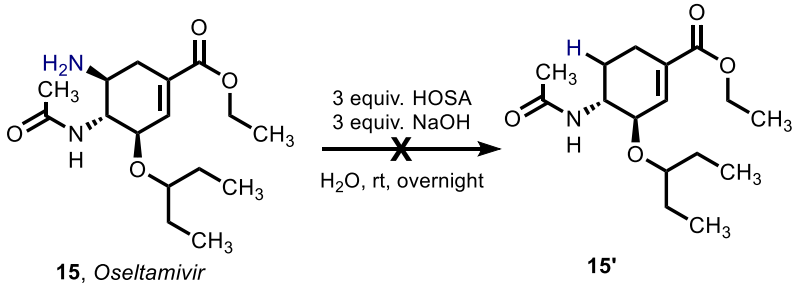

Scheme 3.7. Comparison of HOSA deamination using Oseltamivir.

With the pharmaceutical substrate scope completed, amino acids were then explored (Table 3.5). The carboxylic acid functionality of these compounds typically renders them insoluble in

acetonitrile and thus amino acid methyl esters were utilized. Initial studies by NMR spectroscopy showed that valine methyl ester (**26**) was deaminated by **1**. Methionine methyl ester (**27**) was also deaminated in 74% yield, demonstrating tolerance for a thioester. Phenylalanine methyl ester (**28**) was deaminated and successfully isolated in 96% yield. The deaminated derivative of tryptophan methyl ester (**29**) was also isolated in 71% yield.

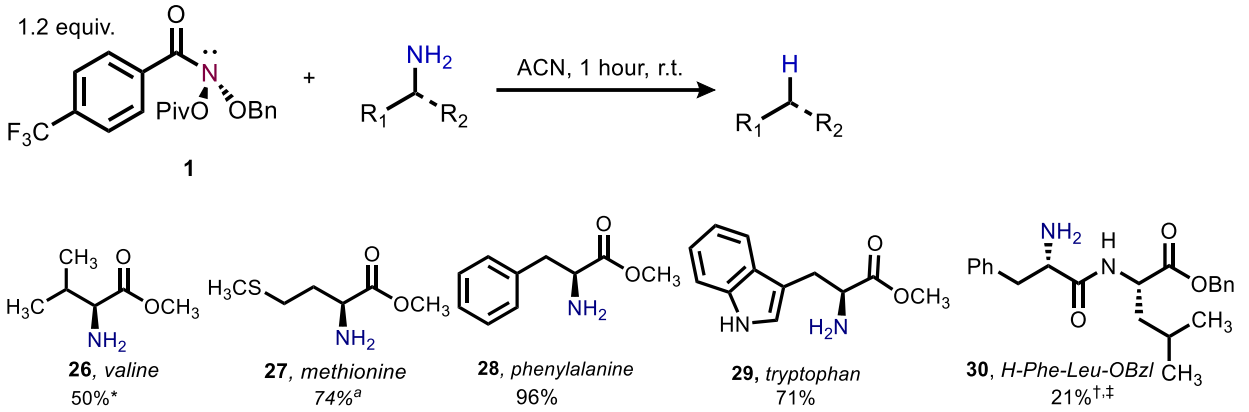

Table 3.5. Scope of amino acid and peptide deamination. *NMR yield; †3 hours; ‡solvent 1:1 DMSO: ACN.

The success of amino acid methyl esters prompted us to try a dipeptide structure. H-Phe-Leu-OBzl (**30**) is a commercially available dipeptide which was selected because it contains UV active functionalities and a protected carboxylic acid. However, the dipeptide was found to be insoluble in acetonitrile. Gratifyingly, the reaction proceeded in 1:1 acetonitrile: DMSO. However, the deaminated product was isolated as a 1:1 mixture with *N*-(benzyloxy)-4-(trifluoromethyl)benzamide, produced by unwanted reduction of the anomeric amide reagent. This mixture was purified by preparative HPLC to obtain the product in 21% yield.

Lysine (**31**) is a particularly intriguing structure because it contains an ε-amino group and an α-amino group, two primary amines with different steric profiles. The reactivity of lysine was initially probed using lysine benzyl ester in order to have a UV active moiety. However, lysine

benzyl ester proved to be difficult to handle. The *O*-benzyl group was a sufficient leaving group to promote cyclization to α-amino caprolactam (**32**). When lysine benzyl ester was treated with **1,** some unwanted cyclization occurred during the reaction, and α-amino caprolactam was subsequently deaminated to give caprolactam (**33**) in a low yield. In order to optimize this serendipitous discovery, lysine was first cyclized in a separate pot using an established literature procedure.[26] Deamination of α-amino caprolactam with **1** then gave caprolactam in 58% isolated yield (Scheme 3.8). A new synthetic route to caprolactam is important because it is a commodity chemical used to produce nylon 6. Caprolactam is traditionally synthesized from cyclohexanone starting material by conversion to an oxime and a subsequent Beckmann rearrangement (Scheme 3.9a).[27] Cyclohexanone (**34**) is a petroleum derived feedstock and an alternative synthesis of caprolactam from biomass is highly desirable. The literature synthesis of caprolactam from lysine requires hydrogenolysis with iridium zeolite at high temperatures (Scheme 3.9b).[28] Thus, the present advance represents a potentially more sustainable procedure.

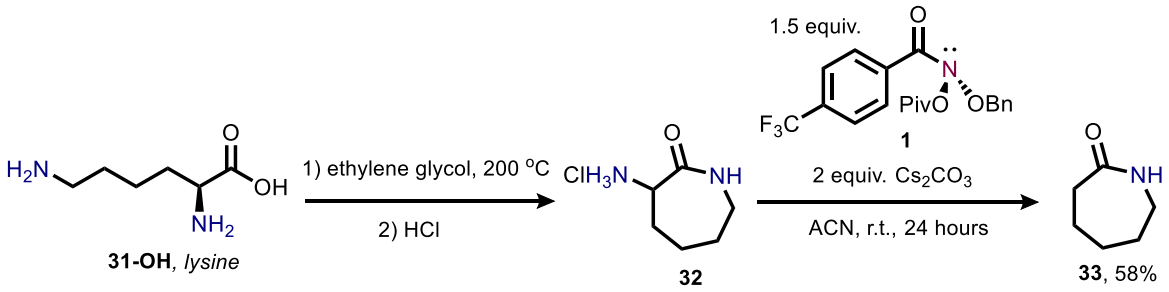

Scheme 3.8. Synthesis of caprolactam from lysine using **1**.

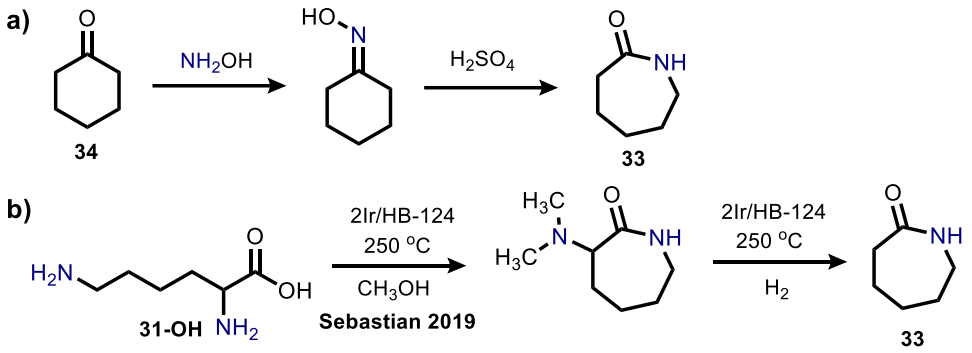

Scheme 3.9. Literature procedures for the synthesis of caprolactam including a) industrial synthesis from petroleum feedstock and b) existing lysine derived synthesis using iridium hydrogenolysis.

Subsequent deamination selectivity studies were conducted using lysine methyl ester (Scheme 3.10). When lysine methyl ester was treated with 0.98 equivalents of **1**, selective deamination of the α-primary primary amine was observed. Norlecuine (**35**) was isolated from the reaction in 69% yield and no methyl 6-aminohexanoate (**35'**) was detected. Addition of 2.1 equivalents of **1** resulted in deamination of both amines to give methyl hexanoate (**36**) in 54% yield.

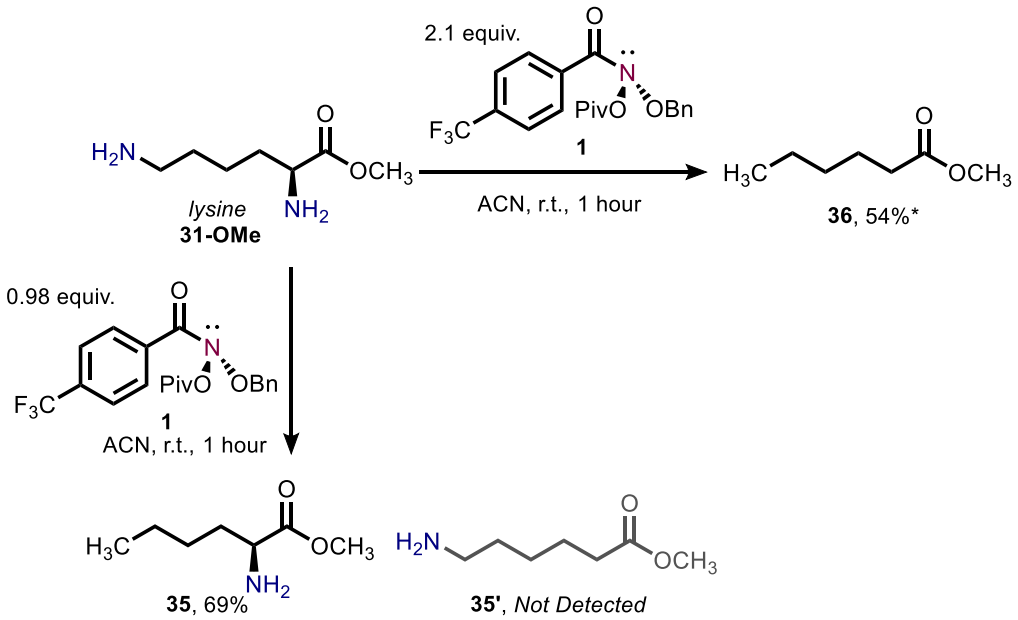

Scheme 3.10. Selectivity of primary amine deletion using lysine methyl ester. *NMR Yield

In addition to amino acids, amino sugars were another class of biomolecule that was of interest. Acetylated β-glucosamine (**37**) was deaminated in 78% yield without erosion of the anomeric stereocenter to give exclusively β-2-deoxyglucose (**β-38**) (Scheme 3.11). The established literature synthesis of β-2-deoxyglucose starts from corresponding glycal precursor **39** and requires hydrohalogenation, followed by nucleophilic isomerization and substitution (Scheme 3.12).[29] Under the acidic conditions of this reaction, epimerization typically occurs and gives an unwanted mixture of β-2-deoxyglucose (**β-38**) and α-2-deoxyglucose (**α-38**) such that the 67% yield reported consisted of a 1.5:1 mixture of α:β anomers.[30] Thus, such a facile and selective synthesis of β-2-deoxyglucose from a biologically ubiquitous amino sugar is quite remarkable.

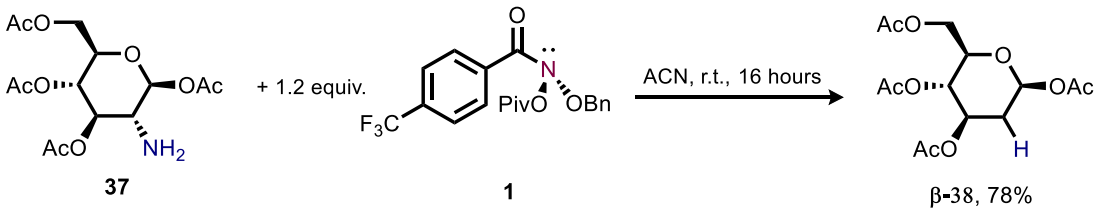

Scheme 3.11. Conversion of acetylated glucosamine to acetylated β-2-deoxyglucose.

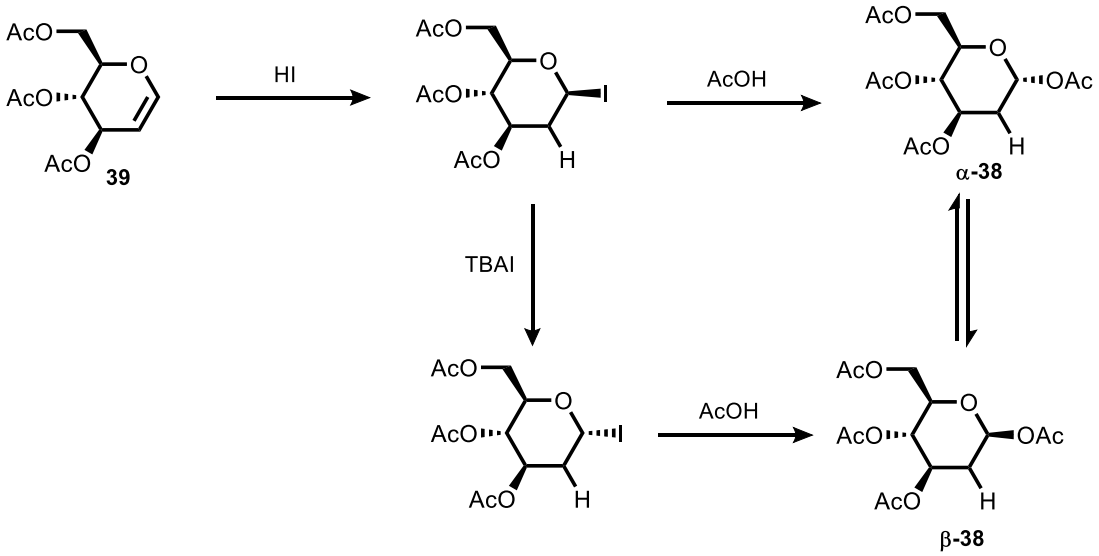

Scheme 3.12. Literature synthesis of β-2-deoxyglucose and unwanted isomerization to α-2-deoxyglucose.

Working in collaboration with Dr. Balu Dherange, he discovered that **1** was capable of deaminating aromatic amines when the reaction was heated to 45 °C. Isolated yields in the range of 53% to 72% were obtained with electron rich arenes **40** - **42** (Table 3.6). The pharmaceutical aminoglutethimide (**43**) was also successfully deaminated in 64% yield.

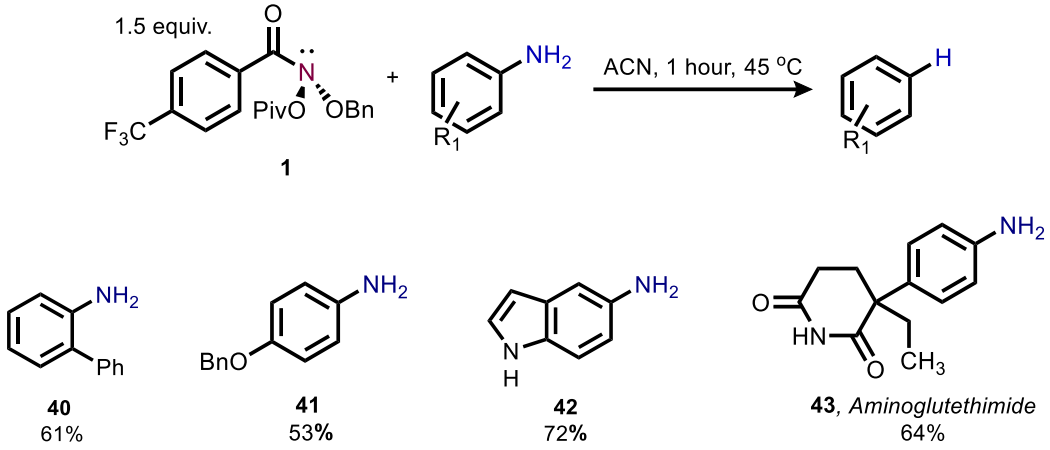

Table 3.6. Scope of aniline deamination obtained by Dr. Balu Dherange.

3.2.4. Additional Synthetic Applications.

Leelamine (**44**) is a diterpene natural product derived from pine trees that has been used as a building block for total syntheses due to its affordability and chiral quaternary centres. For the total synthesis of Chamobtusin A (**46**), Leelamine was first deaminated to give Abietatriene (**45**) – a precursor which is not commercially available (Scheme 3.13).[31] This deamination required formylation, followed by dehydration to an isonitrile species, which was subsequently reduced under harsh conditions using potassium metal. We envisaged the synthesis of Abietatriene in a single step from Leelamine to dramatically simplify its use as a precursor in natural product

synthesis. Excitingly, when Leelamine was treated with **1**, Abietatriene was isolated in 65% yield (Scheme 3.14).

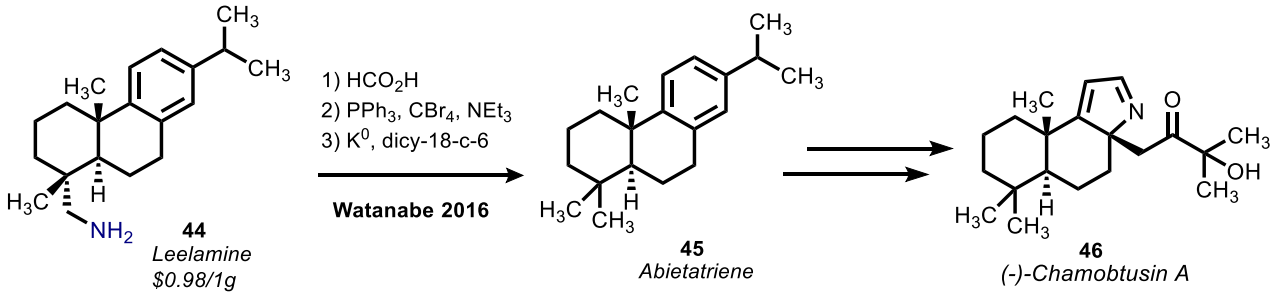

Scheme 3.13. Literature synthesis of (-)-Chamobtusin A from Leelamine involving a three-step deamination.

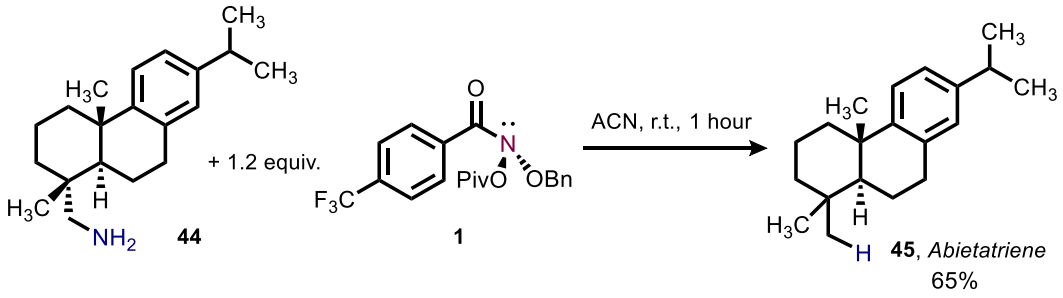

Scheme 3.14. Conversion of Leelamine to Abietatriene in a single step with **1**.

There is a constant need for the development of new antibiotic derivatives. Amines play an interesting role in this field, with a recent study showing that the addition and subtraction of amino moieties can alter whether an antibiotic targets gram-positive or gram-negative bacteria.[32] β-Lactam antibiotics are a common class of antibiotics which includes cephalosporin. Deaminated derivatives of cephalosporin serve as β-lactamase inhibitors which are often co-administered with β-lactam antibiotics to combat antibiotic resistance.[33] Des-amino β-lactam derivatives (**48**) are traditionally synthesized by diazotization of the parent amine (**47**) followed by substitution with bromide and reduction with zinc metal or tin hydride (Scheme 3.15).[34] Diazonium salts are not

desirable synthetic intermediates due to their instability and thus we sought to develop an improved synthesis using our methodology. 7-β-Amino-deacetoxy-cephalosporanic acid *tert*-butyl ester (**48-O*t*Bu**) was deaminated in 43% yield when treated with **1** (Scheme 3.16). The reaction required an elongated time of 16 hours, likely due to the steric bulk of the substrate.

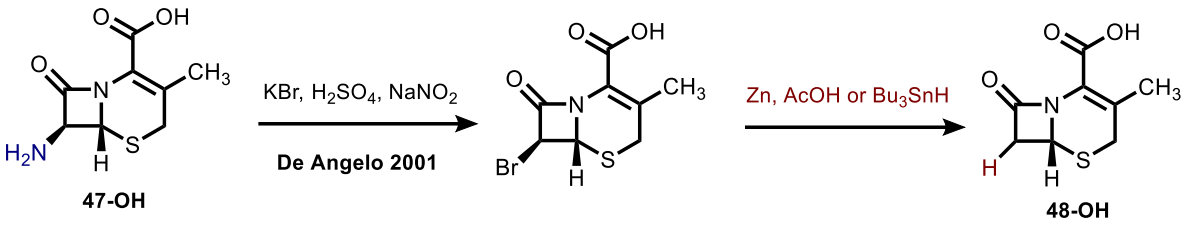

Scheme 3.15. Literature deamination of β-lactam derivatives requires diazotization and reduction.

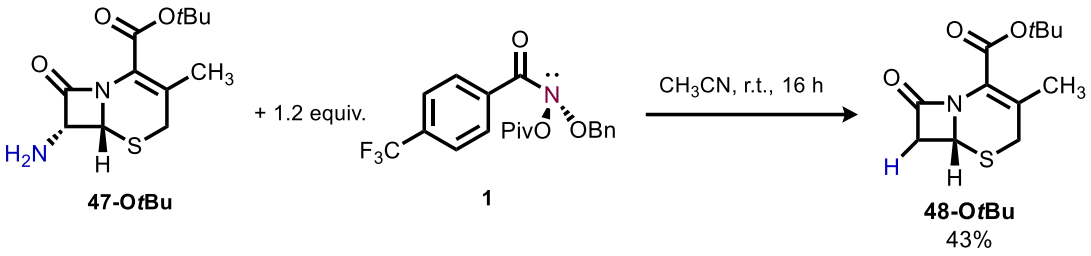

Scheme 3.16. Deamination of 7-β-amino-deacetoxy-cephalosporanic acid *tert*-butyl ester in a single step.

One further application of this methodology involves enabling new synthetic strategies. Reductive amination of ketones is commonly used to synthesize primary amines and thus we envisaged a net conversion of ketones to alkanes using **1**. Gratifyingly, ketone **49** was converted to amine **50** in 97% yield by reductive amination and subsequently deaminated to give the desired alkane (**51**) in 55% yield (Scheme 3.17). In contrast, the direct reduction of a ketone to an alkane using Clemmensen or Wolff-Kishner protocols requires very harsh conditions that would not be suitable for many of the functional groups tolerated by our late-stage deamination procedure.[35]

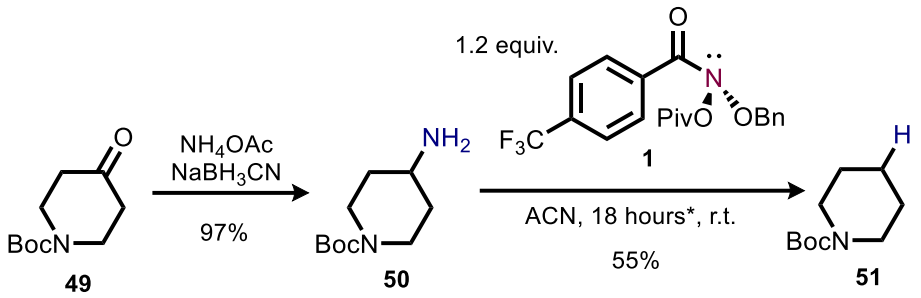

Scheme 3.17. Deoxygenation of ketones in two steps using **1**. *reagent solution added over 3.2 hours using a syringe pump.

Another synthetic application is the net conversion of a nitrile to a methyl group. A Strecker reaction of morpholine and cycloheptanone results nitrile **52**, which can be converted to an α-tertiary amine (**53**) upon reduction.[36] Deamination of **53** resulted in conversion to the requisite methyl analogue (**54**) in 67% yield (Scheme 3.18).

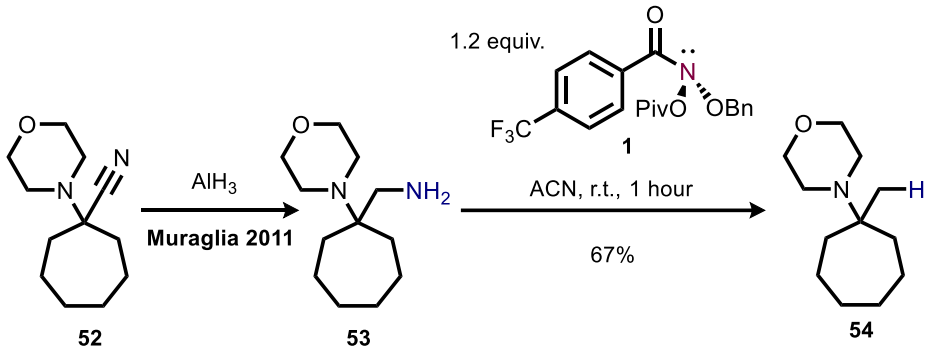

Scheme 3.18. Conversion of a nitrile to a methyl group in two steps using **1**.

Amines are also commonly used as directing groups in metal catalyzed C-H bond activation.[37, 38] We were inspired by a report from Young which uses catalytic palladium to achieve γ-C-H arylation of primary amines.[39] This procedure was used to synthesize **56** from amine **55,** which was then deaminated with **1** (Scheme 3.19). The ability to subsequently remove a primary amine directing group enables a traceless C-H functionalization.

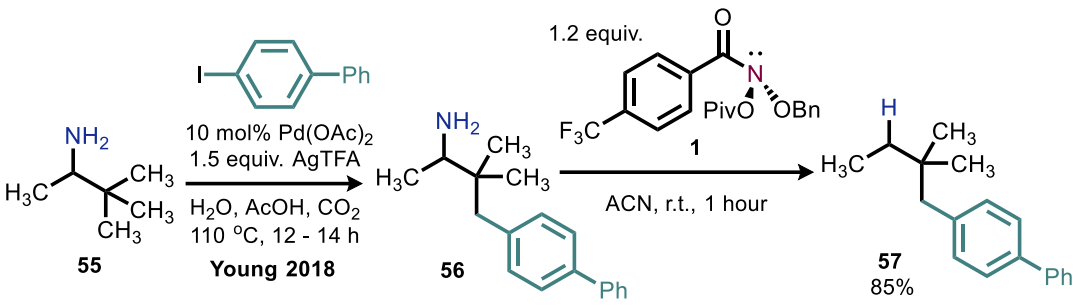

Scheme 3.19. Traceless amine directed C-H arylation.

3.2.5. Mechanistic Studies.

Having thoroughly probed the reaction scope and demonstrated several important synthetic applications, we turned our attention to mechanistic studies. Analogous to secondary amine deletion, primary amines are anticipated to undergo nucleophilic substitution with **1**. The resulting intermediate is then presumed to undergo a rearrangement to yield the proposed primary isodiazene intermediate (see Scheme 3.3). However, the observation in section 3.2.3 that benzylic amines undergo the same 1,2-rearrangement as primary diazene intermediates raised the question as to whether a diazene species was instead generated under our reaction conditions. To probe this, a direct comparison to the Myers allene synthesis[40] was conducted using propargylic alcohol **58** and propargylic amine **60**. The Myers procedure gave allene (**59**) to alkyne (**59'**) products in a ratio of 140 +/- 30 : 1 (Scheme 3.20), whereas the deamination procedure gives the respective products in a ratio of 8.3 +/- 0.6 : 1 (Scheme 3.21). This large difference in the ratio of products suggests that the reaction does not proceed *via* the same intermediate. Work by our computational collaborators Prof. Osvaldo Gutierrez and Mingbin Yuan has shown that rearrangement of a primary isodiazene intermediate to a primary diazene moiety by a 1,2-hydride shift is 50 kcal/mol uphill in energy.[41]

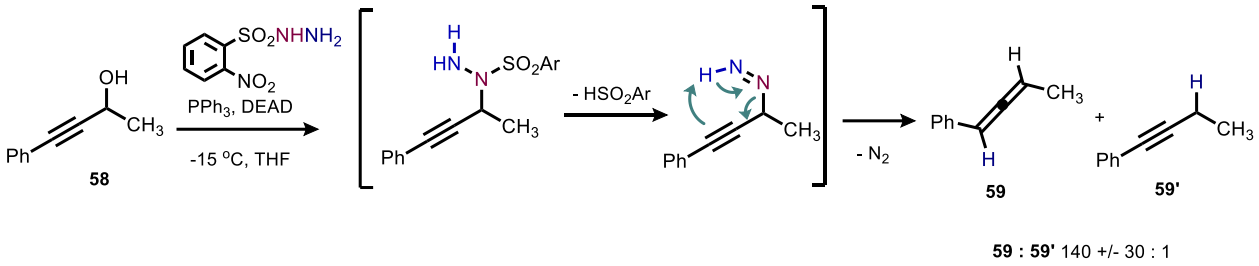

Scheme 3.20. Myers allene synthesis with propargylic alcohol **58** and resulting ratio of products.

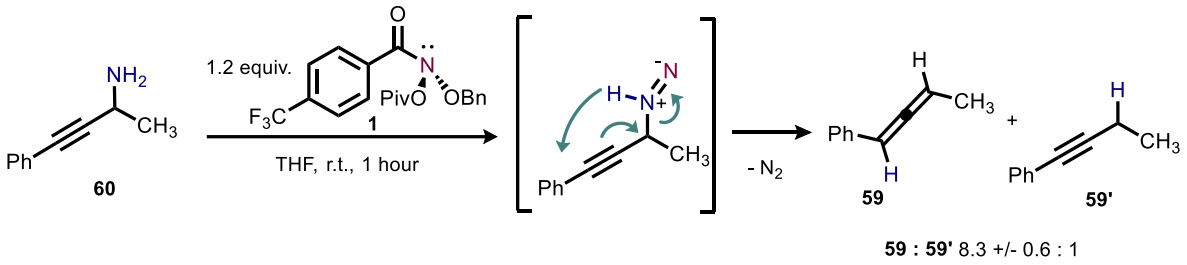

Scheme 3.21. Deamination of propargylic amine **60** with **1** and resulting ratio of products.

Upon generation of a primary isodiazene intermediate, the liberation of dinitrogen results in the reductive deamination product. The preliminary work discussed in section 3.2.1 showed that deamination of deuterated primary amine **2-D$_2$** resulted in deuterium-incorporated deaminated product. This suggested that the source of the hydrogen atom in the product is from the amine -NH_2 and resulting isodiazene intermediate. Working in collaboration with Julia Driscoll, she was able to further demonstrate this deuterium incorporation with a non-benzylic amine substrate (**10-D$_2$**). The percent of deuterium incorporation was variable, ultimately due to sensitivity to adventitious water. Excitingly, *in-situ* deuteration of primary amines and deuterium incorporation into the deaminated product was realized by adding 4% D_2O to the reaction mixture (Table 3.7).

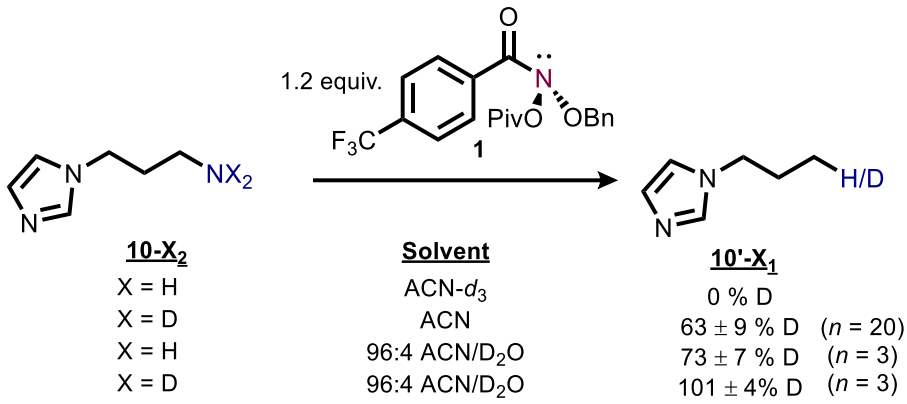

Table 3.7. Percent deuterium incorporation into deaminated product obtained by Julia Driscoll.

We were subsequently interested in whether the nature of this rearrangement to lose dinitrogen proceeded *via* a radical mechanism. Julia Driscoll was able to show that radical clock substrate **61** rearranged upon deamination, providing evidence for a radical intermediate (Scheme 3.22). This clock rearranges with a rate of 4.9 x 10^7 s^{-1},[42] which is slower than the rate that radical species can diffuse from the solvent cage. This finding suggests that free radical species are formed during the reaction, in contrast to secondary amine deletion which was shown to proceed *via* an in-cage recombination. Julia also detected TEMPO trapped adducts of alkyl radicals derived from **10** and **6** as the sole products of the reaction when this radical scavenger was added. No reductive deamination product was observed under these conditions.

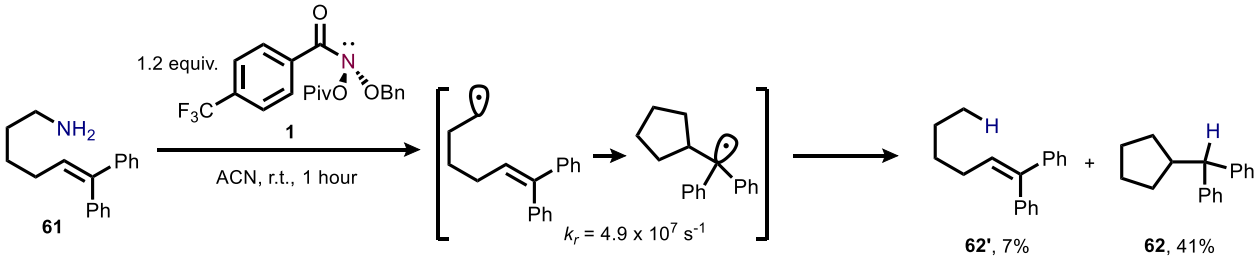

Scheme 3.22. Aliphatic amine clock substrate rearranges suggesting radical intermediates by Julia Driscoll.

Working in collaboration with Dr. Balu Dherange, the deamination of aromatic amines was also demonstrated to proceed *via* a radical mechanism. Using an analogous aromatic amine radical clock substrate (**63**),[42] the rearranged product **64** was detected in 72% yield (Scheme 3.23). TEMPO trapping experiments with 4-methylaniline (**65**) also resulted in the isolation of TEMPO trapped adducts.

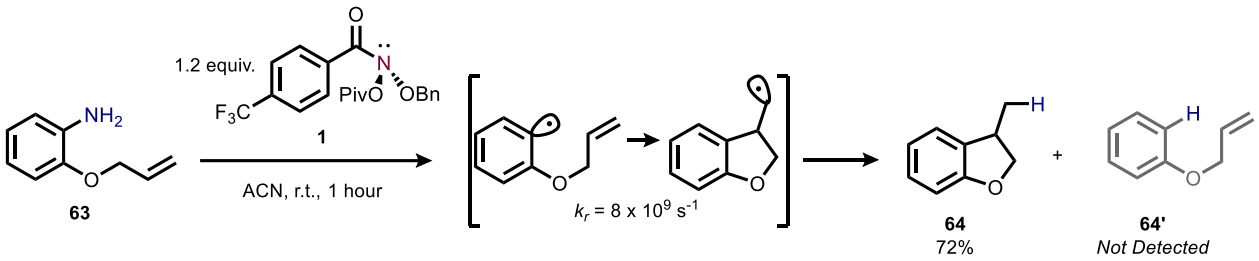

Scheme 3.23. Aromatic amine clock substrate rearranges suggesting radical intermediates by Dr. Balu Dherange.

In collaboration with Professor Osvaldo Gutierrez and Mingbin Yuan, the mechanism was also probed computationally at the DLPNO-CCSD(T) level of theory and provided evidence for a radical chain mechanism (Figure 3.3).[41] Calculations show that following nucleophilic substitution, alkoxyhydrazine **A** undergoes an asynchronous, concerted reductive elimination to afford an isodiazene intermediate **B**. Radical chain initiation occurs from the isodiazene to generate an alkyl radical species (**D**) which undergoes propagation with **B** by an exceptionally fast hydrogen atom transfer process. The resulting diazenyl radical **C** can liberate dinitrogen and regenerate propagating alkyl radical species **D**. Non-chain termination between **D** and **E** was predicted to be diffusion controlled or essentially barrierless, however the high barrier to initiation and experimental evidence of free radical species suggests that an exclusively non-chain pathway would be unlikely.

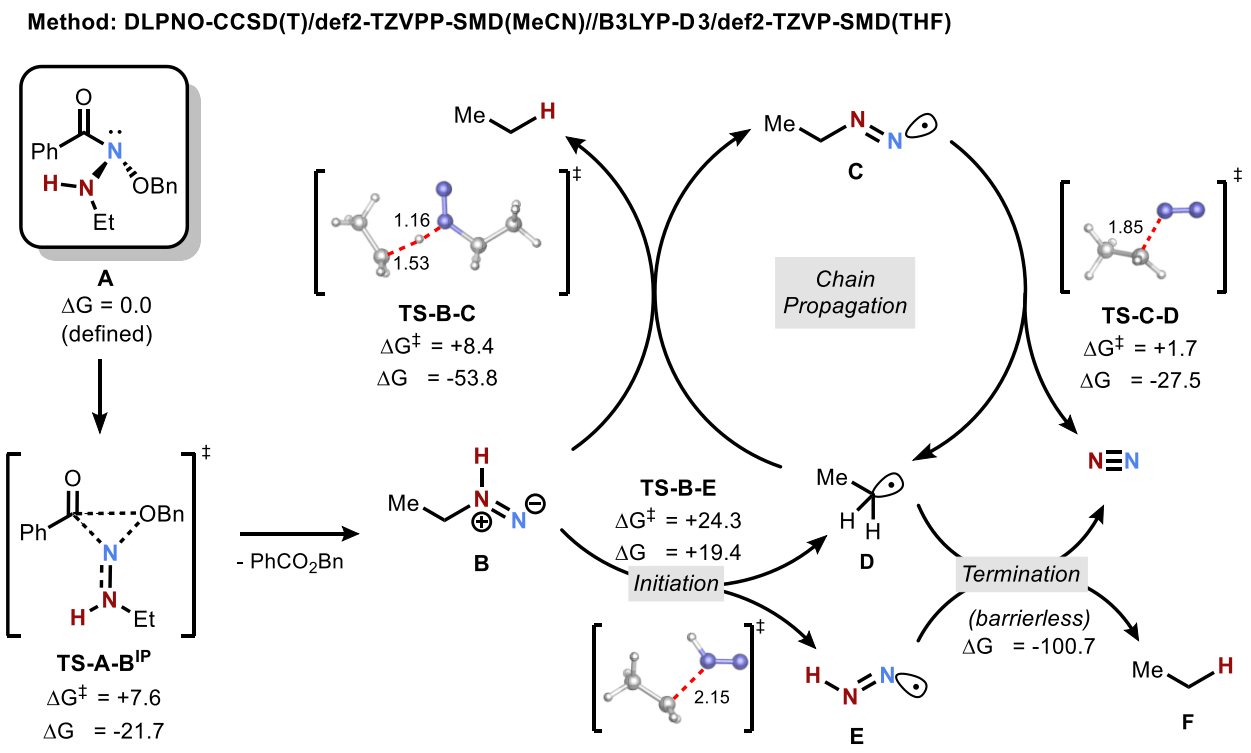

Figure 3.3. Computational mechanism by Mingbin Yuan shows evidence for a radical chain pathway.

Having verified the reaction proceeds by a free radical mechanism, we were interested in intercepting deaminated alkyl species with radical acceptors. This would result in the net conversion of a C-N bond to a C-C or C-heteroatom bond. Electron deficient olefins such as diethyl ethylidene malonate and ethyl acrylate were added, with the hope of obtaining Giese coupling of deaminated alkyl radical species. However, these attempts were largely unsuccessful, with unwanted Michael addition of amine starting material with the activated alkene moieties. Minisci type coupling was also pursued using isoquinoline as the radical acceptor. The addition of ten equivalents of isoquinoline did not result in any radical trapped adducts. It was reasoned that increasing the concentration of this radical acceptor would favour the Minisci coupled product

(**67**). However, when the reaction was run above 0.5 M, unwanted side production of the corresponding *N*-alkyl-4-(trifluoromethyl)benzamide derivative **66** was observed (Scheme 3.24).

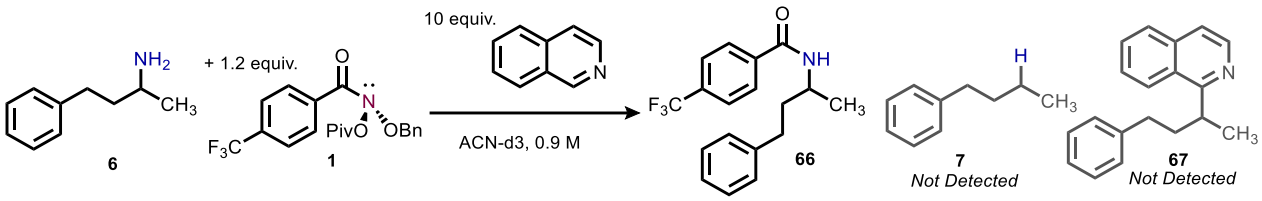

Scheme 3.24. Unsuccessful Minisci coupling resulting in *N*-alkyl-4-(trifluoromethyl)benzamide product derivative.

3.3. Conclusion.

This chapter has presented a novel reaction for the direct deamination of primary amines. In contrast to the previously reported strategies for this transformation, the present method exhibits exceptional functional group tolerance and proceeds rapidly under mild conditions without need for pre-functionalization of the amine. A substrate scope containing multiple pharmaceuticals and biomolecules was developed.

Several synthetic applications of this methodology were presented. These include single step routes to both the natural product precursor Abietatriene and the antibiotic class of des-aminocephalosporins. The use of deamination for other synthetic strategies was explored, including ketone deoxygenation and the conversion of nitriles to methyl isosteres. Traceless C-H arylation was also demonstrated using amine directed palladium catalyzed C-H arylation and subsequently deleting the amine.

Deuterium labelling studies showed that the source of the hydrogen atom in the product is from the primary amine -NH_2. Additionally, mechanistic endeavors provided evidence for a previously unknown primary isodiazene intermediate which participates in radical chain

processes. This is a diversion from the mechanism observed for secondary amine deletion, in which free radical species are not generated. In comparison with secondary amine deletion, the primary amine deletion was also shown to proceed at a faster rate. This is an interesting observation considering that secondary amines are more nucleophilic than primary amines. While steric constraints may play a role in this discrepancy, it is possible that the initial nucleophilic substitution of **1** is not the rate determining step. The free radical nature of primary amine substitution may also account for the difference in rate, if the propagating isodiazene and diazenyl intermediates accumulate in concentration during the chain reaction. These hypotheses are the subject of additional computational studies. Future work will also focus on trapping the alkyl radical species to facilitate the conversion of C-N to C-C and C-heteroatom bonds. Initial attempts with heteroarenes and electron-deficient olefins were largely unsuccessful, however there are many other moieties that have been demonstrated to intercept radical intermediates that can be explored.

3.4. Experimental.

3.4.1. General Procedures.

Unless noted otherwise, all reactions were performed in oven-dried or flame-dried glassware under an atmosphere of dry N_2. THF, Et_2O, DCM, Toluene, ACN, Et_3N, and Pentane were dried by passing these previously degassed solvents through a PPT Solvent Purificatiton System, and all other solvents were dried over molecular sieves (4 Å) and degassed prior to use or purchased anhydrous and sealed under N_2 (e.g. VWR Dri-solv or equivalent). Reaction temperatures were reported as the temperatures of the bath surrounding the flasks or vials. Sensitive reagents and solvents were transferred under nitrogen into a nitrogen-filled glovebox with standard techniques. Unless otherwise noted, all reagents were used as received. Analytical

thin-layer chromatography (TLC) was carried out using 0.2 mm commercial silica gel plates (silica gel 60, F254) and visualized by UV irradiation or staining as indicated.

Low resolution mass spectra were recorded on either an Agilent 6530 LC Q-TOF mass spectrometer using electrospray ionization with fragmentation voltage set at 115 V or an Agilent SQ GC-MMS with a 7890B GC using an Agilent HP-5MS column with a temperature gradient of 50 ^{o}C to 200 ^{o}C over 15 minutes and a 5977A single quad MS using electron ionization. High resolution mass spectra were recorded on either an Agilent 6224 TOF High Resolution Accurate MS with electrospray ionization or an Agilent 7200B QTOF High Resolution Accurate Mass GCMS using an Agilent HP-5MS column with a temperature gradient of 50 ^{o}C to 200 ^{o}C over 15 minutes and electron ionization. All mass spectra were processed with an Agilent MassHunter Operating System. Nuclear magnetic resonance spectra (^{1}H-NMR, ^{13}C-NMR and ^{19}F-NMR) were recorded with Bruker spectrometers operating at 400 or 500 MHz for ^{1}H. Chemical shifts are reported in parts per million (ppm, δ), downfield from tetramethylsilane (TMS, δ=0.00 ppm) and are referenced to residual solvent ($CDCl_3$, δ=7.26 ppm (^{1}H) and 77.160 ppm (^{13}C)). Coupling constants were reported in Hertz (Hz). Data for ^{1}H-NMR spectra were reported as follows: chemical shift (ppm, s = singlet, d = doublet, t = triplet, q = quartet, quin = quintet, dd = doublet of doublets, td = triplet of doublets, ddd = doublet of doublet of doublets, m = multiplet, coupling constant (Hz), and integration).

N-(benzyloxy)-*N*-(pivaloyloxy)-4-(trifluoromethyl)benzamide) (**1**) was prepared according to the optimized procedure in chapter 4. 2-Aminocaprolactam HCl (**32**) was synthesized from lysine according to the literature with the exception that ethylene glycol was used as solvent.[26] 7-amino-3-methyl-8-oxo-5-thia-1-azabicyclo[4.2.0]oct-2-ene-2-carboxylic acid *tert*-butyl ester (**47-O*t*Bu**) was synthesized from 7-aminocephalosporanic acid (**47-O*t*Bu**) according to the

literature.[43] 4-(1,1'-biphenyl-4-yl)-3,3-dimethylbutan-2-amine (**56**) was synthesized according to the literature.[39] 4-phenyl-but-3-yn-2-ol (**58**) and 4-phenylbut-3-yn-2-amine (**60**) were synthesized according to the literature procedures.[44, 45] Leelamine (**44**) was purified according to the literature procedure.[46] 6,6-diphenylhex-5-en-1-amine (**61**) was synthesized according to the literature procedure from ethyl 6-bromohexanoate.[47] Unless otherwise specified, all amines were purchased from the appropriate suppliers and used without further purification. Rimantidine HCl (**17**), Primaquine phosphate (**14**), Oseltamivir phosphate (**15**), Sitagliptin phosphate (**18**), β-1,3,4,6-tetra-O-acetyl-D-glucosamine HCl (**β-38**), phenylalanine methyl ester HCl (**28**) and tryptophan methyl ester HCl (**29**) were freebased before use according to the following procedure: the amine HCl salt was suspended in DCM, 1 M NaOH solution was added and the amine was extracted to DCM, washed with brine, dried over sodium sulfate, filtered and the volatiles were removed *in vacuo*. Lysine methyl ester dihydrochloride (**20**) and excess cesium carbonate were suspended in acetonitrile, stirred for 4 hours and filtered with a sintered glass frit. The filtrate was collected and the solvent was removed *in vacuo* to yield freebase lysine methyl ester.

3.4.2. Isolation of Deaminated Substrates.

General procedure: To a round bottom flask equipped with a stir bar under a nitrogen atmosphere was added the anomeric amide reagent (1.2 equiv.) and anhydrous acetonitrile. Under a nitrogen atmosphere, the primary amine (1 equiv.) was dissolved anhydrous acetonitrile and the solution of amine was added dropwise over 10 minutes to the flask containing the anomeric amide reagent. For select reactions, the reverse addition was performed as noted. The total volume of solvent is such that the concentration of anomeric amide in the reaction is 0.1 M. The reaction was stirred at room temperature for 1 hour. The reaction was quenched with saturated aqueous $NaHCO_3$ solution and extracted to DCM. The combined organic layers were washed with brine

and dried with sodium sulphate. The volatiles were removed *in vacuo* and the crude product purified by silica gel chromatography.

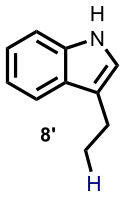

3-ethyl-1H-indole (8'): Synthesized according to the general procedure from tryptamine (**8**) (56 mg, 0.365 mmol). The title compound was obtained in 65% yield (34 mg, 0.237 mmol) after purification by silica gel chromatography. $\mathbf{R_f}$ = 0.45 (1:1 hexanes/EtOAc). **^{1}H NMR** (400 MHz, $CDCl_3$): δ 7.89 (br s, 1H), 7.62 (d, J = 7.8 Hz, 1H), 7.36 (d, J = 8.3 Hz, 1H), 7.19 (dt, J = 8.3 Hz, 1.0 Hz, 1H), 7.11 (dt, J= 7.6 Hz, 0.9 Hz, 1H), 6.98 (m, 1H), 2.80 (qd, J = 7.2 Hz, 1.1 Hz, 2H), 1.34 (t, J = 7.5 Hz, 3H). Spectroscopic data are in agreement with those in the literature.[48]

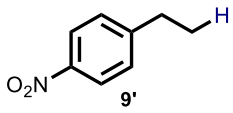

1-ethyl-4-nitrobenzene (9'): Synthesized according to the general procedure by Julia Driscoll from 2-(4-nitrophenyl)ethan-1-amine (**9**) (47.5 mg, 0.286 mmol). The title compound was obtained in 55% yield (23.7 mg) after purification by silica gel chromatography. $\mathbf{R_f}$ = 0.67 (6:4 hexanes/EtOAc). **^{1}H NMR** (400 MHz, CDCl3) δ 8.14 (d, J = 8.7 Hz, 2H), 7.34 (d, J = 8.8 Hz, 2H), 2.76 (q, J = 7.6 Hz, 2H), 1.28 (t, J = 7.6 Hz, 3H). Spectroscopic data are in agreement with those in the literature.[49]

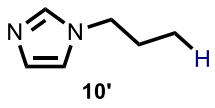

1-propyl-1H-imidazole (10'): Synthesized according to the general procedure by Julia Driscoll from 3-(1H-imidazol-1-yl)propan-1-amine (**10**) (146.9 mg, 1.17 mmol). The title compound was obtained in 81% yield (105.03 mg) after purification by silica gel chromatography. $\mathbf{R_f}$ = 0.56 (6:4 hexanes/EtOAc). **^{1}H NMR** (400 MHz, CD_3CN): δ7.43 (s, 1H), 6.99 (d, J = 1.2 Hz, 1H), 6.90 (d, J = 1.1 Hz, 1H), 3.89 (t, J = 7.1 Hz, 2H), 1.74 (h, J = 7.3 Hz, 2H), 0.85 (t, J = 7.4 Hz, 3H). Spectroscopic data are in agreement with those in the literature.[50]

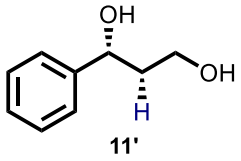

11'

***(R)*-1-phenylpropane-1,3-diol (11'):** Synthesized according to the general procedure by Julia Driscoll from (1S,2S)-2-amino-1-phenyl-1,3-diol (**11**) (35.4 mg, 0.212 mmol), by slow addition of the anomeric amide reagent solution to the solution of (1S,2S)-2-amino-1-phenyl-1,3-diol. The title compound was obtained in 74% yield (24.0 mg) with full stereo-retention after purification by silica gel chromatography. $\mathbf{R_f}$ = 0.17 (6:4 hexanes/EtOAc). **^{1}H NMR** (400 MHz, 1:1 MeOD/CDCl3) δ 7.35 – 7.26 (m, 4H), 7.24 – 7.17 (m, 1H), 4.81 (dd, J = 8.4, 4.8 Hz, 1H), 3.75 – 3.60 (m, 2H), 2.01 – 1.83 (m, 2H). Spectroscopic data are in agreement with those in the literature.[51] A racemic sample of 1-phenylpropane-1,3-diol was synthesized according to the literature procedure from ethyl benzoyl acetate.[52] Both the enantiopure and racemic diol samples were then converted to 2,2-dimethyl-4-phenyl-1,3-dioxane by treatment with camphorsulfonic acid (10 mol%) in 2,2-dimethoxypropane (50 mL/mg) for 20 h at room temperature. The enantiomeric excess of the chiral sample was then determined to be 99 using a chiral Agilent 6850 Network GC System with an Agilent J&W cycloSil-B GC 30 m, 0.25 mm, 0.25 µm, 7 inch cage column.

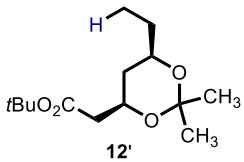

12'

***tert*-butyl 2-((*4R,6R*)-6-ethyl-2,2-dimethyl-1,3-dioxan-4-yl)acetate (12'):** Synthesized according to the general procedure from (4R,6R)-*tert*-Butyl-6-(2-aminoethyl)-2,2-dimethyl-1,3-dioxane-4-acetate (**12**) (200 mg, 0.732 mmol). As separating the title compound from benzyl 4-(trifluoromethyl)benzoate is difficult by column chromatography, saponification of benzyl 4-(trifluoromethyl)benzoate to sodium 4-trifluoromethylbenzoate was performed. After the standard workup, the crude product mixture was dissolved in 9 ml of 3:1 THF:H_2O in a round bottom flask equipped with a stir bar. NaOH (0.8 equiv., 23.4 mg, 0.59 mmol) was added and the solution was refluxed for 3 hours. The solvent was removed *in vacuo* and 10 ml diethyl ether was added to the residue, resulting in a dark yellow

precipitate. The precipitate was removed by filtration, the filtrate containing the title compound was collected and the solvent was removed *in vacuo*. The crude residue was purified by silica gel chromatography, yielding the title compound in 63% yield (189 mg, 0.461 mmol). $\mathbf{R_f}$ = 0.81 (5:1 hexanes/EtOAc). **^{1}H NMR** (Figure 3.12) (400 MHz, $CDCl_3$): δ 4.27 – 4.20 (m, 1H), 3.78 – 3.72 (m, 1H), 2.46 – 2.26 (m, 2H), 1.57 (dt, J = 11.9 Hz, 3.1 Hz, 1H), 1.55 – 1.48 (m, 1H), 1.45 (s, 12H), 1.38 (s, 3H), 1.14 (q, J = 12.2 Hz, 2H), 0.90 (t, J = 7.6 Hz, 3H). **^{13}C{^{1}H}** NMR (Figure 3.13) (101 MHz, $CDCl_3$): δ 170.4, 98.6, 80.6, 70.2, 66.3, 42.8, 36.0, 30.2, 29.7, 29.2, 28.1, 19.8, 9.3. **HR-MS** (ESI) calculated 258.1831 for $C_{14}H_{26}O_4$, found 258.1827.

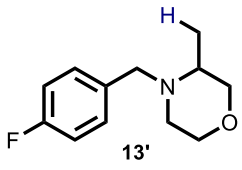

13'

4-[(4-fluorophenyl)methyl]-3-methylmorpholine (13'): Synthesized according to the general procedure from 3-aminomethyl-4-(4-fluorobenzyl)morpholine (**13**) (100 mg, 0.446 mmol). The title compound was obtained in 94% yield (88 mg) after purification by silica gel chromatography. $\mathbf{R_f}$ = 0.42 (5:1 hexanes/EtOAc). **^{1}H NMR** (Figure 3.14) (400 MHz, $CDCl_3$): δ 7.32 – 7.27 (m, 2H), 7.01 (t, J = 8.9 Hz, 2H), 3.87 – 3.81 (m, 1H), 3.73 – 3.60 (m, 2H), 3.51 – 3.44 (m, 2H), 2.73 – 2.62 (m, 2H), 2.15 (t, J = 9.4 Hz, 1H), 1.83 (t, J = 11 Hz, 1H), 1.13 (d, J = 6.1 Hz, 3H). **^{13}C{^{1}H}** NMR (Figure 3.15) (101 MHz, $CDCl_3$): δ 162.1 (d, $^1J_{C\text{-}F}$ = 246 Hz), 130.7 (d, $^3J_{C\text{-}F}$ = 8 Hz), 115.1 (d, $^2J_{C\text{-}F}$ = 21 Hz), 71.8, 66.7, 62.4, 59.9, 52.8, 19.1. **^{19}F{^{1}H}** NMR (Figure 3.16) (376 MHz, $CDCl_3$): δ -115.7. **HR-MS** (ESI) calculated 209.1216 for $C_{12}H_{16}FNO$, found 209.1215.

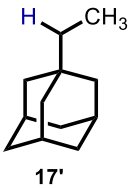

17'

1-ethyladamantane (17'): Synthesized according to the general procedure from rimantadine (**17**) (103 mg, 0.574 mmol). The title compound was obtained in 50% yield (47 mg, 0.287 mmol) after purification by silica gel chromatography. $\mathbf{R_f}$ = 0.8 (5:1 hexanes/EtOAc). **^{1}H NMR** (400 MHz, $CDCl_3$): δ 1.94 (br s, 3H), 1.73 – 1.57 (m, 6H), 1.44

(m, 6H), 1.08 (q, J = 9.0 Hz, 2H), 0.77 (t, J = 8.3 Hz, 3H). Spectroscopic data are in agreement with those in the literature.[53]

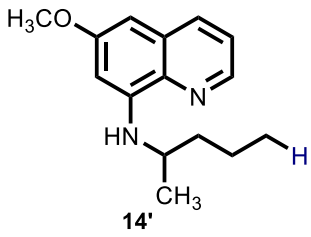

14'

6-methoxy-*N*-(pentan-2-yl)quinolin-8-amine (14'): Synthesized according to the general procedure from primaquine (**14**) (100 mg, 0.386 mmol). The title compound was obtained in 53% yield (49.8 mg, 0.205 mmol) after purification by silica gel chromatography $\mathbf{R_f}$ = 0.58 (5:1 hexanes/EtOAc). **^{1}H NMR** (Figure 3.17) (400 MHz, $CDCl_3$): δ 8.53 (dd, J = 4.1 Hz, 1.6 Hz, 1H), 7.92 (dd, J = 8.33, 1H), 7.32 – 7.28 (m, 1H), 6.33 – 6.28 (m, 2H), 6.02 (br m, 1H), 3.89 (s, 3H), 3.65 – 3.57 (m, 1H), 1.76 – 1.67 (m, 1H), 1.61 – 1.39 (m, 2H), 1.29 (d, J = 6.2 Hz, 3H), 0.94 (t, J = 7.2 Hz, 3H). **^{13}C{^{1}H}** NMR (Figure 3.18) (101 MHz, $CDCl_3$): δ 159.6, 145.3, 144.4, 135.6, 134.9, 130.0, 121.9, 96.6, 91.5, 55.3, 48.0, 39.2, 20.6, 19.6, 14.3. **HR-MS** (ESI) calculated 244.1576 for $C_{15}H_{20}N_2O$, found 244.1594.

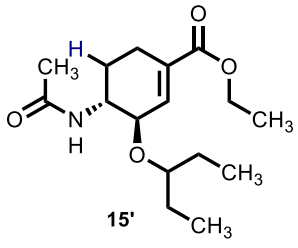

15'

ethyl (*3R,4R*)-4-acetamido-3-(pentan-3-yloxy)cyclohex-1-ene-1-carboxylate (15'): Synthesized according to the general procedure from oseltamivir (**15**) (88 mg, 0.282 mmol) with the exception of a reaction time of 5 hours. The solution of anomeric amide was added dropwise to the solution of oseltamivir and the reaction was stirred at r.t. for 5 hours. The title compound was obtained in 53% yield (44 mg, 0.149 mmol) after purification by silica gel chromatography. $\mathbf{R_f}$ = 0.56 (1:2 hexanes/EtOAc). **^{1}H NMR** (Figure 3.19) (400 MHz, $CDCl_3$): δ 6.84 – 6.81 (m, 1H), 5.41 (d, J = 8.1 Hz, 1H), 4.20 (q, J = 7.6 Hz, 2H), 4.11 – 4.05 (m, 1H), 3.88 – 3.84 (m, 1H), 3.45 (q, J = 6.2 Hz, 1H), 2.53 – 2.43 (m, 1H), 2.27 – 2.16 (m, 1H), 2.09 – 1.99 (m, 1H), 1.96 (s, 3H), 1.81 – 1.72 (m, 1H), 1.58 – 1.46 (m, 4H), 1.29 (t, J = 7.4 Hz, 3H), 0.91 (q, J = 7.4 Hz, 6H). **^{13}C{^{1}H}** (Figure 3.20) (101 MHz, $CDCl_3$): δ 170.0, 166.9, 135.8, 132.8, 81.7, 72.6, 60.9, 47.8, 26.7, 26.6,

23.7, 23.2, 21.3, 14.3, 10.1, 9.5. **HR-MS** (ESI) calculated 297.1940 for $C_{16}H_{27}NO_4$, found 297.1923.

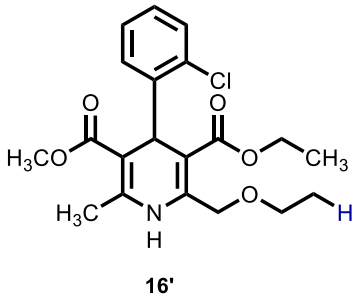

16'

3-ethyl 5-methyl 4-(2-chlorophenyl)-2-(ethoxymethyl)-6-methyl-1,4-dihydropyridine-3,5-dicarboxylate (16'): Synthesized according to the general procedure from amlodipine (**16**) (100 mg, 0.245 mmol). The title compound was obtained in 71% yield (69 mg, 0.174 mmol) after purification by silica gel chromatography. $\mathbf{R_f}$ = 0.21 (1:1 hexanes/EtOAc). **^{1}H NMR** (Figure 3.21) (400 MHz, $CDCl_3$): δ 7.37 (dd, J = 7.9 Hz, 2.0 Hz, 1H), 7.23 (dd, J = 7.8 Hz, 1.3 Hz, 1H), 7.12 (td, J = 7.6, 1.4 Hz, 1H), 7.10 (br s, 1H), 7.06 – 7.01 (m, 1H), 5.40 (s, 1H), 4.69 (q, J = 16.6 Hz, 2H), 4.05 (qd, J = 6.9Hz, 2.4 Hz, 2H), 3.67 – 3.59 (m, 5H), 2.34 (s, 3H), 1.29 (t, J = 7.0 Hz, 3H), 1.18 (t, J = 7.1 Hz, 3H). **^{13}C{^{1}H}** (Figure 3.22) (101 MHz, $CDCl_3$): δ 168.1, 167.2, 145.9, 145.6, 143.8, 132.3, 131.4, 129.4, 129.2, 129.1, 128.8, 127.3, 126.9, 104.0, 101.2, 68.2, 67.4, 67.0, 59.6, 50.8, 37.1, 27.2, 19.6, 15.1, 14.3. **HR-MS** (ESI) calculated 393.1343 for $C_{20}H_{24}ClNO_5$, found 393.1321.

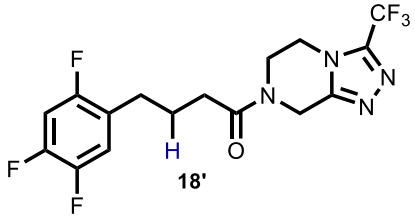

18'

1-(3-(trifluoromethyl)-5,6-dihydro-[1,2,4]triazolo[4,3-*a*]pyrazin-7(8H)-yl-(4(2,4,5-trifluorophenyl)butan-1-one (18'): Synthesized according to the general procedure from sitagliptin (**18**) (200 mg, 0.490 mmol). The title compound was obtained in 52% yield (100 mg, 0.255 mmol) after purification by silica gel chromatography. $\mathbf{R_f}$ = 0.75 (100% EtOAc). **^{1}H NMR** (Figure 3.23) (400 MHz, $CDCl_3$): δ 7.05 – 6.96 (m, 1H), 6.90 – 6.82 (m, 1H), 5.08 – 4.85 (m, 2H), 4.25 – 3.87 (m, 4H), 2.66 (t, J = 7.6 Hz, 2H), 2.43 (t, J = 7.0 Hz, 2H), 2.02 – 1.92 (m, 2H). **^{13}C{^{1}H}** (Figure 3.24a-d) (101 MHz, CD_3CN): δ 172.4, 157.9 (dd, J_{C-F} = 10.0 Hz, 2.5 Hz), 156.0 (dd, J_{C-F}

= 9.6 Hz, 2.4 Hz), 152.2, 151.7, 150.1 (t, J_{C-F} = 13.9 Hz), 148.5 (dd, J_{C-F} = 12.9, 3.7 Hz), 148.2 (t, J_{C-F} = 13.6 Hz), 146.5 (dd, J_{C-F} = 12.3 Hz, 4.3 Hz), 144.2 (q, J_{C-F} = 40.6 Hz), 126.6 (dt, J_{C-F} = 18.6, 5.2 Hz), 119.9 (q, J_{C-F} = 268.7 Hz), 119.2 (dd, J_{C-F} = 19.1, 6.7 Hz), 106.3 (d, J_{C-F} = 20.9 Hz), 106.1 (d, J_{C-F} = 21.1 Hz), 44.7, (major), 44.2 (minor), 43.0 (minor), 42.1 (major), 39.6 (major), 38.7 (minor), 32.8 (minor), 32.5 (major), 28.2 (major), 25.7 (major). **^{19}F{^{1}H}** NMR (Figure 3.25) (376 MHz, $CDCl_3$): δ -63.1, -120.4 (d, J = 16 Hz), -136.6 (d, J = 23 Hz), -143.2 (m). **HR-MS** (ESI) calculated 383.1115, found 383.1119.

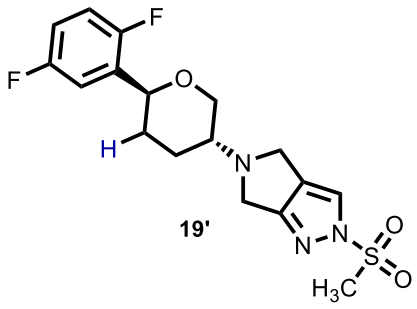

5-((*3R,6S*)-6-(2,5-difluorophenyl)tetrahydro-*2H*-pyran-3-yl)-2-(methylsulfonyl)-2,4,5,6-tetrahydropyrrolo[3,4-*c*]pyrazole (19'): Synthesized according to the general procedure from omarigliptin (**19**) (50 mg, 0.125 mmol). The title compound was obtained in 77% (37 mg, 0.096 mmol) yield after purification by silica gel chromatography. **R_f** = 0.20 (1:1 hexanes: EtOAc). **^{1}H NMR** (Figure 3.26) (400 MHz, $CDCl_3$): δ 7.69 (s, 1H), 7.22 – 7.16 (m, 1H), 7.00 – 6.87 (m, 2H), 4.59 (d, J = 10.6 Hz, 1H), 4.32 (dq, J = 10.7 Hz, 2.4 Hz, 1H), 3.92 – 3.82 (m, 4H), 3.48 (t, J = 11.4 Hz, 1H), 3.27 (s, 3H), 2.91 – 2.82 (m, 1H), 2.28 – 2.20 (m, 1H), 2.10 – 2.02 (m, 1H), 1.70 (qd, J = 12.0 Hz, 3.7 Hz, 1H), 1.59 (qd, J = 13.8 Hz, 3.7 Hz, 1H). **^{19}F{^{1}H}** NMR (Figure 3.27) (376 MHz, $CDCl_3$): δ -118.5 (d, J = 17.8 Hz), -125.6 (d, J = 18.5 Hz). **^{13}C{^{1}H}** NMR (Figure (3.28) (101 MHz, $CDCl_3$): δ 164.2, 159.0 (dd, $^{1}J_{C-F}$ = 242 Hz, $^{4}J_{C-F}$ = 1 Hz), 155.2 (dd, $^{1}J_{C-F}$ = 242 Hz, $^{4}J_{C-F}$ = 1 Hz), 131.4 (dd, $^{2}J_{C-F}$ = 16 Hz, $^{3}J_{C-F}$ = 8 Hz), 124.4, 123.5, 116.2 (dd, $^{2}J_{C-F}$ = 12 Hz, $^{3}J_{C-F}$ = 8 Hz), 115.0 (dd, $^{2}J_{C-F}$ = 13 Hz, $^{3}J_{C-F}$ = 9 Hz), 113.7 (dd, $^{2}J_{C-F}$ = 13 Hz, $^{3}J_{C-F}$ = 5 Hz), 73.2, 71.7, 59.3, 48.7, 48.2, 41.5, 31.7, 29.4. **HR-MS** (ESI) calculated 392.1072, found 392.1089.

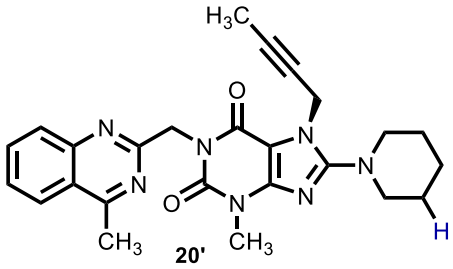

20'

7-(but-2-yn-1-yl)-3-methyl-1-((4-methylquinazolin-2-yl)methyl)-8-(piperidin-1-yl)-3,7-dihydro-1*H*-purine-2,6-dione (20'): Synthesized according to the general procedure from linagliptin (**20**) (10 mg, 0.0212 mmol) with the exception that 1:1 acetonitrile: DMSO was used as the solvent and the reaction was stirred overnight, then washed with 3x 10 ml brine to remove the DMSO. The title compound was obtained in 65% yield (6.3 mg, 0.0138 mmol) after purification by silica gel chromatography. $\mathbf{R_f}$ = 0.3 (1:3 hexanes: EtOAc). **^{1}H NMR** (Figure 3.29) (400 MHz, $CDCl_3$): δ 8.01 (d, J = 8.1 Hz, 1H), 7.89 – 7.84 (m, 1H), 7.78 – 7.73 (td, J = 7.8, 1.5 Hz, 1H), 7.51 (t, J = 7.3 Hz, 1H), 5.56 (s, 2H), 4.85 (m, 2H), 3.55 (s, 3H), 3.40 – 3.35 (m, 3H), 2.88 (s, 3H), 1.81 – 1.58 (m, 10H). **^{13}C{^{1}H}** (Figure 3.30) (101 MHz, $CDCl_3$): δ 168.5, 161.2, 156.9, 154.4, 152.0, 150.0, 148.2, 133.2, 129.0, 126.7, 124.9, 123.2, 81.1, 73.3, 51.2, 46.4, 41.0, 35.9, 29.8, 27.2, 25.8, 24.2, 22.0, 21.8, 3.80. **HR-MS** (ESI) calculated 457.2226 for $C_{25}H_{27}N_7O_2$, found 457.2226.

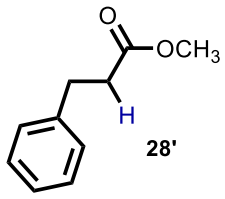

28'

3-phenylpropanoic acid methyl ester (28'): Synthesized according to the general procedure from L-phenylalanine methyl ester (**28**) (100 mg, 0.464 mmol). The title compound was obtained in 96% yield (73 mg, 0.445 mmol) after purification by silica gel chromatography. $\mathbf{R_f}$ = 0.57 (5:1 hexanes/EtOAc). **^{1}H NMR** (400 MHz, $CDCl_3$): δ 7.31 – 7.26 (m, 2H), 7.23 – 7.17 (m, 3H), 3.67 (s, 3H), 2.96 (t, J = 8.3 Hz, 2H), 2.64 (t, J = 7.0 Hz, 2H). Spectroscopic data are in agreement with those in the literature.[54]

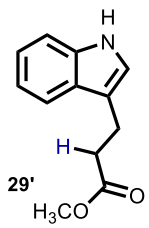

29'

Methyl indole-3-propionate (29'): Synthesized according to the general procedure from L-tryptophan methyl ester (**29**) (100 mg, 0.458 mmol). The title compound was obtained in 71% yield (66 mg, 0.325 mmol) after purification by silica gel chromatography. $\mathbf{R_f}$ = 0.7 (1:5 hexanes/EtOAc). **^{1}H NMR** (400 MHz, $CDCl_3$): δ 7.95

(br s, 1H), 7.61 (d, J = 8.0 Hz, 1H), 7.36 (d, J = 8.0 Hz, 1H), 7.20 (t, J = 7.4 Hz, 1H), 7.12 (t, J = 7.5 Hz, 1H), 7.02 (m, 1H), 3.68 (s, 1H), 3.11 (t, J = 8.2 Hz, 2H), 2.73 (t, J = 7.1 Hz, 2H). Spectroscopic data are in agreement with those in the literature.[55]

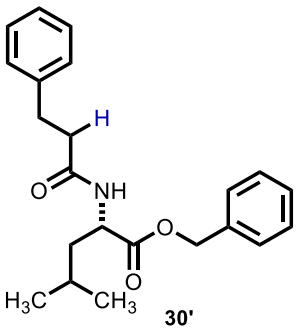

30'

benzyl (3-phenylpropanoyl)-*L*-leucinate (30'): Synthesized according to the general procedure from H-Phe-Leu-OBzl (**30**) (207.6 mg, 0.5634 mmol) with the exception that 1:1 acetonitrile: DMSO as the solvent and the reaction was stirred for 3 hours, diluted with DCM and then washed with 3x 10 ml brine. The volatiles were removed *in vacuo* and crude material was purified by reverse-phase preparative HPLC with an Agilent 5 Prep C18 P/N 446905-702 column using water/acetonitrile with the gradient 0-0.5 min, 10% B; 0.5-10.5 min, 10-95% B; 10.5-11.5 95% B. The title compound was obtained in 21% yield (41.8 mg, 0.1183 mmol), retention time 8.17 min. $\mathbf{R_f}$ = 0.73 (1:1 hexanes/EtOAc). **^{1}H NMR** (Figure 3.31) (400 MHz, $CDCl_3$): δ 7.39 – 7.31 (m, 5H), 7.29 – 7.25 (m 2H), 7.22 – 7.17 (m, 3H), 5.72 (d, J = 8.3 Hz, 1H), 5.15 (s, 2H), 4.71 – 4.64 (m, 1H), 3.03 – 2.91 (m, 2H), 2.59 – 2.46 (m, 2H), 1.64 – 1.40 (m, 3H), 0.89 – 0.85 (m, 6H). **^{13}C{^{1}H}** (Figure 3.32) (101 MHz, $CDCl_3$): δ 173.1, 171.9, 140.8, 135.5, 128.8, 128.7, 128.6, 128.5, 128.4, 126.4, 67.2, 50.9, 41.8, 38.4, 31.6, 24.8, 22.9, 22.1. **HR-MS** (ESI) calculated 353.1991 for $C_{22}H_{27}NO_3$, found 353.1998.

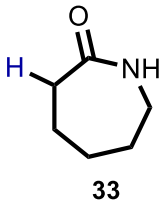

33

caprolactam (33): A 20 ml vial equipped with a stir bar was charged with 2-aminocaprolactam HCl (**32**) (20 mg, 0.121 mmol), 2 ml acetonitrile and cesium carbonate (79 mg, 0.242 mmol, 2 equiv.). Under a nitrogen atmosphere, a 1 ml solution of the anomeric amide reagent (58 mg, 0.146 mmol, 1.2 equiv.) was added dropwise and the reaction was subsequently stirred overnight. The crude reaction mixture was purified by silica gel chromatography and the title compound was obtained in 58% yield (8 mg, 0.07 mmol). $\mathbf{R_f}$ =

0.13 (1:3 hexanes: EtOAc). **^{1}H NMR** (400 MHz, $CDCl_3$): δ 6.29 (br s), 3.19 (q, J = 5.9 Hz, 2H), 2.47 – 2.42 (m, 2H), 1.78 – 1.60 (m, 6H). Spectroscopic data are in agreement with those in the literature.[56]

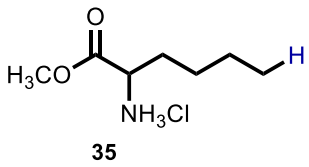

35

norleucine methyl ester hydrochloride (35): Synthesized according to the general procedure from lysine methyl ester (**31-OMe**) (150 mg, 0.936 mmol) with the exception that 0.98 equivalents of anomeric amide was used. After 1 hour, 1.1 equiv. of 4 M HCl in dioxane solution (230 µl) was added dropwise by syringe to the crude reaction mixture. 50 ml of diethyl ether was added and the reaction was extracted with 5x 50 ml water. Water was removed by vacuum and the residue was dissolved in DCM, dried over sodium sulphate, filtered and the volatiles were removed *in vacuo* to give the title compound in 69% yield (117 mg, 0.65 mmol). **^{1}H NMR** (400 MHz, DMSO): δ 8.47 (br s, 3H), 4.03 – 3.97 (m, 1H), 3.75 (s, 3H), 1.83 – 1.74 (m, 2H), 1.40 – 1.21 (m, 4H), 0.87 (t, J = 7.2 Hz, 3H). Spectroscopic data are in agreement with those in the literature.[57]

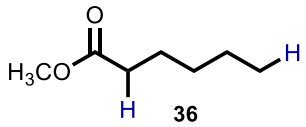

36

methyl hexanoate (36): Synthesized according to the general procedure from lysine methyl ester (**31-OMe**) (20 mg, 0.125 mmol) with the exception that 2.1 equivalents of anomeric amide were used. After 1 hour, internal standard 1,3,5-trimethoxybenzene (6.4 mg, 0.038 mmol) was added and the volatiles were removed *in vacuo* and the residue was dissolved in $CDCl_3$ and the NMR yield of the title compound was determined to be 54%. **^{1}H NMR** (400 MHz, $CDCl_3$): δ 3.66 (s, 3H), 2.30 (t, J = 7.6 Hz, 2H), 1.68 – 1.59 (m, 2H), 1.33 – 1.27 (m, 4H), 0.90 (t, J = 7.2 Hz, 3H). Spectroscopic data are in agreement with those in the literature.[58]

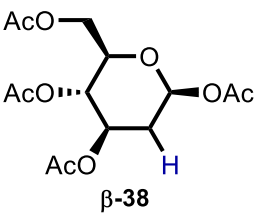

β-38

β-1,3,4,6-Tetra-O-acetyl-2-deoxy-D-glucose (β-38): Synthesized according to the general procedure from β-1,3,4,6-tetra-O-acetyl-D-glucosamine (**37**) (200 mg, 0.576 mmol) with the exception that the reaction was stirred overnight. The title compound was obtained in 78% yield (149 mg, 0.449 mmol) after purification by silica gel chromatography. $\mathbf{R_f}$ = 0.54 (1:1 hexanes: EtOAc). **^{1}H NMR** (400 MHz, $CDCl_3$): δ 5.80 (dd, J = 10.1 Hz, 2.2 Hz, 1H), 5.11 – 5.00 (m, 2H), 4.32 (dd, J = 12.6 Hz, 4.7 Hz,1H), 4.09 (dd, J = 12.3 Hz, 2.4 Hz, 1H), 3.76 – 3.72 (m, 1H), 2.38 – 2.32 (m, 1H), 2.12 (s, 3H), 2.09 (s, 3H), 1.91 – 1.82 (m, 1H). Spectroscopic data are in agreement with those in the literature.[59]

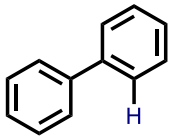

40'

Biphenyl (40'): Synthesized according to the general procedure by Dr. Balu Dherange from 2-aminobiphenyl (**40**) (50 mg, 0.29 mmol) with the exception that 1.5 equiv. of **1** was used and the reaction was heated to 45 ^oC. The title compound was obtained in 61% yield (28 mg, 0.18 mmol) after purification by silica gel chromatography $\mathbf{R_f}$ = 0.7 (24:1 hexanes/EtOAc). **^{1}H NMR** (400 MHz, $CDCl_3$) δ 7.65 – 7.56 (m, 4H), 7.50 – 7.41 (m, 4H), 7.40 – 7.33 (m, 2H). Spectroscopic data are in agreement with those in the literature.[60]

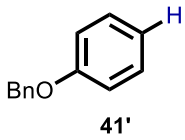

41'

(Benzyloxy)benzene (41'): Synthesized according to the general procedure by Dr. Balu Dherange from 4-benzyloxy aniline (**41**) (40 mg, 0.2 mmol) with the exception that 1.5 equiv. of **1** was used. The title compound was obtained in 53% yield (19.6 mg, 0.11 mmol) after purification by silica gel chromatography $\mathbf{R_f}$ = 0.5 (24:1 hexanes/EtOAc). **^{1}H NMR** (400 MHz, $CDCl_3$) δ 7.49 – 7.43 (m, 2H), 7.43 – 7.37 (m, 2H), 7.37 – 7.28 (m, 3H), 7.05 – 6.94 (m, 3H), 5.08 (s, 2H). Spectroscopic data are in agreement with those in the literature.[61]

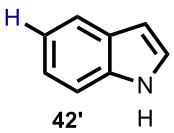

42'

Indole (42'): Synthesized according to the general procedure by Dr. Balu Dherange from 5-aminoindole (**42**) (50 mg, 0.38 mmol) with the exception that 1.5 equiv. of **1** was used and the reaction was heated to 45 °C. The title compound was obtained in 72% yield (32 mg, 0.27 mmol) after purification by silica gel chromatography $\mathbf{R_f}$ = 0.4 (9:1 hexanes/EtOAc). **^{1}H NMR** (400 MHz, $CDCl_3$) δ 8.01 (br. S, 1H), 7.68 (dq, *J* = 7.8, 0.9 Hz, 1H), 7.41 (dq, *J* = 8.1, 1.0 Hz, 1H), 7.25 – 7.19 (m, 2H), 7.15 (ddd, *J* = 8.0, 7.1, 1.1 Hz, 1H), 6.58 (ddd, *J* = 3.2, 2.1, 1.0 Hz, 1H). Spectroscopic data are in agreement with those in the literature.[62]

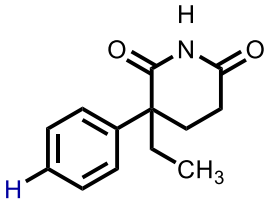

43'

3-ethyl-3-phenylpiperidine-2,6-dione (43'): Synthesized according to the general procedure by Dr. Balu Dherange from aminoglutetimide (**43**) (60 mg, 0.26 mmol) with the exception that 1.5 equiv. of **1** was used and the reaction was heated to 45 °C. The title compound was obtained in 64% yield (36 mg, 0.17 mmol) after purification by silica gel chromatography $\mathbf{R_f}$ = 0.5 (3:2 hexanes/EtOAc). **^{1}H NMR** (Figure 3.33) (400 MHz, $CDCl_3$) δ 8.37 – 7.90 (m, 1H), 7.42 – 7.33 (m, 2H), 7.29 (tt, *J* = 8.3, 1.3 Hz, 3H), 2.68 – 2.54 (m, 1H), 2.47 – 2.34 (m, 2H), 2.23 (td, *J* = 14.0, 4.4 Hz, 1H), 2.07 (dq, *J* = 14.8, 7.4 Hz, 1H), 1.92 (dq, *J* = 14.6, 7.4 Hz, 1H), 0.88 (t, *J* = 7.4 Hz, 3H). **^{13}C{^{1}H} NMR** (Figure 3.34) (101 MHz, $CDCl_3$) δ 175.3, 172.5, 138.9, 129.2, 127.7, 126.3, 51.3, 33.0, 29.4, 27.2, 9.2. **HR-MS** (ESI) calculated 218.1176 for $C_{13}H_{16}NO_2$ (M+H), found 218.1172.

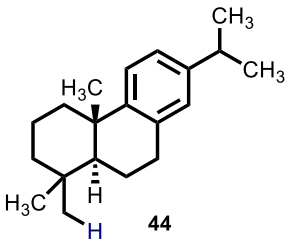

44

Abietatriene (45): Synthesized according to the general procedure from Leelamine (**44**) (100 mg, 0.350 mmol) with the exception that the solution of anomeric amide was added to the solution of Leelamine by careful dropwise addition. The title compound was obtained in 65% yield (62

mg, 0.228 mmol) after purification by silica gel chromatography. $\mathbf{R_f}$ = 0.65 (100% hexanes). **^{1}H NMR** (400 MHz, $CDCl_3$): δ 7.20 – 7.16 (m, 1H), 6.99 (dd, J = 8.4 Hz, 1.5 Hz), 6.89 (m, 1H), 2.96 – 2.78 (m, 3H), 2.27 (d, J = 13.0 Hz, 1H), 1.91 – 1.32 (m, 8H), 1.23 (d, J = 7.2 Hz, 3H), 1.18 (s, 3H), 0.95 (s, 3H), 0.93 (s, 3H). Spectroscopic data are in agreement with those in the literature.[31]

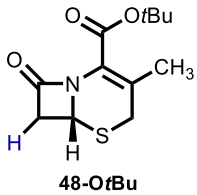

48-O*t*Bu

***tert*-butyl-3-methyl-8-oxo-5-thia-1-azabicyclo[4.2.0]oct-2-ene-2-carboxylate (48-O*t*Bu):** Synthesized according to the general procedure from 7-amino-3-methyl-8-oxo-5-thia-1-azabicyclo[4.2.0]oct-2-ene-2-carboxylic acid *tert*-butyl ester (**47-O*t*Bu**) (40 mg, 0.187 mmol) with the exception that the reaction was stirred overnight. The title compound was obtained in 43% yield (19.8 mg, 0.078 mmol) after purification by silica gel chromatography. $\mathbf{R_f}$ = 0.21 (5:1 hexanes/EtOAc). **^{1}H NMR** (Figure 3.35) (400 MHz, $CDCl_3$): δ 4.65 – 4.63 (dd, J = 5.1 Hz, 2.3 Hz, 1H), 3.57 – 3.48 (m, 2H), 3.14 (d, J = 18.0 Hz, 1H), 2.90 (dd, J = 15.6 Hz, 2.2 Hz, 1H), 2.05 (s, 3H), 1.55 (s, 9H). **^{13}C{^{1}H}** (Figure 3.36) (101 MHz, $CDCl_3$): δ 162.3, 161.3, 125.3, 124.3, 82.7, 48.7, 44.5, 31.5, 28.0, 19.5, 1.0. **HR-MS** (ESI) calculated 255.0929 for $C_{12}H_{17}NO_3S$, found 255.0928.

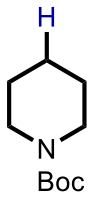

51

***tert*-butyl piperidinecarboxylate (51):** Synthesized according to the general procedure from 1-(*t*-butoxycarbonyl)-4-aminopiperidine (**50**) (20 mg, 0.096 mmol) with the exception that 0.1 M solution of anomeric amide reagent was added dropwise *via* syringe pump to a 0.1 M solution of amine at a rate of 300 µl/h and the reaction was subsequently stirred overnight. The crude reaction mixture was purified by silica gel chromatography and the title compound was obtained in 55% yield (9.8 mg, 0.052 mmol). $\mathbf{R_f}$ = 0.85 (7:3 hexanes/EtOAc). **^{1}H NMR** (400 MHz, $CDCl_3$): δ 3.37 – 3.32 (m, 4H), 1.58 – 1.53 (m, 2H), 1.52 – 1.47 (m, 4H), 1.44 (s, 9H). Spectroscopic data are in agreement with those in the literature.[63]

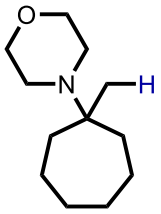

54

4-(1-methylcycloheptyl)morpholine (54): Synthesized according to the general procedure from (1-morpholin-4-ylcycloheptyl)methanamine (**53**) (100 mg, 0.471 mmol). The title compound was obtained in 67% yield (62 mg, 0.316 mmol) after purification by silica gel chromatography. $\mathbf{R_f}$ = 0.4 (1:1 hexanes/ethyl acetate). **^{1}H NMR** (Figure 3.37) (400 MHz, $CDCl_3$): δ 3.71 – 3.66 (m, 4H), 2.54 – 2.50 (m, 4H), 1.82 – 1.75 (m, 2H), 1.64 – 1.55 (m, 4H), 1.53 – 1.44 (m, 2H), 1.43 – 1.28 (m, 4H), 0.90 (s, 3H). **^{13}C{^{1}H}** (Figure 3.38) (101 MHz, $CDCl_3$): δ 68.0, 58.8, 46.3, 38.0, 29.6, 22.9, 22.1. **HR-MS** (ESI) calculated 197.1780 for $C_{12}H_{23}NO$, found 197.1764.

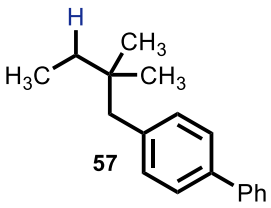

57

2,2-dimethyl-1-biphenylbutane (57): Synthesized according to the general procedure from 4-(1,1'-biphenyl-4-yl)-3,3-dimethylbutan-2-amine (**56**) (16.8 mg, 0.0663 mmol). The title compound was obtained in 85% yield (13.4 mg, 0.056 mmol) after purification by silica gel chromatography. $\mathbf{R_f}$ = 0.5 (100% hexanes). **^{1}H NMR** (400 MHz, $CDCl_3$): δ 7.61 (, J = 7.5 Hz, 2H), 7.51 (d, J = 8.3 Hz, 2H), 7.44 (t, J = 7.8 Hz, 2H), 7.33 (t, J = 7.6 Hz, 1H), 7.21 (J = 8.1 Hz, 2H), 2.55 (s, 2H), 1.31 (q, J = 7.7 Hz, 2H), 0.93 (t, J = 7.4 Hz, 3H), 0.88 (s, 6H). Spectroscopic data are in agreement with those in the literature.[64]

3.4.3. Synthesis of Starting Materials.

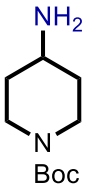

50

***tert*-butyl 4-aminopiperidine-1-carboxylate (50):** To a 50 ml round bottom flask equipped with a stir bar was added 10 ml methanol, 1-Boc-4-piperidone (500 mg, 2.41 mmol), and ammonium acetate (2.23 g, 28.9 mmol, 12 equiv.). The flask was stirred for 10 minutes at room temperature and $NaBH_3CN$ (606 mg, 9.64 mmol, 4 equiv.) was added in a single portion. A reflux condenser was attached to the flask and the reaction was heated at 60 ^{o}C for 16 hours. The flask was cooled to room temperature and the volatiles were removed *in*

vacuo. To the residue was added 30 ml of 1 M NaOH solution and the product was extracted with ethyl acetate (6 x 20 ml), dried over sodium sulfate and the volatiles were removed *in vacuo* to give the title compound in 97% yield (468 mg, 2.33 mmol). **^{1}H NMR** (400 MHz, $CDCl_3$): δ 4.09 – 3.97 (br s, 1H), 3.74 – 3.64 (m, 1H), 2.84 – 2.72 (m, 2H), 1.87 – 1.73 (m, 1H), 1.45 (s, 9H), 1.29 – 1.17 (m, 2H). Spectroscopic data are in agreement with those in the literature.[65]

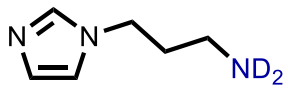

10-D$_2$

Deuterated 1-(3-aminopropyl) imidazole (10-D$_2$): 1-(3-aminopropyl) imidazole (**10-H$_2$**) (53.5 mg, 427 mmol) was added to a vial and purged with nitrogen. The amine was dissolved in dichloromethane (640 mL), triethylamine (120 mL, 2 equiv) was added, and the mixture was cooled to 0 °C. To a separate vial,1,2-bis(chlorodimethylsilyl)ethane (92 mg, 1 equiv) was added and purged with nitrogen. The silane was dissolved in dichloromethane (850 mL) and the solution was added dropwise to the reaction (Scheme 3.X). The reaction stirred for 2 hours at room temperature then diethyl ether was added and the mixture was filtered. The filtrate was concentrated *in vacuo* then dissolved in CD_3OD and stirred overnight in a capped vial at 40 °C. The methanol was removed *in vacuo* and the deuterated amine was stored under nitrogen and used without further purification.

3.4.4. Diazene and Isodiazene Comparison.

Myers allene synthesis was performed according to the previously reported procedure.[40] To a deoxygenated solution of triphenylphosphine (269 mg, 1.026 mmol, 1.5 equiv.) in 2 ml THF was added DEAD (40 wt% solution in toluene, 202 µl, 1 equiv.) and the flask was cooled to -15 ^oC using 1:3 mass sodium chloride ice water bath. Deoxygenated solutions of 4-phenylbut-3-yn-2-ol (**58**) (100mg, 0.684 mmol, 1 equiv.) in 2 ml THF and NBSH[66] (223 mg, 1.026 mmol, 1.5

equiv.) in 2ml THF were subsequently added dropwise. The reaction was stirred at -15 °C for 2 hours and then allowed to warm to room temperature overnight. The volatiles were removed *in vacuo* and the crude material was purified by silica gel chromatography to yield **59** and **59'** in 37% yield (33 mg, 0.253 mmol). The product was analyzed by NMR spectroscopy and the ratio of **59** to **59'** was determined by comparison to literature spectra of the compounds.[40, 67] This procedure was repeated three times and the average ratio of **59** to **59'** was 140 +/- 30 : 1 (Figure 3.4).

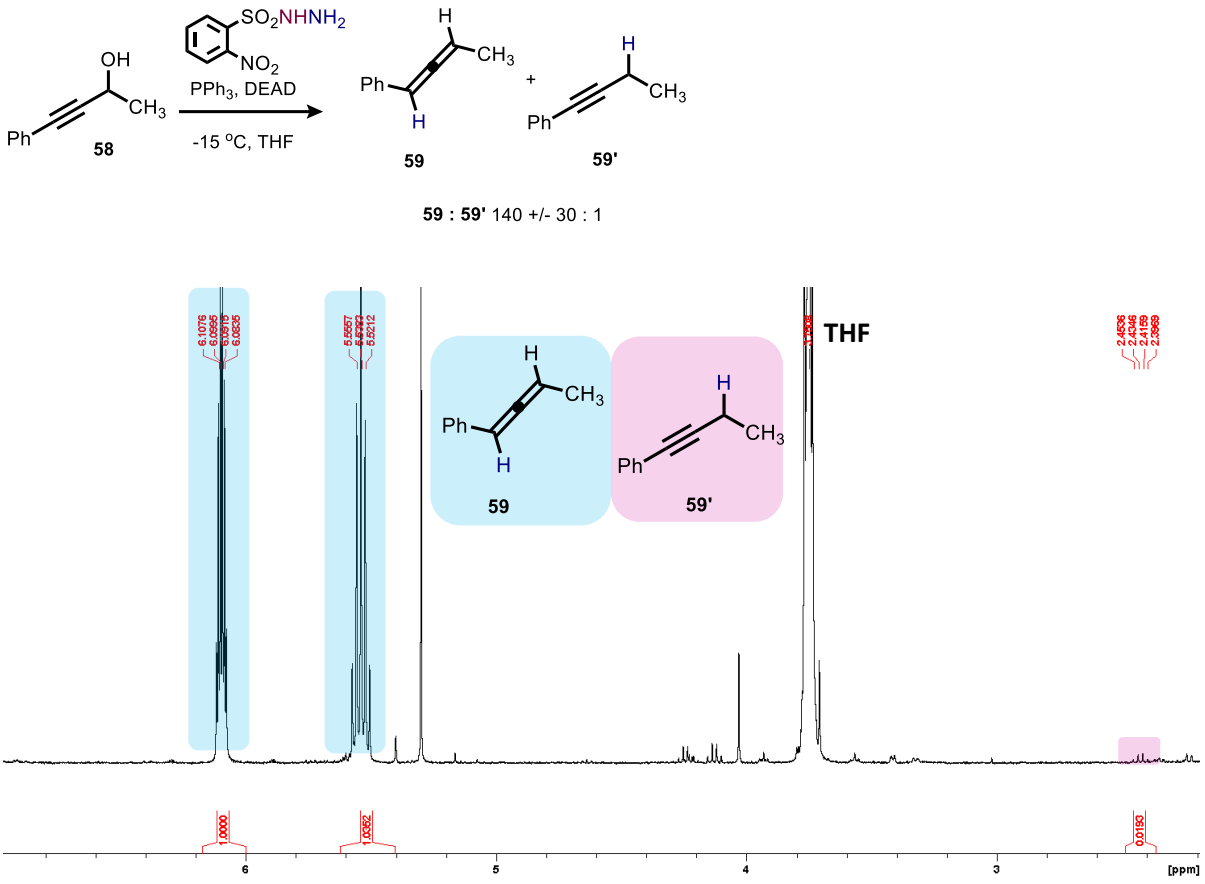

Figure 3.4. Crude ^{1}H NMR spectrum of Myers allene synthesis products in $CDCl_3$, 400 MHz.

To a deoxygenated solution of anomeric amide (326 mg, 0.826 mmol, 1.2 equiv.) in 4 ml THF was added a deoxygenated solution of 4-phenylbut-3-yn-2-amine (**60**) (100 mg, 0.689 mmol) in 4 ml THF over 15 minutes and the solution was stirred at room temperature for 1 hour. The

volatiles were removed *in vacuo* and the crude material was purified by silica gel chromatography to yield **59** and **59'** in 7% yield (6.3 mg, 0.0482 mmol). The product was analyzed by NMR spectroscopy and the ratio of **59** to **59'** was determined by comparison to literature spectra of the compounds.[40, 67] This procedure was repeated three times and the average ratio of **59** to **59'** was 8 +/- 0.6 : 1 (Figure 3.5).

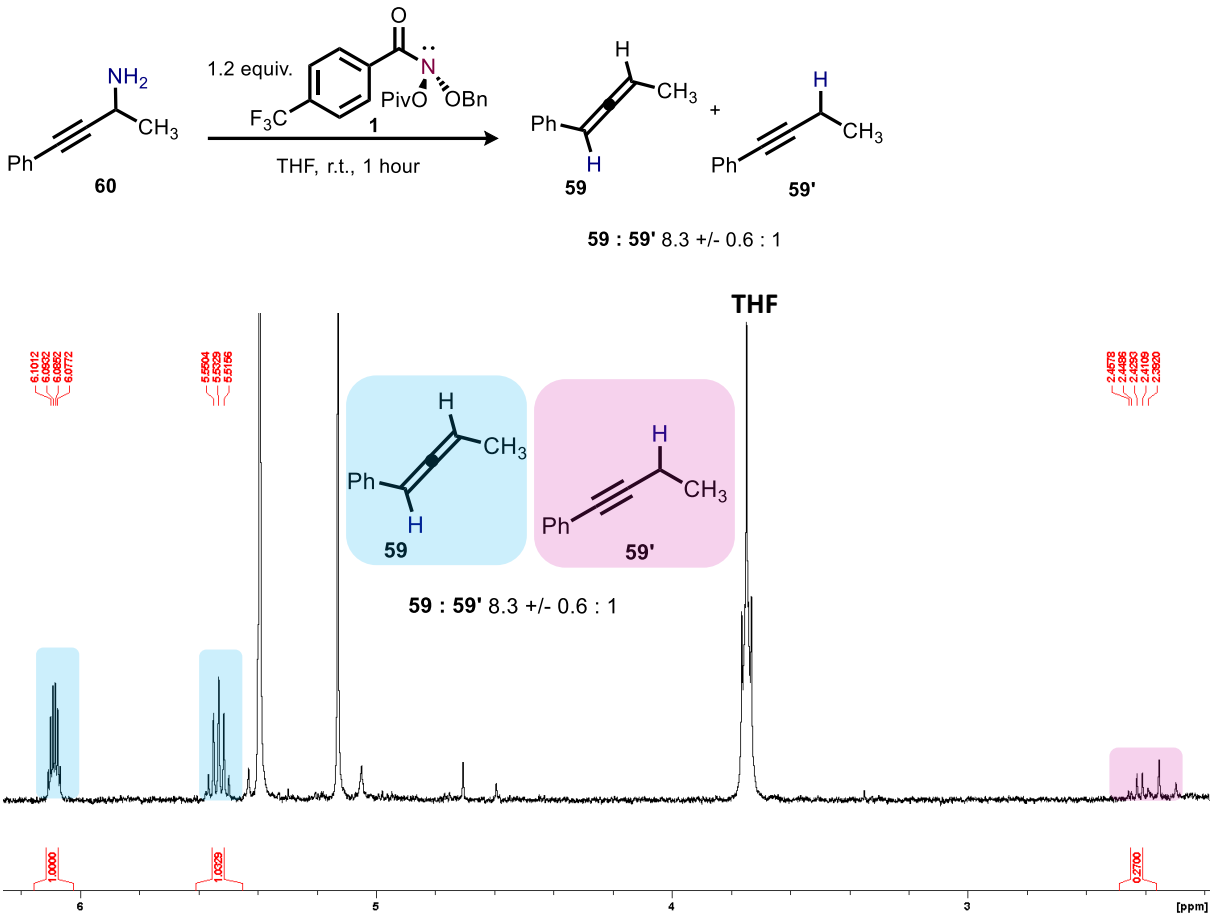

Figure 3.5. ^{1}H NMR spectrum of propargylic amine deletion products in $CDCl_3$, 400 MHz.

3.4.5. Deuterium Labelling Studies.

To a 0.5-dram vial was added 100 mL 3-(1H-imidazol-1-yl)propan-1-amine (**10-D$_2$**) solution in acetonitrile (0.2 M) followed by 100 mL **1** solution in acetonitrile (0.24 M in **1**), added

slowly under nitrogen. After 1 hour, CD_3CN was added (400 mL) and the deuterium incorporation was assessed by NMR. After multipoint baseline correction, the deuterium content was assessed by integration against the methylene indicated by Julia Driscoll (Figure 3.6).

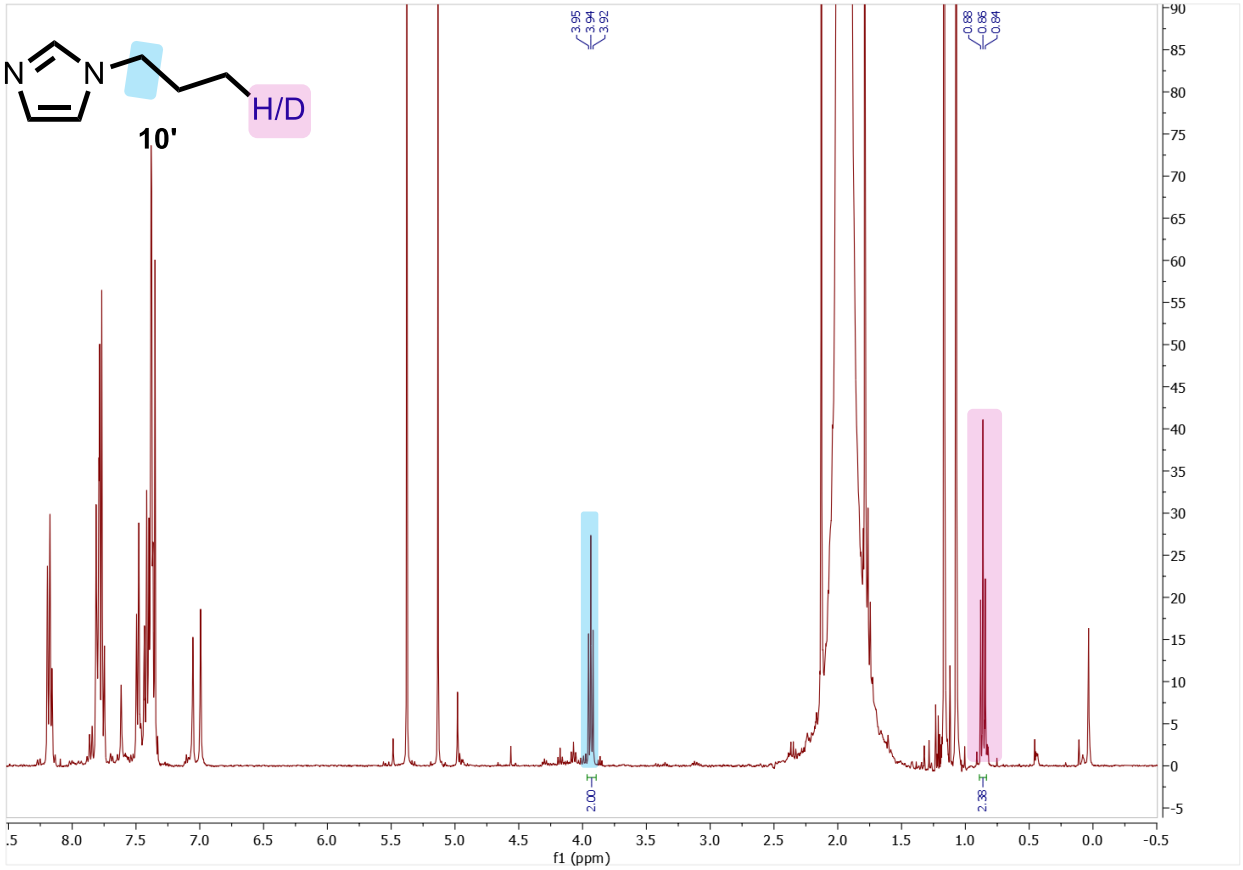

Figure 3.6. ^1H NMR spectrum of deuterium labelling experiment products in CD_3CN, 400 MHz by Julia Driscoll.

3.4.6. TEMPO Trapping Experiments.

To a 1-dram screw cap vial equipped with a stir bar and PTFE/white silicone septum was added *p*-toluidine (**65**) (12 mg, 0.11 mmol, 1 equiv), TEMPO free radical (21 mg, 0.13 mmol, 1.2 equiv.) and dry CD_3CN (0.5 mL) under nitrogen. The anomeric amide (65 mg, 0.16 mmol, 1.5 equiv) and dry CD_3CN (0.5 mL) was added to a second vial and this solution was then transferred to the first vial containing *p*-toluidine under nitrogen and stirred at 45 °C for 24 hours. After 24 h,

1,3,5-trimethoxybenzene (100 µL solution in CD_3CN, 0.01 mmol) was added to the crude reaction mixture as internal standard. The ^1H NMR yield was 55% yield for **65'**[68] and 15% yield for **65"** by Dr. Balu Dherange (Figure 3.7).

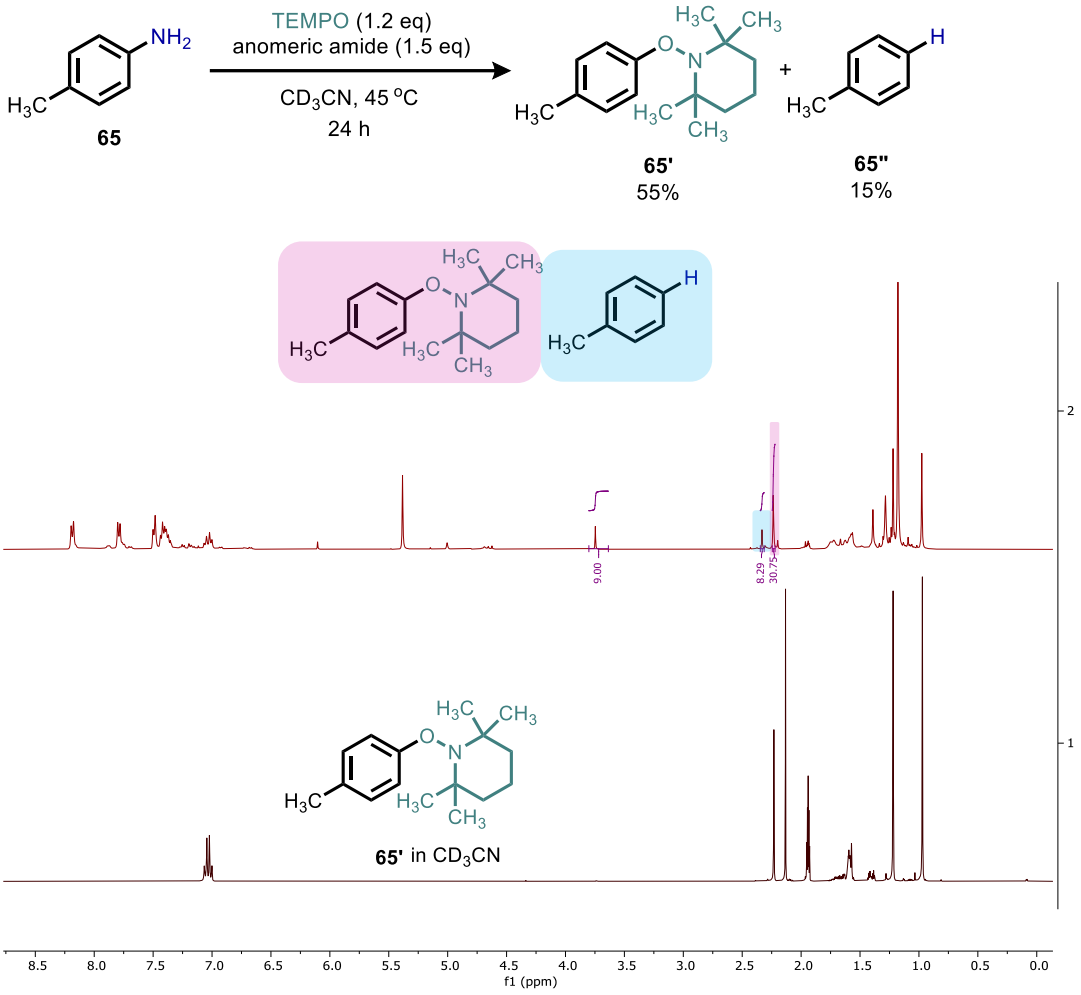

Figure 3.7. ^1H NMR spectrum showing TEMPO trapping of aryl amine in CD_3CN at 400 MHz by Dr. Balu Dherange.

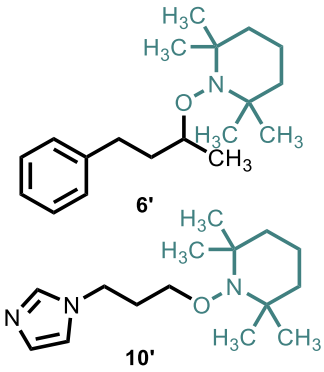

To a 0.5-dram vial was added 100 mL **6** (Figure 3.8) or **10** (Figure 3.9) solution in CD_3CN (0.4 M) followed by 100 mL TEMPO radical solution in CD_3CN (0.48 M). A 200 mL solution of **1** in CD_3CN (0.24 M in **1**) was then added slowly under nitrogen. After 1 hour, 1,3,5-trimethoxybenzene was added as an internal standard to determine the yield by ^{1}H-NMR. Spectroscopic data for **6'** is in agreement with the literature[69] and **10'** was isolated and fully characterized.

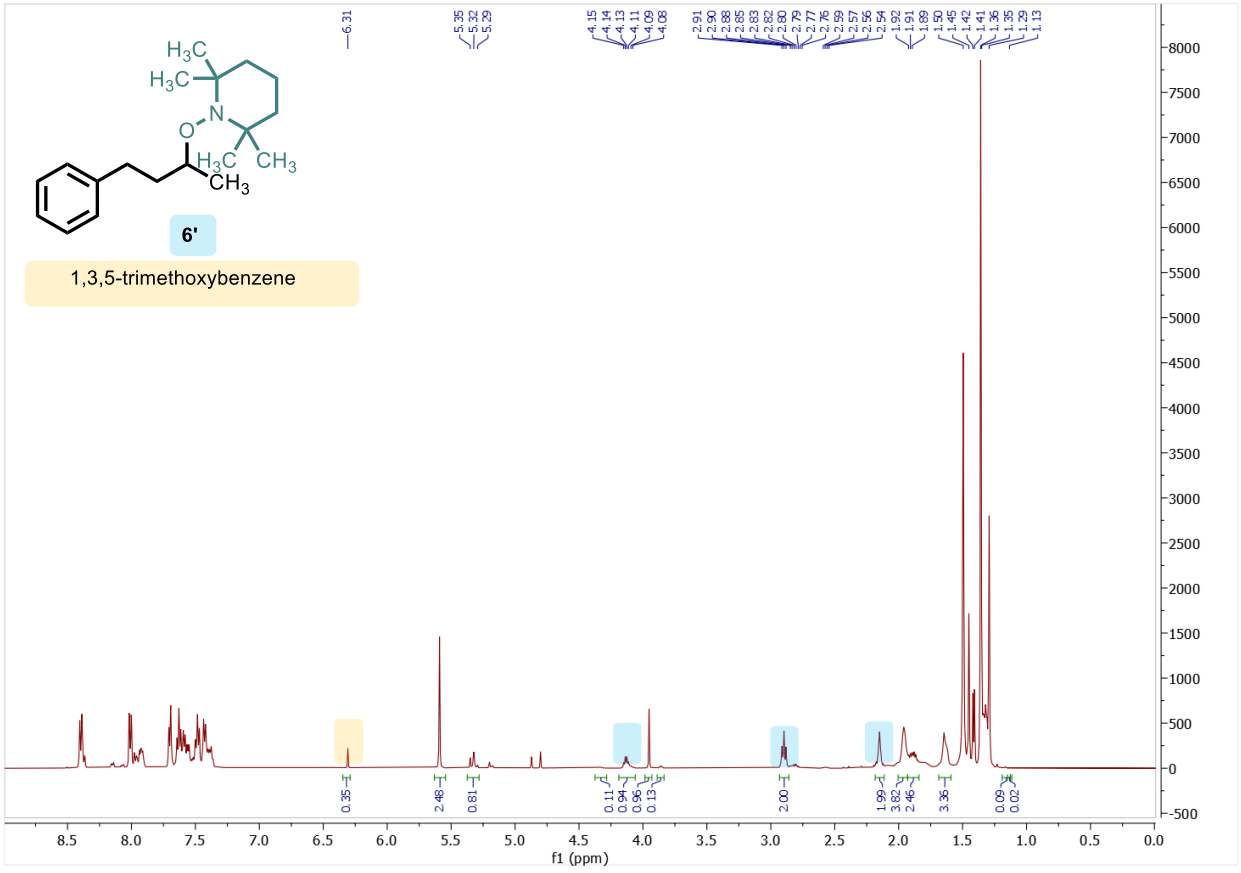

Figure 3.8. ^{1}H NMR spectrum showing TEMPO trapping of α-secondary primary amine by Julia Driscoll in CD_3CN at 400 MHz.

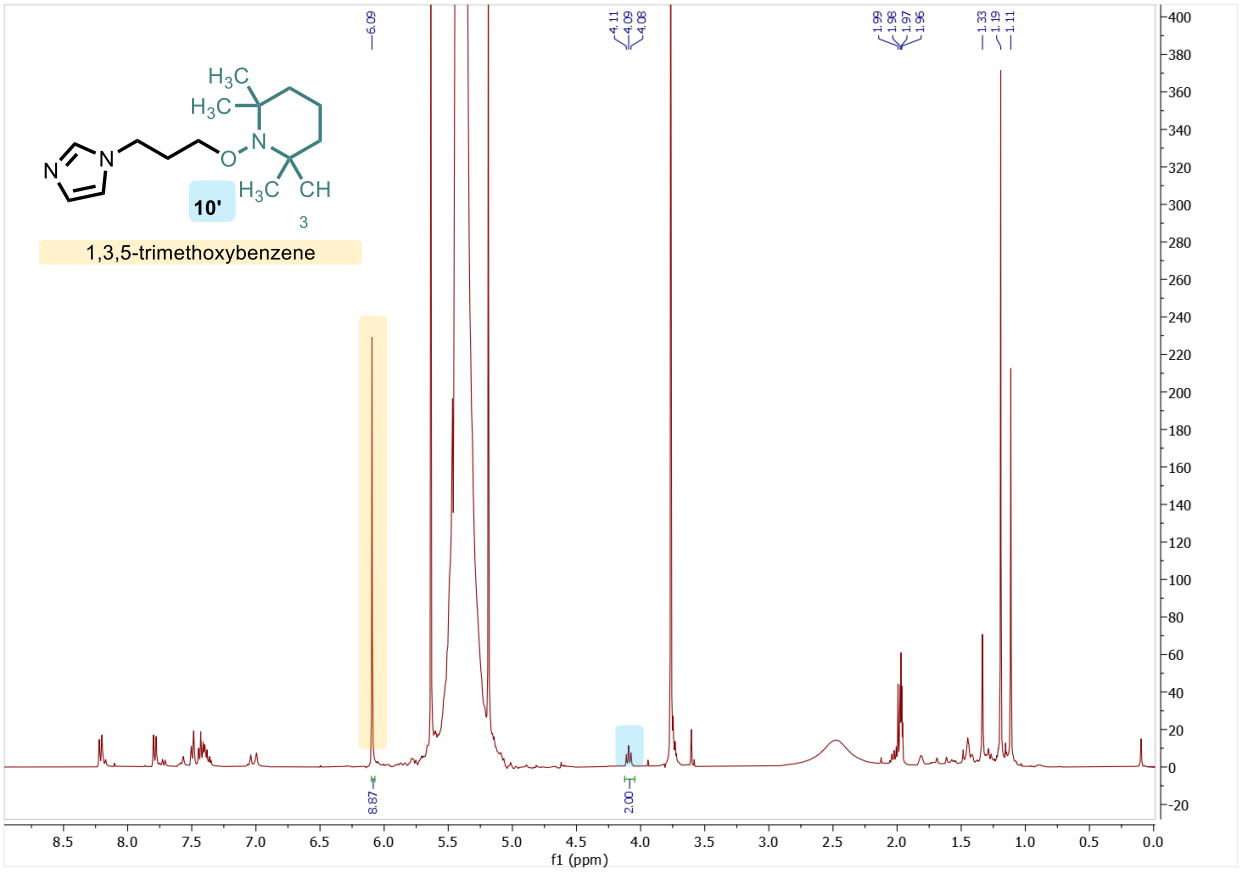

Figure 3.9. ^{1}H NMR Spectrum showing TEMPO trapping of α-primary primary amine by Julia Driscoll in CD_3CN at 400 MHz.

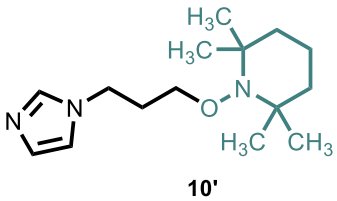

1-(3-(1H-imidazol-1-yl)propoxy)-2,2,6,6-tetramethylpiperidine (10'): ^{1}H NMR (Figure 3.39) **(400 MHz, $CDCl_3$)** δ 7.47 (s, 1H), 7.02 (s, 1H), 6.90 (s, 1H), 4.07 – 3.98 (m, 2H), 3.72 (t, J = 6.0 Hz, 2H), 2.02 – 1.94 (m, 2H), 1.57 – 1.44 (m, 1H), 1.39 (m, 4H), 1.32 – 1.24 (m, 1H), 1.07 (s, 6H), 1.06 (s, 6H). **^{13}C{^{1}H} NMR** (Figure 3.40) **(101 MHz, $CDCl_3$)** δ 137.11, 129.34, 118.78, 77.48, 77.16, 76.84, 72.87, 59.73, 44.36, 39.56, 33.08, 30.56, 20.09, 17.05. **HR-MS** (ESI): calculated 265.2154 for $C_{15}H_{27}N_3O$, found 265.2171.

3.4.7. Radical Clock Experiments.

To a 1-dram screw cap vial equipped with a stir bar and PTFE/white silicone septum was added *2*-(allyloxy)aniline (**63**) (15 mg, 0.1 mmol, 1 equiv) and dry CD_3CN (0.5 mL) under nitrogen. The anomeric amide (59 mg, 0.15 mmol, 1.5 equiv) and dry CD_3CN (0.5 mL) was added to a second vial and this solution was then transferred to the first vial containing *p*-toluidine under nitrogen and stirred at 45 °C for 24 hours. After 24 h, 1,3,5-trimethoxybenzene (100 µL solution in CD_3CN, 0.01 mmol) was added to the crude reaction mixture as internal standard. 72% yield of **64** was obtained *via* ^{1}H NMR by Dr. Balu Dherange (Figure 3.10).

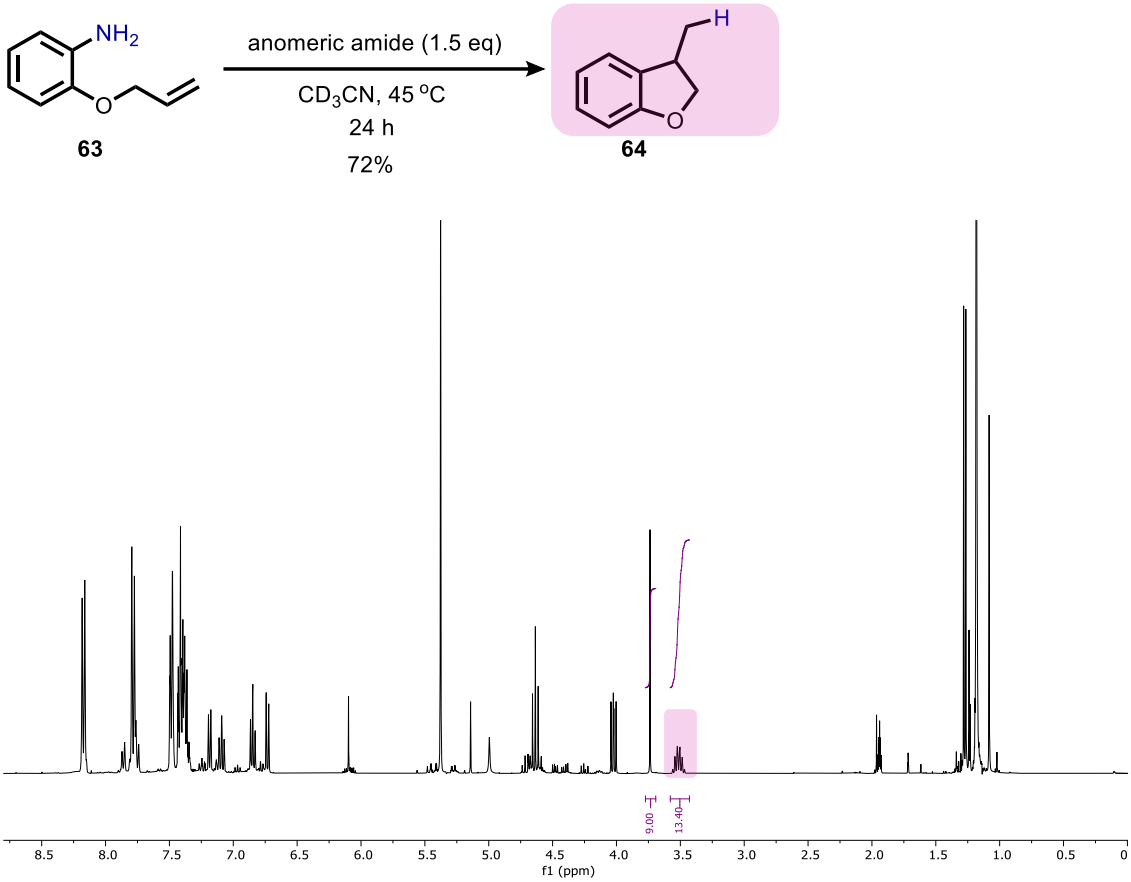

Figure 3.10. ^{1}H NMR spectrum from radical clock experiment with aryl amine substrate in CD_3CN at 400 MHz by Dr. Balu Dherange.

To a 1-dram screw cap vial equipped with a stir bar and PTFE/white silicone septum was added 6,6-diphenylhex-5-en-1-amine (**61**) (10.2 mg, 39.8 mmol, 1 equiv) and dry CD_3CN (0.4 mL) under nitrogen. The anomeric amide (20.4 mg, 1.3 equiv) and dry CD_3CN (0.4 mL) was added to a second vial and this solution was then transferred to the first vial under nitrogen and stirred at room temperature for 1 hour. Then, 1,3,5-trimethoxybenzene (2.2 mg) was added to the crude reaction mixture as internal standard. 41% yield of **62** and 7% yield of **62'** were obtained *via* ^{1}H NMR by Julia Driscoll (Figure 3.11).

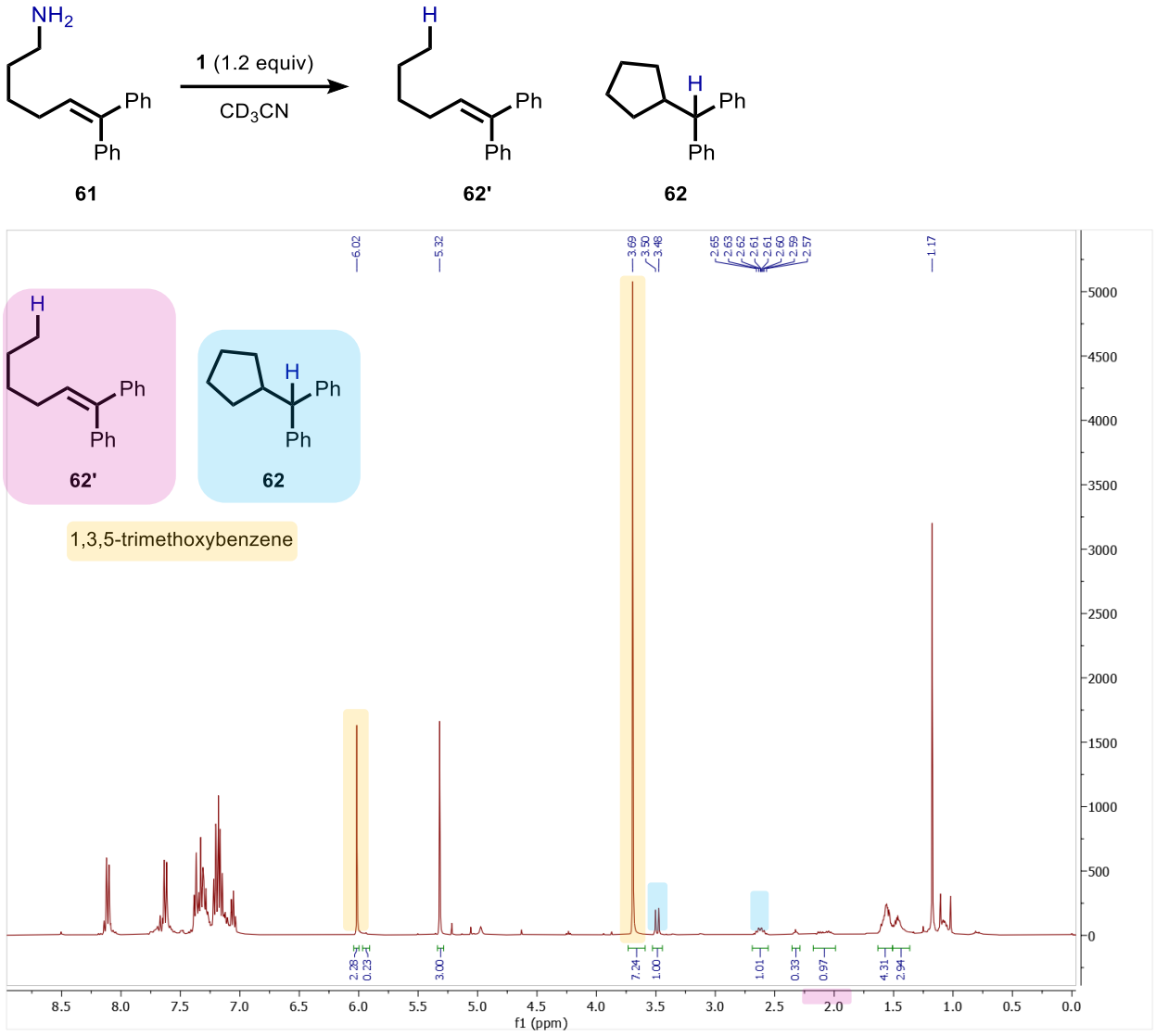

Figure 3.11. ^{1}H NMR spectrum of aliphatic clock reaction in CD_3CN, 400 MHz.

3.4.8. NMR Spectra of New Compounds.

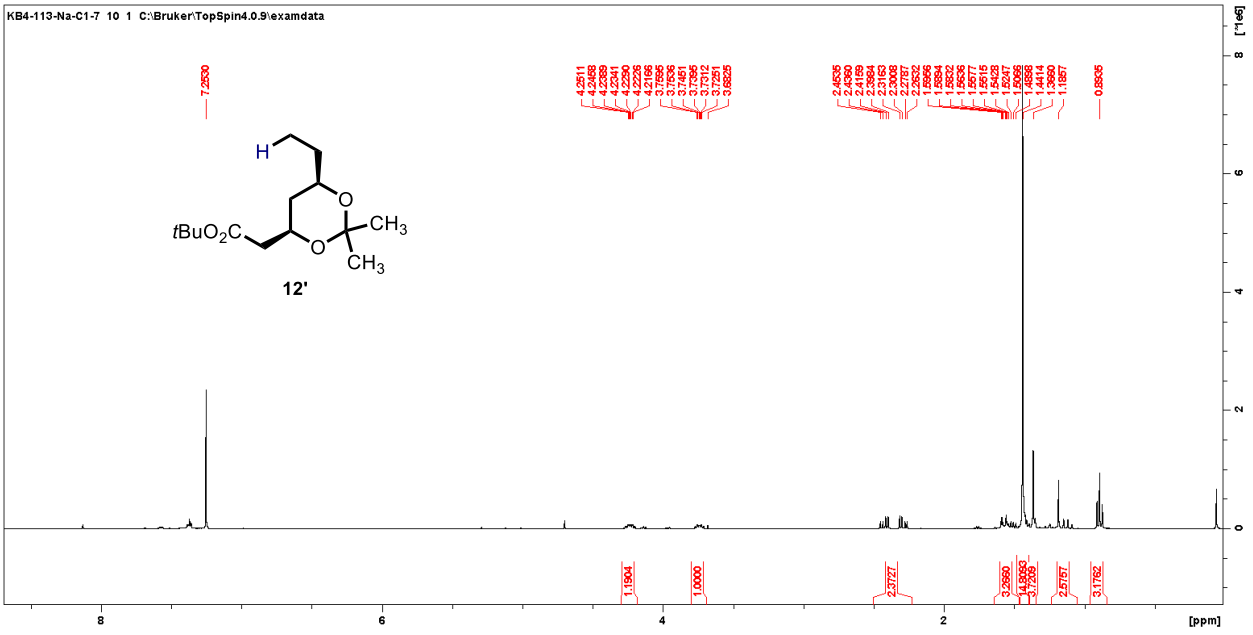

Figure 3.12. ^{1}H NMR spectrum of *tert*-butyl 2-((*4R,6R*)-6-ethyl-2,2-dimethyl-1,3-dioxan-4-yl)acetate (**12'**) in $CDCl_3$, 400 MHz.

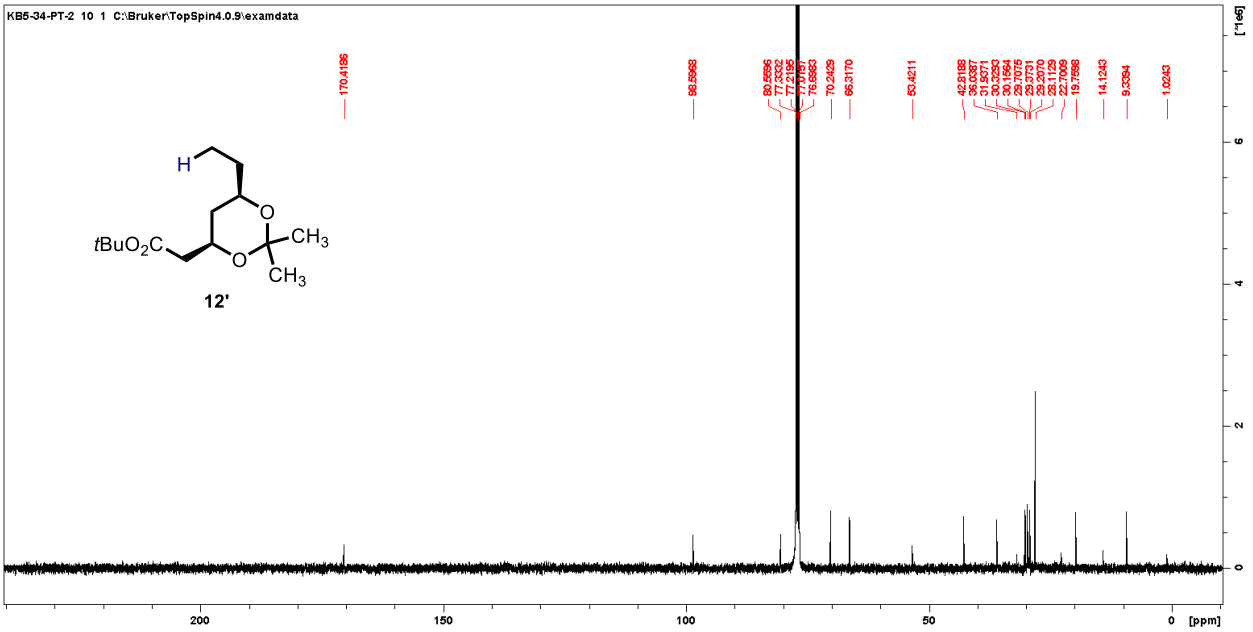

Figure 3.13. $^{13}C\{^{1}H\}$ NMR spectrum of *tert*-butyl 2-((*4R,6R*)-6-ethyl-2,2-dimethyl-1,3-dioxan-4-yl)acetate (**12'**) in $CDCl_3$, 100 MHz.

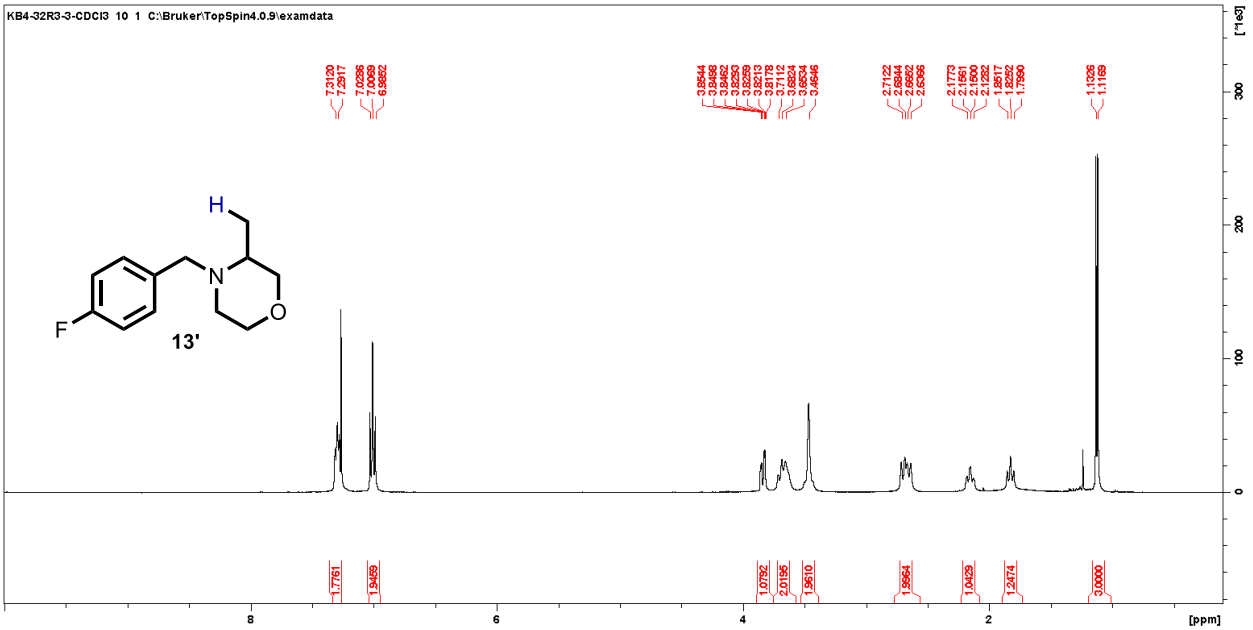

Figure 3.14. ^{1}H NMR spectrum of 4-[(4-fluorophenyl)methyl]-3-methylmorpholine (**13'**) in $CDCl_3$, 400 MHz.

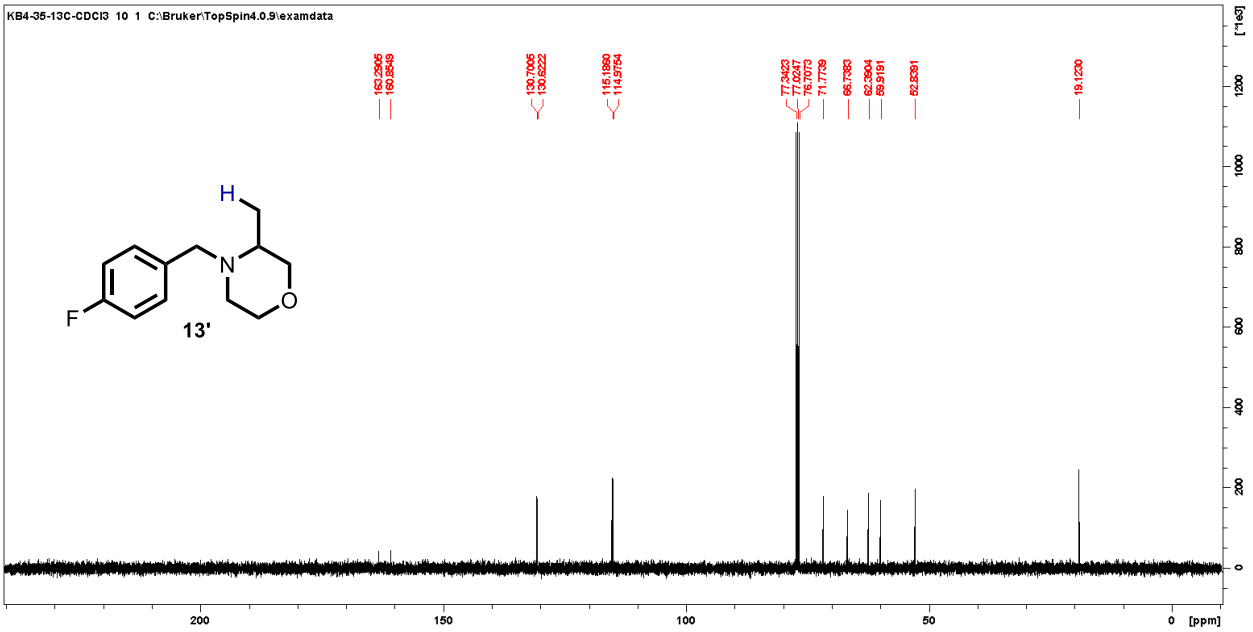

Figure 3.15. ^{13}C{^{1}H} NMR spectrum of 4-[(4-fluorophenyl)methyl]-3-methylmorpholine (**13'**) in $CDCl_3$, 100 MHz.

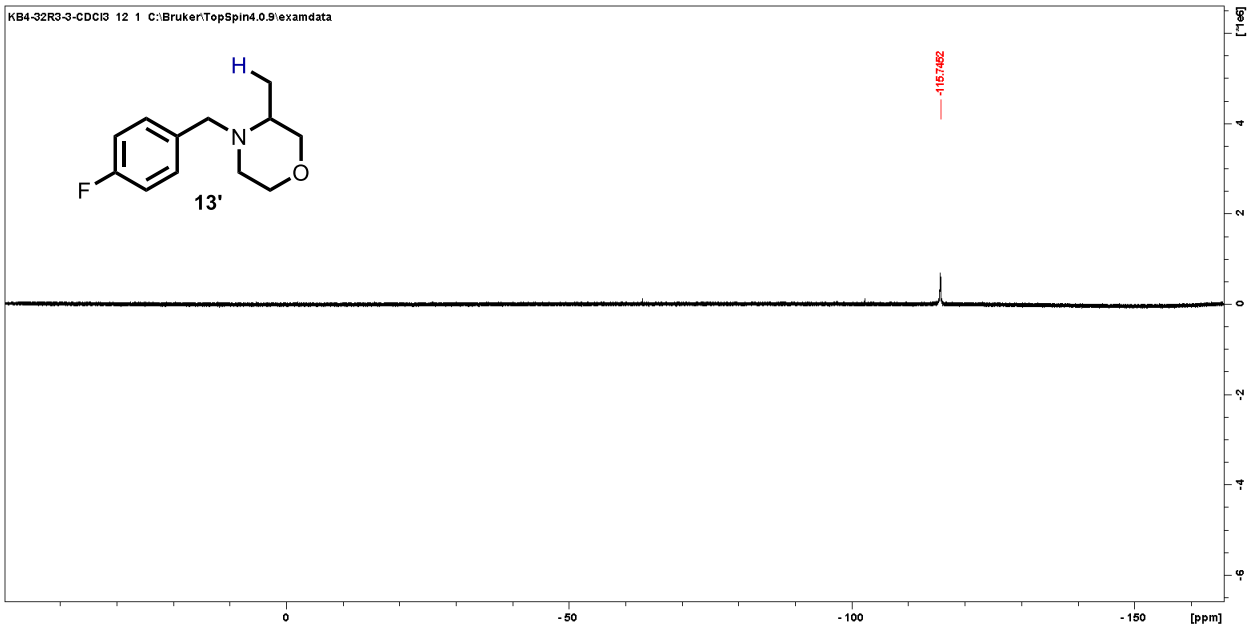

Figure 3.16. $^{19}F\{^{1}H\}$ NMR spectrum of 4-[(4-fluorophenyl)methyl]-3-methylmorpholine (**13'**) in $CDCl_3$, 376 MHz.

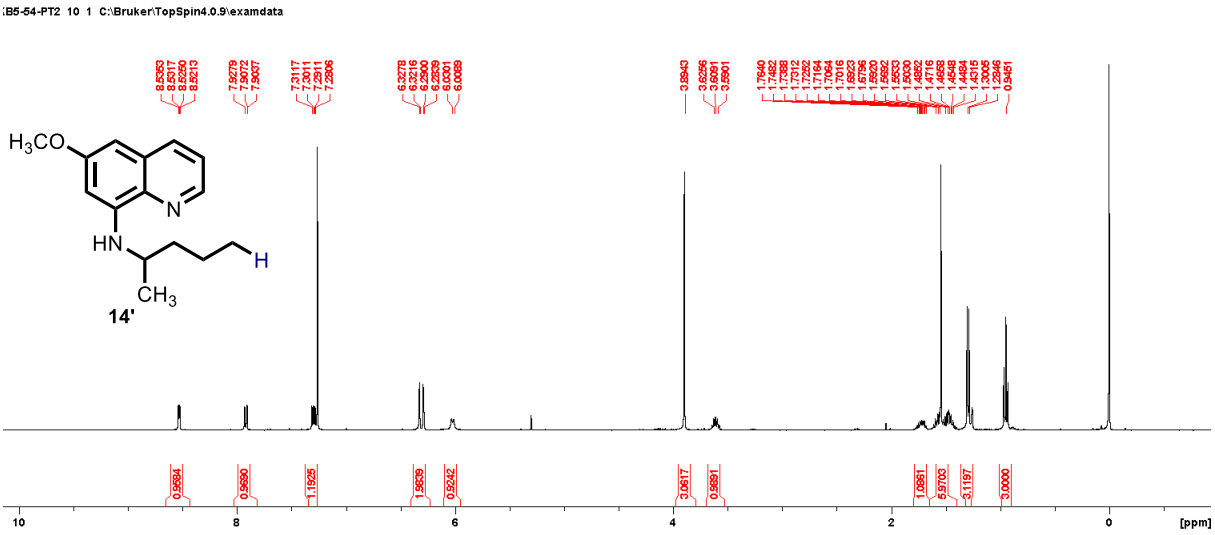

Figure 3.17. ^{1}H NMR spectrum of 6-methoxy-*N*-(pentan-2-yl)quinolin-8-amine (**14'**) in $CDCl_3$, 400 MHz.

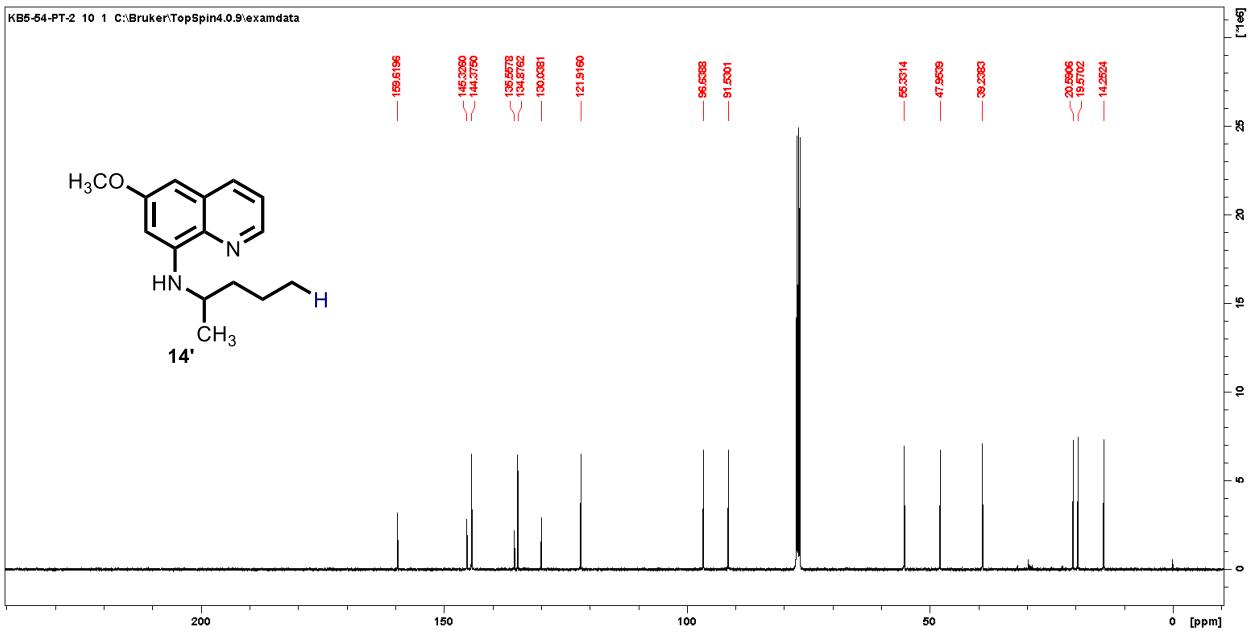

Figure 3.18. $^{13}C\{^{1}H\}$ NMR spectrum of 6-methoxy-*N*-(pentan-2-yl)quinolin-8-amine (**14'**) in $CDCl_3$, 100 MHz.

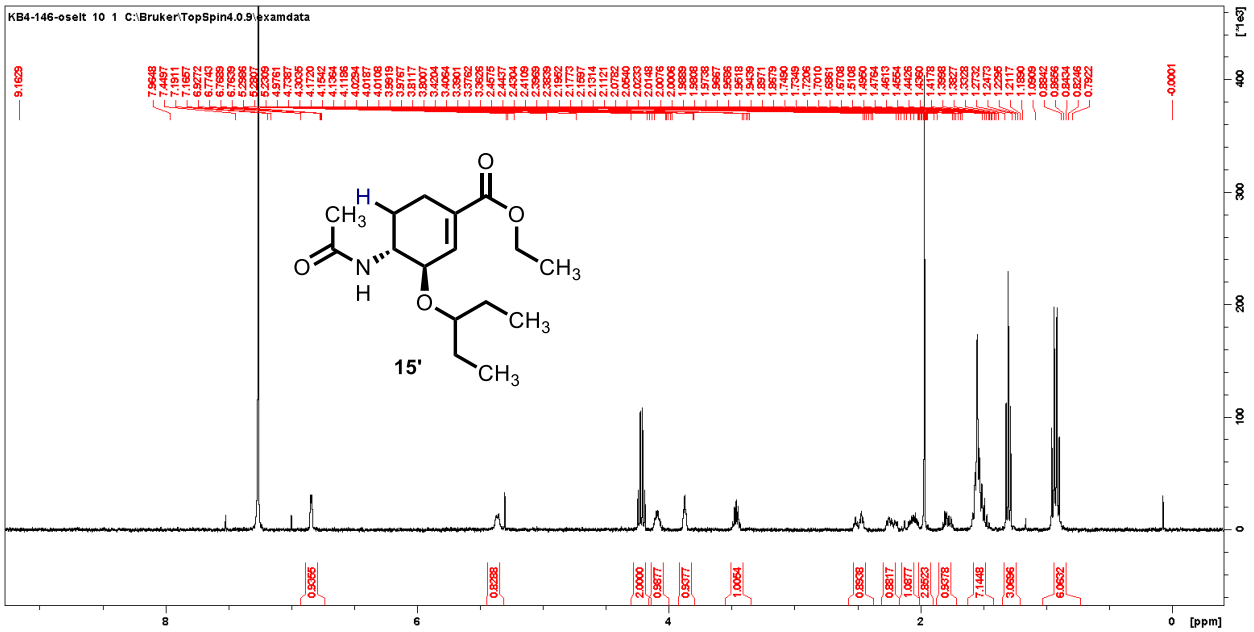

Figure 3.19. ^{1}H NMR spectrum of ethyl (*3R,4R*)-4-acetamido-3-(pentan-3-yloxy)cyclohex-1-ene-1-carboxylate (**15'**) in $CDCl_3$, 400 MHz.

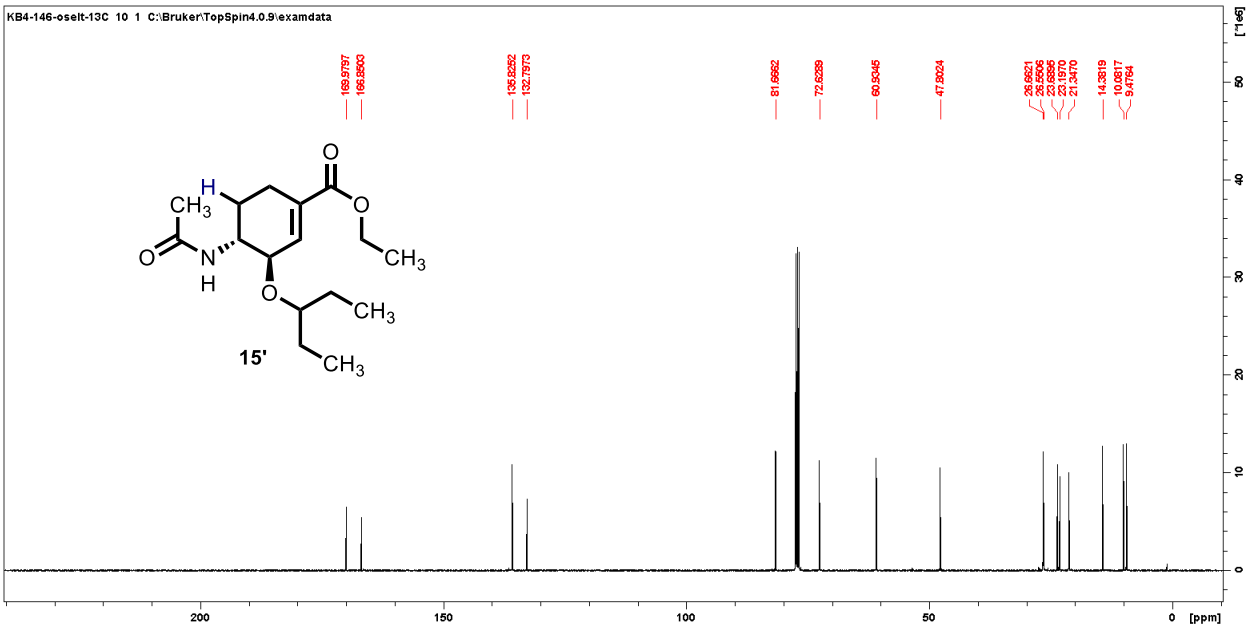

Figure 3.20. $^{13}C\{^{1}H\}$ NMR spectrum of ethyl (*3R,4R*)-4-acetamido-3-(pentan-3-yloxy)cyclohex-1-ene-1-carboxylate (**15'**) in $CDCl_3$, 100 MHz.

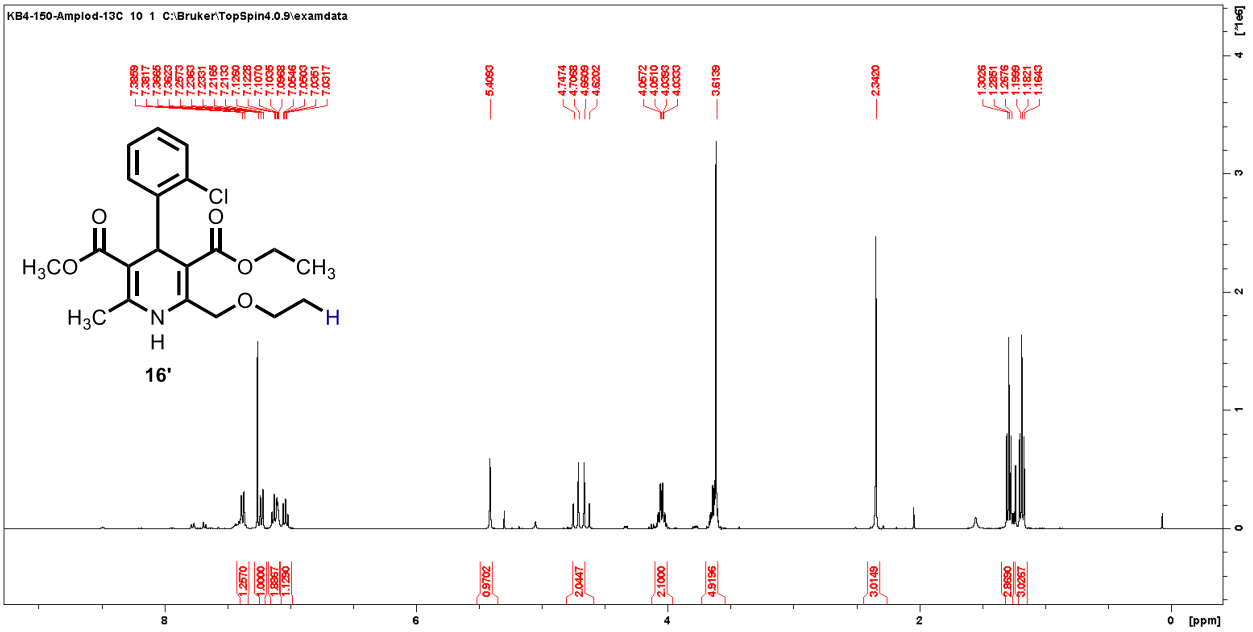

Figure 3.21. ^{1}H NMR spectrum of 3-ethyl 5-methyl 4-(2-chlorophenyl)-2-(ethoxymethyl)-6-methyl-1,4-dihydropyridine-3,5-dicarboxylate (**16'**) in $CDCl_3$, 400 MHz.

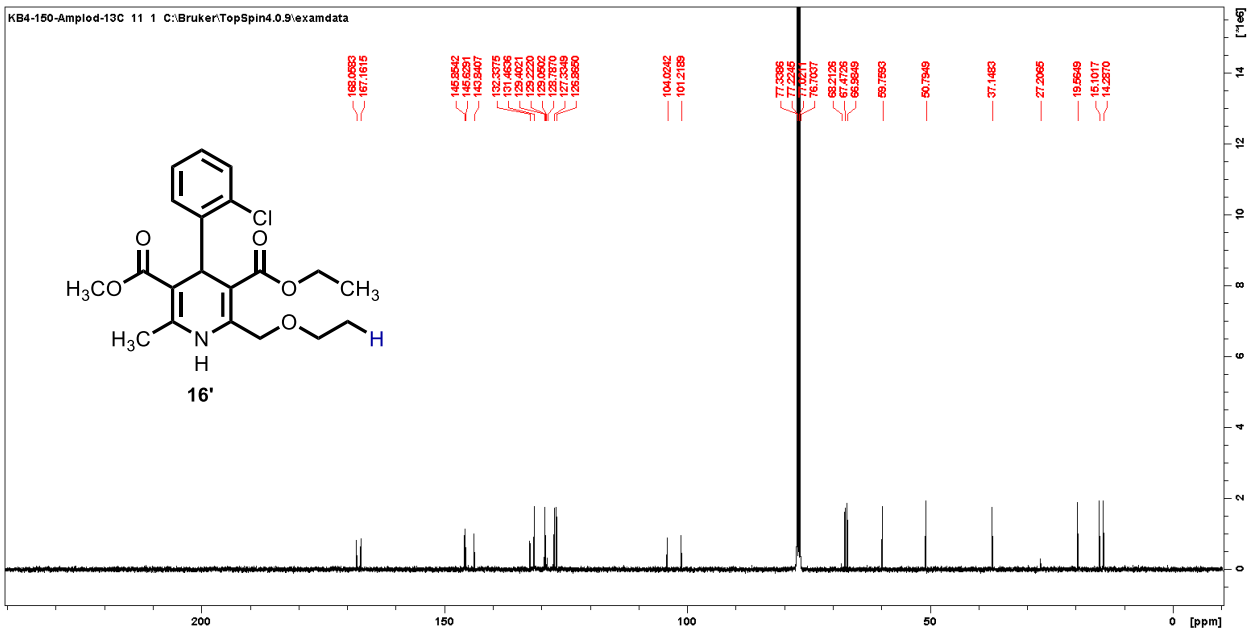

Figure 3.22. $^{13}C\{^{1}H\}$ NMR spectrum of 3-ethyl 5-methyl 4-(2-chlorophenyl)-2-(ethoxymethyl)-6-methyl-1,4-dihydropyridine-3,5-dicarboxylate (**16'**) in $CDCl_3$, 100 MHz.

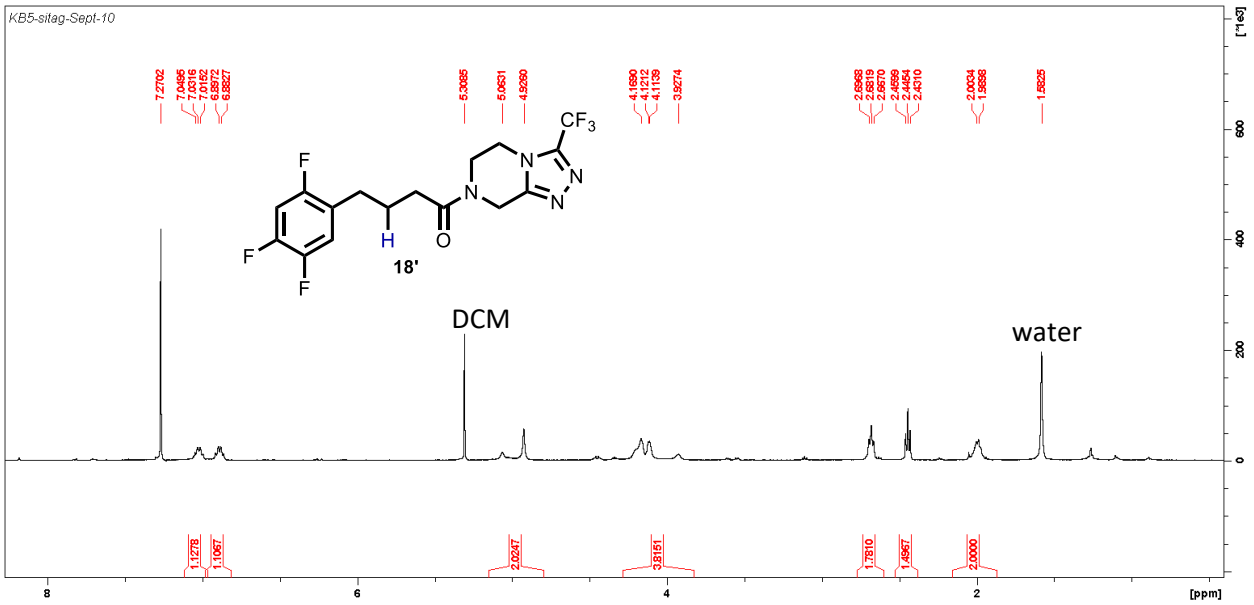

Figure 3.23. ^{1}H NMR spectrum of 1-(3-(trifluoromethyl)-5,6-dihydro-[1,2,4]triazolo[4,3-*a*]pyrazin-7(8H)-yl-(4(2,4,5-trifluorophenyl)butan-1-one (**18'**) in $CDCl_3$, 400 MHz.

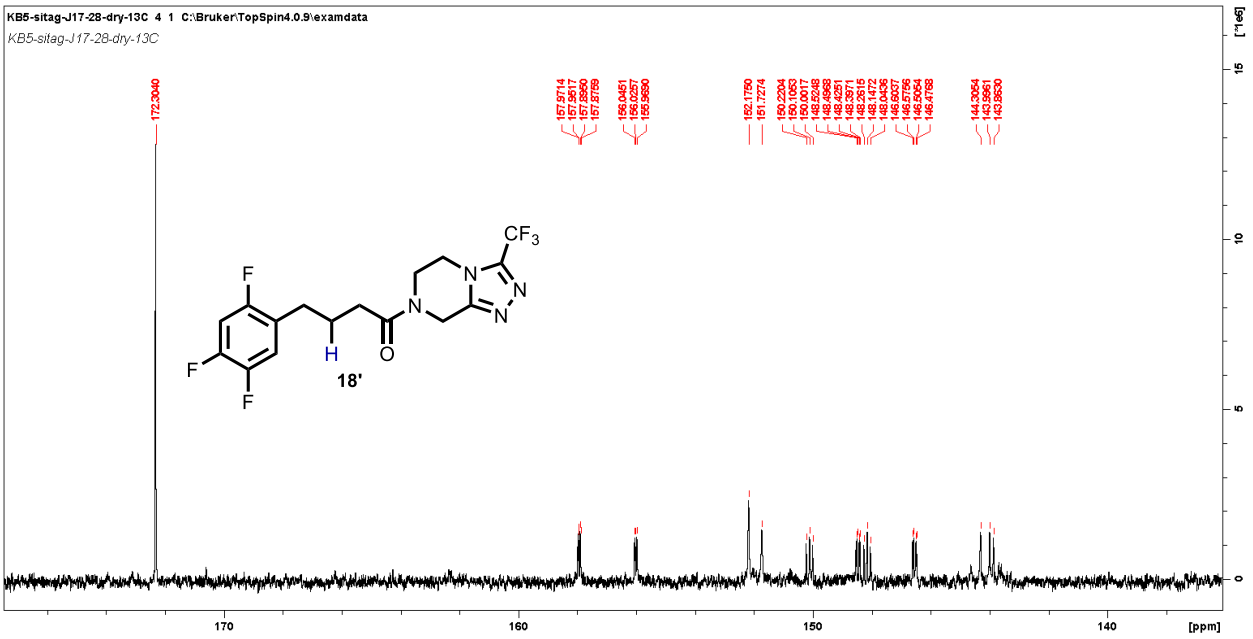

Figure 3.24a. $^{13}C\{^{1}H\}$ NMR spectrum aromatic zoom 1 of 1-(3-(trifluoromethyl)-5,6-dihydro-[1,2,4]triazolo[4,3-*a*]pyrazin-7(8H)-yl-(4(2,4,5-trifluorophenyl)butan-1-one (**18'**) in CD_3CN, 100 MHz.

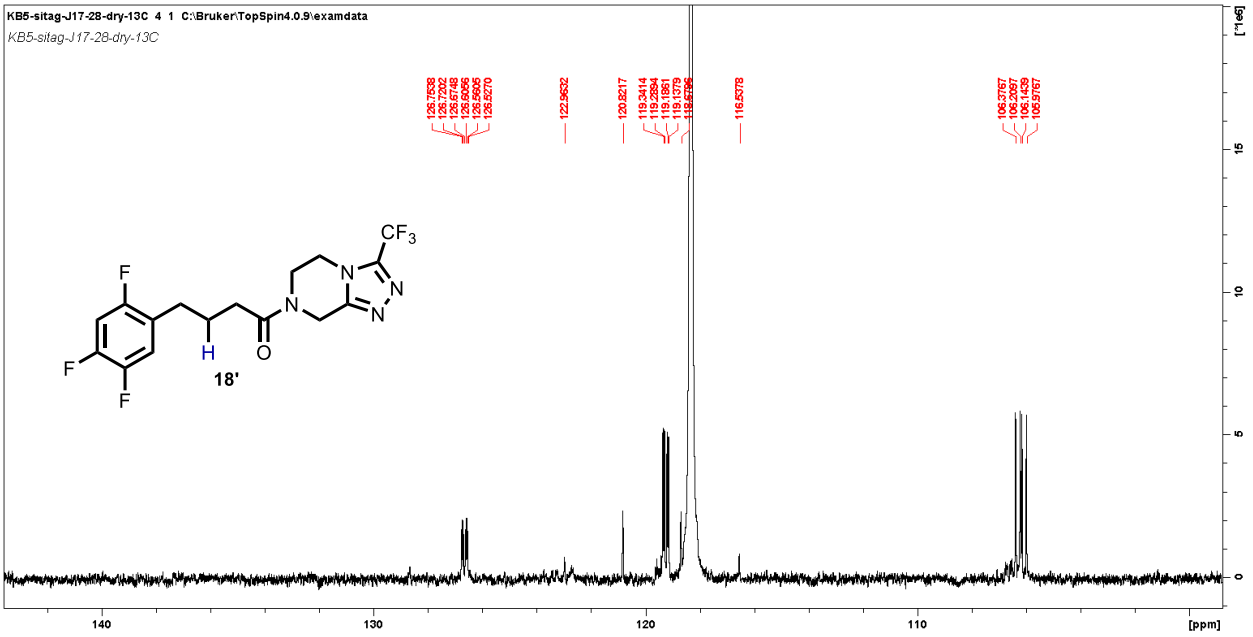

Figure 3.24b. $^{13}C\{^{1}H\}$ NMR spectrum aromatic zoom 2 of 1-(3-(trifluoromethyl)-5,6-dihydro-[1,2,4]triazolo[4,3-*a*]pyrazin-7(8H)-yl-(4(2,4,5-trifluorophenyl)butan-1-one (**18'**) in CD_3CN, 100 MHz.

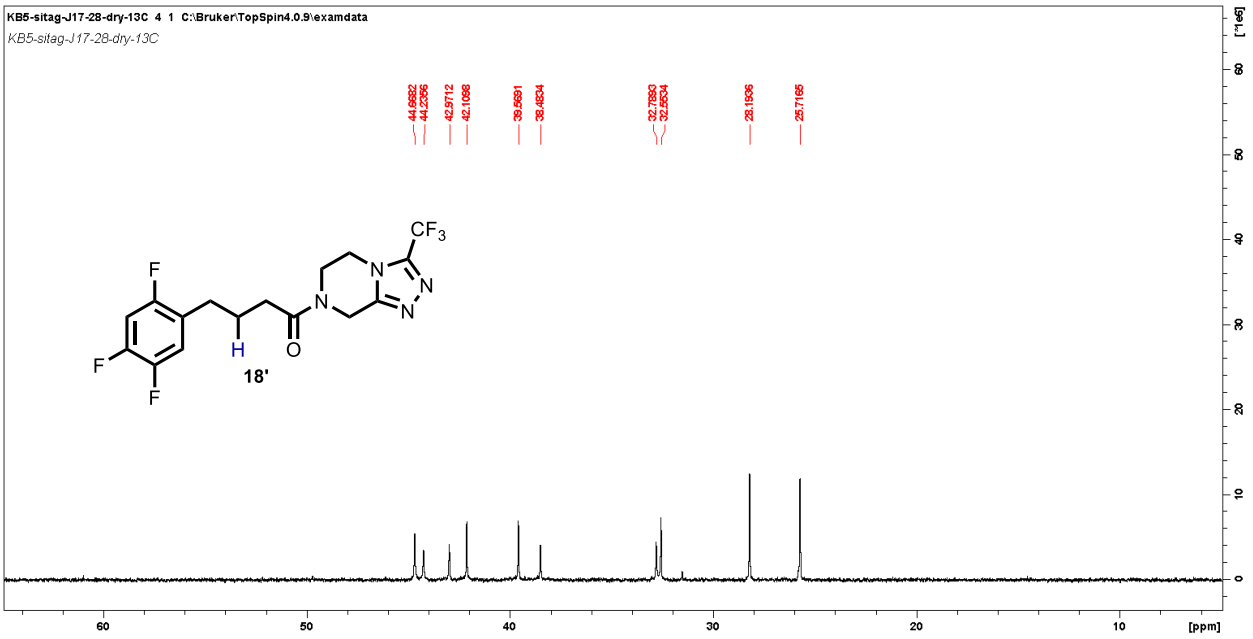

Figure 3.24c. $^{13}C\{^{1}H\}$ NMR spectrum aliphatic zoom of 1-(3-(trifluoromethyl)-5,6-dihydro-[1,2,4]triazolo[4,3-*a*]pyrazin-7(8H)-yl-(4(2,4,5-trifluorophenyl)butan-1-one (**18'**) in CD_3CN, 100 MHz.

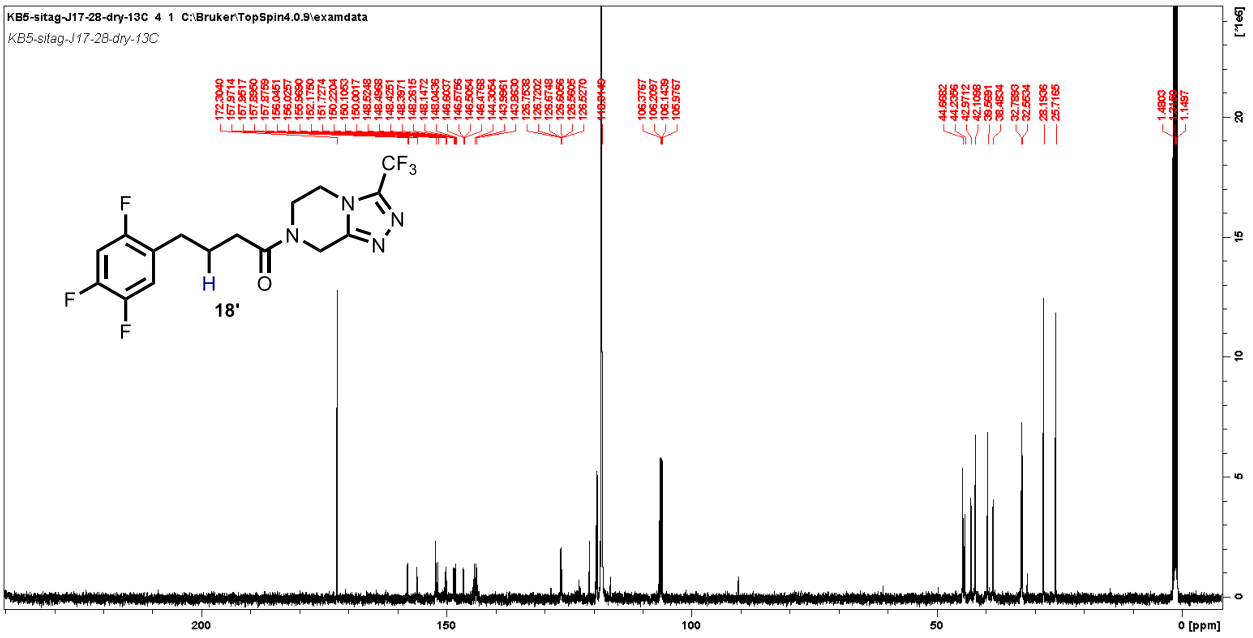

Figure 3.24d. $^{13}C\{^{1}H\}$ NMR full spectrum of 1-(3-(trifluoromethyl)-5,6-dihydro-[1,2,4]triazolo[4,3-*a*]pyrazin-7(8H)-yl-(4(2,4,5-trifluorophenyl)butan-1-one (**18'**) in CD_3CN, 100 MHz.

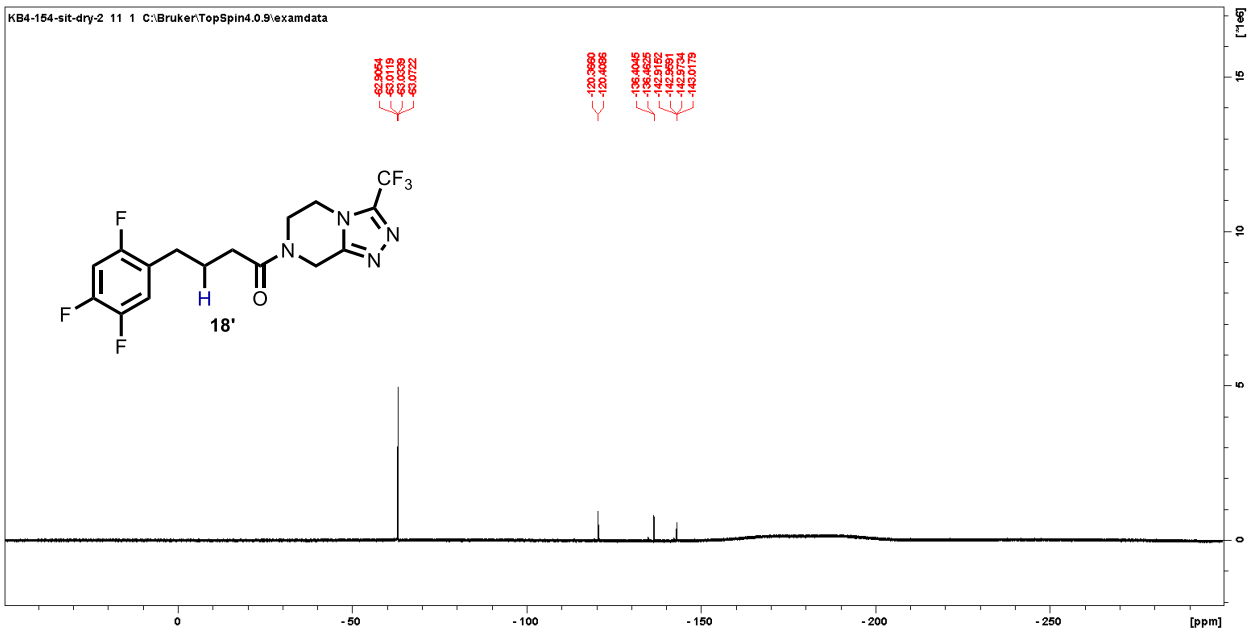

Figure 3.25. $^{19}F\{^{1}H\}$ NMR spectrum of 1-(3-(trifluoromethyl)-5,6-dihydro-[1,2,4]triazolo[4,3-*a*]pyrazin-7(8H)-yl-(4(2,4,5-trifluorophenyl)butan-1-one (**18'**) in $CDCl_3$, 376 MHz.

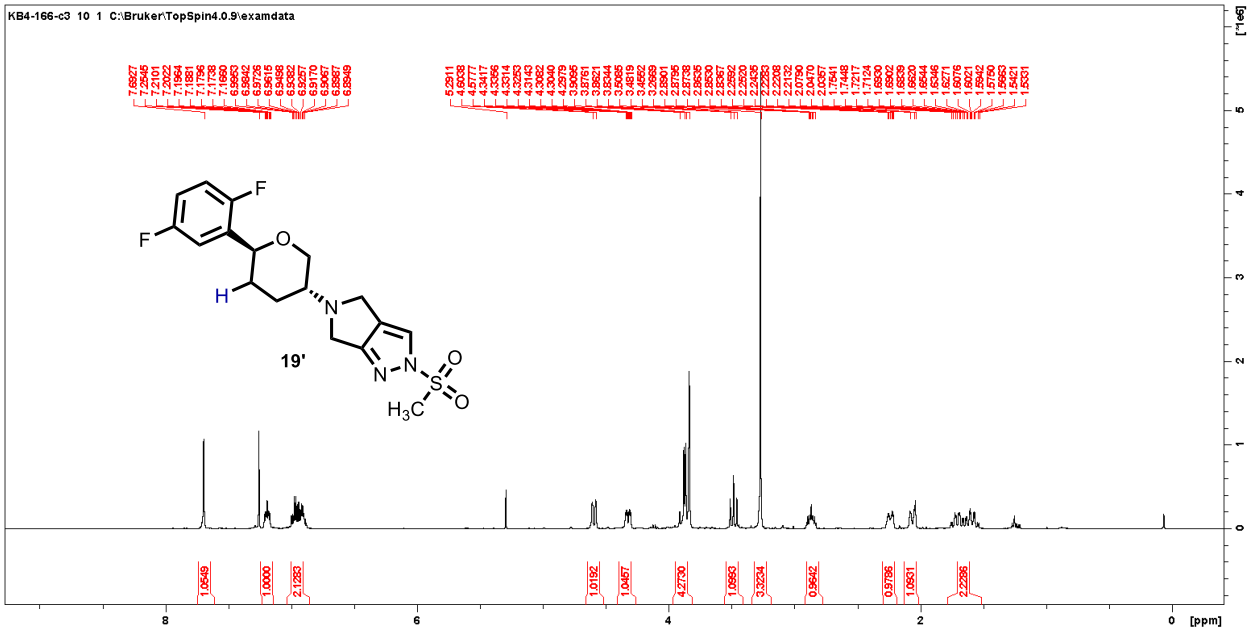

Figure 3.26. ^{1}H NMR spectrum of 5-((*3R,6S*)-6-(2,5-difluorophenyl)tetrahydro-*2H*-pyran-3-yl)-2-(methylsulfonyl)-2,4,5,6-tetrahydropyrrolo[3,4-*c*]pyrazole (**19'**) in $CDCl_3$, 400 MHz.

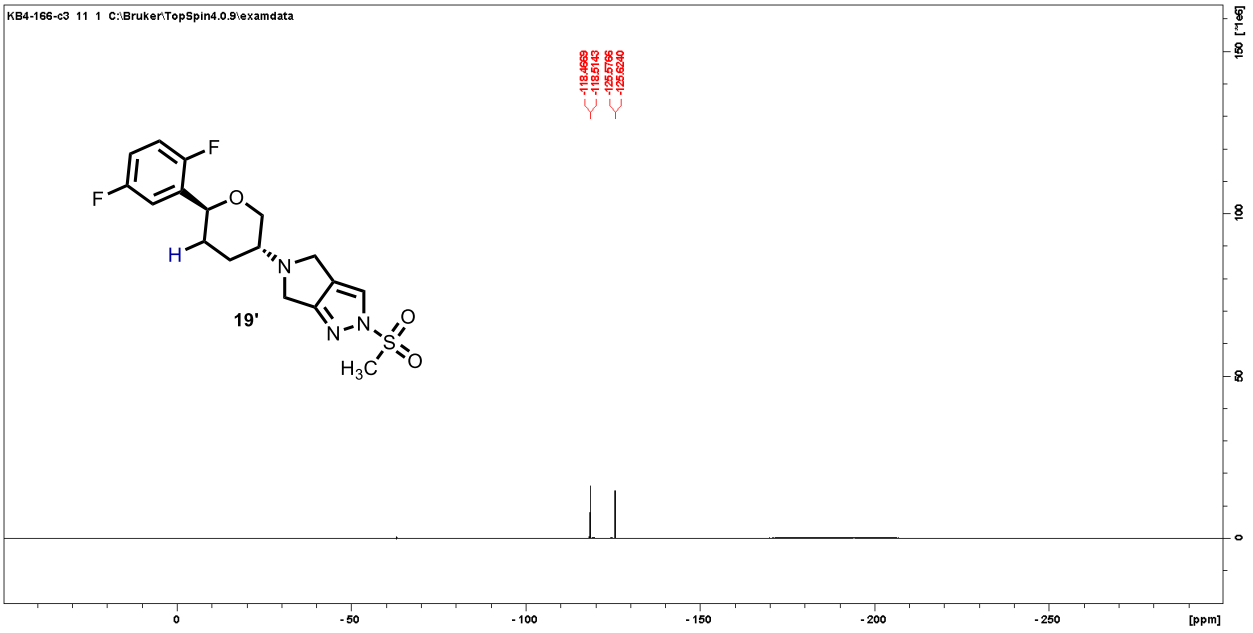

Figure 3.27. $^{19}F\{^{1}H\}$ NMR spectrum of 5-((*3R,6S*)-6-(2,5-difluorophenyl)tetrahydro-*2H*-pyran-3-yl)-2-(methylsulfonyl)-2,4,5,6-tetrahydropyrrolo[3,4-*c*]pyrazole (**19'**) in $CDCl_3$, 376 MHz.

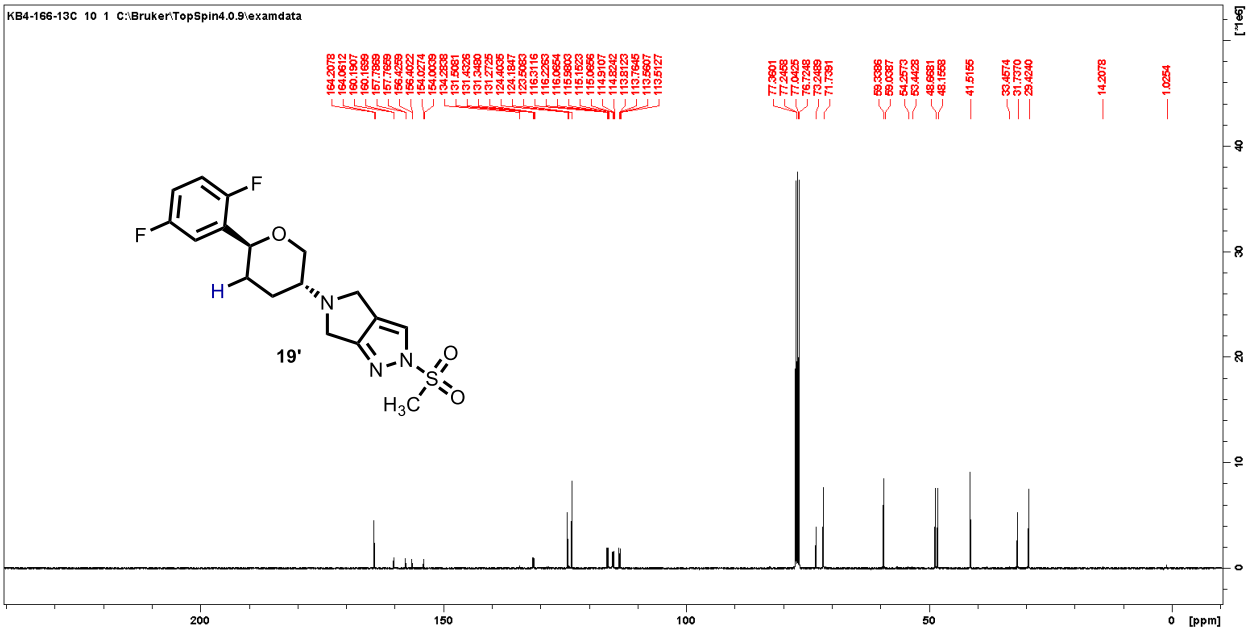

Figure 3.28. $^{13}C\{^{1}H\}$ NMR spectrum of 5-((*3R,6S*)-6-(2,5-difluorophenyl)tetrahydro-*2H*-pyran-3-yl)-2-(methylsulfonyl)-2,4,5,6-tetrahydropyrrolo[3,4-*c*]pyrazole (**19'**) in $CDCl_3$, 100 MHz.

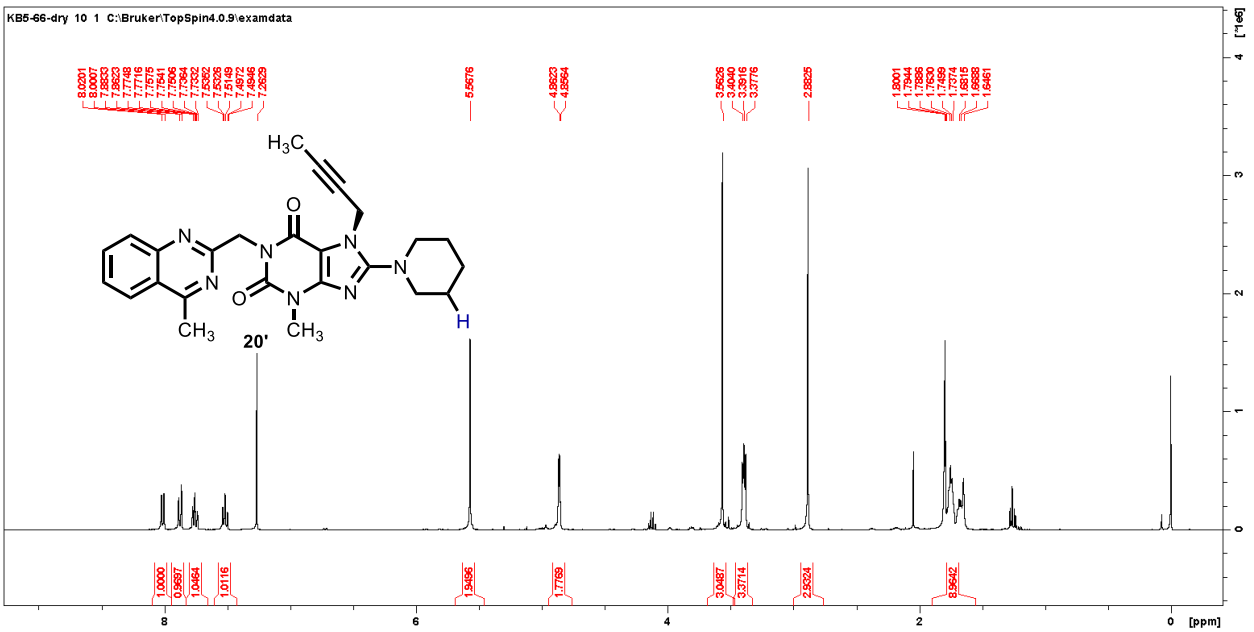

Figure 3.29. ^{1}H NMR spectrum of 7-(but-2-yn-1-yl)-3-methyl-1-((4-methylquinazolin-2-yl)methyl)-8-(piperidin-1-yl)-3,7-dihydro-1*H*-purine-2,6-dione (**20'**) in $CDCl_3$, 400 MHz.

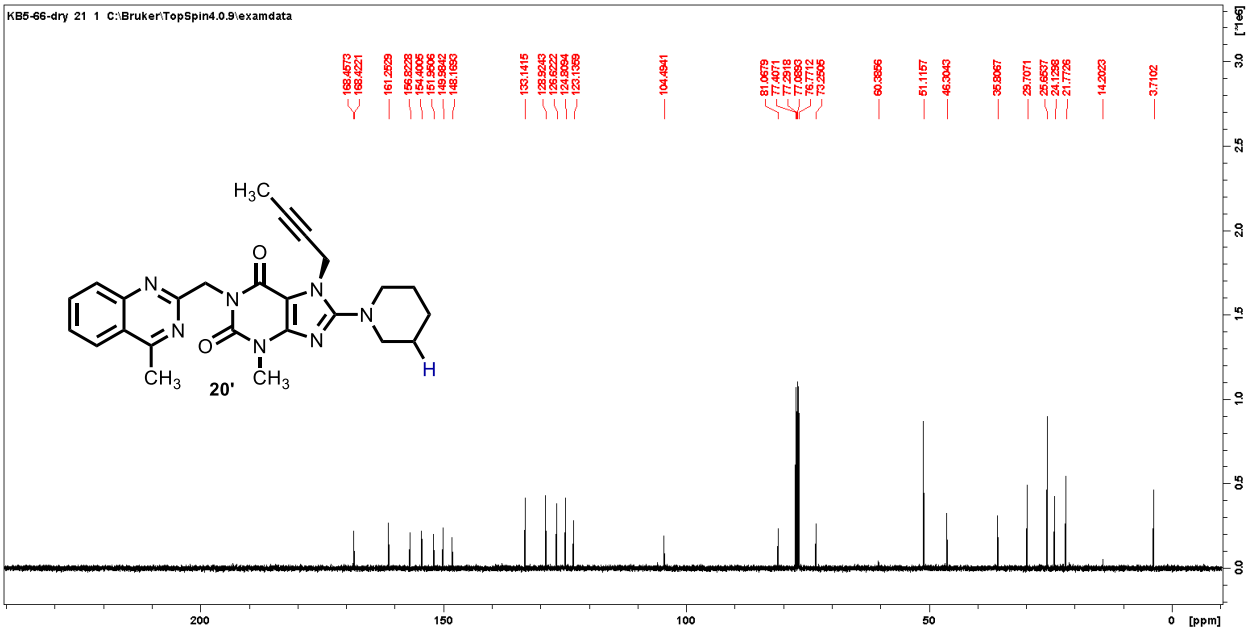

Figure 3.30. ^{13}C{^{1}H} NMR spectrum of 7-(but-2-yn-1-yl)-3-methyl-1-((4-methylquinazolin-2-yl)methyl)-8-(piperidin-1-yl)-3,7-dihydro-1*H*-purine-2,6-dione (**20'**) in $CDCl_3$, 100 MHz.

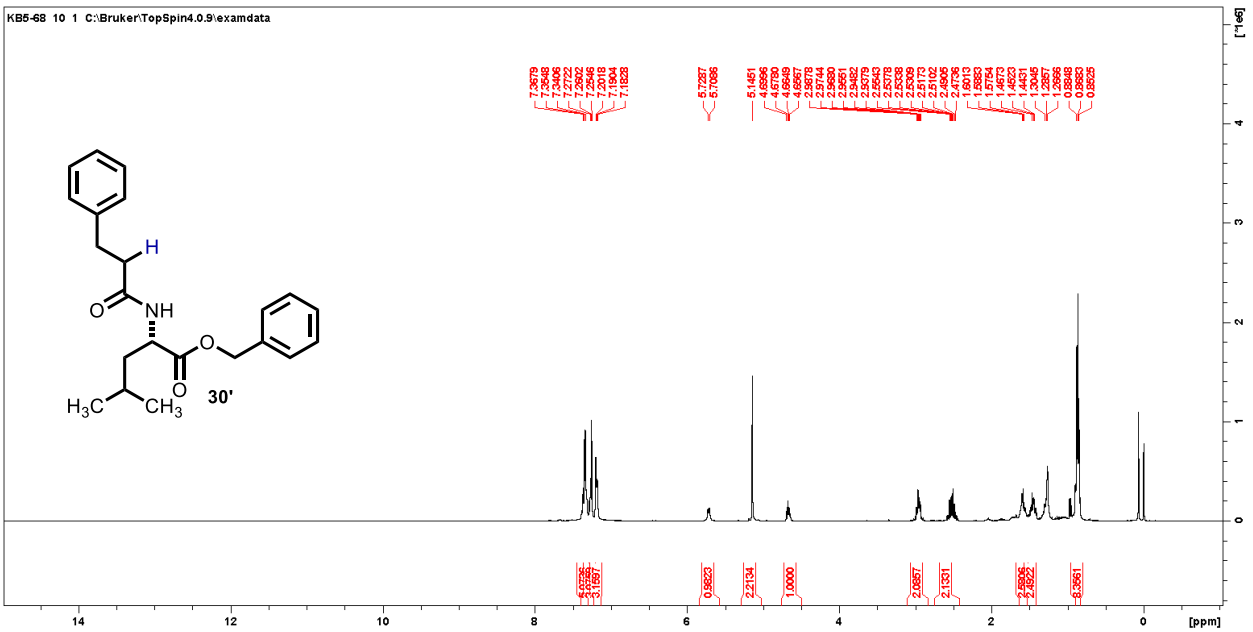

Figure 3.31. ^{1}H NMR spectrum of benzyl (3-phenylpropanoyl)-*L*-leucinate (**30'**) in $CDCl_3$, 400 MHz.

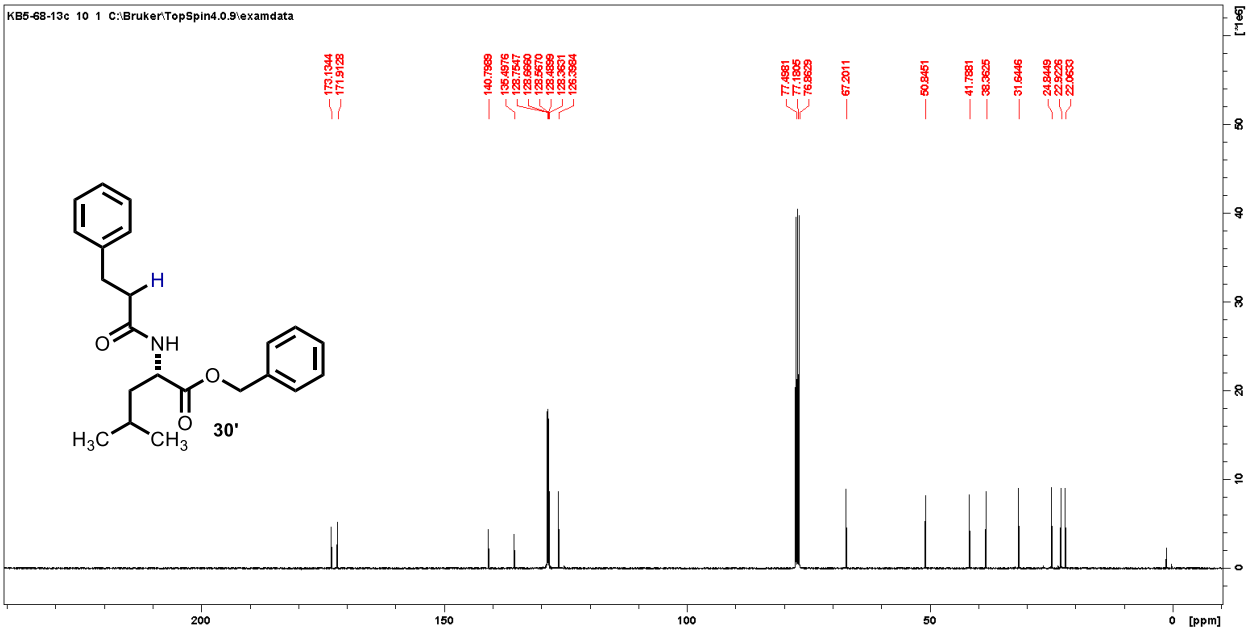

Figure 3.32. ^{13}C{^{1}H} NMR spectrum of benzyl (3-phenylpropanoyl)-*L*-leucinate (**30'**) in $CDCl_3$, 100 MHz.

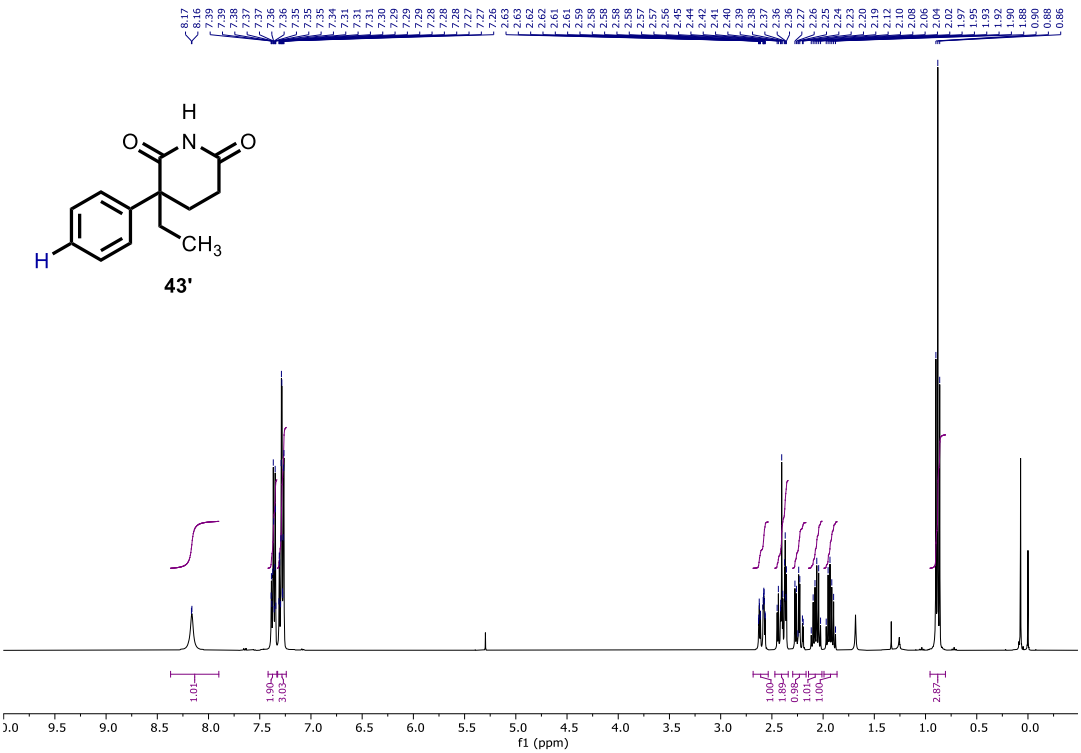

Figure 3.33. ^{1}H NMR spectrum of 3-ethyl-3-phenylpiperidine-2,6-dione (**43'**) in $CDCl_3$, 400 MHz.

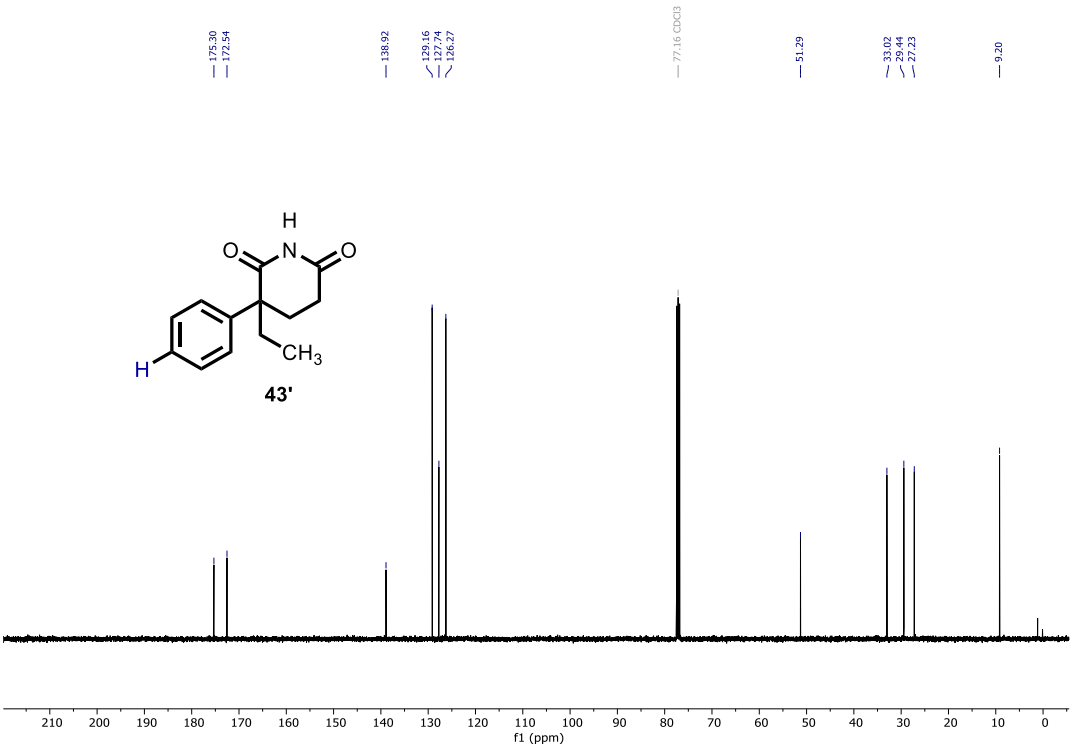

Figure 3.34. $^{13}C\{^{1}H\}$ NMR spectrum of 3-ethyl-3-phenylpiperidine-2,6-dione (**43'**) in $CDCl_3$, 100 MHz.

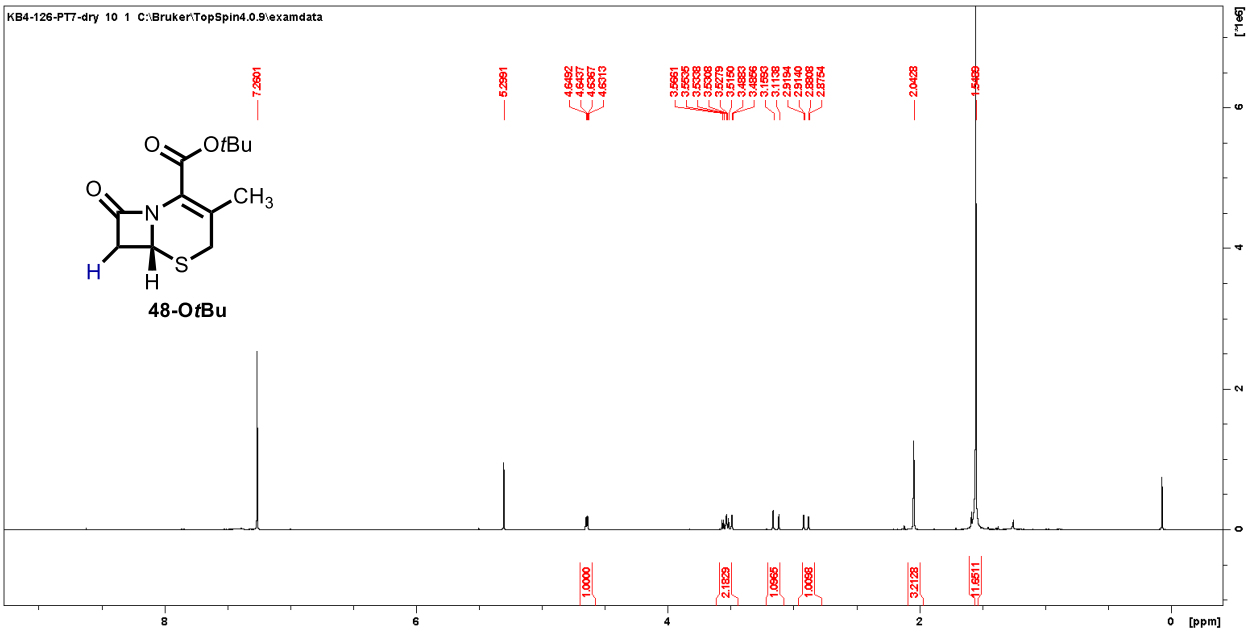

Figure 3.35. ^{1}H NMR spectrum of *tert*-butyl-3-methyl-8-oxo-5-thia-1-azabicyclo[4.2.0]oct-2-ene-2-carboxylate (**48-O*t*Bu**) in $CDCl_3$, 400 MHz.

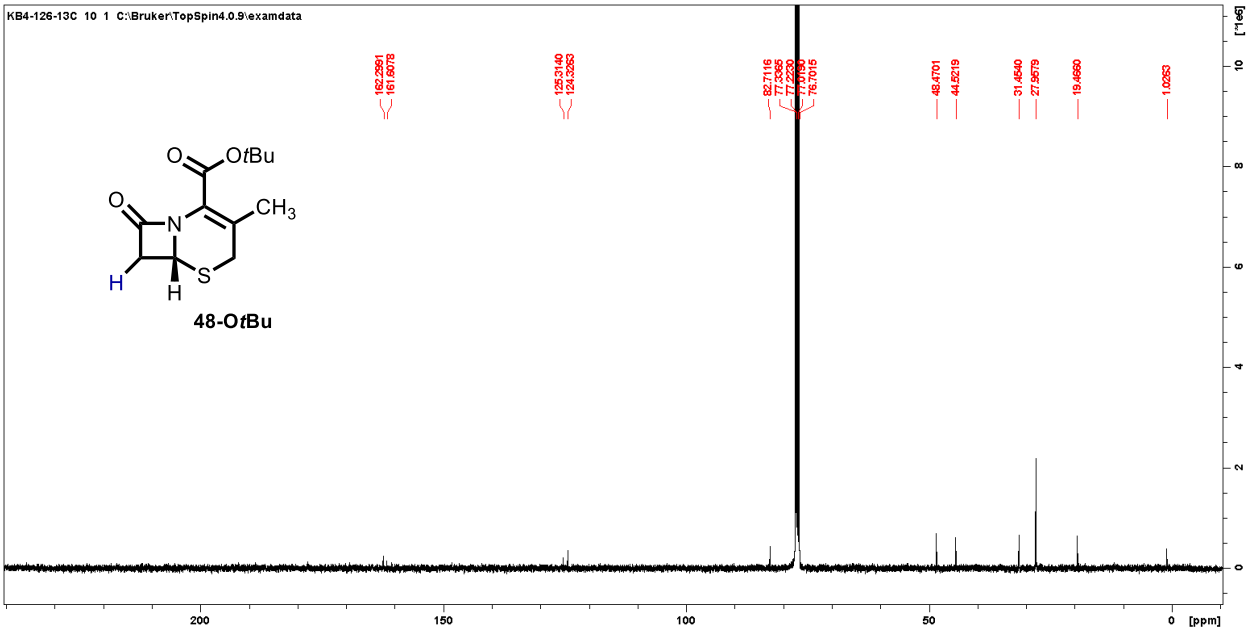

Figure 3.36. ^{13}C{^{1}H} NMR spectrum of *tert*-butyl-3-methyl-8-oxo-5-thia-1-azabicyclo[4.2.0]oct-2-ene-2-carboxylate (**48-O*t*Bu**) in $CDCl_3$, 100 MHz.

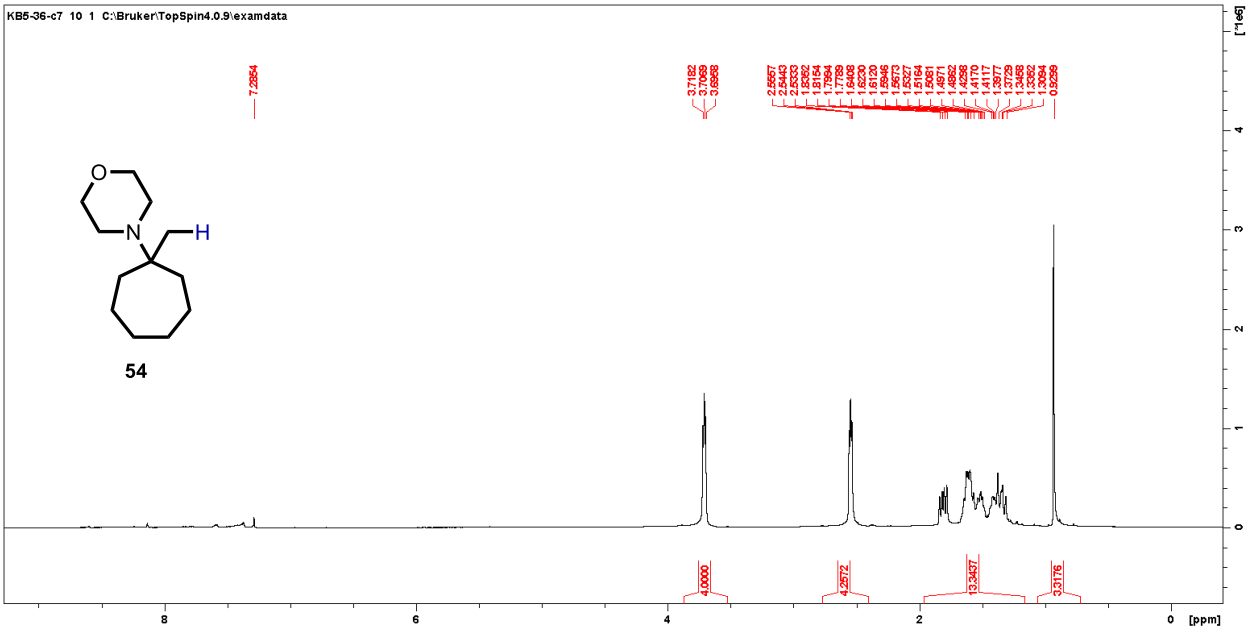

Figure 3.37. ^{1}H NMR spectrum of 4-(1-methylcycloheptyl)morpholine (**54**) in $CDCl_3$, 400 MHz.

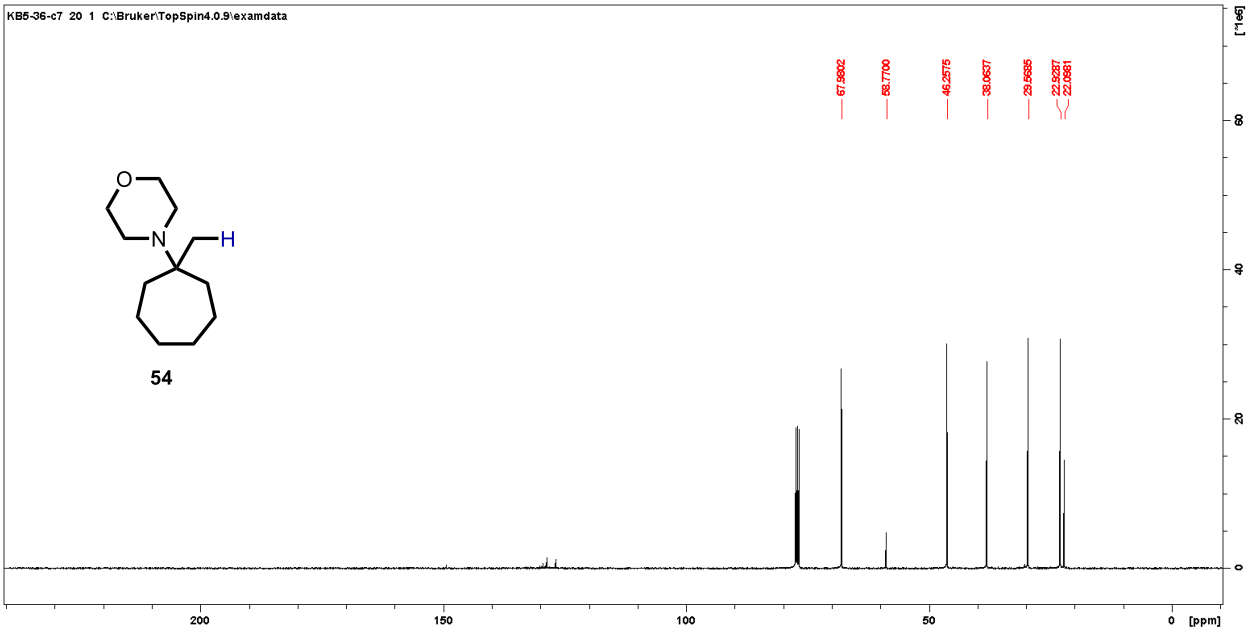

Figure 3.38 ^{13}C{^{1}H} NMR spectrum of 4-(1-methylcycloheptyl)morpholine (**54**) in $CDCl_3$, 100 MHz.

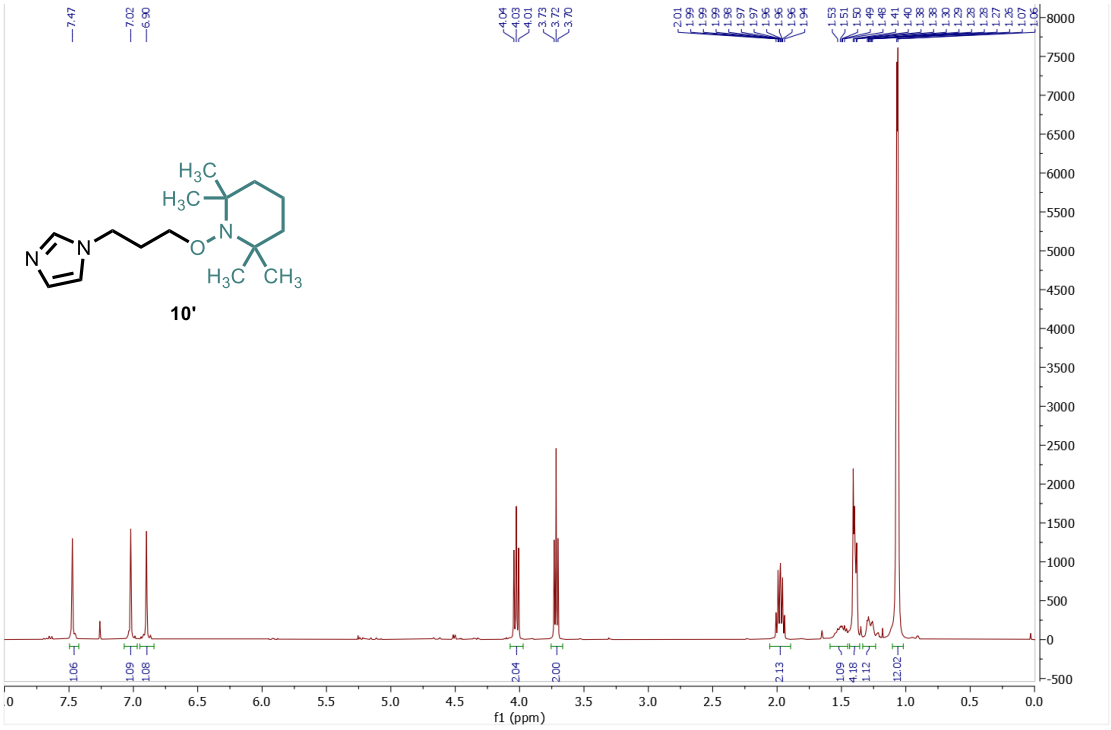

Figure 3.39. ^{1}H NMR spectrum of 1-(3-(1H-imidazol-1-yl)propoxy)-2,2,6,6-tetramethylpiperidine (**10'**) in $CDCl_3$, 400 MHz.

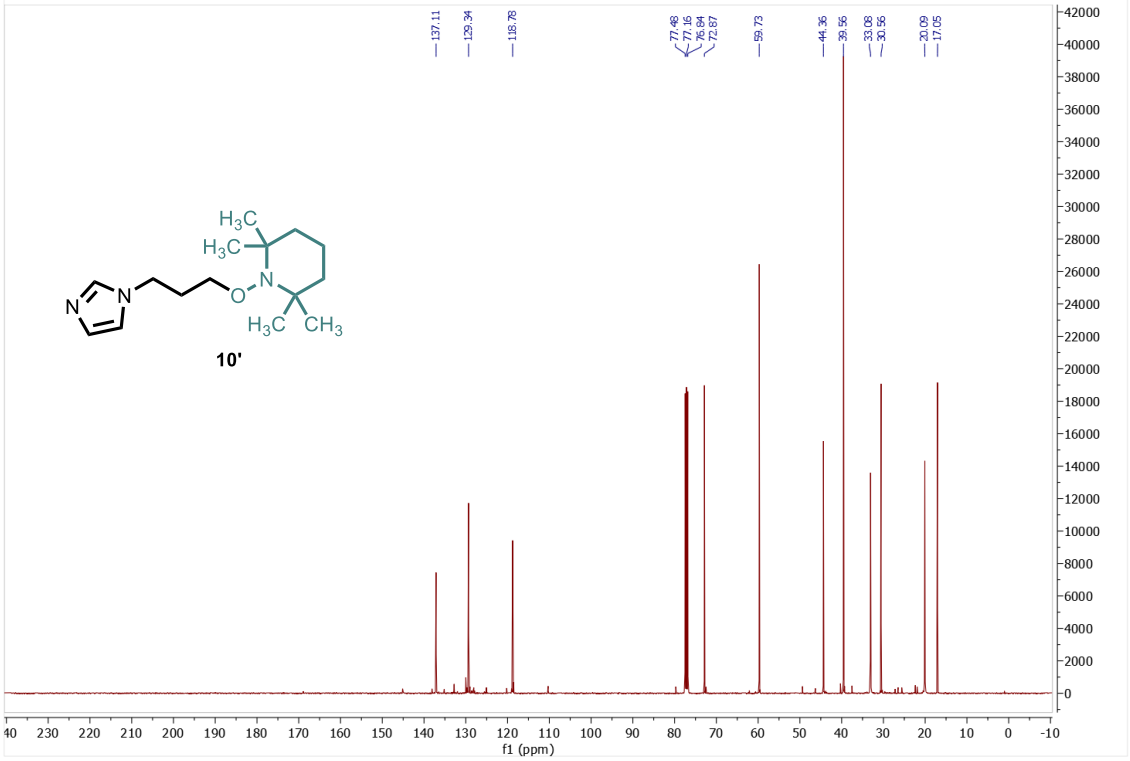

Figure 3.40. $^{13}C\{^{1}H\}$ NMR spectrum of 1-(3-(1H-imidazol-1-yl)propoxy)-2,2,6,6-tetramethylpiperidine (**10'**) in $CDCl_3$, 100 MHz.

3.5. References.

1. Berger, K. J.; Levin, M. D. Reframing Primary Alkyl Amines as Aliphatic Building Blocks. *Org. Biomol. Chem.* **2021,** *19* (1), 11-36.

2. Fang, H.; Oestreich, M. Reductive Deamination with Hydrosilanes Catalyzed by $B(C_6F_5)_3$. *Angew. Chem. Int. Ed.* **2020,** *59* (28), 11394-11398.

3. Basch, C. H.; Liao, J.; Xu, J.; Piane, J. J.; Watson, M. P. Harnessing Alkyl Amines as Electrophiles for Nickel-Catalyzed Cross Couplings *via* C–N Bond Activation. *J. Am. Chem. Soc.* **2017,** *139* (15), 5313-5316.

4. Guan, W.; Liao, J.; Watson, M. P. Vinylation of Benzylic Amines *via* C–N Bond Functionalization of Benzylic Pyridinium Salts. *Synthesis.* **2018,** *50* (16), 3231-3237.

5. Plunkett, S.; Basch, C. H.; Santana, S. O.; Watson, M. P. Harnessing Alkylpyridinium Salts as Electrophiles in Deaminative Alkyl–Alkyl Cross-Couplings. *J. Am. Chem. Soc.* **2019,** *141* (6), 2257-2262.

6. Liao, J.; Basch, C. H.; Hoerrner, M. E.; Talley, M. R.; Boscoe, B. P.; Tucker, J. W.; Garnsey, M. R.; Watson, M. P. Deaminative Reductive Cross-Electrophile Couplings of Alkylpyridinium Salts and Aryl Bromides. *Org. Lett.* **2019,** *21* (8), 2941-2946.

7. Klauck, F. J. R.; James, M. J.; Glorius, F. Deaminative Strategy for the Visible-Light-Mediated Generation of Alkyl Radicals. *Angew. Chem. Int. Ed.* **2017,** *56* (40), 12336-12339.

8. Wu, J.; He, L.; Noble, A.; Aggarwal, V. K. Photoinduced Deaminative Borylation of Alkylamines. *J. Am. Chem. Soc.* **2018,** *140* (34), 10700-10704.

9. Wu, J.; Grant, P. S.; Li, X.; Noble, A.; Aggarwal, V. K. Catalyst-Free Deaminative Functionalizations of Primary Amines by Photoinduced Single-Electron Transfer. *Angew. Chem. Int. Ed.* **2019,** *58* (17), 5697-5701.

10. Katritzky, A. R.; Horvath, K.; Plau, B. Reductive Deamination of Primary Amines. *J. Chem. Soc. Perkin Trans. I.* **1980,** 2554-2560.

11. Katritzky, A. R.; Horvath, K.; Plau, B. Reductive Deamination of Alkyl and Aryl Primary Amines *via* 1,4-Dihydropyridines and a Note on the Mechanism of Reductive Deamination of Benzylamine *via* a 1,2-Dihydropyridine. *J. Chem. Soc. Chem. Commun.* **1979,** (6), 300-301.

12. Barton, D. H. R.; Bringman, G.; Lamotte, G.; Hay Motherwell, R. S.; Motherwell, W. B. Radical Deamination Reactions of Relevance to Aminoglycoside Chemistry. *Tet. Lett.* **1979,** *20* (24), 2291-2294.

13. Barton, D. H. R.; Bringmann, G.; Motherwell, W. B. Radical-Induced Reductive Deamination of Amino Acid Esters. *Synthesis.* **1980,** *1980* (1), 68-70.

14. DeChristopher, P. J.; Adamek, J. P.; Lyon, G. D.; Galante, J. J.; Haffner, H. E.; Boggio, R. J.; Baumgarten, R. J. Approach to Deamination. III. High-yield Conversion of Primary Aliphatic Amines into Alkyl Halides and Alkenes *via* the Use of Sulfonimide Leaving Groups. *J. Am. Chem. Soc.* **1969,** *91* (9), 2384-2385.

15. Guziec, F. S.; Wei, D. Convenient Halodeamination and Hydrodeamination of Primary Amines. *J. Org. Chem.* **1992,** *57* (14), 3772-3776.

16. Bumgardnera, C. L.; Liebmanb, J. F. Considerations of the Mechanism of Reductive Deamination of Primary Amines with HNF_2. *J. Fluor. Chem.* **1993,** *65* (1), 7-9.

17. Guttieri, M. J.; Maier, W. F. Selective Cleavage of Carbon-Nitrogen Bonds with Platinum. *J. Org. Chem.* **1984,** *49* (16), 2875-2880.

18. Maier, W. F.; Grubmüller, P.; Thies, I.; Stein, P. M.; McKervey, M. A.; von Ragué Schleyer, P. Direct Removal of Functional Groups by Catalytic Hydrogenolysis. *Angew. Chem. Int. Ed.* **1979,** *18* (12), 939-940.

19. Audubert, C.; Lebel, H. Mild Esterification of Carboxylic Acids *via* Continuous Flow Diazotization of Amines. *Org. Lett.* **2017,** *19* (16), 4407-4410.

20. Doldouras, G. A.; Kollonitsch, J. A Direct, Selective, and General Method for Reductive Deamination of Primary Amines. *J. Am. Chem. Soc.* **1978,** *100* (1), 341-342.

21. Sylwester, A. P.; Dervan, P. B. Low-Temperature Matrix Isolation of the 1,1-Diazene H_2NN. Electronic and Infrared Characterization. *J. Am. Chem. Soc.* **1984,** *106* (16), 4648-4650.

22. Li, J.; Liu, Q.; Shen, H.; Huang, R.; Zhang, X.; Xiong, Y.; Chen, C. Ethers as Hydrogen Sources in $BF_3{\cdot}OEt_2$ Promoted Reduction of Diphenylmethyl Alcohols, Ethers and Esters to Hydrocarbons. *RSC Adv.* **2015,** *5* (104), 85291-85295.

23. Eliel, E. L.; Manoharan, M.; Pietrusiewicz, K. M.; Hargrave, K. D. Carbon-13 NMR Spectra of Saturated Heterocycles: XI—Tetrahydropyrans (Oxanes). *Org. Magn. Reson.* **1983,** *21* (2), 94-107.

24. Jin, X.; Pybus, B. S.; Marcsisin, S. R.; Logan, T.; Luong, T. L.; Sousa, J.; Matlock, N.; Collazo, V.; Asher, C.; Carroll, D.; Olmeda, R.; Walker, L. A.; Kozar, M. P.; Melendez, V. An LC–MS Based Study of the Metabolic Profile of Primaquine, an 8-Aminoquinoline Antiparasitic Drug, with an *in-vitro* Primary Human Hepatocyte Culture Model. *Eur. J. Drug Metab. Pharmacokinet.* **2014,** *39* (2), 139-146.

25. Myers, A. G.; Movassaghi, M.; Zheng, B. Single-Step Process for the Reductive Deoxygenation of Unhindered Alcohols. *J. Am. Chem. Soc.* **1997,** *119* (36), 8572-8573.

26. Frost, J. W. Synthesis of Caprolactam from Lysine. US7399855B2, Dec. 29, 2005.

27. Kumar, R.; Shah, S.; Paramita Das, P.; Bhagavanbhai, G. G. K.; Al Fatesh, A.; Chowdhury, B. An Overview of Caprolactam Synthesis. *Catal. Rev.* **2019,** *61* (4), 516-594.

28. Sebastian, J.; Zheng, M.; Jiang, Y.; Zhao, Y.; Wang, H.; Song, Z.; Li, X.; Pang, J.; Zhang, T. One-pot Conversion of Lysine to Caprolactam Over Ir/H-Beta Catalysts. *Green Chem.* **2019,** *21* (9), 2462-2468.

29. Lam, S. N.; Gervay-Hague, J. Efficient Route to 2-Deoxy β-O-Aryl-d-Glycosides *via* Direct Displacement of Glycosyl Iodides. *Org. Lett.* **2003,** *5* (22), 4219-4222.

30. Bennett, C. S.; Galan, M. C. Methods for 2-Deoxyglycoside Synthesis. *Chem. Rev.* **2018,** *118* (17), 7931-7985.

31. Mori, N.; Kuzuya, K.; Watanabe, H. Synthesis of (−)-Chamobtusin A from (+)-Dehydroabietylamine. *J. Org. Chem.* **2016,** *81* (23), 11866-11870.

32. Jones, S. Permeability Rules for Antibiotic Design. *Nat. Biotechnol.* **2017,** *35* (7), 639-639.

33. Essack, S. Y. The Development of β-Lactam Antibiotics in Response to the Evolution of β-Lactamases. *Pharm. Res.* **2001,** *18* (10), 1391-1399.

34. De Angelis, F.; Attorrese, G.; Cavicchio, G.; Ciampa, S.; Di Tullio, A.; Fattori, D.; Nicoletti, R.; Domenici, E. Synthesis and Preliminary Biological Evaluation of 3′-Substituted Cephem Sulfones as Potential β-Lactamase Inhibitors. *Eur. J. Org. Chem.* **2001,** *2001* (16), 3075-3081.

35. Burton, J. W. 8.12 Reduction of CX to CH_2. In *Comprehensive Organic Synthesis (Second Edition)*, Knochel, P. Ed; Elsevier: Amsterdam, 2014; pp 446-478.

36. Muraglia, E.; Ontoria, J. M.; Branca, D.; Dessole, G.; Bresciani, A.; Fonsi, M.; Giuliano, C.; Llauger Bufi, L.; Monteagudo, E.; Palumbi, M. C.; Torrisi, C.; Rowley, M.; Steinkühler, C.; Jones, P. *N*-(2-alkylaminoethyl)-4-(1,2,4-oxadiazol-5-yl)piperazine-1-carboxamides as Highly Potent Smoothened Antagonists. *Bioorg. Med. Chem. Lett.* **2011,** *21* (18), 5283-5288.

37. Dong, Z.; Wang, J.; Dong, G. Simple Amine-Directed Meta-Selective C–H Arylation *via* Pd/Norbornene Catalysis. *J. Am. Chem. Soc.* **2015,** *137* (18), 5887-5890.

38. Chen, Y.-Q.; Wang, Z.; Wu, Y.; Wisniewski, S. R.; Qiao, J. X.; Ewing, W. R.; Eastgate, M. D.; Yu, J.-Q. Overcoming the Limitations of γ- and δ-C–H Arylation of Amines through Ligand Development. *J. Am. Chem. Soc.* **2018,** *140* (51), 17884-17894.

39. Kapoor, M.; Liu, D.; Young, M. C. Carbon Dioxide-Mediated $C(sp^3)$–H Arylation of Amine Substrates. *J. Am. Chem. Soc.* **2018,** *140* (22), 6818-6822.

40. Myers, A. G.; Zheng, B. New and Stereospecific Synthesis of Allenes in a Single Step from Propargylic Alcohols. *J. Am. Chem. Soc.* **1996,** *118* (18), 4492-4493.

41. Berger, K. J.; Driscoll, J. L.; Yuan, M.; Dherange, B. D.; Gutierrez, O.; Levin, M. D. Direct Deamination of Primary Amines *via* Isodiazene Intermediates. *J. Am. Chem. Soc.* **2021,** *143* (42), 17366-17373.

42. Newcomb, M. Radical Kinetics and Clocks. In *Encyclopedia of Radicals in Chemistry, Biology and Materials*. Chatgilialoglu, C.; Studer, A. Eds.; John Wiley & Sons, Ltd.: Hoboken, New Jersey, 2012; 1-18.

43. Grigan, N.; Musel, D.; Veinberg, G. A.; Lukevics, E. A Simple Preparative Method for *tert*-Butyl Protection of Aminocephalosporanic Acid. *Synth. Commun.* **1996,** *26* (6), 1183-1185.

44. Oshimoto, K.; Tsuji, H.; Kawatsura, M. Synthesis of Benzoxazoles *via* the Copper-Catalyzed Hydroamination of Alkynones with 2-Aminophenols. *Org. Biomol. Chem.* **2019,** *17* (17), 4225-4229.

45. Chinta, B. S.; Baire, B. Formal Total Synthesis of Selaginpulvilin D. *Org. Biomol. Chem.* **2017,** *15* (28), 5908-5911.

46. Laaksonen, T.; Heikkinen, S.; Wähälä, K. Synthesis and Applications of Secondary Amine Derivatives of (+)-Dehydroabietylamine in Chiral Molecular Recognition. *Org. Biomol. Chem.* **2015,** *13* (42), 10548-10555.

47. Rodes Solanes, R. G. D., Neftali; Lopez Ortega, Beatriz; Alvarez de mon Soto, Melchor; De la Hera Martinez, Antonio; Munoz Munoz, Ana; Ledo Gomez, Francisco. Diphenyl-amine Derivatives: Uses, Process of Synthesis and Pharmaceutical Compositions. WO2012069442A1, May 31, 2012.

48. Borghs, J. C.; Zubar, V.; Azofra, L. M.; Sklyaruk, J.; Rueping, M. Manganese-Catalyzed Regioselective Dehydrogenative *C- versus N*-Alkylation Enabled by a Solvent Switch: Experiment and Computation. *Org. Lett.* **2020,** *22* (11), 4222-4227.

49. Cummings, S. P.; Le, T.-N.; Fernandez, G. E.; Quiambao, L. G.; Stokes, B. J. Tetrahydroxydiboron-Mediated Palladium-Catalyzed Transfer Hydrogenation and Deuteriation of Alkenes and Alkynes Using Water as the Stoichiometric H or D Atom Donor. *J. Am. Chem. Soc.* **2016,** *138* (19), 6107-6110.

50. Arai, T. M.; Yasuhiro, M.; Udagawa, S.; Iseki, K.; Izumimoto, N. Cyclic Amine Derivatives and Pharmaceutical Uses Thereof. SG11201705701UA, Sept. 1, 2016.

51. Merkley, N.; Warkentin, J. Thermolysis of a Spiro-fused Oxadiazoline: The Carbonyl Ylide Cyclic Carbene Diradical Sequence. *Can. J. Chem.* **2002,** *80* (9), 1187-1195.

52. Lee, Y.; Shabbir, S.; Jeong, Y.; Ban, J.; Rhee, H. Formal Synthesis of Fesoterodine by Acid-Facilitated Aromatic Alkylation. *Bull. Korean Chem. Soc.* **2015,** *36* (12), 2885-2889.

53. Maazaoui, R.; Pin-Nó, M.; Gervais, K.; Abderrahim, R.; Ferreira, F.; Perez-Luna, A.; Chemla, F.; Jackowski, O. Domino Methylenation/Hydrogenation of Aldehydes and Ketones by

Combining Matsubara's Reagent and Wilkinson's Catalyst. *Eur. J. Org. Chem.* **2016,** *2016* (34), 5732-5737.

54. Broggi, J.; Jurčík, V.; Songis, O.; Poater, A.; Cavallo, L.; Slawin, A. M. Z.; Cazin, C. S. J. The Isolation of [Pd{OC(O)H}(H)(NHC)(PR_3)] (NHC = N-Heterocyclic Carbene) and Its Role in Alkene and Alkyne Reductions Using Formic Acid. *J. Am. Chem. Soc.* **2013,** *135* (12), 4588-4591.

55. Porcu, S.; Rodriguez, C. A.; Frongia, A.; Secci, F. A. Catalytic One-Pot Synthesis of Indolyl Cyclobutanones. *Synthesis.* **2021,** *53* (05), 925-932.

56. Gao, Y.; Liu, J.; Li, Z.; Guo, T.; Xu, S.; Zhu, H.; Wei, F.; Chen, S.; Gebru, H.; Guo, K. Dichloroimidazolidinedione-Activated Beckmann Rearrangement of Ketoximes for Accessing Amides and Lactams. *J. Org. Chem.* **2018,** *83* (4), 2040-2049.

57. Ganellin, C. R.; Bishop, P. B.; Bambal, R. B.; Chan, S. M. T.; Law, J. K.; Marabout, B.; Luthra, P. M.; Moore, A. N. J.; Peschard, O.; Bourgeat, P.; Rose, C.; Vargas, F.; Schwartz, J.-C. Inhibitors of Tripeptidyl Peptidase II. 2. Generation of the First Novel Lead Inhibitor of Cholecystokinin-8-Inactivating Peptidase: A Strategy for the Design of Peptidase Inhibitors. *J. Med. Chem.* **2000,** *43* (4), 664-674.

58. Jiang, X.; Zhang, J.; Zhao, D.; Li, Y. Aldehyde Effect and Ligand Discovery in Ru-Catalyzed Dehydrogenative Cross-Coupling of Alcohols to Esters. *Chem. Commun.* **2019,** *55* (19), 2797-2800.

59. Beale, T. M.; Moon, P. J.; Taylor, M. S. Organoboron-Catalyzed Regio- and Stereoselective Formation of β-2-Deoxyglycosidic Linkages. *Org. Lett.* **2014,** *16* (13), 3604-3607.

60. Bandari, R.; Höche, T.; Prager, A.; Dirnberger, K.; Buchmeiser, M. R. Ring-Opening Metathesis Polymerization Based Pore-Size-Selective Functionalization of Glycidyl Methacrylate Based Monolithic Media: Access to Size-Stable Nanoparticles for Ligand-Free Metal Catalysis. *Chem. Eur. J.* **2010,** *16* (15), 4650-4658.

61. Zhang, M.; Flynn, D. L.; Hanson, P. R. Oligomeric Benzylsulfonium Salts: Facile Benzylation *via* High-Load ROMP Reagents. *J. Org. Chem.* **2007,** *72* (9), 3194-3198.

62. Chen, X.; Zhou, X.-Y. Decarboxylation of Indole-3-carboxylic Acids Under Metal-free Conditions. *Synth. Commun.* **2020,** *50* (6), 805-812.

63. Li, H.; Tang, X.; Pang, J. H.; Wu, X.; Yeow, E. K. L.; Wu, J.; Chiba, S. Polysulfide Anions as Visible Light Photoredox Catalysts for Aryl Cross-Couplings. *J. Am. Chem. Soc.* **2021,** *143* (1), 481-487.

64. Liu, Z.; Cao, S.; Yu, W.; Wu, J.; Yi, F.; Anderson, E. A.; Bi, X. Site-Selective C–H Benzylation of Alkanes with *N*-Triftosylhydrazones Leading to Alkyl Aromatics. *Chem.* **2020,** *6* (8), 2110-2124.

65. Shibutani, S.; Kodo, T.; Takeda, M.; Nagao, K.; Tokunaga, N.; Sasaki, Y.; Ohmiya, H. Organophotoredox-Catalyzed Decarboxylative C(sp^3)–O Bond Formation. *J. Am. Chem. Soc.* **2020,** *142* (3), 1211-1216.

66. Myers, A. G.; Zheng, B.; Movassaghi, M. Preparation of the Reagent *o*-Nitrobenzenesulfonylhydrazide. *J. Org. Chem.* **1997,** *62* (21), 7507-7507.

67. Zhang, Y.; Torker, S.; Sigrist, M.; Bregović, N.; Dydio, P. Binuclear Pd(I)–Pd(I) Catalysis Assisted by Iodide Ligands for Selective Hydroformylation of Alkenes and Alkynes. *J. Am. Chem. Soc.* **2020,** *142* (42), 18251-18265.

68. Natarajan, P.; Bala, A.; Mehta, S. K.; Bhasin, K. K. Visible-light Photocatalyzed Synthesis of 2-aryl *N*-methylpyrroles, Furans and Thiophenes Utilizing Arylsulfonyl Chlorides as a Coupling Partner. *Tetrahedron* **2016,** *72* (19), 2521-2526.

69. Liu, X.-G.; Dong, C.-S.; Li, F.; Zhang, B. Manganese-Mediated Direct Functionalization of Hantzsch Esters with Alkyl Iodides *via* an Aromatization–Dearomatization Strategy. *Org. Lett.* **2021,** *23* (10), 4002-4007.

CHAPTER 4

Development of New Anomeric Amide Derivatives and Optimization of a Large-Scale Synthesis of *N*-(benzyloxy)-*N*-(pivaloyloxy)-4-(trifluoromethyl)benzamide

4.1. Introduction.

Amides in which the nitrogen moiety is bonded with two electronegative heteroatoms exhibit intriguing properties. In order to satisfy the electron demand of these substituents, the resonance of the nitrogen lone pair with the carbonyl is dramatically reduced (Figure 4.1).[1-5] This results in sp^3 hybridization at nitrogen, as evidenced by pyramidalization in geometry, a decreased barrier to amide bond rotation and a high IR carbonyl vibration frequency in the range of 1710 – 1715 cm^{-1}.[1, 2, 4, 5] These findings have been demonstrated with *N*-acyloxy-*N*-alkoxyamides (**1**),[2, 6] *N*-chloro-*N*-alkoxyamides (**2**),[1] *N*,*N*-dialkoxyamides (**3**),[7, 8] and *N*-alkoxy-*N*-aminoamides (**4**) (Figure 4.2).[1, 9] An anomeric stabilization is also observed between the lone pair of one heteroatom substituent and the σ* orbital of the bond between the amide nitrogen and the other heteroatom substituent, analogous to the anomeric effect commonly observed in sugars.[3-5, 10, 11] Thus, these amides are referred to as anomeric amides. If an amide is substituted with two electronegative heteroatoms (*X*N*Y*), two possible anomeric interactions could in principle occur between either $n_Y – \sigma^*_{NX}$ or $n_X – \sigma^*_{NY}$ (n_X and n_Y represent lone pairs on X or Y and σ^*_{NXorY} represents the antibonding orbital from the N-X or N-Y bonds) (Figure 4.3).[5, 10] Unless both electronegative substituents are identical, one of these interactions is preferential and results in the shortening of one bond and elongation of the other. In *N*-acyloxy-*N*-alkoxyamides, the anomeric effect is observed between the alkoxy oxygen lone pair and the anti-bonding orbital of the *N*-acyloxy bond.[10] Thus, the *N*-acyloxy bond is weakened and the acyloxy group acts as a good leaving group.

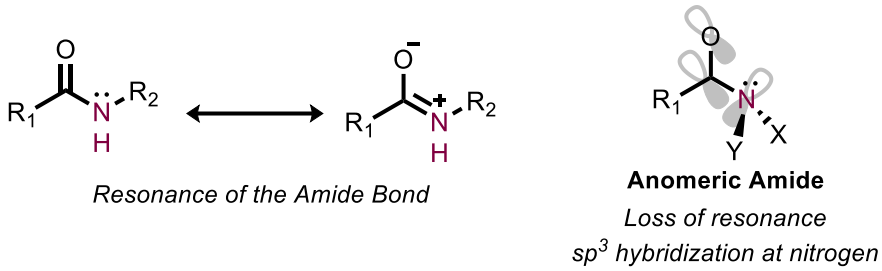

Figure 4.1. Resonance typically observed in amides is impeded by two electronegative substituents (X, Y) at oxygen.

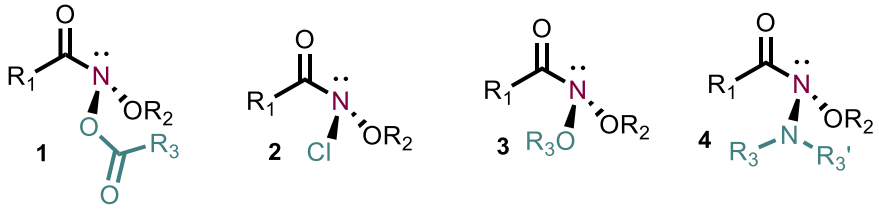

Figure 4.2. Four known classes of anomeric amides.

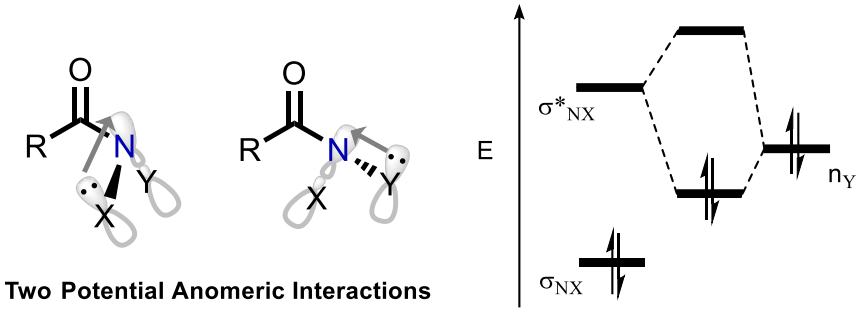

Figure 4.3. a) Two potential anomeric interactions and b) molecular orbital diagram demonstrating an anomeric stabilization.

This anomeric effect is responsible for the interesting reactivity and decomposition pathways exhibited by this class of molecules. Amides which exhibit a strong anomeric stabilization (**5**) may undergo elimination to yield a stabilized nitrenium moiety (**6**) (Scheme 4.1).[1] Additionally with *N*-acyloxy-*N*-alkoxyamides (**1**), radical homolysis of the *N*-acyloxy bond been demonstrated experimentally upon thermolysis in toluene at 90 °C (Scheme 4.2).[2] The resulting alkoxyamidyl radical (**7**) is a long-lived radical species due to the captodative

stabilization by the adjacent acyl and alkoxy moieties. Dimerization of these intermediates to form a hydrazine product (**8**) is known to occur.[2] These hydrazine species can subsequently liberate dinitrogen, resulting in the formation of two equivalents of ester product (**9**).[2, 9] Alkoxyamidyl intermediates undergo several other decomposition pathways, including the formation of **11** by hydrogen atom abstraction from the alkoxy α carbon.[2]

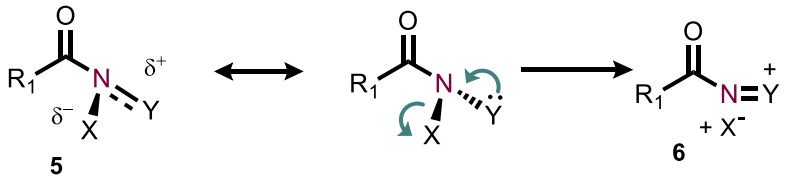

Scheme 4.1. Elimination reaction of anomeric amides yields a nitrenium cation.

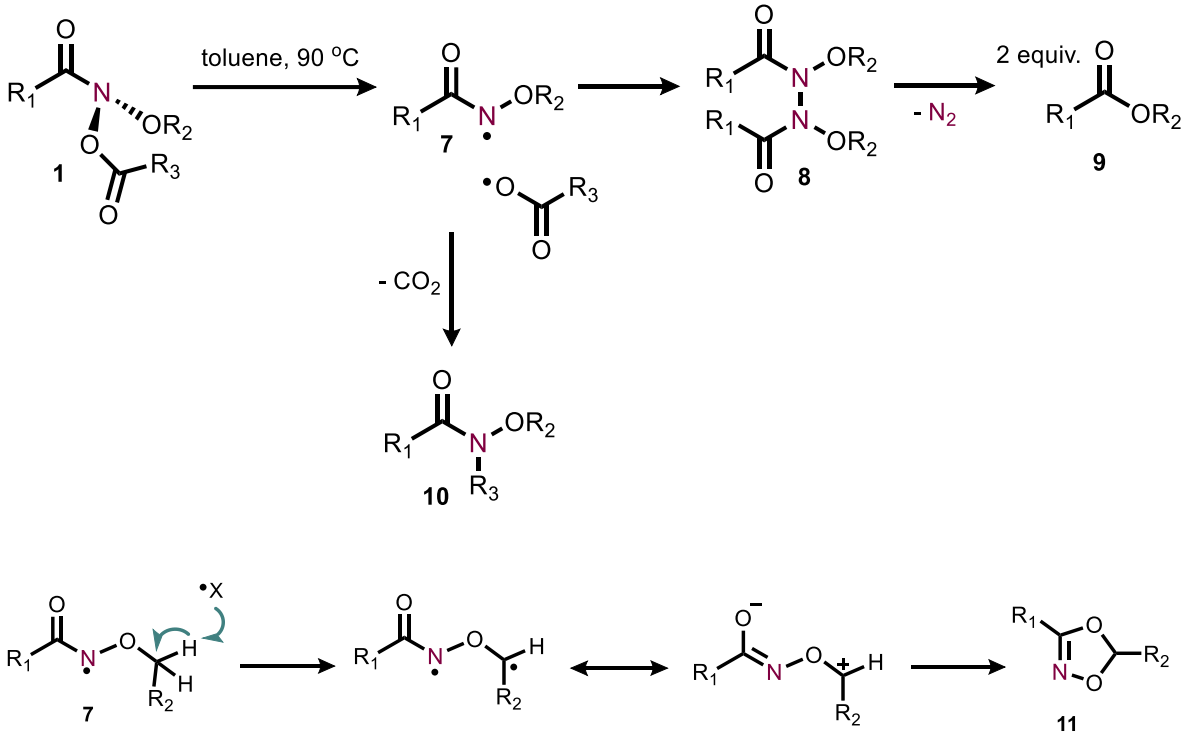

Scheme 4.2. Radical homolysis of anomeric amides yields an alkoxyamidyl radical intermediate, which undergoes several decomposition pathways.

Substitution *via* an S_N2 mechanism has been observed with azide, thiol and amine nucleophiles (Scheme 4.3).[1, 6, 12] Indeed, *N*-acyloxy-*N*-alkoxyamides were first discovered as

mutagenic agents which bind to DNA at the nucleophilic N7 position of guanine in studies with *Salmonella typhimurium*.[13, 14] Kinetic analysis has shown that nucleophilic substitution with anilines is bimolecular in nature and computational modelling has demonstrated a bimolecular transition state (**12**) which exhibits significant charge separation.[6] Substitution has been demonstrated to be sensitive to the sterics of the reagent, with branching α to the amide carbonyl and α to the alkoxy oxygen impeding reactivity and mutagenicity.[6, 13] The sterics of the acyloxy leaving group were shown to be less significant, consistent with an S_N2 mechanism.[13, 15]

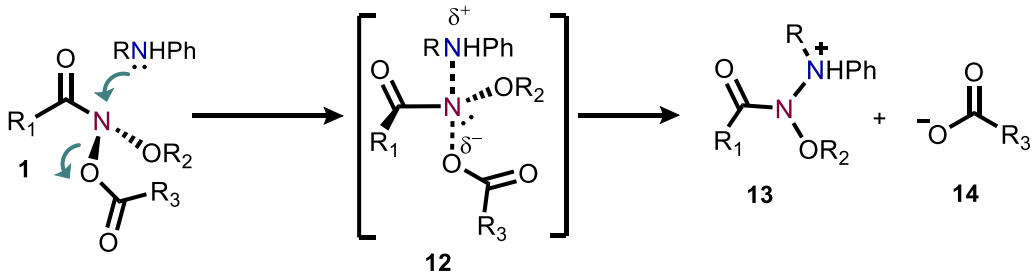

Scheme 4.3. Nucleophilic substitution of anomeric amides.

If the anomeric amide bears a poor leaving group, the anomeric destabilization of this bond can result in a formal reductive elimination, often referred to in these systems as a Heteroatom Rearrangement On Nitrogen (HERON) reaction.[2, 3, 5, 7, 9, 10] This rearrangement involves migration of one heteroatom to the amide carbonyl by liberation of a stabilized nitrene species. In the case of *N*-acyloxy-*N*-alkoxyamides, this results in the formation of an anhydride (**16**) and an alkoxynitrene moiety (**15**), which leads to numerous decomposition products (**17** – **25**) that have been detected experimentally by NMR spectroscopy and GC-MS (Scheme 4.4).[2] Thermolysis of *N*-acyloxy-*N*-alkoxyamides (**1**) has demonstrated this rearrangement occurs in competition with decomposition by radical homolysis of the *N*-acyloxy bond.[2] Substitution of *N*-acyloxy-*N*-alkoxyamides (**1**) with amine nucleophiles results in the formation of *N*-alkoxy-*N*-

aminoamides (**4**), which subsequently undergo a HERON rearrangement preferentially due to the poor leaving group nature of the amino substituent.[10, 12] Since the amine is also a better pi-donor, the aminonitrene moiety is also more stabilized than the corresponding alkoxynitrene product. This rearrangement results in the formation of an isodiazene and an ester side product (see scheme 2.7).[10, 12]

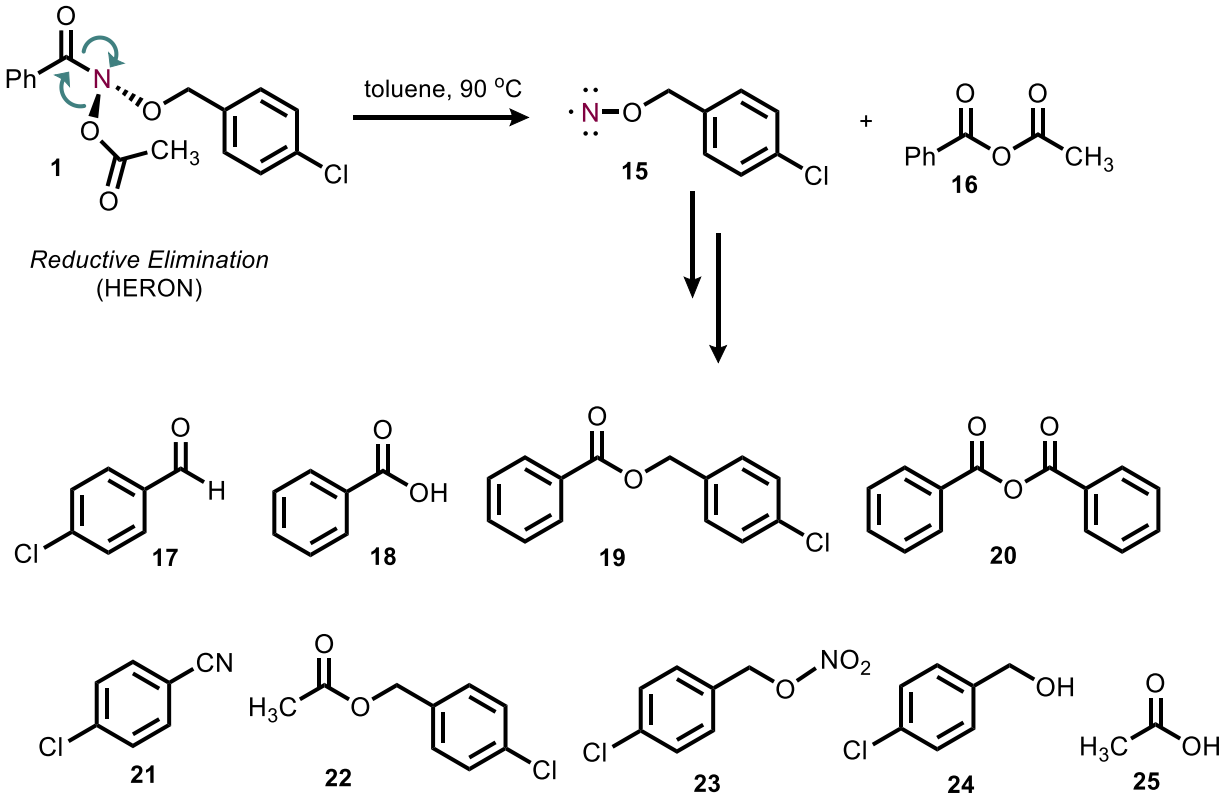

Scheme 4.4. Thermolysis of anomeric amides results in HERON migration and resulting decomposition products.

Chapters 2 and 3 of this thesis describe the use of an *N*-acyloxy-*N*-alkoxy derived anomeric amide reagent (*N*-(benzyloxy)-*N*-(pivaloyloxy)-4-(trifluoromethyl)benzamide for nitrogen 'deletion' of secondary and primary amines, respectively. This anomeric amide reagent was optimized by addition of a *p*-trifluoromethyl group to the benzamide ring, which was found

to increase the rate that initial nucleophilic substitution occurs, as well as the addition of a bulky pivalate derived leaving group to prevent unwanted *N*-acetylation of amines (see Table 2.1). While this reagent was effective at mediating nitrogen deletion reactions of a wide range of amine substrates, we sought to explore the effects of further modifications to the reagent structure. This chapter describes our modular approach to reagent derivatization and the consequences of these modifications with respect to nitrogen deletion chemistry. Additionally, the use of *N*-(benzyloxy)-*N*-(pivaloyloxy)-4-(trifluoromethyl)benzamide for the chemistry presented in chapters 2 and 3 prompted us to develop a robust large-scale synthesis of this reagent. The optimization of this synthesis is discussed in detail in section 4.2.

4.2. Results and Discussion for the Large-Scale Optimization of *N*-(benzyloxy)-*N*-(pivaloyloxy)-4-(trifluoromethyl)benzamide Synthesis.

Throughout our amine deletion studies, the optimized anomeric amide reagent was prepared *via* a three-step synthesis originally developed by Dr. Sean Kennedy (Scheme 4.5). 4-Trifluoromethylbenzoyl chloride (**26**) is first converted to *N*-(benzyloxy)-4-(trifluoromethyl)benzamide (**28**) by addition of *O*-benzylhydroxylamine hydrochloride (**27**) following an established literature procedure.[16] Compound **28** is then treated with *tert*-butylhypochlorite to yield *N*-chloramide intermediate **29**, which undergoes substitution with sodium pivalate to give the desired reagent (**30**).[2, 6, 14, 15, 17, 18] This initial route was robust for quantities up to 1 g but resulted in variable purity of the final compound as the scale was increased. Thus, we wished to conduct a process-chemistry-like optimization of this synthetic route amenable to reproducible large scale synthesis.

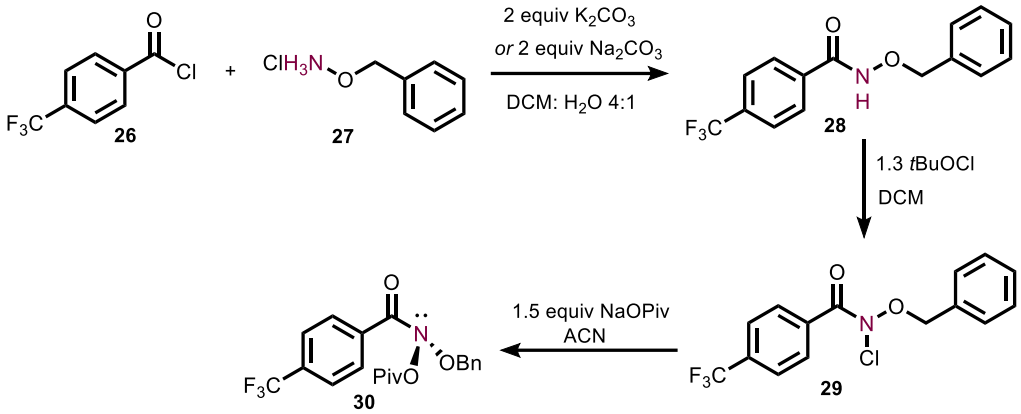

Scheme 4.5. Initial synthetic route to *N*-(benzyloxy)-*N*-(pivaloyloxy)-4-(trifluoromethyl)benzamide **30**.

The synthesis of *N*-(benzyloxy)-4-(trifluoromethyl)benzamide (**28**) was first investigated. Two equivalents of base are added to the reaction to deprotonate *O*-benzylhydroxylamine hydrochloride (**27**) and to neutralize the equivalent of HCl produced during the substitution. Sodium carbonate and potassium carbonate have been used interchangeably as the base for this reaction on a 5 to 10 g scale. *O*-benzylhydroxylamine hydrochloride and the requisite base are dissolved in a solvent mixture of 4:1 DCM:H_2O and the reaction is stirred at 0 ^oC. Neat 4-Trifluoromethylbenzoyl chloride (**26**) is added dropwise, resulting in the precipitation of the product as a white solid (Figure 4.4). Upon completion, the DCM is removed by rotary evaporation and the product solids are isolated by filtration, washing with water and diethyl ether. On a 20 g scale, it was found that potassium carbonate is preferrable over sodium carbonate due to the increased solubility of the byproduct potassium salts during the water wash. This optimized procedure was repeated twice on a 20 g scale and both times a yield of 94% and a purity of 98% as determined by NMR spectroscopy (relative to the internal standard 1,3,5-trimethoxybenzene) were obtained for **28** (Figure 4.5). DMSO-*d6* should be used as the NMR solvent because **28** exists as a mixture of two rotamers in $CDCl_3$ (Figure 4.6).

Figure 4.4. Optimized large scale synthesis of *N*-(benzyloxy)-4-(trifluoromethyl)benzamide **28**.

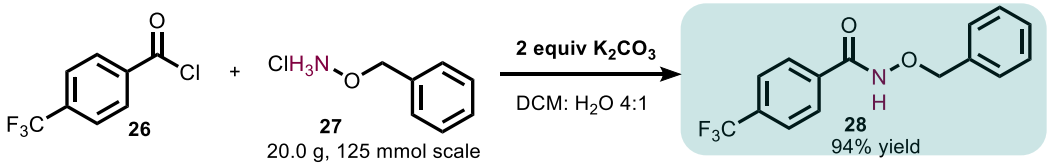

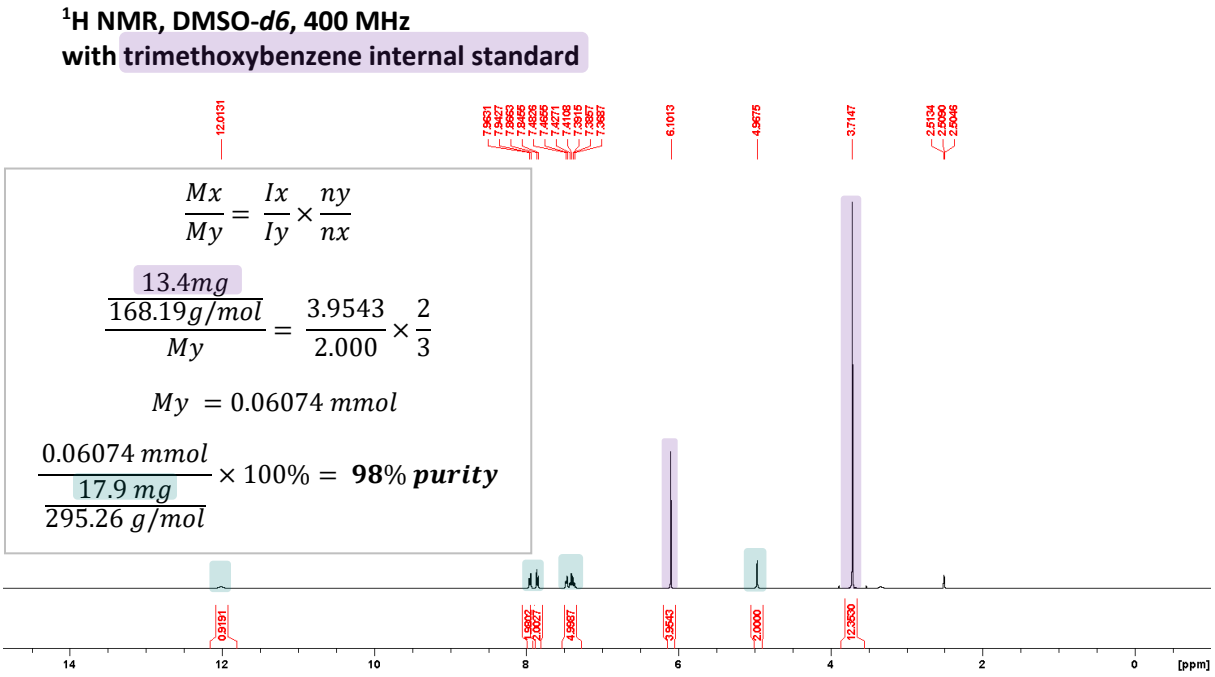

Figure 4.5. Product NMR spectrum of *N*-(benzyloxy)-4-(trifluoromethyl)benzamide **28** demonstrating 98% purity.

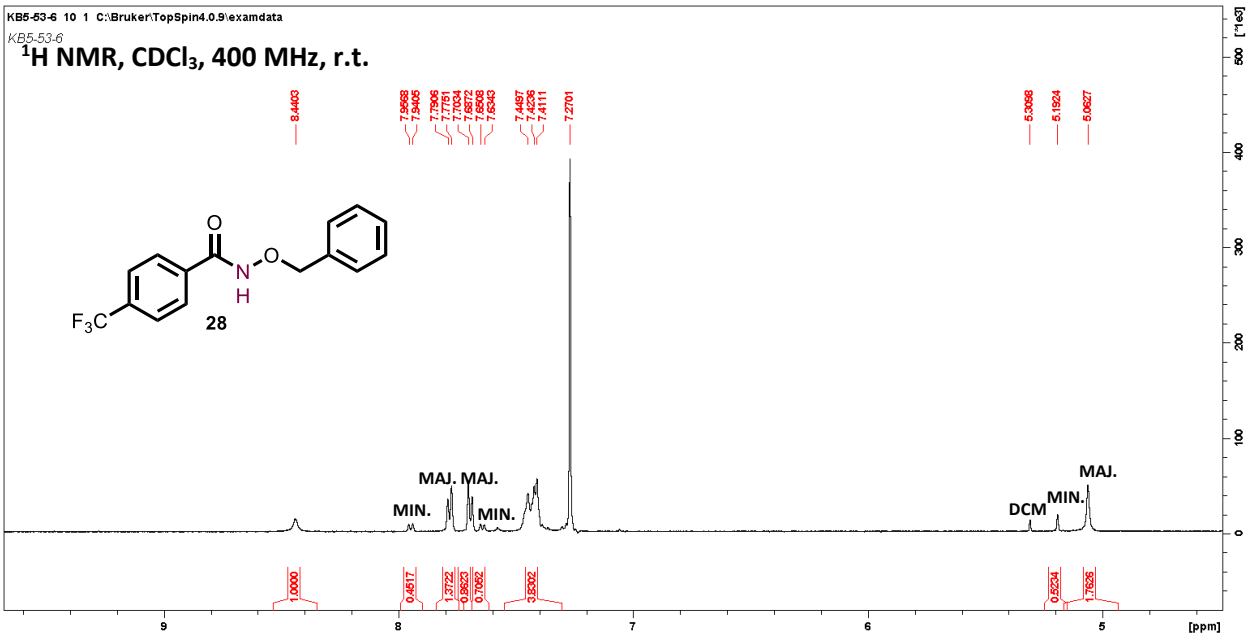

Figure 4.6. NMR spectrum of pure *N*-(benzyloxy)-4-(trifluoromethyl)benzamide **28** in $CDCl_3$ demonstrating major and minor rotamers at room temperature.

With 98% pure *N*-(benzyloxy)-4-(trifluoromethyl)benzamide in hand, the chlorination step was subsequently optimized. In the original procedure, **28** is suspended in DCM and 1.3 equivalents of *tert*-butylhypochlorite are added. Upon completion, DCM is removed by rotary evaporation and excess *tert*-butylhypochlorite is also removed during this process due to its volatility. The crude *N*-chloramide **29** is immediately taken forwards to the next step, as it was observed to decompose if stored. However, there were some safety concerns about scaling up this procedure. In addition to its low boiling point and noxious vapours, *tert*-butylhypochlorite is a heat and light sensitive compound.[19] Thus, we wished to avoid removing excess *tert*-butylhypochlorite by rotary evaporation. An alternative procedure was developed in which *tert*-butylhypochlorite is used as the limiting reagent and fully consumed upon completion of the reaction. However, a method for removing unreacted excess **28** was required. We discovered that the *N*-chloramide intermediate is soluble in pentane, and thus the DCM is removed from the flask by rotary evaporation and pentane is added. The resulting suspension of unreacted **28** is

filtered and pentane is subsequently removed from the filtrate to yield the *N*-chloramide product (Figure 4.7).

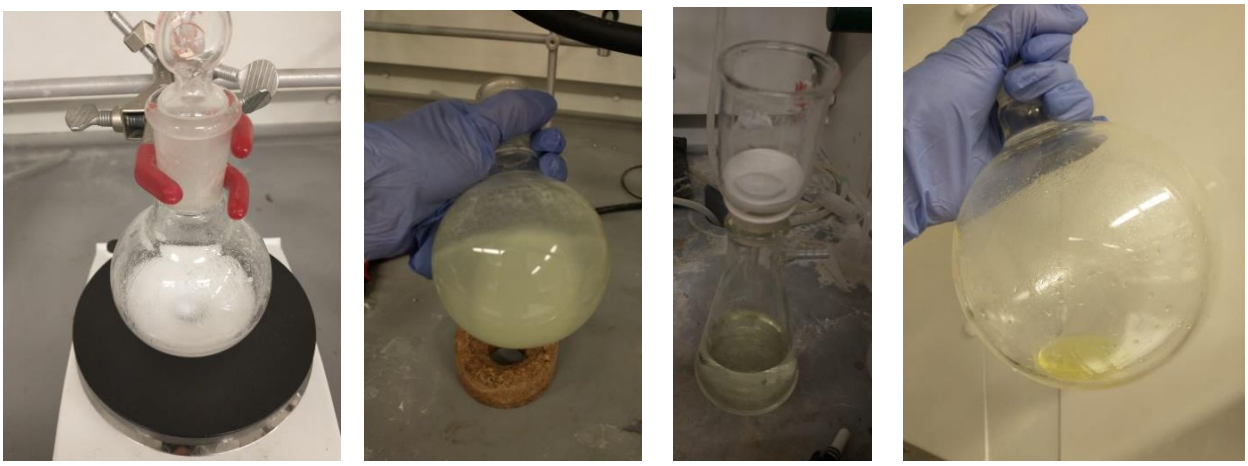

Figure 4.7. Synthesis of *N*-chloramide intermediate **29** using *tert*-butylhypochlorite as the limiting reagent.

Initial trials of this procedure found that the *N*-chloramide **29** is produced in sufficient purity as determined by NMR spectroscopy relative to internal standard (either mesitylene or dodecane must be used as the internal standard because the *N*-chloramide will react with trimethoxybenzene to give 2,4,6-trimethoxychlorobenzene). However, subsequent testing found that some batches produced were 70 – 80 % pure. Dr. Balu Dherange detected the presence of a polar impurity spot by TLC, which we hypothesized might correspond to an *N*-OH impurity. Thus, we wondered if the decrease in purity could be attributed to adventitious water. In order to probe this, the reaction was spiked with several equivalents of water. Surprisingly, this addition of water resulted in product with a purity of 97%. It is possible that water increases the purity by mitigating an exotherm, or that it acts to protonate the transiently formed *tert*-butoxy anion and prevents this intermediate from reacting with the *N*-chloramide product.

Another drawback to the use of *tert*-butyl hypochlorite is that it must be prepared fresh before conducting the *N*-chlorination step. The literature procedure for its synthesis also utilizes household bleach,[19] which is not a standardized chemical and introduces more variables which could potentially affect the reproducibility of our procedure. Thus, we wished to explore other chlorinating reagents. Trichloroisocyanuric acid (TCICA) is a preferable oxidant because it is commercially available and a solid, which is safer to handle. Initially studies with this oxidant found that **29** is not produced in sufficient purity (defined as ≥ 97% throughout this chapter). However, the observation that addition of water to the *tert*-butylhypochlorite synthesis increased product purity prompted us to explore this procedure with TCICA. Dr. Balu Dherange found that using TCICA results in 97% pure product (Figure 4.8) when three equivalents of water are added and the reaction is cooled to 0 ^{o}C. The pentane filtration procedure is also successful in removing excess TCICA and its byproducts (Figure 4.9). When the reaction is conducted with TCICA at 0 ^{o}C without water, the corresponding product was determined to be 91% pure. We observed that water causes the excess TCICA and its byproducts to aggregate during the reaction. It is possible that this inhibits the formation of unwanted side products, such as those formed from the interaction of the corresponding TCICA anion and **29**. Using the optimized *N*-chlorination procedure, **29** should be immediately carried through to the final substitution with sodium pivalate. We observed that **29** undergoes decomposition upon storage, even at -20 ^{o}C, likely due to the thermal and light sensitivity of the N-Cl bond.

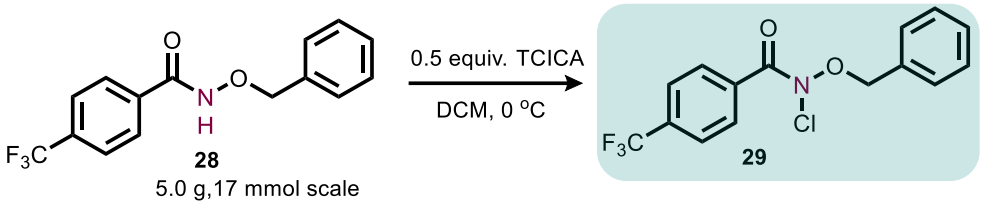

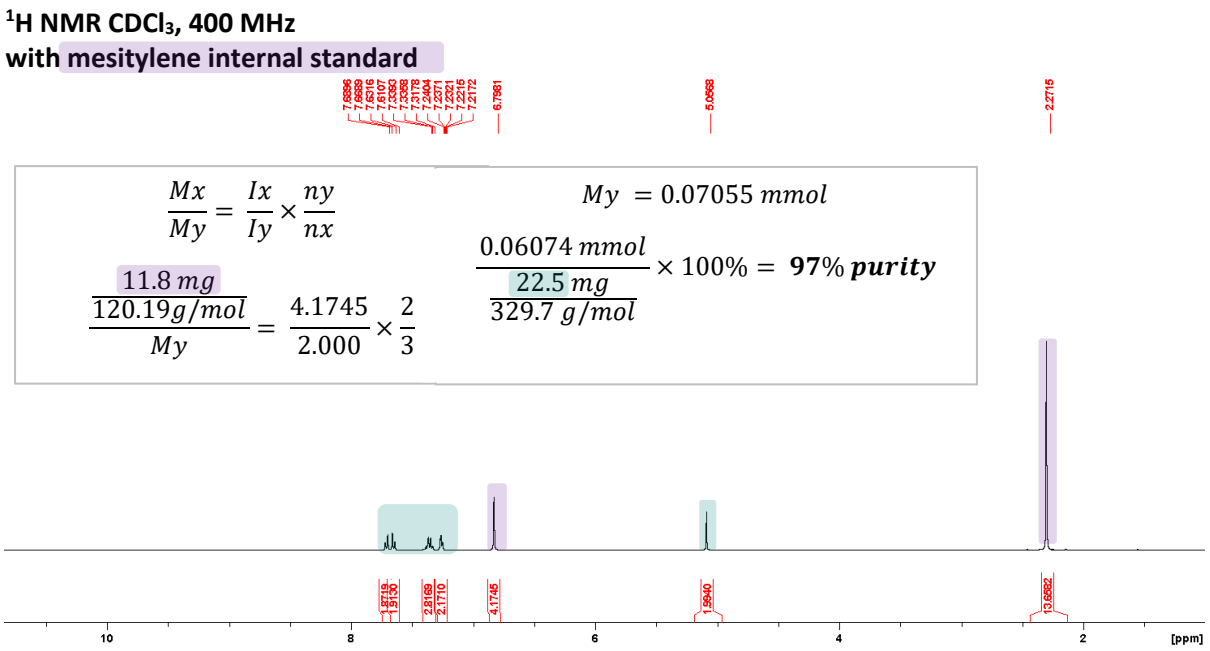

Figure 4.8. Product NMR spectrum of *N*-chloramide **29** demonstrating 97% purity.

Figure 4.9. Synthesis of *N*-chloramide intermediate **29** with TCICA.

The final substitution with sodium pivalate was the most challenging component of the synthesis to scale up. This is likely because the reaction is a suspension and not a homogeneous solution, and reactions of suspended solids are known to be sensitive to mass transport effects that are variable at scale.[20] The reaction is also air sensitive and must be conducted using appropriate air-free techniques (see Figure 4.11). When the reaction is run under air, the purity of the product is dramatically decreased and the presence of aldehyde-containing impurities are visible in the product NMR spectrum, indicating unwanted oxidation. The original procedure involved dissolving the *N*-chloramide intermediate **29** in acetonitrile and adding 1.5 equiv. of sodium pivalate to form a suspension, which is stirred vigorously for 2 hours. Diethyl ether is added and the suspension is filtered over a small plug of silica. The solvent is removed from the filtrate by rotary evaporation to yield **30**. When the reaction was conducted on a 5 to 10 g scale, the presence of two impurity peaks which are not produced on a 1 g scale were detected by NMR spectroscopy. These impurities were identified as pivalic acid (**31**) and pivalic anhydride (**32**) in comparison with literature NMR spectra (Figure 4.10).[21, 22] Initially, we wished to develop a purification procedure for **30** that would simply remove these impurities. Efforts to purify **30** by chromatography on a number of supports and with a wide variety of mobile phases proved fruitless because **30** undergoes significant decomposition. Both deactivated silica and alumina were explored and found to be unsuccessful. Indeed, Glover has reported purification of anomeric amide derivatives using centrifugal liquid-liquid chromatography,[8] however this technique is not widely available to most synthetic organic chemists.

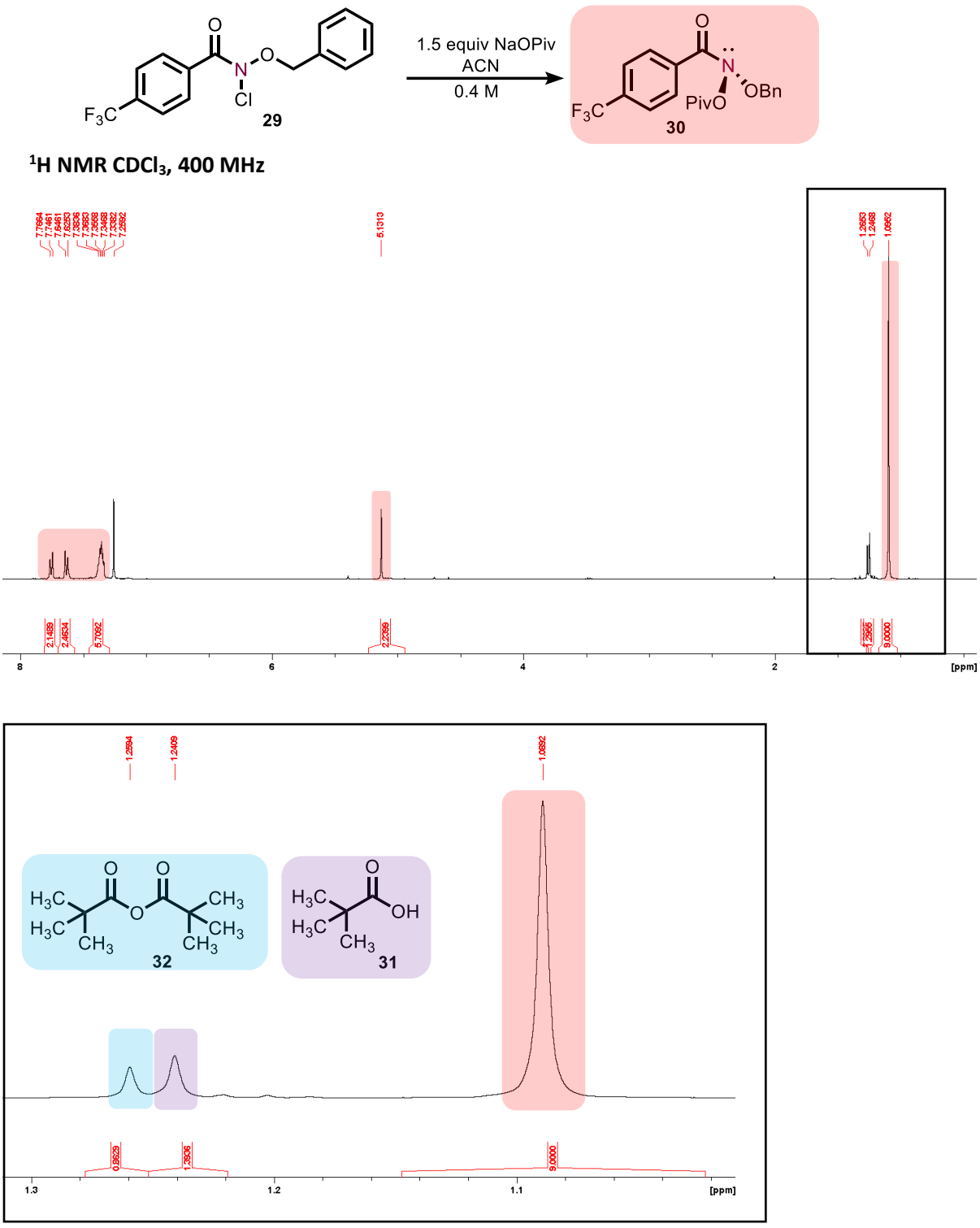

Figure 4.10. ^{1}H NMR Spectrum of *N*-(benzyloxy)-*N*-(pivaloyloxy)-4-(trifluoromethyl)benzamide **30** demonstrating impurity peaks.

Recrystallization was also explored. However, this posed additional challenges because **30** is very nonpolar and soluble in pentane even at low temperatures. Undergraduate student Megan Morales found that using our -80 ^{o}C freezer, **30** precipitates from a concentrated solution of pentane as an amorphous solid. We explored repeat precipitations at -80 ^{o}C, however the pivalic anhydride impurity appeared to co-precipitate with **30**, as it is very non-polar. It was also very challenging to filter the precipitate because as the temperature increases from -80 ^{o}C, the product goes back into solution in pentane.

Thus, some alternative procedures for removing these two impurities were explored. We found that after dissolving in pentane, **30** could be extracted to acetonitrile. By extracting once, 50% of the pivalic anhydride impurity is removed. However, 10% of the product is also lost to the pentane fraction. Thus, we reasoned that this extraction procedure is not acceptably efficient to purify the product from pivalic anhydride. In order to remove the pivalic acid impurity, the product was dissolved in hexanes and washed once with saturated aqueous sodium bicarbonate solution. This wash is successful in completely removing the pivalic acid impurity, however 10% of **30** degrades when exposed to the wash.

Since all of these purification attempts were unsuccessful, we sought to mitigate the formation of these impurities during the large-scale synthesis. In the initial procedure developed by Dr. Sean Kennedy, the substitution with sodium pivalate is conducted at 0.4 M. We hypothesized that the formation of the two impurities is concentration dependent. Indeed, when the reaction is increased to 0.7 M, the integration of the two impurities is approximately doubled. Decreasing the concentration below 0.4 M was then explored. At 0.2 M the purity was found to be 98%. However, conducting the reaction at 0.1 M did not result in any further increase in purity.

The mitigation of these impurities at 0.2 M concentration was a promising result, however this finding was not fully reproducible between batches, with some still exhibiting unacceptable levels. We hypothesized that the formation of these impurities on a large scale might be due to an exotherm which was dissipated better on a small scale.[23] The reaction was conducted at 0 °C using an ice bath and excitingly, the formation of these impurities is fully inhibited under these conditions (Figure 4.11). Using the optimized concentration and temperature, this procedure reproducibly gives >97% pure anomeric amide on a 5 g scale (Figure 4.12). After filtration of excess sodium pivalate and removal of solvent, product **30** should be isolated as a clear oil, which solidifies upon storage at 5 °C to form a white solid. Typically, a yellow discoloration indicates the presence of pivalic acid and pivalic anhydride impurities. The product was isolated in 89% yield across two steps, calculated from *N*-(benzyloxy)-4-(trifluoromethyl)benzamide starting material (**28**).

Figure 4.11. Optimized synthesis of *N*-(benzyloxy)-*N*-(pivaloyloxy)-4-(trifluoromethyl)benzamide **30**.

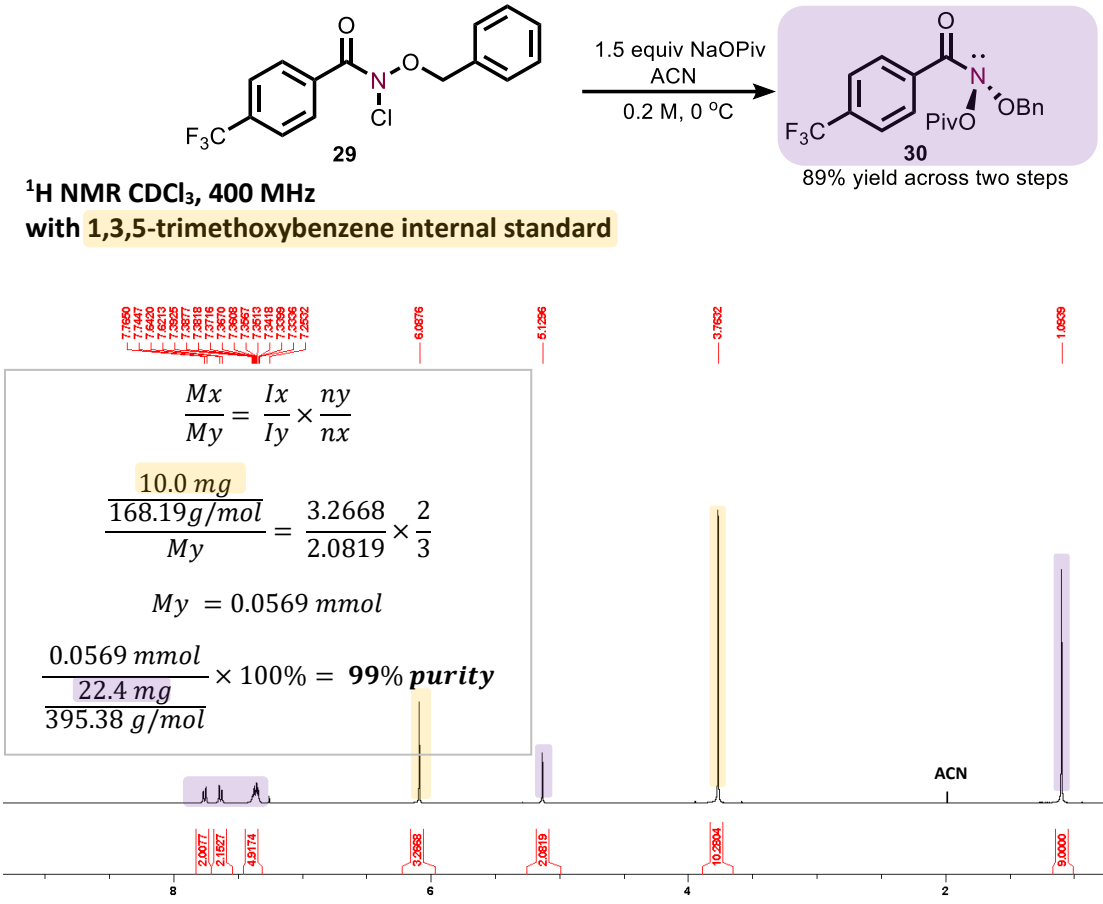

Figure 4.12. NMR spectrum of *N*-(benzyloxy)-*N*-(pivaloyloxy)-4-(trifluoromethyl)benzamide **30** showing 99% purity.

The source of sodium pivalate has also been analyzed. We previously prepared sodium pivalate in house by treating a water solution of pivalic acid with sodium hydroxide. Acetone is added to precipitate sodium pivalate and the requisite salt is isolated by filtration. The sodium pivalate is subsequently dried under high vacuum to remove any water. While this suffices for small scale synthesis of anomeric amides, on a large scale it is cumbersome to repeat. We thus investigated commercial sources of sodium pivalate. The use of commercial anhydrous sodium pivalate produces anomeric amide product in 97% purity. An NMR spectrum of the sodium pivalate batch in deuterated water also verified that there were no pivalic acid or pivalic anhydride impurities. Storage in a vacuum oven at 100 °C ensures the sodium pivalate remains anhydrous. Sodium pivalate monohydrate is also commercially available and the use of this was

investigated. We found that sodium pivalate monohydrate results in anomeric amide which is only 90% pure. This decrease is due to an increase in the amount of the pivalic acid impurity in the product, which likely because of the equivalent of water.

4.3. Results and Discussion for the Synthesis of New Anomeric Amide Derivatives.

Throughout the primary and secondary amine deletion studies a variety of new reagent derivatives were also explored. Anomeric amides can be thought of as containing three entities which affect reactivity, the benzoyl or acyl group, the *O*-benzyl or *O*-alkyl group, and the leaving group (Figure 4.13).[13] A modular approach was taken to reagent development, in which each of these components were varied independently, and the properties of the resulting anomeric amide were then studied. Figure 4.14 summarizes the anomeric amide derivatives that were explored throughout this investigation. The following sections discuss the rationale for and outcome of these different anomeric amide derivatizations. Modifications to the amide bond itself were also considered and attempts to synthesize derivatives containing carbonyl isosteres are discussed in section 4.3.4.

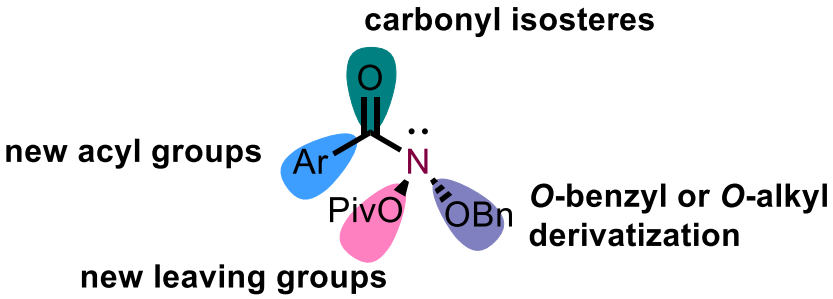

Figure 4.13. Modular approach for the development of new anomeric amide derivatives.

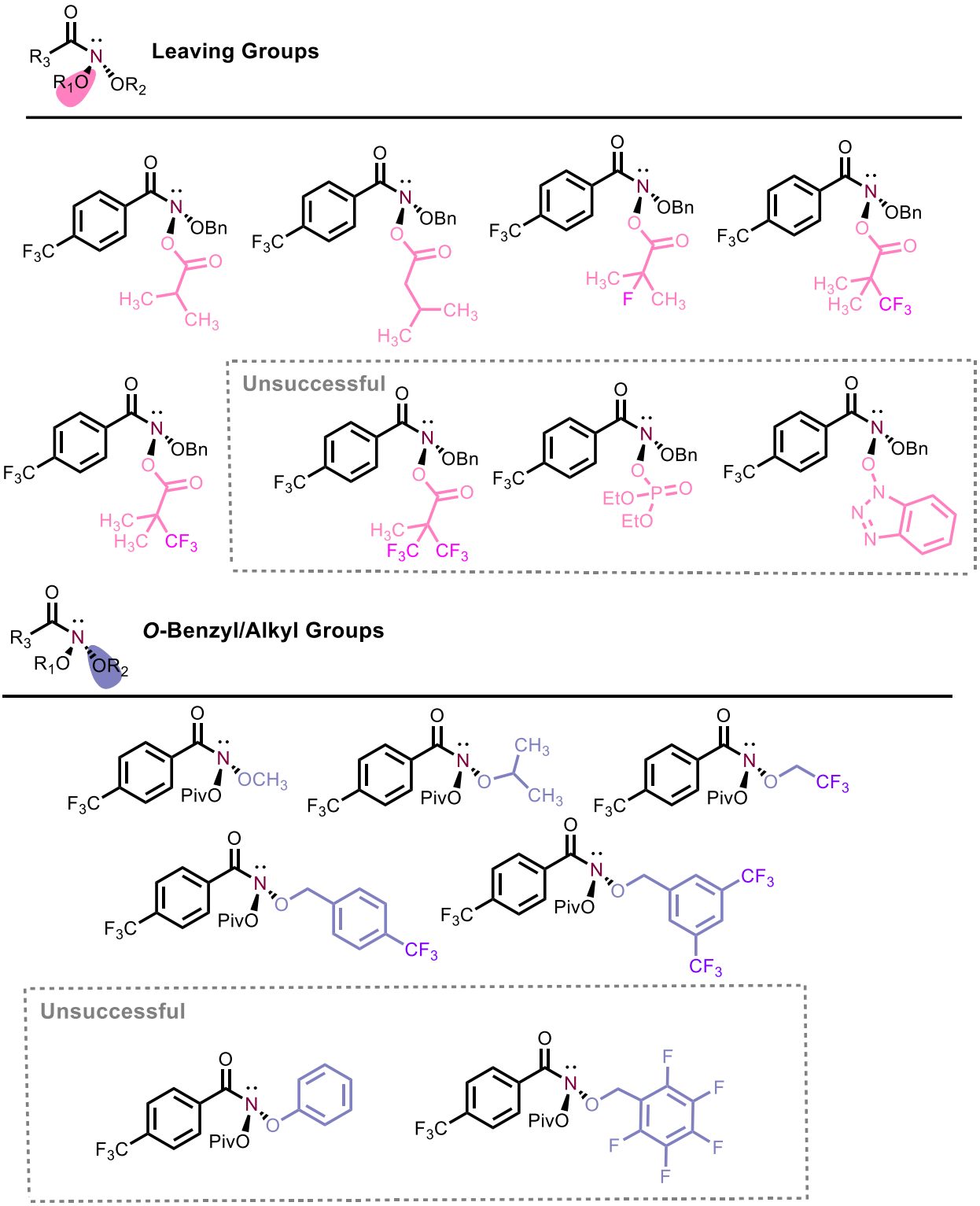

Figure 4.14. Summary of anomeric amide derivatives studied. *Additional derivatives prepared for the Hammett plot analysis are summarized in figure 2.2.

Figure 4.14 continued. Summary of anomeric amide derivatives studied. *Additional derivatives prepared for the Hammett plot analysis are summarized in figure 2.2.

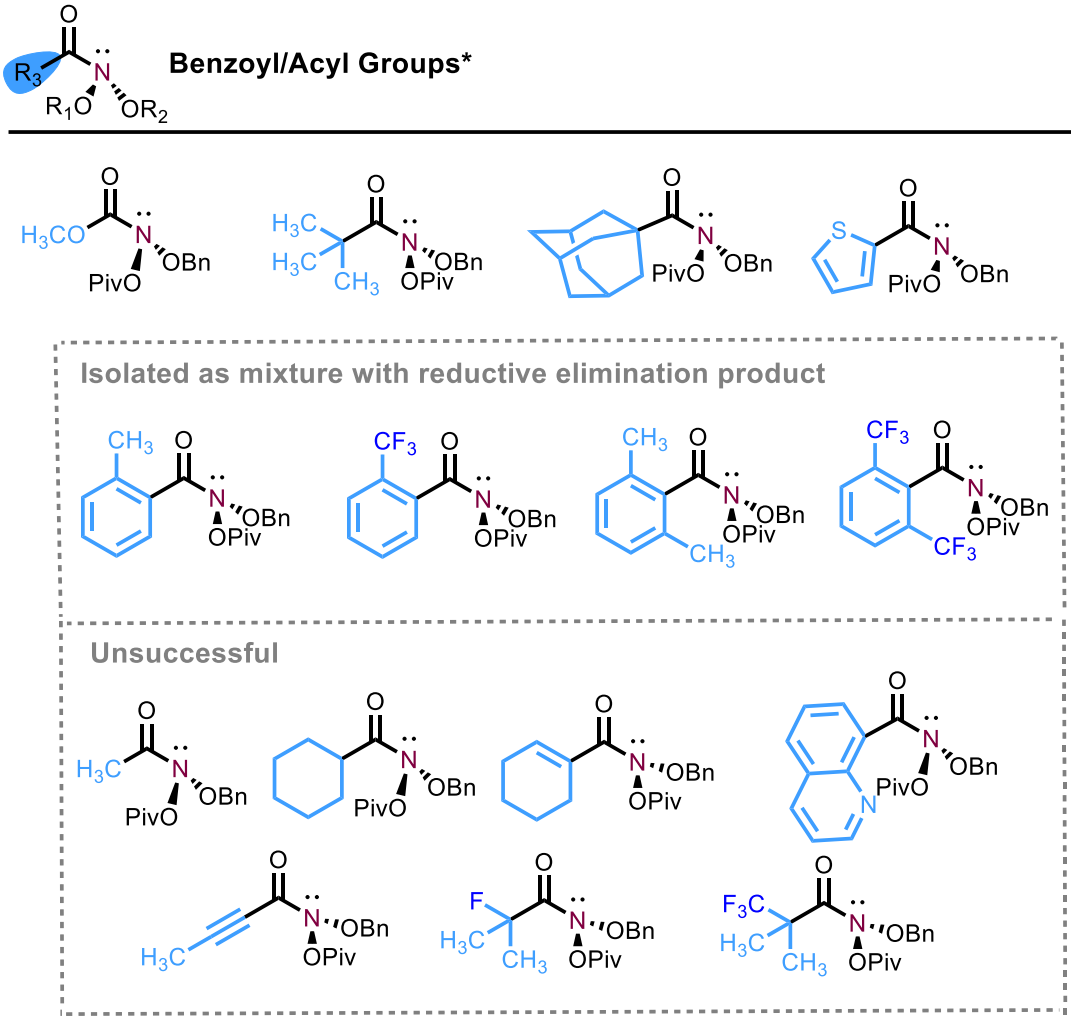

4.3.1. Anomeric Amides Containing New Leaving Groups.

The addition of a bulky pivalate group to the optimized anomeric amide reagent was successful in preventing unwanted attack by the amine at the acyl carbonyl. However, as discussed in section 2.2.1, sterically bulky secondary amine moieties were unable to react with this anomeric amide. Thus, we sought to further probe the sterics of the reagent. Isopropyl derived **33** and isobutyl derived **34** were successfully synthesized by substitution of the *N*-chloramide precursor **29** with the requisite sodium salt (Scheme 4.6). These reagents were

reacted with model secondary amine substrate bis(4-bromobenzyl)amine (**35**). The nitrogen deletion product **36** was produced in 64% yield using reagent **33** and 51% yield using reagent **34** (Table 4.1). These results demonstrate a trend of decreased yield of desired product with decreased steric bulk at the leaving group carbonyl. Additionally, these new reagents were explored with α-tertiary secondary amines (**37**) that were unreactive with the optimized reagent (see Scheme 2.14) and found to be similarly ineffective at mediating this transformation (Scheme 4.7). Glover has also reported that the nucleophilic substitution of anomeric amides is less sensitive to sterics at the leaving group compared to the sterics of the alkoxy and acyl groups.[6, 15] Consequently, the synthesis of derivatives with decreased steric bulk at the leaving group was not pursued further.

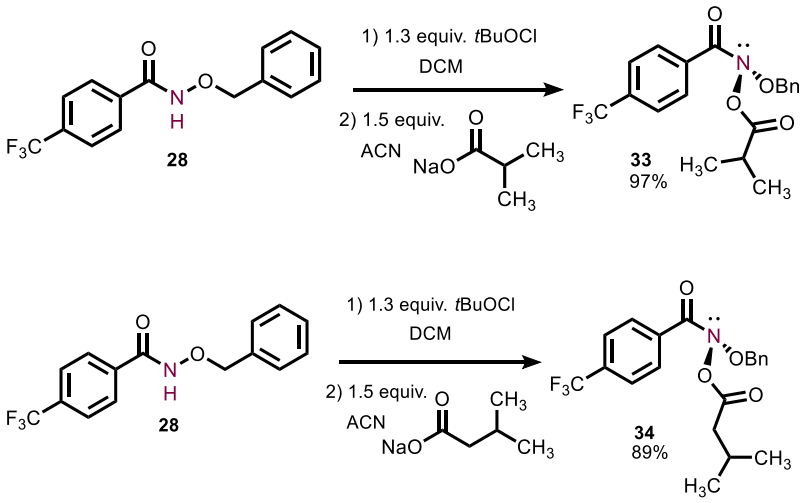

Scheme 4.6. Synthesis of anomeric amides with new leaving groups including a) isopropyl and b) isobutyl derivatives.

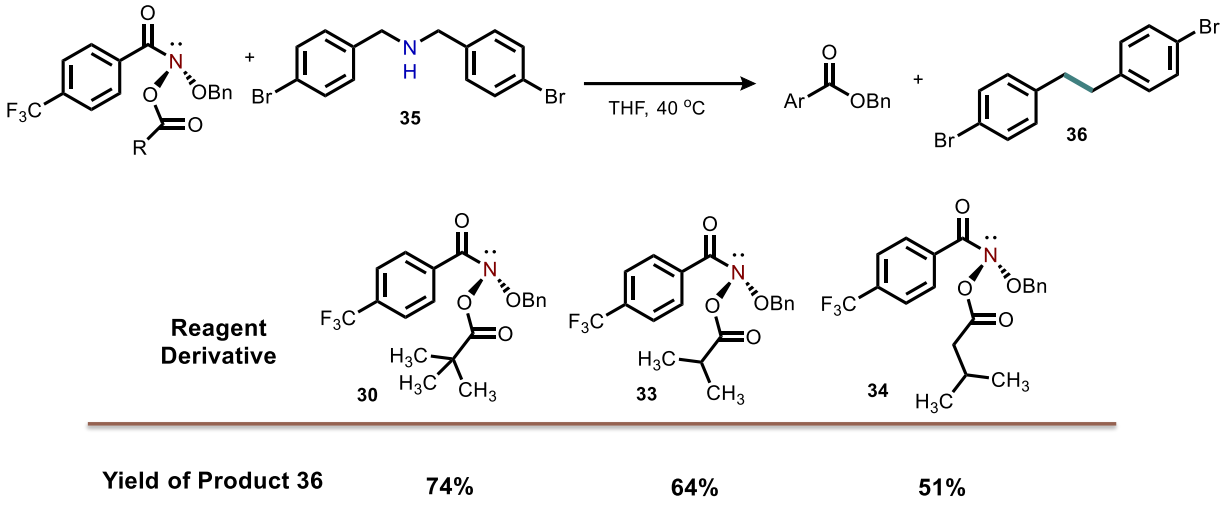

Table 4.1. Yield of nitrogen deletion product decreases with decreased steric bulk at the leaving group carbonyl.

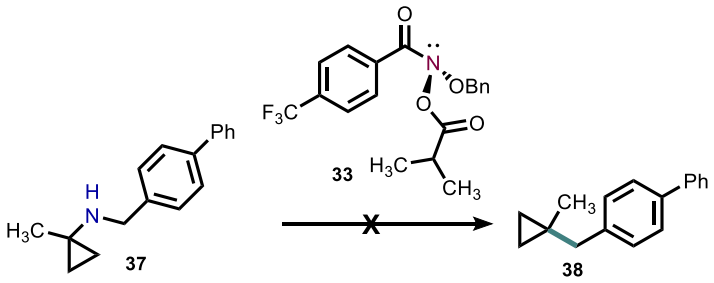

Scheme 4.7. Anomeric amide **33** with isopropyl derived leaving group is unreactive with an α-tertiary amine substrate.

Electron-withdrawing leaving groups were also of interest because it was hypothesized that they would increase the rate of substitution. Previous studies have shown that the rate of substitution of anomeric amides increases as the pKa of the leaving group decreases.[6, 15] The *N*-chloramide precursor was successfully substituted with sodium 2-fluoroisobutyrate to give anomeric amide **39** (Table 4.2). However, when secondary amine **44** was treated with amide **39**, the yield of deletion product after 1 hour compared with the previously optimized reagent was dramatically decreased, suggesting that the rate of substitution is much slower (Table 4.3). It is possible that this is because the leaving group carbonyl oxygen plays a role in stabilizing the transition state. Trifluoromethyl substitutions were also probed and a 3,3,3-trifluoro-2,2-dimethylpropanoyl derivative (**40**) was successfully prepared (Table 4.2). However, the

synthesis of a derivative bearing two trifluoromethyl groups (**41**) was not successful. The rate of substitution of secondary amines with reagent **40** compared to the previously optimized reagent was also studied by comparing the initial rates using the yield of deaminated product after 1 hour (Table 4.4). Derivative **40** resulted in 4.7% yield of nitrogen deletion product compared to 12.0% with optimized reagent **30**, suggesting that derivative **40** exhibits a slower rate of substitution. This finding is in agreement with the decreased rate observed with the 2-fluoroisobutyrate derived reagent and consequently, the addition of other electron-withdrawing leaving groups was not pursued. Phosphate and HOBt derived leaving groups were also explored but the respective reagents (**42** and **43**) were not successfully synthesized (Table 4.2).

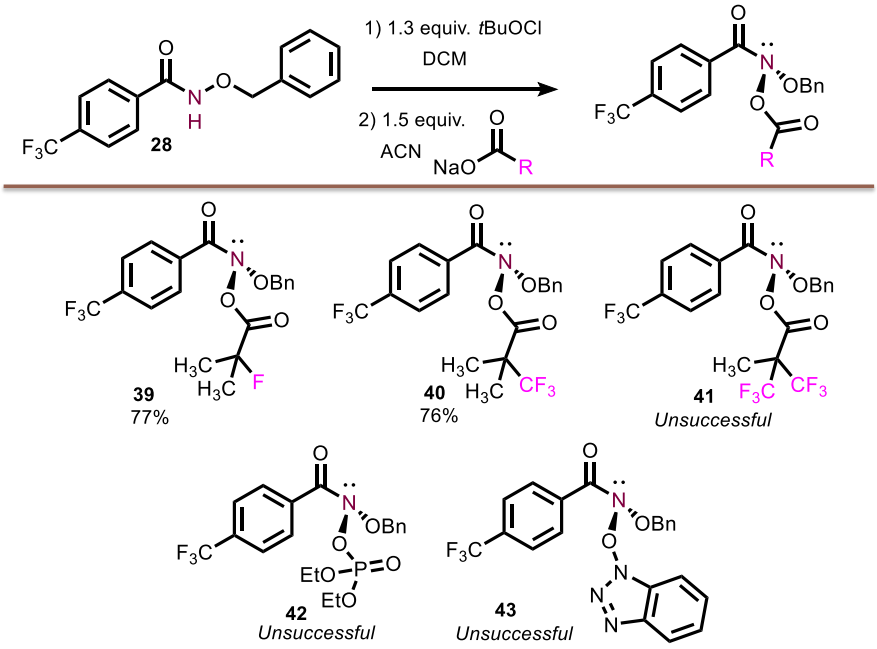

Table 4.2. Synthesis of reagents containing new leaving groups

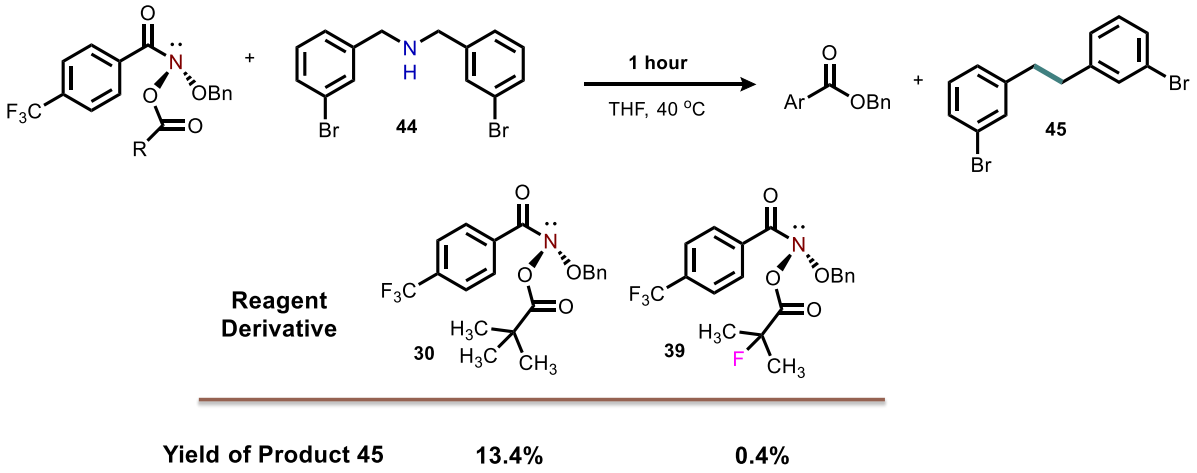

Table 4.3. Initial rate studies of reagents **30** and **39** by analyzing product yield after 1 hour.

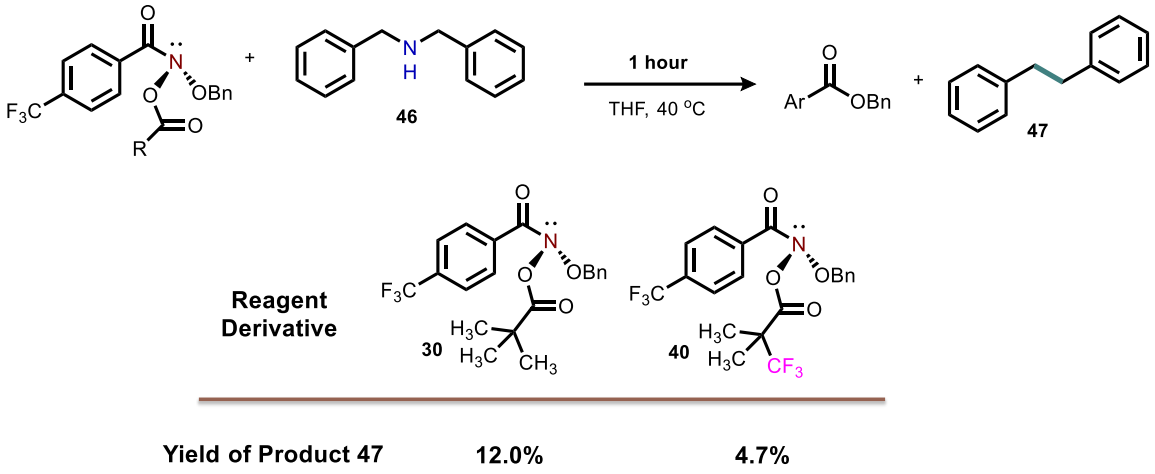

Table 4.4. Initial rate studies of reagents **30** and **40** by analyzing product yield after 1 hour.

4.3.2. Anomeric Amides Containing New Alkoxy and *O*-Benzyl Groups.

The previously optimized reagent *N*-(benzyloxy)-*N*-(pivaloyloxy)-4-(trifluoromethyl)benzamide (**30**) contains an *O*-benzyl group. Preliminary optimizations by Dr. Sean Kennedy demonstrated that this moiety resulted in a slightly faster reaction rate compared to a reagent containing an *O*-methyl group. An *O*-isopropyl derivative was also prepared, which was used for the crossover study (see Scheme 2.16) and resulted a slower reaction rate compared

to the optimized reagent. This finding corroborates the work from the Glover laboratory which found that substitution of anomeric amides is impeded by branching at the alkoxy α carbon.[6, 15]

The thermal instability of *N*-(benzyloxy)-*N*-(pivaloyloxy)-4-(trifluoromethyl)benzamide (**30**) above 45 °C is a limitation of this reagent because the nitrogen deletion reaction could not be heated to higher temperatures to induce substitution with less reactive substrates (see Scheme 2.13). One hypothesis to account for the thermal instability of this reagent is that decomposition to form *N*-centered radical alkoxyamidyl species **48** occurs (Scheme 4.8).[2] This radical is captodatively stabilized by the electron-withdrawing nature of the *p*-trifluoromethylbenzamide moiety and the electron-donating *O*-benzyl moiety, which may account for the low decomposition temperature.[24-26] Alternatively, *N*-acyloxy-*N*-alkoxyamides can also decompose by undergoing the HERON rearrangement when heated, and this transition state has been shown to be stabilized by electron-donation from the *O*-benzyl moiety (Figure 4.15).[2]

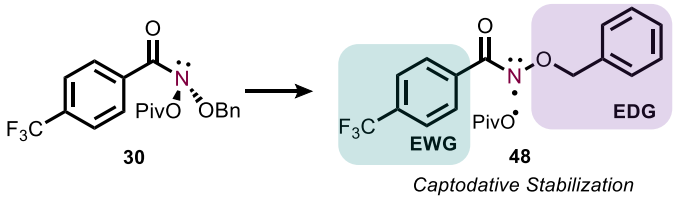

Scheme 4.8. Generation of a captodatively stabilized radical species as a decomposition product of **30**.

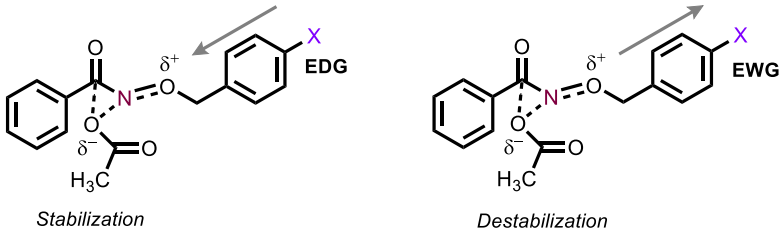

Figure 4.15. Substitution of *O*-benzyl moiety affects stabilization of HERON transition state.

Thus, we sought to add electron-withdrawing substituents to the *O*-benzyl moiety to mitigate either the captodative radical stabilization or the stabilized HERON transition state. *O*-

Benzyl hydroxylamine hydrochloride derivatives containing electron-withdrawing substituents on the aromatic ring are either not commercially available or are expensive to purchase. Thus, instead of substitution of *p*-trifluoromethylbenzoyl chloride (**26**) with *O*-benzyl hydroxylamine derivatives, an alternative synthetic route was pursued. *p*-Trifluoromethylbenzoyl chloride (**26**) was first converted to *N*-hydroxy-4-(trifluoromethyl)benzamide (**49**), which is able to undergo substitution with a variety of benzyl bromides to yield the desired *N*-(benzyloxy)-4-(trifluoromethyl)benzamide derivatives. To this end, *p*-trifluoromethylbenzyl bromide, 3,5-bis(trifluoromethyl)benzyl bromide and pentafluorobenzyl bromide were successfully employed to synthesize the requisite *N*-(benzyloxy)-4-(trifluoromethyl)benzamides (**50** – **52**) containing electron-withdrawing groups on the benzyl ring (Table 4.5).

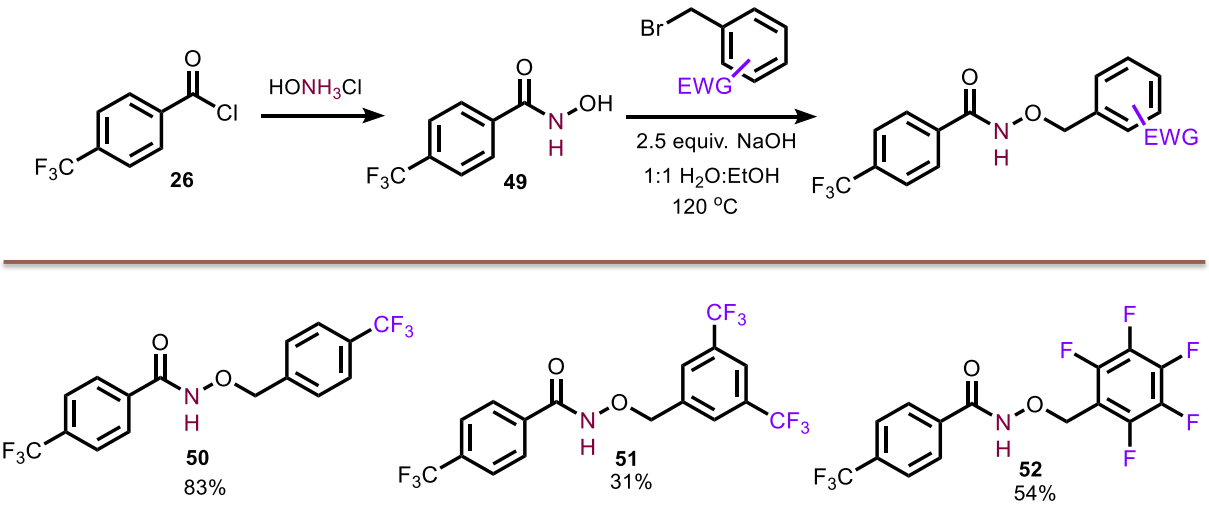

Table 4.5. Synthesis of hydroxamates containing new O-benzyl groups.

Subsequent treatment with *tert*-butylhypochlorite followed by substitution with sodium pivalate resulted in the synthesis of anomeric amides **53** and **54** (Table 4.6). However, pentafluorobenzyl derivative **55** was not successfully obtained. It is likely that the use of an *O*-

benzyl derivative that is strongly electron-withdrawing destabilizes the anomeric amide by decreasing donation of the oxygen lone pair to the *N*-acyloxy σ* orbital. Future work will involve studying the reactivity and thermal stability of these derivatives.

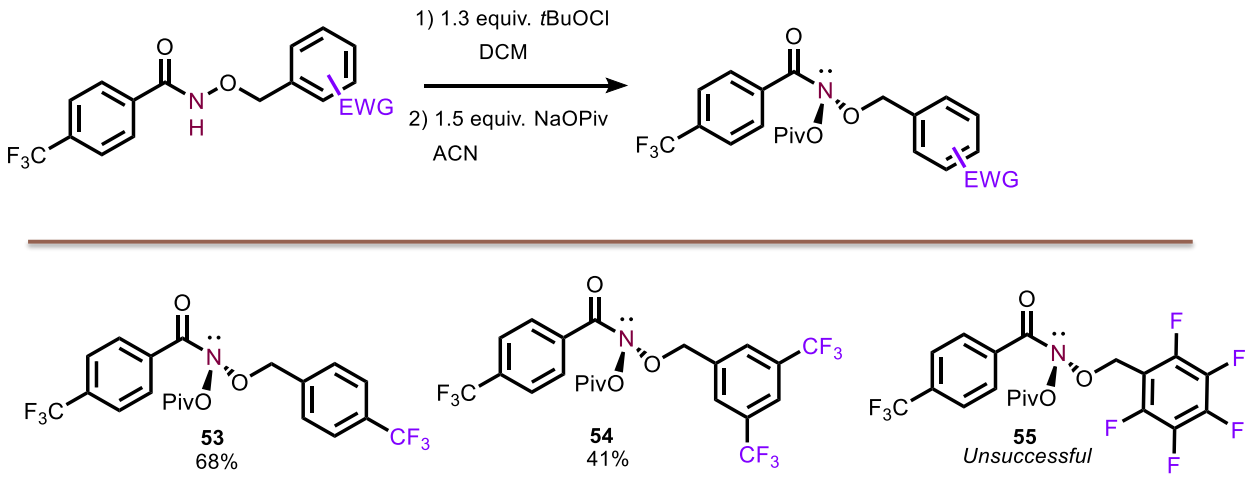

Table 4.6. Synthesis of anomeric amides containing new *O*-benzyl groups.

However, while **53** and **54** contain electron-withdrawing groups, the location of the fluorine moieties is still relatively distant from *O*-benzyl oxygen. Thus, we sought to prepare an additional derivative bearing an α-trifluoromethyl moiety. The commercially available precursor 2,2,2-trifluoroethoxyamine hydrochloride (**56**) was reacted with *p*-trifluoromethylbenzoyl chloride (**26**) to yield the requisite *N*-(alkoxy)-benzamide derivative **57** (Scheme 4.9). Compound **57** was treated with *tert*-butylhypochlorite followed by successful substitution with sodium pivalate to give the desired anomeric amide **58**. With **58** in hand, we then studied its thermal stability. A THF solution of **58** was heated to 40 °C overnight in the absence of any amine nucleophiles. Decomposition was assessed by NMR spectroscopy relative to internal standard and 39% of the initial amount of **58** remained. A solution of the optimized anomeric

amide reagent **30** was also heated at 40 °C overnight under identical conditions, and it was calculated that 53% of the initial amount remained. Thus, it appears that the addition of a trifluoromethyl group to the alkoxy α carbon does not lead to an increase in thermal stability. A reagent derived from *O*-phenyl hydroxylamine (**59**) was also explored, however the pivalate leaving group was not successfully installed on precursor **60** (Scheme 4.10).

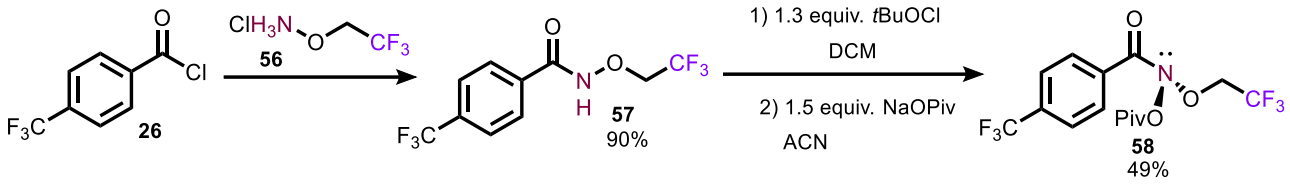

Scheme 4.9. Synthesis of anomeric amide **58** bearing an alkoxy group with an α-trifluoromethyl group.

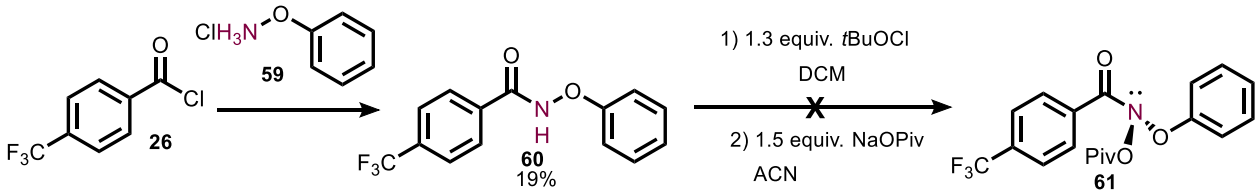

Scheme 4.10. Synthesis of an *O*-phenyl derived anomeric amide is unsuccessful.

4.3.3. Anomeric Amides Containing New Acyl Substituents.

The optimized anomeric amide contains a *p*-trifluoromethyl group, which was demonstrated to increase the reaction rate. The Hammett plot analysis described in section 2.2.2 demonstrated that this increase in rate is due to both inductive and resonance effects. As part of this study, a variety of reagent derivatives containing electron-withdrawing or electron-donating substituents on the benzamide ring were synthesized (see Figure 2.2). In addition to these compounds, several other derivatives containing additional substituents on the benzamide ring were explored. The observation in section 3.2.3 that sterically bulky α-secondary primary amines sometimes exhibit unwanted attack at the amide carbonyl prompted us to explore *ortho*-substituted benzamide moieties as a means of blocking this side reaction. Four derivatives (**62** –

65) were prepared according to Table 4.7. Following the substitution with sodium pivalate, for each of these derivatives the product was isolated as a mixture of desired amide and the reductive elimination ester byproduct (**66**) (Figure 4.16). Although the reactions were not clean, it was exciting to detect some production of these anomeric amides because Glover has reported that a 2,6-dimethylbenzamide derivative (**67**) could not be synthesized (Figure 4.17).[15] It is possible that *ortho*-substituents cause twisting to relieve steric constraints which may destabilize the anomeric amide and drive HERON rearrangement to occur spontaneously at room temperature. These *ortho*-substituted reagents were tested with α-secondary primary amines to explore whether increasing steric bulk around the amide carbonyl prevented unwanted nucleophilic attack. However, these reagents were unsuccessful in mediating primary amine deletion in any appreciable yield. Consequently, *ortho*-substituted anomeric amides were not pursued any further.

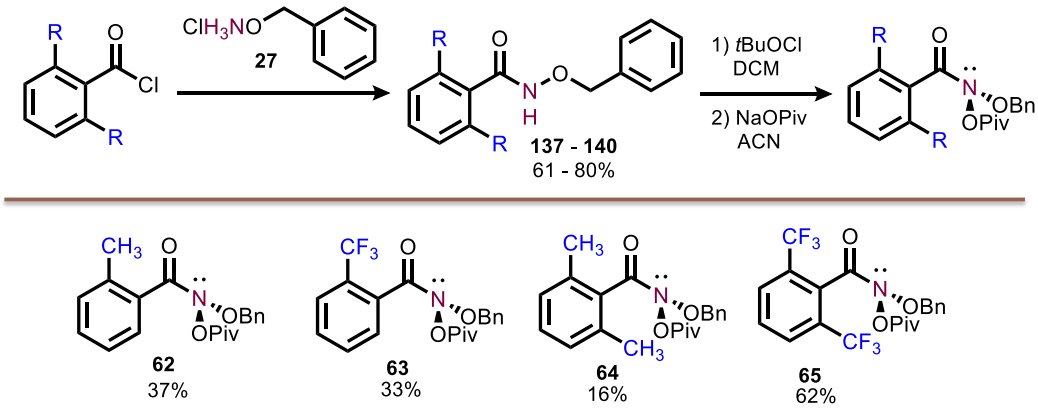

Table 4.7. Synthesis of anomeric amide derivatives with *ortho*-benzamide substituents.

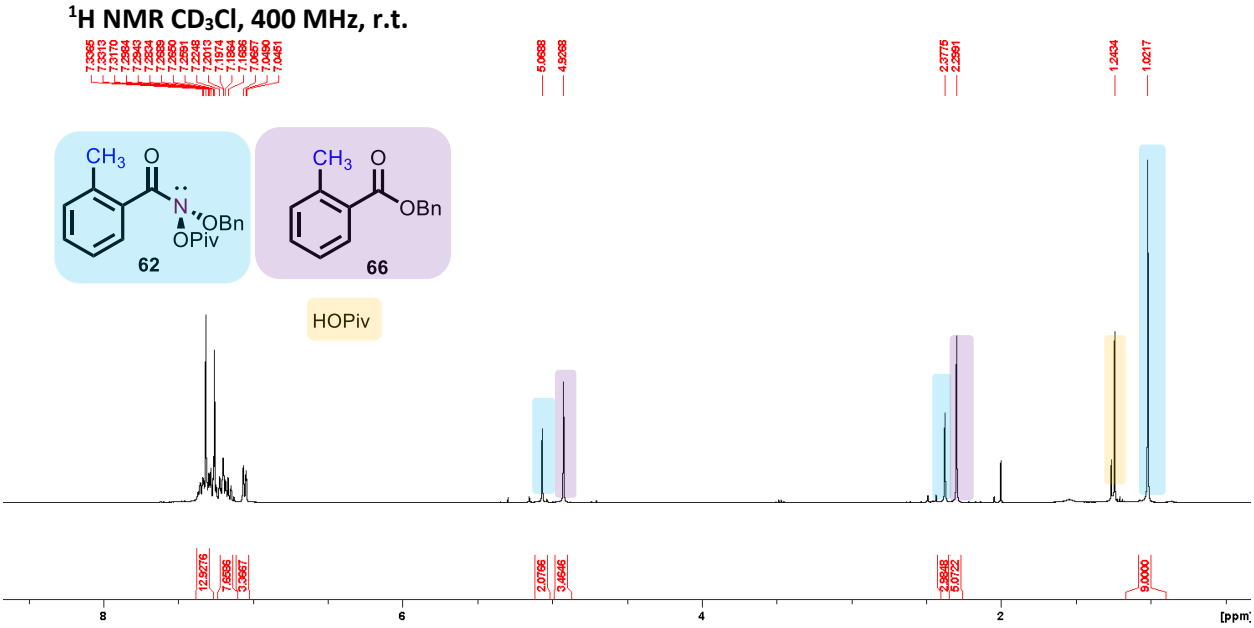

Figure 4.16. ^{1}H NMR spectrum of product mixture demonstrating both *ortho*-substituted anomeric amide **62** and reductive elimination ester byproduct **66**.

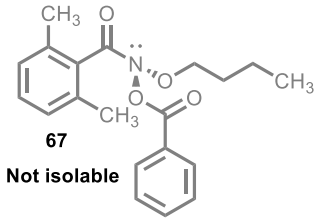

Figure 4.17. Previous literature attempt at a bulky benzamide derivative is unsuccessful.

While benzamide derived anomeric amides mediate amine deletion on a wide range of substrates, we were interested in exploring aliphatic amide derivatives because they have been less explored in the literature. A simple methyl derived reagent was first explored using acetyl chloride precursor (**68**). While *N*-benzyloxyacetamide (**69**) is easily prepared and underwent facile chlorination with *tert*-butylhypochlorite, substitution with sodium pivalate was unsuccessful. Instead, dimerization of an *N*-centered radical intermediate occurred to give *N*'-acetyl-*N*,*N*'-bis(benzyloxy)acetohydrazide product (**70**) (Scheme 4.11), as evidenced by NMR spectroscopy.[9] The diastereotopicity of the benzylic protons results in a distinctive 2 x d[AB system] in the product NMR spectrum.[9] If the amide substituent does not bear sufficient electron

density to stabilize the electron demand from the electronegative oxygen moieties at nitrogen, the resulting anomeric amide is unstable. This was previously observed by Dr. Sean Kennedy, who found that while the addition of a *p*-trifluoromethyl group resulted in increased reactivity, a reagent containing 3,5-bis(trifluoromethyl) substituents could not be successfully prepared. Dimerization of a variety of *N*-acyl-*N*-alkoxy derivatives has been reported by Glover.[2, 9] The initial discovery of these moieties was by oxidation of the requisite hydroxamate *O*-alkyl esters with lead tetraacetate (Scheme 4.12).[27-29] This oxidation has also been reported with cerium ammonium nitrate or nickel peroxide.[30] Dimerized products are stabilized by $n_N - \sigma^*_{NO}$ anomeric effects, which results in a significantly shorter N-N bond compared to other hydrazine moieties.[9] Consequently, these moieties are remarkable stable and isolable at room temperature, although thermolysis results in liberation of dinitrogen and production of two equivalents of ester (see Scheme 4.2).[2, 30] Glover has found that electron donating groups on the acyl side chain and electron withdrawing groups on the benzyloxy substituent accelerate the rate of this decomposition.[9]

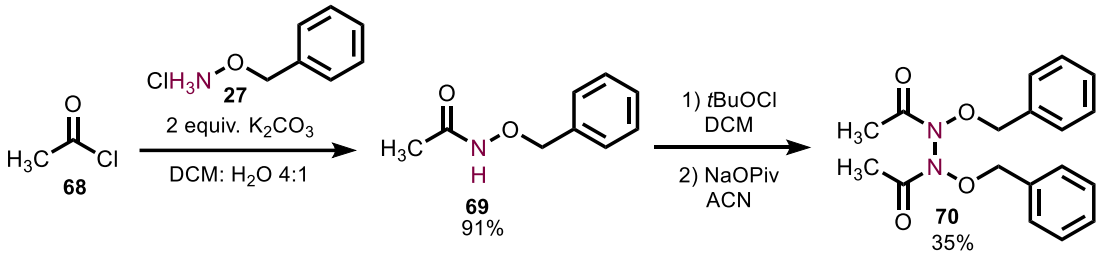

Scheme 4.11. Dimerization observed during attempted synthesis of acetamide derived reagent.

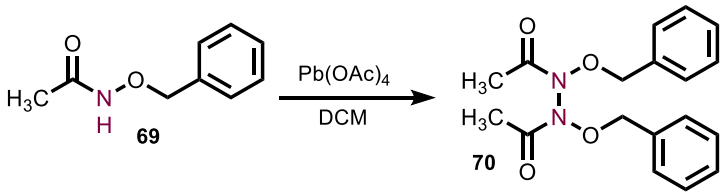

Scheme 4.12. Literature synthesis of dimerized hydrazine product.

We then explored replacement of the methyl substituent with a methoxy group, motivated by the idea that an electron-donating oxygen moiety would stabilize the resulting anomeric amide and destabilize formation of a dimerized hydrazine product. This carbamate reagent (**73**) was indeed isolable (Scheme 4.13), however subsequent studies demonstrated that this reagent was unreactive to primary and secondary amines. Unreacted starting material and **73** were observed and heating the reaction did not result in any nitrogen deletion product. Thus, it seems that a large increase in electron density at the amide increases stability but renders the amide unreactive towards nucleophilic substitution.

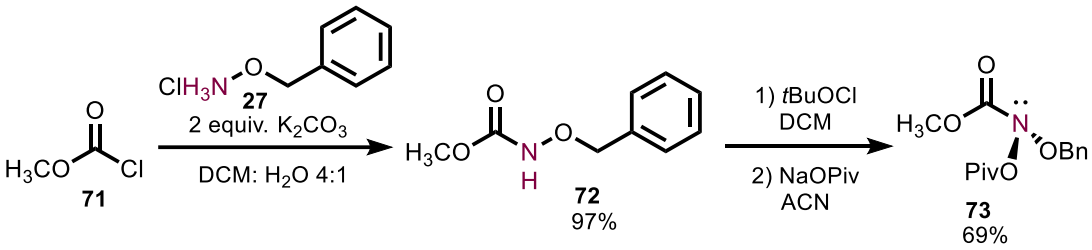

Scheme 4.13. Synthesis of a methoxy derived anomeric amide.

It was reasoned that aliphatic acyl substituents with more electron density than a methyl group may help stabilize the corresponding anomeric amide without being as electron-donating and inactivating as a methoxy group. Working in collaboration with my undergraduate Megan Morales, a cyclohexyl derivative (**77**) was pursued. However, analogous to the acyl synthesis, the preparation of a cyclohexyl derivative was also unsuccessful (Scheme 4.14). While the cyclohexyl group may not be sufficiently electron-rich to stabilize the corresponding anomeric amide, we were curious if the hydrogen atom alpha to the carbonyl could potentially undergo abstraction resulting in an alternate decomposition pathway. Thus, a *tert*-butyl derived reagent

(**81**) was then explored. Gratifyingly, the *N*-chloramide precursor (**80**) was prepared and successfully substituted with sodium pivalate to the requisite anomeric amide **81** (Scheme 4.15).

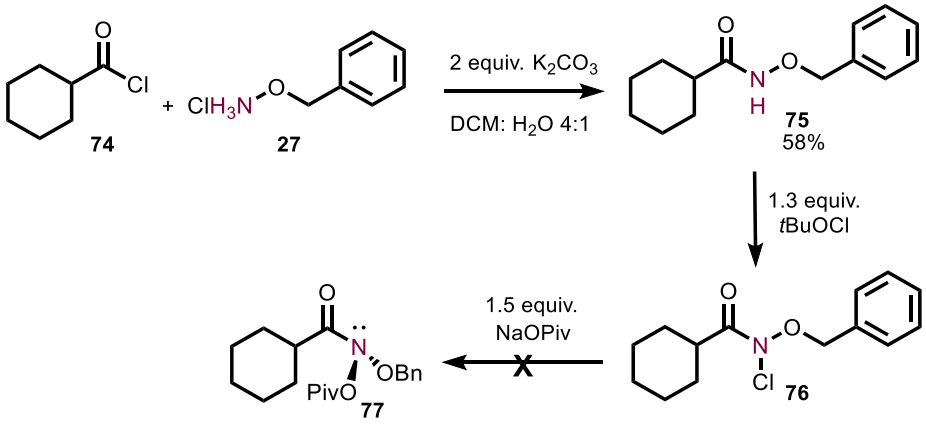

Scheme 4.14. Unsuccessful synthesis of a cyclohexyl derived anomeric amide reagent.

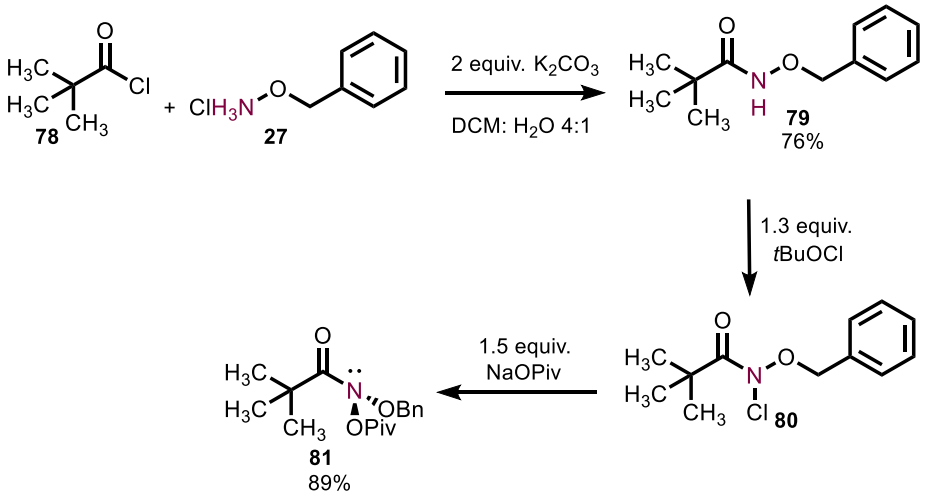

Scheme 4.15. Successful synthesis of a *tert*-butyl derived reagent.

Megan then conducted thermal stability studies with *tert*-butyl derived reagent **81** compared with previously optimized anomeric amide **30**. A temperature screen was conducted with solutions of reagent by heating overnight in the absence of any amine substrates. It was found that **81** could be heated to 60 °C with minimal decomposition observed by NMR spectroscopy. Compared to **30**, which can only be heated to 40 °C under the same conditions before significant decomposition is observed, this increase in thermal stability was exciting

because there might be an increased driving force for substitution with more challenging amine substrates at higher temperatures. Unfortunately, Megan found that the model secondary amine substrate **35** did not react with the *tert*-butyl derived reagent to produce the nitrogen deletion product **36** in any appreciable yield (Scheme 4.16a). This is likely due to the increased steric bulk of the *tert*-butyl moiety, which has been shown by Glover to hinder nucleophilic attack.[6, 13, 15] Primary amine deletion was observed with dodecylamine (**82**) to give **83** (Scheme 4.16b), with unwanted attack at the amide carbonyl resulting in *N*-dodecyl-4-(trifluoromethyl)benzamide (**84**), which also detected in the product mixture by GC-MS.

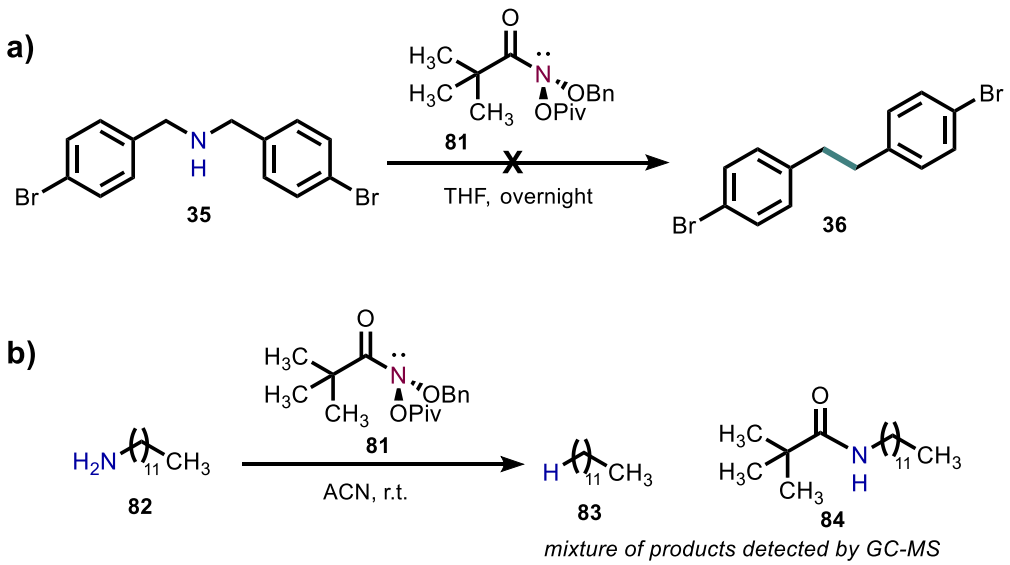

Scheme 4.16. Reactivity studies of *tert*-butyl derived amide **81** with a) secondary and b) primary amines.

We reasoned that an adamantyl derived anomeric amide would also be isolable and may be more reactive than the *tert*-butyl derived reagent due to its conformational rigidity. Anomeric amide **88** was successfully synthesized by substitution of the *N*-chloramide intermediate (**87**) with sodium pivalate by Megan Morales (Scheme 4.17). Reagent **88** could be heated to 40 ^{o}C before decomposition was observed, a decrease in thermal stability compared to what was observed with reagent **81**. Additionally, this reagent was similarly unreactive to secondary

amines. When **81** was treated with dodecylamine, the desired nitrogen deletion product was produced in 34% yield (Scheme 4.18).

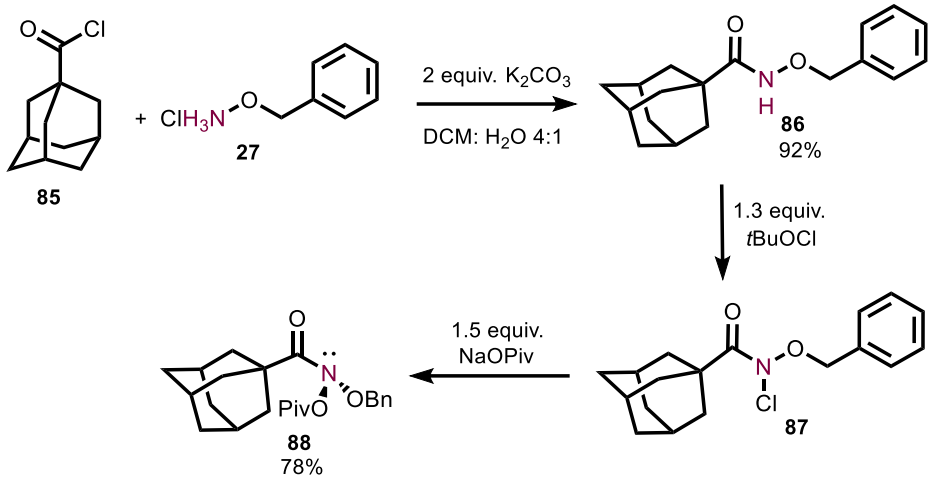

Scheme 4.17. Successful synthesis of an adamantyl derived reagent.

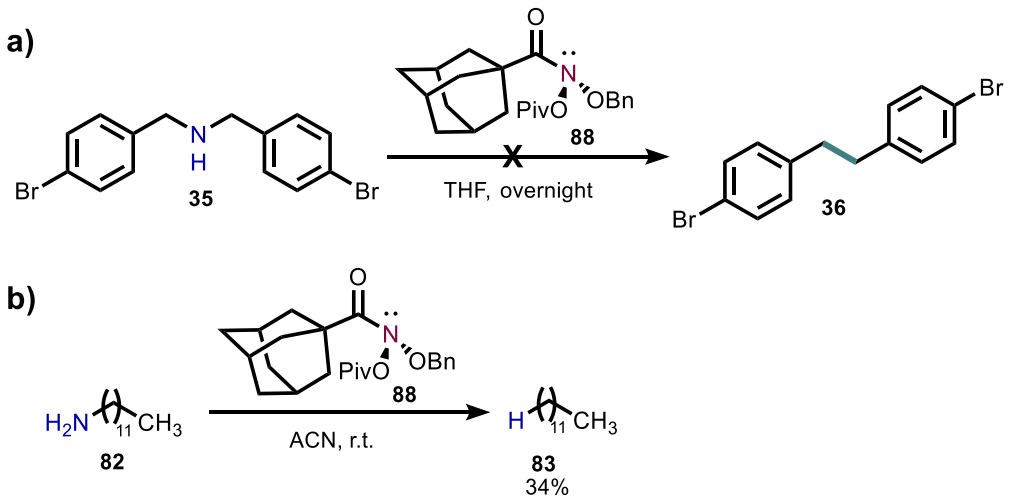

Scheme 4.18. Reactivity studies of adamantyl derived amide **88** with a) secondary and b) primary amines.

Interestingly, Glover has previously reported the isolation of five anomeric amide derivatives with aliphatic acyl groups (**89** – **93**) (Figure 4.18).[6, 13] These moieties contain benzoate leaving groups that were successfully installed by substitution of the *N*-chloramide

precursor. In contrast to our findings with the unsuccessful synthesis of a cyclohexyl derived reagent, isopropyl, *sec*-butyl and ethyl derivatives were successfully isolated. This suggests that the presence of an α hydrogen atom should not impede the formation of a stable anomeric amide reagent. However, the overall effect on stability by replacing both the *O*-benzyl and pivalate moieties with *O*-butyl and benzoate, respectively, is less clear. The isopropyl, adamantyl and *tert*-butyl derived reagents (**89** – **91**) were shown to be resistant to substitution with *N*-methylaniline.[6] The neopentyl derived reagent (**93**) was susceptible to substitution chemistry, demonstrating tolerance for β-branching, although the reaction rate was slower compared to the propyl derivative (**92**).[6]

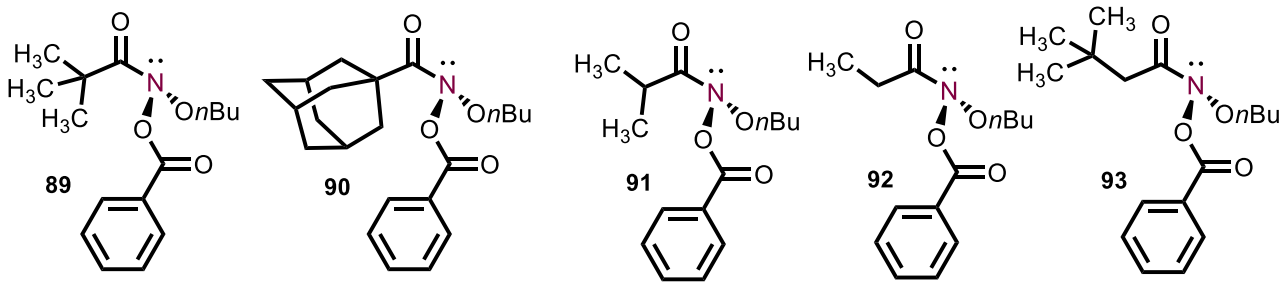

Figure 4.18. Literature reports of alkyl derived anomeric amides isolated by Glover.

As we previously found that the reactivity of benzamide derived reagents increased with the addition of electron-withdrawing moieties to the aromatic ring, the synthesis of fluorinated α-tertiary acyl derived reagents was subsequently explored. 2-Fluoro-2-methylpropanoyl chloride (**95**) was successfully converted to *N*-(benzyloxy)-2-fluoro-2-methylpropanamide (**96**), which was chlorinated with *tert*-butylhypochlorite but subsequent substitution with sodium pivalate to give **98** was unsuccessful (Scheme 4.19). It is likely that the electron-withdrawing nature of the α-fluorine moiety destabilizes the desired anomeric amide. Consequently, a 3,3,3-trifluoro-2,2-dimethylpropanoyl derivative (**103**) was pursued because this bulkier group may be able to

stabilize the resulting anomeric amide while still containing an electron-withdrawing moiety to increase reactivity. *N*-(benzyloxy)-3,3,3-trifluoro-2,2-dimethylpropanamide (**101**) was also successfully prepared and chlorinated, however the desired product **103** was not isolated following substitution with sodium pivalate (Scheme 4.20). Future work should include exploring the synthesis of fluorinated acyl derivatives bearing benzoate and *O*-butyl moieties, analogous to the acyl derivatives that were successfully isolated by Glover.[6, 15]

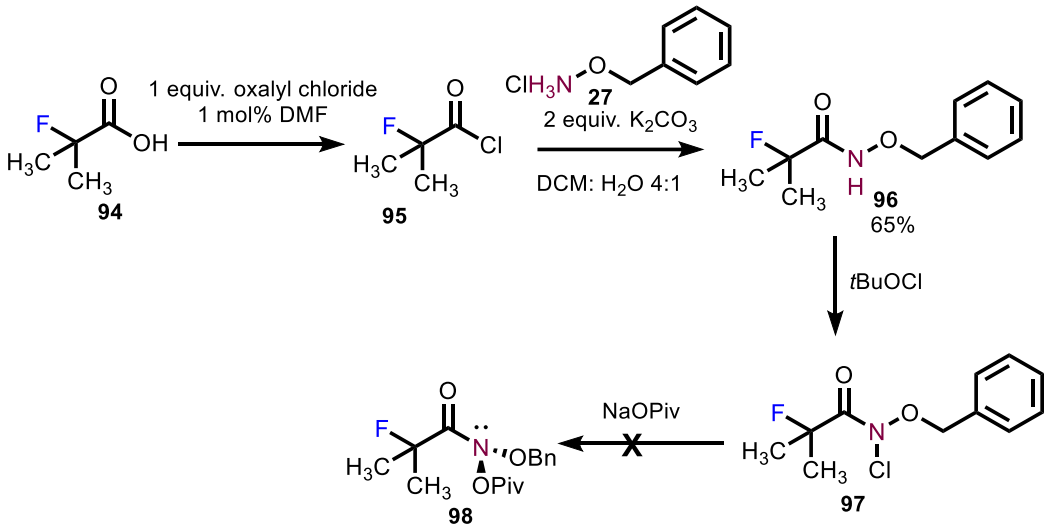

Scheme 4.19. Unsuccessful synthesis of a 2-fluoro-2-methylpropanoyl derived reagent.

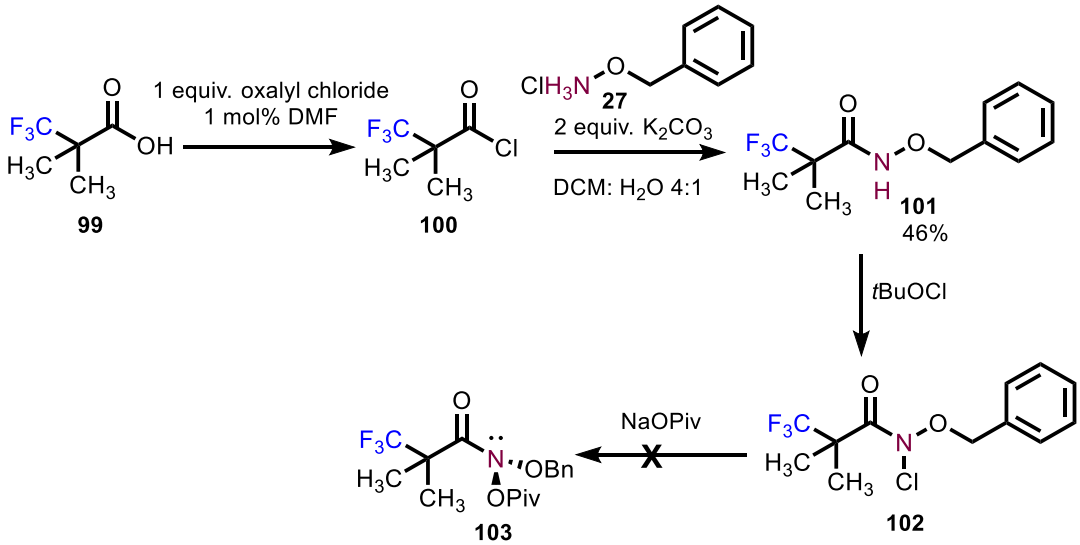

Scheme 4.20. Unsuccessful synthesis of a 3,3,3-trifluoro-2,2-dimethyl derived reagent.

While the inability to isolate fluorinated α-tertiary acyl anomeric amide derivatives was disappointing, we became interested in comparing unsaturated aliphatic substituents with the parent benzamide derived reagents. Alkynes have been utilized by the medicinal chemistry community as benzene isosteres[31] and thus it was reasoned they might be able stabilize a corresponding anomeric amide derivative. But-2-ynoyl chloride (**105**) was successfully prepared and converted to *N*-(benzyloxy)but-2-ynamide (**106**) upon treatment with *O*-benzylhydroxylamine. Analogous to the results observed with a wide variety of aliphatic acyl substituents, the corresponding *N*-chloramide species **107** was prepared but failed to undergo substitution with sodium pivalate to give **108** (Scheme 4.21). An olefin is another unsaturated moiety that has not been previously explored. Cyclohex-1-ene was of interest because this moiety is similar to the cyclohexyl derivative (see Scheme 4.14) but without an α-hydrogen atom, which we hypothesized might be able to undergo unwanted abstraction. *N*-(benzyloxy)cyclohex-1-ene-1-carboxamide (**111**) was prepared and underwent chlorination but the corresponding anomeric amide (**113**) was not successfully obtained upon substitution with sodium pivalate (Scheme 4.22). This suggests that the presence of an α-hydrogen atom does not account for the instability observed with the cyclohexyl derivative, however it is possible that cyclohex-1-ene can participate as a Michael acceptor resulting in an alternate unwanted decomposition pathway.

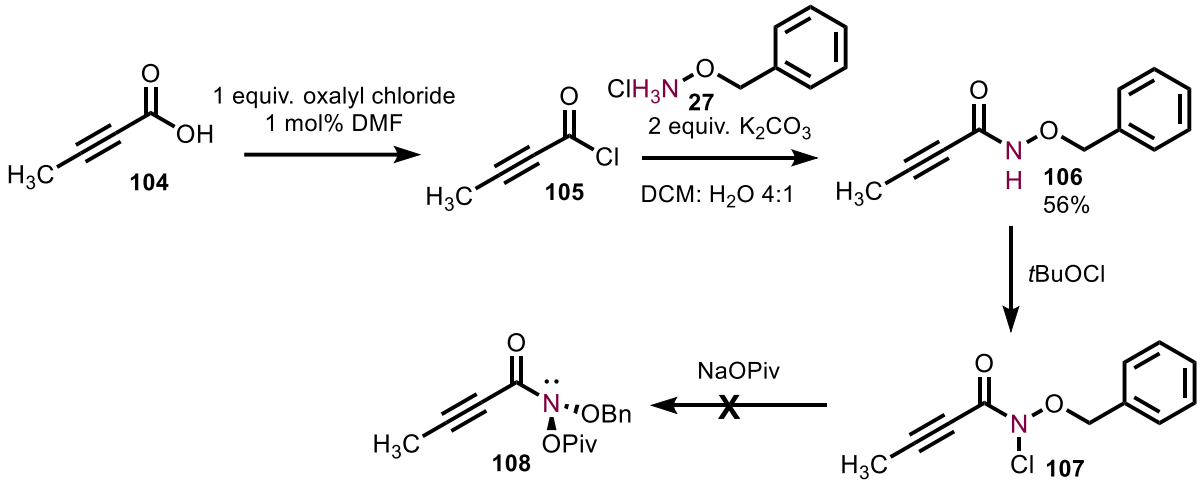

Scheme 4.21. Unsuccessful synthesis of an alkyne derived anomeric amide.

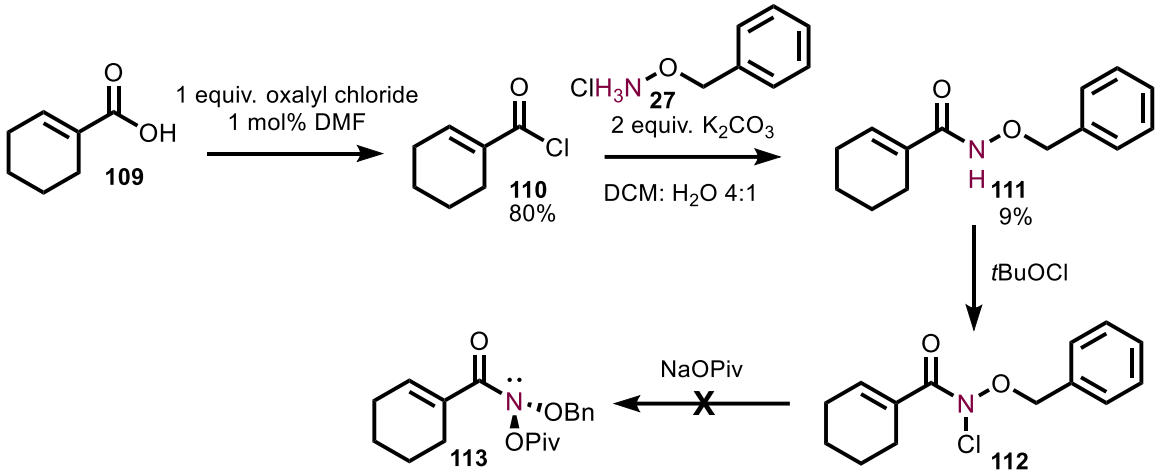

Scheme 4.22. Unsuccessful synthesis of an alkene derived anomeric amide.

Given the limited success of aliphatic anomeric amide derivatives, heterocyclic aromatic derivatives were then explored. Preliminary work by Dr. Sean Kennedy demonstrated that a 2-pyridyl derived anomeric amide was not isolable. It was reasoned that an 8-quinoline derived reagent (**118**) might stabilize the corresponding anomeric amide while still bearing the electron-withdrawing nitrogen substituent. Quinoline-8-carboxylic acid (**114**) was treated with oxalyl chloride and the resulting acyl chloride was isolated as the HCl salt (**115**). This precursor was converted to *N*-(benzyloxy)quinoline-8-carboxamide (**116**) using an extra equivalent of base.

However, attempts to chlorinate **116** using *tert*-butylhypochlorite were unsuccessful (Scheme 4.23). This finding is unusual because the other anomeric amide derivatives that could not be isolated underwent chlorination but failed at the substitution step with sodium pivalate. It is possible that the quinoline nitrogen moiety interacts with the amide N-H and this disrupts chlorination reaction.

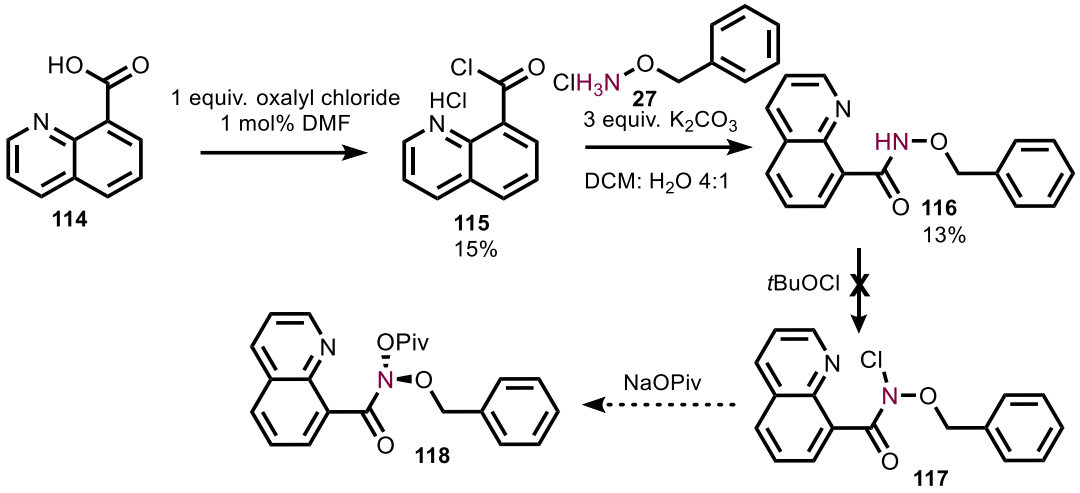

Scheme 4.23. Unsuccessful synthesis of quinoline derived anomeric amide.

Another heterocycle of interest was a thiophene moiety, which had not been previously explored. Excitingly, the corresponding anomeric was prepared by chlorination and substitution with sodium pivalate (Scheme 4.24). Thiophene containing reagent **121** was shown to react with secondary amines, and model substrate **35** gave the nitrogen deletion product in 66% yield (Scheme 4.25). We were interested in comparing the rate of this reagent with previously optimized anomeric amide **30** (Table 4.8). The yields of nitrogen deletion product after 2 hours were compared, and **30** appears to react significantly faster than thiophene derived **121**. Indeed, the reaction with the optimized anomeric amide reagent approaches completion after 2 hours, whereas the yield of deletion product with reagent **121** was just 12.8%. Future studies involving the addition of electron-withdrawing trifluoro moieties to the thiophene ring may be required to

develop a more reactive reagent. While thiophene derived **121** is not as reactive as the original reagent **30**, the observed reactivity with secondary amines was still quite an exciting find because as demonstrated in this chapter, very few derivatives can mediate this chemistry.

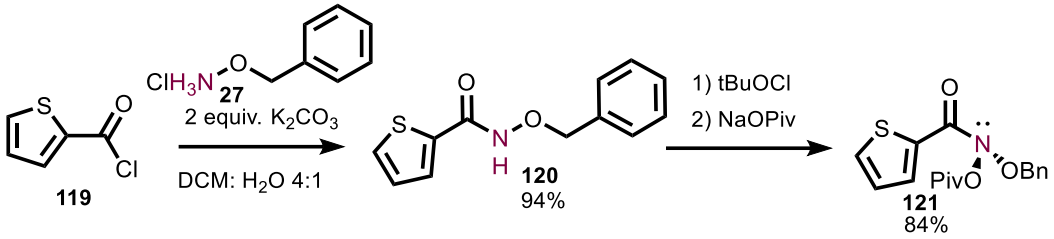

Scheme 4.24. Synthesis of thiophene derived anomeric amide **121**.

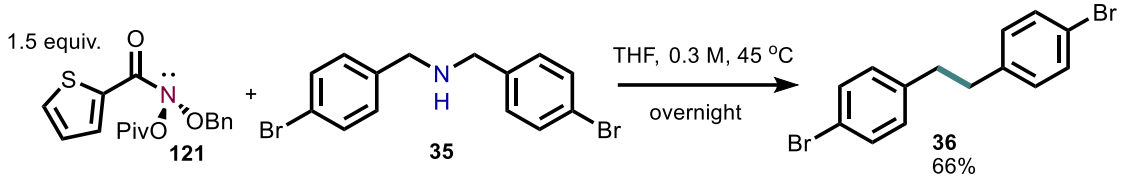

Scheme 4.25. Reactivity of thiophene derived reagent **121** with secondary amine substrates.

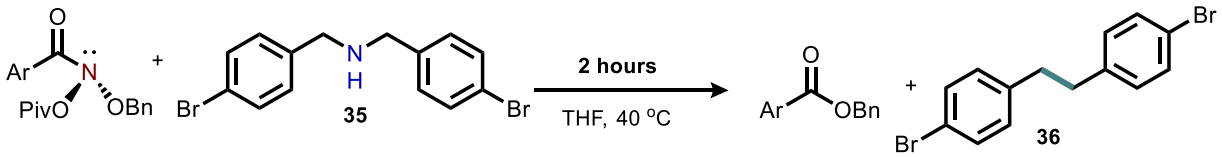

Reagent Derivative	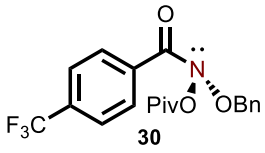	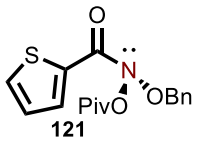
Yield of Product 36	**76.9%**	**12.8%**

Table 4.8. Initial rate studies for comparison of secondary amine deletion between **121** and **30**.

4.3.4. Exploration of Carbonyl Isosteres.

While there are many possible derivatizations to the leaving group, *O*-alkyl and benzamide moieties that can be explored, we were also interested in modifying the amide core itself. A thiocarbonyl is an interesting carbonyl isostere because its elongated bond length and decreased resonance stabilization with amide nitrogen would likely increase the electrophilicity of the resulting anomeric amide.[32] To this end, benzothioyl chloride (**123**) was prepared and reacted with *O*-benzylhydroxylamine to generate *N*-(benzyloxy)benzothioamide (**124**). The maintenance of the thiocarbonyl was confirmed by high resolution mass spectrometry and carbon NMR spectroscopy, from which the spectrum demonstrated the presence of a thiocarbonyl carbon. However, when **124** was treated with *tert*-butylhypochlorite and substituted with sodium pivalate, *N*-(benzyloxy)-*N*-(pivaloyloxy)benzamide (**126**) was produced (Scheme 4.26). The carbon NMR spectrum matched that of the anomeric amide bearing the oxygen containing carbonyl, even when the reaction was conducted under rigorous air and moisture free conditions. Thus, it is possible that the oxygen incorporation is due to *tert*-butylhypochlorite, however we cannot be certain without conducting a labelling experiment. Future work will explore the use of other reagents for chlorination or oxidation to produce a thiocarbonyl derivative.

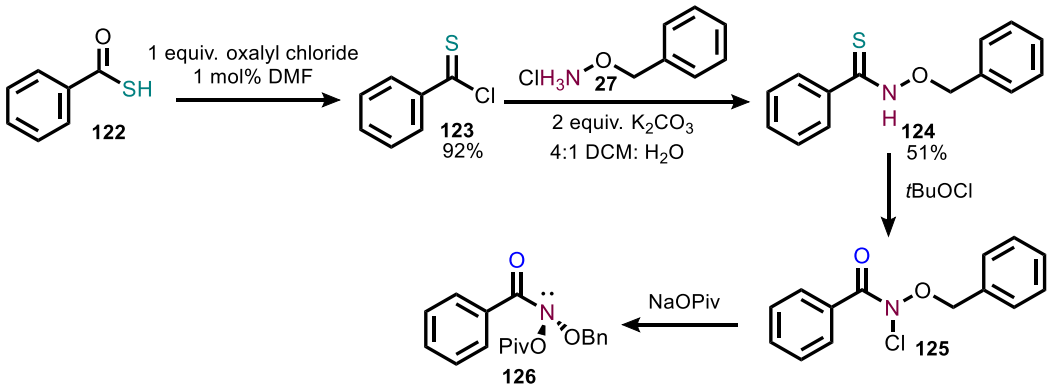

Scheme 4.26. Attempted synthesis of an anomeric amide containing a thiocarbonyl isostere results in isolation of *N*-(benzyloxy)-*N*-(pivaloyloxy)benzamide.

Another isostere of interest was a sulfonamide group. *O*-Benzyl hydroxylamine hydrochloride was treated with 4-(trifluoromethyl)benzenesulfonyl chloride (**127**), resulting in the desired *N*-(benzyloxy)benzenesulfonamide derivative **128** (Scheme 4.27). Chlorination with *tert*-butylhypochlorite was successful, however the *N*-chlorosulfonamide product **129** appeared to exhibit increased stability compared to the other *N*-chloramides synthesized in this chapter. Substitution with sodium pivalate under standard conditions was unsuccessful, but instead of resulting in the typically observed decomposition, unreacted starting material was recovered. These findings mirror the results of early work by Rudchenko, who synthesized *N*-chlorosulfonamide derivative **131** and found that it is thermally stable and inert to substitution with sodium methoxide (Scheme 4.28).[33, 34]

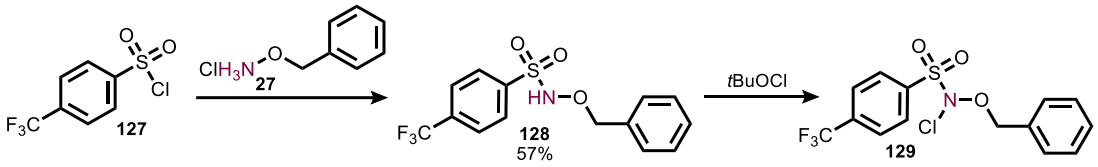

Scheme 4.27. Attempted synthesis of an anomeric amide containing a sulfonamide isostere.

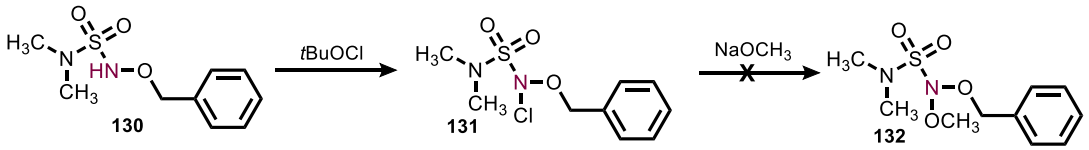

Scheme 4.28. Literature report of *N*-chlorosulfonamide derivate which is inert to substitution chemistry.

4.4. Conclusion.

This chapter has presented a reproducible 5 g scale synthesis for *N*-(benzyloxy)-*N*-(pivaloyloxy)-4-(trifluoromethyl)benzamide (**30**) in 97% purity in three steps. Starting from 4-trifluoromethylbenzoyl chloride, substitution with *O*-benzylhydroxylamine yields *N*-(benzyloxy)-4-(trifluoromethyl)benzamide (**28**). This reaction can be conducted on a 20 g scale and results in a 94% yield of product, which is 98% pure. Subsequent chlorination can be

conducted with either *tert*-butylhypochlorite or TCICA to give the *N*-chloramide intermediate. TCICA is the recommended oxidant for a large-scale synthesis because it is safer to handle. Using the optimized TCICA procedure, the *N*-chloramide intermediate is produced in 97% purity on a 5g scale. This intermediate should be immediately taken forward to the substitution with sodium pivalate to give **30**. The preliminary procedure for the synthesis of **30** resulted in the formation of pivalic acid and pivalic anhydride impurities. Optimization of concentration and temperature was effective at mitigating the formation of these impurities and **30** was isolated in 97% purity, and in 89% yield across two steps from *N*-(benzyloxy)-4-(trifluoromethyl)benzamide (**28**).

In addition to the optimized synthesis of **30**, a range of other anomeric amide derivatives were synthesized throughout the course of our investigation. A modular approach was taken to reagent derivatization in which the effect of modifications to the leaving group, acyl and *O*-alkyl moieties were explored separately. Anomeric amides containing isopropyl and isobutyl derived leaving groups were successfully synthesized but were shown to result in a decreased yield of secondary amine deletion product compared to the previously optimized reagent. Derivatives bearing 2-fluoro-2-methylpropanoate and 3,3,3-trifluoro-2,2-dimethylpropanoate leaving groups were also prepared but demonstrated a decreased reaction rate with secondary amines. Three anomeric amides bearing electron-withdrawing moieties on the *O*-alkyl group were also successfully prepared. A range of acyl derivatives were explored and many were unsuccessful in stabilizing the resulting anomeric amide. However, α-tertiary acyl derivatives were isolable. A *tert*-butyl derived reagent was prepared and this reagent exhibited stability at temperatures 20 ^{o}C higher than the previously optimized reagent. Reactivity with secondary amines was inhibited by

the increased steric bulk of the reagent. An adamantyl derived reagent was also prepared but this did not alleviate the steric clash with secondary amine nucleophiles.

4.5. Experimental.

4.5.1. General Procedures.

Unless noted otherwise, all reactions were performed in oven-dried or flame-dried glassware under an atmosphere of dry N_2. THF, Et_2O, DCM, Toluene, ACN, Et_3N, and Pentane were dried by passing these previously degassed solvents through a PPT Solvent Purificatiton System, and all other solvents were dried over molecular sieves (4A) and degassed prior to use or purchased anhydrous and sealed under N_2 (e.g. VWR Dri-solv or equivalent). Reaction temperatures were reported as the temperatures of the bather surrounding the flasks or vials. Sensitive reagents and solvents were transferred under nitrogen into a nitrogen-filled glovebox with standard techniques. Analytical thin-layer chromatography (TLC) was carried out using 0.2 mm commercial silica gel plates (silica gel 60, F254) and visualized by UV irradiation or staining as indicated.

Low resolution mass spectra were recorded on either an Agilent 6530 LC Q-TOF mass spectrometer using electrospray ionization with fragmentation voltage set at 115 V or an Agilent SQ GC-MMS with a 7890B GC using an Agilent HP-5MS column with a temperature gradient of 50 ^oC to 200 ^oC over 15 minutes and a 5977A single quad MS using electron ionization. High resolution mass spectra were recorded on either an Agilent 6224 TOF High Resolution Accurate MS with electrospray ionization or an Agilent 7200B QTOF High Resolution Accurate Mass GCMS using an Agilent HP-5MS column with a temperature gradient of 50 ^oC to 200 ^oC over 15 minutes and electron ionization. All mass spectra were processed with an Agilent MassHunter Operating System. Nuclear magnetic resonance spectra (^{1}H-NMR, ^{13}C-NMR and ^{19}F-NMR) were recorded with Bruker spectrometers operating at 400 or 500 MHz for 1H. Chemical shifts

are reported in parts per million (ppm, δ), downfield from tetramethylsilane (TMS, δ=0.00 ppm) and are referenced to residual solvent ($CDCl_3$, δ=7.26 ppm (1H) and 77.160 ppm (^{13}C)). Coupling constants were reported in Hertz (Hz). Data for ^{1}H-NMR spectra were reported as follows: chemical shift (ppm, s = singlet, d = doublet, t = triplet, q = quartet, quin = quintet, dd = doublet of doublets, td = triplet of doublets, ddd = doublet of doublet of doublets, m = multiplet, coupling constant (Hz), and integration).

Unless otherwise noted, all reagents were used as received. *t*BuOCl was prepared according to the literature.[19] *N*-hydroxy-4-(trifluoromethyl)benzamide (**49**),[35] *N*-(benzyloxy)pivalamide (**79**),[36] *N*-(benzyloxy)adamantane-1-carboxamide (**86**),[30] and methyl (benzyloxy)carbamate (**72**),[37] *N*-(benzyloxy)cyclohexanecarboxamide (**75**)[38] and *N*-benzyloxyacetamide (**69**)[16] were prepared according to the literature. Note on safety: 2-fluoroisobutyric acid should be handled with caution as it is fatal if inhaled.

4.5.2. Large Scale Synthesis of *N*-(benzyloxy)-*N*-(pivaloyloxy)-4-(trifluoromethyl)benzamide.

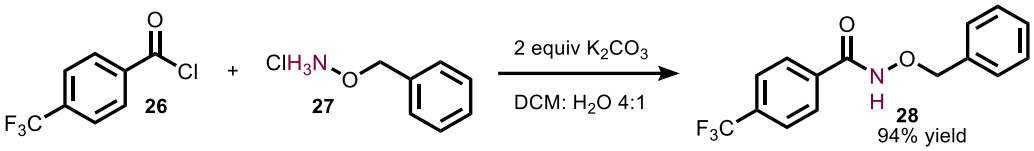

***N*-(benzyloxy)-4-(trifluoromethyl)benzamide (28):** In air, an oven-dried 1 L round bottom flask (24/40 joint) equipped with a 3 x 1.5 cm Teflon-coated egg-shaped stir bar is charged with *o*-benzyl hydroxylamine hydrochloride (20.0 g, 0.125 mol, 1 equiv.), potassium carbonate (34.64 g, 0.251 mol, 2 equiv.) and 4:1 DCM:H_2O (0.25 M, 400 ml DCM (ACS grade), 100 ml de-ionized water). The flask is immersed in an ice/water bath and stirred for 15 minutes with Heidolph MR Hei-Mix L stirplate at a rate of 1400 rpm. A 250 ml addition funnel (24/40 joint) is attached to the flask and charged with *p*-trifluoromethyl benzoyl chloride (18.6 ml, 0.1253

mol, 1 equiv.). A septum and a balloon of nitrogen gas with a needle adaptor are affixed to the top of the addition funnel and the *p*-trifluoromethyl benzoyl chloride is added dropwise over 10 minutes while stirring. A white precipitate rapidly appears. Once the addition is complete, the addition funnel is removed, the flask is sealed with a septum and the reaction is removed from the ice bath. The reaction is stirred for five hours at room temperature. DCM is removed by rotary evaporation (A Buchi rotovap R-100 was used with a bath temperature of 40 ^{o}C and vacuum at 100 mbar) and diethyl ether (ACS grade) (200 ml) is added to the resulting water suspension. The mixture is vacuum filtered with a Synthware 150 ml (7.2 cm diameter) fine porosity filter frit attached to a 500 ml filter flask using a rubber filter adaptor. The white solids are washed with 100 ml diethyl ether, followed by 2 x 100 ml de-ionized water, each time breaking the solids in the filter with a spatula and mixing thoroughly before applying vacuum. The solids are washed with an addition 100 ml diethyl ether and then transferred to a tared 250 ml round bottom flask using a spatula. The product is dried under high vacuum in a round bottom flask using a 24/40 joint to hose adaptor. The round bottom flask was immersed in a heating bath with a temperature of 70 ^{o}C. High vacuum was established with a vacuum pump provided by Welch. After drying overnight, a pressure of 50 mTorr was achieved and product **1** was isolated as a white solid in 94% yield (34.68 g, 0.117 mol). **^{1}H NMR** (400 MHz, DMSO-*d6*): δ 12.01 (br s, 1 H), 7.95 (d, J = 8.2 Hz, 2 H), 7.83 (d, J = 8.1 Hz, 2 H), 7.50 – 7.32 (m, 5 H), 4.96 (s, 2 H). **^{19}F{^{1}H} NMR** (376 MHz, DMSO-*d6*): δ -61.49. **^{13}C{^{1}H} NMR** (101 MHz, DMSO-*d6*): 136.6, 136.4, 131.9 (q, $^{2}J_{C-F}$ = 33 Hz), 129.4, 128.8, 128.5, 125.9 (q, $^{3}J_{C-F}$ = 4 Hz), 124.3 (q, $^{1}J_{C-F}$ = 274 Hz), 77.5. **IR** (diamond ATR, neat) 3175, 1647, 1329, 1167, 1109, 1123, 1070, 1069, 1042, 1016, 901, 856, 745, 700, 621 cm^{-1}. **HR-MS** (ESI) calculated 295.0820 for $C_{15}H_{12}F_3NO_2$, found 295.0814. **mp:** 170.8 – 172.3 ^{o}C.

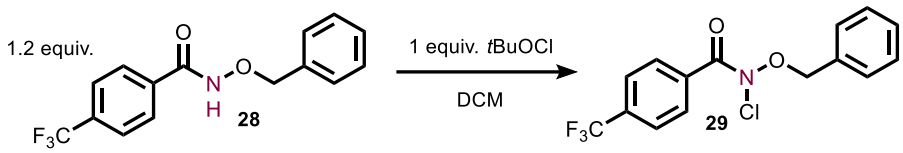

***N*-(benzyloxy)-*N*-chloro-4-(trifluoromethyl)benzamide (29) (procedure A using *t*BuOCl):**

In air, an oven-dried 250 ml round bottom flask (24/40 joint) equipped with a 2.5 cm diameter Teflon-coated egg-shaped stir bar is charged with **28** (5.0 g, 0.01695 mol, 1.2 equiv.) and dichloromethane (ACS grade) (0.042 M, 40 ml). The flask is stirred for 5 minutes, resulting in a white suspension using a Heidolph MR Hei-Mix L stir plate with a rate of 750 rpm. The flask is wrapped in aluminum foil (the reaction is light sensitive and the fumehood light was turned off) and *t*-butylhypochlorite (1.6 ml, 0.0141 mol, 1 equiv.) is added in a single portion using a 5 ml syringe. The flask is sealed with a ground glass stopper (24/40 joint) and stirred at room temperature for 4 hours (Note 17) over which time a yellow solution forms. DCM is removed by rotary evaporation using a Buchi rotovap R-100 with a bath temperature of 40 ^{o}C and vacuum at 100 mbar. 50 ml pentane (ACS grade) is then added and the flask is stirred for 5 minutes to form an even mixture of yellow solution and suspended white solids. The mixture is vacuum filtered with a Synthware 60 ml fine porosity filter frit attached to a 500 ml filter flask using a rubber filter adaptor. White solids (excess **28**) are collected in the frit and the flask is rinsed with an addition 50 ml of pentane, which is subsequently poured through the filter frit. The clear yellow solution in the filter flask is transferred to a 1 L round bottom flask (24/40 joint). The filter flask is rinsed with an additional 50 ml of pentane which is then transferred to the 1 L round bottom flask. Pentane is removed from the flask by rotary evaporation to yield **29** as a yellow oil. Product **29** is immediately used in the next step without further purification.

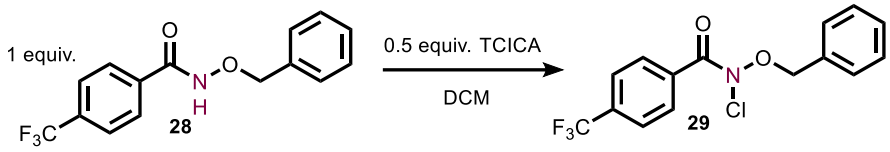

***N*-(benzyloxy)-*N*-chloro-4-(trifluoromethyl)benzamide (29) (procedure B using TCICA):**

An oven-dried 250 ml round bottom flask (24/40 joint) equipped with a 2.5 cm diameter Teflon-coated egg-shaped stir bar is charged with **28** (5.0 g, 16.9 mmol, 1 equiv.), dichloromethane (ACS grade, 0.4 M, 40 ml) and de-ionized water (915 µL, 50.8 mmol). The flask is submersed in an ice bath stirred for 5 minutes (Heidolph MR Hei-Mix L stir plate with a rate of 750 rpm) at 0 ^{o}C, resulting in a white suspension. The flask is wrapped in aluminum foil (the reaction is light sensitive and the fumehood light was turned off) and trichloroisocyanuric acid (TCICA) (1.97 g, 8.47 mmol, 0.5 equiv.) is added in portions over 15 min. This is performed by dividing the TCICA into 7 equal portions of 281 mg and adding one portion every two minutes using a timer. The flask is then sealed with a glass stopper (24/40 joint) and stirring is continued for 1 h at 0 ^{o}C at a rate of 750 rpm. DCM is removed by rotary evaporation (water bath temp kept 20 ^{o}C). Pentane (ACS grade, 50 ml) is added and the flask is stirred for 2 minutes to form an even mixture of yellow solution and suspended white solids. The mixture is vacuum filtered with a Synthware 60 ml fine porosity filter frit, loaded with celite (3 cm height) attached to a 250 ml round bottom flask using glass adaptor. White solids (excess TCICA and byproducts) are collected in the frit and the flask is rinsed with an addition 40 ml of pentane twice, which is subsequently passed through celite. Pentane is removed from the round bottom flask by rotary evaporation (Buchi rotovap R-100 with a bath temp 20 ^{o}C). Once pentane is removed (visibly) from the flask, the rotovap recovery flask is emptied. Evaporation of the flask is then continued at the maximal vacuum of the rotovap (down to 30 mBar, bath temp 20 ^{o}C) for 5 min to yield **29** as a yellow solid. Product **29** is immediately used in the next step without

further purification. **^{1}H NMR** (400 MHz, $CDCl_3$): δ 7.71 (d, J = 8.1 Hz, 2H), 7.65 (d, J = 8.4 Hz, 2H), 7.37 – 7.32 (m, 3H), 7.26 (d, J = 7.7 Hz, 2H), 5.10 (s, 2H). **^{19}F{^{1}H} NMR** (376 MHz, $CDCl_3$): δ -63.16. **^{13}C{^{1}H} NMR** (101 MHz, $CDCl_3$): δ 172.5, 134.7, 134.0 (q, $^{2}J_{C-F}$ = 32 Hz), 132.9, 129.8, 129.6, 129.4, 128.7, 125.3 (q, $^{3}J_{C-F}$ = 4 Hz), 123.5 (q, $^{1}J_{C-F}$ = 272 Hz), 76.7. **IR** (diamond ATR, neat) 1722, 1410, 1321, 1258, 1182, 1128, 1065, 997, 935, 862, 754, 698, 604, 507 cm^{-1}. **HR-MS** (ESI) calculated 329.0430 for $C_{15}H_{11}ClF_3NO_2$, found 329.0427. **mp:** 39.7 – 40.3 °C.

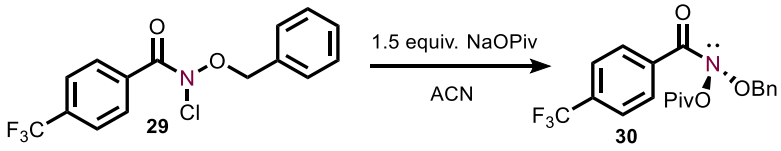

***N*-(benzyloxy)-*N*-(pivaloxy)-4-(trifluoromethyl)benzamide (30):**

In air, an oven dried 200 ml pear shaped Schlenk flask (14/20 joint; ground glass socket and hose adaptor) equipped with a 3.2 cm diameter Teflon-coated cylindrical stir bar is charged with anhydrous sodium pivalate (2.63 g, 0.0212 mol, 1.5 equiv.). The Schlenk flask joint is sealed with a rubber septum and the socket to the hose adaptor is sealed with a ground glass key. The key was greased with Dow Corning high vacuum grease and secured to the flask using a metal spring and retainer clip. The flask was attached to a Schlenk line using the hose adaptor and Tygon A-60-G vacuum tubing. The flask is evacuated with a vacuum line and refilled with dinitrogen to obtain an inert atmosphere. Vacuum was established with a vacuum pump provided by Welch. Five cycles of evacuating the flask to a pressure of 100 mTorr and refilled with dinitrogen gas were performed. Dry, degassed acetonitrile (50 ml, HPLC grade degassed with argon and dried by passing through a PPT Solvent Purification System) is transferred to the Schlenk flask under inert atmosphere in two portions using a syringe equipped with an oven

dried Luer-lok 12 inch reusable needle. The flask containing the white solids and acetonitrile is submersed in an ice/water bath and stirred *vigorously* (Heidolph MR Hei-Mix L stir plate with a rate of 1400 rpm) to form a white suspension equilibrated to 0 ^{o}C. In air, an oven dried 250 ml round bottom flask (24/40 joint) was charged with **29** and 40 ml dry, degassed acetonitrile to form a yellow solution. The round bottom flask is covered in aluminum foil due to the potential light sensitivity of the *N*-chloramide intermediate. The round bottom flask is sealed with a septum which is pierced with a vent needle (Exel 18G x 1 inch pink disposable needle) and an inlet needle (a Luer-lok 12 inch reusable needle) attached to a nitrogen line. The solution is thoroughly sparged with dinitrogen gas for 15 minutes and the vent needle is subsequently removed. The inlet needle should remain in the round bottom flask to maintain positive dinitrogen flow while syringe transferring the degassed solution. The degassed solution of **29** is transferred under inert atmosphere using a 50 ml syringe equipped with an oven dried Luer-lok 12 inch reusable needle to the cooled Schlenk flask while stirring at 1400 rpm. The solution of **29** is added slowly over 10 minutes to form a yellow solution with white suspended solids. The round bottom flask is rinsed with an additional 10 ml of dry, degassed acetonitrile (the final volume of solvent in the reaction is 100 ml, 0.14 M) which is transferred to the Schlenk flask under inert atmosphere using a 50 ml syringe equipped with an oven dried Luer-lok 12 inch reusable needle. The Schlenk flask is covered with aluminum foil and the reaction is *vigorously* stirred at 1400 rpm under positive flow of dinitrogen gas for 2 hours at 0 ^{o}C. In air, the white suspension is vacuum filtered with through a plug of silica 2 cm in height using a Synthware 60 ml fine porosity filter frit attached to a 500 ml filter flask using a rubber filter adaptor. White solids (sodium chloride) are collected in the frit and the flask is rinsed with 100 mL of diethyl ether (ACS grade), which is subsequently poured through the silica plug. The clear filtrate is

transferred from the filter flask to a 500 ml round bottom flask (24/40 joint). The filter flask is rinsed with an additional 20 ml diethyl ether which is transferred to the round bottom flask. The solvents are removed by rotary evaporation (using a Buchi rotovap R-100 with a bath temperature of 40 ^{o}C and vacuum at 100 mbar) to yield **30** as a clear oil in 89% yield (5.93 g, 15.0 mmol). Storage of **30** at 5 ^{o}C results in a waxy, off-white solid. **^{1}H NMR** (400 MHz, $CDCl_3$): δ 7.77 (d, J = 8.3 Hz, 2H), 7.65 (d, J = 8.0 Hz, 2H), 7.41 – 7.34 (m, 5H), 5.15 (s, 2H), 1.11 (s, 9H). **^{19}F{^{1}H} NMR** (376 Hz, $CDCl_3$): δ -63.16. **^{13}C{^{1}H} NMR** (101 Hz, $CDCl_3$): δ 175.3, 173.2, 135.5, 134.7, 133.8 (q, $^{2}J_{C-F}$ = 32 Hz), 129.3, 129.2, 128.9, 128.5, 125.1 (q, $^{3}J_{C-F}$ = 4 Hz), 123.5 (q, $^{1}J_{C-F}$ = 272 Hz), 77.9, 38.4, 26.6. **HR-MS** (ESI) calculated 395.1344 for $C_{20}H_{20}F_3NO_4$ $[M]^+$, found 395.1333. **mp:** 38.7 – 39.5 ^{o}C.

4.5.3. Synthesis and Characterization of Anomeric Amides Derived from *N*-(benzyloxy)-4-(trifluoromethyl)benzamide Containing New Leaving Groups.

General procedure for synthesis of anomeric containing new leaving groups:

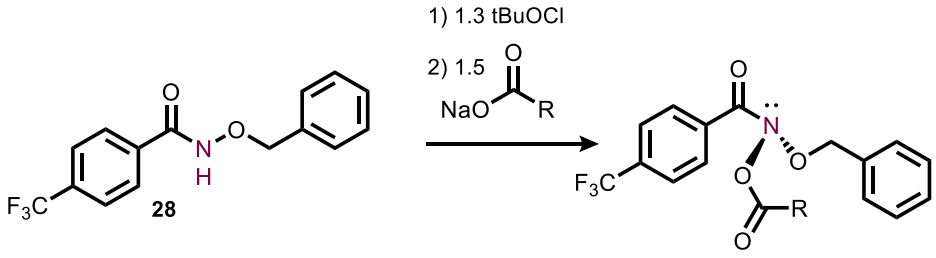

To a stirred suspension of *N*-(benzyloxy)-4-(trifluoromethyl)benzamide (1 g, 3.89 mmol, 1 equivalent) in CH_2Cl_2 (8 mL) in a 50 ml round bottom flask was added freshly prepared *t*-BuOCl (478 mg, 4.40 mmol, 1.3 equiv) in a single portion. The reaction was shielded from ambient light and stirred at room temperature for 2 hours (consumption of starting material by TLC). The solution was concentrated *in vacuo* to afford *N*-(benzyloxy)-*N*-chloro-4-(trifluoromethyl)benzamide product as a yellow liquid, which was immediately used in the next

step. To a suspension of the requisite sodium carboxylate salt (1.09 mmol, 1.5 equiv.) in dry acetonitrile (2ml) under a nitrogen atmosphere was added a degassed solution of *N*-(benzyloxy)-*N*-chloro-4-(trifluoromethyl)benzamide (240 mg, 0.727 mmol, 1 equiv.) in 3 ml dry acetonitrile. The reaction was shielded from light and stirred vigorously at ambient temperature for 2 hours. Upon completion (consumption of starting material monitored by TLC), the reaction mixture was diluted with 20 ml diethyl ether and vacuum filtered to remove a white salt (sodium chloride). The filtrate was concentrated in vacuo to yield the anomeric amide product.

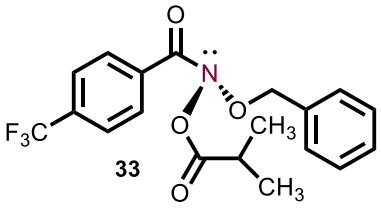

33

***N*-(benzyloxy)-*N*-(isobutyryloxy)-4-(trifluoromethyl)benzamide (33):** Synthesized according to the general procedure from *N*-(benzyloxy)-*N*-chloro-4-(trifluoromethyl)benzamide (240 mg, 0.727 mmol, 1 equiv.) and sodium isopropoxide (120.1 mg, 1.09 mmol, 1.5 equiv.). The title compound was obtained as a pale yellow oil (270 mg, 0.71 mmol, 97% yield). **^{1}H NMR** (400 MHz, $CDCl_3$): δ 7.76 (d, J = 8.5 Hz, 2H), 7.64 (d, J = 8.1 Hz, 2H), 7.38 – 7.33 (m, 5H), 5.14 (s, 2H), 2.55 (sept, J = 7.0 Hz, 1H), 1.09 (d, J = 7.0 Hz, 2H). **^{19}F{^{1}H}** NMR (376 MHz, $CDCl_3$): δ -63.18. **^{13}C{^{1}H} NMR** (101 MHz, $CDCl_3$): δ 174.1, 173.1, 135.4, 134.6, 133.8 (q, $^{2}J_{C\text{-}F}$ = 32 Hz), 129.3, 129.2, 128.8, 128.5, 125.1 (q, $^{3}J_{C\text{-}F}$ = 4 Hz), 123.5 (q, $^{1}J_{C\text{-}F}$ = 237 Hz), 77.7, 32.2, 18.4. **HRA-MS:** Calculated 381.1188 for $C_{19}H_{18}F_3NO_4$, found 381.1188.

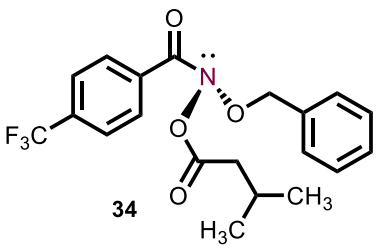

34

***N*-(benzyloxy)-*N*-((3-methylbutanoyl)oxy)-4-(trifluoromethyl)benzamide (34):** Synthesized according to the general procedure from *N*-(benzyloxy)-*N*-chloro-4-(trifluoromethyl)benzamide (240 mg, 0.727 mmol, 1 equiv.) and sodium isovalerate (194 mg, 1.09 mmol). The title compound was obtained as a pale yellow

liquid (257 mg, 0.65 mmol, 89% yield). **^{1}H NMR** (400 MHz,$CDCl_3$): δ 7.77 (d, J = 8.3 Hz, 2H), 7.63 (d, J = 8.2 Hz, 2H), 7.35 (s, 5H), 5.13 (s, 2H), 2.10 – 2.02 (m, 1H), 1.02 – 0.97 (m, 2H), 0.90 (d, J = 6.7 Hz, 6H). **^{19}F{^{1}H} NMR** (376 MHz, $CDCl_3$): δ -63.21. **^{13}C{^{1}H} NMR** (101 MHz, $CDCl_3$): δ 173.0, 170.2, 135.4, 134.5, 133.9 (q, $^{2}J_{C-F}$ = 33 Hz), 129.3, 128.9, 128.6, 125.2 (q, $^{3}J_{C-F}$ = 4 Hz), 78.9, 40.7, 25.7, 22.2. **HRA-MS:** Calculated 395.1344 for $C_{20}H_{20}F_3NO_4$, found 395.1338.

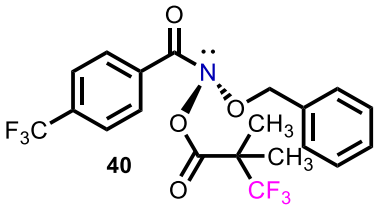

40

***N*-(benzyloxy)-*N*-((3,3,3-trifluoro-2,2-dimethylpropanoyl)oxy)-4-(trifluoromethyl)benzamide (40):** Synthesized according to the general procedure from *N*-(benzyloxy)-*N*-chloro-4-(trifluoromethyl)benzamide (100 mg, 0.414 mmol, 1 equiv.) and sodium 3,3,3-trifluoro-2,2-dimethylpropanoate (111 mg, 0.621 mmol, 1.5 equiv.). The product was obtained as a pale yellow oil (141 mg, 0.314 mmol, 75.8% yield). **^{1}H NMR** (400 MHz, $CDCl_3$): δ 7.75 (d, J = 8.2 Hz, 2H), 7.65 (d, J = 8.4 Hz, 2H), 7.36 – 7.34 (m, 5H), 5.13 (s, 2H), 1.36 (s, 6H). **^{19}F{^{1}H} NMR** (376 MHz, $CDCl_3$): δ -63.25, -74.65. **^{13}C{^{1}H} NMR** (101 MHz, $CDCl_3$): δ 171.0, 166.0, 132.9, 132.3, 127.8, 127.4, 126.9, 123.5 (q, $^{3}J_{C-F}$ = 4 Hz), 76.4, 46.7 (q, $^{2}J_{C-F}$ = 27 Hz), 17.5 (q, $^{3}J_{C-F}$ = 2 Hz). **HRA-MS:** calculated 449.1062 for $C_{20}H_{17}F_6NO_4$, found 449.1065.

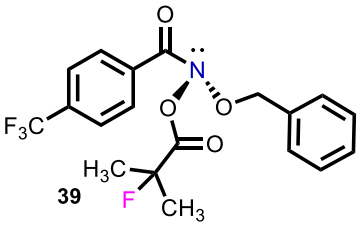

39

***N*-(benzyloxy)-*N*-((2-fluoro-2-methylpropanoyl)oxy)-4-(trifluoromethyl)benzamide (39):** Synthesized according to the general procedure from *N*-(benzyloxy)-*N*-chloro-4-(trifluoromethyl)benzamide (172 mg, 0.521 mmol, 1 equiv.) and sodium 2-fluoro-2-methylpropanoate (100 mg, 0.781 mmol, 1.5 equiv.). The product was obtained as a pale yellow oil (179.9 mg, 0.4004 mmol, 76.8% yield). **^{1}H NMR** (400 MHz,

$CDCl_3$): δ 7.77 (d, J = 8.1 Hz, 2H), 7.66 (d, J = 8.7 Hz, 2H), 7.37 – 7.35 (m, 5H), 5.16 (s, 2H), 1.51 (d, $^2J_{C-F}$ = 21.8 Hz, 6H). **^{19}F NMR** (376 MHz, $CDCl_3$): δ -63.23, -147.50 (sept, $^2J_{C-F}$ = 21.8 Hz). **^{13}C{^{1}H} NMR** (101 MHz, $CDCl_3$): δ 171.1, 167.7 (d, $^2J_{C-F}$ = 26 Hz), 132.5, 127.7, 127.6, 127.3, 126.9, 123.6 (q, $^3J_{C-F}$ = 4 Hz), 90.6 (d, $^1J_{C-F}$ = 184 Hz), 76.5, 22.9 (d, $^2J_{C-F}$ = 24 Hz). **HRA-MS:** calculated 339.1094 for $C_{19}H_{17}F_4NO_4$, found 399.1118.

General procedure for synthesis of sodium carboxylate salts:

A 20 ml vial was charged with a stirbar, sodium hydroxide (233 mg, 5.83 mmol, 1 equiv.) and 1 ml water. The vial was stirred at room temperature until all of the solids dissolved. The requisite carboxylic acid (5.83 mmol, 1 equiv.) was added portion-wise with a spatula and the vial was stirred at room temperature for 2 hours. The water was removed under vacuum and the sodium carboxylate salt was obtained as a white solid which, which was washed with ethyl acetate and dried overnight under high vacuum.

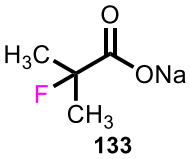

133

Sodium 2-fluoro-2-methylpropanoate (133): Synthesized according to the general procedure from 2-fluoroisobutyric acid (200 mg, 1.885 mmol). The title compound was obtained as a white solid (231 mg, 1.80 mmol, 96% yield). **^{1}H NMR** (400 MHz, D_2O): δ 1.52 (d, J = 21.9 Hz, 6H). **^{19}F{^{1}H} NMR** (376 MHz, D_2O): δ -137.98 (br. s). **^{13}C{^{1}H} NMR** (101 MHz, D_2O): δ 181.01 (d, $^2J_{C-F}$ = 23 Hz), 95.8 (d, $^1J_{C-F}$ = 177 Hz), 24.7 (d, $^2J_{C-F}$ = 25 Hz). **HR-MS:** Calculated 105.0352 for $C_4H_6FO_2$, found 105.0351.

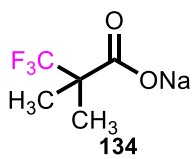

134

Sodium 3,3,3-trifluoro-2,2-dimethylpropanoate (134): Synthesized according to the general procedure from 3,3,3-trifluoro-2,2-dimethylpropanoic acid (1.0 g,

6.41 mmol). The title compound was obtained as a white solid (1.1 g, 6.3 mmol, 98% yield). **^{1}H NMR** (400 MHz, D_2O): δ 1.33. **^{19}F{^{1}H} NMR** (376 MHz, D_2O): δ -74.33. **^{13}C{^{1}H} NMR** (101 MHz, D_2O): δ 178.4, 128.0 (q, $^{2}J_{C-F}$ = 278), 49.2 (q, $^{1}J_{C-F}$ = 24 Hz), 19.9 (q, $^{3}J_{C-F}$ =3 Hz). **HR-MS:** Calculated 155.032 for $C_5H_6F_3O_2$, found 155.0334.

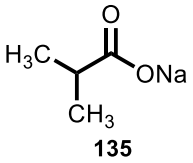

135

Sodium isobutyrate (135): Synthesized according to the general procedure from isobutyric acid (2.0 g, 0.0227 mol) with the exception that sodium hydroxide was used as the limiting reagent (0.825 g, 0.0206 mmol, 0.91 equiv.). The title compound was obtained as a white solid (2.27 g, 0.0206 mmol, 100% yield) after rinsing with ethyl acetate to remove excess isobutyric acid. **^{1}H NMR** (400 MHz, D_2O): δ 2.39 (sept, J = 7.0 Hz, 1H), 1.06 (d, J = 7.0 Hz, 6H). Spectroscopic data were in agreement with the literature.[39]

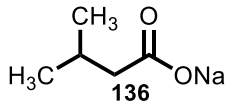

136

Sodium isovalerate (136): Synthesized according to the general procedure from isovaleric acid (2.0 g, 0.0196 mol, 1 equiv.) with the exception that sodium hydroxide was used as the limiting reagent (0.712 g, 0.0178 mol, 0.91 equiv.). The title compound was obtained as a white solid (2.43 g, 0.0178 mol, 100% yield) after rinsing with ethyl acetate to remove excess isovaleric acid. **^{1}H NMR** (400 MHz, D_2O) δ 2.08 – 2.05 (m, 2H), 1.97 (nonet, J = 6.95, 1H), 0.91 (d, J = 6.7 Hz, 6H). Spectroscopic data were in agreement with the literature.[40]

4.5.4. Synthesis and Characterization of Anomeric Amides Containing New Alkoxy Groups.

General procedure for synthesis of substituted benzyloxy derivatives of *N*-(benzyloxy)-4-(trifluoromethyl)benzamide:

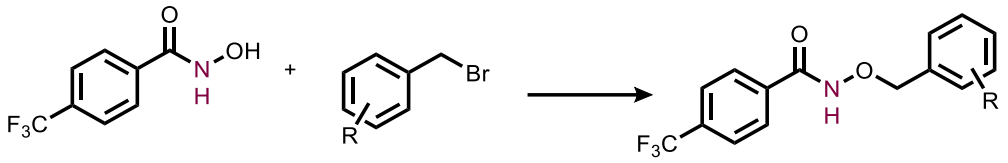

A 50 ml pear shaped round bottom flask equipped with a stir bar was charged with *N*-hydroxy-4-(trifluoromethyl)benzamide (2.44 mmol, 1.5 equiv.), the requisite benzyl bromide (1.63 mmol, 1 equiv.) and 2 ml of ethanol. A 20 ml vial was charged with sodium hydroxide (4.07 mmol 2.5 equiv.) and 2 ml deionized water was added. The sodium hydroxide solution was slowly pipetted into the round bottom flask. A reflux condenser was affixed to the flask and the reaction was refluxed at 120 °C for 18 hours. The reaction was subsequently cooled to room temperature and ethanol was removed by rotary evaporation. The remaining residue was acidified with 10 ml of a 3M HCl solution and extracted with 3 x 10 ml ethyl acetate. The organic fractions were combined, washed with brine, dried over sodium sulfate and filtered. The volatiles were removed by rotary evaporation to yield the requisite *N*-(benzyloxy)benzamide which was taken forward without further purification.

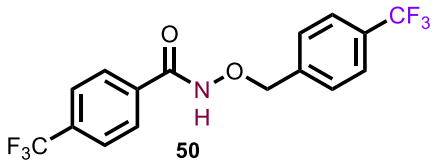

50

4-(trifluoromethyl)-*N*-((4-(trifluoromethyl)benzyl)oxy)benzamide (50): Synthesized according to the general procedure from *N*-hydroxy-4-(trifluoromethyl)benzamide (500 mg, 2.44 mmol) and 1-(bromomethyl)-4-(trifluoromethyl)benzene (388 mg, 1.625 mmol). The product was obtained as a white solid (300 mg, 83% yield). **^{1}H NMR** (400 MHz, DMSO-*d6*): δ 12.08 (br s, 1H), 7.94 (d, J = 8.7 Hz, 2H), 7.87 (d, J = 8.4 Hz, 2H), 7.78 (d, J = 8.1 Hz, 2H), 7.71 (d, J = 8.7 Hz, 2H), 5.06 (s, 2H). **^{19}F{^{1}H} NMR** (376 MHz, DMSO-*d6*): δ -61.03, -61.50. **^{13}C{^{1}H} NMR** (101 MHz, DMSO-*d6*): δ 163.8,

141.1, 136.4, 129.8, 128.5, 126.0 (q, J_{C-F} = 4 Hz), 125.7 (q, J_{C-F} = 4 Hz), 123.3, 123.0, 76.6. **HR-MS:** Calculated 363.0694 for $C_{16}H_{11}F_6NO_2$, found 363.0690.

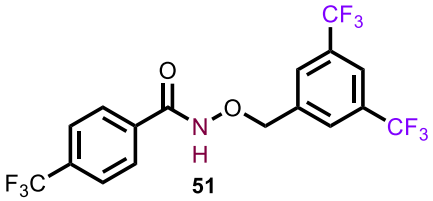

51

***N*-((3,5-bis(trifluoromethyl)benzyl)oxy)-4-(trifluoromethyl)benzamide (51):** Synthesized according to the general procedure from *N*-hydroxy-4-(trifluoromethyl)benzamide (500 mg, 2.44 mmol) and 1-(bromomethyl)-3,5-bis(trifluoromethyl)benzene (899 mg, 2.93 mmol). The product was obtained as a white solid (329.8 mg, 0.765 mmol, 31% yield). **^{1}H NMR** (400 MHz, DMSO-d6): δ 12.15 (br s, 1H), 8.23 (s, 2H), 8.11 (s, 1H), 7.95 – 7.85 (m, 4H), 5.18 (s, 2H). **^{19}F{^{1}H} NMR** (376 MHz, DMSO-d6): δ -61.28, -61.45. **HRA-MS:** Calculated 431.0568 for $C_{17}H_{10}F_9NO_2$, found 431.0581.

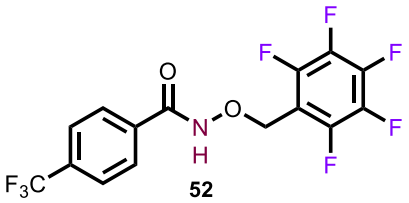

52

***N*-((perfluorophenyl)methoxy)-4-(trifluoromethyl)benzamide (52):** Synthesized according to the general procedure from *N*-hydroxy-4-(trifluoromethyl)benzamide (500 mg, 2.44 mmol) and 1-(bromomethyl)-2,3,4,5,6-pentafluorobenzene (637 mg, 2.44 mmol). The product was obtained as a light brown solid. **^{1}H NMR** (400 MHz, DMSO-d6): δ 12.05 (s, 1H), 7.88 (s, 5H), 5.12 (s, 2H). **^{19}F{^{1}H} NMR** (376 MHz, DMSO-*d6*): δ -61.80, -142.49 (d, J = 23.5 Hz), -153.67 (t, J = 20.1 Hz), -162.95 (td, J = 22.5 Hz, 7.1 Hz). **^{13}C{^{1}H} NMR** (101 MHz, DMSO-*d6*): δ 163.82, 146.2 (d, $^1J_{C-F}$ = 250 Hz), 141.6 (d, $^1J_{C-F}$ = 243 Hz), 138.3, 136.2, 132.1 (q, $^2J_{C-F}$ = 31 Hz), 130.6, 128.5, 126.0, 124.3 (d, $^1J_{C-F}$ = 271), 110.4 (q, $^3J_{C-F}$ = 9 Hz), 64.0. **HRA-MS:** Calculated 385.0349 for $C_{15}H_7F_8NO_2$, found 385.0343.

General procedure for the synthesis of new O-substituted benzamide derivatives using hydroxylamines:

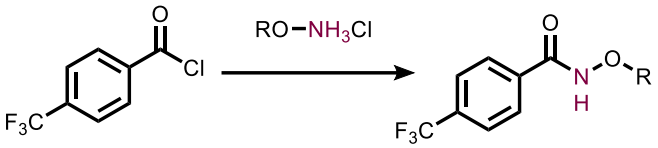

To a 50 ml pear shaped round bottom flask equipped with a stirbar was the requisite *O*-substituted hydroxylamine hydrochloride (1.37 mmol, 1 equiv.), potassium carbonate (379 mg, 2.74 mmol, 2 equiv.) and 4:1 DCM:water (0.25 M, 4.4 ml DCM, 1.1 ml water). The flask was stirred for 20 min at 0 ^{o}C and then 4-(trifluoromethyl)benzoyl chloride (286 mg, 1.37 mmol, 1 equiv.) was added dropwise by syringe at 0 ^{o}C. The ice bath was removed and the flask was stirred at room temperature for 5 hours. The water phase was removed using a separatory funnel and the DCM fraction was washed with brine, dried over sodium sulfate and filtered. The filtrate was concentrated in vacuo to yield the crude product, which was recrystallized from concentrated diethyl ether.

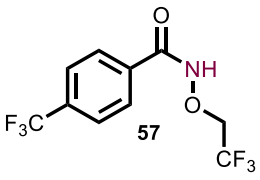

***N*-(2,2,2-trifluoroethoxy)-4-(trifluoromethyl)benzamide (57):** Synthesized according to the general procedure from 2,2,2-Trifluoroethoxyamine hydrochloride (200 mg, 1.32 mmol, 1 equiv.), potassium carbonate (365 mg, 2.64 mmol, 2 equiv.) and 4-(trifluoromethyl)benzoyl chloride (275 mg, 1.32 mmol, 1 equiv.). The title compound was obtained as a white solid after recrystallization from diethyl ether (340.8 mg, 1.187 mmol, 89.9% yield). **^{1}H NMR** (400 MHz, $CDCl_3$): δ 7.92 (d, J = 8.3 Hz, 2H), 7.75 (d, J = 7.74, 2H), 6.32 (br. s, 1H), 4.21 – 4.11 (m, 2H). **^{19}F{^{1}H} NMR** (376 MHz, $CDCl_3$): δ -63.09, -72.26. **^{13}C{^{1}H} NMR** (101 MHz, $CDCl_3$): δ 166.3,

136.4, 134.0 (q, J_{C-F} = 32 Hz), 127.6, 125.9 (q, J_{C-F} = 4 Hz), 124.0 (q, J_{C-F} = 276), 123.6 (q, J_{C-F} = 274 Hz), 41.2 (q, J_{C-F} = 34 Hz). **HR-MS:** Calculated 287.0377 for $C_{10}H_7F_6NO_2$, found 287.0381.

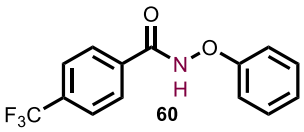

60

***N*-phenoxy-4-(trifluoromethyl)benzamide (60):** Synthesized according to the general procedure from O-phenyl hydroxylamine hydrochloride (200 mg, 1.37 mmol, 1 equiv.), potassium carbonate (379 mg, 2.74 mmol, 2 equiv.) and 4-(trifluoromethyl)benzoyl chloride (286 mg, 1.37 mmol, 1 equiv.). The title compound was obtained as a white solid after recrystallization from diethyl ether (71.5 mg, 0.254 mmol, 18.6% yield). **^{1}H NMR** (400 MHz, DMSO-*d6*): δ 12.74 (br. s, 1H), 8.09 (d, J = 8.3 Hz, 2H), 7.92 (d, J = 7.6 Hz, 2H), 7.37 (t, J = 8.4 Hz, 2H), 7.14 (d, J = 7.7 Hz, 2H), 7.06 (t, J = 7.6 Hz, 1H). **^{19}F{^{1}H} NMR** (376 MHz, DMSO-*d6*): δ -61.43. **^{13}C{^{1}H} NMR** (101 MHz, DMSO-*d6*): δ 159.9, 130.0, 128.8, 128.7, 126.1, 122.9, 113.6. **HRA-MS:** Calculated 281.0664 for $C_{14}H_{10}F_3NO_2$, found 281.0667.

General procedure for synthesis of new substituted *O*-benzyl and *O*-alkyl anomeric amide:

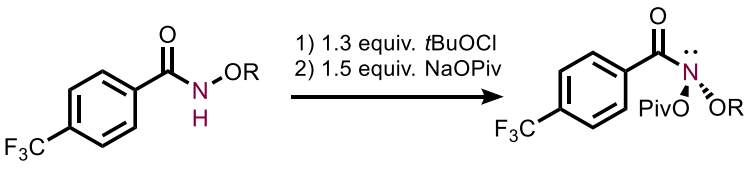

To a stirred suspension of *N*-(benzyloxy)-4-(trifluoromethyl)benzamide derivative (1 g, 3.89 mmol, 1 equivalent) in CH_2Cl_2 (8 mL) in a 50 ml round bottom flask was added freshly prepared t-BuOCl (478 mg, 4.40 mmol, 1.3 equiv) in a single portion. The reaction was shielded from ambient light and stirred at room temperature for 2 hours (consumption of starting material by

TLC). The solution was concentrated in vacuo to afford *N*-(benzyloxy)-*N*-chloro-4-(trifluoromethyl)benzamide derivative as a yellow liquid, which was immediately used in the next step. To a suspension of the requisite sodium carboxylate salt (1.09 mmol, 1.5 equiv.) in dry acetonitrile (2ml) under a nitrogen atmosphere was added a degassed solution of *N*-(benzyloxy)-*N*-chloro-4-(trifluoromethyl)benzamide derivative (240 mg, 0.727 mmol, 1 equiv.) in 3 ml dry acetonitrile. The reaction was shielded from light and stirred vigorously at ambient temperature for 2 hours. Upon completion (consumption of starting material monitored by TLC), the reaction mixture was diluted with 20 ml diethyl ether and vacuum filtered to remove a white salt (sodium chloride). The filtrate was concentrated in vacuo to yield the anomeric amide product.

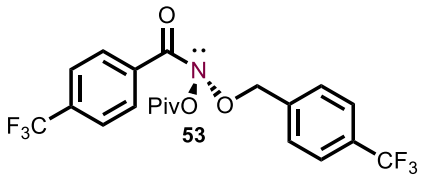

***N*-(pivaloyloxy)-4-(trifluoromethyl)-*N*-((4-(trifluoromethyl)benzyl)oxy)benzamide (53):** Synthesized according to the general procedure from 4-(trifluoromethyl)-*N*-((4-(trifluoromethyl)benzyl)oxy)benzamide (100 mg, 0.275 mmol, 1 equiv.). The title compound was obtained as a pale yellow oil (86.5 mg, 0.187 mmol, 67.8%). **^{1}H NMR** (400 MHz, $CDCl_3$): δ 7.75 (d, J = 8.5 Hz, 2H), 7.67 – 7.59 (m, 4H), 7.51 (d, J = 8.0 Hz, 2H), 5.19 (s, 2H), 1.05 (s, 9H). **^{19}F{^{1}H} NMR** (376 MHz, $CDCl_3$): δ -62.74, -63.21. **HRA-MS:** Calculated 363.0694 for $C_{16}H_{11}F_6NO_2$, found 363.0666.

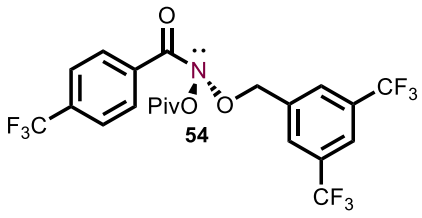

***N*-((3,5-bis(trifluoromethyl)benzyl)oxy)-*N*-(pivaloyloxy)-4-(trifluoromethyl)benzamide (54):** Synthesized according to the general procedure from *N*-((3,5-

bis(trifluoromethyl)benzyl)oxy)-4-(trifluoromethyl)benzamide (100 mg, 0.232 mmol, 1 equiv.). The title compound was isolated as a yellow oil (50.6 mg, 0.095 mmol, 41% yield). **^{1}H NMR** (400 MHz, $CDCl_3$): δ 7.82 (s, 2H), 7.79 (s, 1H), 7.70 (d, J = 8.2 Hz, 2H), 7.60 (d, J = 8.3 Hz, 2H), 5.21 (s, 2H), 0.98 (s, 9H).

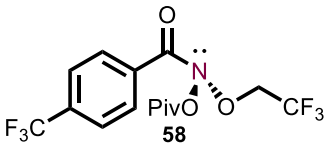

58

***N*-(pivaloyloxy)-N-(2,2,2-trifluoroethoxy)-4-(trifluoromethyl)benzamide (58):** Synthesized according to the general procedure from *N*-(2,2,2-trifluoroethoxy)-4-(trifluoromethyl)benzamide (78 mg, 0.271 mmol, 1 equiv.). The title compound was isolated as a yellow oil (52.8 mg, 0.133 mmol, 49% yield). **^{1}H NMR** (400 MHz, $CDCl_3$): δ 7.76 (d, J = 8.4 Hz, 2H), 7.63 (d, J = 8.3 Hz, 2H), 4.52 (q, J_{C-F} = 8.1 Hz, 2H), 1.01 (s, 9H).

4.5.5. Synthesis and Characterization of Anomeric Amides Containing New Acyl Derivatives.

General procedure for the synthesis of acyl chloride derivatives:

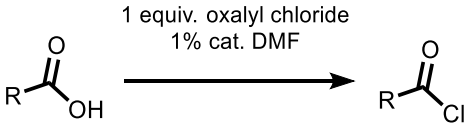

A 100 ml Schlenk flask equipped with a stirbar was charged with the requisite carboxylic acid (3.96 mmol, 1 equiv.). The flask was evacuated and refilled with dinitrogen to obtain an inert atmosphere. Dry, degassed DCM (20 ml) was added and the flask was stirred at 0 ^oC for 15 minutes. Oxalyl chloride (2.0M solution in DCM, 1.98 ml, 3.96 mmol, 1 equiv.) was added dropwise with a syringe. Catalytic DMF (3.1 µl, 0.0396 mmol, 0.01 equiv.) was added by syringe, the ice bath was removed and the reaction was stirred at room temperature overnight. The solvent was removed *in vacuo* to obtain the acyl chloride which was immediately taken forward for the synthesis of the *O*-benzyl hydroxamate derivative. For volatile acyl chlorides,

the crude reaction solution was taken forward without removal of solvent and isolation. This was necessary for 2-fluoro-2-methylpropanoyl chloride, 3,3,3-trifluoro-2,2-dimethylpropanoyl chloride, 2-butynoyl chloride.

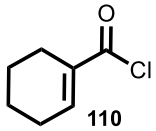

110

cyclohex-1-ene-1-carbonyl chloride (110): Synthesized according to the general procedure from cyclohex-1-ene-1-carboxylic acid (500 mg, 3.96 mmol, 1 equiv.). The product was obtained as a yellow oil (458 mg, 3.18 mmol, 80.3% yield). **^{1}H NMR** (400 MHz, $CDCl_3$): δ 7.45 – 7.42 (m, 1H), 2.37 – 2.30 (m, 4H), 1.73 – 1.60 (m, 4H). The spectroscopic data are in agreement with the literature.[41]

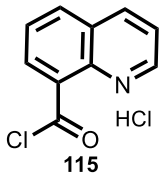

115

quinoline-8-carbonyl chloride HCl (115): Synthesized according to the general procedure from quinoline-8-carboxylic acid (604.8 mg, 3.49 mmol, 1 equiv.). The product was obtained as a purple solid (222.3 mg, 0.535 mmol, 15.3% yield). **^{1}H NMR** (400 MHz, DMSO-d6): δ 9.18 (dd, J = 4.7 Hz, 1.7 Hz, 1H), 8.89 (dd, J = 8.5 Hz, 1.4 Hz, 1H), 8.63 (7.4 Hz, 1.6 Hz, 1H), 8.45 (dd, J = 8.0 Hz, 1.2 Hz, 1H), 7.94 – 7.89 (m, 2H). **^{13}C{^{1}H} NMR** (101 MHz, DMSO-d6): δ 167.01, 149.8, 143.1, 141.7, 135.6, 134.6, 128.8, 128.2, 123.7, 123.1. **HRA-MS:** Calculated 156.0446 for $C_{10}H_6NO$ $[M\text{-}Cl]^+$, found 156.0451.

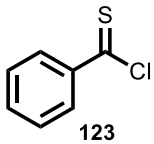

123

thiobenzoyl chloride (123): Synthesized according to the general procedure from thiobenzoic acid (1.0 g, 7.24 mmol, 1 equiv.). The title compound was obtained an amber oil (1.044 g, 6.662 mmol, 92% yield). **^{1}H NMR** (400 MHz, $CDCl_3$): δ 8.13 (d, J = 8.4 Hz, 2H), 7.69 (t, J = 7.6 Hz, 1H), 7.52 (t, J = 7.6 Hz, 2H). Spectroscopic data are in agreement with the literature.[42]

General procedure for the synthesis of *O*-benzyl hydroxamate derivatives:

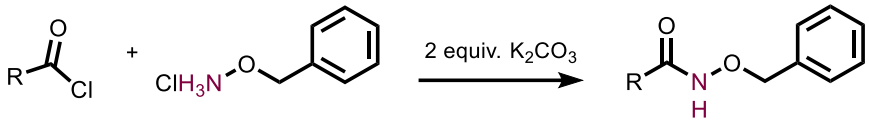

A 50 ml round bottom flask equipped with a stir bar was charged with a *O*-benzyl hydroxylamine hydrochloride (1.09 g, 6.82 mmol, 1 equiv.), potassium carbonate (1.885 g, 13.64 mmol, 2 equiv.) and 4:1 DCM:water (0.25 M, 22 ml DCM, 5 ml water). The flask was stirred for 20 min at 0 °C and then the requisite acyl chloride (6.82 mmol, 1.2 equiv.) was added dropwise by syringe at 0 °C. The ice bath was removed and the flask was stirred at room temperature for 5 hours. The water phase was removed using a separatory funnel and the DCM fraction was washed with brine, dried over sodium sulfate and filtered. The filtrate was concentrated in vacuo to yield the crude product, which was typically of sufficient purity. **Note:** Some acyl chloride derivatives were too volatile to be isolated and the crude product solution was taken forward without isolation, thus for some of the products below the stoichiometry is calculated using the amount of carboxylic acid precursor which must first treated with oxalyl chloride according to the procedure above.

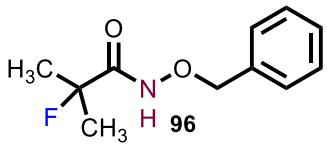

96

***N*-(benzyloxy)-2-fluoro-2-methylpropanamide (96):** Synthesized according to the general procedure from 2-fluoro-2-methylpropanoic acid (201.6 mg, 1.90 mmol, 1 equiv), *O*-benzylhydroxylamine HCl (253 mg, 1.583 mmol, 0.83 equiv) and potassium carbonate (438 mg, 3.166 mmol, 1.7 equiv). The title compound was isolated as a white solid (259 mg, 1.23 mmol, 65% yield). **^{1}H NMR** (400 MHz, $CDCl_3$): δ 9.02 (br. s, 1H), 7.34 – 7.23 (m, 5H), 4.83 (s, 2H), 1.46 (d, J = 22.6 Hz, 6H). **^{13}C{^{1}H} NMR** (101 MHz, $CDCl_3$): δ 170.2 (d, J = 20.5 Hz), 134.9, 129.3, 128.9, 128.6, 96.3 (d, J = 179 Hz), 78.3, 25.0 (d, J = 24 Hz). **^{19}F NMR** (376 MHz, $CDCl_3$): δ -151.6 (hd, J = 22.7, 3.3 Hz). **HRA-MS:** Calculated 211.1009 for $C_{11}H_{14}FNO_2$, found 211.1008.

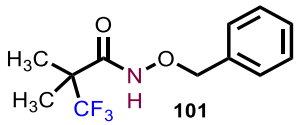

***N*-(benzyloxy)-3,3,3-trifluoro-2,2-dimethylpropanamide (101):** Synthesized according to the general procedure from 3,3,3-trifluoro-2,2-dimethylpropanoic acid (500 mg, 2.865 mmol, 1 equiv.), *O*-benzylhydroxylamine HCl (416 mg, 2.605 mmol, 0.83 equiv.), and potassium carbonate (720 mg, 5.21 mmol, 1.7 equiv.). The title compound was isolated as a white solid (343 mg, 1.32 mmol, 46% yield). **^{1}H NMR** (400 MHz, $CDCl_3$): δ 8.49 (br. s, 1H), 7.41 – 7.35 (m, 5H), 4.91 (s, 2H), 1.37 (s, 6H). **^{13}C{^{1}H} NMR** (101 MHz, $CDCl_3$): δ 167.0, 134.7, 129.5, 129.0, 128.6, 126.8 (q, J = 282 Hz), 78.3, 47.8 (q, J = 26 Hz), 19.7 (q, J = 2.3 Hz). **^{19}F NMR** (376 MHz, $CDCl_3$): δ -73.94. **HRA-MS:** calculated 261.0977 for $C_{12}H_{14}F_3NO_2$, found 261.0978.

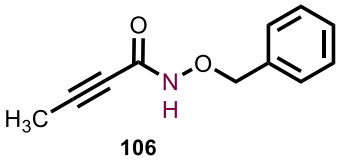

***N*-(benzyloxy)but-2-ynamide (106):** Synthesized according to the general procedure from 2-butynoic acid (300 mg, 3.568 mmol, 1 equiv.), *O*-benzylhydroxylamine HCl (475 mg, 2.973 mmol, 0.83 equiv.), and potassium carbonate (822 mg, 5.946 mmol, 1.7 equiv.). The title compound was isolated in 56% yield. (315.9 mg, 1.67 mmol). **^{1}H NMR** (400 MHz, $CDCl_3$): δ 9.24 (br. s, 1H), 7.32 – 7.20 (m, 5H), 4.79 (s, 2H), 1.78 (s, 3H). **^{13}C{^{1}H} NMR** (101 MHz, $CDCl_3$): δ 152.0, 135.0, 129.2, 128.7, 128.6, 86.7, 78.3, 71.9, 3.6. **HR-MS:** Calculated 189.0790 for $C_{11}H_{11}NO_2$, found 189.0789.

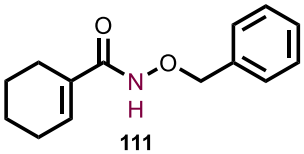

***N*-(benzyloxy)cyclohex-1-ene-1-carboxamide (111)**: Synthesized according to the general procedure from *O*-benzyl hydroxylamine hydrochloride (1.09 g, 6.82 mmol, 1 equiv.), potassium carbonate (1.885 g, 13.64 mmol, 2 equiv.) and 1-cyclohexenoyl chloride (573 mg, 3.96 mmol). The product was purified by automated column chromatography using silica gel and hexanes/ethyl acetate to obtain a white solid (84 mg, 0.36 mmol, 9% yield). **^{1}H NMR** (400 MHz, $CDCl_3$): δ

8.04 (br. s, 1H), 7.45 – 7.35 (m, 5H), 6.49 (sept, 1H), 4.95 (s, 2H), 2.19 – 2.09 (m, 4H), 1.69 – 1.55 (m, 5H). **$^{13}C\{^{1}H\}$ NMR** (101 MHz, $CDCl_3$): δ 135.1, 134.5, 131.4, 129.3, 128.7, 128.6, 78.1, 25.3, 24.0, 22.7, 21.9, 21.4. **HRA-MS:** Calculated 231.1259 for $C_{14}H_{17}NO_2$, found 231.1261.

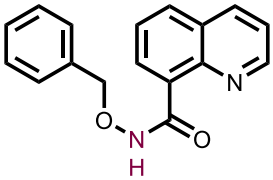

116

***N*-(benzyloxy)quinoline-8-carboxamide (116):** Synthesized according to the general procedure from *O*-benzyl hydroxylamine hydrochloride (159.61 mg, 0.98 mmol, 1 equiv.) with the exception that quinoline-8-carbonyl chloride HCl (222.3 mg, 0.98 mmol, 1 equiv.) was added to the reaction flask as a solid in a single portion and 3 equivalents of sodium carbonate (311 mg, 2.93 mmol) were used. The product was purified by column chromatography and isolated as a yellow solid (34.3 mg, 0.123 mmol, 13% yield). **^{1}H NMR** (400 MHz, $CDCl_3$): δ 13.47 (br s), 8.85 (d, J = 7.3 Hz, 1H), 8.69 (dd, J = 4.2 Hz, 1.5 Hz, 1H), 8.26 (dd, J = 8.4 Hz, 1.0 Hz, 1H), 7.97 (d, J = 8.2 Hz, 1H), 7.69 (t, J = 7.9 Hz, 1H), 7.56 – 7.52 (m, 2H), 7.47 – 7.43 (m, 1H), 7.41 – 7.35 (m, 3H), 5.15 (s, 2H). **$^{13}C\{^{1}H\}$ NMR** (101 MHz, $CDCl_3$): δ 171.1, 164.2, 149.3, 144.7, 137.8, 136.1, 133.8, 132.1, 129.3, 128.5, 128.4, 138.3, 126.7, 121.1, 78.1. **HRA-MS:** Calculated 263.0946 for $C_{17}H_{14}N_2O_2$, found 263.0956.

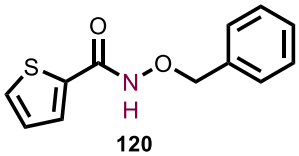

120

***N*-(benzyloxy)thiophene-2-carboxamide (120):** Synthesized according to the general procedure from *O*-benzyl hydroxylamine hydrochloride (1.09 g, 6.82 mmol, 1 equiv.), potassium carbonate (1.885 g, 13.64 mmol, 2 equiv.) and thiophene-2-carbonyl chloride (1 g, 6.82 mmol, 1 equiv.). The product was obtained as a waxy off-white solid (1.49 g, 6.42 mmol, 94% yield). **^{1}H NMR** (400 MHz, $CDCl_3$): δ 8.33 (br s, 1H), 7.62 (br s, 1H), 7.54 (d, J = 5.0 Hz, 1H), 7.46 – 7.37 (m,

5H), 7.10 - 7.07 (m, 5H), 5.01 (s, 2H). The spectroscopic data are in agreement with the literature.[43]

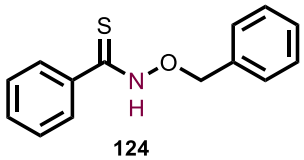

124

***N*-(benzyloxy)benzothioamide (124):** Synthesized according to the general procedure from thiobenzoyl chloride (500 mg, 3.1922 mmol, 1.2 equiv.), *O*-benzyl hydroxylamine hydrochloride (159.61 mg, 0.98 mmol, 1 equiv.). The title compound was obtained as a yellow solid after purification by column chromatography (398.6 mg, 1.638 mmol, 51.3%). **^{1}H NMR** (400 MHz, $CDCl_3$): δ 8.94 (br s.), 7.67 (d, J = 8.1 Hz, 2H), 7.48 (t, J = 7.7 Hz, 1H), 7.44 – 7.34 (m, 7H). 5.00 (s, 2H). **^{13}C{^{1}H} NMR** (101 MHz, $CDCl_3$): δ 135.3, 132.1, 132.0, 129.3, 128.8, 128.7, 128.6, 127.1, 78.4. **HRA-MS:** calculated 243.0718 for $C_{14}H_{13}NOS$, found 243.0712.

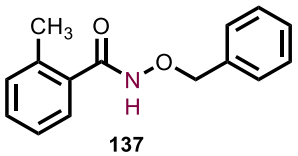

137

***N*-(benzyloxy)-2-methylbenzamide (137):** Synthesized according to the general procedure from 2-methylbenzoyl chloride (448 mg, 2.898 mmol, 1 equiv.), *O*-benzyl hydroxylamine hydrochloride (463 mg, 2.898 mmol, 1 equiv.) and potassium carbonate (801 mg, 5.796 mmol, 2 equiv.). The title compound was obtained by recrystallization from a concentrated ether solution at 5 ^{o}C to yield a white crystalline solid (558.2 mg, 2.313 mmol, 80% yield). **^{1}H NMR** (400 MHz, $CDCl_3$): δ 8.47 (br. s, 1H), 7.49 – 7.12 (m, 9H), 5.04 (s, 2H), 2.40 (s, 3H). **^{13}C{^{1}H} NMR** (101 MHz, $CDCl_3$): δ 168.0, 136.9, 135.2, 132.8, 131.0, 130.5, 129.3, 128.8, 128.7, 127.1, 125.6. **HR-MS:** Calculated 241.1103 for $C_{15}H_{15}NO_2$, found 241.1103.

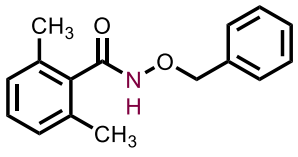

138

***N*-(benzyloxy)-2,6-dimethylbenzamide (138):** Synthesized according to the general procedure from 2,6-dimethylbenzoyl chloride (200 mg, 1.186 mmol, 1 equiv.), *O*-benzyl hydroxylamine hydrochloride (189.3 mg, 1.186 mmol, 1 equiv.) and potassium carbonate (327.8 mg, 2.372 mmol, 2 equiv.). The title

compound was isolated as a pale-yellow solid (185.4 mg, 0.723 mmol, 61% yield). **^{1}H NMR** (400 MHz, $CDCl_3$): δ 7.35 – 7.15 (m, 6H), 7.03 (t, J = 7.8 Hz, 1H), 6.85 (d, J = 7.6 Hz, 2H), 4.92 (s, 2H), 2.14 (s, 6H). **^{13}C{^{1}H} NMR** (400 MHz, $CDCl_3$): δ 167.41, 135.4, 129.5, 129.7, 128.8, 128.6, 128.5, 128.4, 127.5, 78.4, 19.02. **HR-MS:** Calculated 255.1259 for $C_{16}H_{17}NO_2$, found 255.1263.

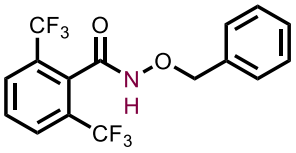

139

***N*-(benzyloxy)-2,6-bis(trifluoromethyl)benzamide (139):** Synthesized according to the general procedure from 2,6-bis(trifluoromethyl)benzoyl chloride (200 mg, 0.723 mmol, 1 equiv.), *O*-benzyl hydroxylamine hydrochloride (115 mg, 0.723 mmol, 1 equiv.) and potassium carbonate (200.4 mg, 1.45 mmol, 2 equiv.). The title compound was isolated as a white solid (71 mg, 0.195 mmol, 27% yield). **^{1}H NMR** (400 MHz, $CDCl_3$): δ 7.90 (d, J = 7.9 Hz, 2H), 7.72 (t, J = 8.0 Hz, 1H), 7.31 – 7.22 (m, 5H), 5.32 (br. s., 1H), 4.63 (s, 2H).

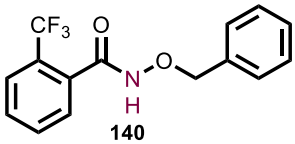

140

***N*-(benzyloxy)-2-(trifluoromethyl)benzamide (140):** Synthesized according to the general procedure from 2-(trifluoromethyl)benzoyl chloride (500 mg, 2.397 mmol, 1 equiv.), *O*-benzyl hydroxylamine hydrochloride (382.6 mg, 2.397 mmol, 1 equiv.) and potassium carbonate (663 mg, 4.8 mmol, 2 equiv.). The title compound was isolated as a white crystalline solid (499 mg, 1.689 mmol, 71% yield) after recrystallization from diethyl ether at 5 ^{o}C. **^{1}H NMR** (400 MHz, $CDCl_3$): δ 8.59 (br. s, 1H), 7.60 – 7.21 (m, 9H), 4.91 (s, 2H). **^{19}F{^{1}H} NMR** (376 MHz, $CDCl_3$): δ -58.81. **^{13}C{^{1}H} NMR** (101 MHz, $CDCl_3$): δ 165.2, 135.0, 132.0, 130.5, 129.3, 129.1, 128.8, 128.6, 126.5 (q, J_{C-F} = 4.7 Hz), 78.3. **HRA-MS:** Calculated 295.0820 for $C_{15}H_{12}F_3NO_2$, found 295.0820.

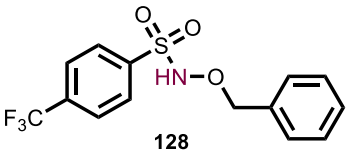

128

***N*-(benzyloxy)-4-(trifluoromethyl)benzenesulfonamide (128):** A 100 ml round bottom flask equipped with a stirbar was charged with *O*-benzyl hydroxylamine hydrochloride (653 mg, 4.088 mmol, 1 equiv.), 7.5 ml water and 5 ml methanol. A solution of potassium carbonate (565 mg, 4.088 mmol, 1 equiv.) in 7 ml water was added dropwise and the reaction flask was stirred vigorously for 1 hour. Ice cold methanol (50 ml) was poured into the flask and 4-(trifluoromethyl)benzenesulfonyl chloride (1 g, 4.088 mmol) was added to the reaction portion-wise using a spatula. The reaction was stirred for 5 hours and the methanol was removed *in vacuo*. The remaining water mixture was acidified with 3 M HCl solution and the product was extracted to ethyl acetate. The organic layers were combined, washed with brine, dried over sodium sulphate and filtered. The filtrate was concentrated *in vacuo* to yield the title compound as a faintly pink solid (767 mg, 2.32 mmol, 57%). **^{1}H NMR** (400 MHz, $CDCl_3$): δ 8.06 (d, J = 8.6 Hz, 2H), 7.80 (d, J = 9.1 Hz, 2H), 7.38 – 7.33 (m, 5H), 7.00 – 6.98 (br s, 1H), 5.00 (s, 2H). **^{19}F{^{1}H} NMR** (376 MHz, $CDCl_3$): δ -63.23. **^{13}C{^{1}H} NMR** (101 MHz, $CDCl_3$): δ 140.11, 135.34 (q, $^{2}J_{C-F}$ = 33.1 Hz), 134.94, 129.4, 129.1, 128.9, 128.6, 126.21 (q, $^{3}J_{C-F}$ = 3.9 Hz), 123.2 (q, $^{1}J_{C-F}$ = 273.3), 79.7. **HRA-MS:** Calculated 331.0490 for $C_{14}H_{12}F_3NO_3S$, found 331.0499.

General procedure for the synthesis of anomeric amides derived from hydroxamates bearing new acyl substituents:

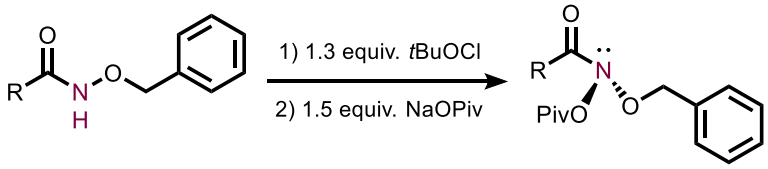

To a stirred suspension of *N*-(benzyloxy)-amide derivative (0.429 mmol, 1 equivalent) in CH_2Cl_2 (2 mL) in a 50 ml pear shaped round bottom flask was added freshly prepared *t*-BuOCl

(61 mg, 0.557 mmol, 1.3 equiv.) in a single portion. The reaction was shielded from ambient light and stirred at room temperature for 2 hours (consumption of starting material by TLC). The solution was concentrated in vacuo to afford the *N*-(benzyloxy)-*N*-chloro-amide product as a yellow liquid, which was immediately used in the next step. To a suspension of sodium pivalate (80 mg, 0.643 mmol, 1.5 equiv.) in dry acetonitrile (2 ml) under a nitrogen atmosphere was added a degassed solution of *N*-(benzyloxy)-*N*-chloro-amide derivative 2 ml dry acetonitrile. The reaction was shielded from light and stirred vigorously at ambient temperature for 2 hours. Upon completion (consumption of starting material monitored by TLC), the reaction mixture was diluted with 10 ml diethyl ether and vacuum filtered to remove a white salt (sodium chloride). The filtrate was concentrated in vacuo to yield the anomeric amide product.

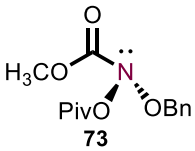

73

***N*-(benzyloxy)-*N*-(pivaloyloxy)-methylcarbamate (73):** Synthesized according to the general procedure from methyl benzyloxycarbamate (750 mg, 4.54 mmol). The title compound was obtained as a clear, colourless oil (878 mg, 3.12 mmol, 69% yield over two steps). **^{1}H NMR** (400 MHz, $CDCl_3$): δ 7.43 – 7.32 (m, 5H), 5.07 (3, 2H), 3.84 (s, 3H), 1.21 (s, 9H). **^{13}C{^{1}H} NMR** (101 MHz, $CDCl_3$): δ 175.4, 158.7, 135.2, 129.2, 128.4, 78.01, 54.9, 38.3, 26.8. **HRMS** (ESI) calculated 281.1263 for $C_{14}H_{19}NO_5$ $[M]^+$, found 281.1257.

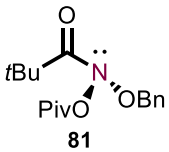

81

***N*-(benzyloxy)-*N*-(pivaloyloxy)pivalamide (81):** Synthesized according to the general procedure from *N*-(benzyloxy)pivalamide (4.0 g, 19.3 mmol, 1 equiv.). The title compound was isolated as a pale yellow oil (5.25 g, 17.1 mmol, 88.6%

yield). **^{1}H NMR** (400 MHz, $CDCl_3$): δ 7.38 – 7.36 (m, 5H), 5.07 (s, 2H), 1.31 (s, 9H), 1.23 (s, 9H). **^{13}C{^{1}H} NMR** (101 MHz, $CDCl_3$): δ 182.7, 175.1, 134.8, 129.2, 128.9, 128.9, 128.7, 77.6, 40.6, 38.6, 27.1, 27.0.

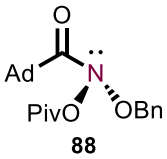

88

***N*-(benzyloxy)-*N*-(pivaloyloxy)adamantane-1-carboxamide (88):** Synthesized according to the general procedure from *N*-(benzyloxy)adamantane-1-carboxamide (1.0 g, 3.49 mmol, 1 equiv.). The title compound was isolated as a pale yellow oil (1.05 g, 2.736 mmol, 78% yield). **^{1}H NMR** (400 MHz, $CDCl_3$): δ 7.41 – 7.33 (m, 5H), 5.07 (s, 2H), 2.04 – 1.99 (m, 8H), 1.75 – 1.64 (m, 7H), 1.23 (s, 9H). **^{13}C{^{1}H} NMR** (100 MHz, $CDCl_3$): δ 182.1, 175.1, 134.6, 129.2, 128.8, 128.6, 127.7, 77.4, 43.1, 37.9, 36.5, 28.0, 26.9.

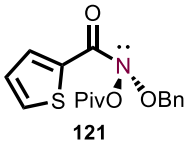

121

***N*-(benzyloxy)-*N*-(pivaloyloxy)thiophene-2-carboxamide (121):** Synthesized according to the general procedure from *N*-(benzyloxy)thiophene-2-carboxamide (100 mg, 0.429 mmol, 1 equiv.). The title compound was obtained as a pale yellow oil (120 mg, 0.36 mmol, 84% yield). **^{1}H NMR** (400 MHz, $CDCl_3$): δ 7.92 (dd, J = 3.8 Hz, 1.3 Hz, 1H), 7.65 (dd, J = 5.1 Hz, 1.3 Hz, 1H), 7.47 – 7.43 (m, 2H), 7.41 – 7.32 (m, 3H), 7.13 – 7.10 (m, 1H), 5.21 (s, 2H), 1.22 (s, 9H). **^{13}C{^{1}H} NMR** (101 MHz, $CDCl_3$): δ 175.1, 166.8, 136.0, 134.6, 134.5, 132.1, 129.5, 128. 9, 128.6, 127.6, 78.3, 26.7. **HRA-MS:** calculated 333.1035 for $C_{17}H_{19}NO_4S$, found 333.1035.

4.5.6. NMR Spectra of New Compounds.

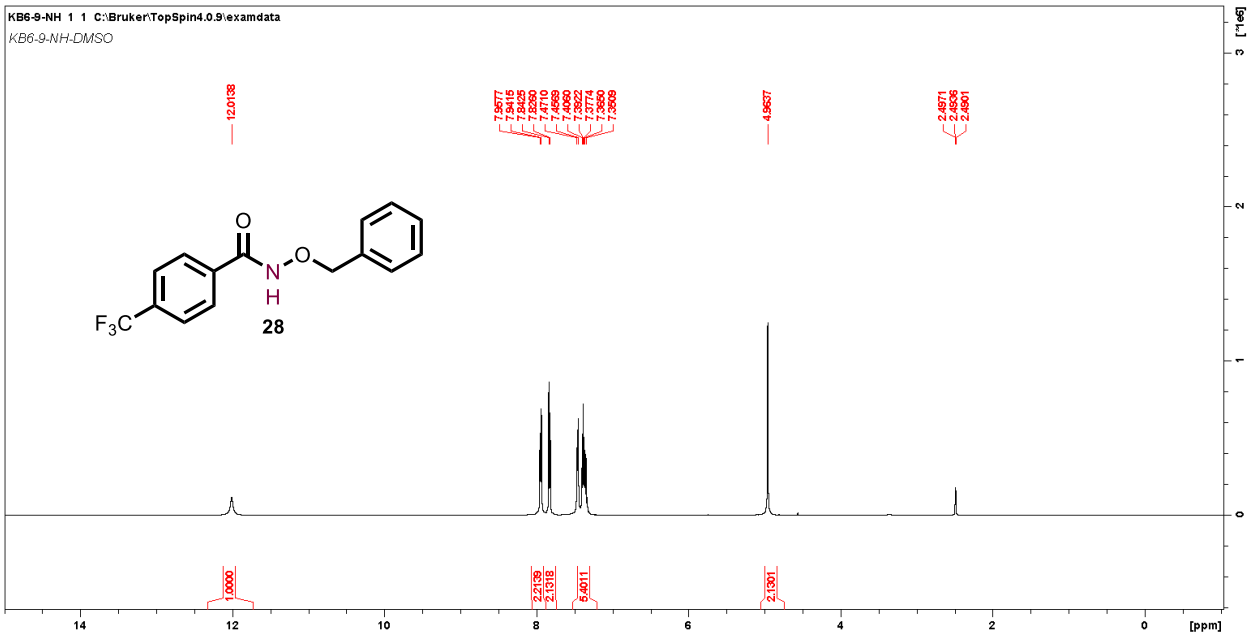

Figure 4.19. ^{1}H NMR spectrum of *N*-(benzyloxy)-4-(trifluoromethyl)benzamide (**28**) in DMSO-*d6*, 400 MHz.

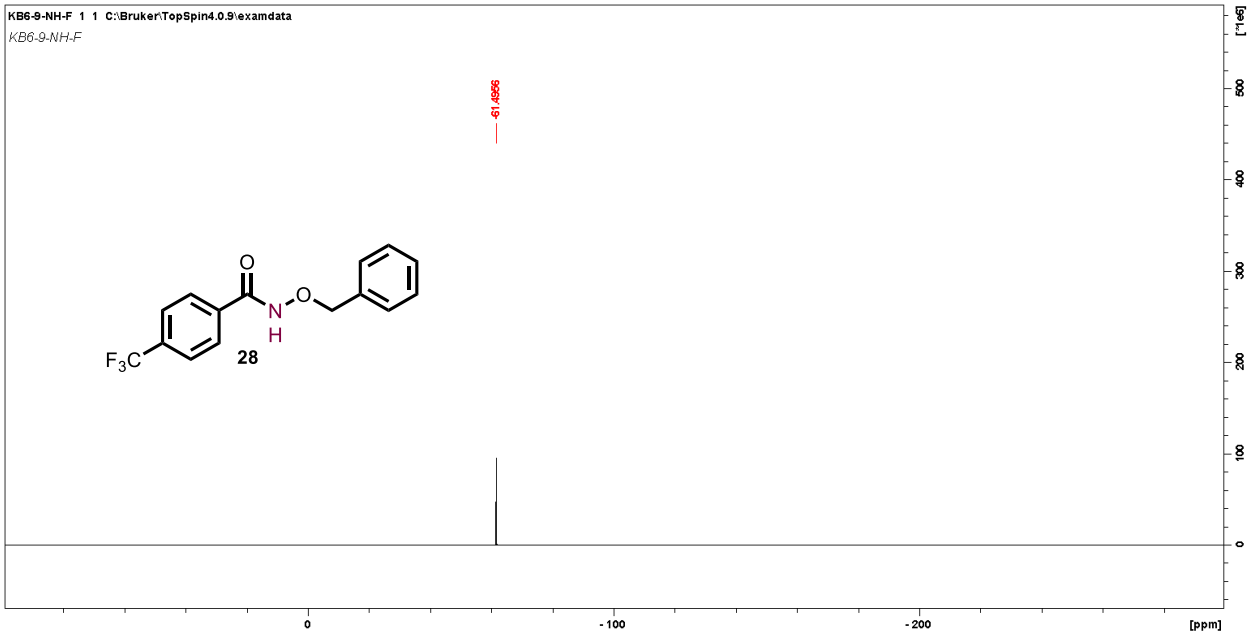

Figure 4.20. ^{19}F{^{1}H} NMR spectrum of *N*-(benzyloxy)-4-(trifluoromethyl)benzamide (**28**) in DMSO-*d6*, 376 MHz.

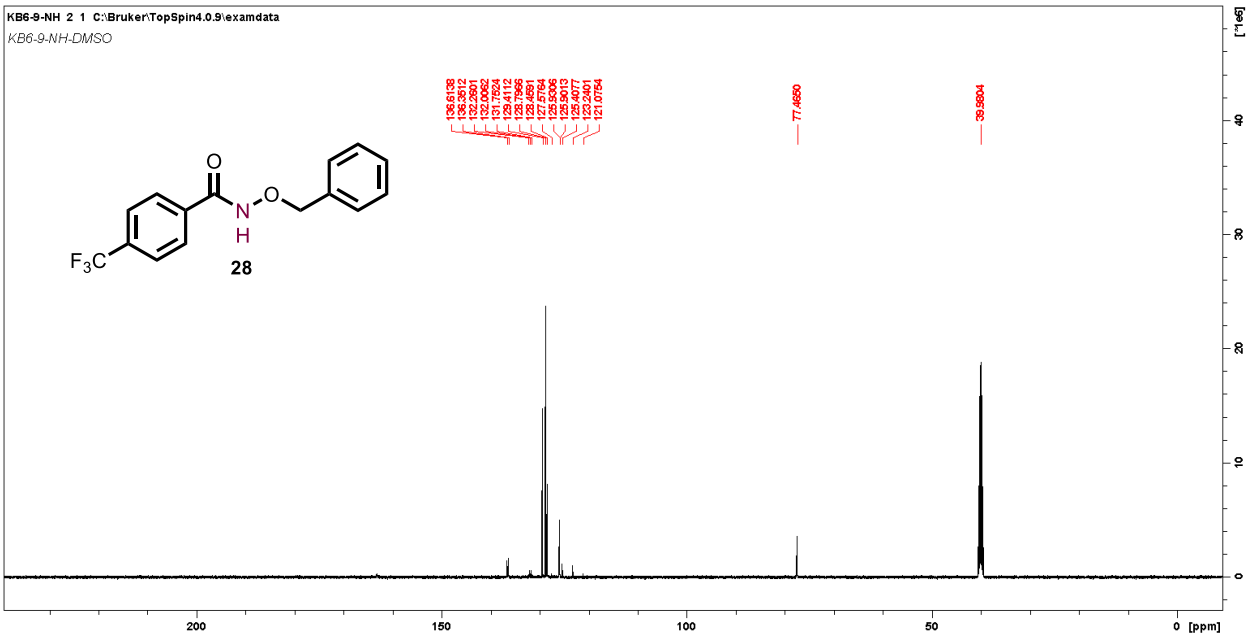

Figure 4.21. $^{13}C\{^{1}H\}$ NMR spectrum of *N*-(benzyloxy)-4-(trifluoromethyl)benzamide (**28**) in DMSO-*d6*, 101 MHz

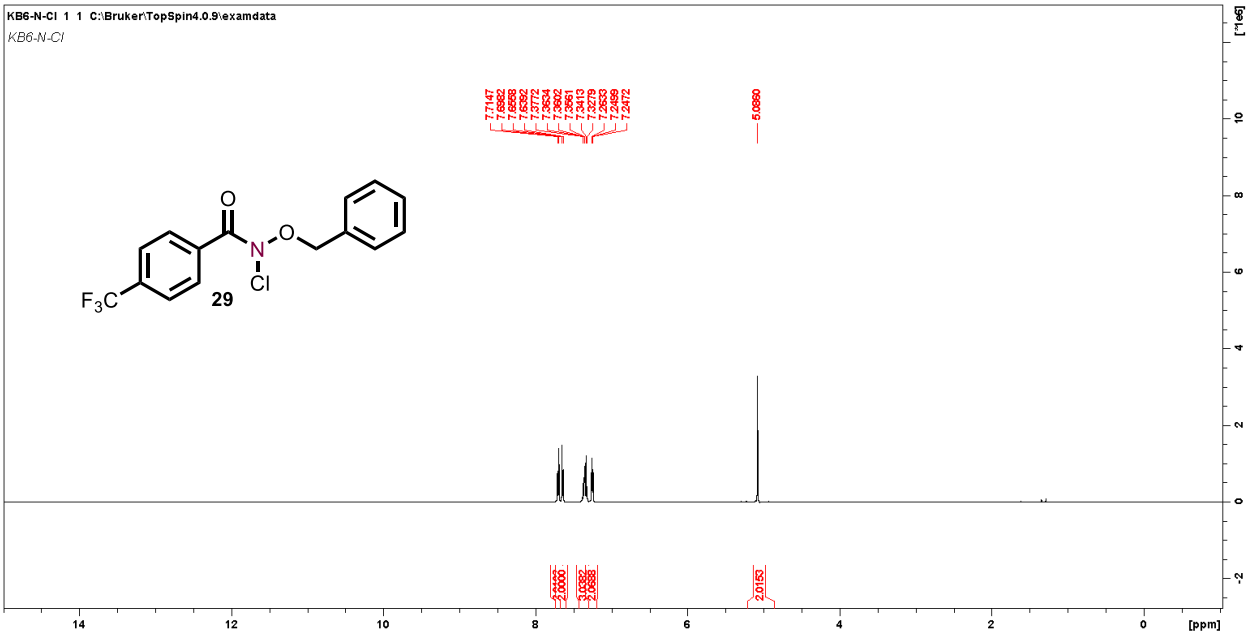

Figure 4.22. ^{1}H NMR spectrum of *N*-(benzyloxy)-*N*-(chloro)-4-(trifluoromethyl)benzamide (**29**) in $CDCl_3$, 400 MHz.

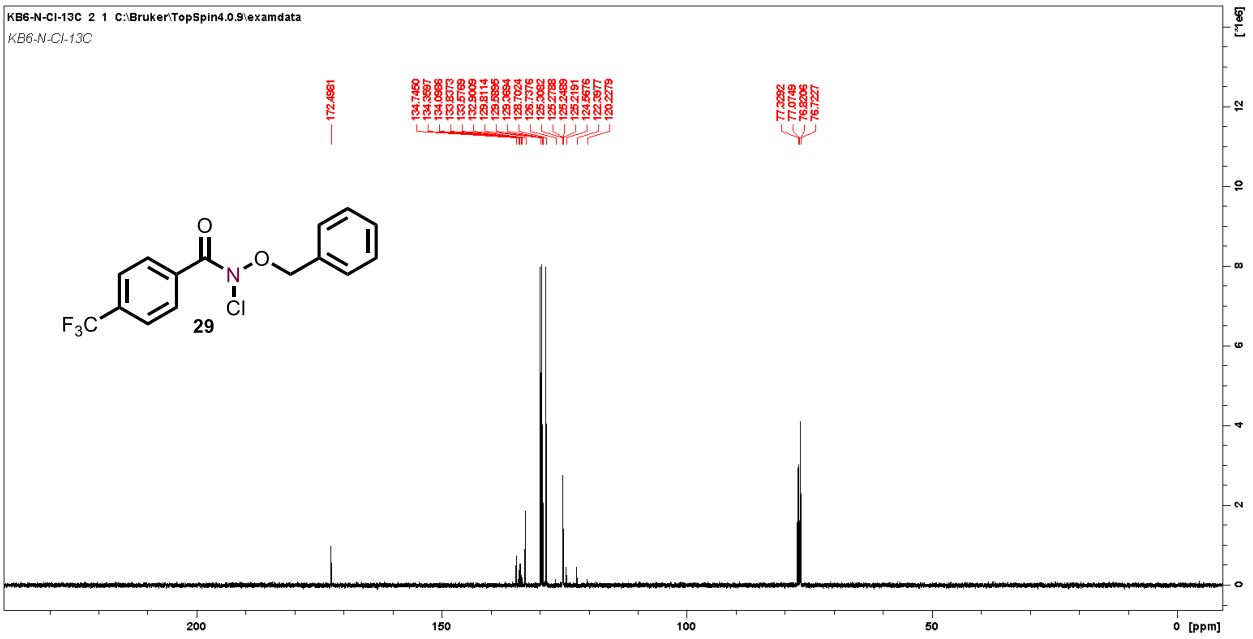

Figure 4.23. $^{13}C\{^{1}H\}$ NMR spectrum of *N*-(benzyloxy)-*N*-(chloro)-4-(trifluoromethyl)benzamide (**29**) in $CDCl_3$, 100 MHz.

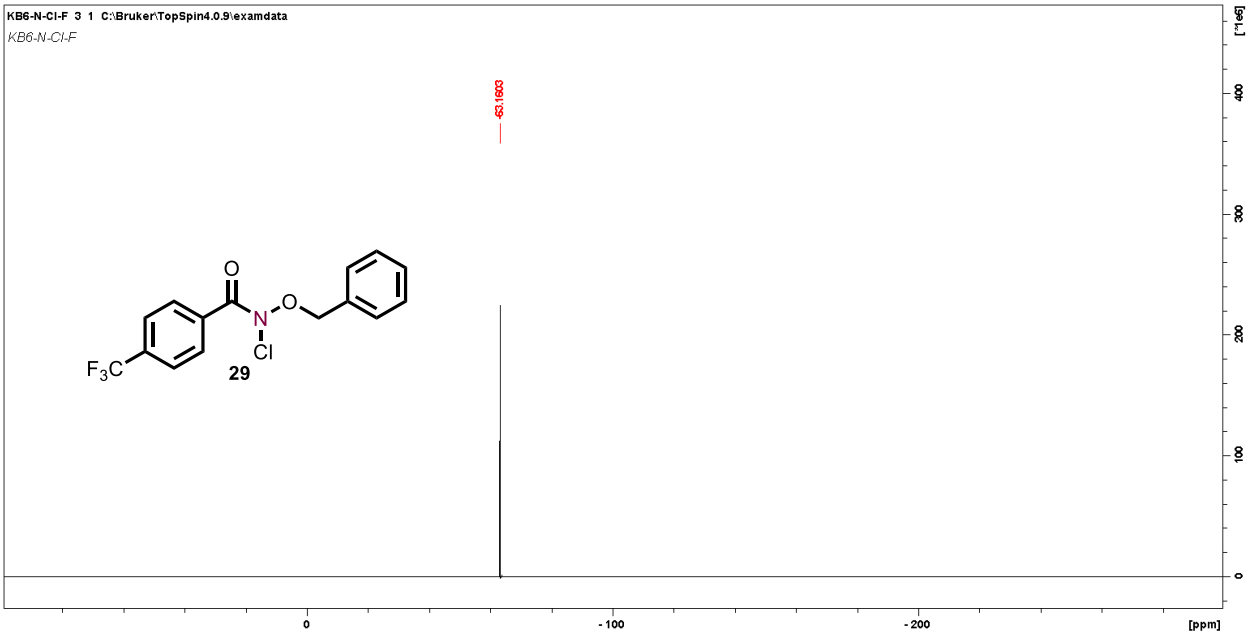

Figure 4.24. $^{19}F\{^{1}H\}$ NMR spectrum of *N*-(benzyloxy)-*N*-(chloro)-4-(trifluoromethyl)benzamide (**29**) in $CDCl_3$, 376 MHz.

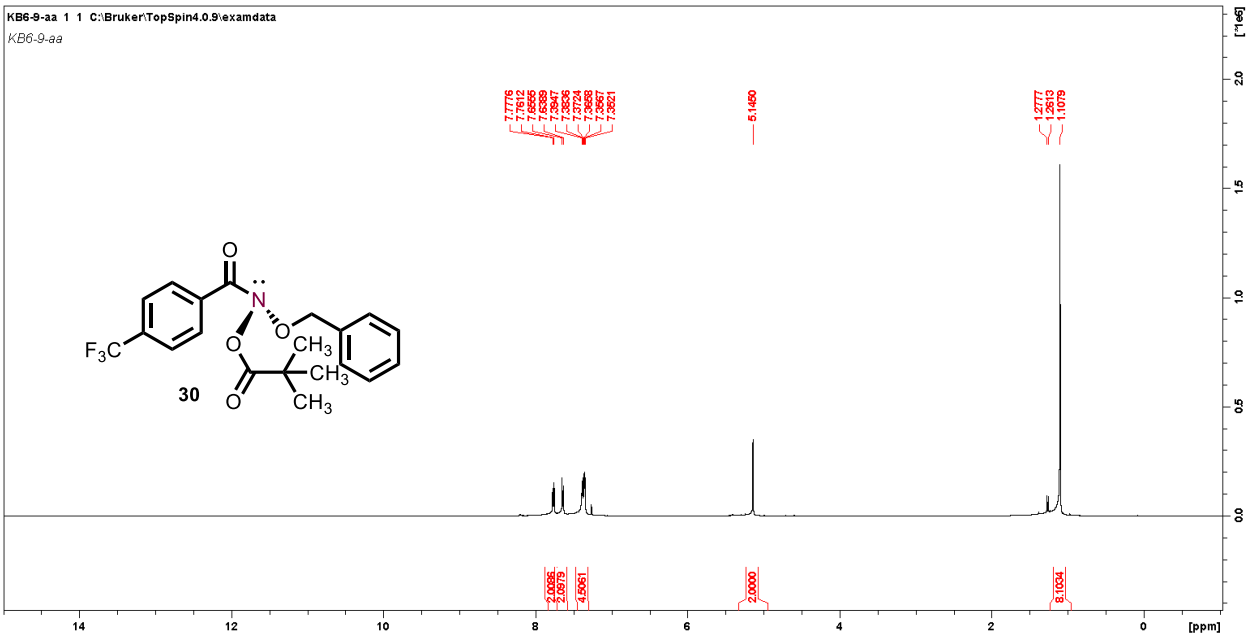

Figure 4.25. ^{1}H NMR spectrum of *N*-(benzyloxy)-*N*-(pivaloyloxy)-4-(trifluoromethyl)benzamide (**30**) in $CDCl_3$, 400 MHz.

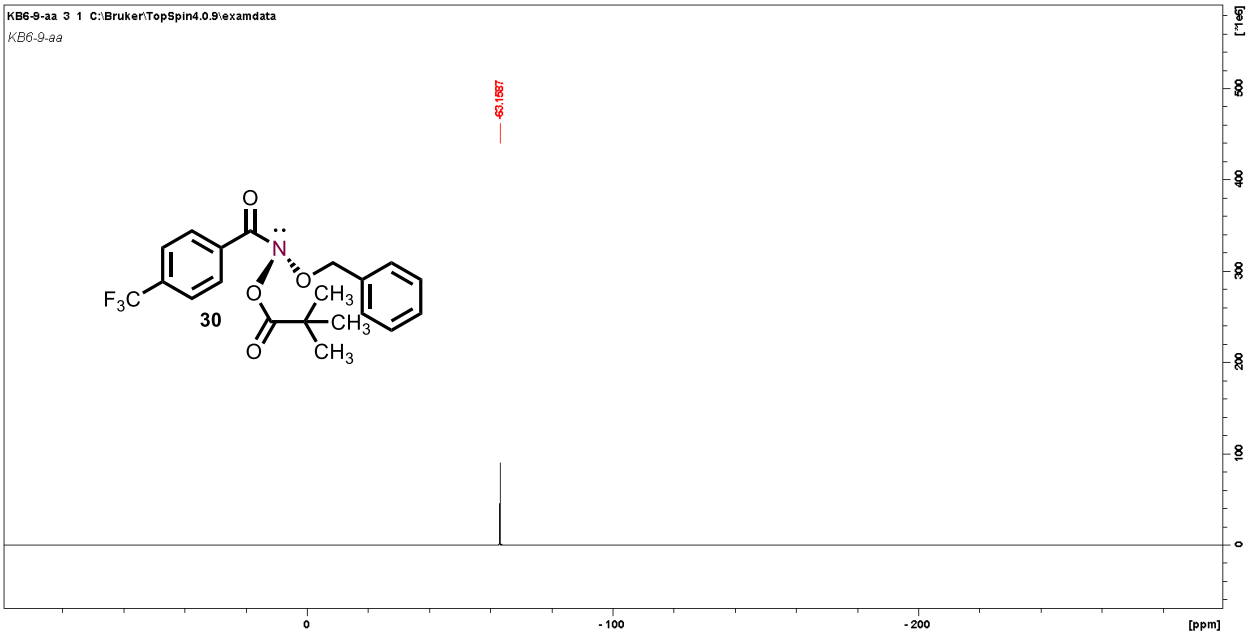

Figure 4.26. ^{19}F{^{1}H} NMR spectrum of *N*-(benzyloxy)-*N*-(pivaloyloxy)-4-(trifluoromethyl)benzamide (**30**) in $CDCl_3$, 376 MHz.

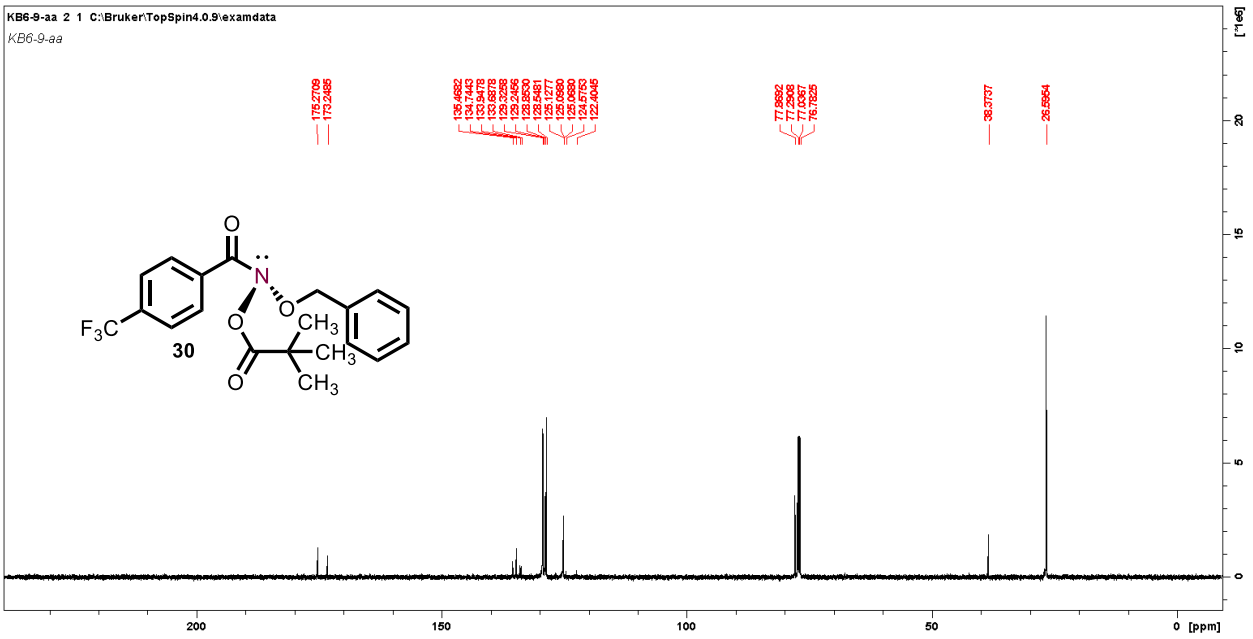

Figure 4.27. $^{13}C\{^{1}H\}$ NMR spectrum of *N*-(benzyloxy)-*N*-(pivaloyloxy)-4-(trifluoromethyl)benzamide (**30**) in $CDCl_3$, 101 MHz.

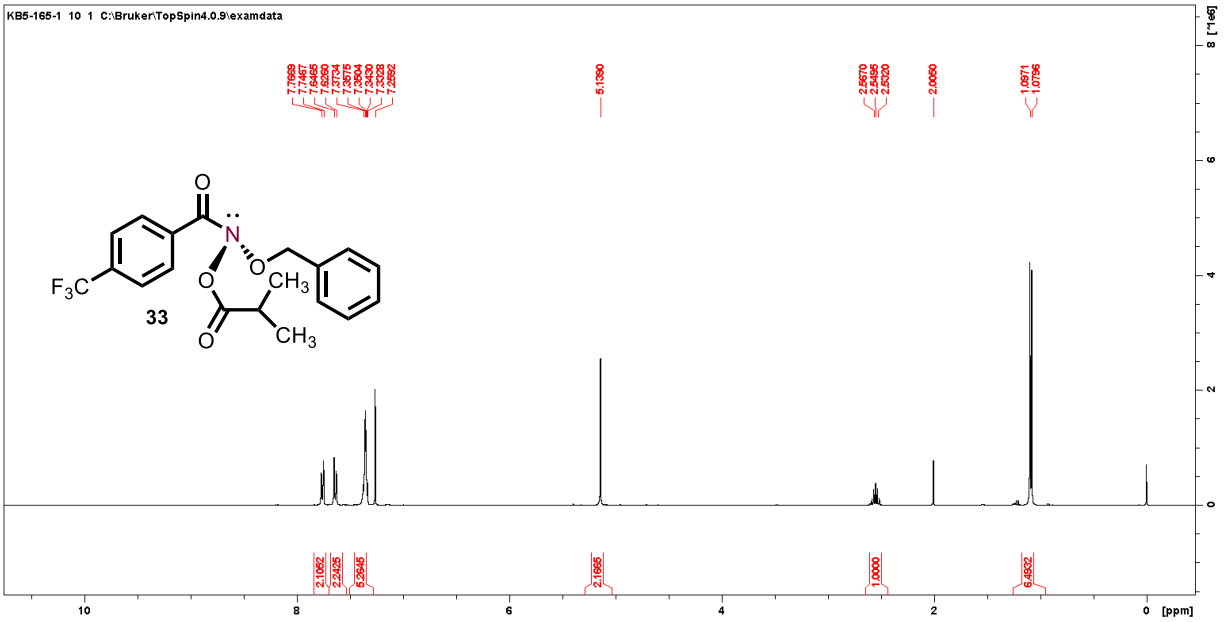

Figure 4.28. ^{1}H NMR spectrum of *N*-(benzyloxy)-*N*-(isobutyryloxy)-4-(trifluoromethyl)benzamide (**33**) in $CDCl_3$, 400 MHz.

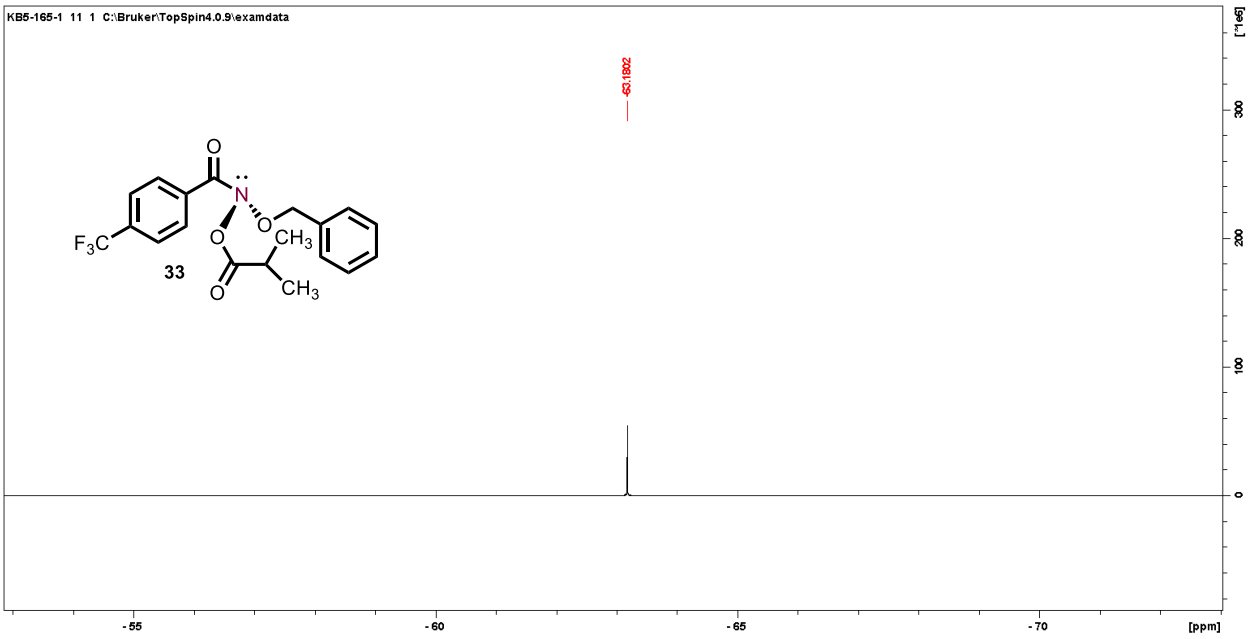

Figure 4.29. $^{19}F\{^{1}H\}$ NMR spectrum of *N*-(benzyloxy)-*N*-(isobutyryloxy)-4-(trifluoromethyl)benzamide (**33**) in $CDCl_3$, 376 MHz.

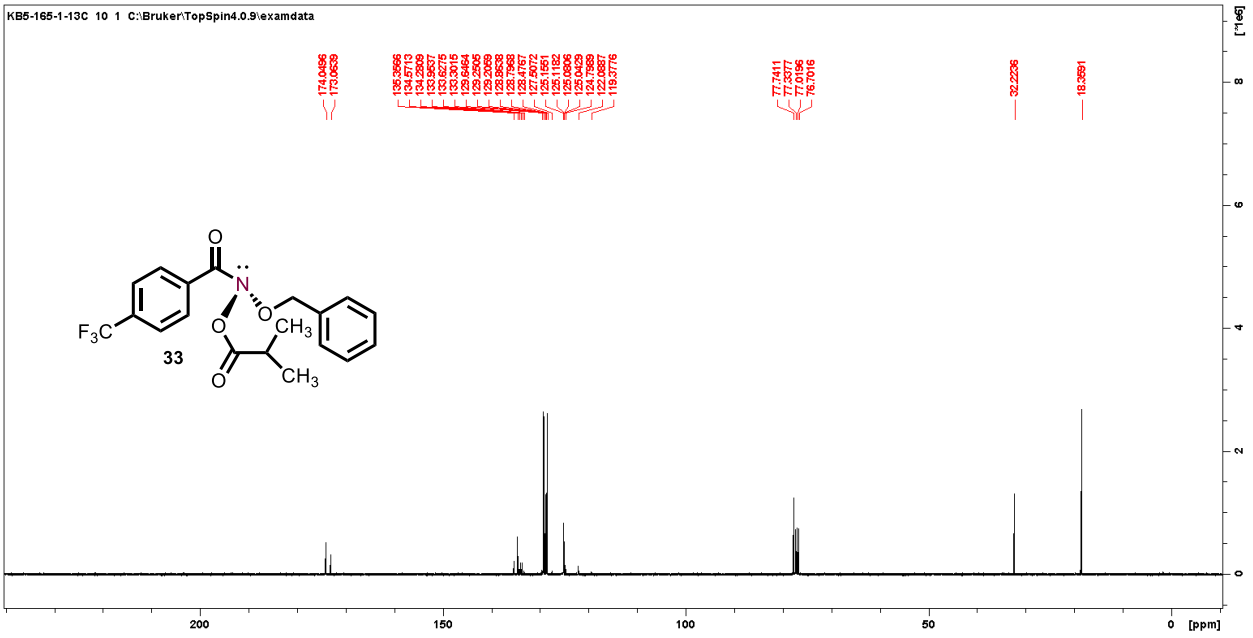

Figure 4.30. $^{13}C\{^{1}H\}$ NMR spectrum of *N*-(benzyloxy)-*N*-(isobutyryloxy)-4-(trifluoromethyl)benzamide (**33**) in $CDCl_3$, 101 MHz.

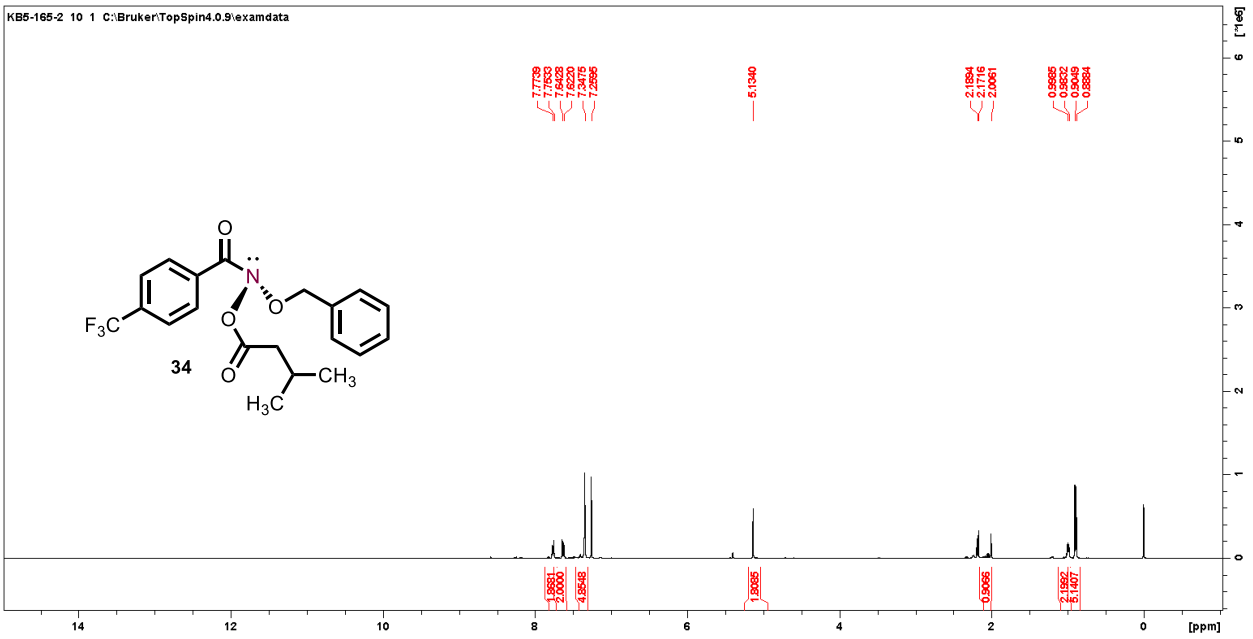

Figure 4.31. ^{1}H NMR spectrum of *N*-(benzyloxy)-*N*-((3-methylbutanoyl)oxy)-4-(trifluoromethyl)benzamide (**34**) in $CDCl_3$, 400 MHz.

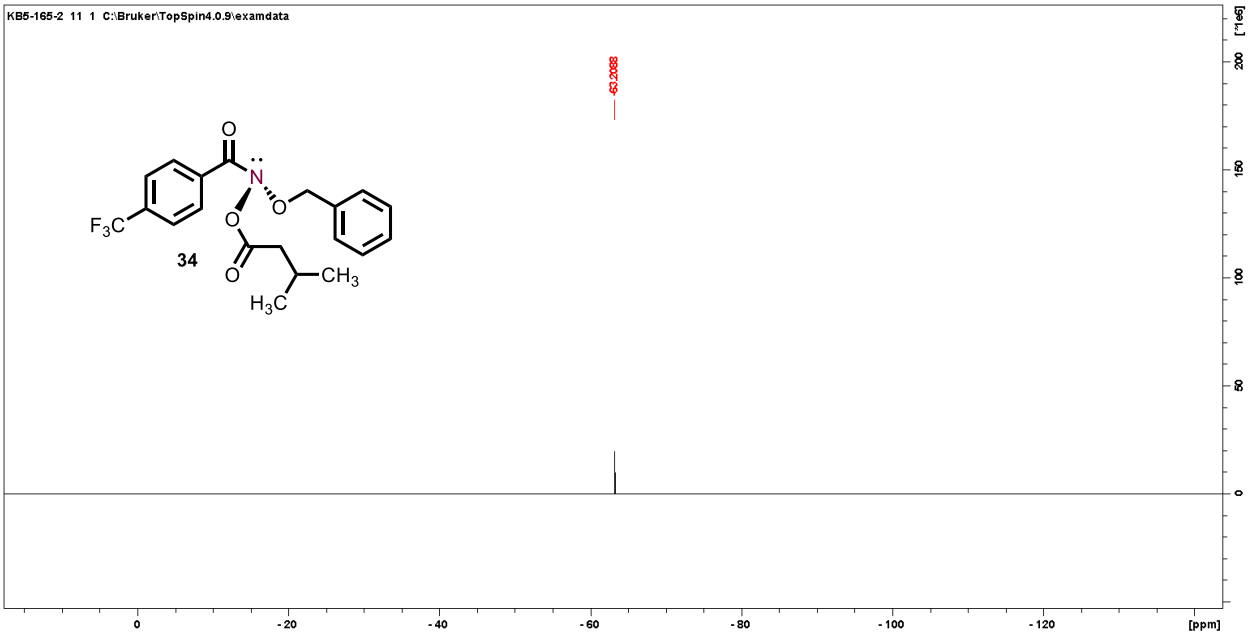

Figure 4.32. ^{19}F{^{1}H} NMR spectrum of *N*-(benzyloxy)-*N*-((3-methylbutanoyl)oxy)-4-(trifluoromethyl)benzamide (**34**) in $CDCl_3$, 376 MHz.

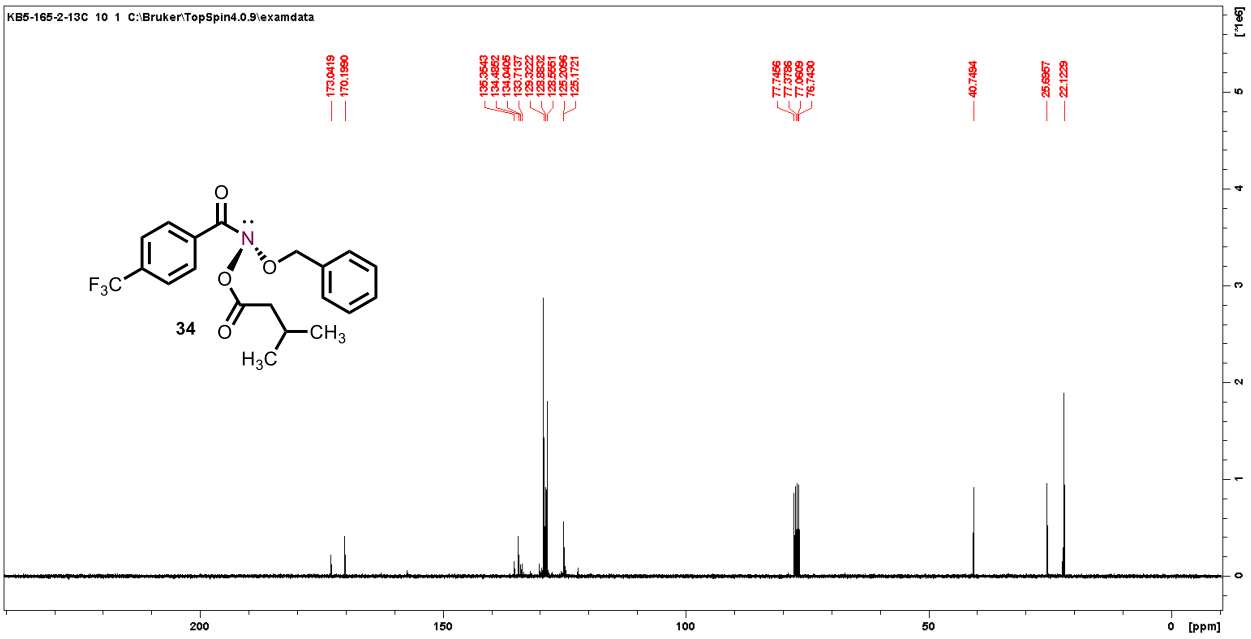

Figure 4.33. $^{13}C\{^{1}H\}$ NMR spectrum of *N*-(benzyloxy)-*N*-((3-methylbutanoyl)oxy)-4-(trifluoromethyl)benzamide (**34**) in $CDCl_3$, 101 MHz.

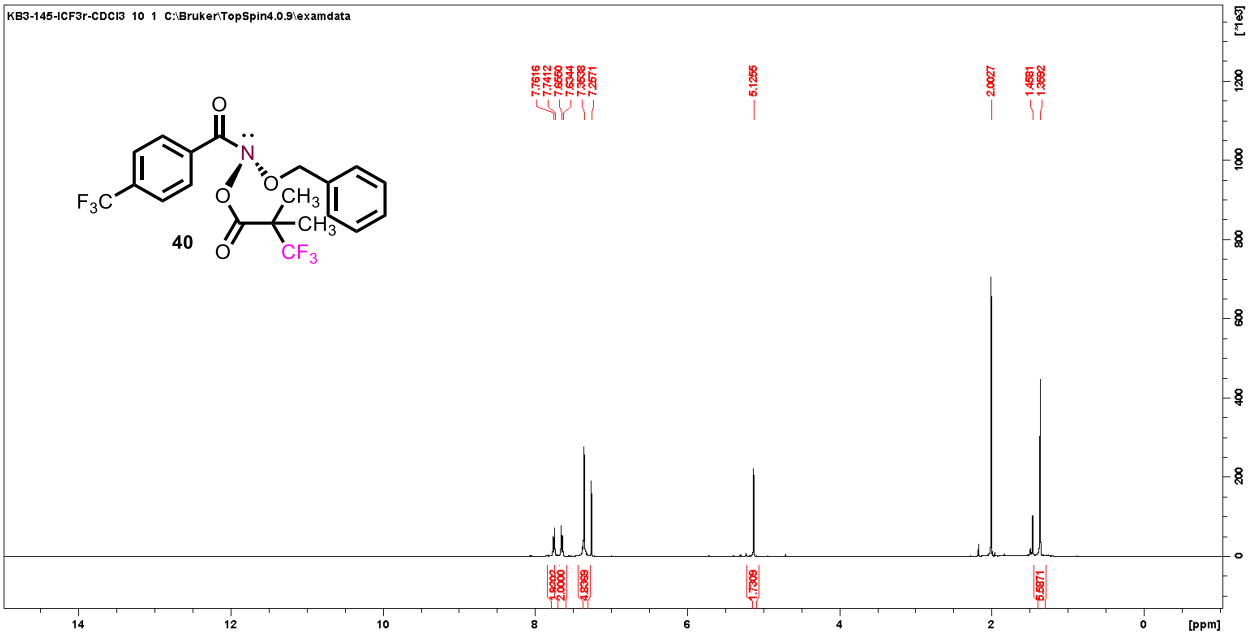

Figure 4.34. ^{1}H NMR spectrum of *N*-(benzyloxy)-*N*-((3,3,3-trifluoro-2,2-dimethylpropanoyl)oxy)-4-(trifluoromethyl)benzamide (**40**) in $CDCl_3$, 400 MHz.

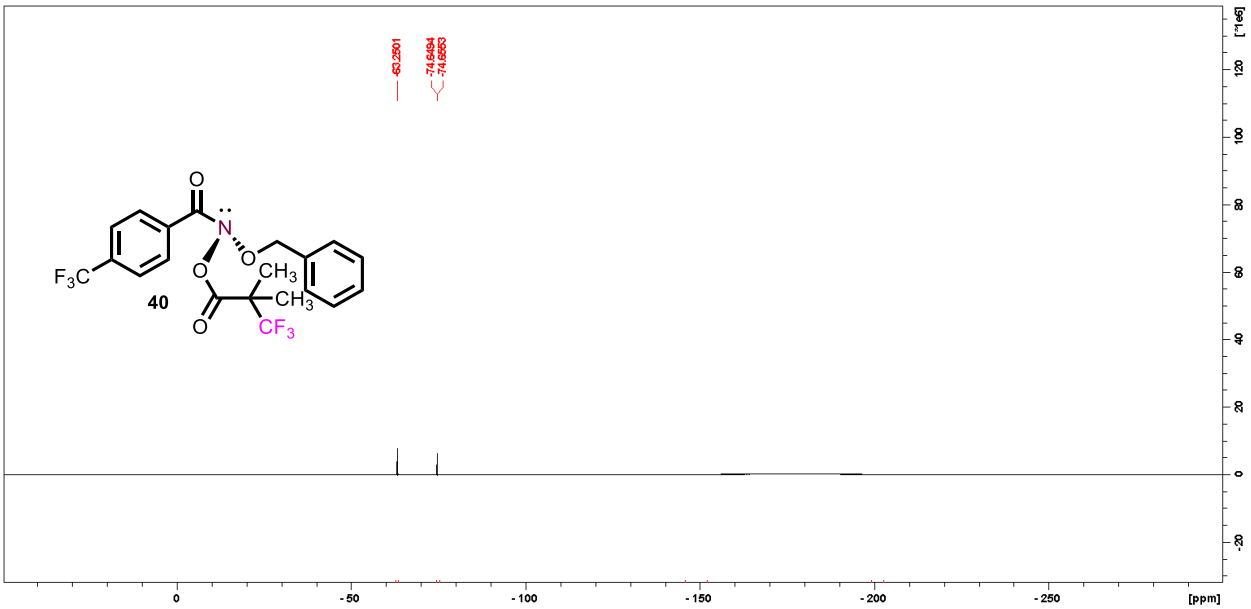

Figure 4.35. $^{19}F\{^{1}H\}$ NMR spectrum of *N*-(benzyloxy)-*N*-((3,3,3-trifluoro-2,2-dimethylpropanoyl)oxy)-4-(trifluoromethyl)benzamide (**40**) in $CDCl_3$, 376 MHz.

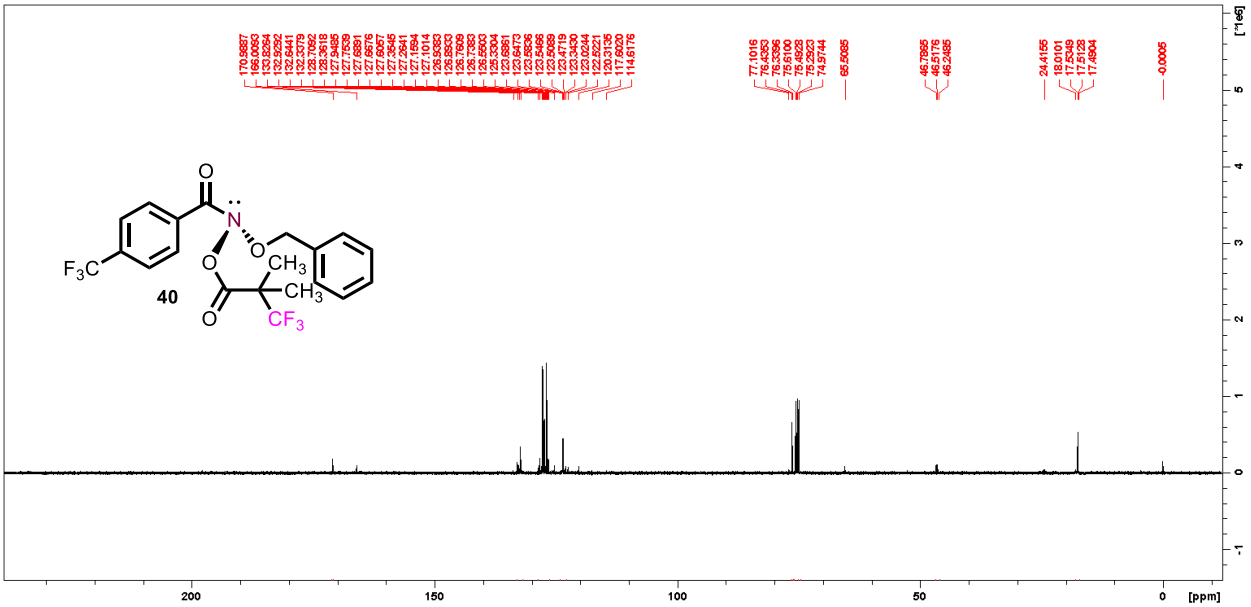

Figure 4.36. $^{13}C\{^{1}H\}$ NMR spectrum of *N*-(benzyloxy)-*N*-((3,3,3-trifluoro-2,2-dimethylpropanoyl)oxy)-4-(trifluoromethyl)benzamide (**40**) in $CDCl_3$, 101 MHz.

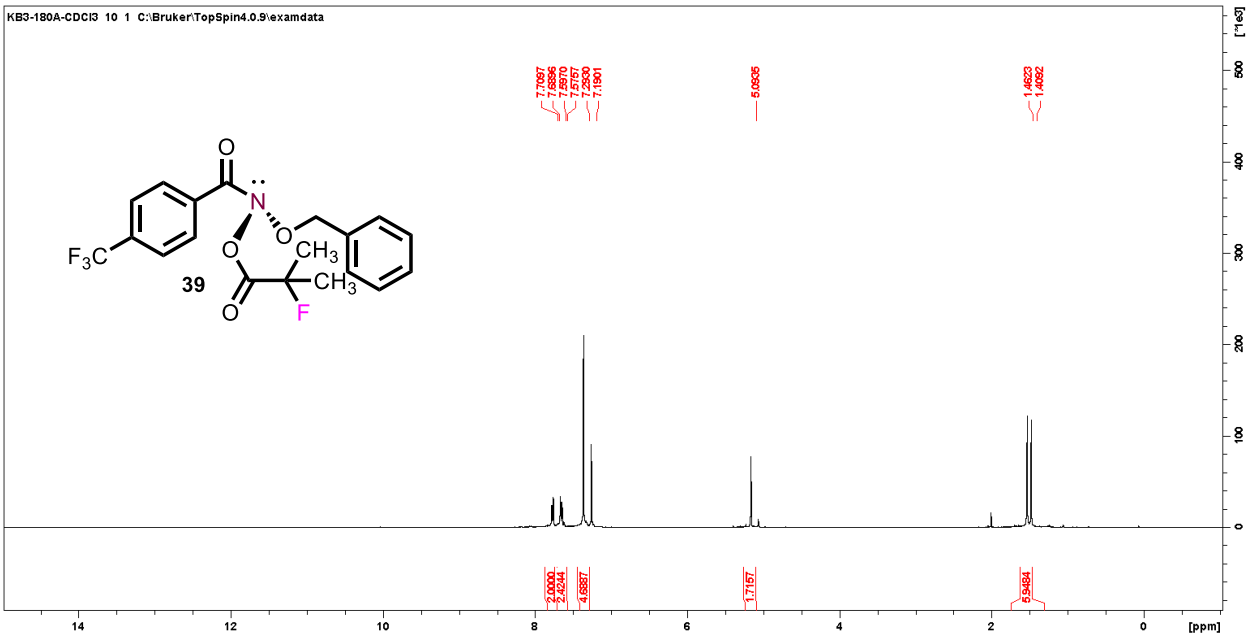

Figure 4.37. ^{1}H NMR spectrum of *N*-(benzyloxy)-*N*-((2-fluoro-2-methylpropanoyl)oxy)-4-(trifluoromethyl)benzamide (**39**) in $CDCl_3$, 400 MHz.

Figure 4.38. ^{19}F NMR spectrum of *N*-(benzyloxy)-*N*-((2-fluoro-2-methylpropanoyl)oxy)-4-(trifluoromethyl)benzamide (**39**) in $CDCl_3$, 376 MHz.

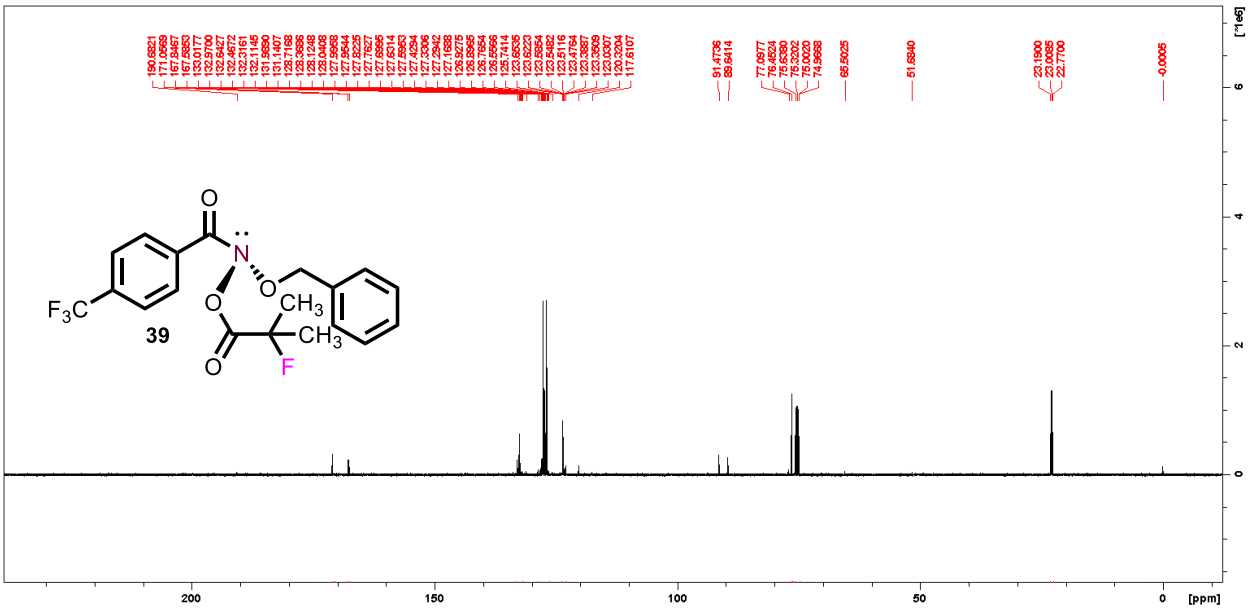

Figure 4.39. $^{13}C\{^{1}H\}$ NMR spectrum of *N*-(benzyloxy)-*N*-((2-fluoro-2-methylpropanoyl)oxy)-4-(trifluoromethyl)benzamide (**39**) in $CDCl_3$, 101 MHz.

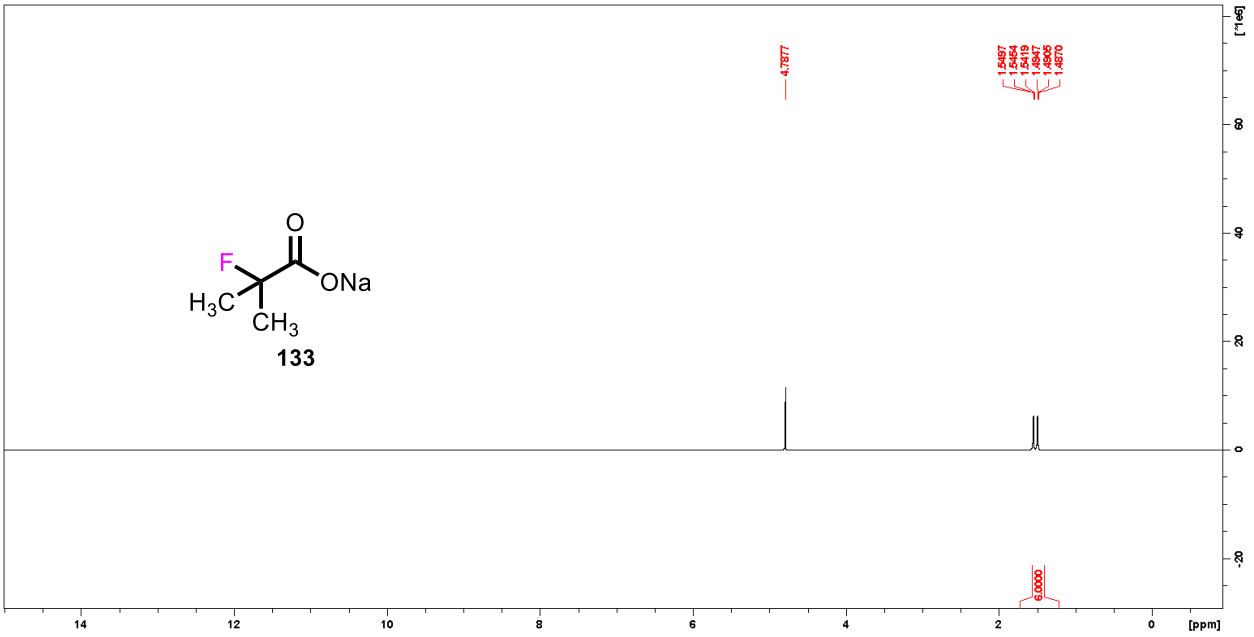

Figure 4.40. ^{1}H NMR spectrum of sodium 2-fluoro-2-methylpropanoate (**133**) in D_2O, 400 MHz.

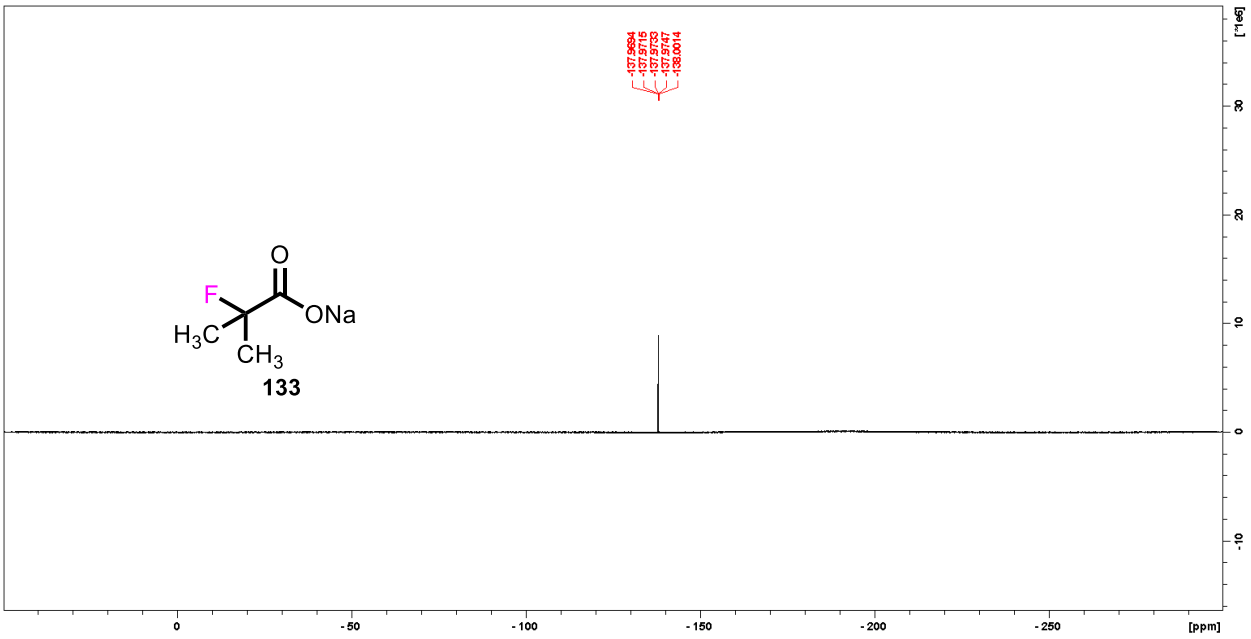

Figure 4.41. ^{19}F NMR spectrum of sodium 2-fluoro-2-methylpropanoate (**133**) in D_2O, 376 MHz.

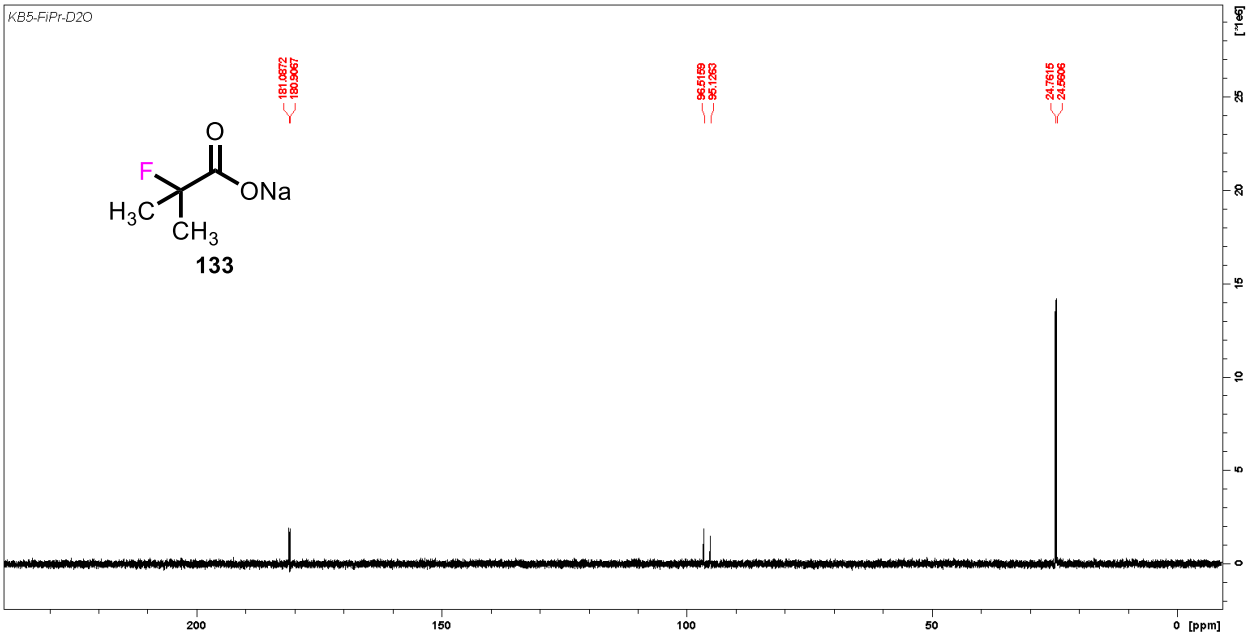

Figure 4.42. $^{13}C\{^1H\}$ NMR spectrum of sodium 2-fluoro-2-methylpropanoate (**133**) in D_2O, 101 MHz.

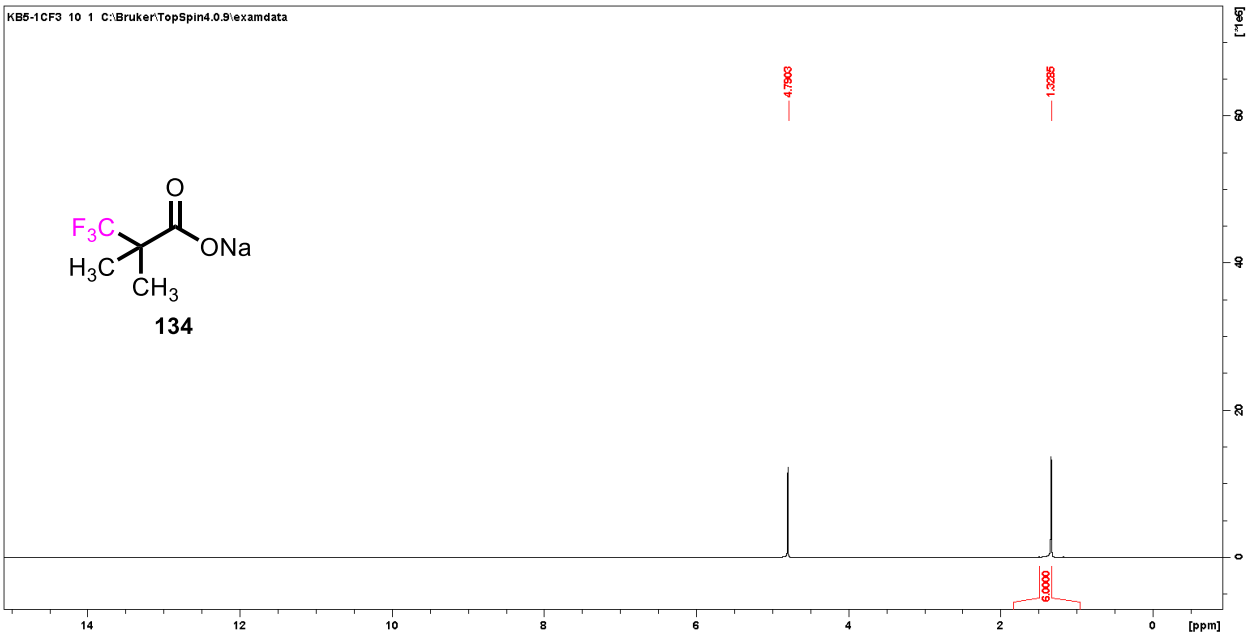

Figure 4.43. ^{1}H NMR spectrum of sodium 3,3,3-trifluoro-2,2-dimethylpropanoate (**134**) in D_2O, 400 MHz.

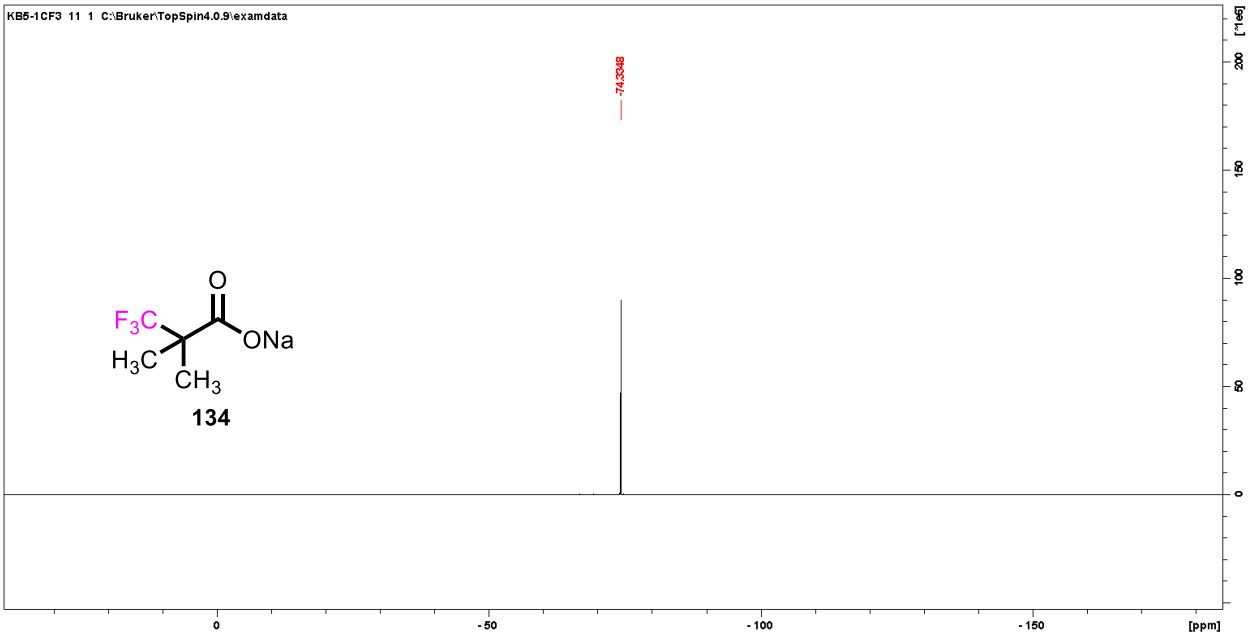

Figure 4.44. ^{19}F{^{1}H} NMR spectrum of *N*-(benzyloxy)-*N*-((2-fluoro-2-methylpropanoyl)oxy)-4-(trifluoromethyl)benzamide (**134**) in D_2O, 376 MHz.

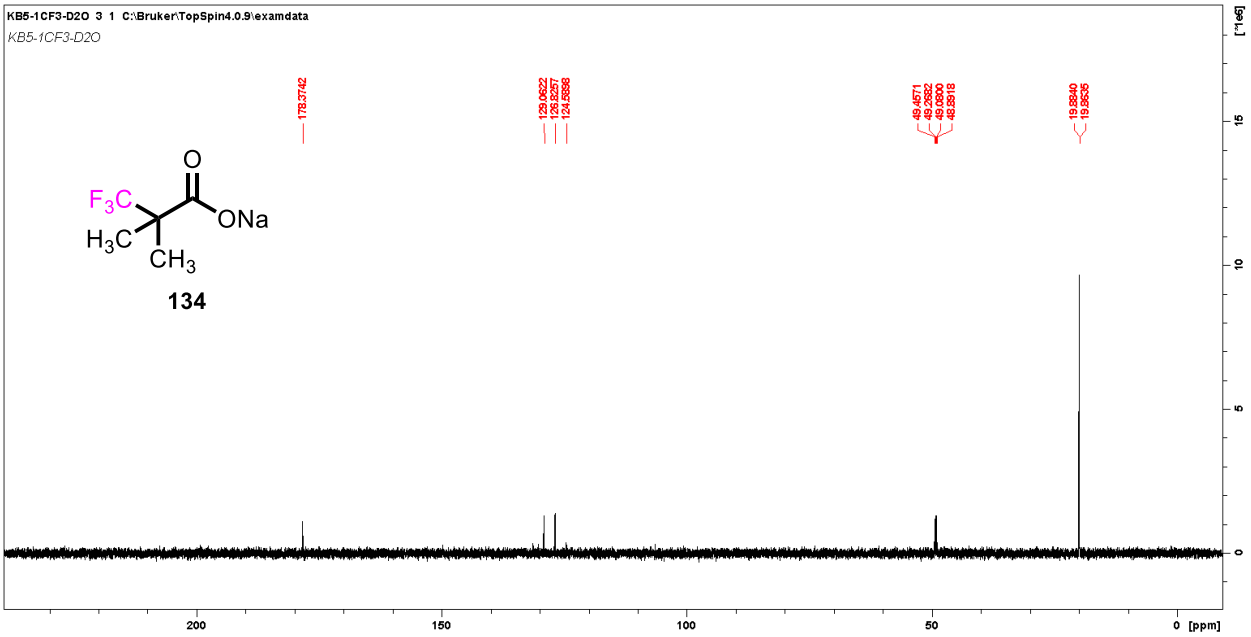

Figure 4.45. $^{13}C\{^{1}H\}$ NMR spectrum of *N*-(benzyloxy)-*N*-((2-fluoro-2-methylpropanoyl)oxy)-4-(trifluoromethyl)benzamide (**134**) in D_2O, 101 MHz.

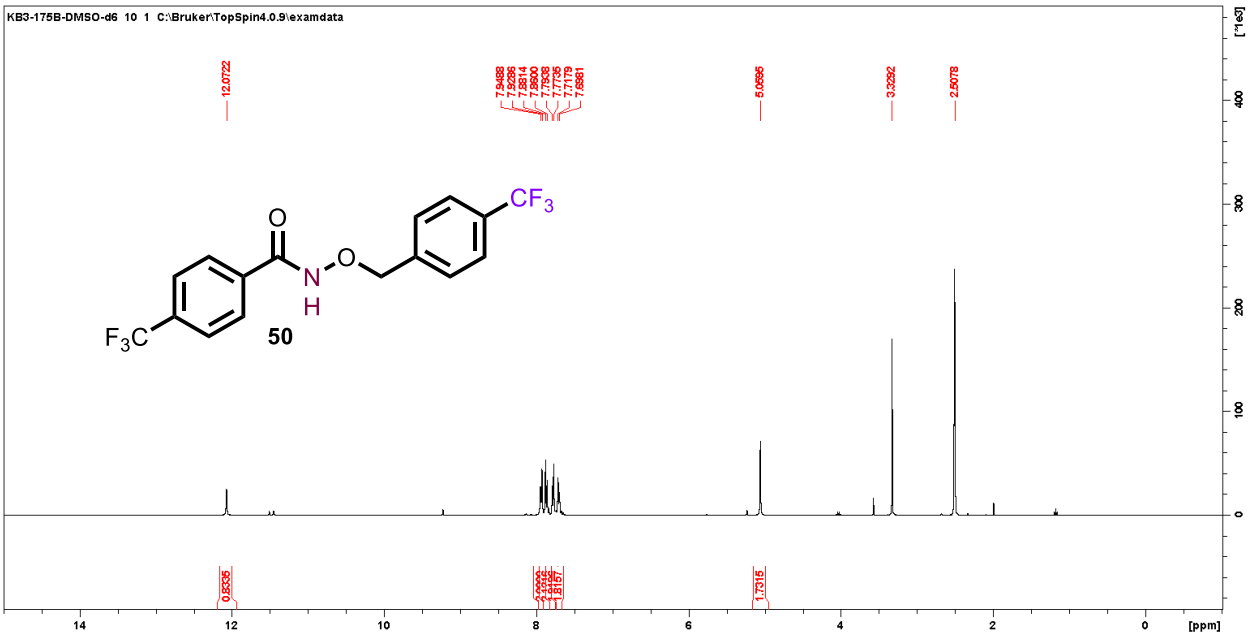

Figure 4.46. ^{1}H NMR spectrum of 4-(trifluoromethyl)-*N*-((4-(trifluoromethyl)benzyl)oxy)benzamide (**50**) in DMSO-*d6*, 400 MHz.

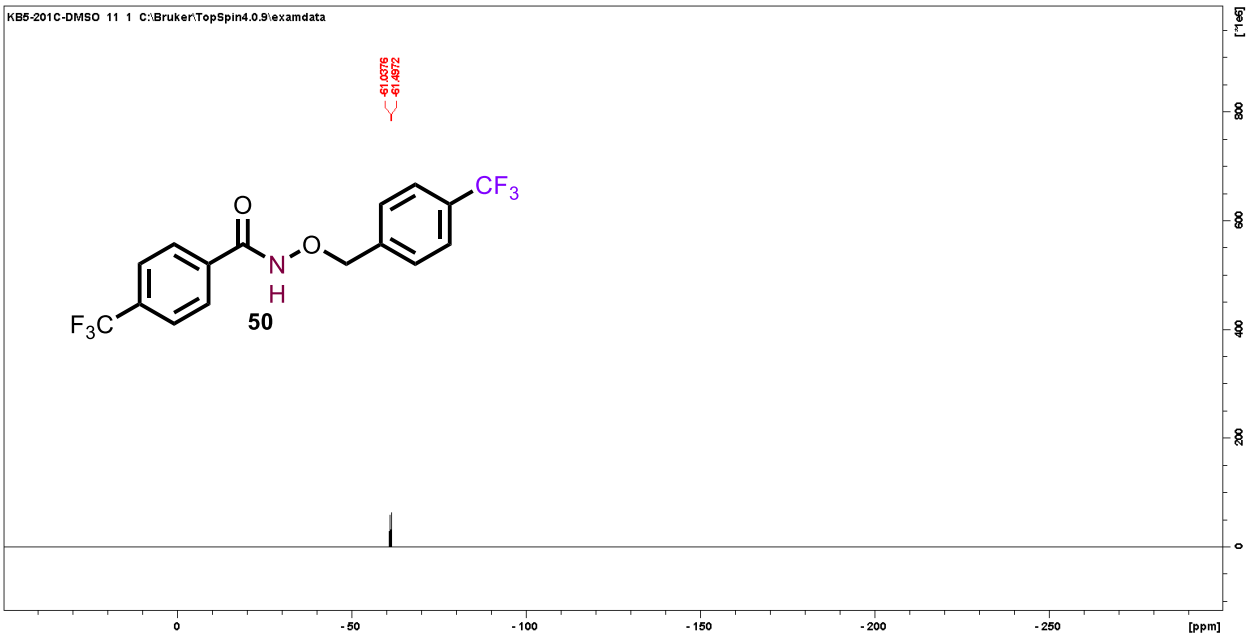

Figure 4.47. $^{19}F\{^{1}H\}$ NMR spectrum of 4-(trifluoromethyl)-*N*-((4-(trifluoromethyl)benzyl)oxy)benzamide (**50**) in DMSO-*d6*, 376 MHz.

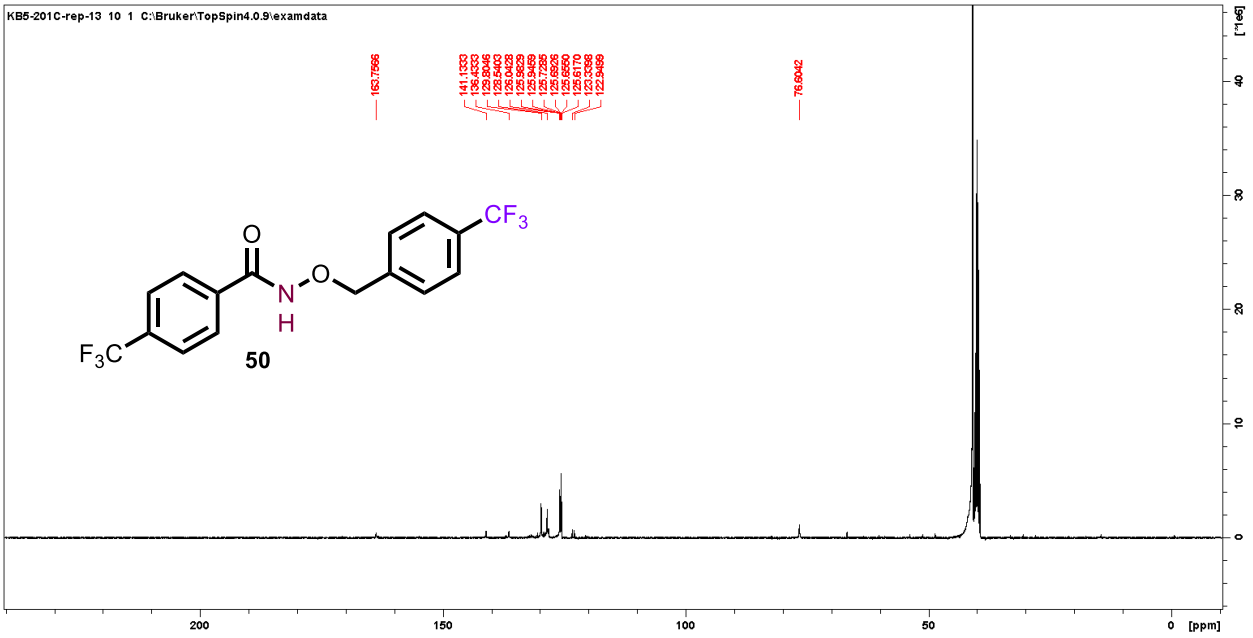

Figure 4.48. $^{13}C\{^{1}H\}$ NMR spectrum of 4-(trifluoromethyl)-*N*-((4-(trifluoromethyl)benzyl)oxy)benzamide (**50**) in DMSO-*d6*, 101 MHz.

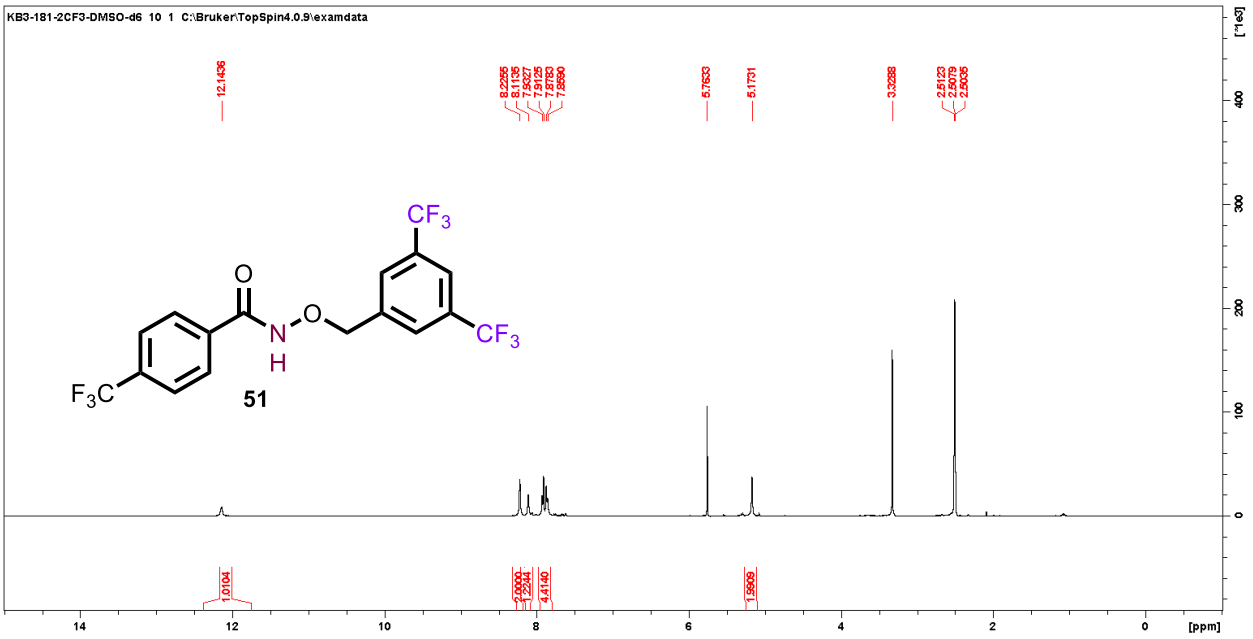

Figure 4.49. ^{1}H NMR spectrum of *N*-((3,5-bis(trifluoromethyl)benzyl)oxy)-4-(trifluoromethyl)benzamide (**51**) in DMSO-*d6*, 400 MHz.

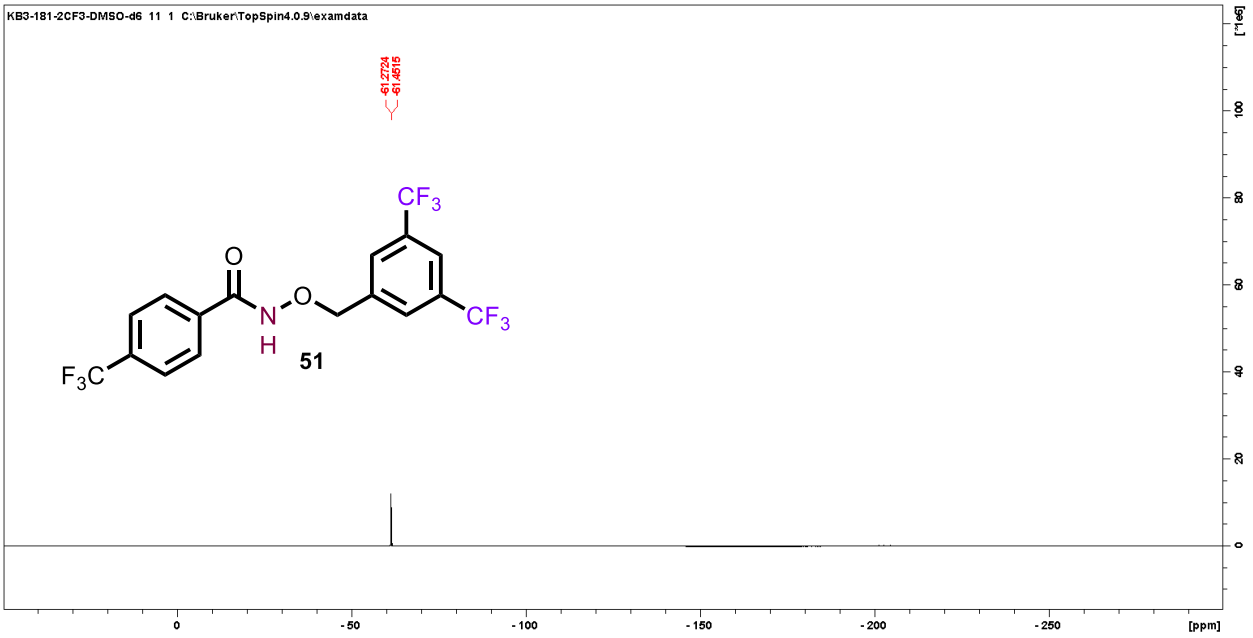

Figure 4.50. ^{19}F{^{1}H} NMR spectrum of *N*-((3,5-bis(trifluoromethyl)benzyl)oxy)-4-(trifluoromethyl)benzamide (**51**) in DMSO-*d6*, 376 MHz.

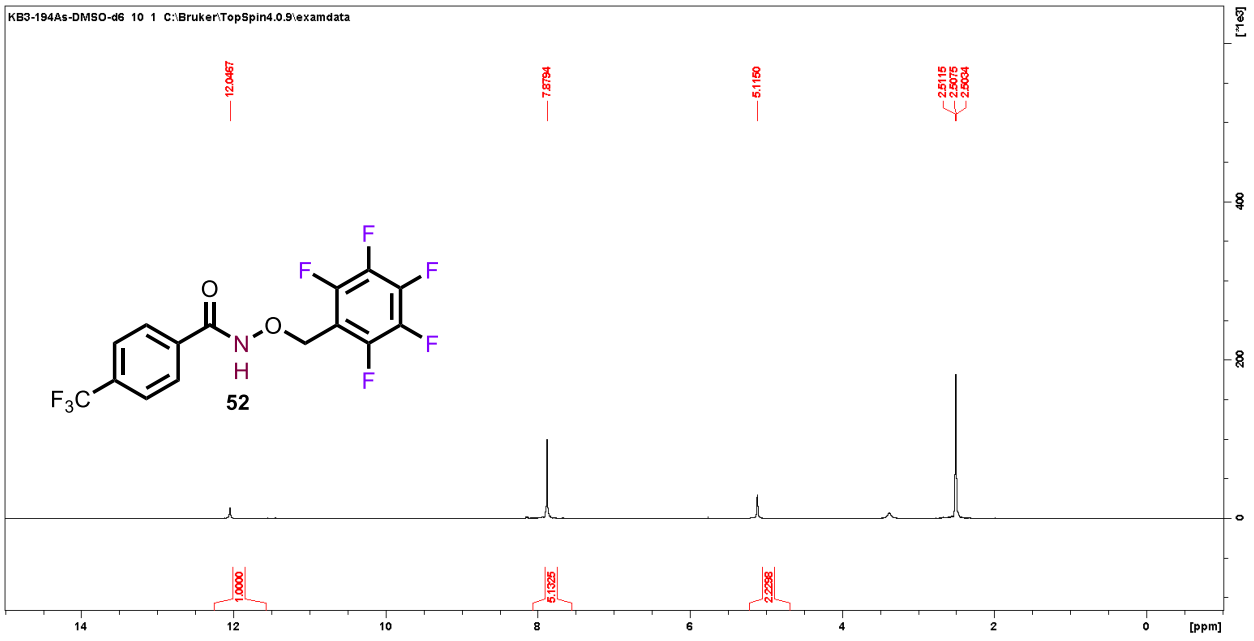

Figure 4.51. ^{1}H NMR spectrum of *N*-((perfluorophenyl)methoxy)-4-(trifluoromethyl)benzamide (**52**) in DMSO-*d6*, 400 MHz.

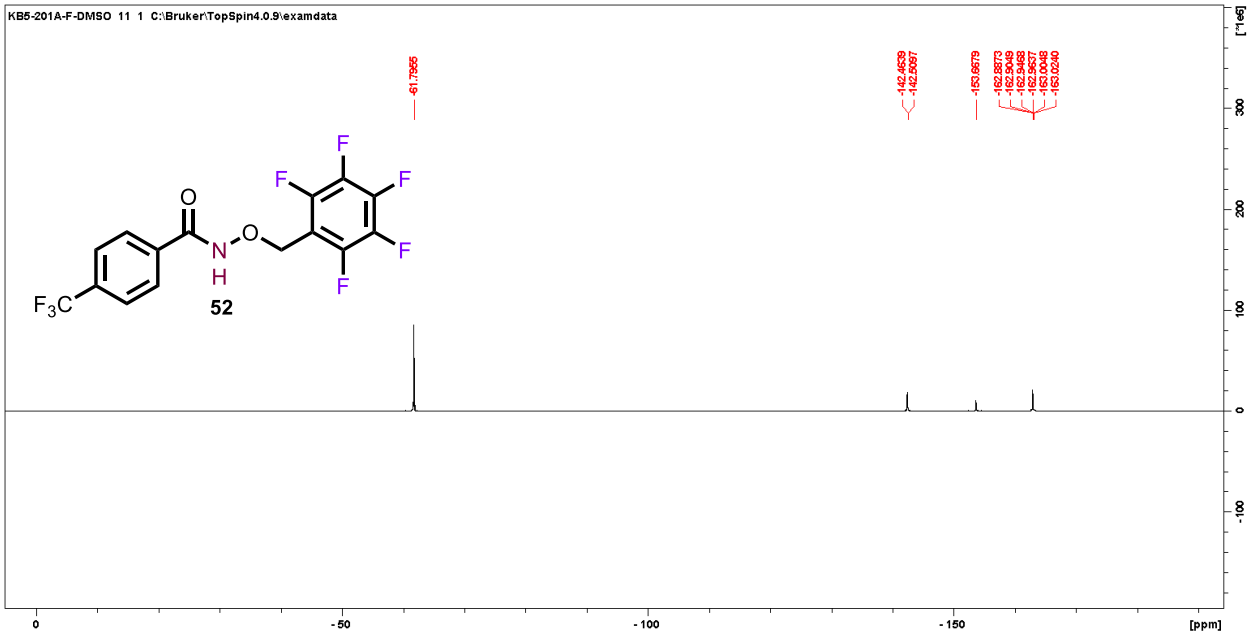

Figure 4.52. ^{19}F{^{1}H} NMR spectrum of *N*-((perfluorophenyl)methoxy)-4-(trifluoromethyl)benzamide (**52**) in DMSO-*d6*, 376 MHz.

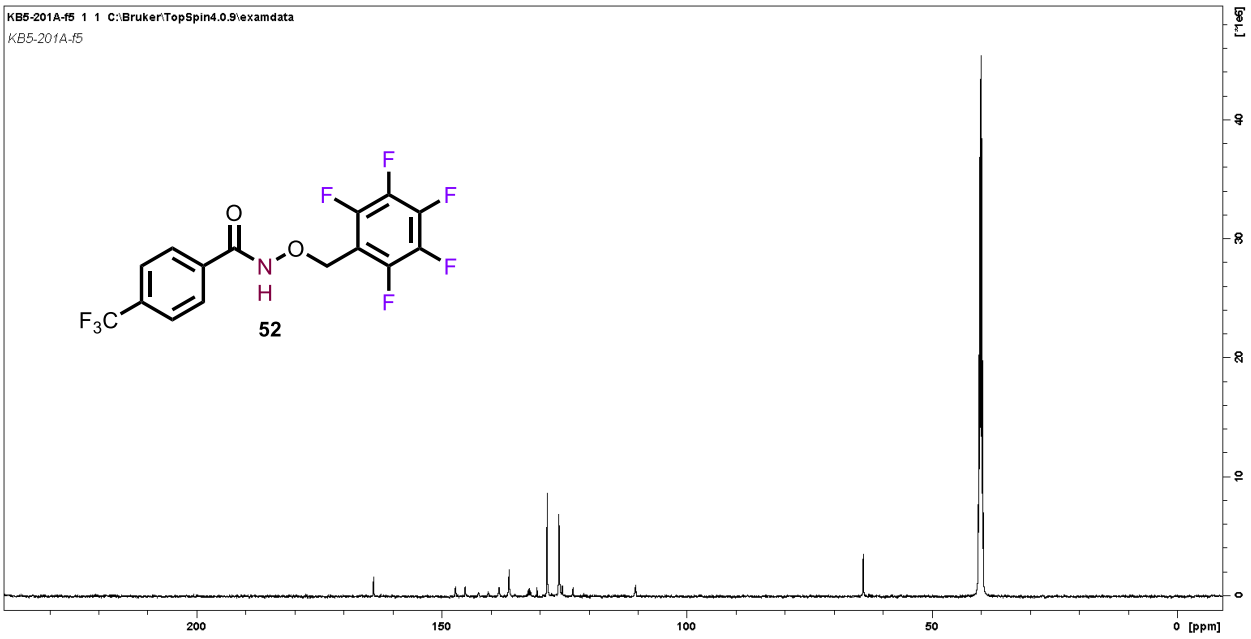

Figure 4.53. $^{13}C\{^{1}H\}$ NMR spectrum of *N*-((perfluorophenyl)methoxy)-4-(trifluoromethyl)benzamide (**52**) in DMSO-*d6*, 101 MHz.

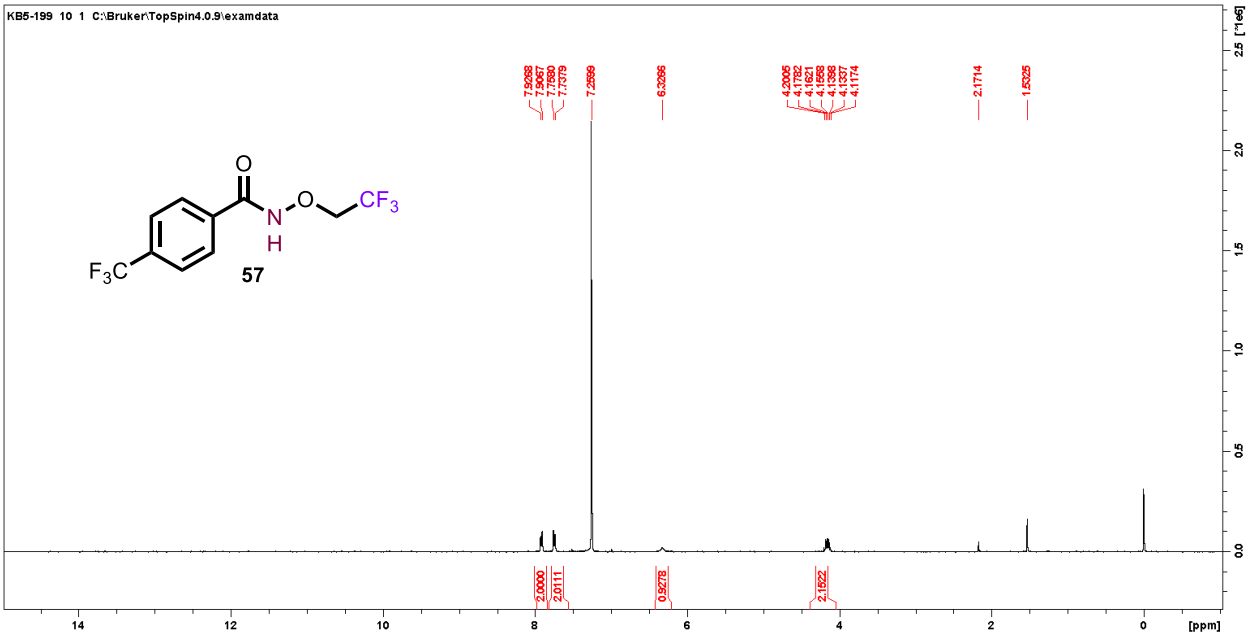

Figure 4.54. ^{1}H NMR spectrum of N-(2,2,2-trifluoroethoxy)-4-(trifluoromethyl)benzamide (**57**) in $CDCl_3$, 400 MHz.

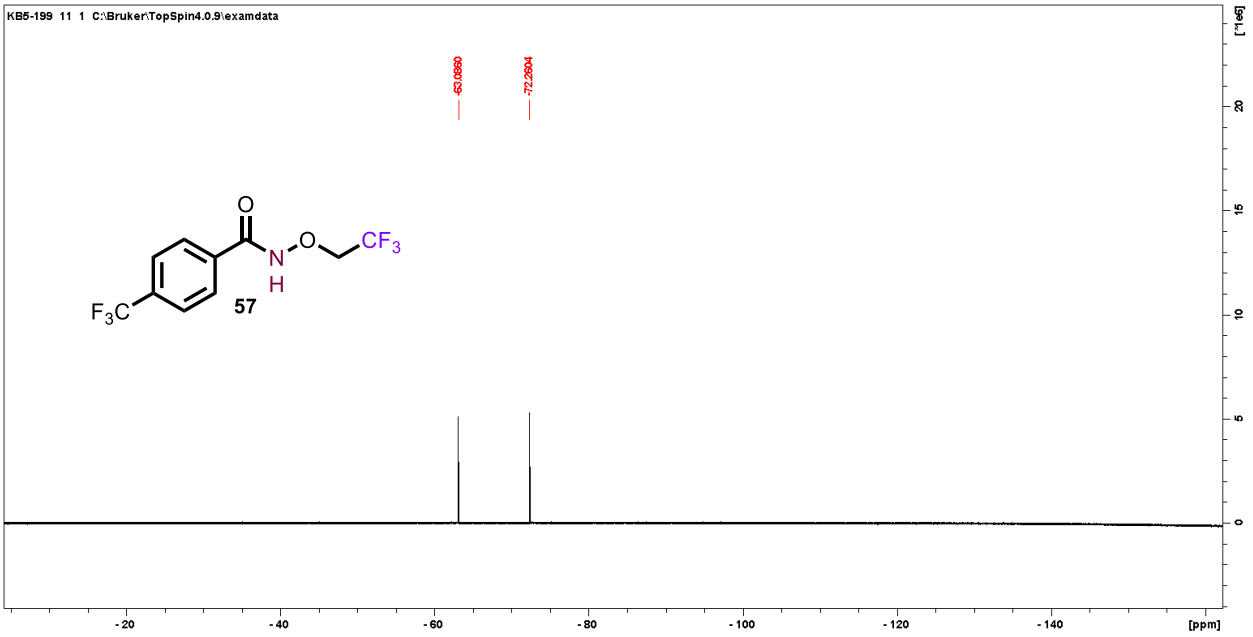

Figure 4.55. $^{19}F\{^{1}H\}$ NMR of N-(2,2,2-trifluoroethoxy)-4-(trifluoromethyl)benzamide (**57**) in $CDCl_3$, 376 MHz.

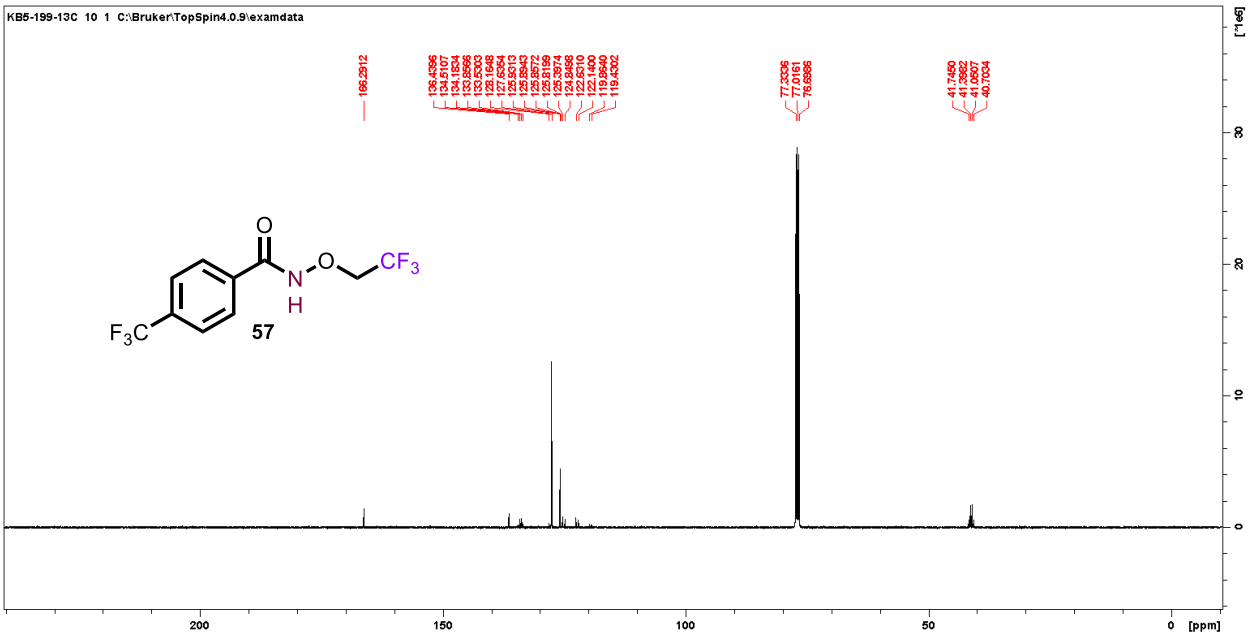

Figure 4.56. $^{13}C\{^{1}H\}$ NMR of N-(2,2,2-trifluoroethoxy)-4-(trifluoromethyl)benzamide (**57**) in $CDCl_3$, 101 MHz.

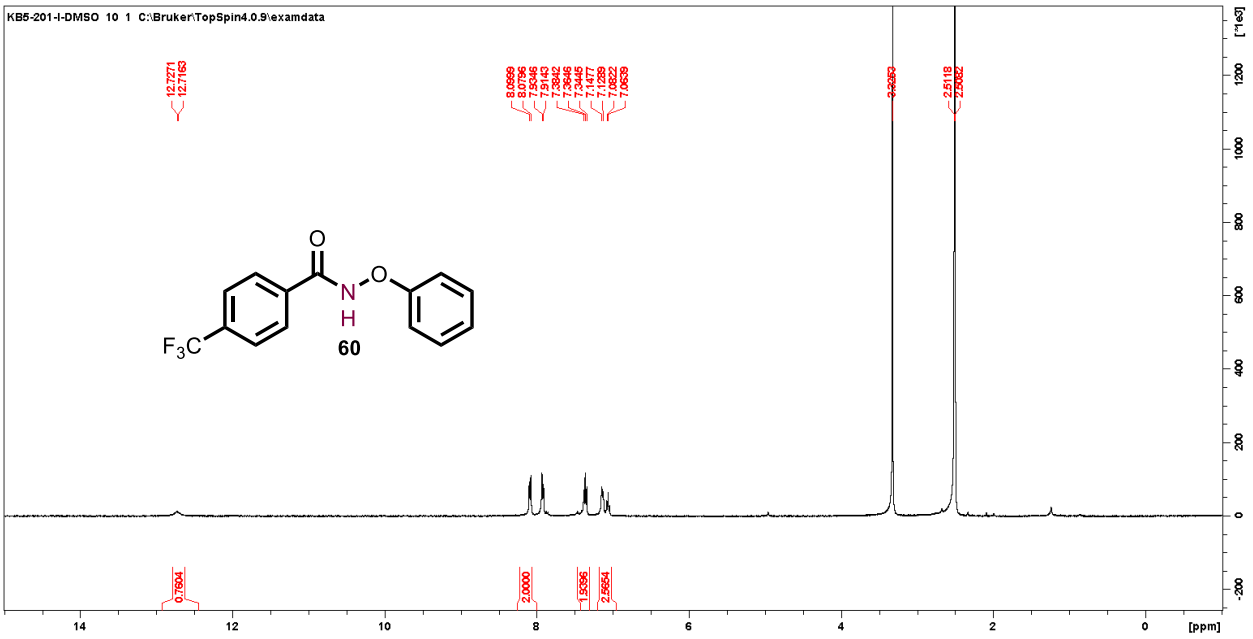

Figure 4.57. ^{1}H NMR of N-phenoxy-4-(trifluoromethyl)benzamide (**60**) in DMSO-*d6*, 400 MHz.

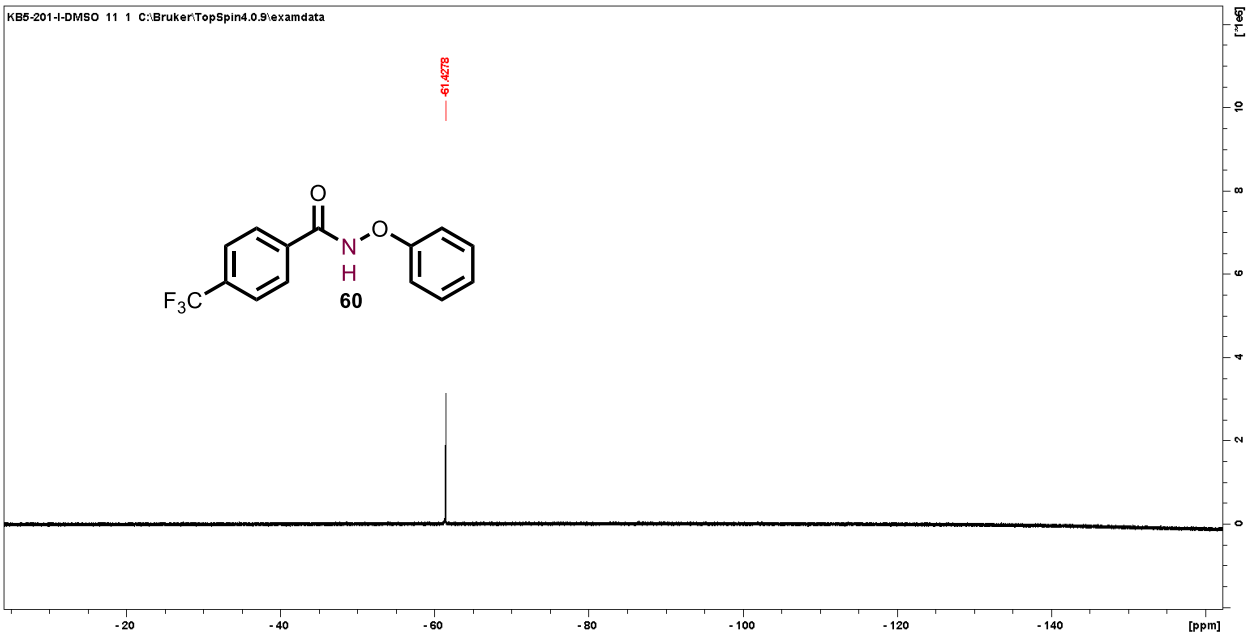

Figure 4.58. ^{19}F{^{1}H} NMR of N-phenoxy-4-(trifluoromethyl)benzamide (**60**) in DMSO-*d6*, 376 MHz.

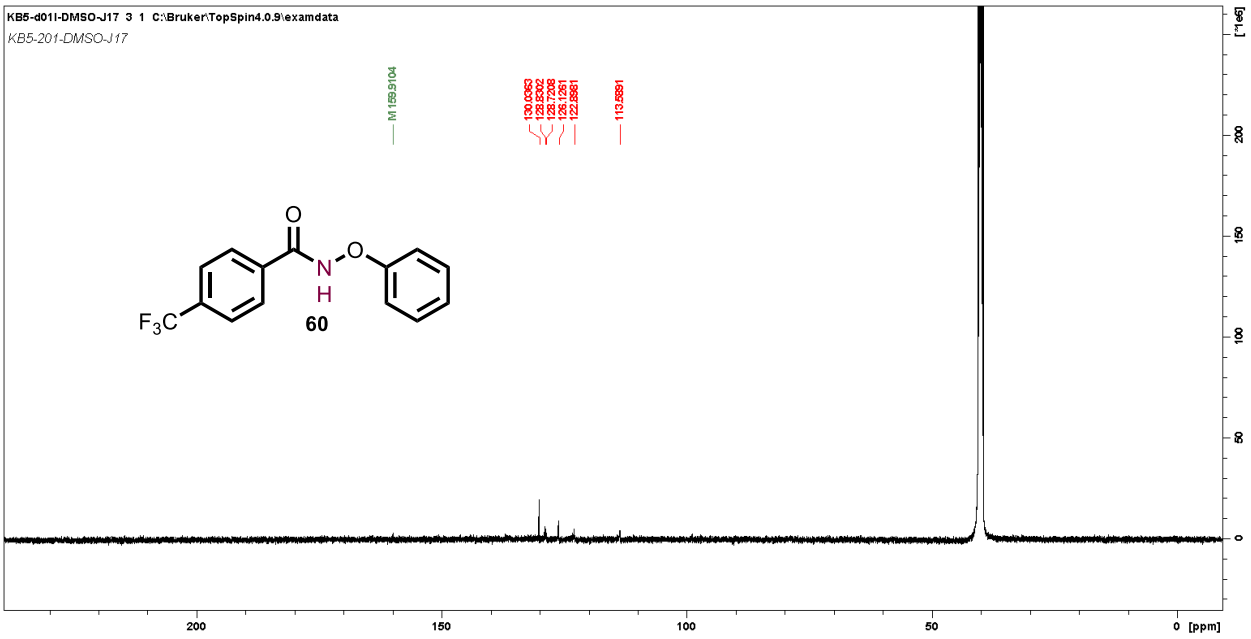

Figure 4.59. $^{13}C\{^{1}H\}$ NMR spectrum of N-phenoxy-4-(trifluoromethyl)benzamide (**60**) in DMSO-*d6*, 101 MHz.

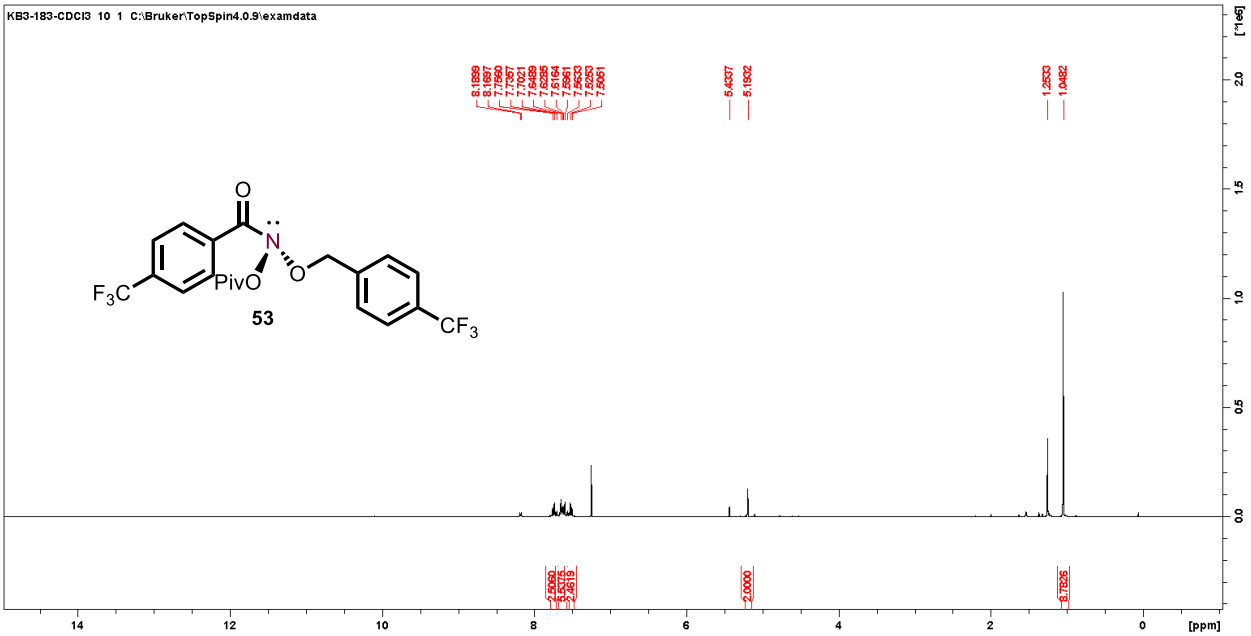

Figure 4.60. ^{1}H NMR spectrum of *N*-(pivaloyloxy)-4-(trifluoromethyl)-*N*-((4-(trifluoromethyl)benzyl)oxy)benzamide (**53**) in $CDCl_3$, 400 MHz.

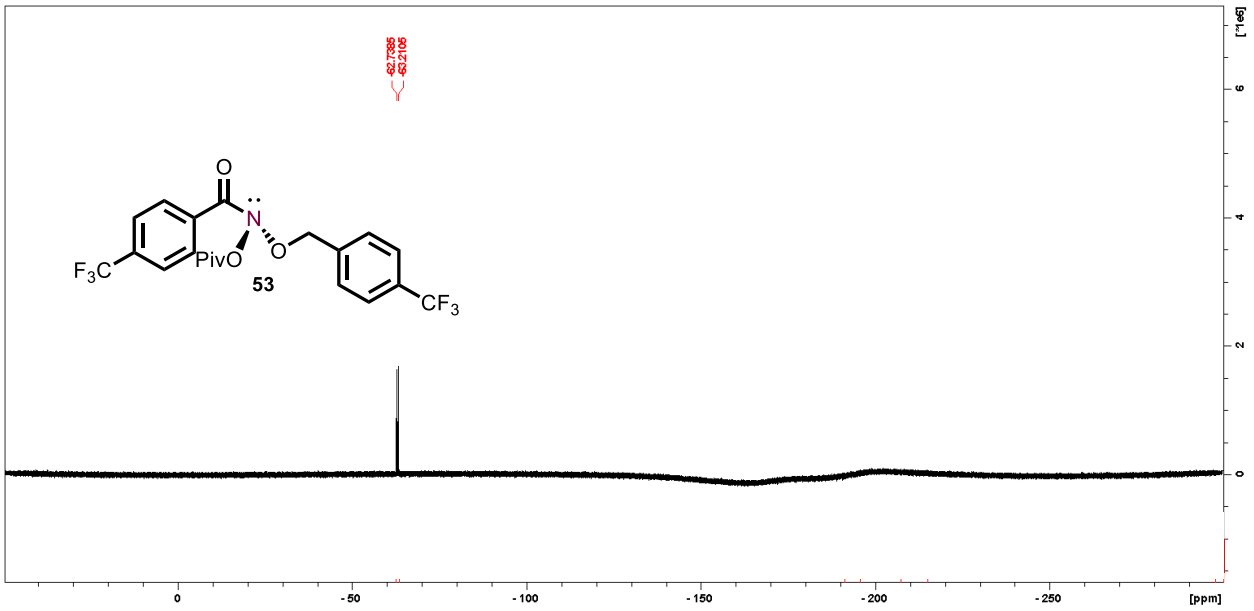

Figure 4.61. $^{19}F\{^{1}H\}$ NMR spectrum of *N*-(pivaloyloxy)-4-(trifluoromethyl)-*N*-((4-(trifluoromethyl)benzyl)oxy)benzamide (**53**) in $CDCl_3$, 376 MHz.

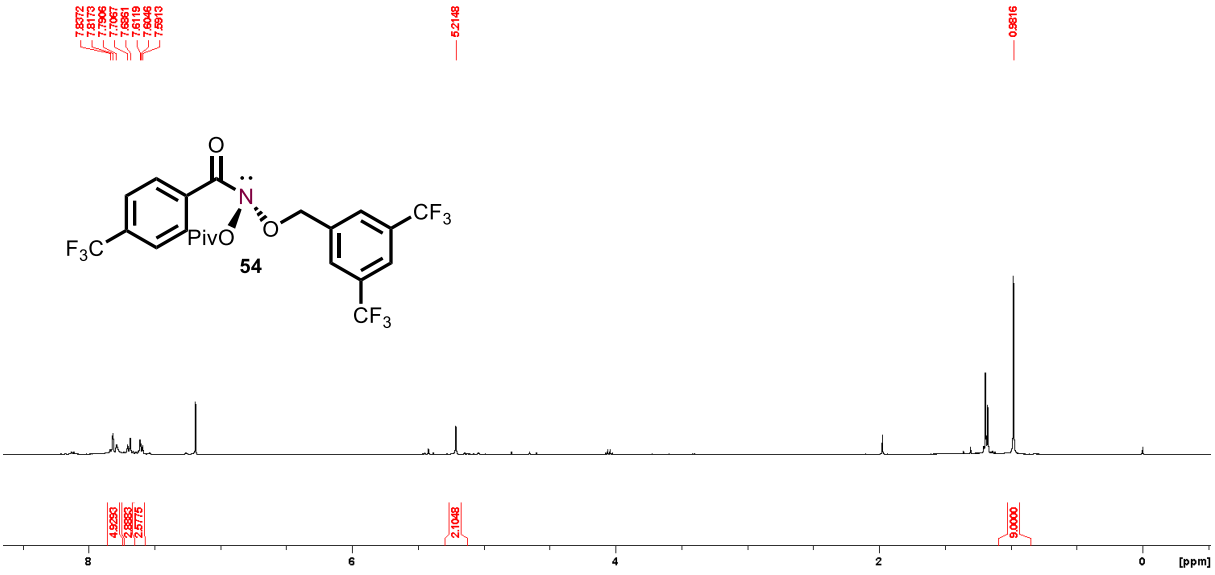

Figure 4.62. ^{1}H NMR spectrum of *N*-((3,5-bis(trifluoromethyl)benzyl)oxy)-*N*-(pivaloyloxy)-4-(trifluoromethyl)benzamide (**54**) in $CDCl_3$, 400 MHz.

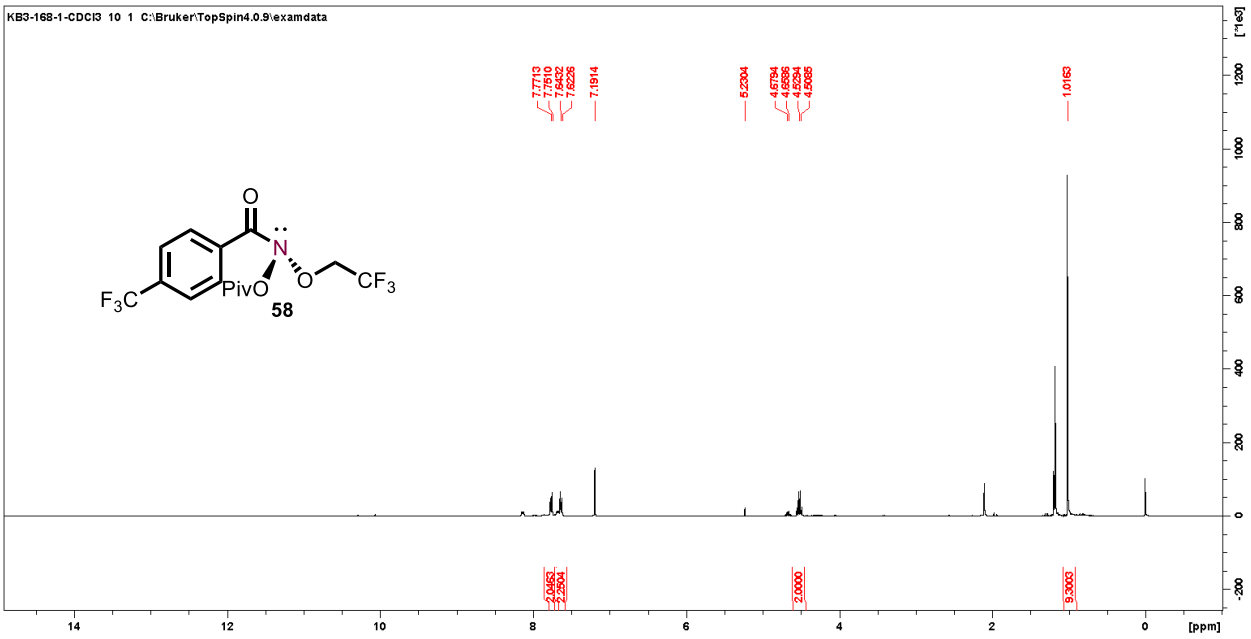

Figure 4.63. ^{1}H NMR spectrum of *N*-(pivaloyloxy)-*N*-(2,2,2-trifluoroethoxy)-4-(trifluoromethyl)benzamide (**58**) in $CDCl_3$, 400 MHz.

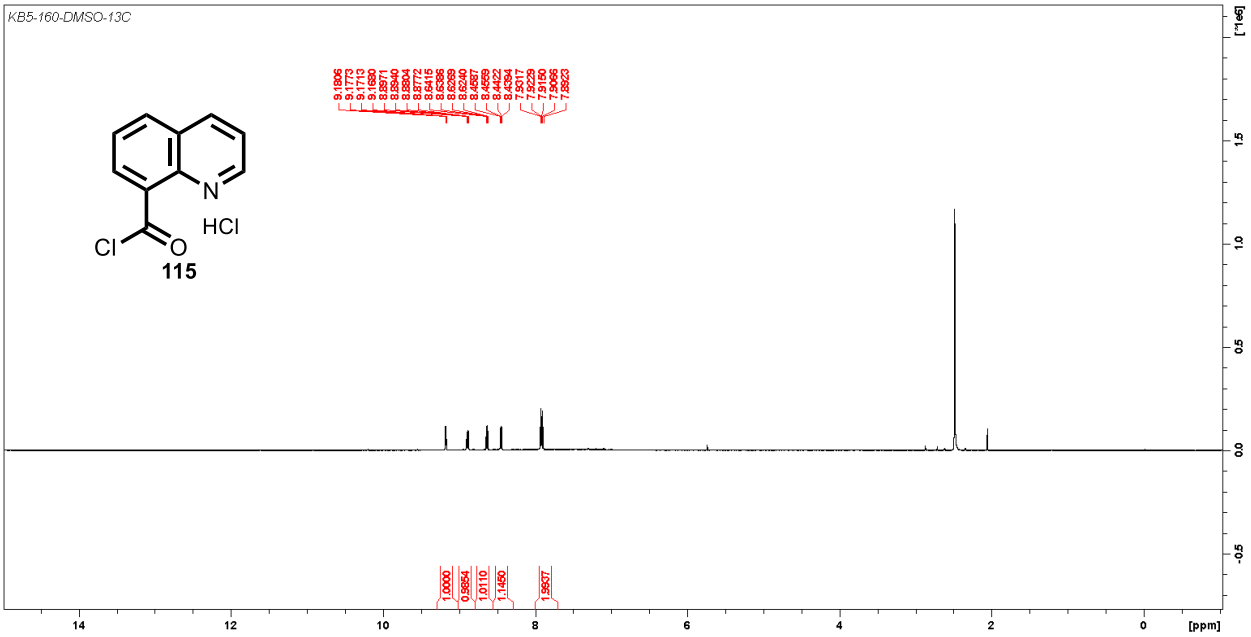

Figure 4.64. ^{1}H NMR spectrum of quinoline-8-carbonyl chloride HCl (**115**) in DMSO-*d6*, 400 MHz.

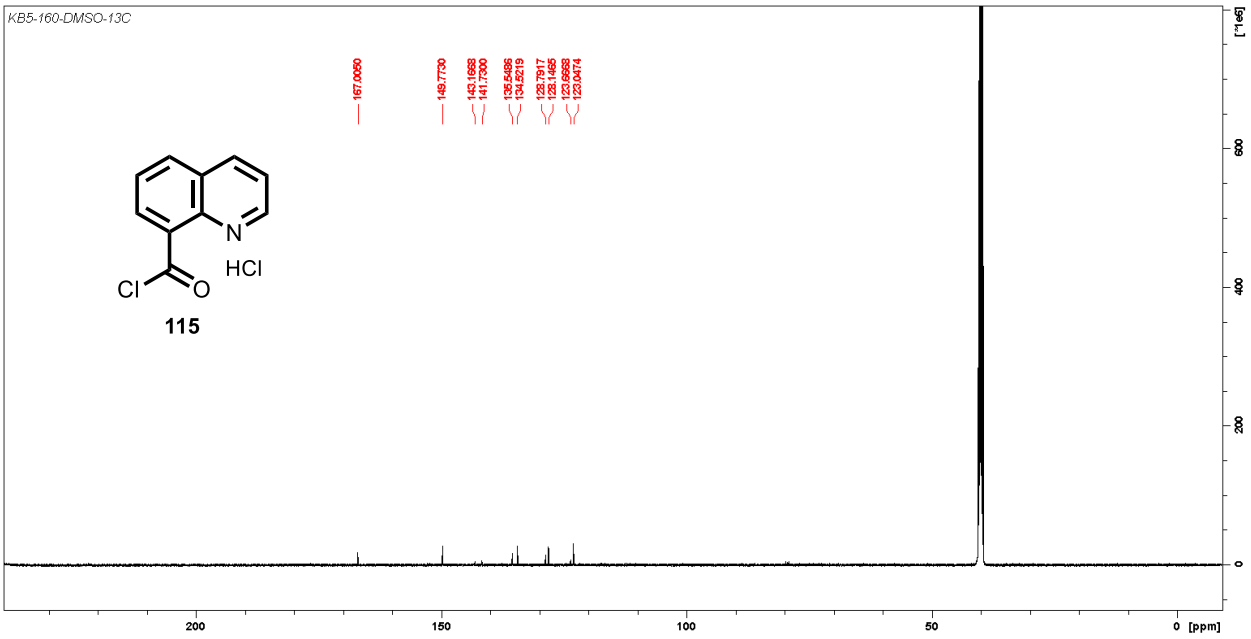

Figure 4.65. $^{13}C\{^{1}H\}$ NMR spectrum of quinoline-8-carbonyl chloride HCl (**115**) in DMSO-*d6*, 101 MHz.

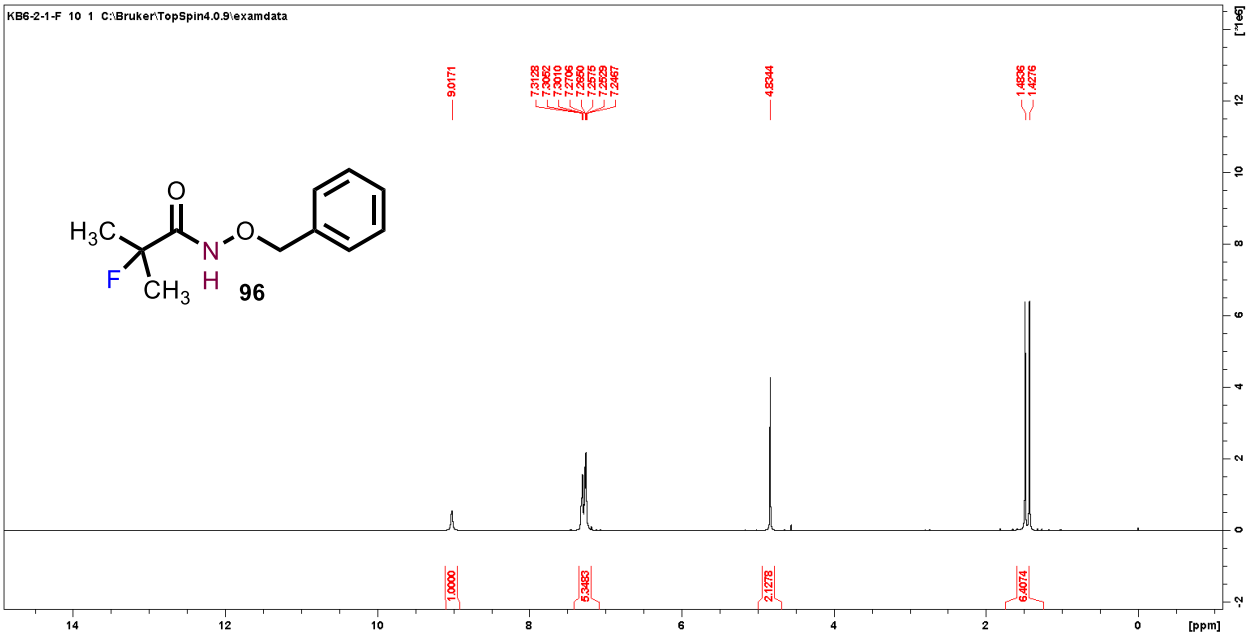

Figure 4.66. ^{1}H NMR spectrum of *N*-(benzyloxy)-2-fluoro-2-methylpropanamide (**96**) in $CDCl_3$, 400 MHz.

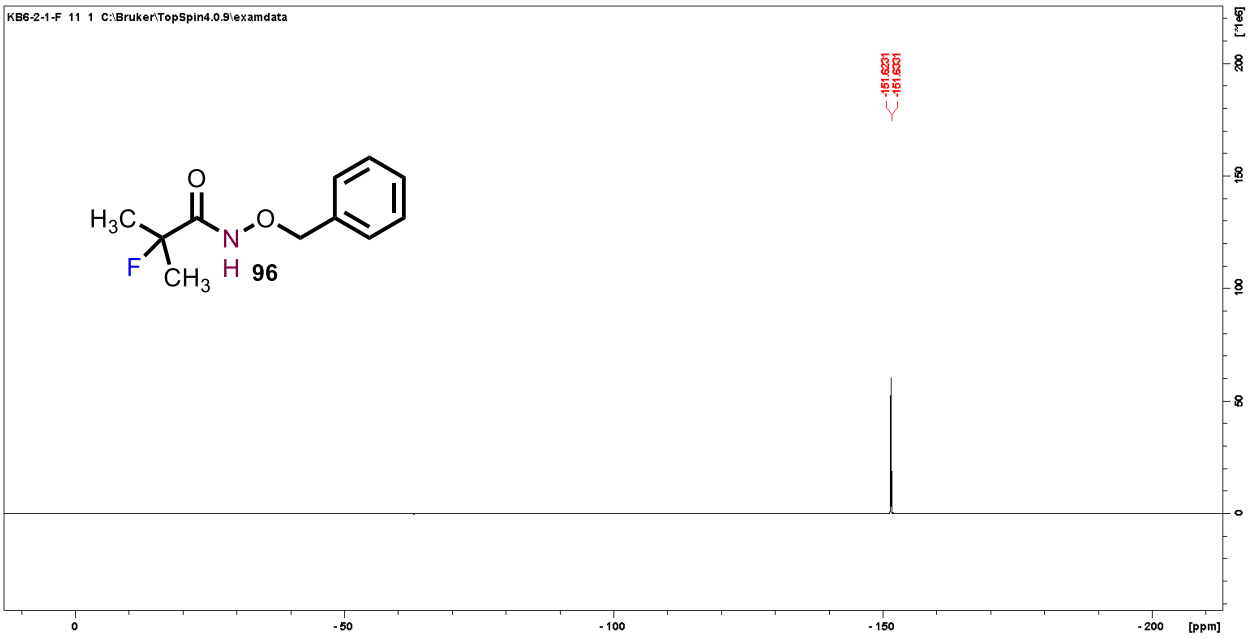

Figure 4.67. ^{19}F NMR spectrum of *N*-(benzyloxy)-2-fluoro-2-methylpropanamide (**96**) in $CDCl_3$, 376 MHz.

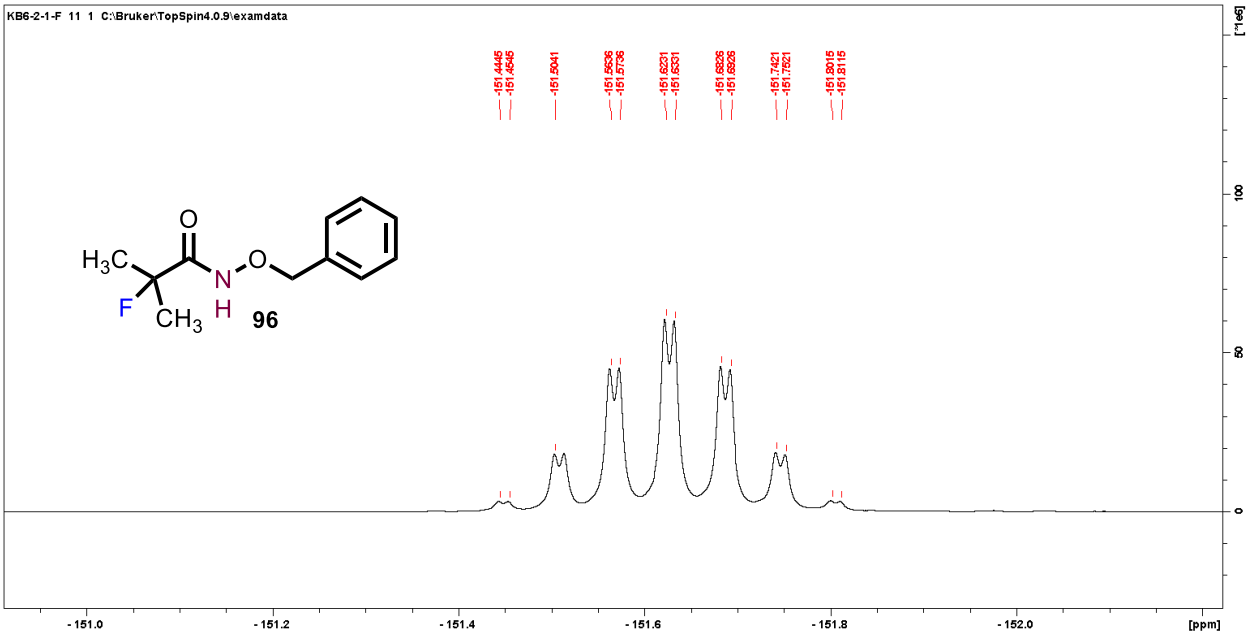

Figure 4.68. ^{19}F NMR spectrum expanded of *N*-(benzyloxy)-2-fluoro-2-methylpropanamide (**96**) in $CDCl_3$, 376 MHz.

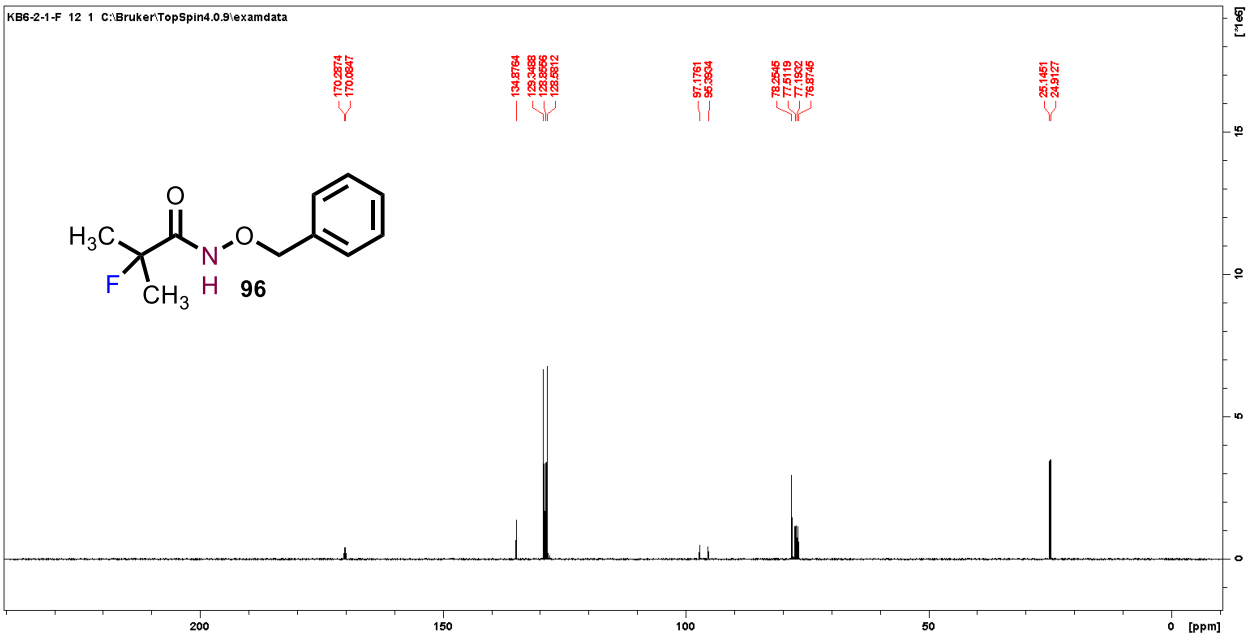

Figure 4.69. $^{13}C\{^{1}H\}$ NMR spectrum of *N*-(benzyloxy)-2-fluoro-2-methylpropanamide (**96**) in $CDCl_3$, 101 MHz.

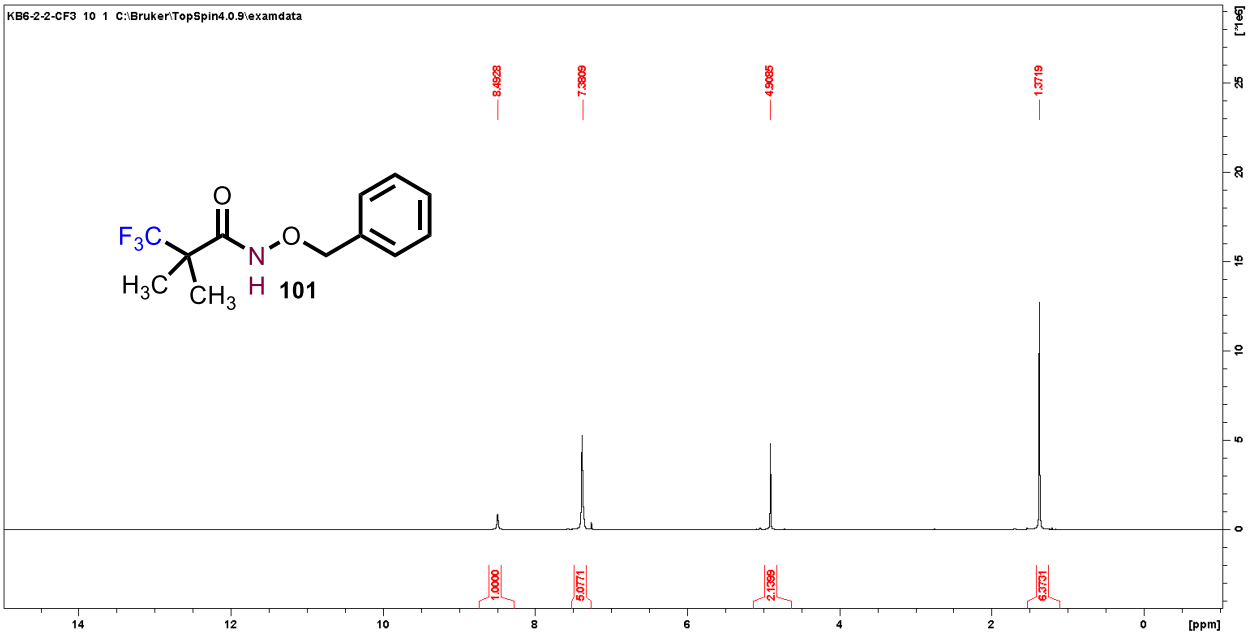

Figure 4.70. ^{1}H NMR spectrum of *N*-(benzyloxy)-3,3,3-trifluoro-2,2-dimethylpropanamide (**101**) in $CDCl_3$, 400 MHz.

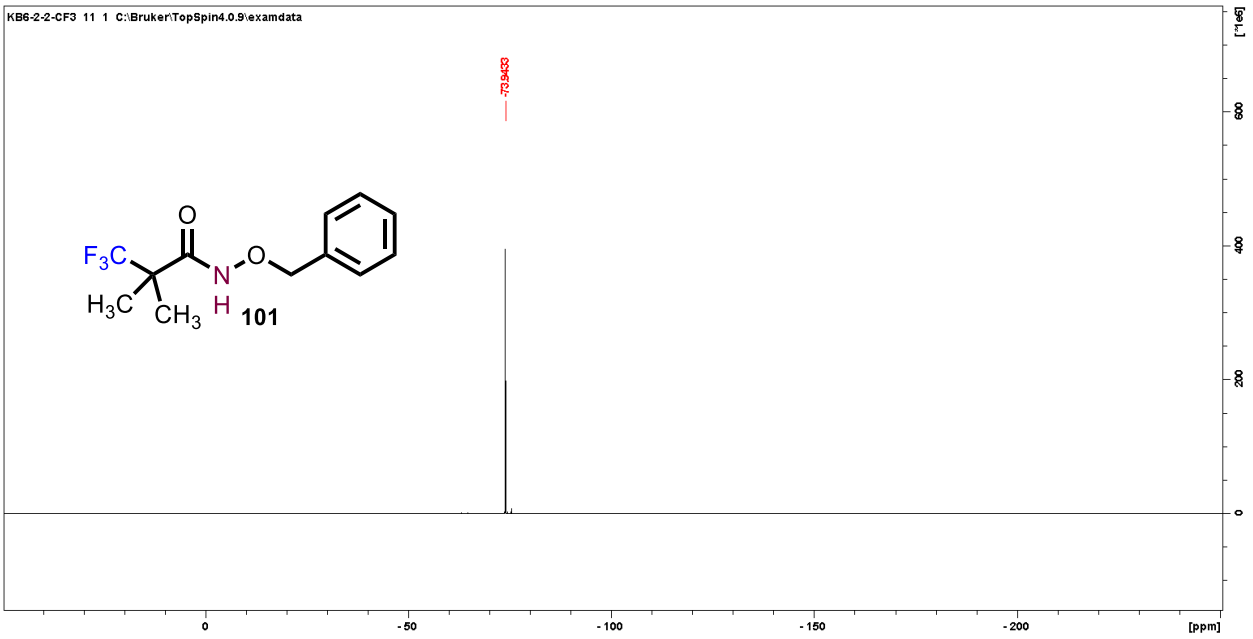

Figure 4.71. $^{19}F\{^{1}H\}$ NMR spectrum of *N*-(benzyloxy)-3,3,3-trifluoro-2,2-dimethylpropanamide (**101**) in $CDCl_3$, 376 MHz.

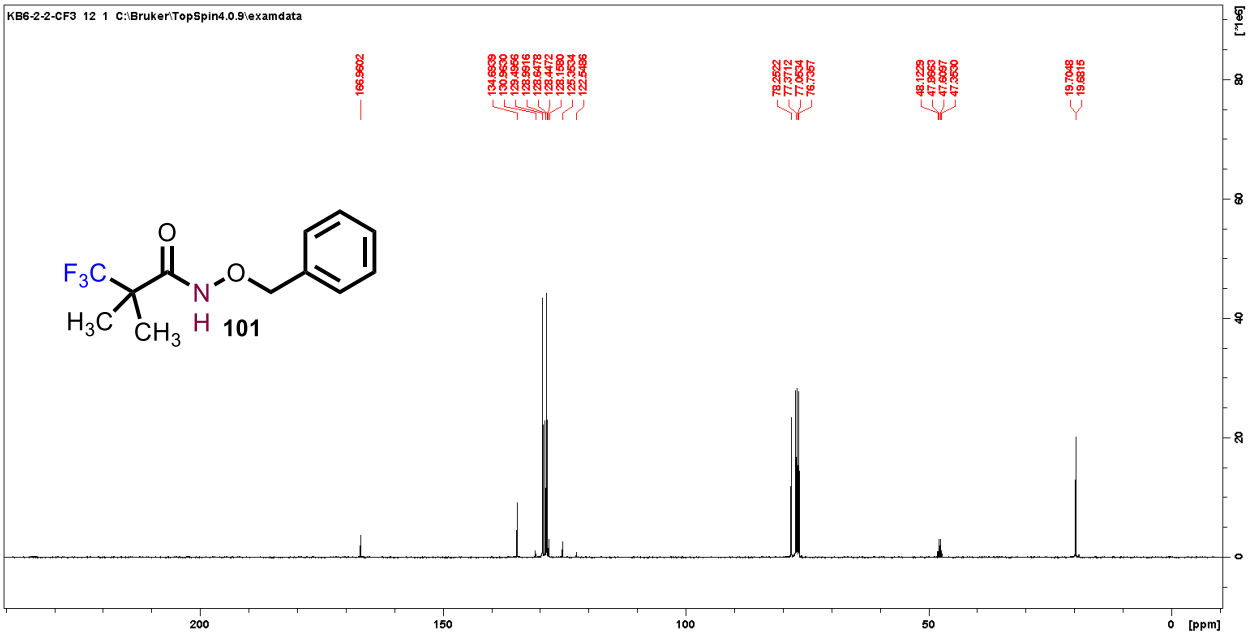

Figure 4.72. $^{13}C\{^{1}H\}$ NMR spectrum of *N*-(benzyloxy)-3,3,3-trifluoro-2,2-dimethylpropanamide (**101**) in $CDCl_3$, 101 MHz.

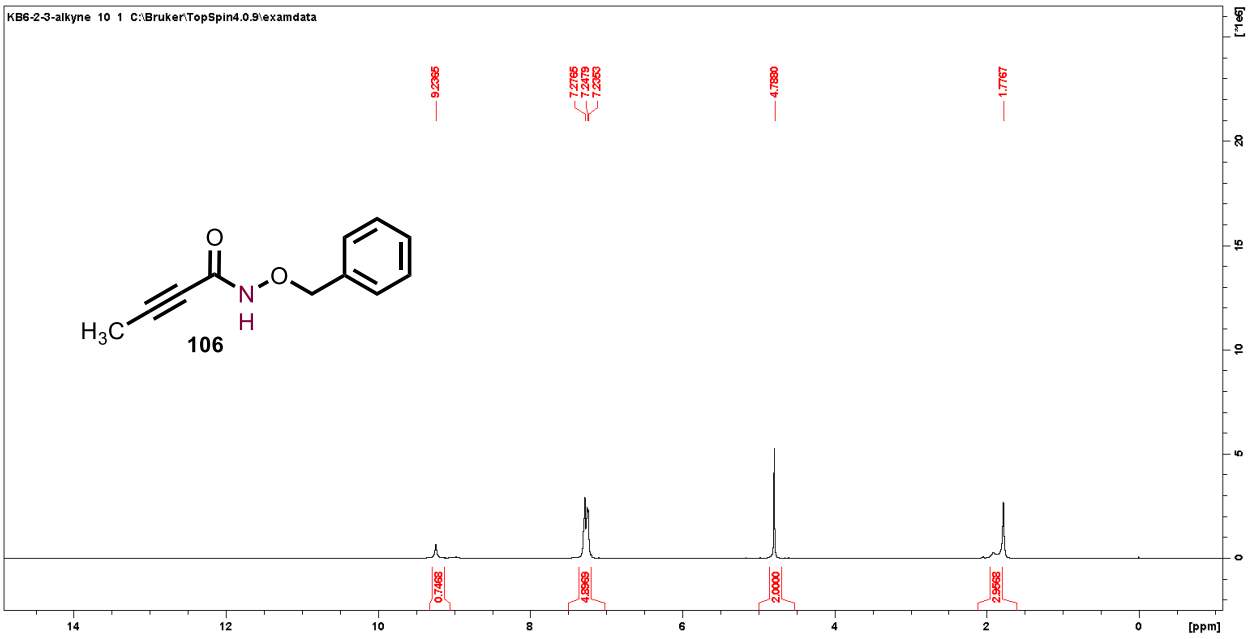

Figure 4.73. ^{1}H NMR spectrum of *N*-(benzyloxy)but-2-ynamide (**106**) in $CDCl_3$, 400 MHz.

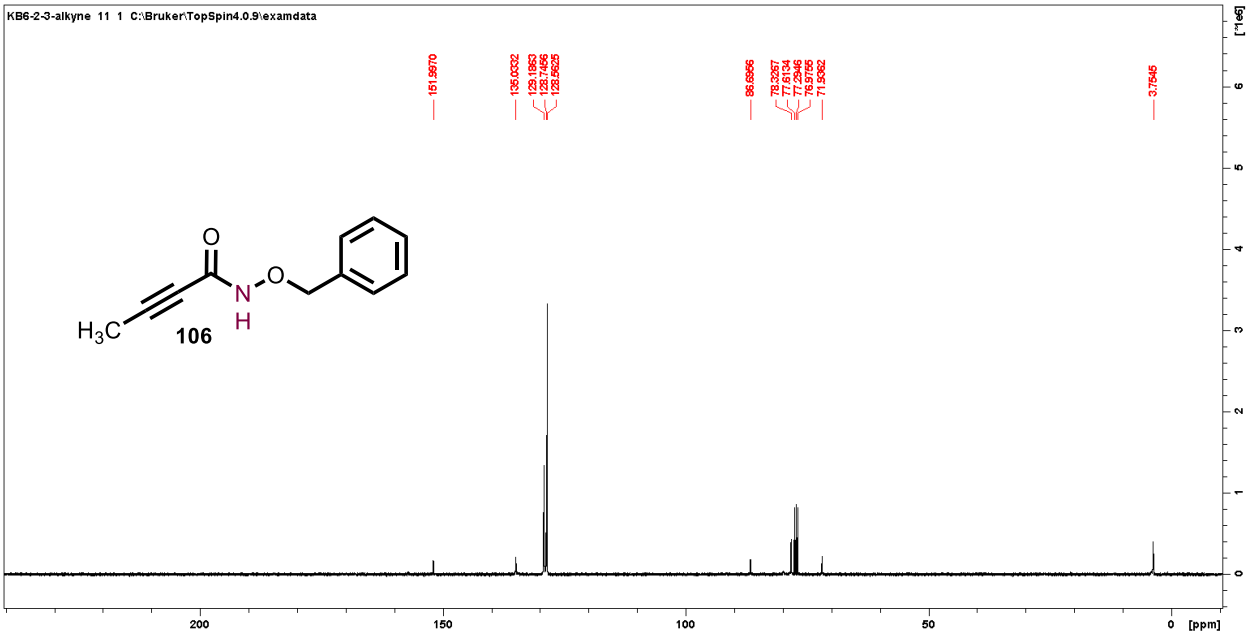

Figure 4.74. ^{13}C{^{1}H} NMR spectrum of *N*-(benzyloxy)but-2-ynamide (**106**) in $CDCl_3$, 101 MHz.

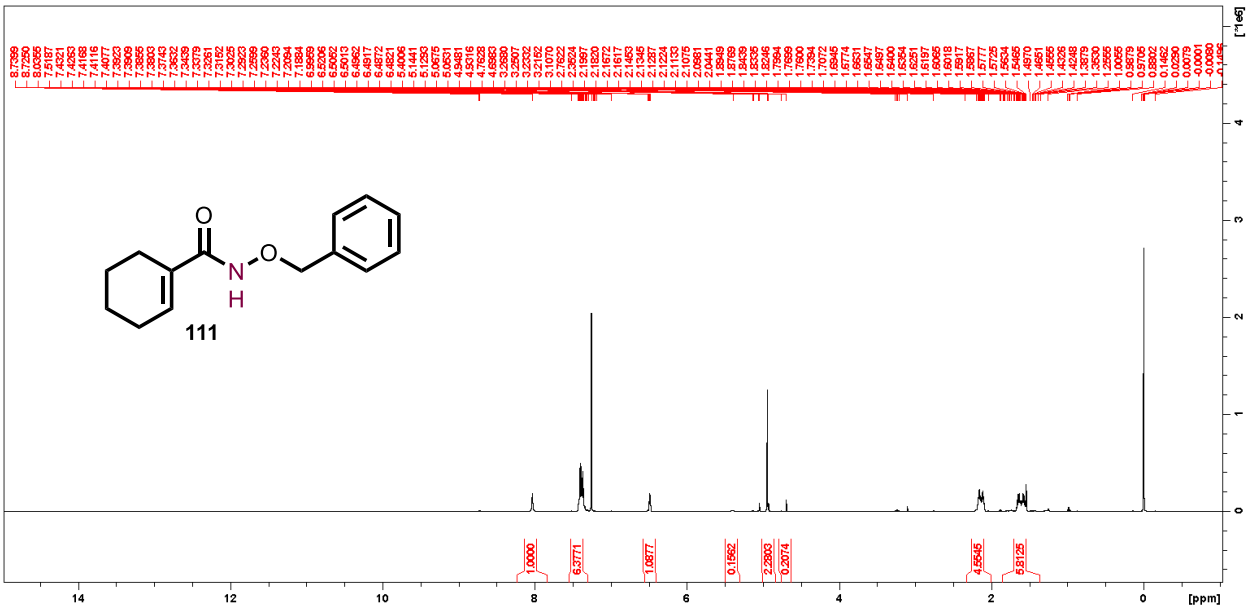

Figure 4.75. ^{1}H NMR spectrum of *N*-(benzyloxy)cyclohex-1-ene-1-carboxamide (**111**) in $CDCl_3$, 400 MHz.

Figure 4.76. ^{13}C{^{1}H} NMR spectrum of *N*-(benzyloxy)cyclohex-1-ene-1-carboxamide (**111**) in $CDCl_3$, 101 MHz.

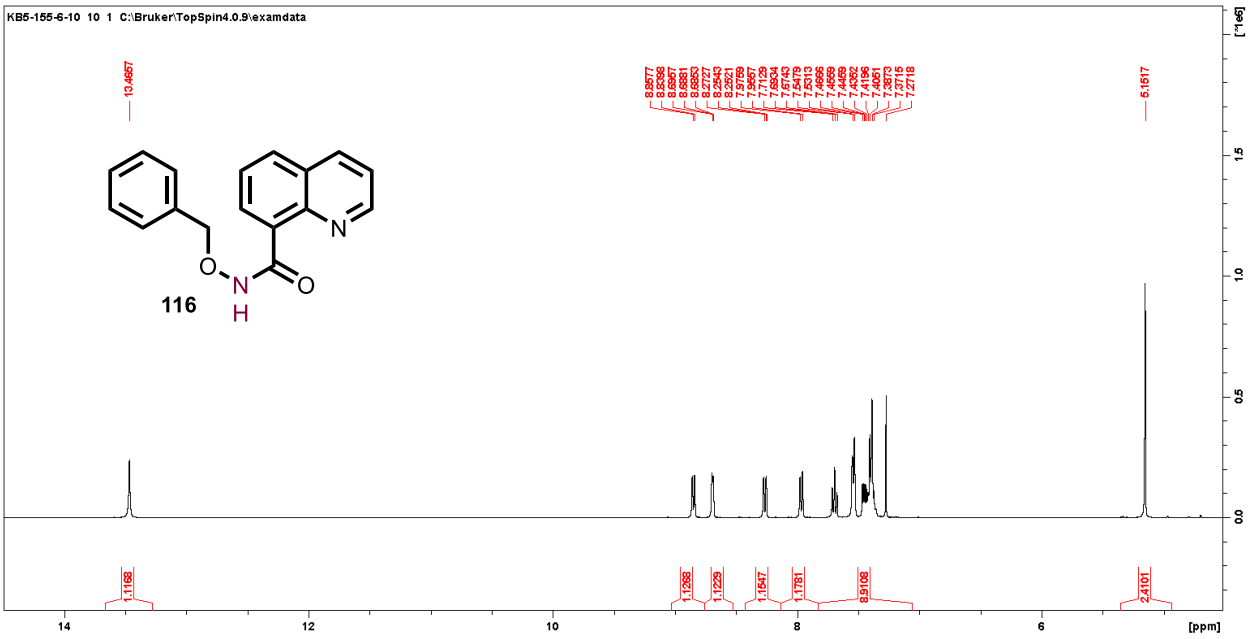

Figure 4.77. ^{1}H NMR spectrum of *N*-(benzyloxy)quinoline-8-carboxamide (**116**) in $CDCl_3$, 400 MHz.

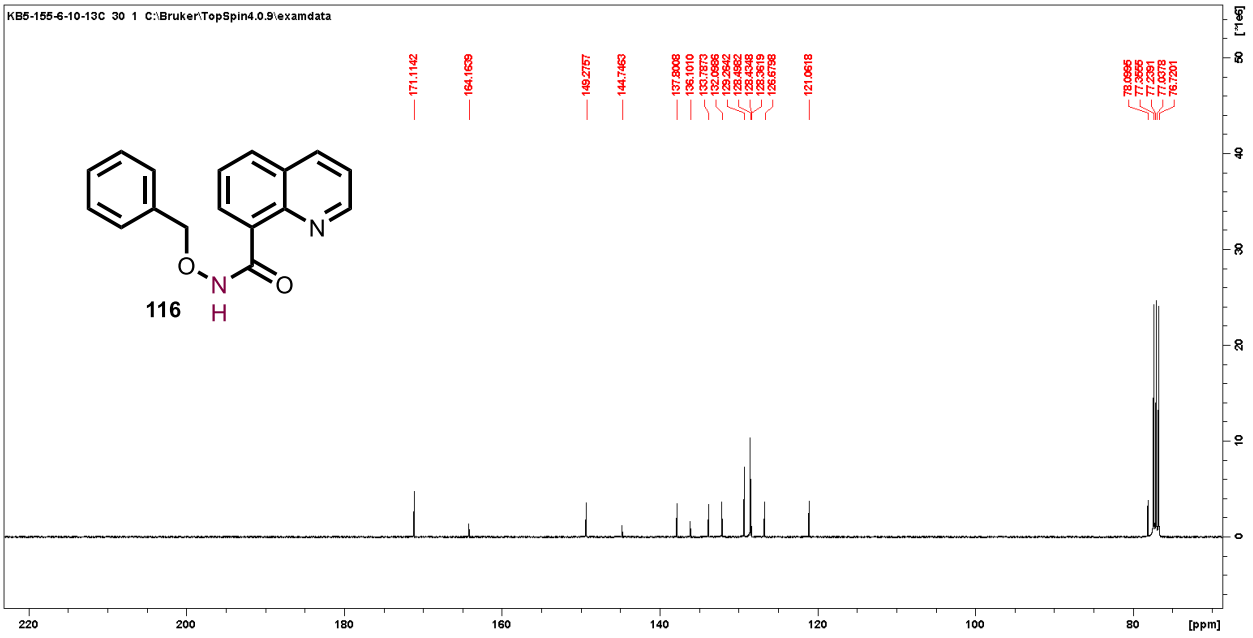

Figure 4.78. $^{13}C\{^{1}H\}$ NMR spectrum of *N*-(benzyloxy)quinoline-8-carboxamide (**116**) in $CDCl_3$, 101 MHz.

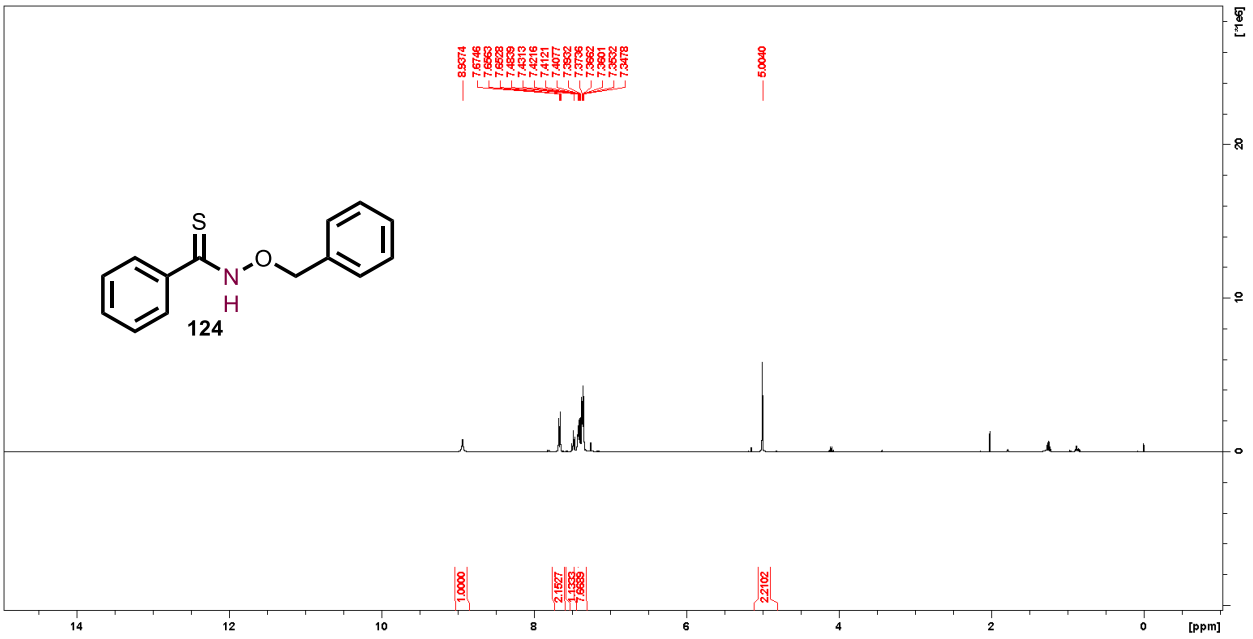

Figure 4.79. ^{1}H NMR spectrum of *N*-(benzyloxy)benzothioamide (**124**) in $CDCl_3$, 400 MHz.

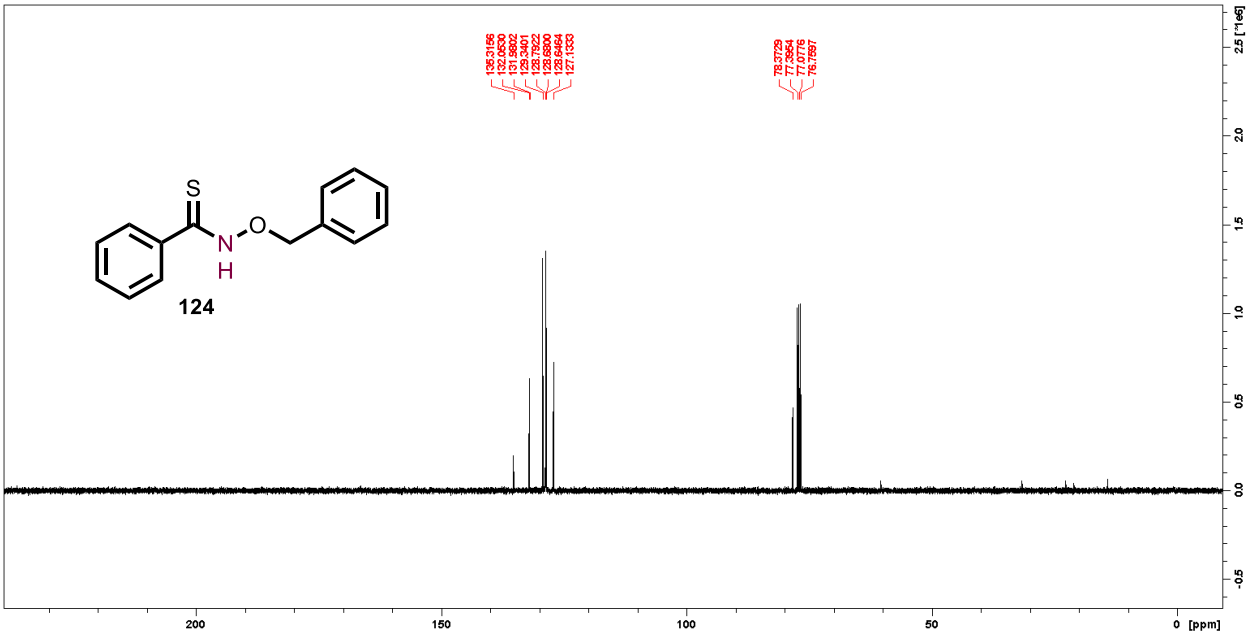

Figure 4.80. ^{13}C{^{1}H} NMR spectrum of *N*-(benzyloxy)benzothioamide (**124**) in $CDCl_3$, 101 MHz.

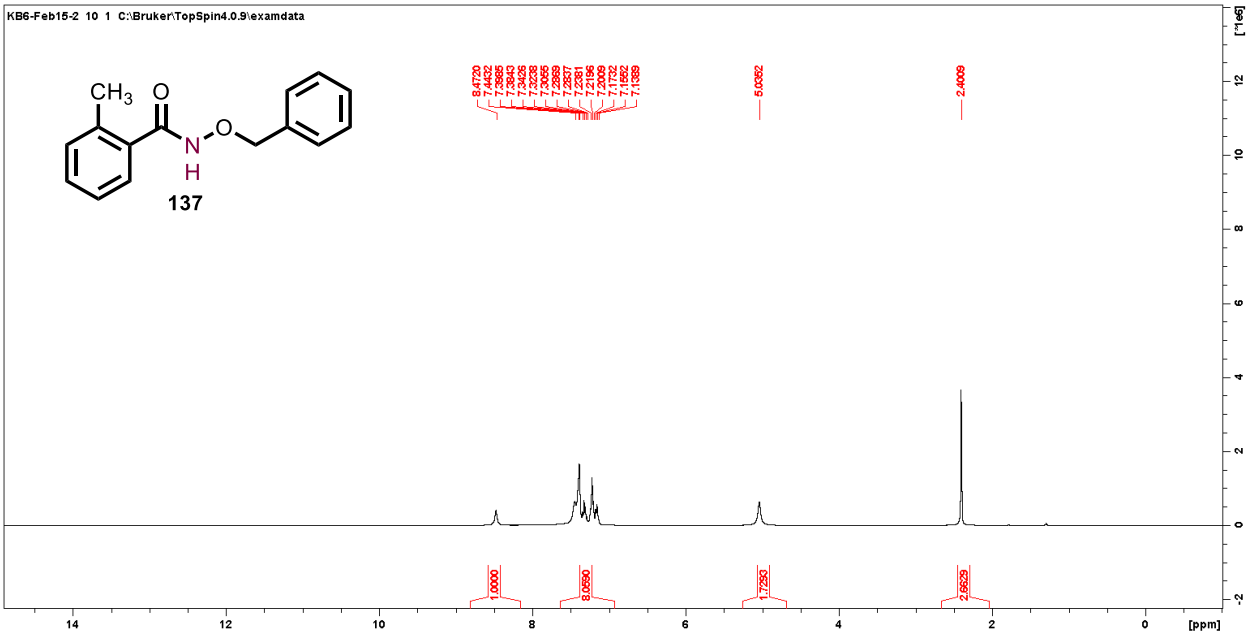

Figure 4.81. ^{1}H NMR spectrum of *N*-(benzyloxy)-2-methylbenzamide (**137**) in $CDCl_3$, 400 MHz.

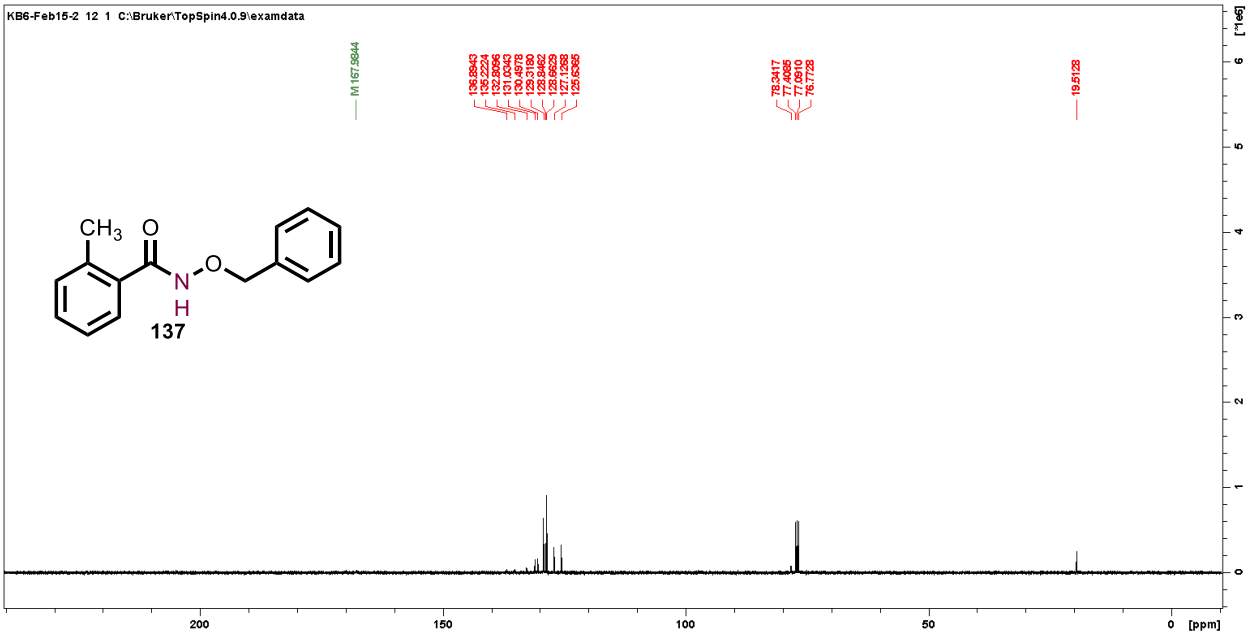

Figure 4.82. ^{13}C{^{1}H} NMR spectrum of *N*-(benzyloxy)-2-methylbenzamide (**137**) in $CDCl_3$, 100 MHz.

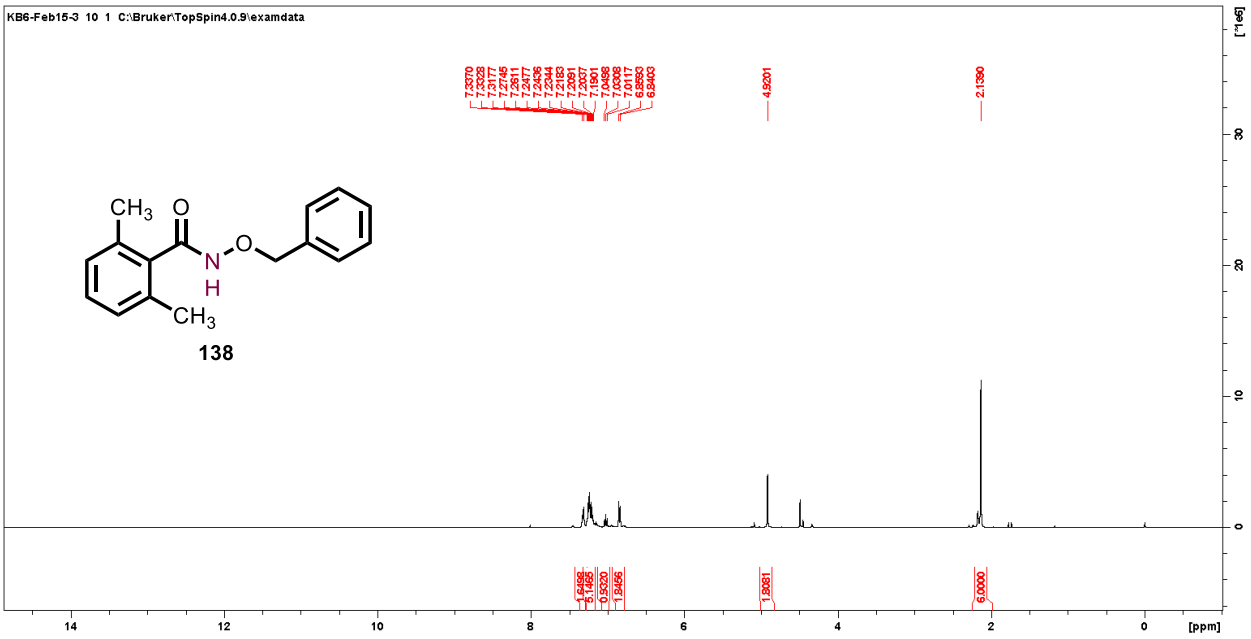

Figure 4.83. ^{1}H NMR spectrum of *N*-(benzyloxy)-2,6-dimethylbenzamide (**138**) in $CDCl_3$, 400 MHz.

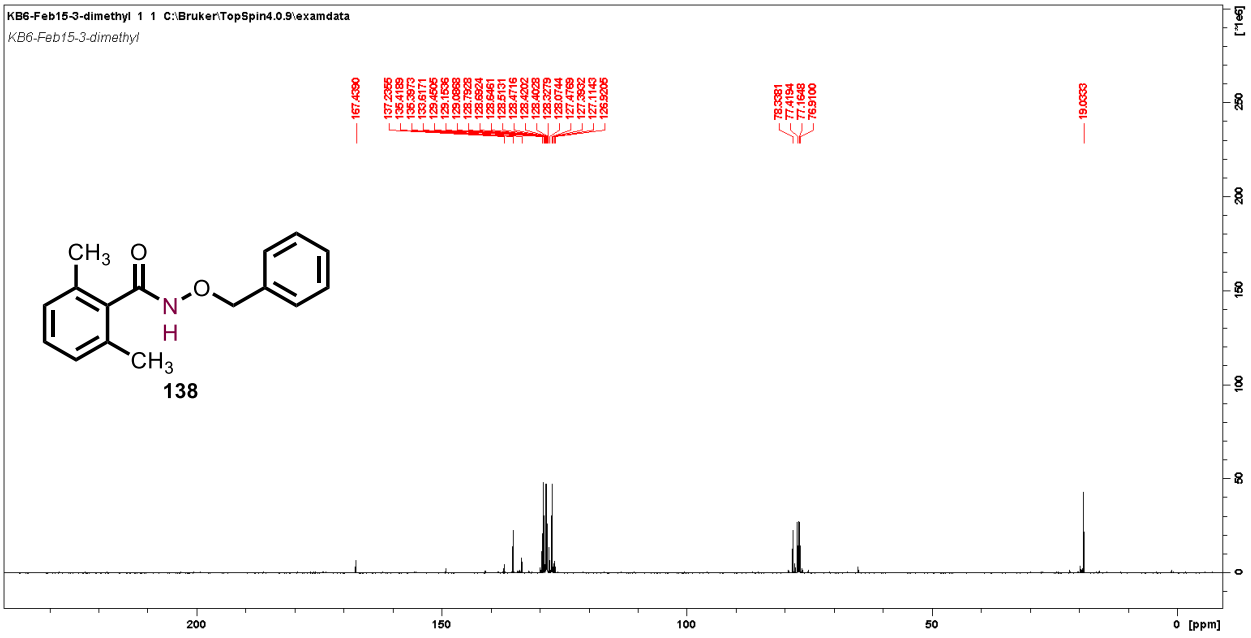

Figure 4.84. ^{13}C{^{1}H} NMR spectrum of *N*-(benzyloxy)-2,6-dimethylbenzamide (**138**) in $CDCl_3$, 100 MHz.

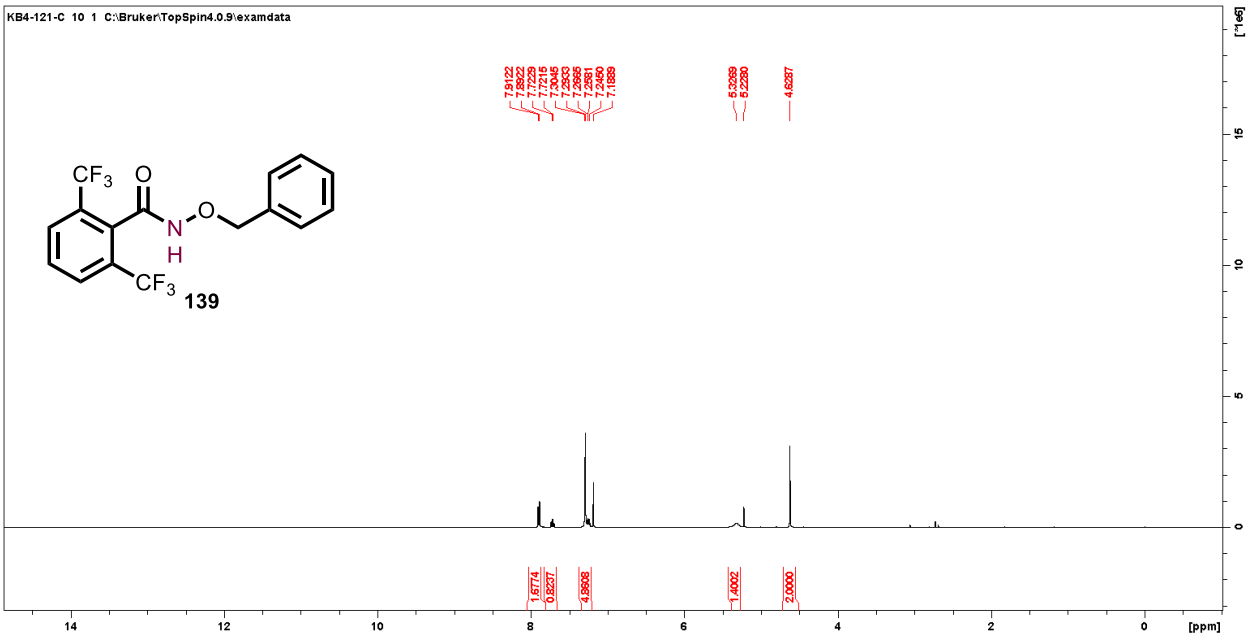

Figure 4.85. ^{1}H NMR spectrum of *N*-(benzyloxy)-2,6-bis(trifluoromethyl)benzamide (**139**) in $CDCl_3$, 400 MHz.

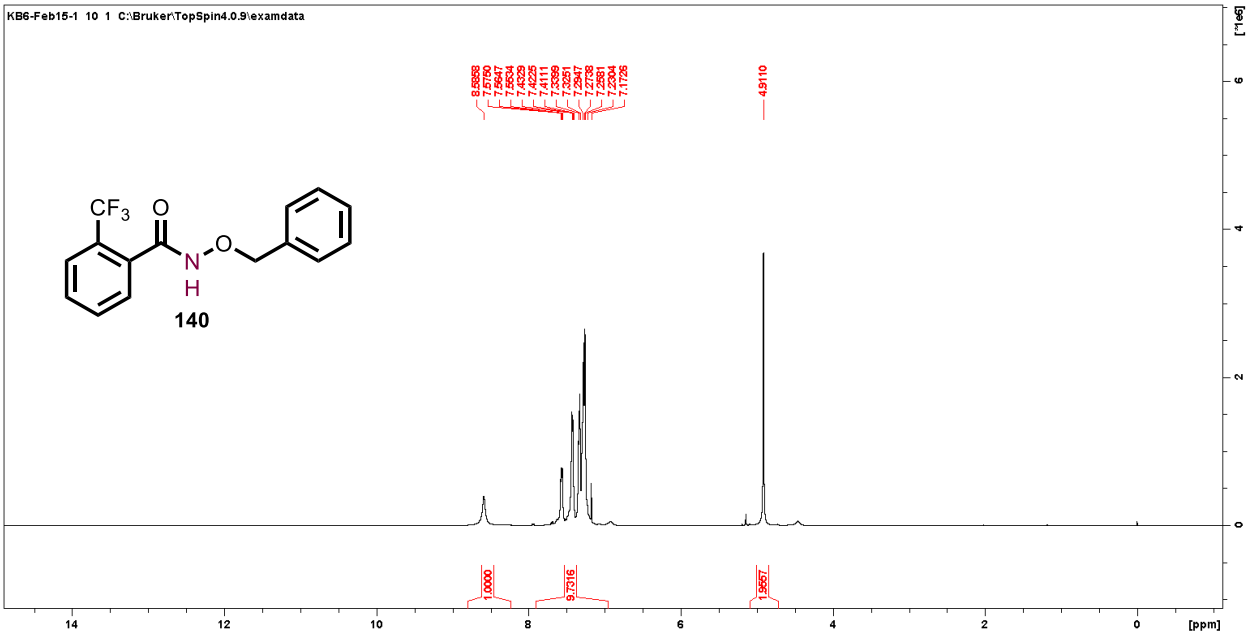

Figure 4.86. ^{1}H NMR spectrum of *N*-(benzyloxy)-2-(trifluoromethyl)benzamide (**140**) in $CDCl_3$, 400 MHz.

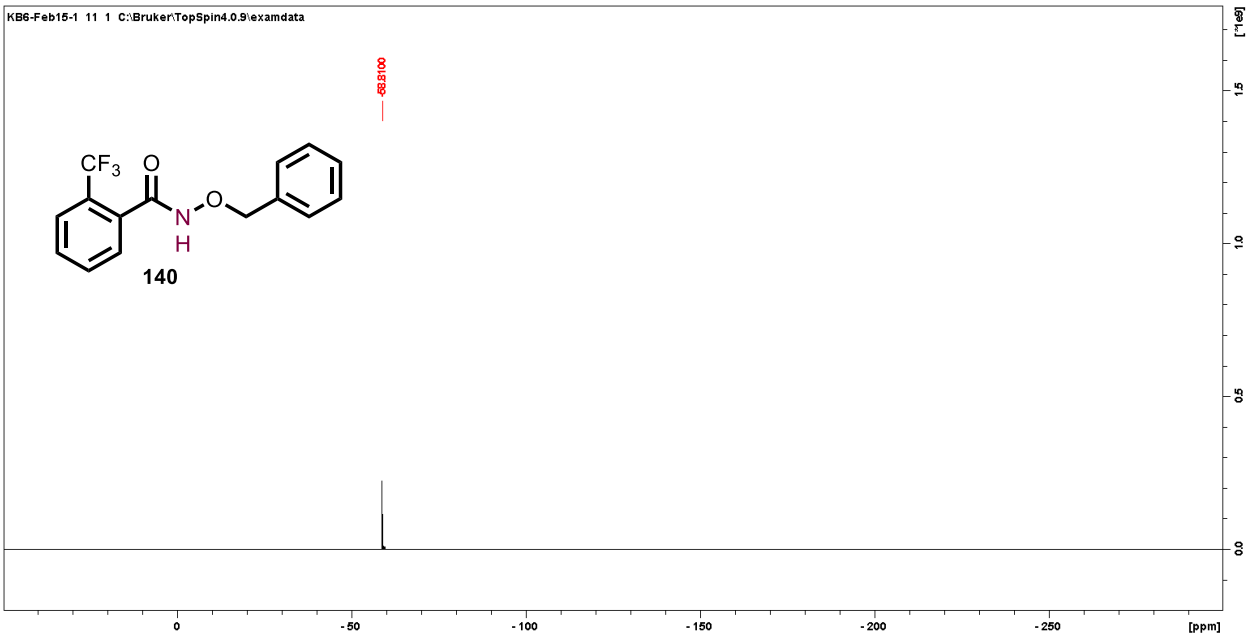

Figure 4.87. $^{19}F\{^{1}H\}$ NMR spectrum of *N*-(benzyloxy)-2-(trifluoromethyl)benzamide (**140**) in $CDCl_3$, 376 MHz.

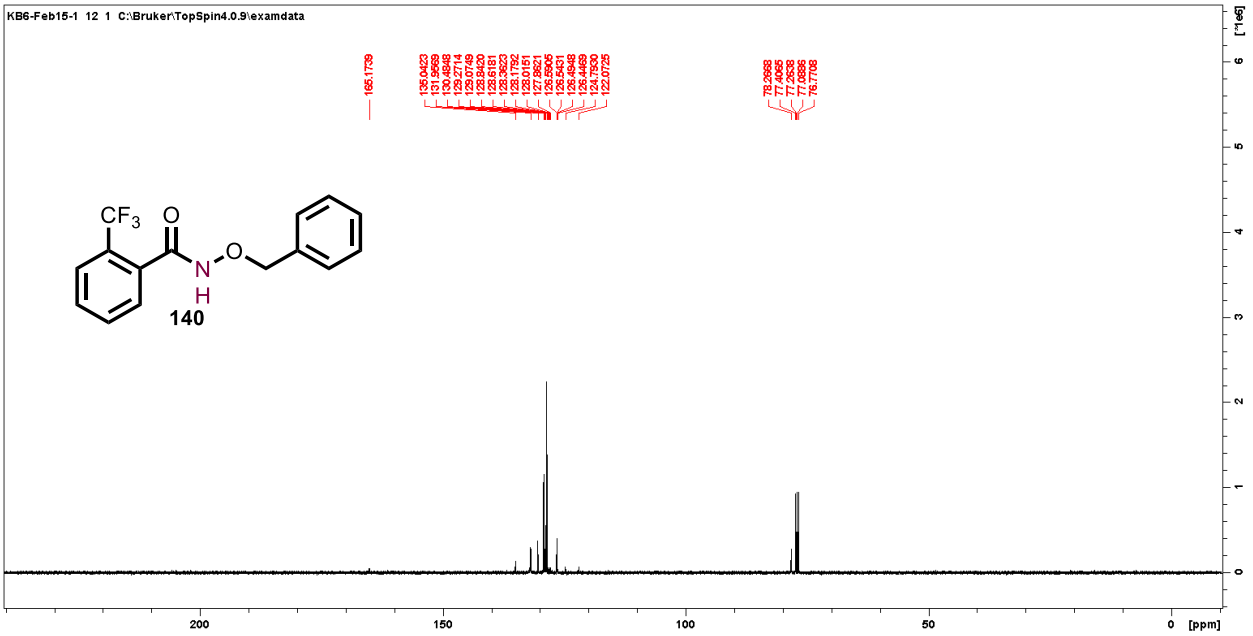

Figure 4.88. $^{13}C\{^{1}H\}$ NMR spectrum of *N*-(benzyloxy)-2-(trifluoromethyl)benzamide (**140**) in $CDCl_3$, 101 MHz.

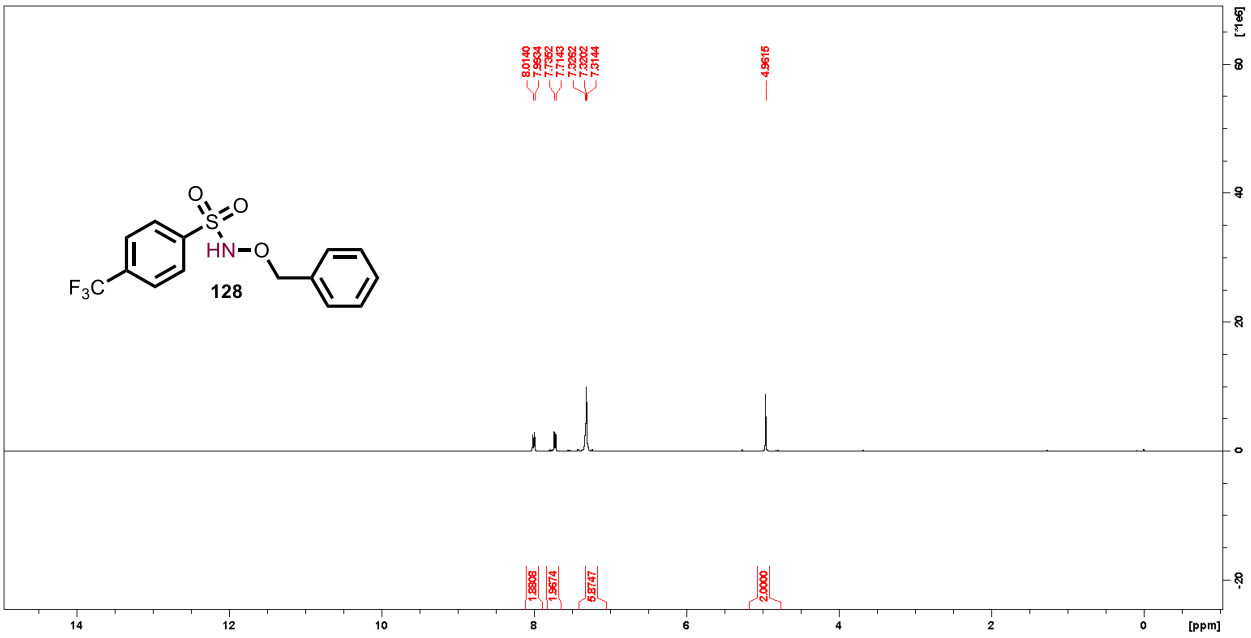

Figure 4.89. ^{1}H NMR spectrum of *N*-(benzyloxy)-4-(trifluoromethyl)benzenesulfonamide (**128**) in $CDCl_3$, 400 MHz.

Figure 4.90. ^{19}F{^{1}H} NMR spectrum of *N*-(benzyloxy)-4-(trifluoromethyl)benzenesulfonamide (**128**) in $CDCl_3$, 376 MHz.

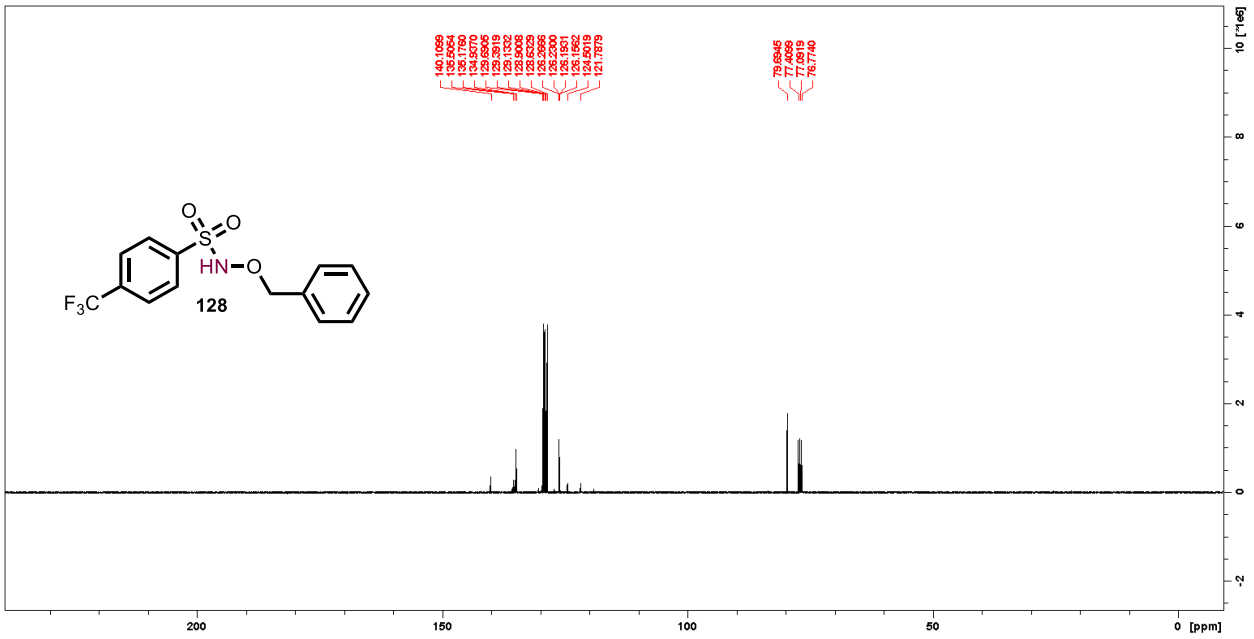

Figure 4.91. $^{13}C\{^{1}H\}$ NMR spectrum of *N*-(benzyloxy)-4-(trifluoromethyl)benzenesulfonamide (**128**) in $CDCl_3$, 100 MHz.

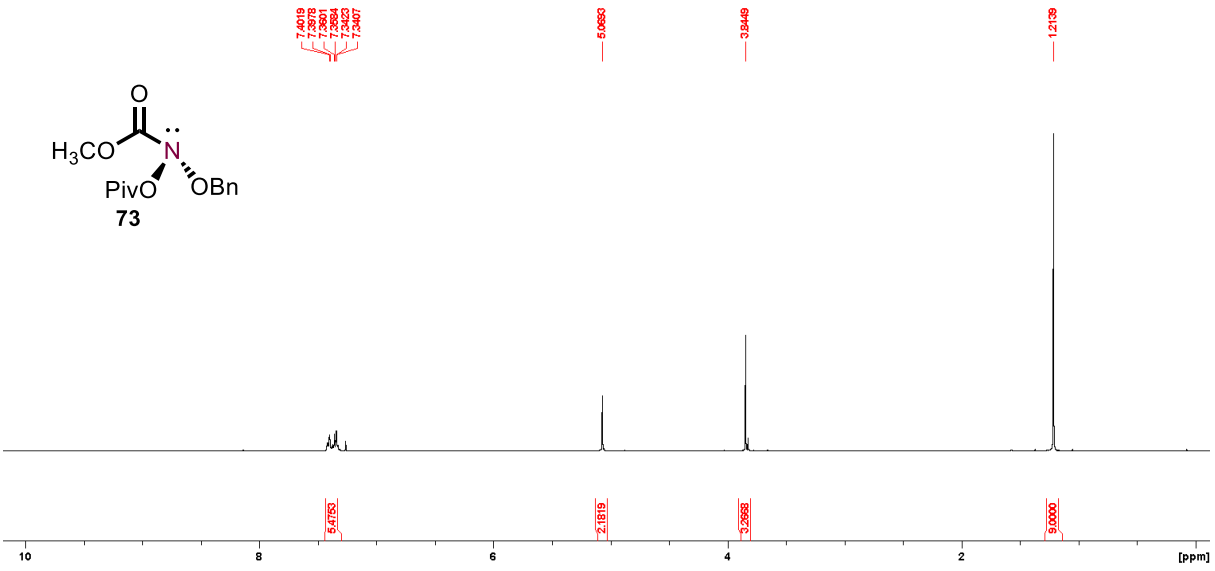

Figure 4.92. ^{1}H NMR spectrum of *N*-(benzyloxy)-*N*-(pivaloyloxy)-methylcarbamate (**73**) in $CDCl_3$, 400 MHz.

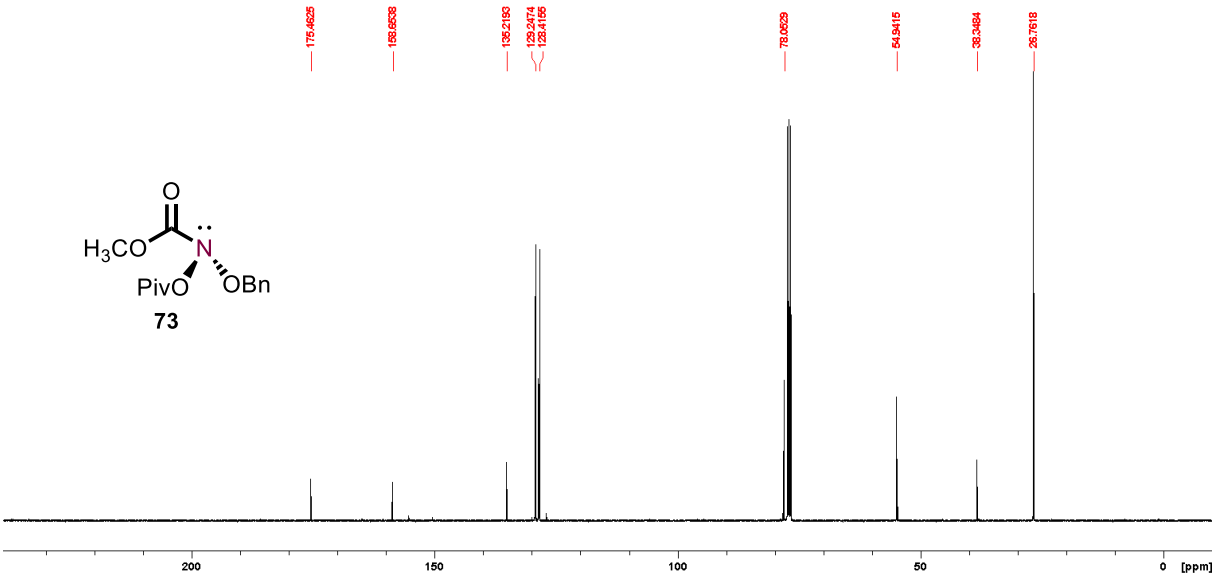

Figure 4.93. $^{13}C\{^{1}H\}$ NMR spectrum of *N*-(benzyloxy)-*N*-(pivaloyloxy)-methylcarbamate (**73**) in $CDCl_3$, 100 MHz.

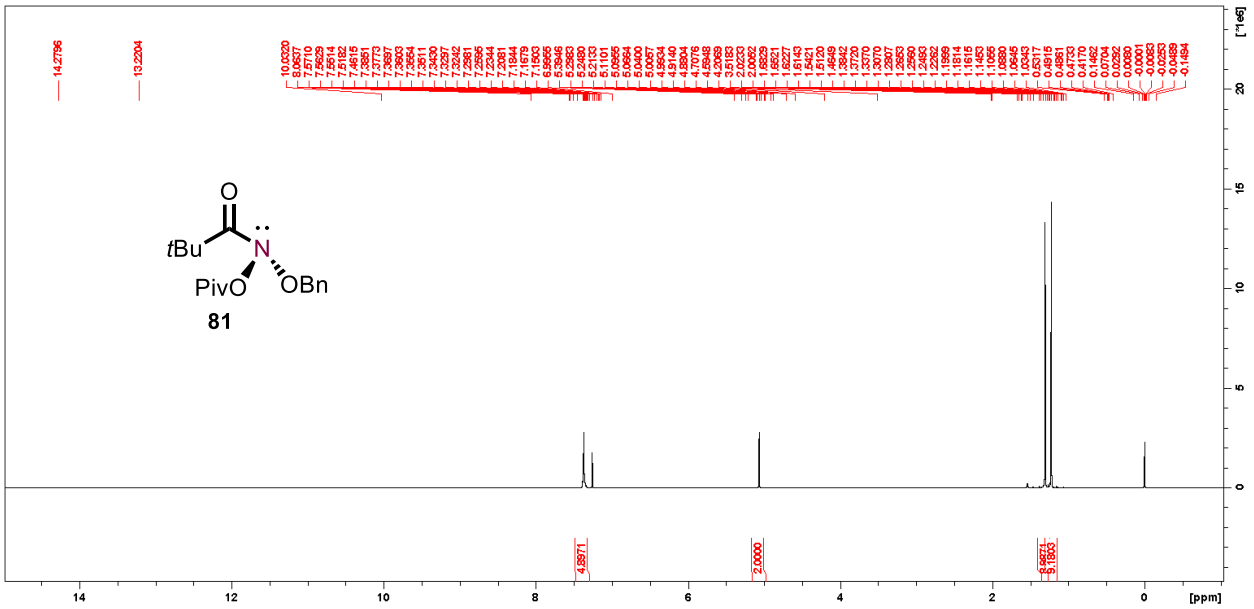

Figure 4.94. ^{1}H NMR spectrum of *N*-(benzyloxy)-*N*-(pivaloyloxy)pivalamide (**81**) in $CDCl_3$, 400 MHz.

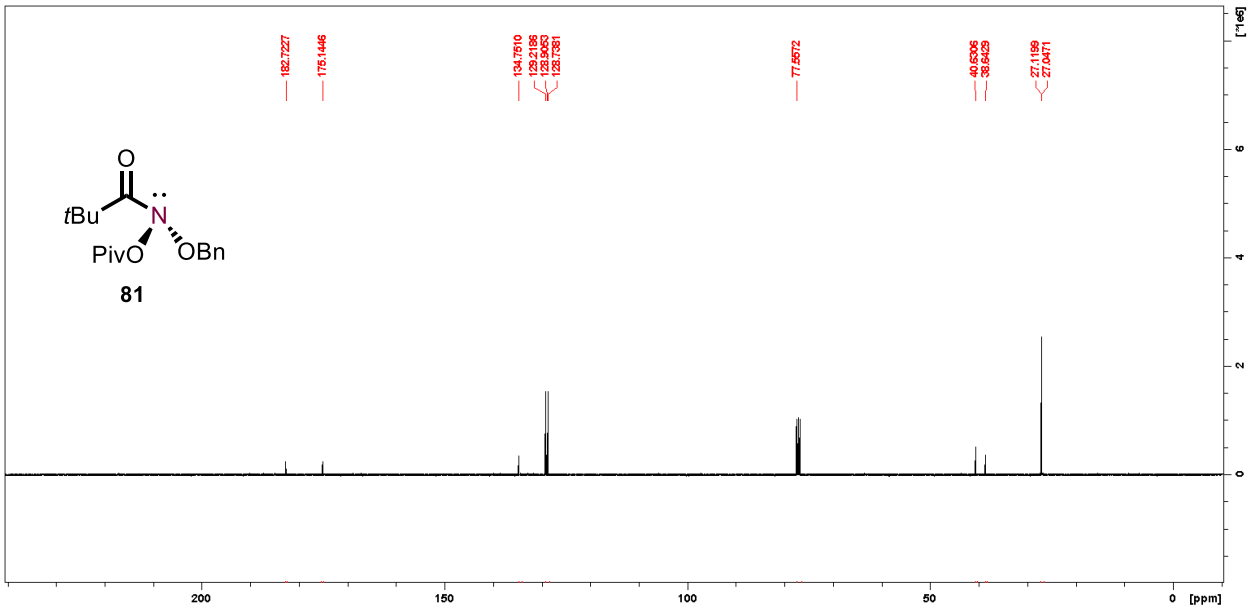

Figure 4.95. $^{13}C\{^{1}H\}$ NMR spectrum of *N*-(benzyloxy)-*N*-(pivaloyloxy)pivalamide (**81**) in $CDCl_3$, 100 MHz.

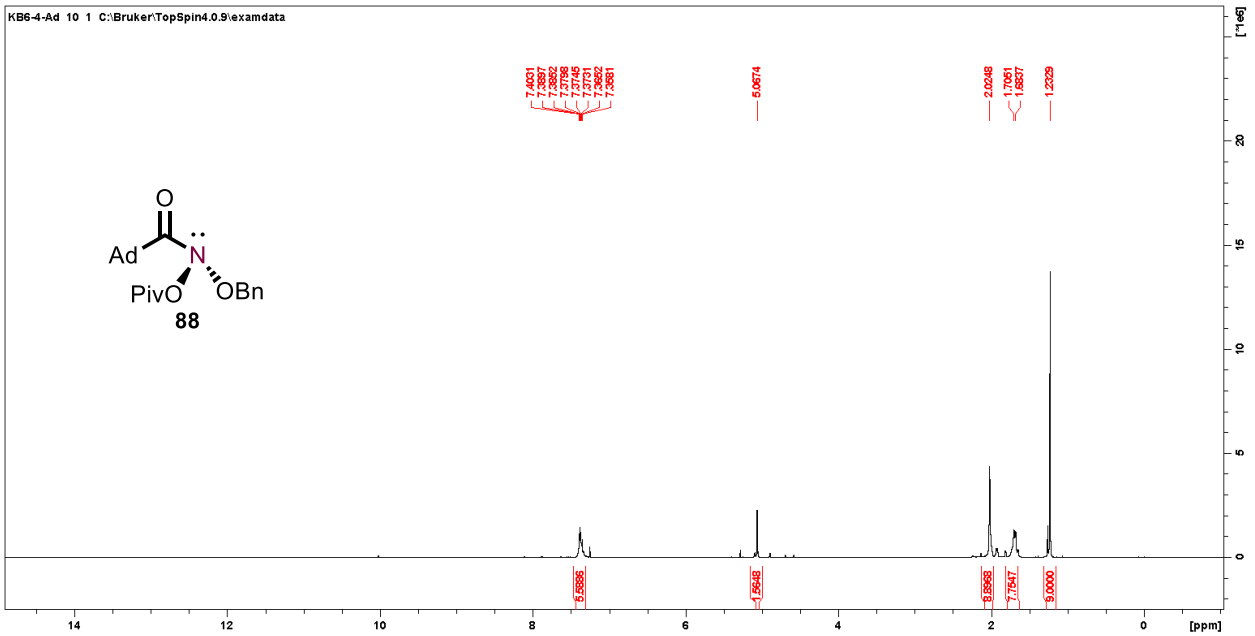

Figure 4.96. ^{1}H NMR spectrum of *N*-(benzyloxy)-*N*-(pivaloyloxy)adamantane-1-carboxamide (**88**) in $CDCl_3$, 400 MHz.

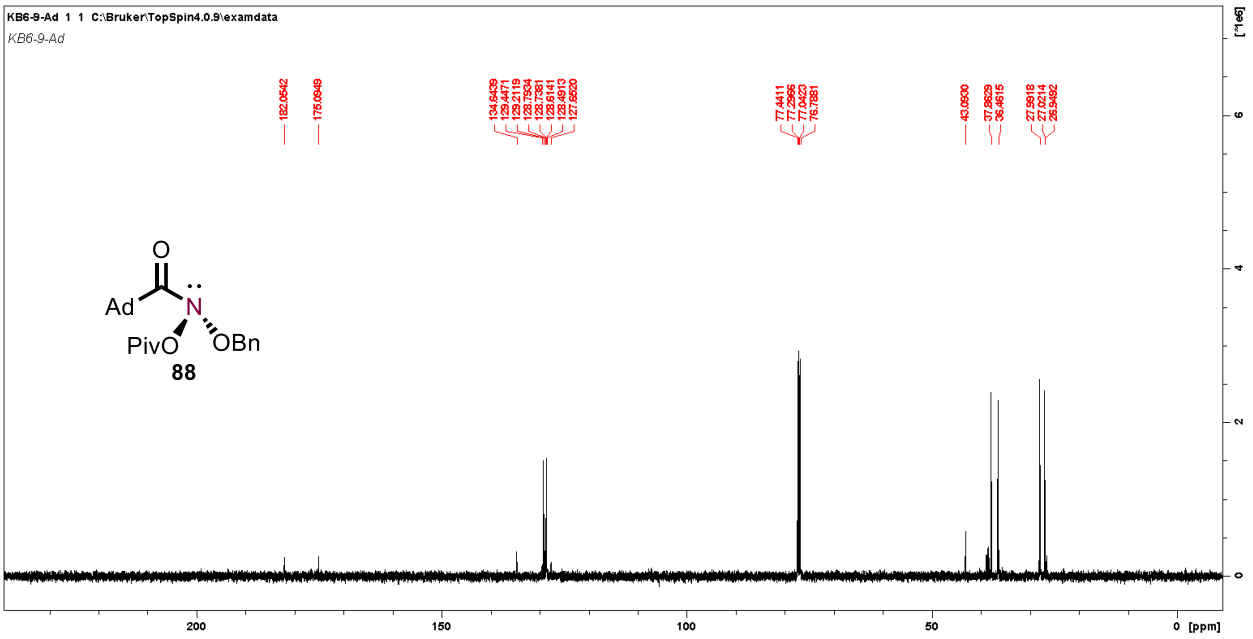

Figure 4.97. $^{13}C\{^{1}H\}$ NMR spectrum of *N*-(benzyloxy)-*N*-(pivaloyloxy)adamantane-1-carboxamide (**88**) in $CDCl_3$, 100 MHz.

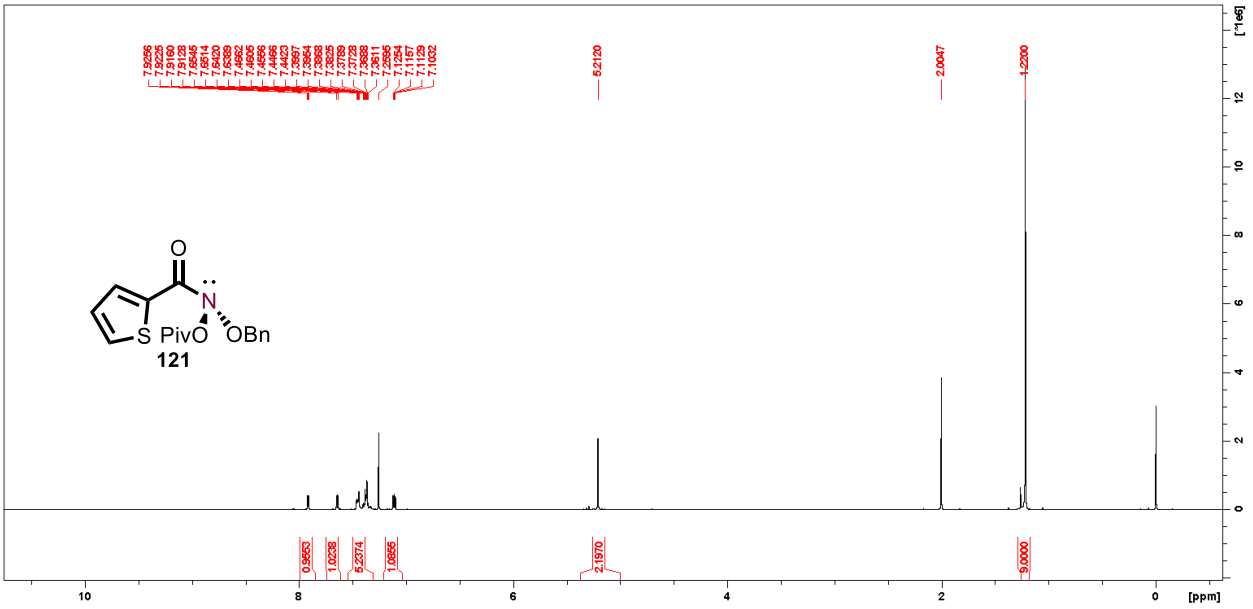

Figure 4.98. ^{1}H NMR spectrum of *N*-(benzyloxy)-*N*-(pivaloyloxy)thiophene-2-carboxamide (**121**) in $CDCl_3$, 400 MHz.

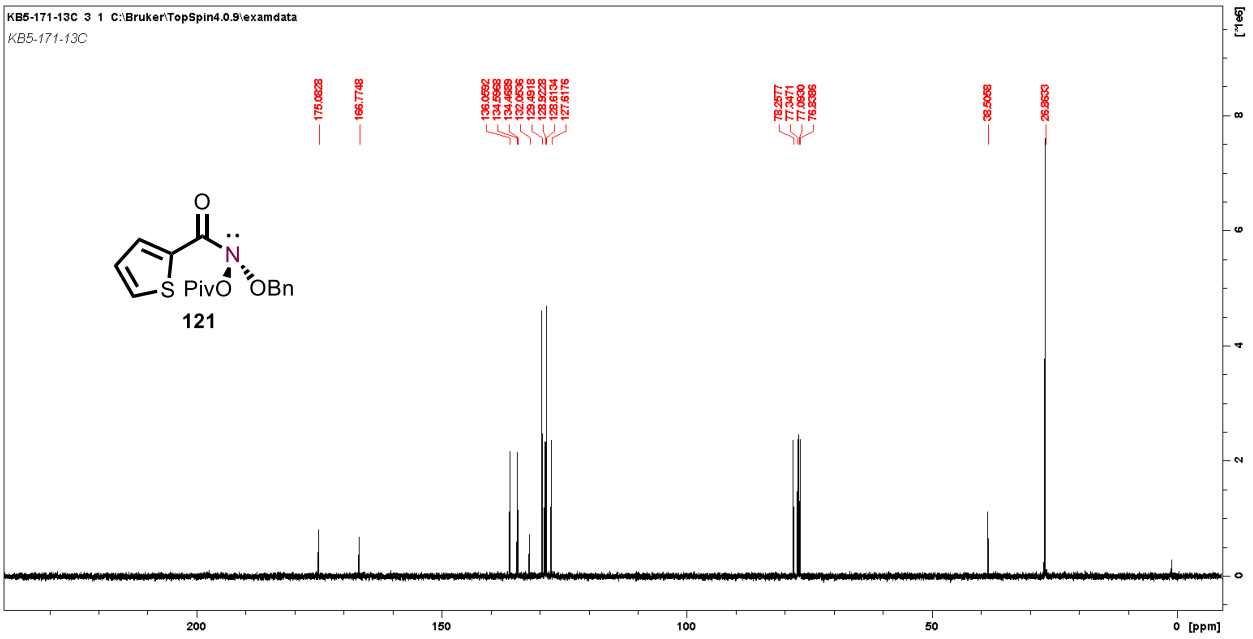

Figure 4.99. $^{13}C\{^{1}H\}$ NMR spectrum of *N*-(benzyloxy)-*N*-(pivaloyloxy)thiophene-2-carboxamide (**121**) in $CDCl_3$, 101 MHz.

4.6. References.

1. Glover, S. A. S_N2 Reactions at Amide Nitrogen – Theoretical Models for Reactions of Mutagenic *N*-acyloxy-*N*-alkoxyamides with Bionucleophiles. *ARKIVOC* **2002,** *2001* (12), 143-160.

2. Johns, J. P.; van Losenoord, A.; Mary, C.; Garcia, P.; Pankhurst, D. S.; Rosser, A. A.; Glover, S. A. Thermal Decomposition of *N*-Acyloxy-*N*-alkoxyamides – A New HERON Reaction. *Aust. J. Chem.* **2010,** *63* (12), 1717-1729.

3. Glover, S. A.; Rauk, A.; Buccigross, J. M.; Campbell, J. J.; Hammond, G. P.; Mo, G.; Andrews, L. E.; Gillson, A.-M. E. The HERON Reaction — Origin, Theoretical Background, and Prevalence. *Can. J. Chem.* **2005,** *83* (9), 1492-1509.

4. Glover, S. A. Anomeric Amides — Structure, Properties and Reactivity. *Tetrahedron* **1998,** *54* (26), 7229-7271.

5. Glover, S. A.; Rosser, A. A. Heteroatom Substitution at Amide Nitrogen—Resonance Reduction and HERON Reactions of Anomeric Amides. *Molecules* **2018,** *23* (11).

6. Cavanagh, K. L.; Glover, S. A.; Price, H. L.; Schumacher, R. R. S_N2 Substitution Reactions at the Amide Nitrogen in the Anomeric Mutagens, *N*-Acyloxy-*N*-alkoxyamides. *Aust. J. Chem.* **2009,** *62* (7), 700-710.

7. Glover, S. A.; Rosser, A. A.; Taherpour, A.; Greatrex, B. W. Formation and HERON Reactivity of Cyclic *N*,*N*-Dialkoxyamides. *Aust. J. Chem.* **2014,** *67* (3), 507-520.

8. Digianantonio, K. M.; Glover, S. A.; Johns, J. P.; Rosser, A. A. Synthesis and Thermal Decomposition of *N*,*N*-Dialkoxyamides. *Org. Biomol. Chem.* **2011,** *9* (11), 4116-4126.

9. Glover, S. A.; Mo, G.; Rauk, A. HERON Rearrangement of *N*,*N*′-diacyl-*N*,*N*′-dialkoxyhydrazines — A Theoretical and Experimental Study. *Tetrahedron* **1999,** *55* (11), 3413-3426.

10. Buccigross, J. M.; Glover, S. A. Molecular Orbital Studies of Novel N to C Migrations in *N*,*N*-bisheteroatom-substituted Amides—HERON Rearrangements. *J. Chem. Soc. Perkin Trans. II.* **1995,** (3), 595-603.

11. Alabugin, I. V.; Kuhn, L.; Krivoshchapov, N. V.; Mehaffy, P.; Medvedev, M. G. Anomeric Effect, Hyperconjugation and Electrostatics: Lessons from Complexity in a Classic Stereoelectronic Phenomenon. *Chem. Soc. Rev.* **2021,** *50* (18), 10212-10252.

12. Campbell, J. J.; Glover, S. A. Bimolecular Reactions of Mutagenic *N*-acetoxy-*N*-alkoxybenzamides and *N*-methylaniline. *J. Chem. Soc. Perkin Trans. II.* **1992,** (10), 1661-1663.

13. Andrews, L. E.; Bonin, A. M.; Fransson, L. E.; Gillson, A.-M. E.; Glover, S. A. The Role of Steric Effects in the Direct Mutagenicity of *N*-acyloxy-*N*-alkoxyamides. *Mutat. Res. Genet. Toxicol. Environ. Mutagen.* **2006,** *605* (1), 51-62.

14. Gerdes, R. G.; Glover, S. A.; ten Have, J. F.; Rowbottom, C. A. *N*-acetoxy-*N*-alkoxyamides - A New Class of Nitrenium Ion Precursors which are Mutagenic. *Tet. Lett.* **1989,** *30* (20), 2649-2652.

15. Glover, S. A.; Schumacher, R. R.; Bonin, A. M.; Fransson, L. E. Steric Effects on the Direct Mutagenicity of *N*-acyloxy-*N*-alkoxyamides—Probes for Drug–DNA Interactions. *Mutat. Res. Genet. Toxicol. Environ. Mutagen.* **2011,** *722* (1), 32-38.

16. Zhang, L.; Geng, Y.; Jin, Z. Transition-Metal-Free Synthesis of *N*-Aryl Hydroxamic Acids via Insertion of Arynes. *J. Org. Chem.* **2016,** *81* (9), 3542-3552.

17. Kikugawa, Y.; Shimada, M. Intramolecular Cyclization with Nitrenium Ions Generated from *N*-Chloro-*N*-methoxyamides in Neutral Conditions. *Chem. Lett.* **1987,** *16* (9), 1771-1774.

18. Kikugawa, Y.; Kawase, M. Electrophilic aromatic substitution with a nitrenium ion generated from N-chloro-N-methoxyamides. Application to the synthesis of 1-methoxy-2-oxindoles. *J. Am. Chem. Soc.* **1984,** *106* (19), 5728-5729.

19. Mintz, M. J.; Walling, C. *t*-Butyl Hypochlorite. *Org. Synth.* **1969,** *49*.

20. Buurman, C.; Resoort, G.; Plaschkes, A. Scaling-up Rules for Solids Suspension in Stirred Vessels. *Chem. Eng. Sci.* **1986,** *41* (11), 2865-2871.

21. Gaspa, S.; Porcheddu, A.; De Luca, L. Metal-free Oxidative Self-coupling of Aldehydes or Alcohols to Symmetric Carboxylic Anhydrides. *Tet. Lett.* **2017,** *58* (26), 2533-2536.

22. Wang, X.-Y.; Shang, Z.-P.; Zha, G.-F.; Chen, X.-Q.; Bukhari, S. N. A.; Qin, H.-L., $[Ru(bpy)_3]Cl_2$-catalyzed Aerobic Oxidative Cleavage β-diketones to Carboxylic Acids under Visible Light Irradiation. *Tet. Lett.* **2016,** *57* (50), 5628-5631.

23. Levin, D. Managing Hazards for Scale Up of Chemical Manufacturing Processes. In *Managing Hazardous Reactions and Compounds in Process Chemistry*, American Chemical Society: 2014; Vol. 1181, pp 3-71.

24. Bordwell, F. G.; Lynch, T. Y. Radical Stabilization Energies and Synergistic (Captodative) Effects. *J. Am. Chem. Soc.* **1989,** *111* (19), 7558-7562.

25. Viehe, H. G.; Janousek, Z.; Merenyi, R.; Stella, L. The Captodative Effect. *Acc. Chem. Res.* **1985,** *18* (5), 148-154.

26. Peterson, J. P.; Winter, A. H. Solvent Effects on the Stability and Delocalization of Aryl Dicyanomethyl Radicals: The Captodative Effect Revisited. *J. Am. Chem. Soc.* **2019,** *141* (32), 12901-12906.

27. Norman, R. O. C.; Purchase, R.; Thomas, C. B.; Aylward, J. B. Reactions of lead(IV). Part XXV. Oxidation of Some Benzyl-substituted Hydrazine Derivatives. *J. Chem. Soc. Perkin Trans. I* **1972,** (0), 1692-1700.

28. Crawford, R. J.; Raap, R. The Synthesis and Reactions of *N,N*'-Dicarbalkoxy-*N,N*'-dialkoxyhydrazines and Some Observations on Carbalkoxylium Ions. *J. Org. Chem.* **1963,** *28* (9), 2419-2424.

29. Cooley, J. H.; Stone, D. M.; Oguri, H. Electronic Effects in Multicenter Rearrangements of Compounds with Nitrogen-Nitrogen Bonds. *J. Org. Chem.* **1977,** *42* (18), 3096-3097.

30. De Almeida, M. V.; Barton, D. H. R.; Bytheway, I.; Ferreira, J. A.; Hall, M. B.; Liu, W.; Taylor, D. K.; Thomson, L. Preparation and Thermal Decomposition of *N,N*'-Diacyl-*N,N*'-Dialkoxyhydrazines: Synthetic Applications and Mechanistic Insights. *J. Am. Chem. Soc.* **1995,** *117* (17), 4870-4874.

31. Subbaiah, M. A. M.; Meanwell, N. A. Bioisosteres of the Phenyl Ring: Recent Strategic Applications in Lead Optimization and Drug Design. *J. Med. Chem.* **2021,** *64* (19), 14046-14128.

32. Abboud, J. L. M.; Mo, O.; de Paz, J. L. G.; Yanez, M.; Esseffar, M.; Bouab, W.; El-Mouhtadi, M.; Mokhlisse, R.; Ballesteros, E. Thiocarbonyl *versus* Carbonyl Compounds: A Comparison of Intrinsic Reactivities. *J. Am. Chem. Soc.* **1993,** *115* (26), 12468-12476.

33. Rudchenko, V. F.; Shevchenko, V. I.; Kostyanovskii, R. G. Geminal systems. Communication 28 Alcoholysis of *N*-chloro-*N*-alkoxyamides and Synthesis of *N,N*-dialkoxyureas. *Bull. Acad. Sci. USSR, Div. Chem. Sci.* **1986,** *35* (3), 543-551.

34. Shtamburg, V. G.; Klots, E. A.; Pleshkova, A. P.; Avramenko, V. I.; Ivonin, S. P.; Tsygankov, A. V.; Kostyanovsky, R. G. Geminal Systems. 50. Synthesis and Alcoholysis of *N*-acyloxy-*N*-alkoxy derivatives of ureas, carbamates, and benzamides. *Russian Chemical Bulletin* **2003,** *52* (10), 2251-2260.

35. Feng, C.; Loh, T.-P. Rhodium-Catalyzed C-H Alkynylation of Arenes at Room Temperature. *Angew. Chem. Int. Ed.* **2014,** *53* (10), 2722-2726.

36. Chen, X.; Han, J.; Zhu, Y.; Yuan, C.; Zhang, J.; Zhao, Y. Transformation of Masked Benzyl Alcohols to *o*-Aminobenzaldehydes through C–H Activation: A Facile Approach to Quinazolines. *Chem. Commun.* **2016,** *52* (67), 10241-10244.

37. Cecere, G.; König, C. M.; Alleva, J. L.; MacMillan, D. W. C. Enantioselective Direct α-Amination of Aldehydes *via* a Photoredox Mechanism: A Strategy for Asymmetric Amine Fragment Coupling. *J. Am. Chem. Soc.* **2013,** *135* (31), 11521-11524.

38. San Jose, G.; Jackson, E. R.; Uh, E.; Johny, C.; Haymond, A.; Lundberg, L.; Pinkham, C.; Kehn-Hall, K.; Boshoff, H. I.; Couch, R. D.; Dowd, C. S. Design of Potential Bisubstrate Inhibitors against *Mycobacterium tuberculosis* (Mtb) 1-Deoxy-d-xylulose 5-Phosphate Reductoisomerase (Dxr)—Evidence of a Novel Binding Mode. *MedChemComm* **2013,** *4* (7), 1099-1104.

39. Ishihara, K.; Katsutani, N.; Aoki, T. A Metabonomics Study of the Hepatotoxicants Galactosamine, Methylene Dianiline and Clofibrate in Rats. *Basic Clin. Pharmacol. Toxicol.* **2006,** *99* (3), 251-260.

40. Manker, D. C.; Faulkner, D. J. Diterpenes from the Marine Pulmonate Trimusculus Reticulatus. *Tetrahedron* **1987,** *43* (16), 3677-3680.

41. Kim, D. E.; Lee, Y. J.; Jun, J. H; Jung, S.-H.; Gong, J. S.; Lee, C. H. Ligand Compound, Transition Metal Compound, and Catalyst Composition Containing Same. WO2018088820, May. 17, 2018.

42. Newton, J.; Driedger, D.; Nodwell, M. B.; Schaffer, P.; Martin, R. E.; Britton, R.; Friesen, C. M. A Convenient Synthesis of Difluoroalkyl Ethers from Thionoesters Using Silver(I) Fluoride. *Chem. Eur. J.* **2019,** *25* (70), 15993-15997.

43. Sharma, N.; Saha, R.; Parveen, N.; Sekar, G. Palladium-Nanoparticles-Catalyzed Oxidative Annulation of Benzamides with Alkynes for the Synthesis of Isoquinolones. *Adv. Synth. Catal.* **2017,** *359* (11), 1947-1958.

CHAPTER 5

Mechanistic Studies of Tungsten-Alkylidyne Photoredox-Catalyzed C-H Arylation Reactions and the Synthesis of a Sterically Protected Tungsten-Alkylidyne Complex

5.1. Introduction.

Photoredox-catalyzed C-H arylation has been highly explored in recent years as a novel method of C-C bond formation.[1-6] Photoredox catalysts are chromophores that absorb light to generate an excited state that is simultaneously a stronger oxidant and reductant relative to the ground state (Figure 5.1).[7] While many photoredox-catalyzed transformations involve the chromophore acting as an oxidant, the focus of this chapter will be chromophores that catalyze C-H arylation *via* photoreduction. The strongest commercially available photoreductant chromophore previously employed for C-H arylation is *fac*-Ir(ppy)$_3$ ($E^{*/ox}$ = −2.15 V vs. $FeCp_2^{0/+}$ in DMF[*]).[7, 8] The excited-state oxidation potential of a photoredox chromophore defines the substrate scope for its synthetic applications. In some instances, this has resulted in the use of easy-to-reduce compounds such as aryl diazonium salts ([PhN_2][PF_6], E^{red} = −0.046 V vs $FeCp_2^{0/+}$ in acetonitrile)[7] and hypervalent iodide salts ([Ph_2I][PF_6], E^{red} = −0.6 V vs $FeCp_2^{0/+}$)[4] as substrates in photoredox-catalyzed C-H arylation reactions.[3, 4, 6] There are significant drawbacks to the use of these substrates; namely the instability of diazonium salts and the cost of hypervalent iodide salts renders these reactions impractical on an industrial scale.[4, 9]

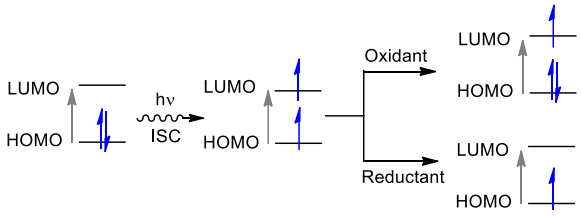

Figure 5.1. Ground-state and excited-state redox potentials of photoredox chromophores.

[*] Literature values reported as referenced to SCE are converted using the solvent dependent conversion factors reported by Connelly and Geiger (Ref. 8).

Unactivated aryl halides are desirable substrates for C-H arylation but have been previously out of range of the excited-state oxidation potentials of available photoreduction chromophores.[3, 10] For example, the reduction potentials of PhI, PhBr and PhCl are −2.63 V in acetonitrile, −2.89 V in DMF, and −3.23 V in DMF vs $FeCp_2^{0/+}$, respectively, which places them ≥0.5 V uphill from $Ir(ppy)_3$*.[11, 12] The Hopkins Group has developed a series of tungsten-alkylidyne visible-light chromophores of the type $W(CAr)L_4X$ (where Ar is an aryl group, L is an equatorial phosphine ligand and X is a halide) with tunable excited state oxidation potentials as low as −3.2 V vs. $FeCp_2^{0/+}$.[13] The tunability of the photoredox potentials of these compounds is based on their symmetry-orthogonal frontier orbitals. The HOMO is d_{xy}, which is of π (or π*) symmetry with respect to the L ligands and nonbonding with respect to the CAr and X ligands, and LUMO is π*(WCAr) and additionally interacts with X. Thus, the energy of the HOMO is controlled by the nature of the L substituents and the energy of the LUMO is controlled by the Ar and X substituents (Figure 5.2a-b).[13] Dr. Hunter Vibbert, a former student in the Hopkins Group, has successfully used these chromophores in visible-light photoredox-catalyzed C-H arylation reactions of unactivated aryl halides.[14] The postulated mechanism for this transformation begins with reduction of an aryl halide by the chromophore to form an aryl radical, which reacts with a radical acceptor (pyrrole, arene) to generate an enyl intermediate. In the presence of the exogenous base 1,1,3,3-tetramethylguanidine (TMG), the chromophore is regenerated and the C-H arylation product is produced (Figure 5.2c).[14] The fine details regarding the conversion of the intermediate to product and the regeneration of the chromophore are not known, however. In this chapter, the mechanism by which the enyl intermediate loses both a proton and an electron to generate C-H arylation product is explored. The experiments are conducted using $W(CPh)(depe)_2Cl$ (**1**) ($E^{*/ox}$ = −2.78 V vs. $FeCp_2^{0/+}$ in THF)[13] (depe, 1,2-bis(diethylphosphino)ethane) because preliminary

results have shown this chromophore has greater air stability than the W(CAr)(dmpe)$_2$Cl chromophores (dmpe = 1,2-bis(dimethylphosphine)ethane) used in the earlier photoredox studies.

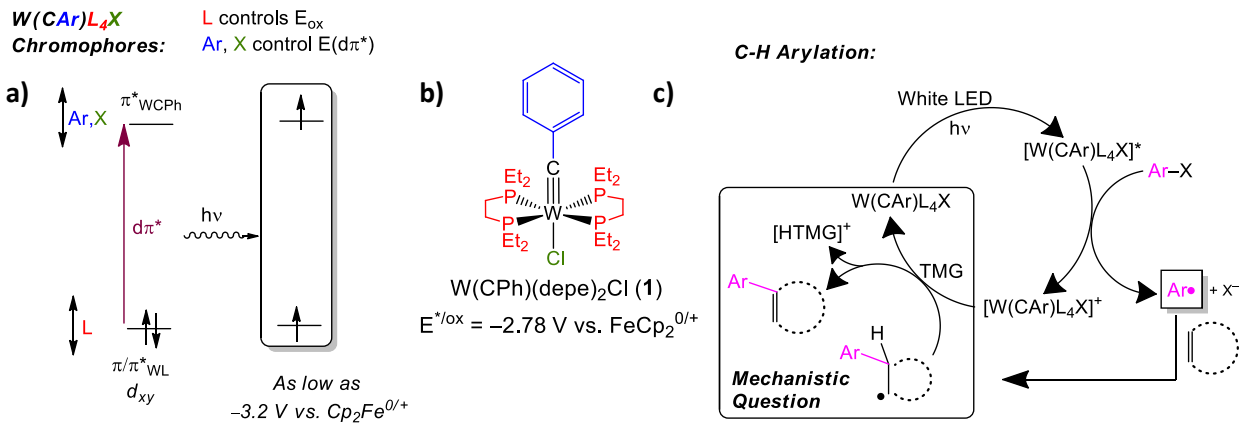

Figure 5.2. a) W(CAr)L$_4$X chromophores with tunable HOMO and LUMO orbitals achieve excited-state oxidation potentials as low as −3.2 V vs. $FeCp_2^{0/+}$. **b)** The tungsten-alkylidyne chromophore W(CPh)(depe)$_2$Cl (**1**) used in this chapter containing equatorial depe ligands. **c)** Proposed catalytic cycle for tungsten photoredox-catalyzed C-H arylation including key mechanistic question addressed in this chapter.

The formation of the C-H arylation product from the enyl intermediate requires either loss of a hydrogen atom or of an electron and proton. This could proceed in one of two ways. One way it could proceed is through a multisite-proton-coupled electron-transfer (PCET) reaction[15, 16] in which the oxidized chromophore [W(CAr)L$_4$X]$^+$ is reduced by the enyl intermediate to regenerate W(CAr)L$_4$X and the exogenous base TMG deprotonates the enyl intermediate (Figure 5.3). In principle, either sequence of these two events—oxidation/deprotonation or deprotonation/oxidation—is possible, with operative sequence being determined by the relative pK_as and redox potentials of the reactants. This multisite-PCET mechanism has been broadly invoked in the literature for photoreduction catalyzed C-H functionalization chemistry.[6, 17-29] Alternatively, the C-H arylation product could be produced by a proton-coupled electron-transfer between the oxidized chromophore and the enyl intermediate to generate the tungsten-hydride complex [HW(CAr)L$_4$X]$^+$. Deprotonation of photogenerated [HW(CAr)L$_4$X]$^+$ by TMG would restore the chromophore (Figure 5.4) and complete the catalytic cycle. Several examples of such

seven-coordinate tungsten–alkylidyne hydride species have been prepared and studied including the ion $[HW(CPh)(dmpe)_2Cl]^+$,[30] which is interconvertible with the photoredox chromophore $W(CPh)(dmpe)_2Cl$ (**2**) employed in earlier studies through reversible Brønsted acid-base reactions. Additionally, our group has previously shown that an analogous oxidized $[W(CPh)(dppe)_2Cl]^+$ complex can react with dihydrogen to generate $[HW(CPh)(dppe)_2Cl]^+$,[31] which is suggestive of a PCET reaction (Figure 5.4). This type of chromophore-centered mechanism has not been reported to occur in C-H arylation reactions catalyzed by visible-light photoreduction chromophores, and if operative would be a novel reaction pathway.

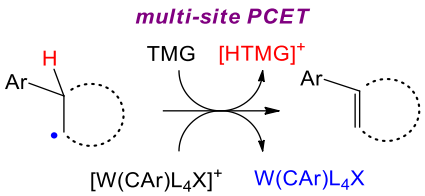

Figure 5.3. Potential multisite-proton-coupled electron-transfer mechanism in which the enyl intermediate loses a proton to the exogenous base and an electron to the oxidized chromophore.

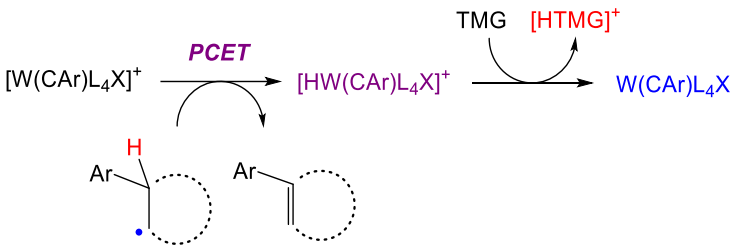

Figure 5.4. Potential proton-coupled electron-transfer mechanism in which the enyl intermediate reacts with oxidized chromophore to generate a tungsten-hydride species.

In this chapter, the $[HW(CPh)(depe)_2Cl]^+$ cation is first isolated to demonstrate that this is a feasible catalytic intermediate. A stoichiometric reaction between $W(CPh)(depe)_2Cl$ and aryl halide in the presence of radical acceptor is conducted and $[HW(CPh)(depe)_2Cl]^+$ and C-H arylation product are produced, suggesting that PCET between an enyl intermediate and oxidized chromophore is a viable reaction pathway. DFT calculations are used to study the possible PCET

mechanisms for this transformation and suggest that ET-PT is thermodynamically favourable while PT-ET is not. Catalytic and stoichiometric reactions are performed with different radical acceptors to determine whether the mechanism is ET-PT or HAT. Additionally, the synthesis of a new, sterically bulky tungsten-alkylidyne complex W(CPh)(diBupe)$_2$Cl (**3**) is discussed.

5.2. Results and Discussion.

5.2.1. Synthesis and Characterization of [HW(CPh)(depe)$_2$Cl][BAr^{F24}] ([1H][BAr^{F24}]).

In view of the mechanistic considerations outlined in the introduction, we were interested in synthesizing the tungsten-alkylidyne hydride complex [HW(CPh)(depe)$_2$Cl] ([**1H**]$^+$), which is a potential intermediate in the photoredox reaction (Figure 5.4). Previous work by the Hopkins and Schrock groups demonstrated that d^2 tungsten-alkylidyne complexes of the type W(CR)L$_4$X are strong Brønsted bases that react with protons to generate seven-coordinate tungsten- alkylidyne hydride complexes of form [HW(CR)L$_4$X]$^+$.[31, 32] Following the method previously by Newsom *et al.*,[31] a THF solution of **1** was treated with ethereal HCl resulting in the bleaching of the colour and the production of a white precipitate, presumably [HW(CPh)(depe)$_2$Cl]Cl ([**1H**]Cl). Salt metathesis with NaBAr^{F24} (BAr^{F24-} = tetrakis(3,5-bis(trifluoromethyl)phenyl)borate)) was used to provide a salt with greater solubility in organic solvents, providing off-white [**1H**][BAr^{F24}] in 30% yield post recrystallization (Scheme 5.1). [**1H**][BAr^{F24}] was characterized with ^{1}H-, ^{31}P{^{1}H}-, ^{13}C{^{1}H}-, and ^{19}F{^{1}H}-NMR spectroscopy as well as HR-MS and single-crystal X-ray diffraction.

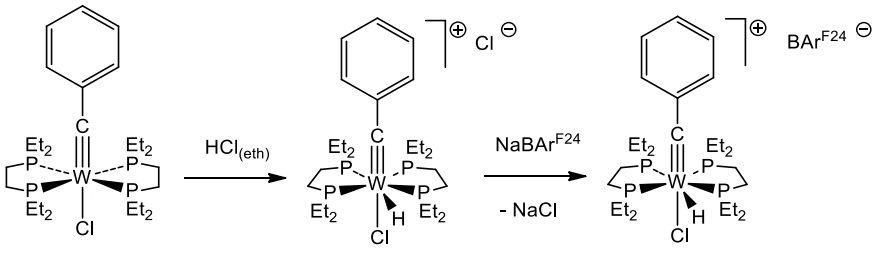

Scheme 5.1. Synthesis of [HW(CPh)(depe)$_2$Cl][BAr^{F24}] ([**1H**][BAr^{F24}]).

The NMR spectra of [**1H**][BAr^{F24}] are consistent with the cation being fluxional, as observed for other $[HW(CR)L_4X]^+$ ions.[30-32] The fluxionality has been described as involving rapid conversion between benzylidyne hydride and benzylidene tautomers on the NMR timescale.[32] The signatures of this for [**1H**][BAr^{F24}] are that the $^{31}P\{^1H\}$ NMR spectrum exhibits one very broad peak at room temperature and the $^{13}C\{^1H\}$ NMR spectrum exhibits two resonances for both the $P\underline{C}H_2CH_3$ and $PCH_2\underline{C}H_3$ functionalities as opposed to four distinct signals (Figure 5.43). This is consistent with the NMR data reported for $[HW(CPh)(dmpe)_2Cl]^+$ ([**2H**]$^+$) by Dr. Chris Hansen.[30] The ^1H NMR resonance of the hydride ligand is not visible due to overlap other resonances in the aliphatic region. The resonance for the hydride ligand may lie under the $PC\underline{H}_2C\underline{H}_2P$ resonance because the latter has an integration of greater than 4 protons (Figure 5.40). The ^1H NMR resonance of the hydride ligand for the analogous complex [**2H**]$^+$ is also shown to be in the aliphatic region.[30] Because the NMR spectra do not allow identification of all nuclei, high resolution mass spectrometry was used to verify that a hydride complex is indeed produced. The experimental *m/z* ratio of 721.2323 closely matches the predicted molecular weight of 721.2361 (Figure 5.48). The X-ray crystal structure was also obtained.

Crystals of [**1H**][BAr^{F24}] were grown from concentrated acetonitrile solution and the structure (Figure 5.5a) is shown to be analogous with the 7-coordinate, pentagonal-bipyramidal geometry found in the crystal structure of $[HW(CPh)(dmpe)_2Cl][BAr^{F20}]$ ([**2H**][BAr^{F20}]) obtained by Dr. Chris Hansen.[30] The chloride and benzylidyne functionalities of [**1H**]$^+$ are linear (C(1)W(1)Cl(1) = 177.0(2)° and occupy the axial sites of the structure, while the phosphine ligands occupy the equatorial sites (C(1)W(1)P(avg) = 91.7[2]°). The hydride atom is not detected or modelled in the crystal structure of [**1H**]$^+$, however the P(1)W(1)P(4) angle of 117.99(6)° matches the angle of 119.13(3)° in the structure of [**2H**][BAr^{F20}], in which the hydride ligand was observed

(Table 5.1).[30] Additionally, the structure of [**1H**]$^+$ was computed by DFT with Gaussian 16[33] using the B3P86 functional (Figure 5.5b).[34] The Dunning (DZP) basis set[35] was used for atoms H, C, P, Cl and the LANL2DZ basis set with effective core potentials was used for W.[36] The geometry of the DFT structure is in reasonable agreement with the geometry of the crystal structure except for the W–Cl bond length, which is substantially longer in the calculated structure than the crystal structure (Table 5.1).

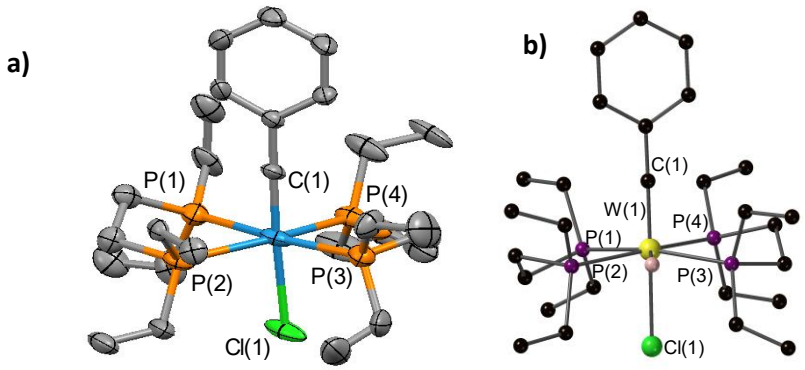

Figure 5.5. a) Molecular structure of [HW(CPh)(depe)$_2$Cl]$^+$ ([**1H**]$^+$) (50% probability ellipsoids). Hydrogen atoms, disordered atoms and BAr^{F24-} counterion omitted for clarity. **b)** DFT computed structure of [HW(CPh)(depe)$_2$Cl]$^+$ ([**1H**]$^+$). Hydrogen atoms removed for clarity.

Parameter	[HW(CPh)(depe)$_2$Cl]$^+$ crystal structure	[HW(CPh)(depe)$_2$Cl]$^+$ DFT structure	[HW(CPh)(dmpe)$_2$Cl]$^+$ crystal structure[30]
W(1)-Cl(1) (Å)	2.555(2)	2.674	2.5362(11)
W(1)-P(1) (Å)	2.462(2)	2.506	2.4466(9)
W(1)-P(2) (Å)	2.550(2)	2.582	2.5600(9)
W(1)-P(3) (Å)	2.549(2)	2.572	2.5599(9)
W(1)-P(4) (Å)	2.490(2)	2.507	2.4623(8)
W(1)-C(1) (Å)	1.804(7)	1.808	1.809(3)
W(1)-H (Å)	-	1.718	1.64(3)
P(1)W(1)P(2) (°)	79.02(7)	77.613	76.94(3)
P(1)W(1)P(4) (°)	86.76(7)	86.347	86.45(3)
P(2)W(1)P(3) (°)	117.99(6)	117.300	119.13(3)
P(2)W(1)P(4) (°)	75.85(6)	77.230	76.96(3)
Σ**PW**(1)**P** (°)	359.62[7]	358.49	359.48[3]
C(1)**W**(1)**P**(avg) (°)	91.7[2]	93.9	92.91[10]
C(1)**W**(1)**Cl**(1) (°)	177.0(2)	177.0	179.09(10)

Table 5.1. Comparison of structural parameters between the crystal structures of [**1H**]$^+$ and [**2H**]$^+$ and the DFT structure of [**1H**]$^+$.

5.2.2. Production of [1H]$^+$ as a C-H Arylation Reaction Intermediate.

The synthesis and characterization of [**1H**][BAr^{F24}] shows that [**1H**]$^+$ is viable as a potential intermediate in photoredox-driven C-H arylation reactions. To determine if [**1H**]$^+$ could be produced under photoredox conditions, a stoichiometric photo-reaction between **1** and an aryl halide in the presence of radical acceptor was conducted in the absence of exogenous base. 2-Chlorobenzonitrile was chosen as the aryl halide and *N*-methylpyrrole was chosen as the radical acceptor because previous studies by Dr. Vibbert demonstrated this reaction quantitatively forms the C-H arylation product at 2 mol% photocatalyst loading in acetonitrile.[14] Irradiation of an NMR-scale reaction mixture of 1 equivalent of 2-chlorobenzonitrile, 1 equivalent of **1**, and 10 equivalents of *N*-methylpyrrole in CD_3CN for 24 hours resulted in complete consumption of 2-chlorobenzonitrile, and formation of [**1H**]$^+$ and the C-H arylation product 2-(1-methyl-1H-pyrrol-2-yl)benzonitrile (**4**) in a 1:1 ratio. As seen in the ^{1}H-NMR spectrum shown in Figure 5.6, the integrated intensities demonstrate molar ratio of 1.03:1. The ^{1}H NMR spectrum is very clean, consistent with the product being formed in high yield. The identity of the C-H arylation product and [**1H**]$^+$ were verified by comparison to authentic samples of **4** and [**1H**][BAr^{F24}] in CD_3CN, respectively (Figures 5.7 - 5.10). This experiment shows that a PCET reaction between an enyl intermediate and [**1**]$^+$ to generate a hydride complex as a catalytic intermediate is a feasible reaction pathway (Figure 5.4).

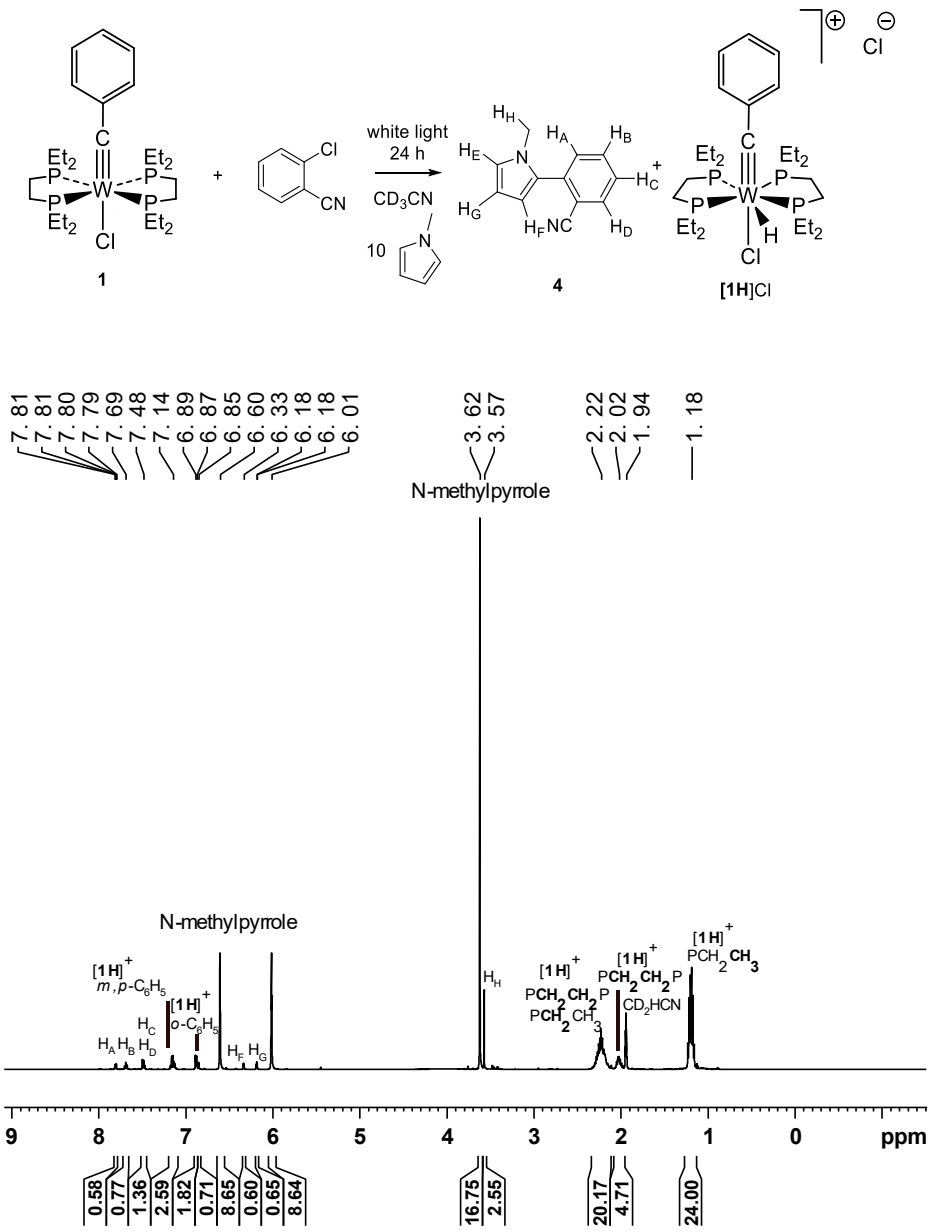

Figure 5.6. ^{1}H NMR spectrum (500.13 MHz, CD_3CN) of the stoichiometric reaction between 2-chlorobenzonitrile and W(CPh)(depe)$_2$Cl (**1**) with 10 equivalents of *N*-methylpyrrole after 24 hours of irradiation with white light shows [HW(CPh)(depe)$_2$Cl]$^+$ [**1H**]$^+$ and C-H arylation product **4**. Expanded spectra are shown in Figures 5.9–5.12.

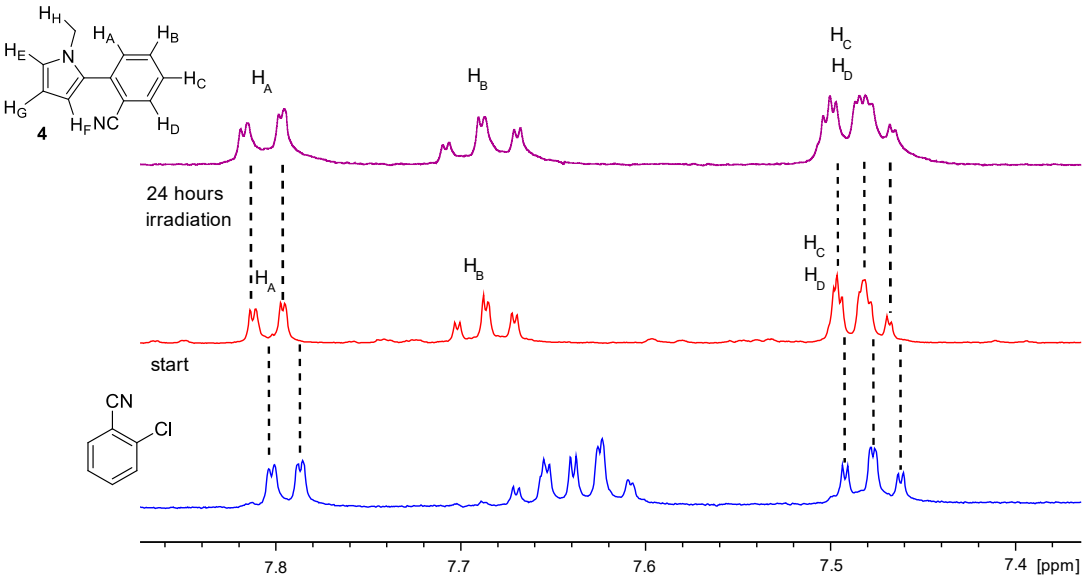

Figure 5.7. ^{1}H NMR spectra (500.13 MHz, CD_3CN) of the aromatic region of the stoichiometric reaction between 2-chlorobenzonitrile and W(CPh)(depe)$_2$Cl (**1**) with 10 equivalents of N-methylpyrrole before (bottom) and after 24 hours of irradiation (middle) shows consumption of 2-chlorobenzonitrile and production of **4** in comparison with authentic product (top).

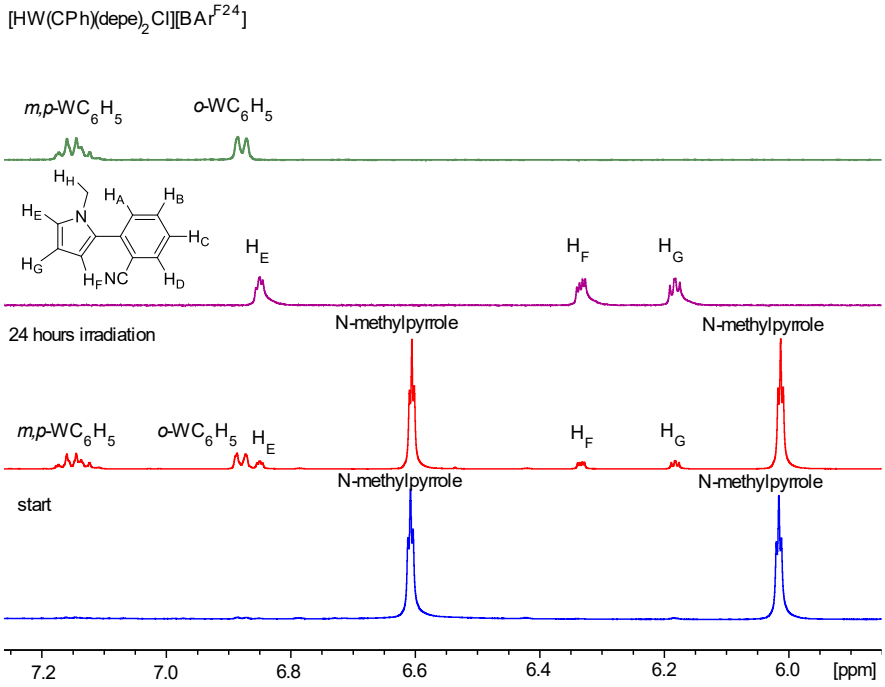

Figure 5.8. Additional ^{1}H NMR spectra (500.13 MHz, CD_3CN) of the aromatic region of the stoichiometric reaction between 2-chlorobenzonitrile and W(CPh)(depe)$_2$Cl (**1**) with 10 equivalents of N-methylpyrrole and the absence of any base before (bottom) and after 24 hours of irradiation (second from bottom) shows production of **4** and [HW(CPh)(depe)$_2$Cl]$^+$ ([**1H**]$^+$) in comparison with authentic products (top two spectra).

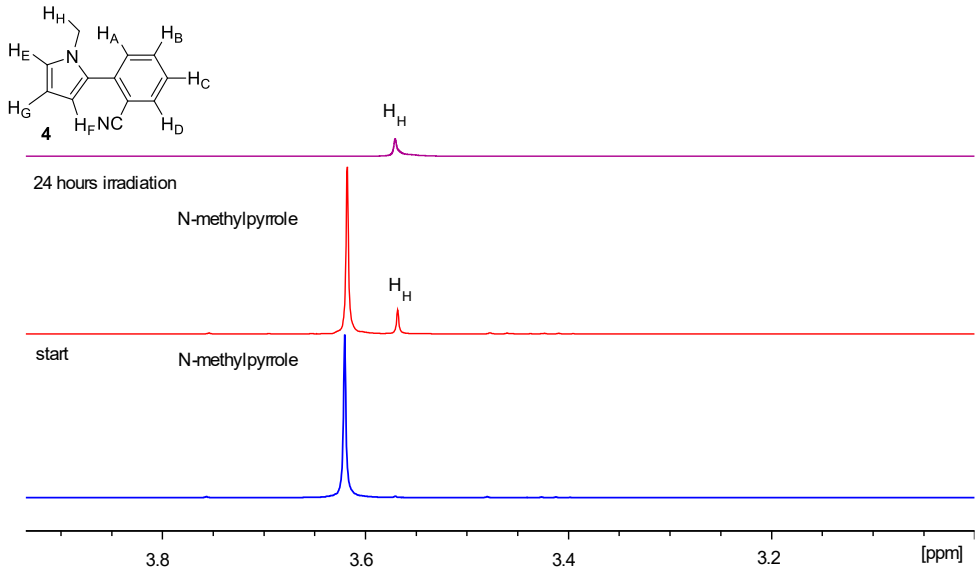

Figure 5.9. ^{1}H NMR spectra (500.13 MHz, CD_3CN) of the aliphatic region of the stoichiometric reaction between 2-chlorobenzonitrile and W(CPh)(depe)$_2$Cl (**1**) with 10 equivalents of N-methylpyrrole and the absence of any base before (bottom) and after 24 hours of irradiation (middle) shows production of **4** in comparison with authentic product (top).

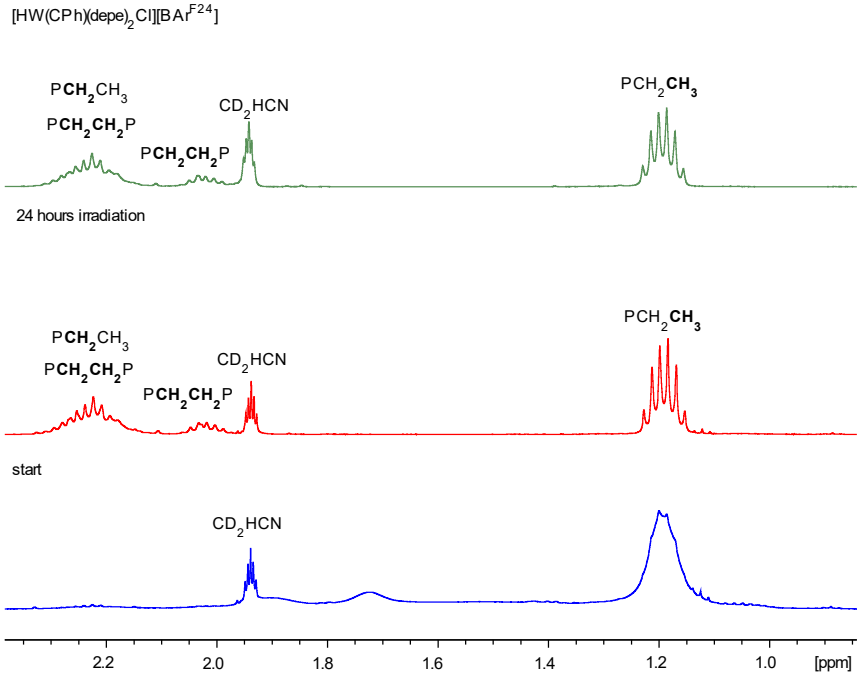

Figure 5.10. Additional ^{1}H NMR spectra (500.13 MHz, CD_3CN) of the aliphatic region of the stoichiometric reaction between 2-chlorobenzonitrile and W(CPh)(depe)$_2$Cl (**1**) with 10 equivalents of N-methylpyrrole and the absence of any base before (bottom) and after 24 hours of irradiation (middle) shows production of [HW(CPh)(depe)$_2$Cl]$^+$ ([**1H**]$^+$) in comparison with authentic product (top).

5.2.3 DFT Calculations of pK_as and Redox Potentials to Assess PCET Mechanistic Possibilities for the Production of $[1H]^+$.

The above sections demonstrated that [HW(CPh)(depe)$_2$Cl] ([**1H**]$^+$) is a stable, isolatable compound and that it forms stoichiometrically in a photo-driven reaction between **1**, haloarene, and radical acceptor in the absence of base. If a PCET pathway involving a [HW(CAr)L$_4$X]$^+$ tungsten-hydride complex is operative under catalytic conditions, there are three PCET mechanisms that must be considered.[37] The first pathway (ET-PT)[37] involves step-wise outer-sphere electron-transfer (ET) between the enyl intermediate and the oxidized chromophore [W(CAr)L$_4$X]$^+$ to regenerate W(CAr)L$_4$X and produce the oxidized intermediate (a carbocation). A subsequent proton-transfer (PT) between the carbocation and W(CAr)L$_4$X produces the C-H arylation product and [HW(CAr)L$_4$X]$^+$ (Figure 5.11). A second possible pathway is step-wise proton-transfer followed by electron-transfer (PT-ET).[37] Unreacted W(CAr)L$_4$X would first deprotonate the enyl intermediate (PT) to generate [HW(CAr)L$_4$X]$^+$ and a carbanion, which could then subsequently reduce [W(CAr)L$_4$X]$^+$ (ET) to regenerate W(CAr)L$_4$X and produce the C-H arylation product (Figure 5.12). The third possible pathway is concerted hydrogen atom transfer (HAT)[37] between the enyl intermediate and [W(CAr)L$_4$X]$^+$ to generate [HW(CAr)L$_4$X]$^+$ and C-H arylation product (Figure 5.13). In all three mechanisms, [HW(CAr)L$_4$X]$^+$ would be deprotonated by exogenous Brønsted base to close the catalytic cycle.

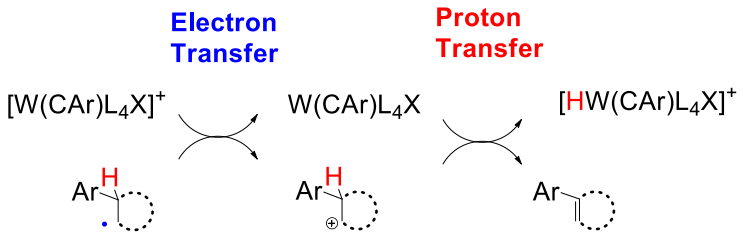

Figure 5.11. Step-wise outer-sphere electron-transfer (ET) followed by proton-transfer (PT) to generate C-H arylation product and a tungsten-hydride complex.

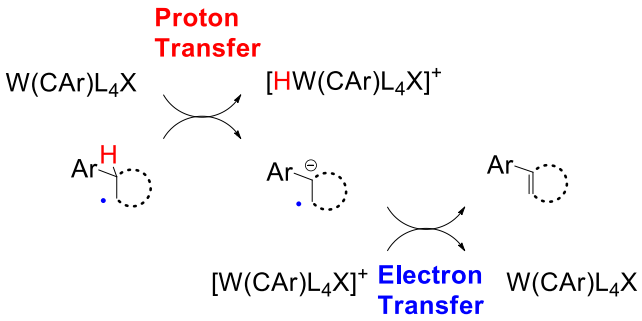

Figure 5.12. Step-wise proton transfer (PT) followed by outer-sphere electron-transfer (ET) to generate C-H arylation product and a tungsten-hydride complex.

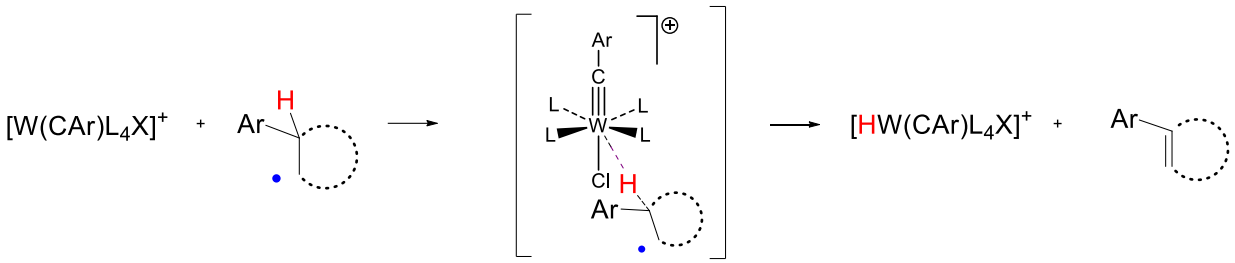

Figure 5.13. Concerted hydrogen atom transfer (HAT) to generate C-H arylation product a tungsten-hydride complex.

In order to assess which PCET pathway is operative, DFT calculations were performed to predict the pK_a and oxidation potential of enyl intermediates. The pK_a calculations were performed by Dr. Vibbert using Gaussian 16[33] with the exchange-correlation functional B3LYP,[38] the basis set 6-31+G* and solvation energies calculated by the IEFPCM model (integral equation formalism polarizable continuum) with acetonitrile (ε = 35.7).[39] The free energies of solvated protonated and deprotonated molecules are calculated and used to determine ΔG_T (T = total) of deprotonation (Figure 5.14, equation 5.1). ΔG_T is related to pK_α by equation 5.2, which is then converted to a corrected pK_a by application of an experimental anchor value for triethylamine (pK_a = 18.8)[40] as shown in equation 5.3. The validity of this method is demonstrated by comparing calculated pK_a values of organic acids in acetonitrile with the experimentally determined values; and a strong correlation was observed. As shown in Table 5.2 (entry i), the pK_a of the enyl

intermediate generated from pyrrole acceptor (**5**) is determined to be 43, which means that W(CPh)(depe)$_2$Cl (**1**) is not a strong enough base to depronotate it (pK_a [**1H**]$^+$ ≅ 23 (*vide infra*)).

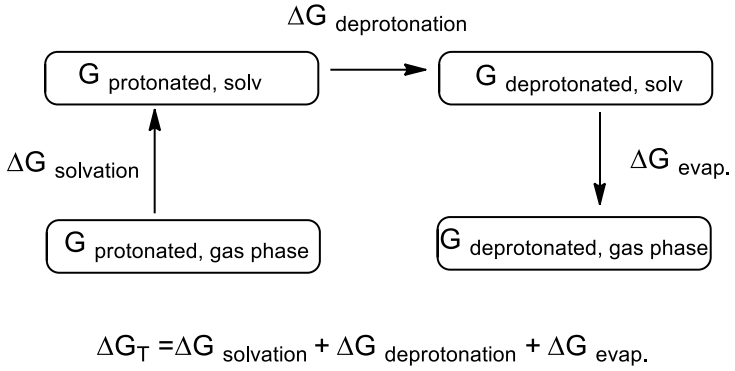

Figure 5.14. Relationship between free energy values used to determine ΔG_T of deprotonation.

$$\Delta G_T = G_{protonated,solv} - G_{deprotonated,solv} \quad (5.1)$$

$$pK_\alpha = \frac{\Delta G_T}{2.303RT} \quad (5.2)$$

$$pK_a^{calc} = \{pK_\alpha(HA) - pK_\alpha(HNEt_3)\} + 18.8 \quad (5.3)$$

Entry	Molecule	pK_a^{calc}
i	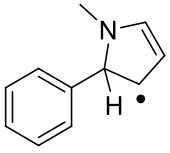 **5**	43
ii	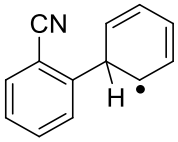 **6**	31
iii	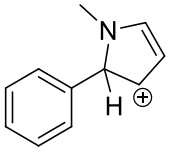 **7**	7

Table 5.2. DFT computed pK_a values of select enyl intermediates in acetonitrile.

Previous work has demonstrated that tungsten-alkylidyne complexes are strong bases.[31, 32] The pKa of $[HW(CPh)(dmpe)_2Cl]^+$ ($[\mathbf{2H}]^+$) was determined to 16.8(1) in THF by Dr. Newsom.[30] The pK_a of $[HW(CPh)(depe)_2Cl]^+$ ($[\mathbf{1H}]^+$) is approximated to be 22–24 in acetonitrile by two methods. First, the deprotonation of [**1H**][BAr^{F24}] by two equivalents of TMG was monitored by UV-vis (Scheme 5.2, Figure 5.15) and the absorbance of the resulting $W(CPh)(depe)_2Cl$ (**1**) product was measured. The absorbance was compared to that of a solution of **1** with known concentration and Beer's law is used to determine the equilibrium concentration of deprotonated complex. The equilibrium concentration of **1** was then used to determine the equilibrium concentration of TMG, $[HTMG]^+$ and $[\mathbf{1H}]^+$, and these concentrations are used to calculate a reaction equilibrium constant of 0.142 (equation 5.4). This provides $pK_a([\mathbf{1H}]^+) = 22.6$ by use of equation 5.5,[41] given that the pK_a of TMG in acetonitrile has been reported as 23.4.[42†] The second method for estimating the pK_a used a Bordwell cycle, which relates the pK_a and W-H bond dissociation free energy of $[HW(CPh)(depe)_2Cl]^+$ with the oxidation potential of $W(CPh)(depe)_2Cl$ (Figure 5.16; Equation 5.6). It was assumed that the W-H BDFE of $[HW(CPh)(depe)_2Cl]^+$ is the same as that previously calculated for $[\mathbf{2H}]^+$, using the Bordwell cycle and the measured pK_a of $[\mathbf{2H}]^+$ and oxidation potential of **2**. The BDFE of $[\mathbf{2H}]^+$ is calculated to be 70.11 in THF[13,30] and the measured oxidation potential ($E_{1/2}^{0/+}$) of **1** is –0.84 V vs. $FeCp_2^{0/+}$ in THF.[13] Using the solvent dependent conversion factor of 54.9 (C_G) for acetonitrile,[37] these values provide $pK_a([\mathbf{1H}]^+) = 23.5$. Taken together, these results eliminate the PT-ET pathway as a mechanistic possibility because **1** is not a strong enough base to deprotonate **5** ($pK_a^{DFT} = 43$). The reverse ET-PT sequence requires that **1** be a strong enough base to deprotonate the oxidized enyl intermediate **7**. A density functional theory calculation predicts that the pK_a of the oxidized intermediate is 7 (Table 5.2, entry iii),

† Value determined experimentally by reference 42 by titration and benchmarking to the pKa values of known phosphazene bases.

indicating it could be deprotonated by **1**. This suggests that an ET-PT pathway may be favourable if the enyl intermediate can be oxidized by [**1**]$^+$.

$$[HW(CPh)(depe)_2Cl][BAr^{F24}] + 2\ TMG \longrightarrow W(CPh)(depe)_2Cl + [HTMG][BAr^{F24}]$$

Scheme 5.2. Experimental deprotonation of [HW(CPh)(depe)$_2$Cl][BAr^{F24}] ([**1H**][BAr^{F24}]) with TMG showing the stoichiometry used to determine the concentrations in equation 5.4.

$$K_{eq} = \frac{[HTMG][W(CPh)(depe)_2Cl]}{[TMG][[HW(CPh)(depe)_2Cl]BAr^{F24}]} \tag{5.4}$$

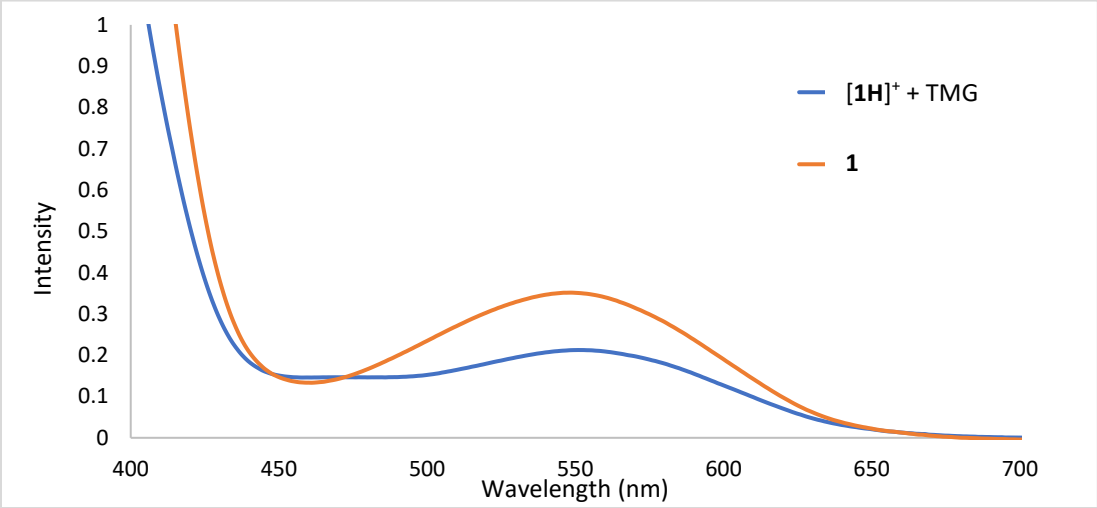

Figure 5.15. Absorption spectra of a reaction mixture of [HW(CPh)(depe)$_2$Cl]$^+$ ([**1H**]$^+$) and TMG compared to W(CPh)(depe)$_2$Cl (**1**).

$$\mathrm{pK}_a([1\mathrm{H}]^+) = \mathrm{pK}_a(\mathrm{TMGH}^+) + -\mathrm{pK}_{eq} \tag{5.5}$$

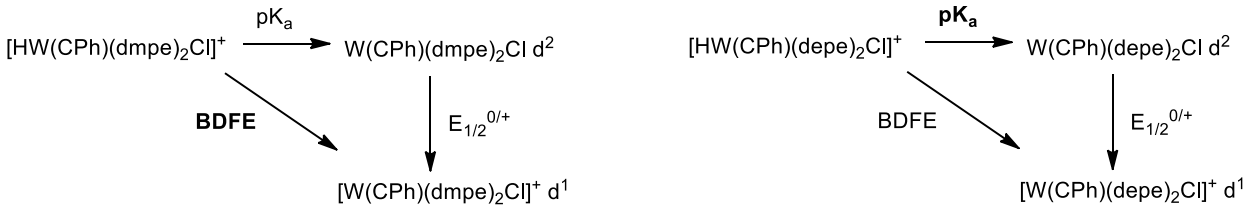

Figure 5.16. Bordwell diagrams illustrating how BDFE can be calculated from pK$_a$ and $E_{1/2}^{0/+}$ values. The BDFE of [HW(CPh)(dmpe)$_2$Cl]$^+$ ([**2H**]$^+$) is used to approximate the pK$_a$ of [HW(CPh)(depe)$_2$Cl]$^+$ ([**1H**]$^+$).[37]

$$BDFE_{sol}(W-H) = 1.37pKa + 23.06E° + C_{G,sol} \quad (5.6)$$

To probe whether the ET-PT pathway is viable, the oxidation potentials of enyl intermediates were calculated using DFT by both myself and Dr. Vibbert. The Born-Haber cycle (Figure 5.17, and equation 5.7) shows the free energies that were calculated. The corresponding ΔG for oxidation is related to the oxidation potential *via* the Nernst equation (equation 5.8, Table 5.3). Using this approach, the oxidation potential of enyl intermediate **11** generated from 2-chlorobenzonitrile radical and pyrrole acceptor is calculated to be –1.04 V vs. $FeCp_2^{0/+}$ (Table 5.3, entry v); this is sufficient to reduce $[W(CPh)(depe)_2Cl]^+$, the oxidized form of the chromophore ($E_{1/2}^{0/+}$ = –0.82 V vs. $FeCp_2^{0/+}$). As noted above, the oxidized enyl intermediate that would result from this reaction is a strong enough acid to protonate **1**. These facts suggest that ET-PT is a favourable pathway for the production of C-H arylation product **4**. The $[\mathbf{1H}]^+$ formed as a result of this reaction can be deprotonated by TMG.

The DFT calculations (Table 5.3) explored variations in both aryl halide and radical acceptors with the aim of understanding whether there were combinations for which the enyl intermediate would not possess an oxidation potential low enough to reduce oxidized chromophore [**1**$^+$]. The calculated oxidation potentials of enyl intermediates **13**, **15** and **6**, formed from 2-chlorobenzonitrile radical and 2,5-dimethoxybenzene, mesitylene and benzene acceptors, show that reduction of [**1**$^+$] is thermodynamically uphill by 0.47 V, 0.34 V and 0.75 V vs. $FeCp_2^{0/+}$, respectively (Table 5.3, entries vii-ix). Thus, it is predicted that these reactions should not proceed from intermediate to product by a ET-PT pathway. (The PT-ET pathway is excluded by the high pK_as of the intermediates.) In contrast, the enyl intermediates formed from reaction between 2-chlorobenzonitrile radical and *N*-methylpyrrole (**11**) or 1,3,5-trimethoxybenzene acceptor (**12**) are thermodynamically downhill for ET to [**1**$^+$] by 0.22 V and 0.34 V vs. $FeCp_2^{0/+}$, respectively (Table

5.3, entry v and vi). Thus, these could proceed from intermediate to product by an ET-PT mechanism.

The fact that the ET-PT mechanism is thermodynamically viable does not preclude the concerted hydrogen-atom transfer mechanism. In order to differentiate between ET-PT and concerted hydrogen atom transfer, both catalytic and stoichiometric reactions were performed with the acceptors outlined above. The presence of C-H arylation product and [**1H**]$^+$ in reactions whose intermediates are uphill for ET would suggest that the mechanism is concerted HAT, and the absence of these products would suggest that the general mechanism is ET-PT.

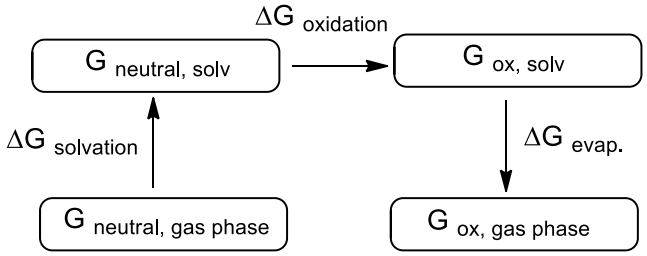

$\Delta G_T = \Delta G_{solvation} + \Delta G_{oxidation} + \Delta G_{evap.}$

Figure 5.17. Relationship between free energy values used to determine ΔG_T (T = total) of oxidation.

$$\Delta G_T = G_{ox,solv} - G_{neutral,solv} \quad (5.7)$$

$$\Delta G_T = -nFE^{ox} \quad (5.8)$$

Entry	Molecule	$E_{1/2}^{calc}$ (V vs. $FeCp_2^{0/+}$)	$\Delta E_{1/2}$ Relative to $[1]^+$
i	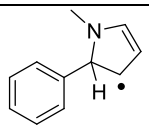 **5**	–1.21	–0.39
ii	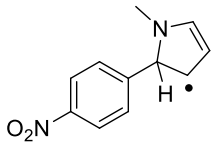 **8**	–1.05	–0.23
iii	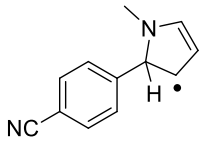 **9**	–1.10	–0.28
iv	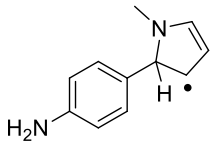 **10**	–1.27	–0.45
v	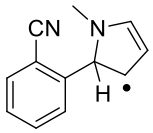 **11**	–1.04	–0.22
vi	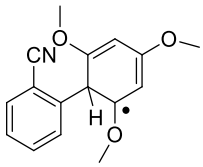 **12**	–1.16	–0.34
vii	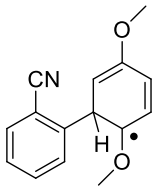 **13**	–0.35	0.47
viii	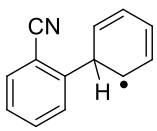 **6**	0.07	0.75
ix	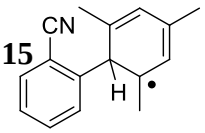 **15**	–0.48	0.34

Table 5.3. DFT computed oxidation potentials of select enyl intermediates.

Table 5.3 continued. DFT computed oxidation potentials of select enyl intermediates.

x	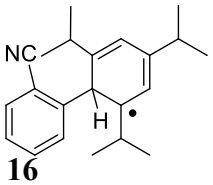 **16**	–0.50	0.32
xi	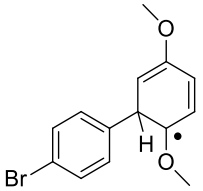 **22**	–0.05	0.77
xii	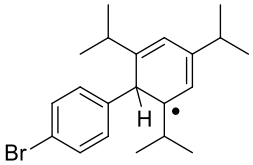 **23**	–0.56	0.26

5.2.4. Comparison of Reactions Under Catalytic Conditions that Generate Enyl Intermediates that are Thermodynamically Downhill or Uphill for Electron-Transfer to $[1]^+$.

In order to differentiate between ET-PT and HAT mechanisms, reactions under catalytic conditions were performed using radical acceptors that generated both uphill and downhill enyl intermediates with respect to reduction of $[\mathbf{1}]^+$. GC-MS scale reactions were performed with 2-chlorobenzonitrile, 40 equivalents of radical acceptor, 2 mol% W(CPh)(depe)$_2$Cl (**1**) and 1.1 equivalents of TMG in acetonitrile under photolysis with white light. The results are set out in Table 5.4. For the acceptor *N*-methylpyrrole, the resulting enyl intermediate **11** is formed. Electron transfer from **11** to $[\mathbf{1}]^+$ is downhill by 0.22 V vs. $FeCp_2^{0/+}$, and C-H arylation product **4** is produced quantitatively (Table 5.4, entry i). For the acceptor 1,3,5-trimethoxybenzene, electron transfer from resulting intermediate **12** to $[\mathbf{1}]^+$ is downhill by 0.34 V vs. $FeCp_2^{0/+}$, and the yield of the C-H arylation product **17** from this reaction is 65% (Table 5.4, entry ii). The sub-quantitative yield may be due to the increased steric bulk of the acceptor, which might decrease the rate of radical coupling relative to other pathways. This is supported by the fact that a trace amount of

benzonitrile is detected in the product sample by NMR spectroscopy and GC-MS. The production of benzonitrile is an off-cycle pathway that does not result in catalyst regeneration.

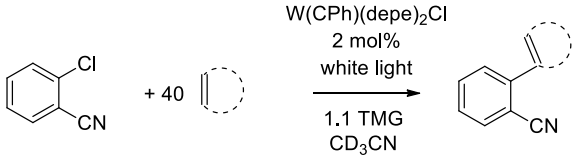

Entry	Acceptor	Potential of Enyl Intermediate Relative to $[1]^+$	GC Yield of Product
i		–0.22	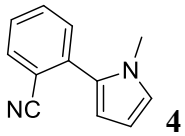 **4** 106%
ii	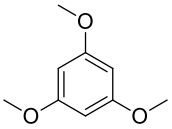	–0.34	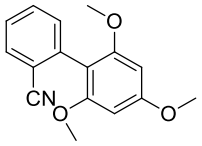 **17** 65%
iii		0.75	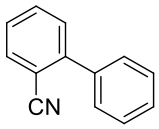 **18** 5%
iv	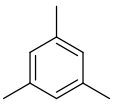	0.34	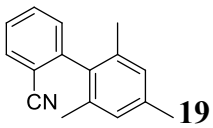 **19** 8%
v	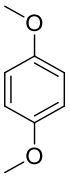	0.47	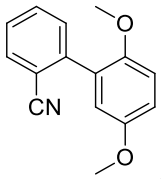 **20** 13%
vi	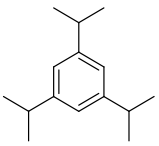	0.32	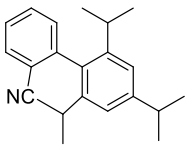 **21** trace

Table 5.4. Catalytic reactions of 2-chlorobenzonitrile with different radical acceptors showing the oxidation potential of the enyl intermediate relative to $[\mathbf{1}]^+$, in comparison with GC yield of product.

We also observed product in reactions where ET from the enyl intermediate is significantly uphill to [**1**]$^+$, indicating a HAT mechanism may be possible. For intermediate **6**, generated from 2-chlorobenzonitrile radical and benzene acceptor, ET to [**1**]$^+$ is uphill by 0.75 V vs. $FeCp_2^{0/+}$. The GC yield of C-H arylation product **18** in this reaction is 5% (Table 5.4, entry iii). The acceptors mesitylene and 2,5-dimethoxybenzene generate intermediates **15** and **13** that are uphill to [**1**]$^+$ by 0.34 V and 0.47 V vs. $FeCp_2^{0/+}$, and the use of these acceptors in the GC scale reactions generated C-H arylation product **19** and **20** with yields of 8% and 13%, respectively (Table 5.4, entries iv and v). These yields exceed the catalyst loading (2 mol%), indicating that there is catalyst turnover.

In order to test whether the low yields for these reactions were intrinsic to the products rather than the mechanistic considerations outlined above, we wished to compare these yields to those provided by different chromophores for which electron transfer from the enyl intermediate is downhill. Ideally, these would use 2-chlorobenzonitrile as the photoredox substrate, but common chromophores are incapable of reducing it. Instead, an easily reduced arene substrate was used. A GC-MS scale photoredox reaction was performed using $[Ru(bpy)_3][PF_6]_2$ chromophore (2 mol%) ($E^{*/ox}$ = –1.21 V vs. $FeCp_2^{0/+}$)[7] and 4-bromobenzenediazonium tetrafluoroborate substrate (E^{red} = –0.46 V vs. $FeCp_2^{0/+}$)[7] with 2,5-dimethoxybenzene as the radical acceptor. Electron transfer from enyl intermediate **22** (E^{ox} = –0.05 V vs. $FeCp_2^{0/+}$) generated in this reaction to oxidized $[(Ru(bpy)_3)]^{3+}$ chromophore ($E_{1/2}^{0/+}$ = 0.89 V vs. $FeCp_2^{0/+}$)[7] is downhill by 0.94 V vs. $FeCp_2^{0/+}$. This reaction is shown to quantitatively produce C-H arylation product **24** by GC-MS (Figure 5.18, 5.19). Because of the steric and electronic differences between 2-chlorobenzonitrile and 4-bromobenzenediazonium tetrafluoroborate, a more closely comparable experiment was performed with $W(CPh)(depe)_2Cl$ (2 mol %) using the substrate 1-bromo-4-iodobenzene and the radical

acceptor 2,5-dimethoxybenzene. This reaction also generates enyl intermediate **22**, from which electron transfer to the oxidized chromophore ([**1**]$^{+}$) is uphill by 0.77 V vs. $FeCp_2^{0/+}$. A significant amount of unreacted aryl halide starting material is observed (Figure 5.20) in addition to some production of C-H arylation product **24**, which is analogous to the low yield of **20** observed with the 2-chlorobenzonitrile substrate. Taken together, these results demonstrate that a much higher product yield is achievable when electron transfer from the enyl intermediate to the oxidized chromophore is downhill than when it is uphill.

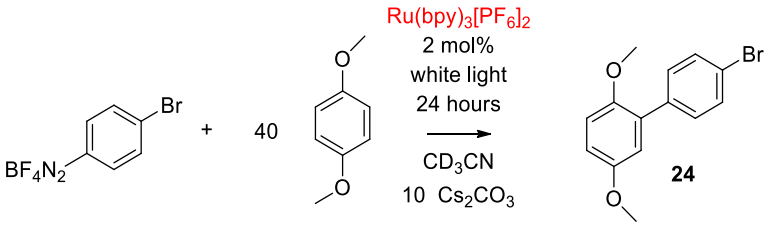

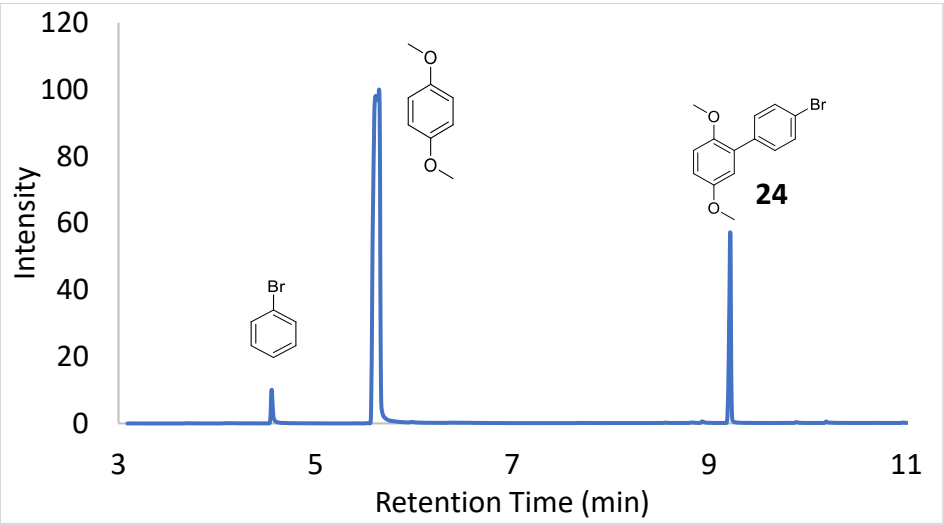

Figure 5.18. GC-MS trace of the reaction between 4-bromobenzenediazonium tetrafluoroborate and 2,5-dimethoxybenzene with $[Ru(bpy)_3]^{2+}$ chromophore shows C-H arylation product **24**.

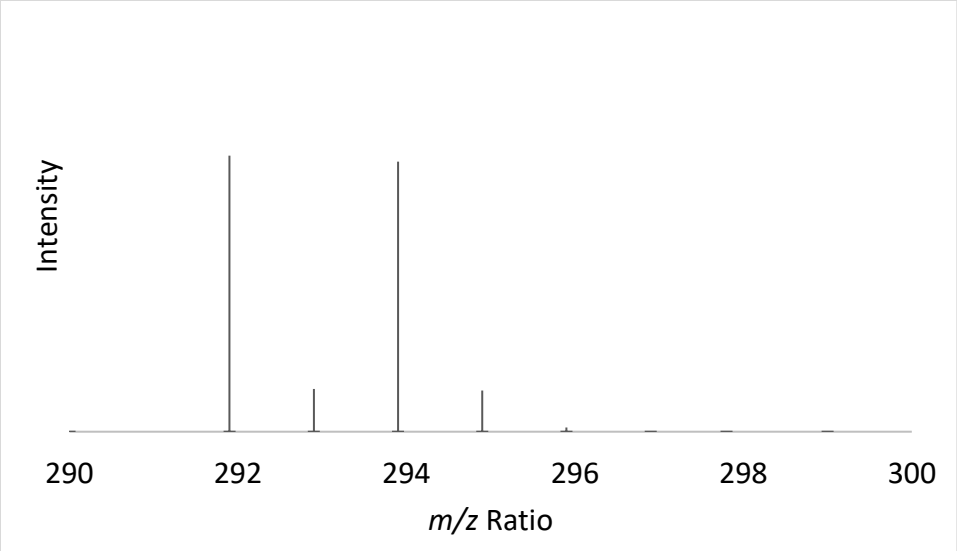

Figure 5.19. MS fragmentation at 9.22 min of the GC-MS trace of the control reaction between 4-bromobenzenediazonium tetrafluoroborate and 2,5-dimethoxybenzene with $[Ru(bpy)_3]^{2+}$ chromophore shows C-H arylation product **24**.

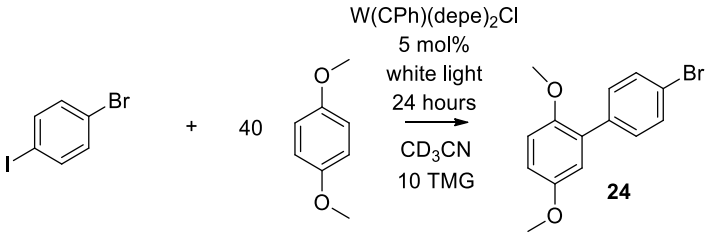

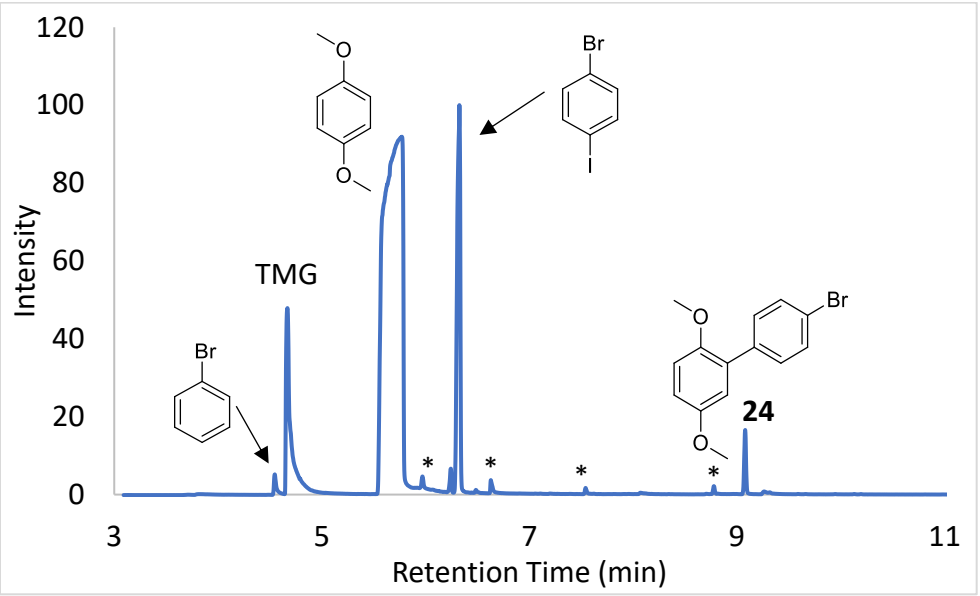

Figure 5.20. GC-MS trace of the reaction between 1-bromo-4-iodobenzene and 2,5-dimethoxybenzene with $W(CPh)(depe)_2Cl$ (**1**) chromophore shows C-H arylation product **24** and unreacted aryl halide. * Represents a peak that could not be identified.

The presence of C-H arylation product in catalytic reactions where electron transfer from the enyl intermediate to [**1**]$^+$ is uphill supports the possibility that a HAT mechanism could be occurring. Unlike the outer-sphere electron transfer step central to the ET-PT mechanism, HAT should be highly sensitive to the steric bulk near the transferred hydrogen atom of the enyl intermediate (Figure 5.21). Thus, the sterics around the enyl intermediate were increased to see if this blocked reaction with [**1**]$^+$. Earlier, it was noted that the photoreaction between **1** (2 mol %), 2-chlorobenzonitrile, and mesitylene provided the C-H arylation product in 8% yield *via* intermediate **15**, for which ET to [**1**]$^+$ is uphill by 0.34 V (Table 5.4, entry iv). The acceptor 1,3,5-triisopropylbenzene is chosen as the bulky acceptor because electron transfer from corresponding enyl intermediate **16** to [**1**$^+$] is uphill by a similar amount (0.32 V; Table 5.4, entry vi). Under catalytic loading of **1**, the reaction between 1,3,5-triisopropylbenzene acceptor and 2-chlorobenzonitrile substrate provided only a trace amount of C-H arylation product **21** ($\leq$0.1%), as detected by GC-MS (Table 5.4, entry vi). This suggests that the chromophore is consumed but cannot be catalytically regenerated if a HAT mechanism is sterically inhibited.

However, it is necessary to ensure that the increased steric bulk of the acceptor does not prevent its coupling with the 2-chlorobenzonitrile radical to generate enyl intermediate **16**. A control experiment was performed using $[Ru(bpy)_3][PF_6]$ with 1,3,5-triisopropylbenzene and 4-bromobenzenediazonium tetrafluoroborate substrate, which generates enyl intermediate **23** (E^{ox} = –0.56 V, Table 5.3 entry xii). Electron transfer from **23** to oxidized $[Ru(bpy)_3]^{3+}$ chromophore ($E_{1/2}^{0/+}$ = 0.89 V vs. $FeCp_2^{0/+}$)[7] is downhill by 1.45 V and C-H arylation product **25** is produced catalytically, demonstrating that the increased sterics do not prevent the radical from coupling with the acceptor (Figures 5.21, 5.22). To ensure the steric profile of this comparison is identical, a parallel reaction was also performed using 1,3,5-triisopropylbenzene acceptor with 1-bromo-4-

iodobenzene substrate instead of 2-chlorobenzonitrile, with 2 mol% W(CPh)(depe)$_2$Cl. This also generates enyl intermediate **23** but electron-transfer to [**1**]$^+$ is uphill by 0.26 V (Table 5.3, entry xii). The reaction provides only a trace of C-H arylation product **25** (Figure 5.23), analogous to the result observed with 2-chlorobenzonitrile substrate.

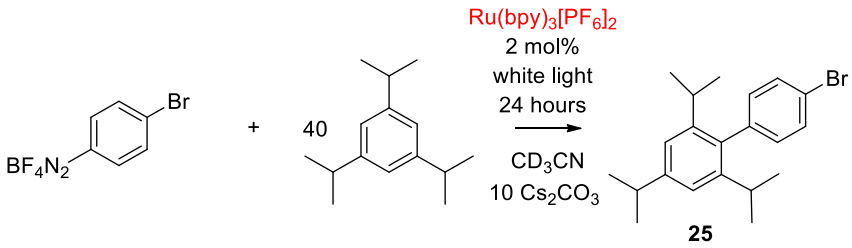

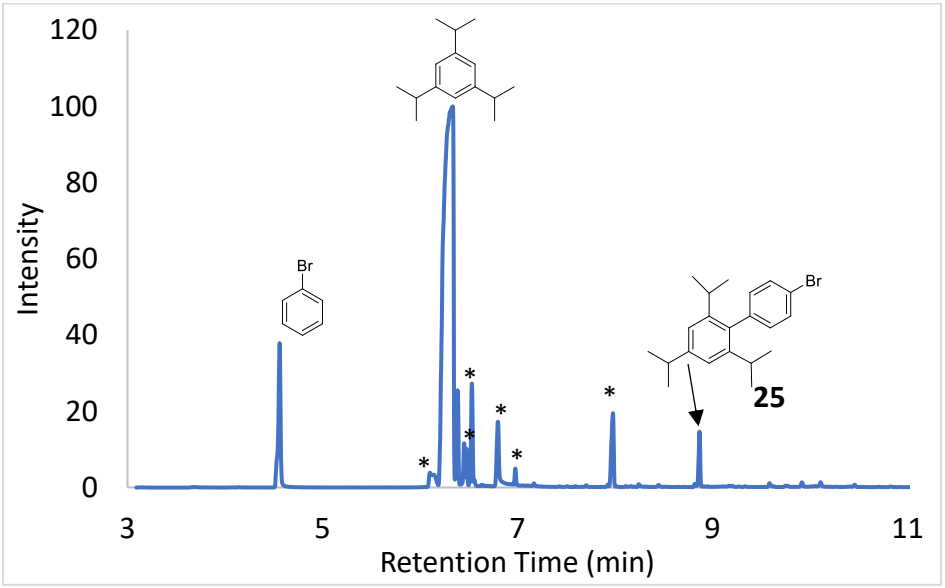

Figure 5.21. GC-MS trace of the reaction between 4-bromobenzenediazonium tetrafluoroborate and 1,3,5-triisopropylbenzene with [Ru(bpy)$_3$]$^{2+}$ chromophore shows C-H arylation product **25**. * Represents a peak that could not be identified.

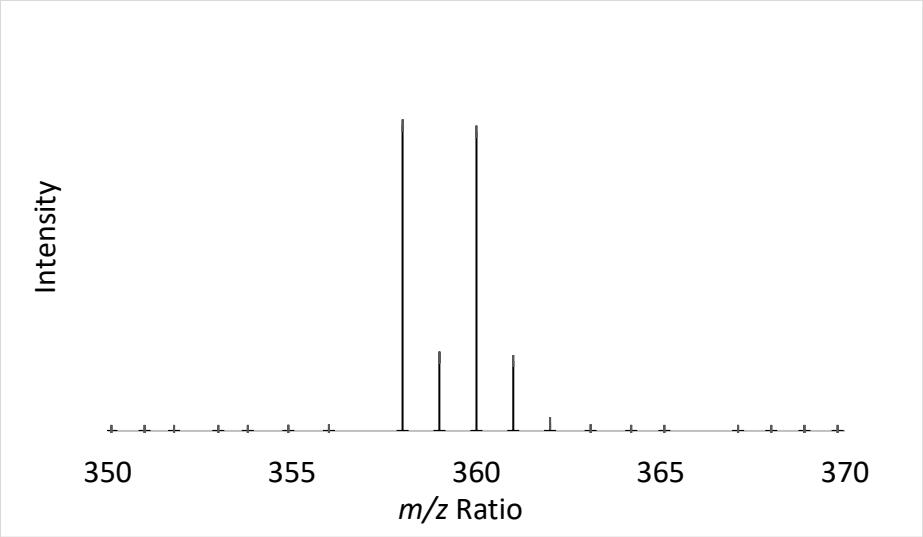

Figure 5.22. MS fragmentation at 8.87 min of the GC-MS trace of the reaction between 4-bromobenzenediazonium tetrafluoroborate and 1,3,5-triisopropylbenzene with $[Ru(bpy)_3]^{2+}$ chromophore shows C-H arylation product **25**.

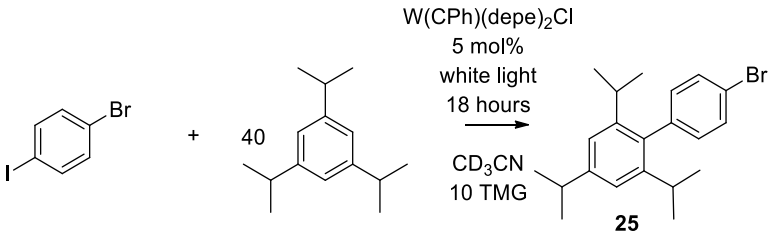

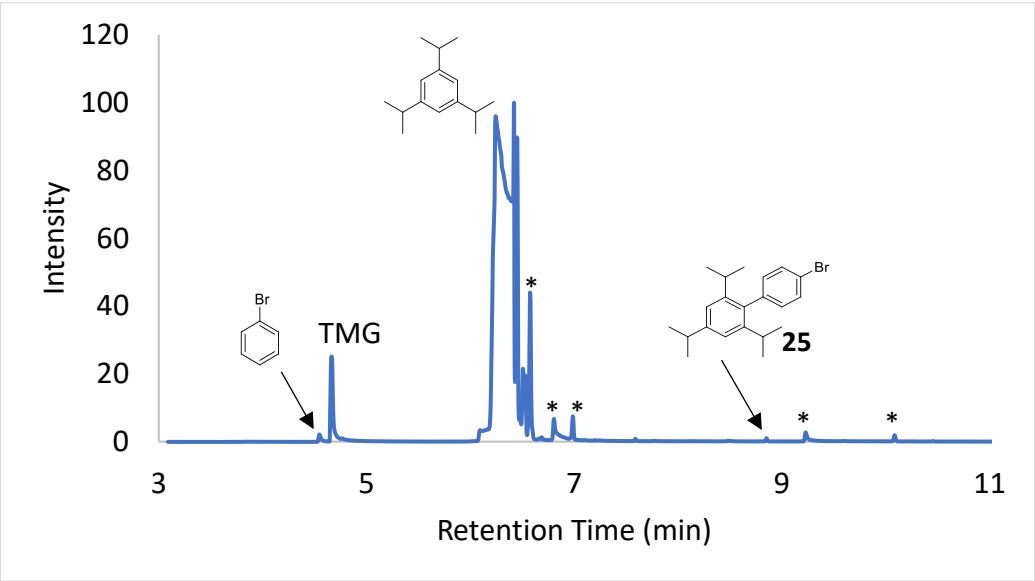

Figure 5.23. GC-MS trace of the control reaction between 1-bromo-4-iodobenzene and 1,3,5-triisopropylbenzene with $W(CPh)(depe)_2Cl$ (**1**) chromophore shows trace C-H arylation product **25**. * Represents a peak that could not be identified.

The results of the experiments comparing C-H arylation yields from the same enyl intermediates with $[Ru(bpy)_3]^{2+}$ and **1** are summarized in Table 5.5. When ET from enyl intermediate **22** to chromophore is made downhill by using $[Ru(bpy)_3]^{2+}$, the substrate is completely consumed and C-H arylation product **24** is produced in high yield (entry i). In contrast, when ET is made uphill by using **1** (entry iv) there is a low yield of **24**. The fact that the reaction occurs at all for **1** is indicative that the mechanism switches from ET-PT to HAT. When the sterics are increased around the acceptor, the yield of C-H arylation product **25** is also highly dependent on chromophore. It is produced catalytically when enyl intermediate **23** is downhill for ET to oxidized $[Ru(bpy)_3]^{3+}$ (entry ii) but produced in trace amount for **1**, because ET is uphill and the HAT mechanism is inhibited by the increased sterics (entry iii). This same result is also observed using 2-chlorobenzonitrile substrate and 1,3,5-triisopropylbenzene acceptor (entry v).

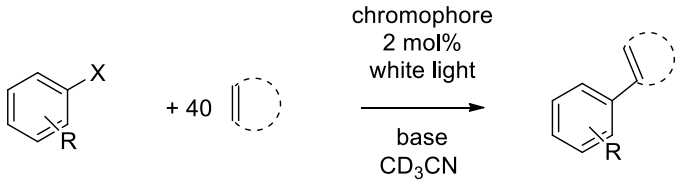

R = CN or Br, X = I or N_2BF_4

Entry	Chromophore	Product	Designation	Result
i	$[Ru(bpy)_3]^{2+}$	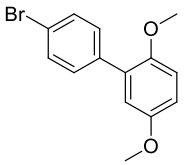 **24**	sterically unhindered, downhill[a]	quant. consumption of substrate
ii	$[Ru(bpy)_3]^{2+}$	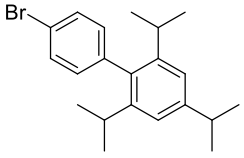 **25**	sterically hindered, downhill	low consumption of substrate
iii	W(CPh)(depe)$_2$Cl (**1**)	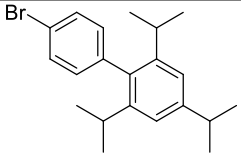 **25**	sterically hindered, uphill	trace conversion only

Table 5.5. Results of reactions under catalytic conditions where enyl intermediates have different steric effects and ET driving forces.

Table 5.5 continued. Results of reactions under catalytic conditions where enyl intermediates have different steric effects and ET driving forces.

iv	W(CPh)(depe)$_2$Cl (**1**)	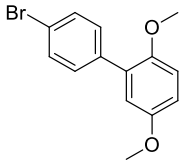 **24**	unhindered, uphill	consumption of substrate
v	W(CPh)(depe)$_2$Cl (**1**)	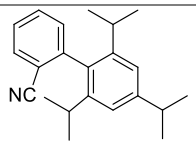 **21**	sterically unhindered, uphill	trace conversion only

a. Represents driving force of enyl radical potential relative to oxidized chromophore.

5.2.5. Stoichiometric Reactions with Benzene and 1,3,5-Triisopropylbenzene Acceptors.

The presence of C-H arylation product in catalytic reactions where the enyl intermediate is uphill for ET to [**1**]$^+$, which is suggestive of an HAT mechanism, raised the question of whether [**1H**]$^+$ would be detected in reactions run under stoichiometric conditions in the absence of base. These reactions are analogous to the stoichiometric reactions described earlier with pyrrole acceptor. A stoichiometric reaction between 2-chlorobenzonitrile and **1** in CD_3CN using 10 equivalents of benzene acceptor was performed. Following irradiation, the ^{1}H NMR spectrum showed the presence of [**1H**]$^+$, C-H arylation product **18**, and the reductive dehalogenation side-product benzonitrile. The identity of these compounds were verified by comparison to ^{1}H NMR spectra of authentic samples in CD_3CN, as well as by mass spectrometry (Figure 5.24 - 5.28). The fate of 92% of the starting material 2-chlorobenzonitrile is accounted for in the product NMR spectrum by integration relative to the internal standard TMS. The C-H arylation product is produced in 16% yield, benzonitrile is produced in 45% yield, and 39% of 2-chlorobenzonitrile is unreacted. The formation of benzonitrile was shown to arise in part from H-atom abstraction from the solvent. Irradiating 2-chlorobenzonitrile with **1** in CD_3CN in the absence of a radical acceptor produces deuterated benzonitrile, as shown by high resolution MS (Figure 5.30- 5.31). We also

probed whether benzonitrile could form as a result of H-atom abstraction from the enyl intermediate (Scheme 5.3). A stoichiometric cross-over photochemical reaction with 2-chlorobenzonitrile substrate, **1**, and benzene acceptor in CD_3CN was analyzed by HR-MS. Benzonitrile is shown to be 52:48 mixture of C_6H_5CN and C_6H_4DCN, suggesting that H-atom abstraction by benzonitrile radical from both solvent abstraction and enyl intermediate **6** is occurring (Figure 5.29). The presence of [**1H**]$^+$ and **18** as products indicates that a HAT mechanism is occurring *via* the enyl intermediate **6** and oxidized chromophore [**1**]$^+$.

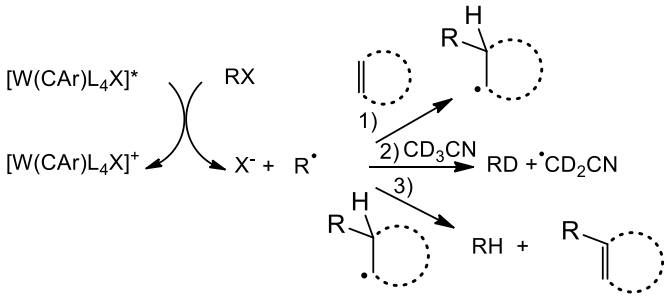

Scheme 5.3. Possible reaction pathways for the aryl radical including 1) reaction with radical acceptor, 2) solvent abstraction and 3) hydrogen atom abstraction from the enyl intermediate.

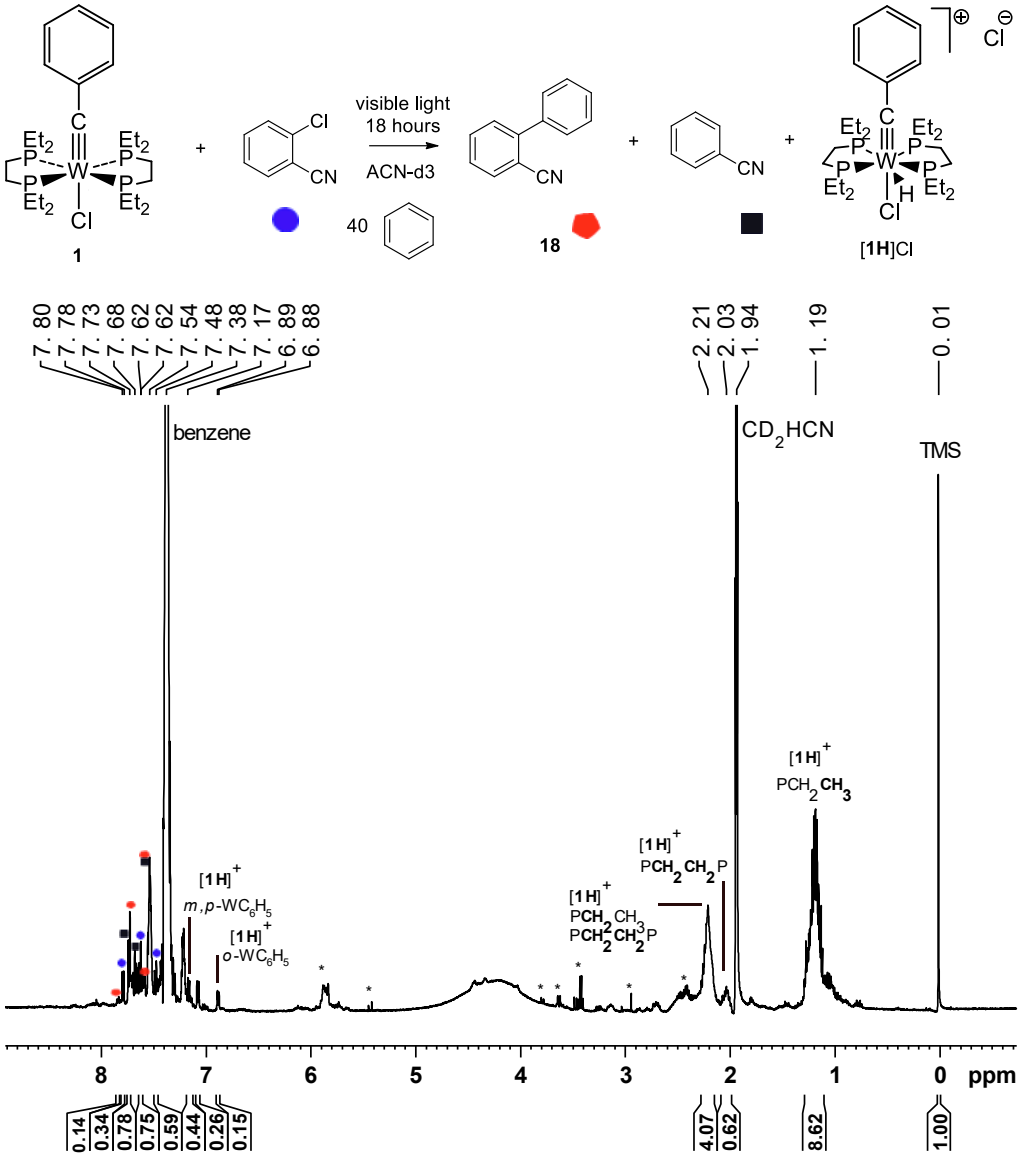

Figure 5.24. ^{1}H NMR spectrum (500.13 MHz, CD_3CN) of the stoichiometric reaction between 2-chlorobenzonitrile and W(CPh)(depe)$_2$Cl (**1**) with 40 equivalents of benzene after 18 hours of irradiation shows production of [HW(CPh)(depe)$_2$Cl]$^+$ ([**1H**]$^+$), [1,1'-biphenyl]-2-carbonitrile (**18**) and benzonitrile. * Represents a peak that could not be identified.

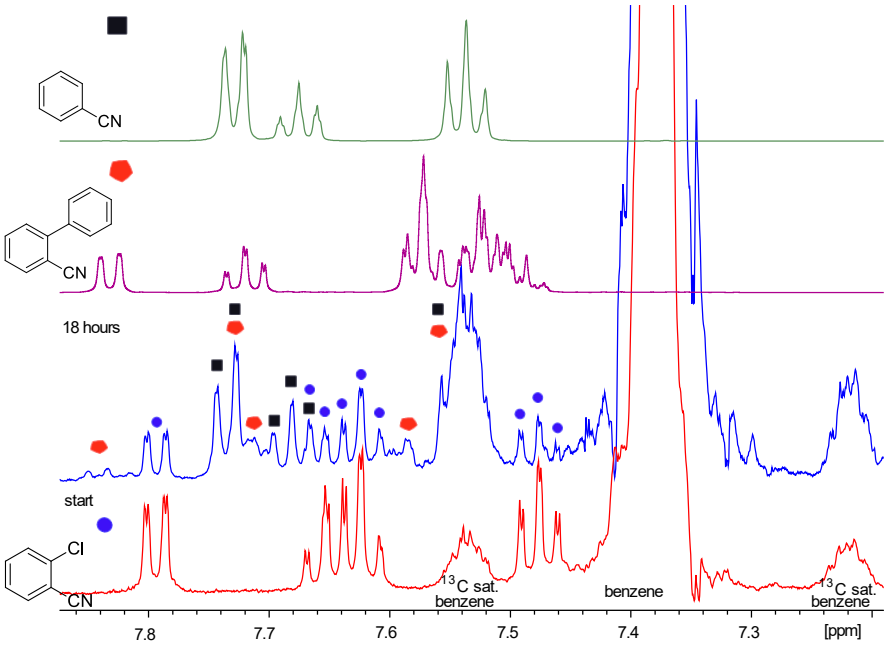

Figure 5.25. ^{1}H NMR spectra (500.13 MHz, CD_3CN) of the aromatic region of the stoichiometric reaction between 2-chlorobenzonitrile and **1** with 40 equivalents of benzene after 18 hours of irradiation shows production of **18** and benzonitrile, in comparison with authentic product.

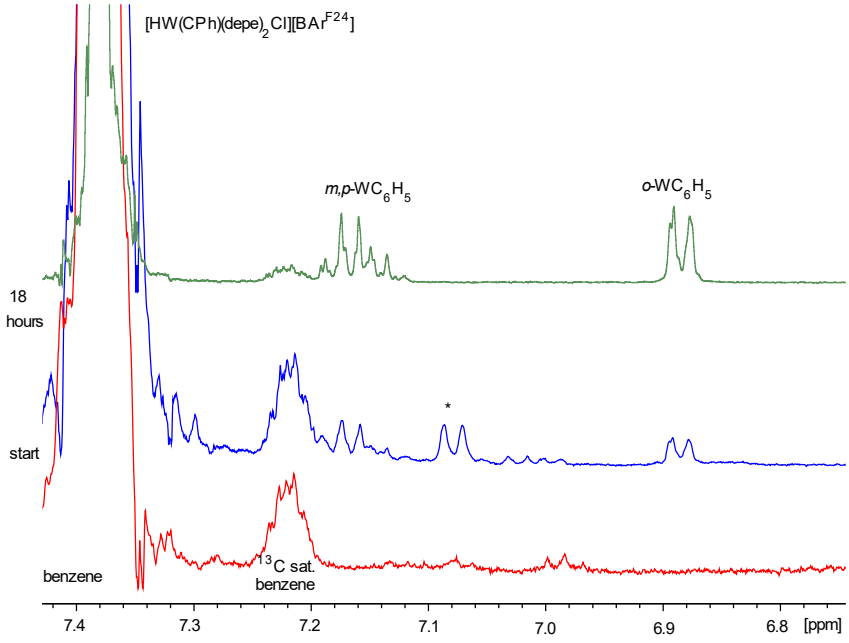

Figure 5.26. ^{1}H NMR spectra (500.13 MHz, CD_3CN) of the aromatic region of the stoichiometric reaction between 2-chlorobenzonitrile and **1** with 40 equivalents of benzene after 18 hours of irradiation shows production of [**1H**]$^{+}$. Benzene is added to the authentic sample of [**1H**][BAr^{F24}] to account for solvent effects on the chemical shift. *Represents a product that could not be identified.

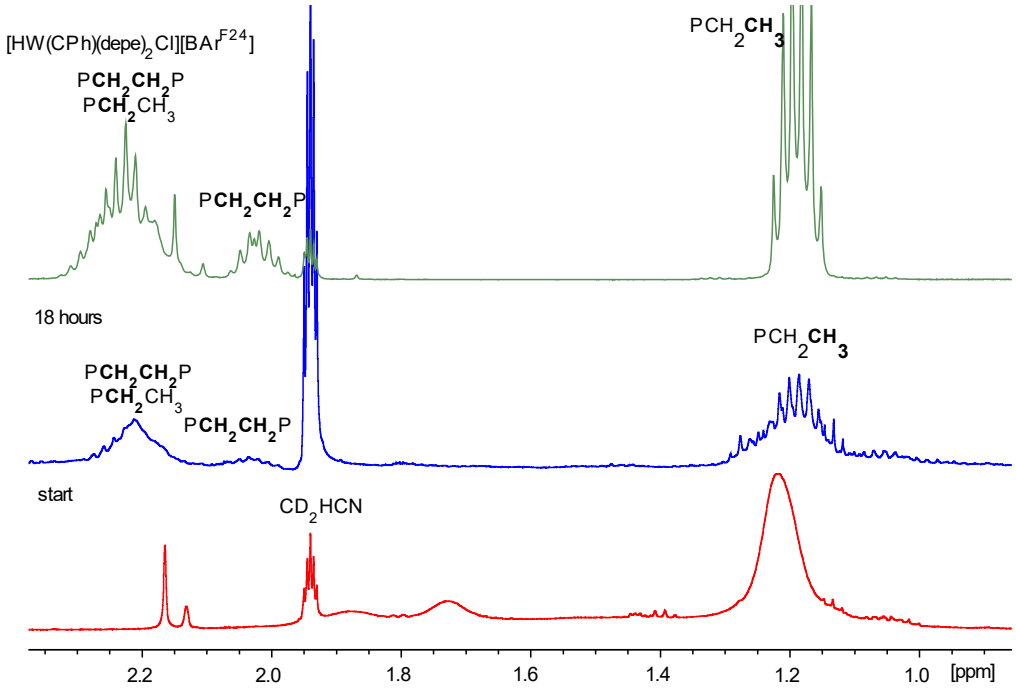

Figure 5.27. ^{1}H NMR spectra (500.13 MHz, CD_3CN) of the aliphatic region of the stoichiometric reaction between 2-chlorobenzonitrile and **1** with 40 equivalents of benzene after 18 hours of irradiation shows production of [**1H**]$^{+}$, in comparison with authentic product.

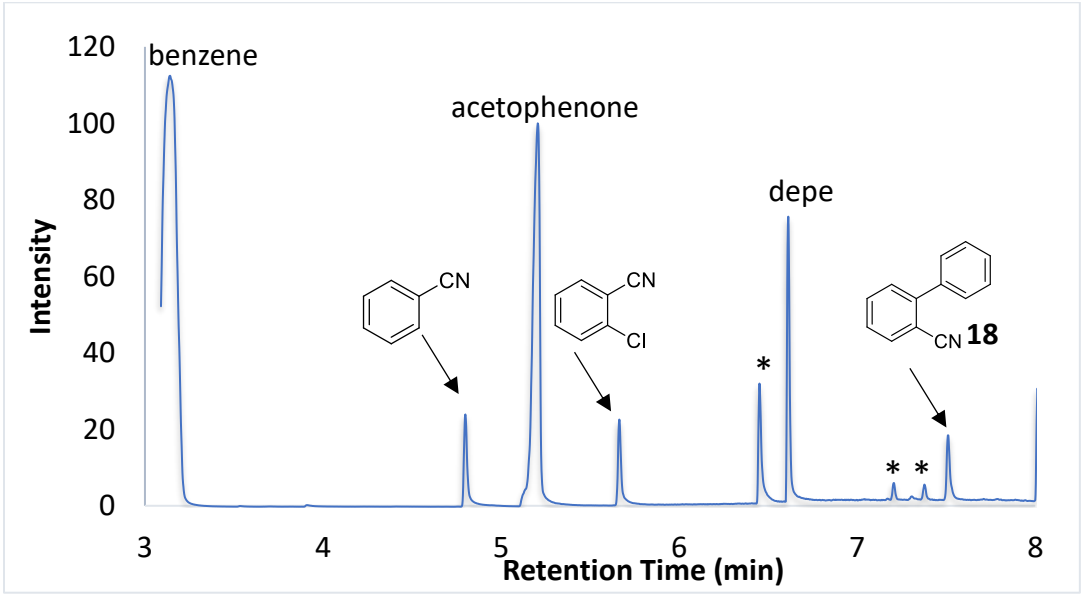

Figure 5.28. GC-MS trace of the stoichiometric reaction between 2-chlorobenzonitrile and **1** with 40 equivalents of benzene after 18 hours of irradiation shows production of **18**, benzonitrile and unreacted 2-chlorobenzonitrile, in comparison with authentic product. *Represents a peak that could not be identified.

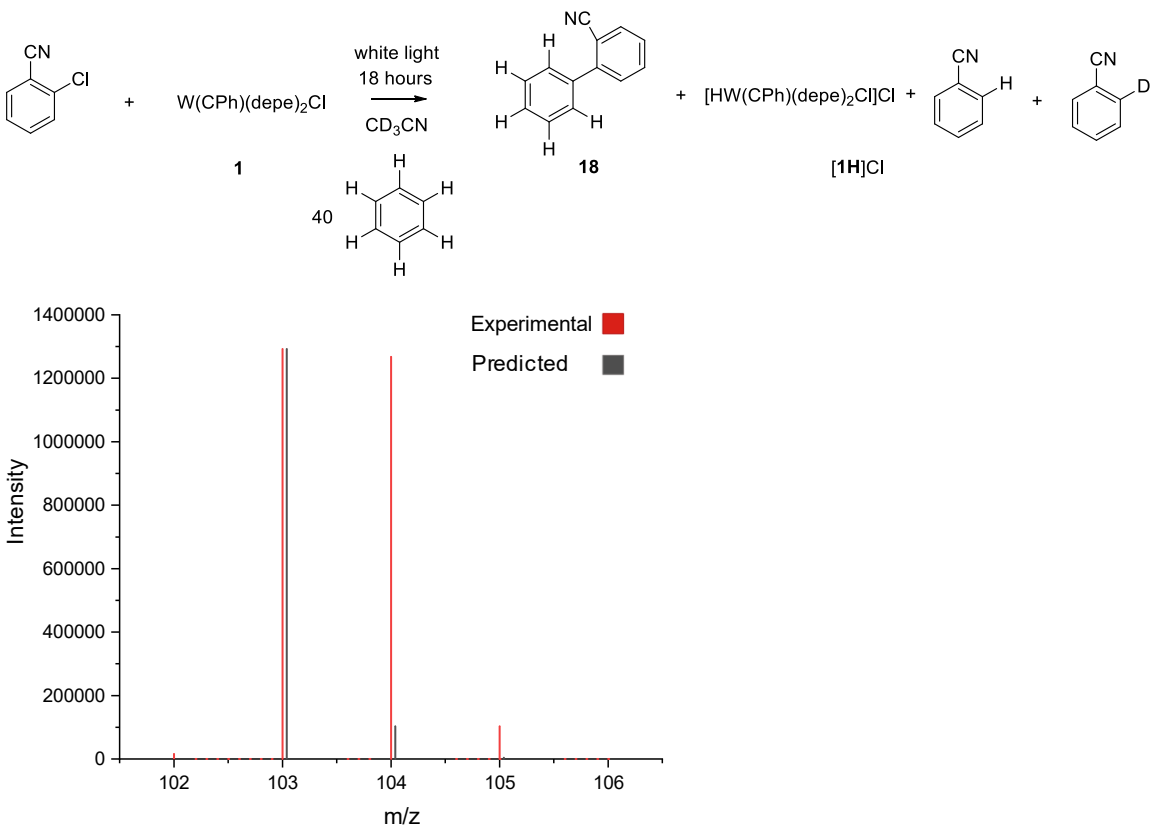

Figure 5.29. HR-MS fragmentation of the GC-MS trace peak at 4.79 min corresponding to benzonitrile shows both h_5- and h_4d_1-benzonitrile in comparison with the predicted isotope splitting for proteo-benzonitrile.

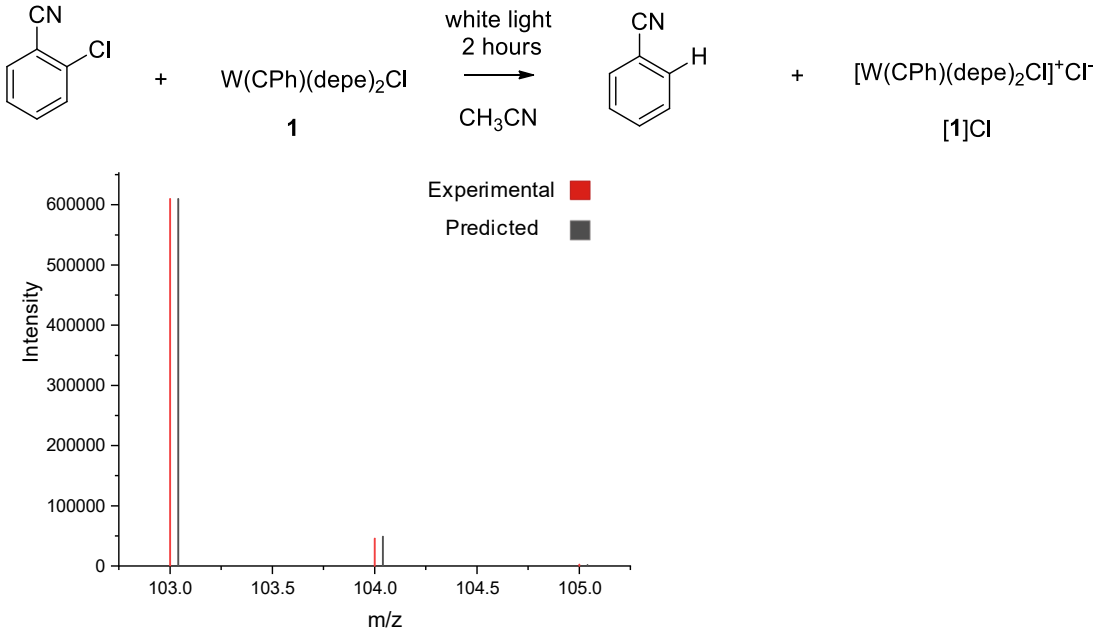

Figure 5.30. HR-MS fragmentation of the GC-MS trace peak at 4.79 min corresponding to benzonitrile shows proteo-benzonitrile in comparison with the predicted isotope splitting for proteo-benzonitrile (Score: 99.82%; Diff (tgt, ppm): –4.58).

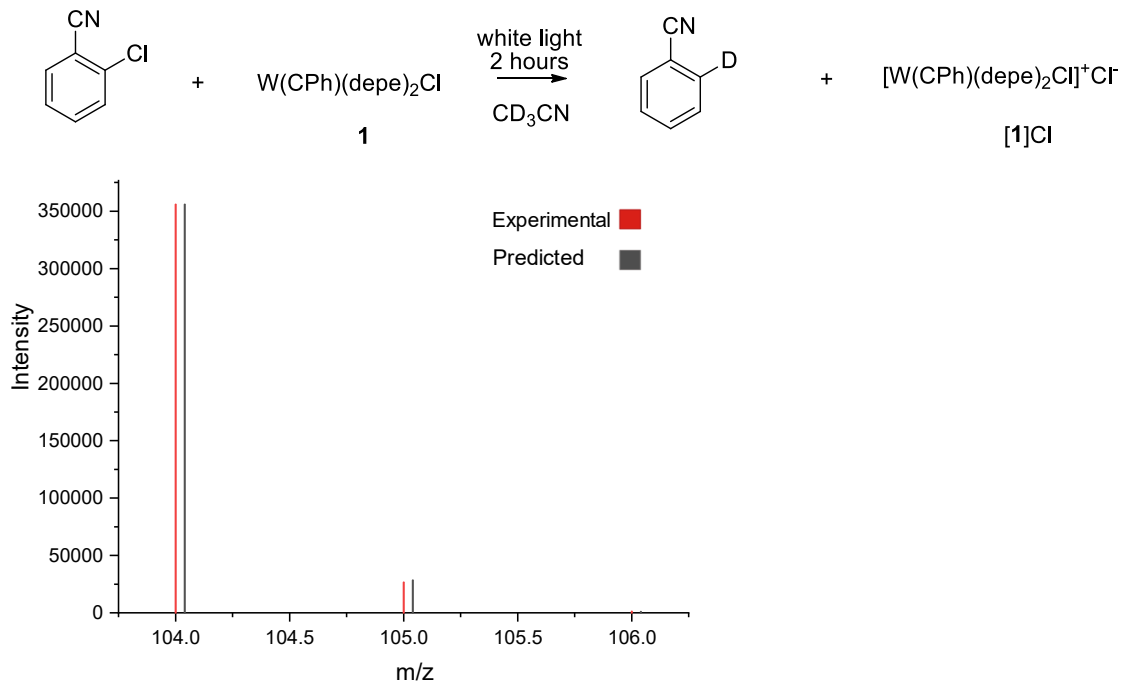

Figure 5.31. HR-MS fragmentation of the GC-MS trace peak at 4.79 min corresponding to benzonitrile shows d_1-benzonitrile in comparison with the predicted isotope splitting for d_1-benzonitrile (Score: 99.81%; Diff (tgt, ppm): -11.2).

The concerted HAT mechanism between [**1**]$^+$ and enyl intermediate **16** generated from 1,3,5-triisopropylbenzene and 2-chlorobenzonitrile appeared to be blocked by the increased sterics of **16**, as evidenced by the trace GC-MS yield of C-H arylation product **21**. A stoichiometric reaction between 2-chlorobenzonitrile and **1** was also performed in the presence of 10 equivalents of 1,3,5-triisopropylbenzene and absence of base in order to determine if the production of [**1H**]$^+$ would be inhibited. C-H arylation product **21** is observed, as evidenced by GC-MS (Figure 5.37) and a new isopropyl septet in the ^{1}H NMR spectrum after 2 hours of irradiation (Figure 5.35), but [**1H**]$^+$ is not observed in the ^{1}H NMR spectrum (Figure 5.32 - 5.36). Because the ET-PT reaction is uphill and the concerted HAT pathway for is inhibited by sterics, the product must form by another pathway. Benzonitrile is also observed in the ^{1}H NMR spectrum with C-H arylation product. HR-MS analysis of this product indicated 87% of the benzonitrile is not deuterated and thus did not form by H-atom abstraction from solvent (Figure 5.38). Instead, it indicates that enyl

intermediate **16** transfers a hydrogen atom to the aryl radical generated from 2-chlorobenzonitrile, producing C-H arylation product **21** and benzonitrile (Scheme 5.3, pathway 3).

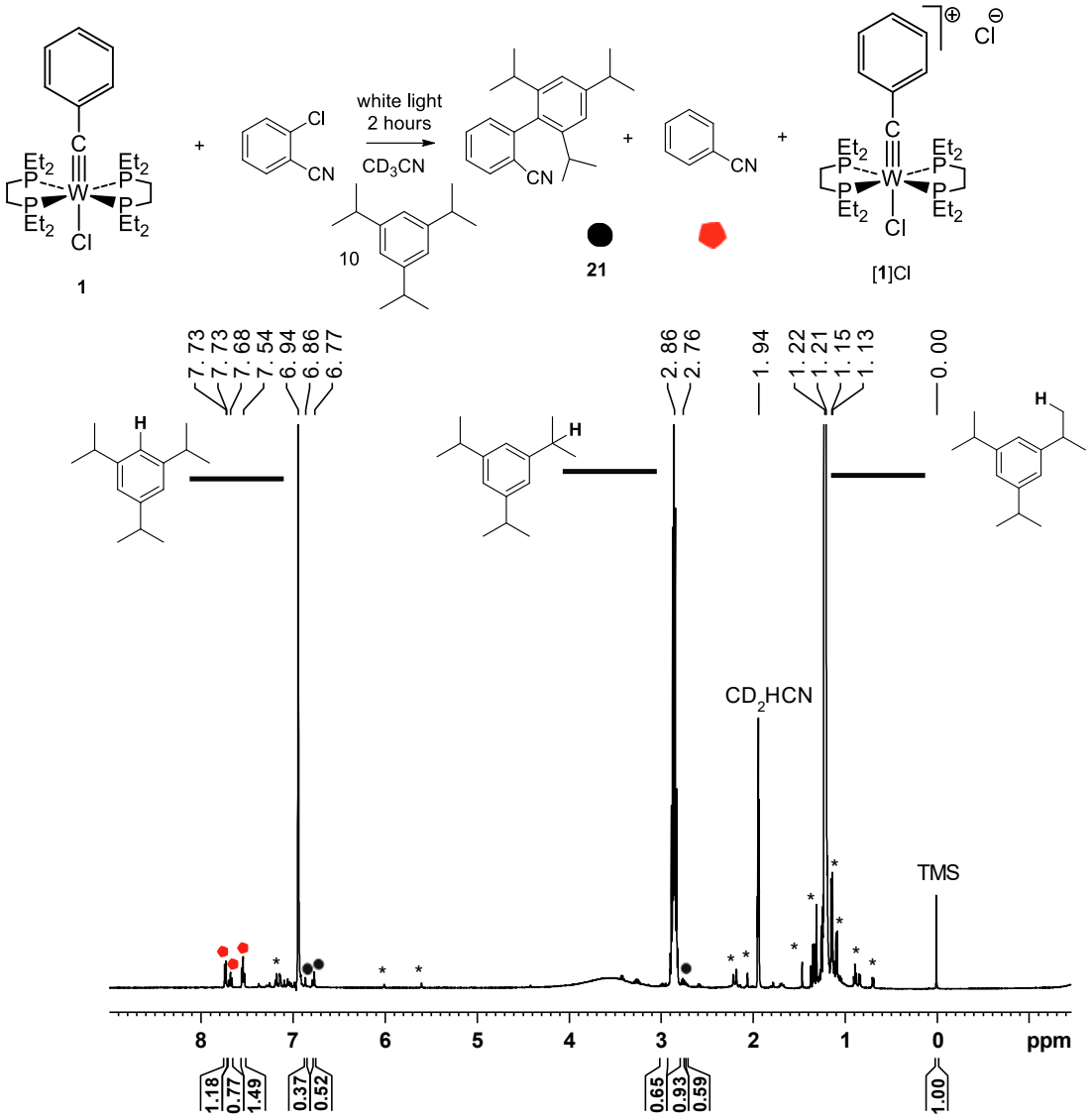

Figure 5.32. ^{1}H NMR spectrum (500.13 MHz, CD_3CN) of the stoichiometric reaction between 2-chlorobenzonitrile and **1** with 10 equivalents of 1,3,5-triisopropylbenzene after 2 hours of irradiation shows production of benzonitrile, **21** and the absence of [**1H**]$^{+}$. * Represents a peak that could not be identified.

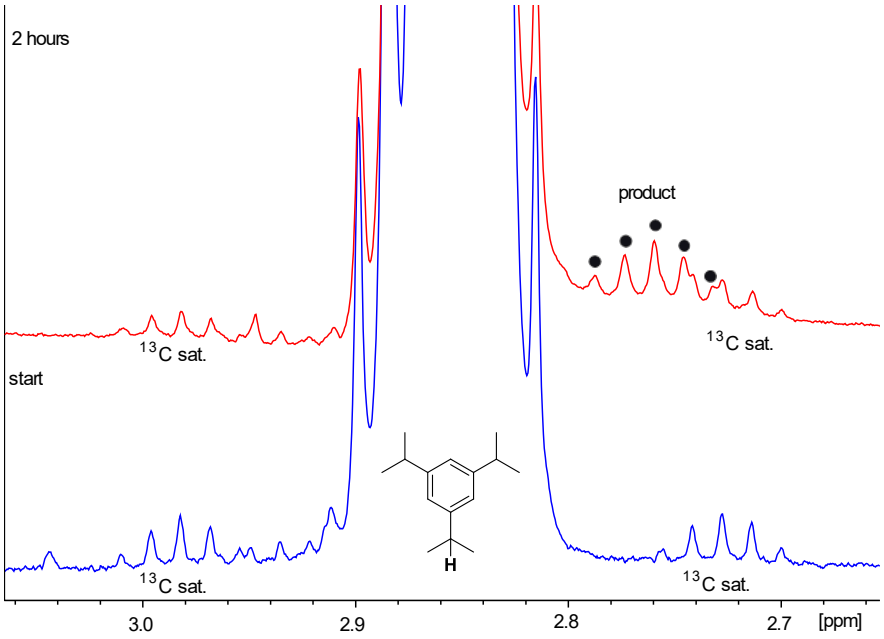

Figure 5.33. ^{1}H NMR spectra (500.13 MHz, CD_3CN) of the aliphatic region of the stoichiometric reaction between 2-chlorobenzonitrile and **1** with 10 equivalents of 1,3,5-triisopropylbenzene after 2 hours of irradiation shows production of an isopropyl-containing product presumed to be **21**.

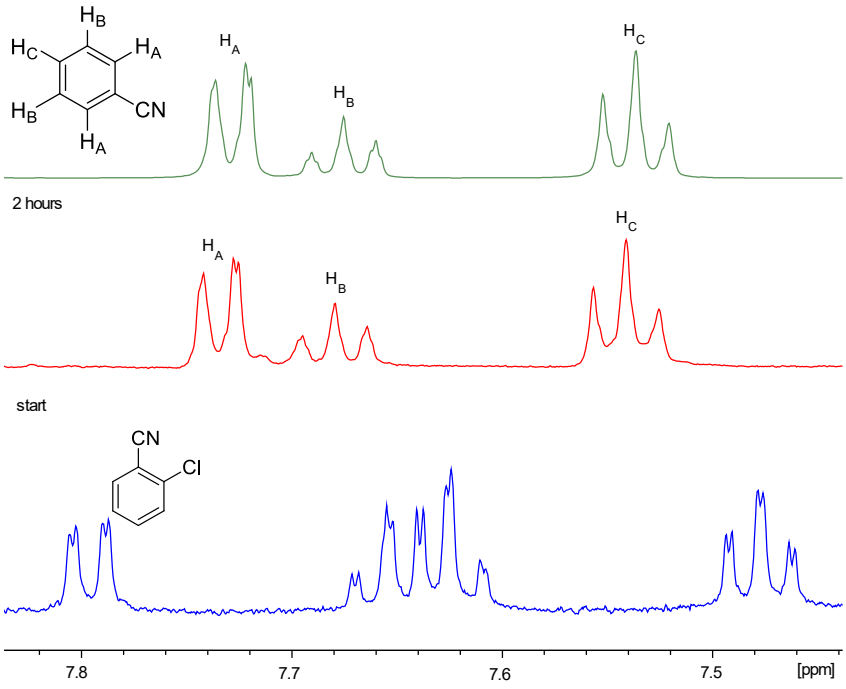

Figure 5.34. ^{1}H NMR spectra (500.13 MHz, CD_3CN) of the aromatic region of the stoichiometric reaction between 2-chlorobenzonitrile and **1** with 10 equivalents of 1,3,5-triisopropylbenzene after 2 hours of irradiation shows production of benzonitrile.

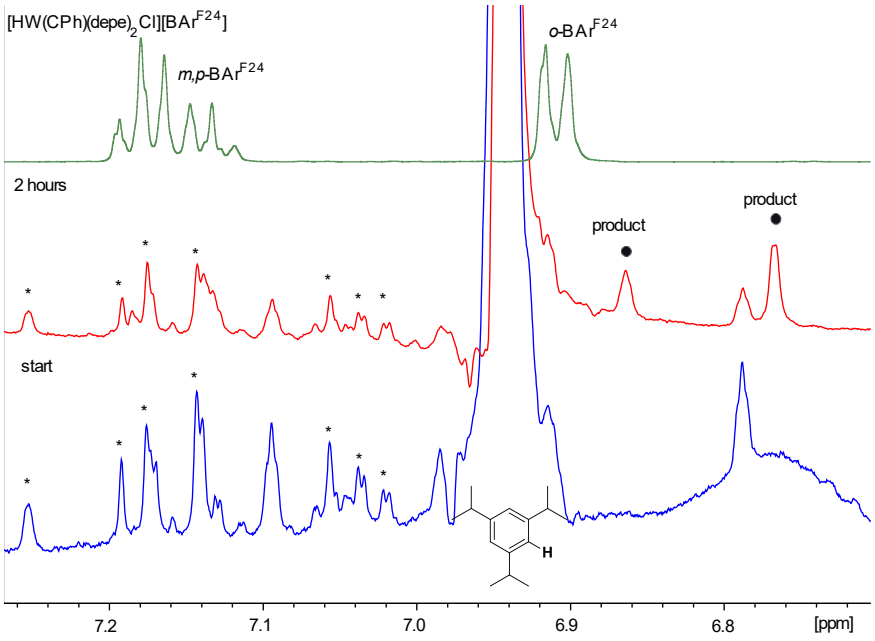

Figure 5.35. ^{1}H NMR spectra (500.13 MHz, CD_3CN) of the aromatic region of the stoichiometric reaction between 2-chlorobenzonitrile and **1** with 10 equivalents of 1,3,5-triisopropylbenzene after 2 hours of irradiation shows product presumed to be **21** and the absence of [**1H**]$^{+}$ in comparison to authentic product. * Represents a 1% impurity in 1,3,5-triisopropylbenzene.

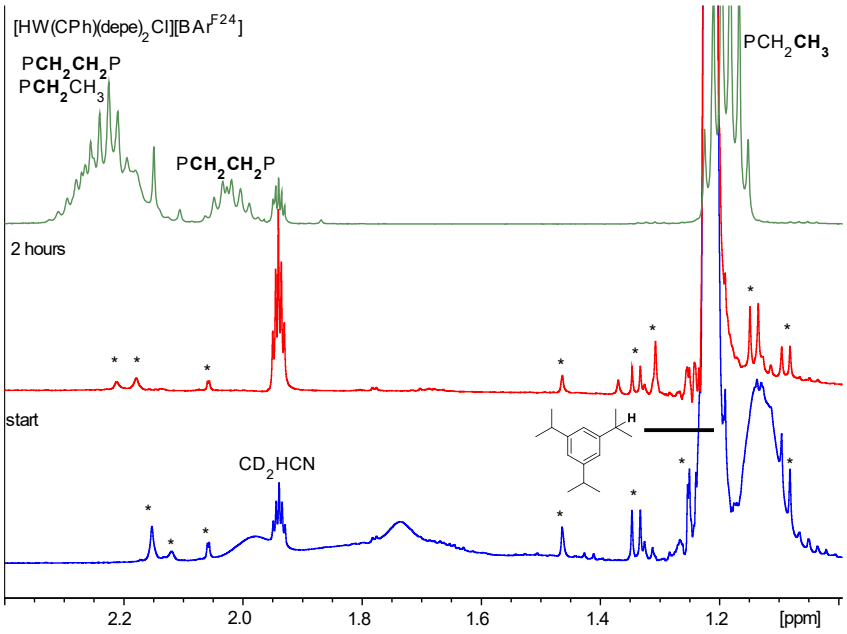

Figure 5.36. ^{1}H NMR spectra (500.13 MHz, CD_3CN) of the aliphatic region of the stoichiometric reaction between 2-chlorobenzonitrile and **1** with 10 equivalents of 1,3,5-triisopropylbenzene after 2 hours of irradiation shows the absence of [**1H**]$^{+}$ in comparison to authentic product. * Represents a peak that could not be identified.

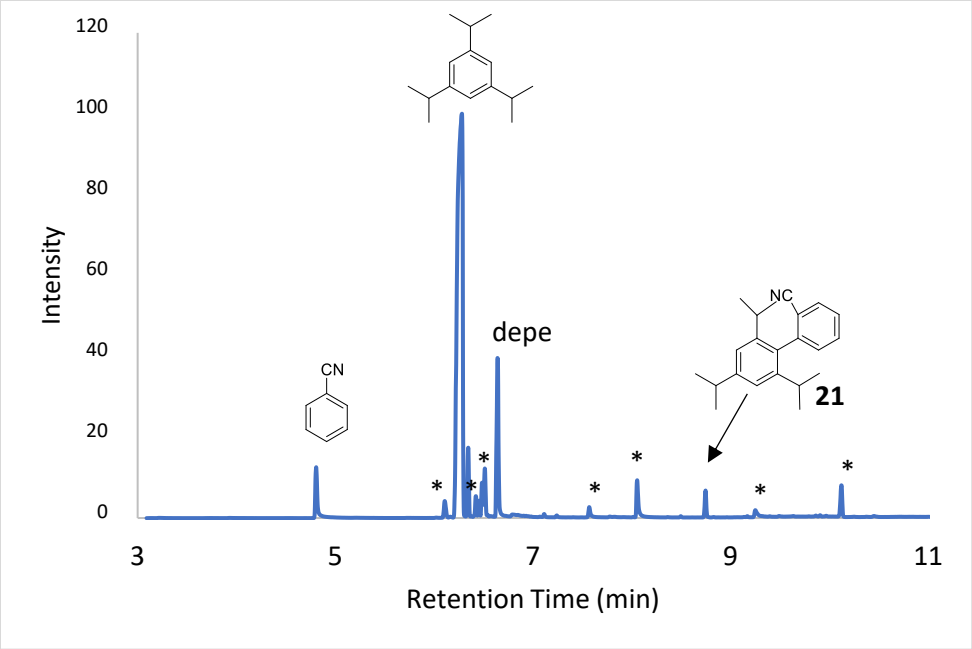

Figure 5.37. GC-MS trace of the stoichiometric reaction between 2-chlorobenzonitrile and W(CPh)(depe)$_2$Cl (**1**) with 10 equivalents of 1,3,5-triisopropylbenzene and the absence of any base after 2 hours of irradiation shows production of 2',4',6'-triisopropyl-[1,1'-biphenyl]-2-caronitrile (**21**).

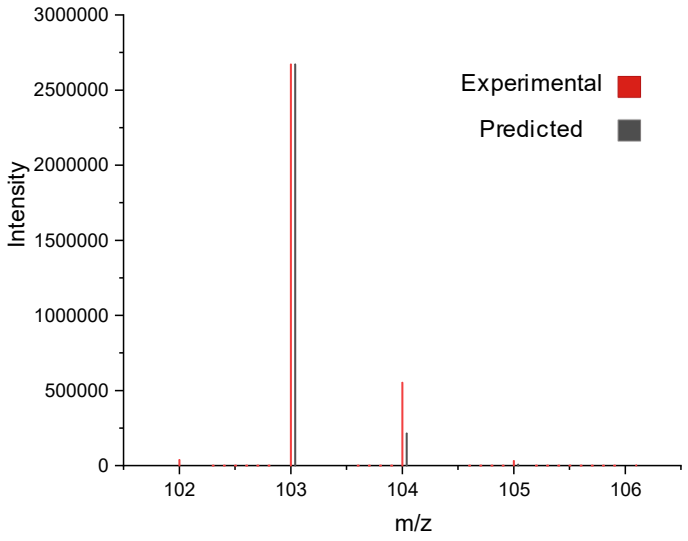

Figure 5.38. HR-MS fragmentation of the GC-MS trace peak at 4.79 min corresponding to benzonitrile shows proteo-benzonitrile and a small amount of deutero-benzonitrile in comparison with the predicted isotope splitting for proteo-benzonitrile.

5.2.6. New Chromophore Development: Synthesis and Characterization of W(CPh)(diBupe)$_2$Cl (3).

The discovery that W(CPh)(depe)$_2$Cl is significantly more stable in air than is W(CPh)(dmpe)$_2$Cl, despite possessing a nearly identical ground-state oxidation potential, suggests that sterically bulky phosphine R groups might impart kinetic aerobic stability to these chromophores. We tested this hypothesis by attempting to synthesize compounds with even bulkier phosphines, because bench-stable chromophores would be of greater practical value than air sensitive chromophores. As previously demonstrated by Dr. Vibbert, W(CPh){P(OMe)$_3$}$_4$Cl can be used as a precursor complex to W(CPh)(dmpe)$_2$Cl (**1**) and W(CPh)(depe)$_2$Cl (**2**) in a ligand substitution reaction with the corresponding bidentate phosphine ligand by refluxing in toluene.[14] We were interested in synthesizing tungsten-alkylidyne complexes with more sterically hindered phosphine ligands *via* this method including W(CPh)(diPrpe)$_2$Cl (diPrpe, 1,2-bis(diisopropylphosphino)ethane) and W(CPh)(diBupe)$_2$Cl (**3**) (diBupe, 1,2-bis(diisobutylphosphino)ethane). All attempts to synthesize W(CPh)(diPrpe)$_2$Cl from W(CPh){P(OMe)$_3$}$_4$Cl were unsuccessful. The structure of W(CPh)(diPrpe)$_2$Cl was calculated using DFT by Dr. Vibbert and shown to possess elongated W-P bonds, suggesting that the complex is too sterically congested to synthesize. To overcome this limitation, the synthesis of **3** was pursued instead. To a room temperature solution of W(CPh){P(OMe)$_3$}$_4$Cl (0.050 g, 0.0621 mmol) in toluene (20 mL) was added 1,2-bis(diisobutylphosphino)ethane (diBupe, 0.042 g, 0.130 mmol, 2.1 equivalents). A reflux condenser was affixed to the flask, the reaction apparatus was removed from the glovebox and the orange solution was heated to reflux. Over the course of 18 hours, the colour of the reaction mixture changed from yellow to brown. An aliquot of reaction mixture analyzed by $^{31}P\{^{1}H\}$ NMR spectroscopy showed evidence of decomposition due to the absence of resonances with tungsten satellites. The reaction was repeated using the solvent *o*-

xylene to achieve more forcing conditions and evidence of decomposition was again observed. Thus, it was reasoned that ligand substitution from a different complex should be explored and the starting material $W(CPh)(pic)_2(CO)_2Cl$ (pic = 4-picoline) was instead pursued. An *o*-xylene solution of $W(CPh)(pic)_2(CO)_2Cl$ and 2.1 equivalents of diBupe ligand were refluxed for 5 hours providing pink $W(CPh)(diBupe)_2Cl$ (**3**) in 48% crude yield (Scheme 5.4). Complex **3** was characterized with ^1H -, $^{31}P\{^1H\}$ -, and $^{13}C\{^1H\}$-NMR spectroscopy, HRA-MS and single-crystal X-ray diffraction.

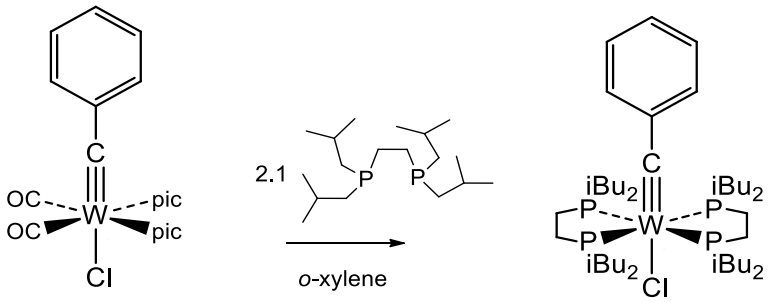

Scheme 5.4. Synthesis of $W(CPh)(diBupe)_2Cl$ (**3**) from $W(CPh)(pic)_2(CO)_2Cl$.

The $^{31}P\{^1H\}$ NMR spectrum of **3** (Figure 5.56) exhibits a singlet at 38.93 ppm with ^{183}W satellites, characteristic of tungsten-alkylidyne complexes with two bidentate phosphine ligands.[43] The ^1H NMR spectrum (Figure 5.51) exhibits four doublets between 0.93 and 1.14 ppm each integrating to 12 protons, assignable to the eight $PCH_2CH(C\underline{H}_3)_2$ moieties. The remainder of the aliphatic region exhibits broad multiplets that were identified by COSY NMR as corresponding to the $PCH_2C\underline{H}(CH_3)_2$, $PC\underline{H}_2CH(CH_3)_2$ and $PC\underline{H}_2C\underline{H}_2P$ resonances (Figure 5.52). The $^{13}C\{^1H\}$ NMR spectrum shows a characteristic multiplet at 247.64 ppm corresponding the alkylidyne carbon (Figure 5.53).[43] High resolution mass spectrometry verified the atomic weight of complex **3** (Anal. 944.4739, Calc. M^+ 944.4790; Figure 5.61).

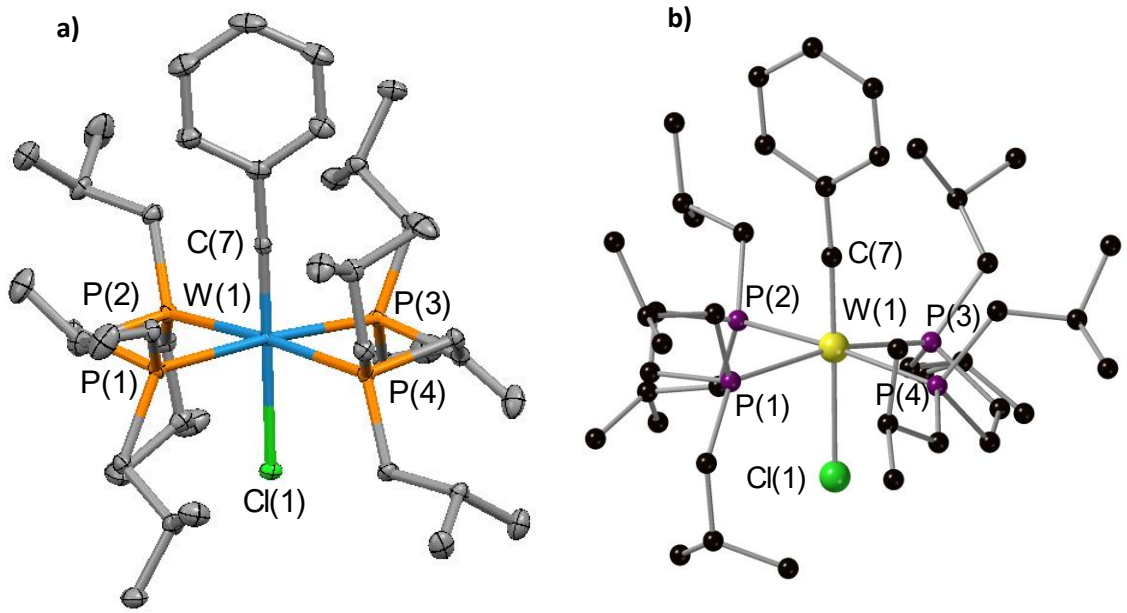

Figure 5.39. a) Molecular structure of W(CPh)(diBupe)$_2$Cl (**3**) (50% probability ellipsoids). Hydrogen atoms omitted for clarity**. b)** DFT computed structure of **3** with hydrogen atoms omitted for clarity.

Parameter	**W(CPh)(diBupe)$_2$Cl (3) crystal structure**	**W(CPh)(depe)$_2$Cl (1) crystal structure**	**W(CPh)(dmpe)$_2$Cl[13] (2) crystal structure**	**W(CPh)(diBupe)$_2$Cl (3) DFT structure**
W(1)-Cl(1) (Å)	2.5997(4)	2.5769(10)	2.5834(5)	2.622
W(1)-P(1) (Å)	2.4472(4)	2.4676(11)	2.4322(6)	2.525
W(1)-P(2) (Å)	2.4801(4)	2.4601(11)	2.4445(6)	2.486
W(1)-P(3) (Å)	2.4734(4)	2.4359(11)	2.4432(6)	2.495
W(1)-P(4) (Å)	2.4662(4)	2.4604(11)	2.4272(6)	2.517
W(1)-P(avg) (Å)	2.4667[4]	2.4560[11]	2.4368[6]	2.506
W(1)-C(7) (Å)	1.8244(16)	1.818(4)	1.829(2)	1.818
P(1)W(1)P(2) (°)	80.608(14)	80.11(4)	80.809(19)	77.4
P(3)W(1)P(4) (°)	80.174(14)	80.49(4)	80.741(19)	80.3
P(1)W(1)P(4) (°)	99.833(15)	97.87 (4)	98.97(2)	96.4
P(3)W(1)P(2) (°)	98.956(14)	100.74(4)	98.565(19)	104.3
C(7)W(1)Cl(1) (°)	179.40(5)	177.89(13)	178.38(6)	178.5
C(7)W(1)P(1) (°)	89.58(5)	95.40(13)	89.04(6)	90.9
C(7)W(1)P(2) (°)	92.24(5)	92.75(13)	93.56(6)	91.4
C(7)W(1)P(3) (°)	95.29(5)	91.13(13)	98.03(6)	95.5
C(7)W(1)P(4) (°)	92.76(5)	94.07(13)	93.77(6)	102.9
C(7)-W(1)-P(°) (avg)	92.47[5]	93.34[13]	93.60[6]	95.175

Table 5.6. Comparison of geometric parameters for the crystal structure and DFT computed structure of **3** with the crystal structures of **1** and **2**.

Crystals of **3** were grown from concentrated ether solution and the crystal structure was obtained (Figure 5.39). Complex **3** is shown to have a pseudo-octahedral structure analogous to the previously studied complexes **1** and **2**. Selected bond lengths and angles for these complexes are reported in Table 5.7. The benzylidyne and chloride ligands are in a linear arrangement (C(7)W(1)Cl(1) = 179.40(5)°) and occupy the axial sites of **3**. The phosphine ligands occupy the equatorial sites (C(7)W(1)P(avg) = 92.47[5]°). The tungsten-carbon bond length is 1.8244(16) Å which provides evidence for a triple bond.[13] In comparing the crystal structures of **1**, **2** and **3**, an observation can be made about the geometry as the steric bulk around the phosphine ligands is increased. The average tungsten phosphorus bond length increases with the steric bulk of the ligand, with 2.4368[6] Å for W(CPh)(dmpe)$_2$Cl (**2**), 2.4560[11] Å for W(CPh)(depe)$_2$Cl (**1**), and 2.4667[4] Å for W(CPh)(diBupe)$_2$Cl (**3**). The differences are statistically significant because they are greater than 3σ. Space-filling models of structures **1**-**3** are illustrate the increasing steric bulk of the ligand (Figure 5.40). In **2**, the benzylidyne α-carbon atom and tungsten center are visible; in **1** and **3**, they are not. Notably, in complex **2** the phenyl plane is oriented with the cleft between the dmpe ligands whereas for **1** and **3** are phenyl plane bisects the phosphine backbone.

Additionally, the structure of **3** was computed by DFT with Gaussian 16[33] using the B3P86 functional (Figure 5.39b).[34] The Dunning (DZP) basis set[35] was used for atoms H, C, P, Cl and the LANL2DZ basis set with effective core potentials was used for W.[36] The computed geometry is in good agreement with the crystal structure parameters (Table 5.6). The energy of the HOMO d_{xy} orbital is determined to be −4.58 eV. Using the relationship reported by Haines *et al.*, this corresponds to a first oxidation potential of $E_{1/2}^{0/+} = -1.00$ V vs. $FeCp_2^{0/+}$.[43] This potential is close to that calculated for **1** ($E_{1/2}^{0/+} = -1.09$ V vs. $FeCp_2^{0/+}$).[13] This is reasonable because of the structural similarity between the two compounds.

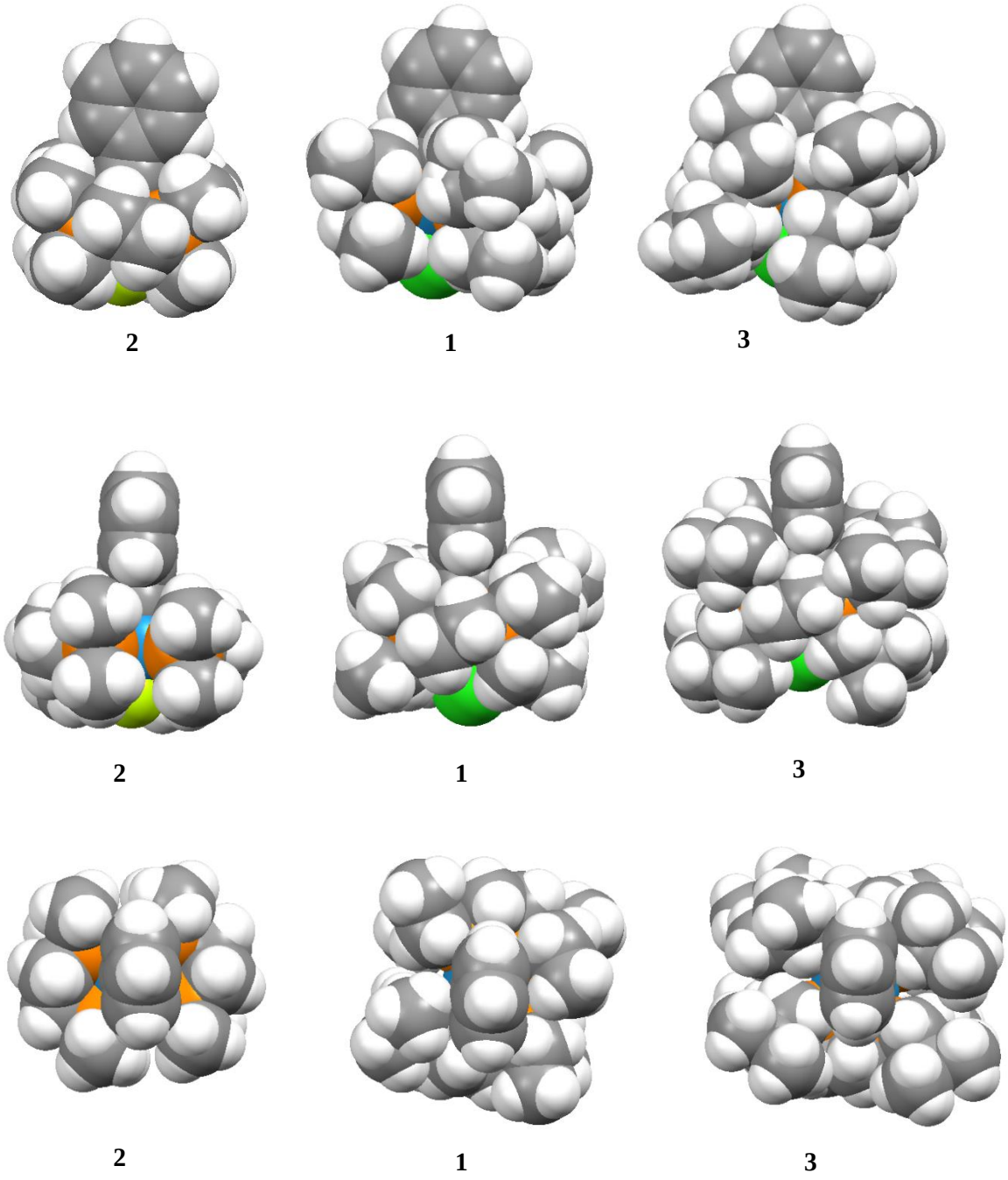

Figure 5.40. Space-filling models of the crystal structures of W(CPh)(dmpe)$_2$Cl (**2**), W(CPh)(depe)$_2$Cl (**1**) and W(CPh)(diBupe)$_2$Cl (**3**). Top row: front view, middle row: side view, bottom row: top view. Color code: Chlorine, green, etc. (note-Cl for 2 is a different color than for 1 and 3)

5.3 Conclusion.

Mechanistic studies of tungsten-alkylidyne catalyzed photoredox C-H arylation reactions were performed and $[HW(CPh)(depe)_2Cl]^+$ ($[\mathbf{1H}]^+$) is shown to be produced in the absence of exogenous base. This suggests that a PCET event between the enyl intermediate and oxidized chromophore may be occurring; this idea was further probed by DFT calculations for the pK_a and redox potentials of various enyl intermediates. Enyl intermediate **5** generated from pyrrole acceptor is calculated to have a pK_a of 43, which is too high for deprotonation by **1** and this eliminats PT-ET as the pathway. ET-PT is shown to be thermodynamically favourable between $[\mathbf{1}]^+$ and several enyl intermediates with sufficient reduction potentials, and these reactions generated a high catalytic yield of C-H arylation product.

ET-PT is also shown to be thermodynamically unfavourable with respect to ET between select enyl intermediates and $[\mathbf{1}]^+$. Catalytic reactions involving these enyl intermediates generate a low yield of C-H arylation product, suggesting an alternative HAT mechanism is possible. Stoichiometric reactions involving these intermediates in the absence of base also generate $[\mathbf{1H}]^+$ as a product, further supporting a HAT mechanism. The possibility of this mechanism is further probed by increasing the sterics around the enyl intermediate, which successfully inhibits the concerted HAT reaction.

A concerted HAT mechanism involving visible-light catalyzed C-H arylation has not been demonstrated before and represents a novel pathway for these reactions. The findings from this study may be used to understand the substrate and acceptor scope that is feasible for tungsten-alkylidyne catalyzed C-H arylation reactions, as well as design new photoredox chromophores. Additionally, a new tungsten-alkylidyne chromophore with sterically bulky phosphine ligands was synthesized and its reactivity in C-H arylation reactions may be studied.

5.4 Experimental Section.

5.4.1 Synthesis and Characterization of New Metal Complexes.

General Procedures. All manipulations were performed under a nitrogen atmosphere using standard glovebox and Schlenk techniques unless otherwise stated. Solvents used for synthesis were HPLC grade and were purified under nitrogen with an anaerobic steel system of either two 4.5 in × 24 in (1 gal) activated A2 alumina columns (CH_3CN, Et_2O, THF) or one column of activated A2 alumina and one column of activated BASF R3-11 catalyst (toluene, pentane). CH_2Cl_2 was sparged with nitrogen gas for 15 minutes and dried over 3 Å molecular sieves. Solvents used for NMR spectroscopy (CD_3CN, $(CD_3)_2SO$, C_6D_6) were used as received and stored in the glovebox over 3 Å molecular sieves in the glovebox. W(CPh){P(OMe)$_3$}$_4$Cl was prepared as previously described.[31] 1,2-bis(diisobutylphosphino)ethane) (diBupe) ligand was prepared according to the literature procedure.[44] N-methylpyrrole was distilled before use. All other reagents were used as received. ^{1}H- , ^{13}C{^{1}H}- , ^{31}P{^{1}H}-, ^{19}F{^{1}H} - NMR spectra were recorded at room temperature using a Bruker AF-500 NMR spectrometer. Chemical shifts were measured relative to residual solvent resonances (^{1}H, ^{13}C) or external standards (^{31}P, 85% v/v H_3PO_4; ^{19}F C_6F_6). ^{13}C{^{1}H}- resonances were identified using H-C HSQC. GC-MS was recorded with either an Agilent SQ GC-MS (5977A single quad MS and 7890B GC) or an Agilent QTOF High Resolution Accurate GC-MS. HR-MS spectra were measured with an Agilent 6224 ToF High Resolution Accurate MS.

Synthesis of [HW(CPh)(depe)$_2$Cl][BAr^{F24}] ([1H][BAr^{F24}]). This procedure is adapted from the synthesis of [HW(CPh)(dppe)$_2$Cl][PF_6].[31] A stirred THF solution (20 mL) of W(CPh)(depe)$_2$Cl (0.300 g, 0.416 mmol) was cooled to 0 ºC with an ice bath and HCl (0.46 mL, 1.0 M in ether, 0.457 mmol) was added dropwise by syringe causing an immediate colour change from pink to light

yellow and the precipitation of off-white solid. After stirring for 2 hours at 0 ºC, the volatile components were removed under vacuum and the remaining yellow film was dissolved in minimal acetonitrile and filtered over Celite. To the filtrate was added $NaBAr^{F24}$ (0.369 g, 0.416 mmol) in acetonitrile (5 mL) slowly while stirring causing a white precipitate (presumably NaCl), which was subsequently filtered to remove. Acetonitrile was removed from the filtrate under vacuum to yield $[HW(CPh)(depe)_2Cl][BAr^{F24}]$ as an off-white solid (0.276 g, 0.383 mmol, 92% crude yield). The solid was dissolved in acetonitrile (2 mL) and recrystallized by cooling to −40 ºC; this provided off-white crystals (0.195 g, 0.123 mmol, 30% yield). ^{1}H NMR (500.13 MHz, CD_3CN): δ 7.70 (s, 8H, *o*-CH BAr^{F24}); 7.67 (s, 4 H *p*-CH BAr^{F24}); 7.13 (m, 3H, *m*,*p*-C_6H_5); 6.88 (d, J_{HH} = 7 Hz, 2H, *o*-C_6H_5); 2.23 (m, 20 H, $PC\underline{H}_2CH_3$, $PC\underline{H}_2C\underline{H}_2P$); 2.02 (m, 5H, $PC\underline{H}_2C\underline{H}_2P$); 1.19 (m, 24 H, $PCH_2C\underline{H}_3$). The W-H resonance could not be identified in the ^{1}H NMR, likely due to its chemical shift overlapping with the aliphatic region.[30] $^{13}C\{^1H\}$ NMR (125.75 MHz, CD_3CN): δ 260.47 (m, $^2J_{CP}$ = 12 Hz, $W\underline{C}C_6H_5$), 162.77 (q, $^1J_{CB}$ = 50 Hz, $B\underline{C}Ar$), 135.62 (*o*-BCAr), 131.20 (*o*-WCC_6H_5), 129.76 (q, $^1J_{CF}$ = 31 Hz, BCAr-$\underline{C}F_3$), 128.75 (*m/p*-WCC_6H_5), 128.08 (m/*p*-WCC_6H_5), 118.64 (*p*-BCAr), 23.23 (m, $P\underline{C}H_2CH_3$), 22.41 (br m., $P\underline{C}H_2CH_3$), 17.66 (m, $P\underline{C}H_2\underline{C}H_2P$), 9.43 ($PCH_2\underline{C}H_3$), 8.56 ($PCH_2\underline{C}H_3$). ^{19}F NMR (471 MHz, CD_3CN): δ -63.22 (s, BAr^{F24}). HR MS: 721.2323 m/z (M^+, calc, 721.2361).

Synthesis of $W(CPh)(diBupe)_2Cl$ (3). $W(CPh)(pic)_2(CO)_2Cl$ (0.100 g, 0.182 mmol) was suspended in o-xylene (1.2 mL) and 1,2-bis(diisobutylphosphino)ethane (diBupe, 0.122 g, 0.381 mmol, 2.1 equivalents) was added. A refluxed condenser was affixed to the flask, the reaction apparatus was removed from the glovebox and the yellow solution was heated to reflux. Over the course of 5 hours, the colour of the reaction mixture changed from yellow to red. The reaction was cooled to room temperature, and the volatile components were removed under vacuum. The

remaining red film was extracted into ether (50 mL) and filtered over Celite. The volatile components were removed from the filtrate by vacuum to yield a pink solid (0.083 g, 0.088 mmol, 48% crude yield). The solid was dissolved in ether (1 mL) and cooled to -40 ºC; this provided pink crystals (0.030 g, 0.032 mmol, 17% yield). ^{1}H NMR (500.13 MHz, C_6D_6): δ 6.95 (m, 3H, *m,p*-C_6H_5); 6.86 (m, 2H, *o*-C_6H_5); 2.41 (m, 4H, $PC\underline{H_2}CH(CH_3)_2$); 2.33, 2.27 (two overlapping br m, 8H, $PCH_2C\underline{H}(CH_3)_2$); 2.14 (br m, 8H, $PC\underline{H_2}CH(CH_3)_2$); 2.04, 1.99 (two overlapping br m, 8H, $PC\underline{H_2}CH(CH_3)_2$, $PC\underline{H_2}C\underline{H_2}P$); 1.82 (br m, 4H, $PC\underline{H_2}C\underline{H_2}P$); 1.13 (d, J_{HH} = 7 Hz, 12H, $PCH_2CH(C\underline{H_3})_2$); 1.09 (d, J_{HH} = 7 Hz, 12H, $PCH_2CH(C\underline{H_3})_2$); 1.05 (d, J_{HH} = 7 Hz, 12H, $PCH_2CH(C\underline{H_3})_2$); 0.94 (d, J_{HH} = 7 Hz, 12H, $PCH_2CH(C\underline{H_3})_2$). ^{31}P{^{1}H} NMR (202.45 MHz, C_6D_6): δ 38.93 (s with ^{183}W satellites, $^{1}J_{WP}$ = 273 Hz). ^{13}C{^{1}H} NMR (125.75 MHz, C_6D_6): δ 247.64 (m, $W\underline{C}C_6H_5$);129.32 (*o*-C_6H_5), 127.63 (*m/p*-C_6H_5); 122.78 (*m/p*-C_6H_5); 43.28 (m, $P\underline{C}H_2CH(CH_3)_2$); 37.51 (m, $P\underline{C}H_2CH(CH_3)_2$); 29.53 (m, $P\underline{C}H_2\underline{PC}H_2P$); 26.88 ($PCH_2\underline{C}H(CH_3)_2$); 26.47 ($PCH_2\underline{C}H(CH_3)_2$); 26.41 ($PCH_2CH(\underline{C}H_3)_2$); 26.41 ($PCH_2CH(\underline{C}H_3)_2$); 25.99 ($PCH_2CH(\underline{C}H_3)_2$); 25.92 ($PCH_2CH(\underline{C}H_3)_2$). HR MS: 944.4739 m/z ($M^+$, calc, 944.4790).

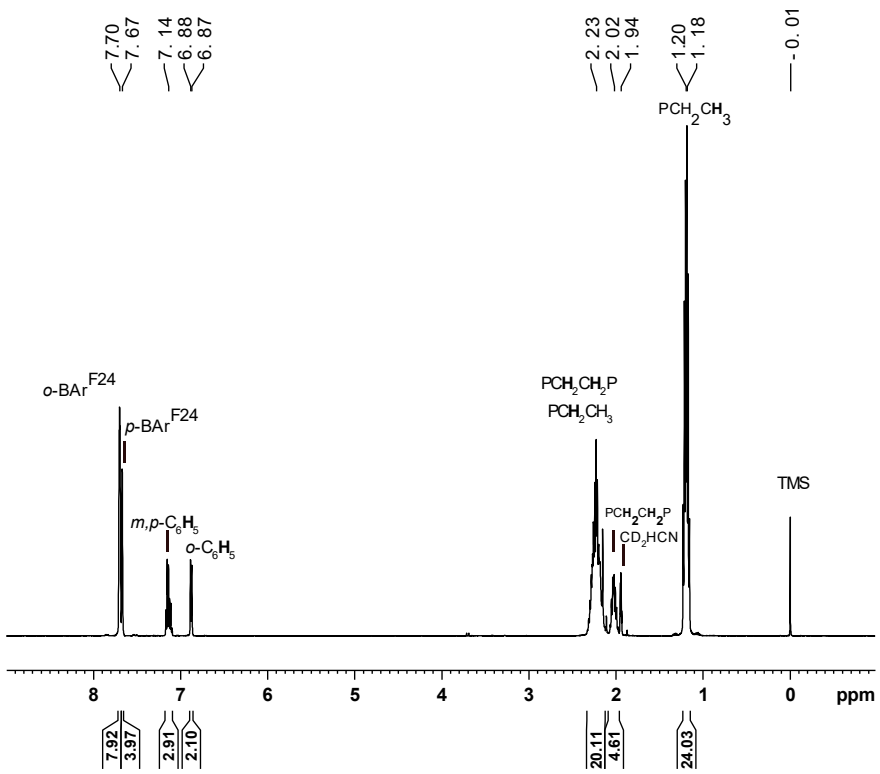

Figure 5.41. ^{1}H NMR spectrum (500.13 MHz) of [HW(CPh)(depe)$_2$Cl][BAr^{F24}] ([**1H**][BAr^{F24}]) in CD_3CN.

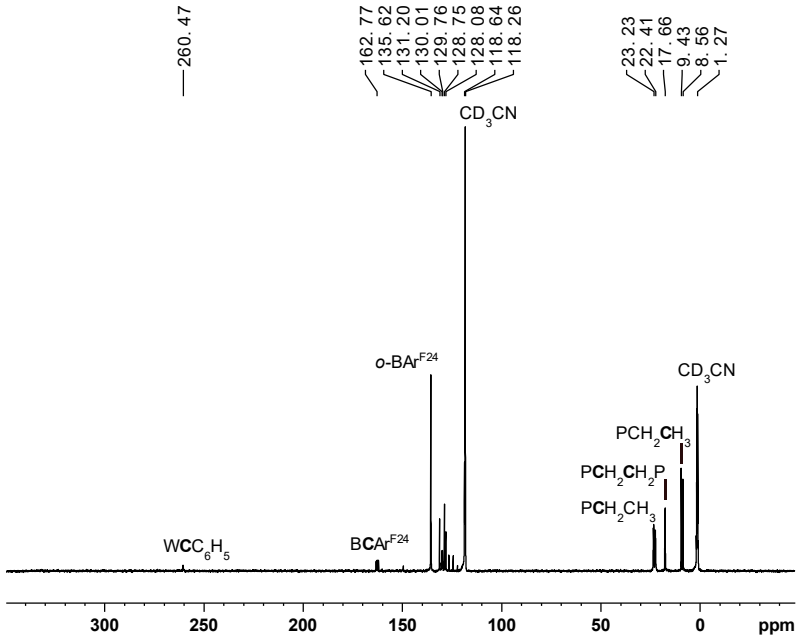

Figure 5.42. ^{13}C{^{1}H} NMR spectrum (125.75 MHz) of [HW(CPh)(depe)$_2$Cl][BAr^{F24}] ([**1H**][BAr^{F24}]) in CD_3CN.

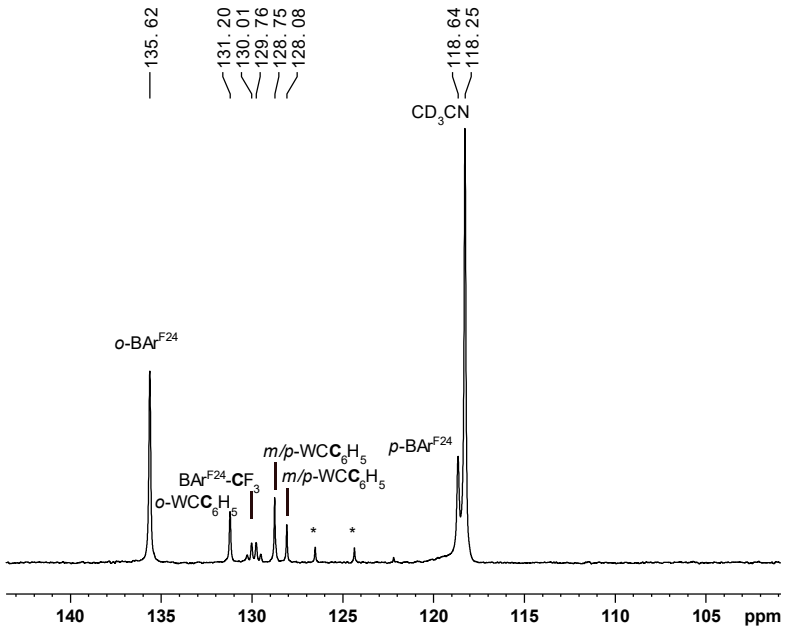

Figure 5.43. Aromatic region of the $^{13}C\{^{1}H\}$ NMR spectrum (125.75 MHz) of [HW(CPh)(depe)$_2$Cl][BAr^{F24}] ([**1H**][BAr^{F24}]) in CD_3CN. * Represents an impurity that could not be removed.

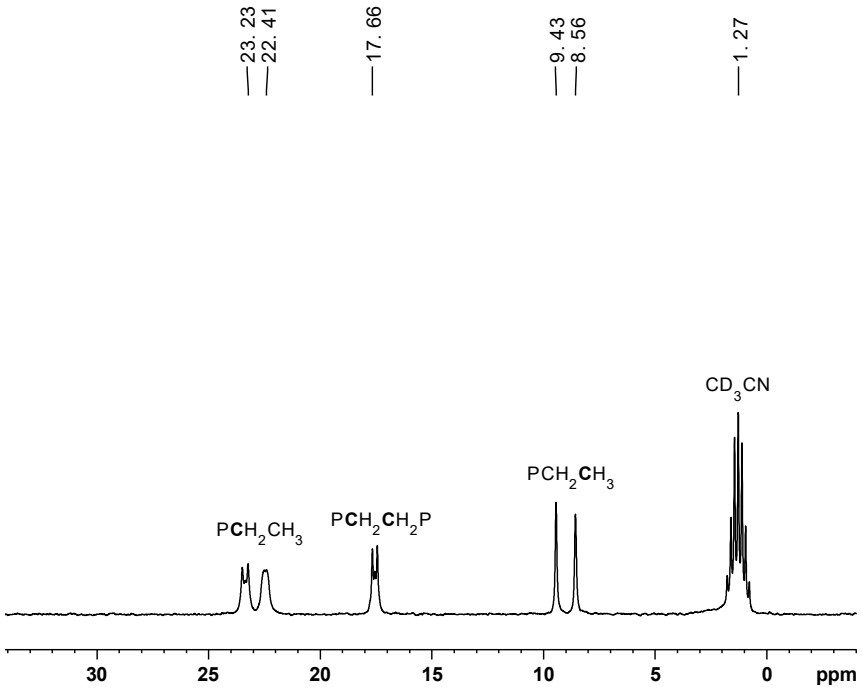

Figure 5.44. Aliphatic region of the $^{13}C\{^{1}H\}$ NMR spectrum (125.75 MHz) of [HW(CPh)(depe)$_2$Cl][BAr^{F24}] ([**1H**][BAr^{F24}]) in CD_3CN.

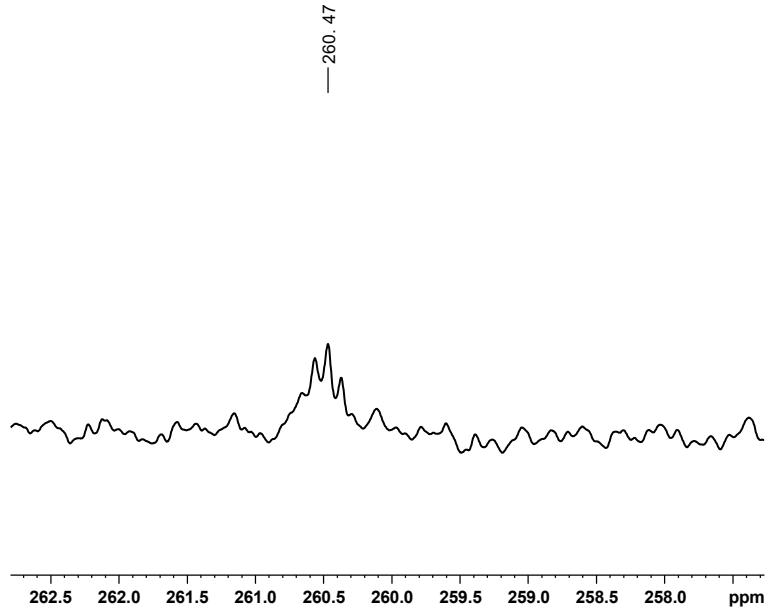

Figure 5.45. Alkylidyne resonance of the $^{13}C\{^{1}H\}$ NMR spectrum (125.75 MHz) of $[HW(CPh)(depe)_2Cl][BAr^{F24}]$ ($[\mathbf{1H}][BAr^{F24}]$) in CD_3CN.

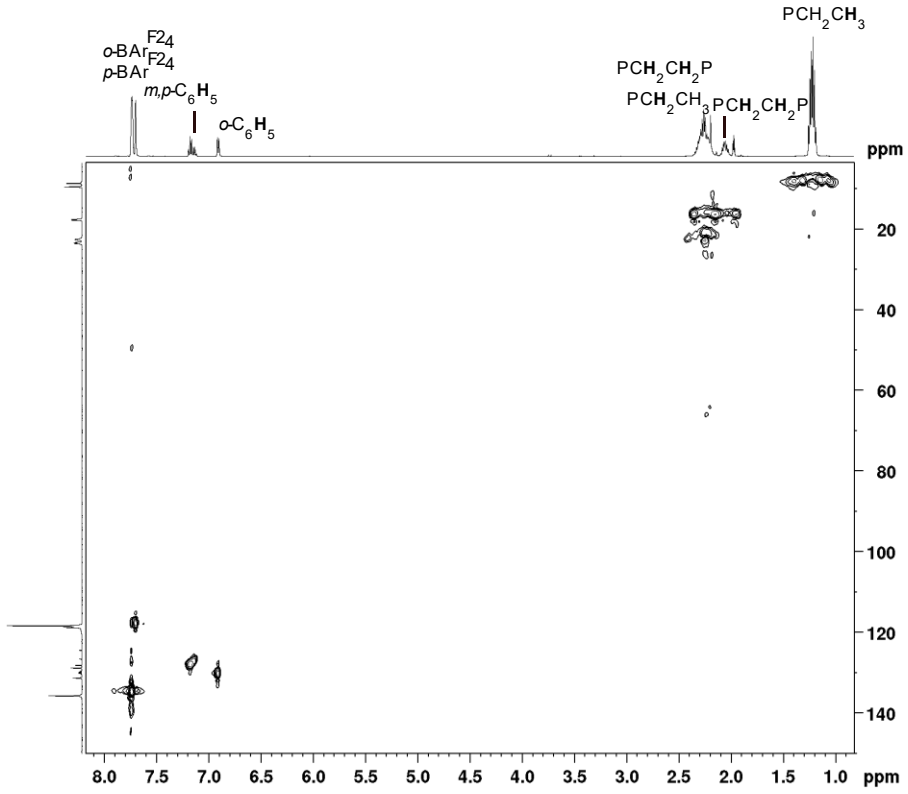

Figure 5.46. HSQC spectrum (CD_3CN) of $[HW(CPh)(depe)_2Cl][BAr^{F24}]$ ($[\mathbf{1H}][BAr^{F24}]$).

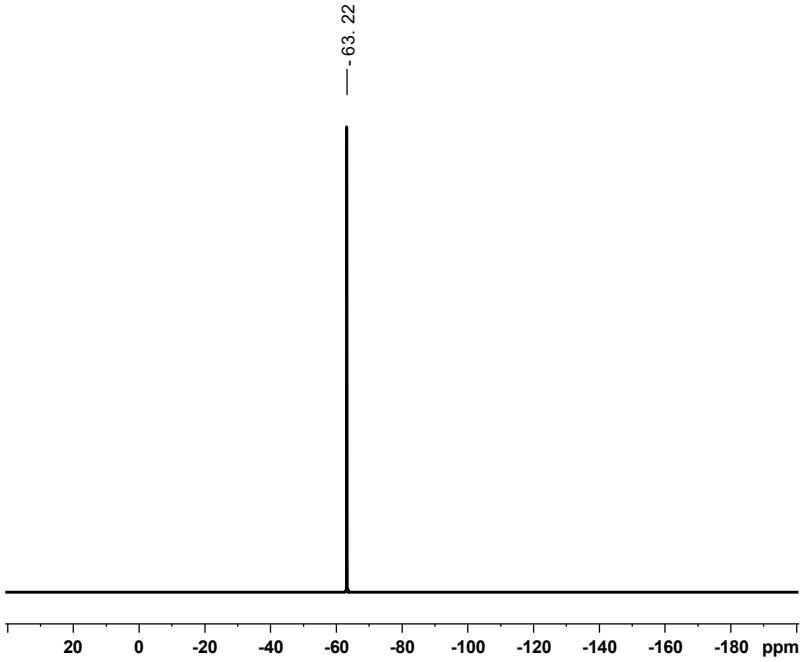

Figure 5.47. $^{19}F\{^{1}H\}$ NMR spectrum (470.60 MHz) of $[HW(CPh)(depe)_2Cl][BAr^{F24}]$ ([**1H**][BAr^{F24}]) in CD_3CN.

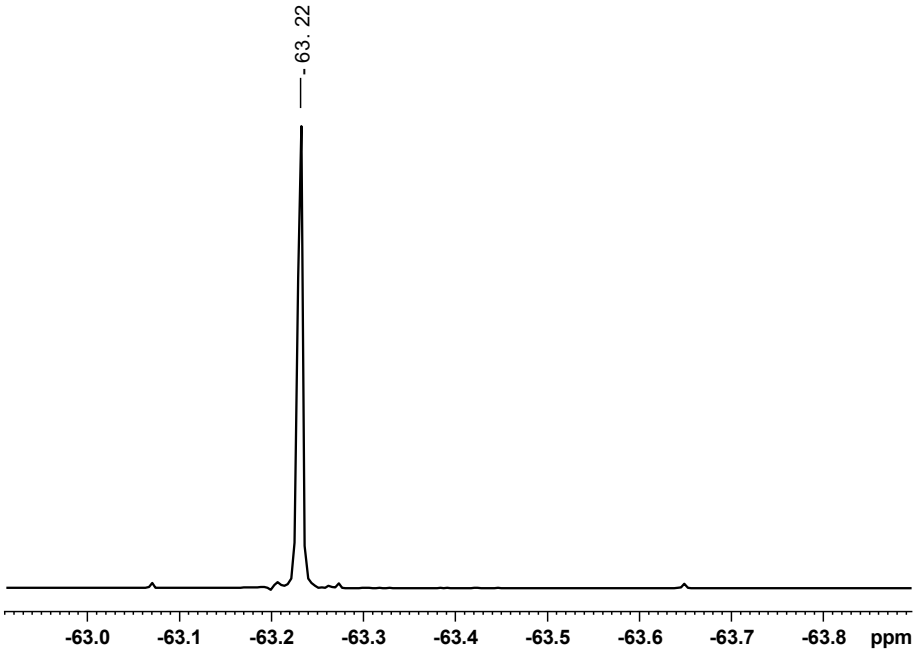

Figure 5.48. Expanded $^{19}F\{^{1}H\}$ NMR spectrum (470.60 MHz) of $[HW(CPh)(depe)_2Cl][BAr^{F24}]$ ([**1H**][BAr^{F24}]) in CD_3CN.

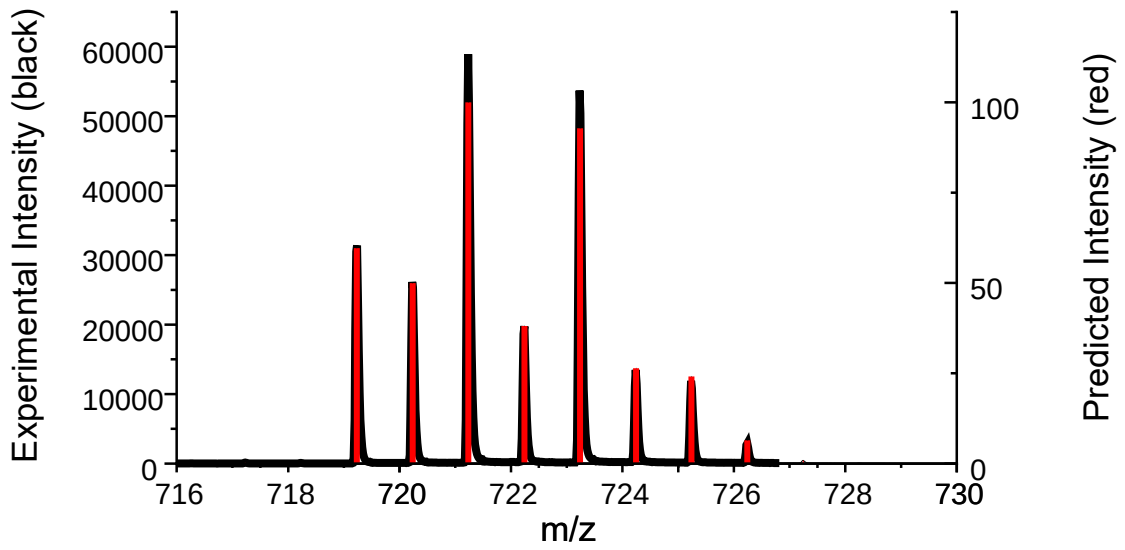

Figure 5.49. HR-MS (acetonitrile, 298 K) of [HW(CPh)(depe)$_2$Cl][BAr^{F24}] ([**1H**][BAr^{F24}]). Anal. M$^+$ 721.2323; Calc. M$^+$ 721.2361.

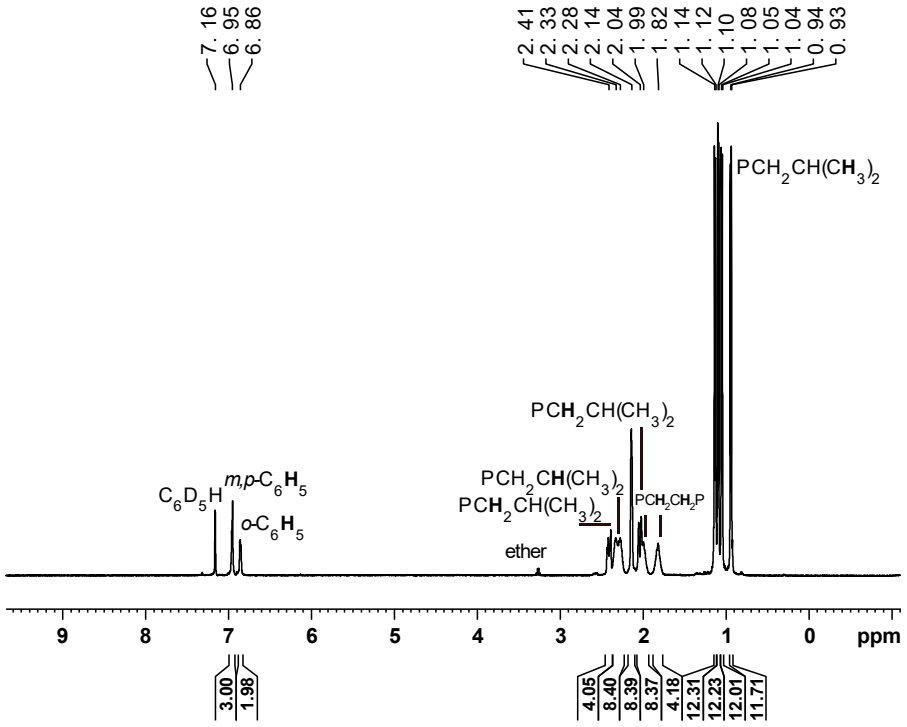

Figure 5.50. ^{1}H NMR spectrum (500.13 MHz) of W(CPh)(diBupe)$_2$Cl (**3**) in C_6D_6.

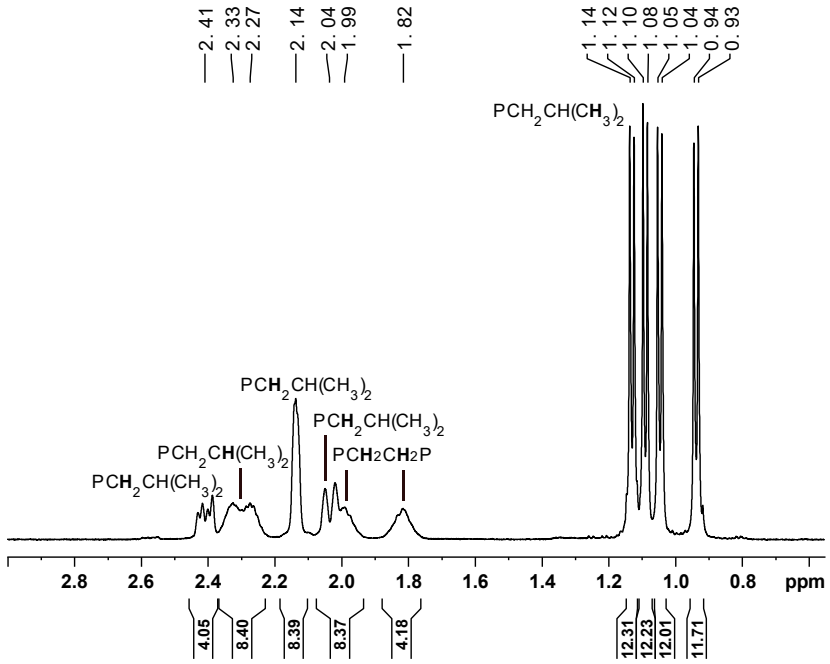

Figure 5.51. Expanded aliphatic region of the ^{1}H NMR spectrum (500.13 MHz) of W(CPh)(diBupe)$_2$Cl (**3**) in C_6D_6.

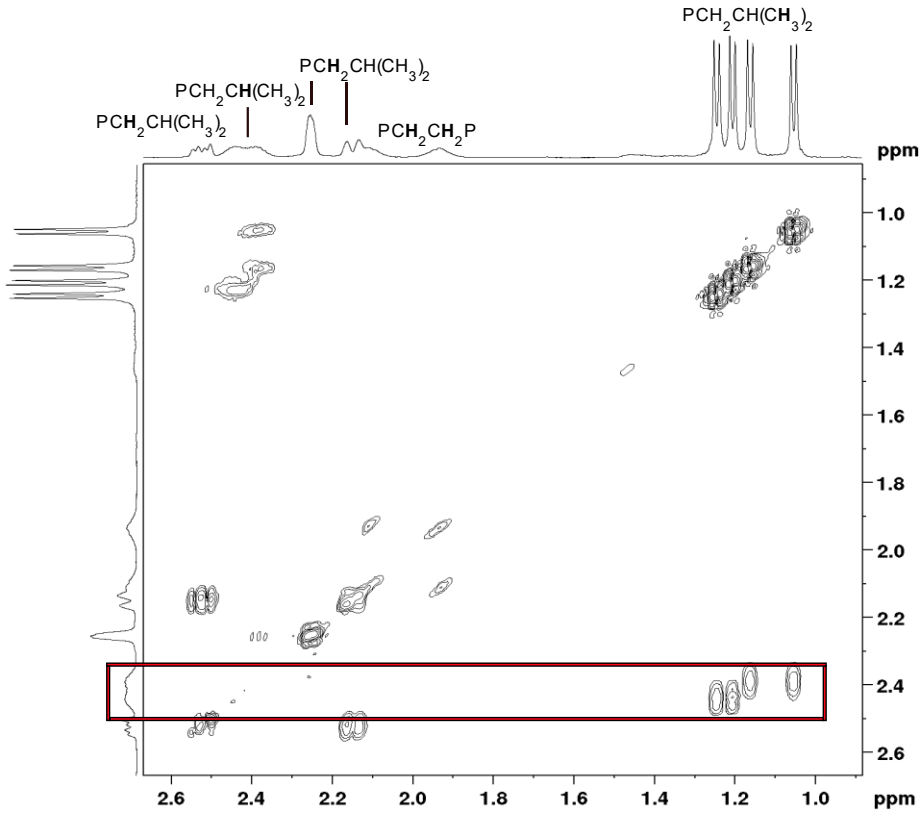

Figure 5.52. Aliphatic region of COSY spectrum (C_6D_6) of W(CPh)(diBupe)$_2$Cl (**3**) showing the correlation that identifies the isopropyl proton resonance.

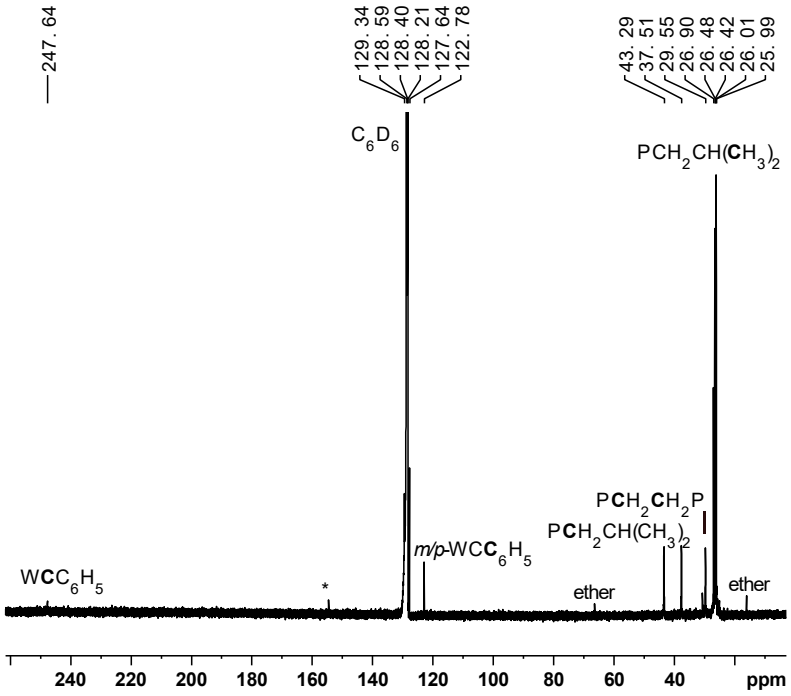

Figure 5.53. $^{13}C\{^{1}H\}$ NMR spectrum (125.75 MHz) of W(CPh)(diBupe)$_2$Cl (**3**) in C_6D_6. * Represents an impurity that could not be removed.

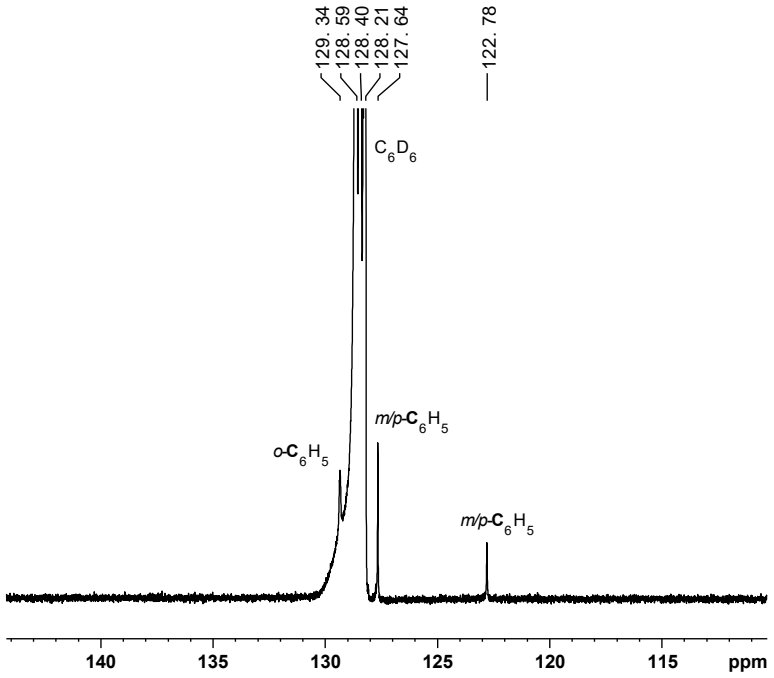

Figure 5.54. Expanded aromatic region of $^{13}C\{^{1}H\}$ NMR spectrum (125.75 MHz) of W(CPh)(diBupe)$_2$Cl (**3**) in C_6D_6.

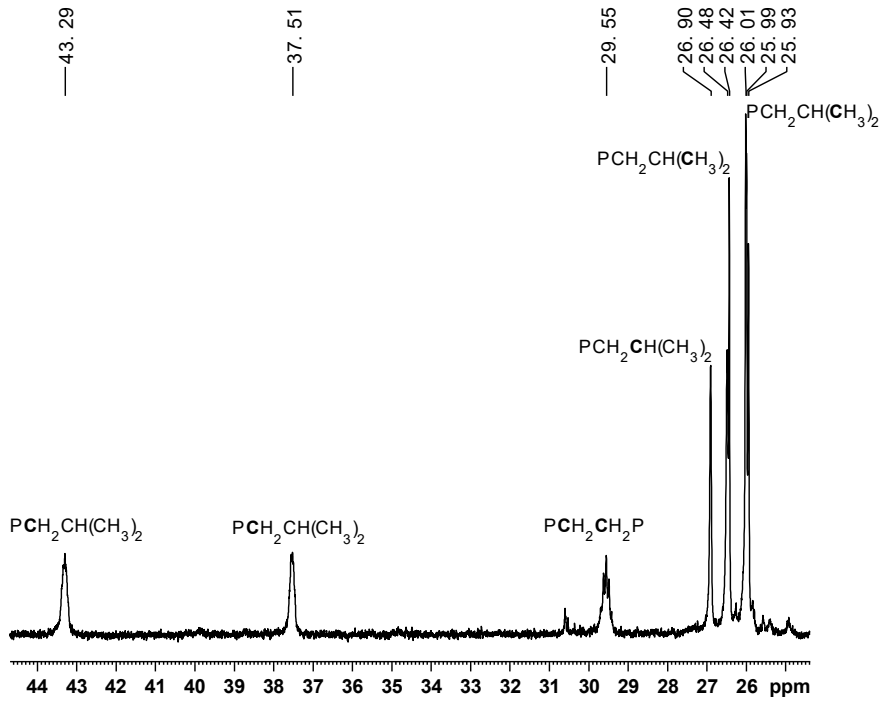

Figure 5.55. Expanded aliphatic region of $^{13}C\{^{1}H\}$ NMR spectrum (125.75 MHz) of W(CPh)(diBupe)$_2$Cl (**3**) in C_6D_6.

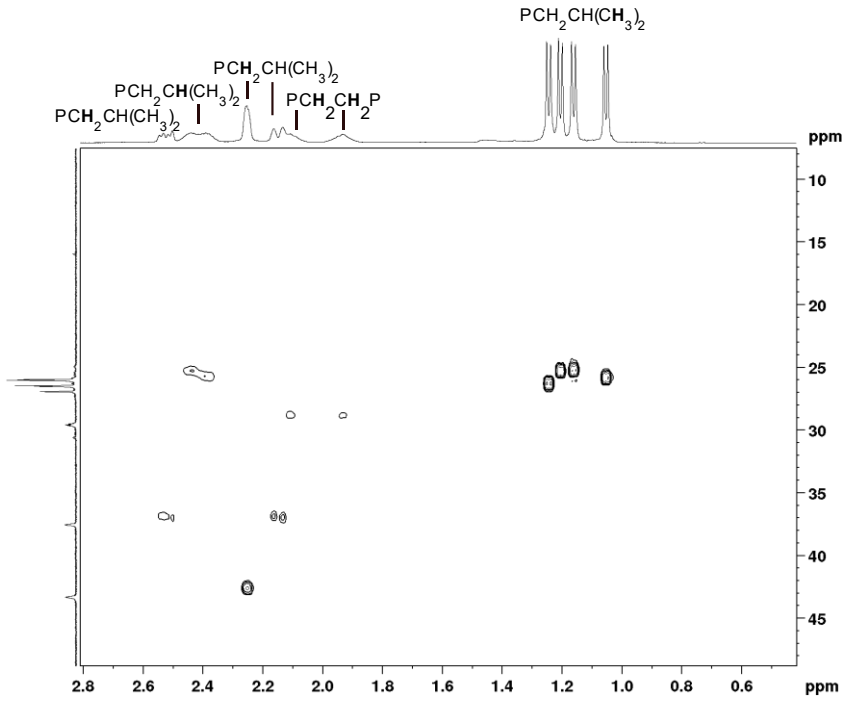

Figure 5.56. HSQC spectrum (C_6D_6) of W(CPh)(diBupe)$_2$Cl (**3**).

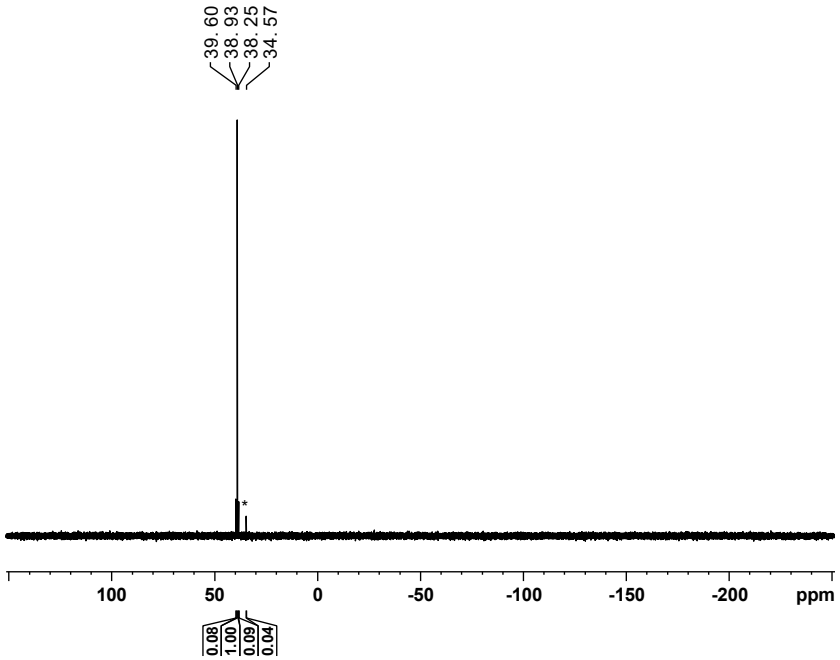

Figure 5.57. $^{31}P\{^{1}H\}$ NMR spectrum (202.45 MHz) of W(CPh)(diBupe)$_2$Cl (**3**) in C_6D_6. * Represents an impurity that could not be removed.

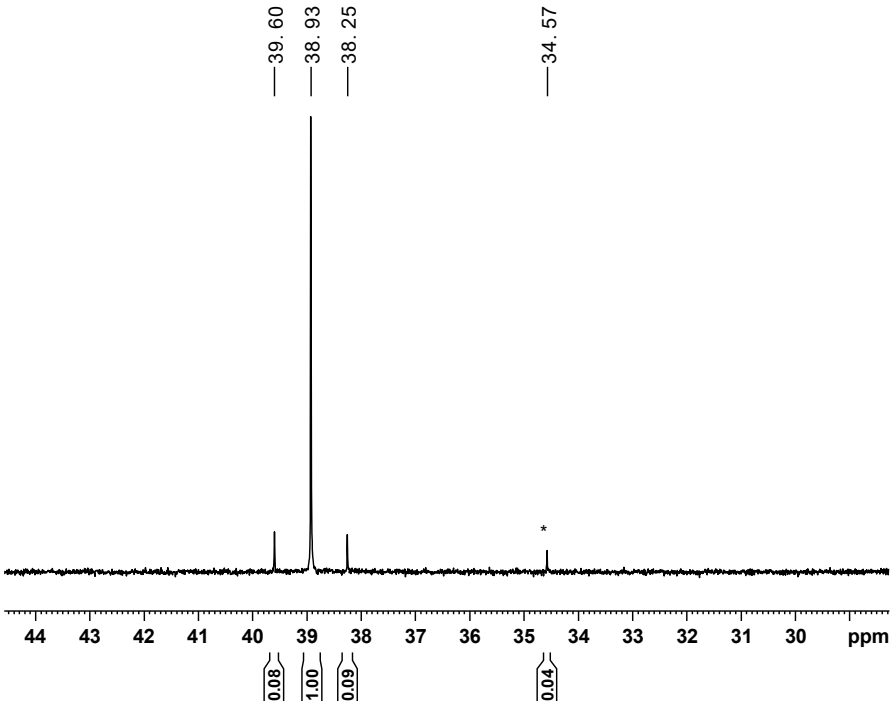

Figure 5.58. Expanded $^{31}P\{^{1}H\}$ NMR spectrum (202.45 MHz) of W(CPh)(diBupe)$_2$Cl (**3**) in C_6D_6. * Represents an impurity that could not be removed.

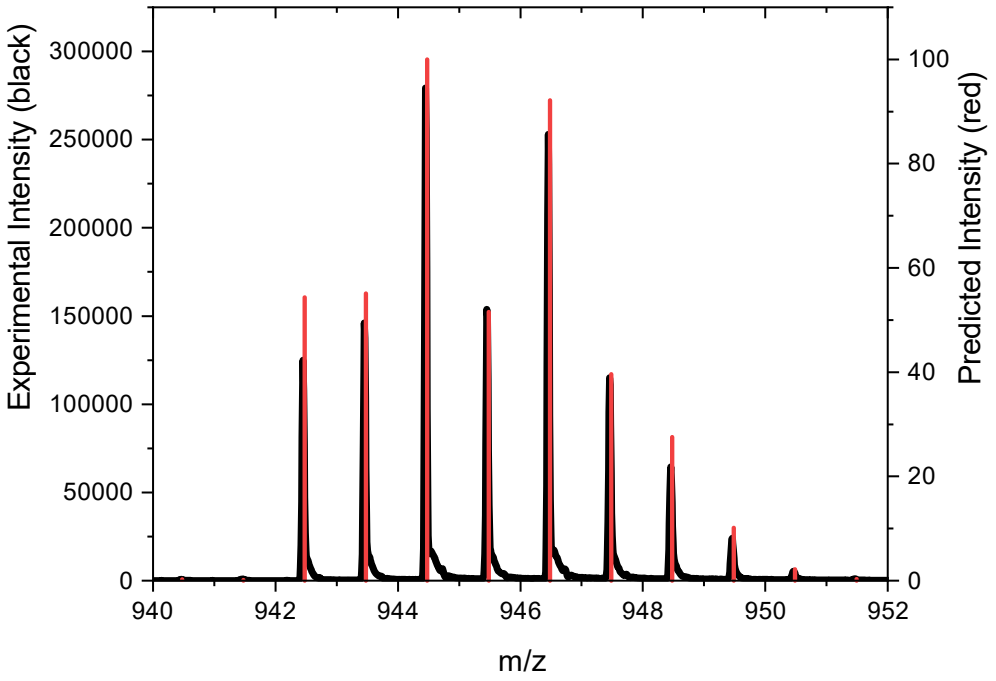

Figure 5.59. HR-MS (THF, 298 K) of W(CPh)(diBupe)$_2$Cl (**3**). Anal. M^+ 944.4739; Calc. M^+ 944.4790.

5.4.2 Single-Crystal X-ray Diffraction Studies.

General Procedures. Crystals were coated with Fluorolube, attached to the tip of a glass fiber and mounted under nitrogen at 100 K in the X-ray beam with a video camera. The diffraction data were measured with a Bruker D8 VENTURE diffractometer with a microfocus Mo-target X-ray tube (λ = 0.71073 Å) and a PHOTON 100 CMOS detector. The data were collected with φ and ω scans surveying a hemisphere of reciprocal space. The reduction and integration of the data were performed with the Bruker APEX3 software (Bruker AXS, version 2017.3-0, 2018). Data was scaled and corrected for absorption effects with the multi-scan SADABS procedure (Bruker AXS, version 2014/5).[45] Structures were solved with SHELXT Version 2014/5[46] and refined with a full-matrix least-squares procedure[47] using OLEX2.[48] Crystal structure data and refinement parameters are included in Table 5.7.

Crystal Structure of [HW(CPh)(depe)$_2$Cl][BAr^{F24}] ([1H]BAr^{F24}). The hydride atom of [**1H**]$^+$ was not detected or modelled. Atoms were refined with anisotropic thermal parameters except the disordered part of the phosphine ligand, of which the ratio of parts is 65:35. The BAr^{F24}- counterion contained several CF_3 groups that were disordered and each was modelled individually. The geometric restraints used for the disordered parts include SADI and DFIX, and the thermal constraints were RIGU, SIMU and EADP. Hydrogen atoms were included in idealized positions for structure factor calculations. The molecular structure of [**1H**]$^+$ is shown in Figure 5.5 and structural parameters are detailed in Table 5.1.

Crystal Structure of W(CPh)(diBupe)$_2$Cl (3). All atoms were refined with anisotropic thermal parameters. Hydrogen atoms were included in idealized positions for structure factor calculations. The molecular structure of **3** is shown in Figure 5.39 and structural parameters are detailed in Table 5.6.

Parameter	**[1H][BAr^{F24}]**	**3**
Empirical Formula	$C_{59}H_{65}BClF_{24}P_4W$	$C_{43}H_{85}ClP_4W$
Formula Weight	1584.10	945.28
Temperature (K)	100(2)	100(2)
Crystal System	triclinic	monoclinic
Space Group	P-1	$P2_{1/c}$
***a* (Å)**	13.5663(9)	12.2995(7)
b (Å)	14.4714(9)	24.1887(13)
c (Å)	17.0473(11)	16.4815(9)
***α* (deg)**	94.470(2)	90
***β* (deg)**	101.618(2)	105.221(2)
***γ* (deg)**	96.027(2)	90
Volume (Å^3)	3243.2(4)	4731.4(5)
Z	2	4
ρ_{calc} (g/cm^3)	1.622	1.327

Table 5.7. Crystal Data and Refinement Parameters for [HW(CPh)(depe)$_2$Cl][BAr^{F24}] ([**1H**]BAr^{F24}) and W(CPh)(diBupe)$_2$Cl (**3**).

Table 5.7 continued. Crystal Data and Refinement Parameters for [HW(CPh)(depe)$_2$Cl][BAr^{F24}] ([**1H**]BAr^{F24}) and W(CPh)(diBupe)$_2$Cl (**3**).

Abs coeff μ (mm^{-1})	2.028	2.660
***F*(000)**	1582.0	1976.0
Crystal dimensions (mm^3)	0.28×0.18×0.12	0.36×0.24×0.21
2θ range for data collection (deg)	4.33 to 52.882	4.808 to 61.302
***h, k, l* ranges collected**	$-16 \leq h \leq 16$ $-18 \leq k \leq 18$ $-21 \leq l \leq 21$	$-17 \leq h \leq 17$ $-34 \leq k \leq 34$ $-23 \leq l \leq 23$
Reflections collected	79773	179898
Independent reflections	13316 [R_{int}[a]= 0.0591, R_{sigma} = 0.0501]	14596 [R_{int}[a]= 0.0505, R_{sigma} = 0.0230]
Data/restraints/parameters	13316/1511/1083	14596/0/458
Goodness-of-fit on F^2 [d]	1.039	1.070
Final *R* indexes (I ≥ 2σ(*I*))	R_1[b] = 0.0599, wR_2[c] = 0.1270	R_1[b] = 0.0216, wR_2[c] = 0.0452
Final *R* indexes (all data)	R_1[b] = 0.0888, wR_2[c] = 0.1423	R_1[b] = 0.0296, wR_2[c] = 0.0472
Largest diff. peak/hole (e•Å^{-3})	3.27/–1.99	1.15/–0.47

[a] $R_{int} = \Sigma(|Fo^2 - \langle Fo^2 \rangle|) / \Sigma |Fo^2|$
[b] $R_1 = \Sigma ||Fo| - |Fc|| / \Sigma |Fo|$
[c] $wR_2 = \{\Sigma [w(Fo^2 - Fc^2)^2] / \Sigma [w(Fo^2)^2]\}^{1/2}$
[d] Goodness–of–fit = $[[w(Fo^2 - Fc^2)^2] / (Nrefl - Nparams)^{1/2}$

5.4.3. Photoredox C-H Arylation Reactions.

General Procedure for GC-MS Scale Reactions. The reactions were performed in screw cap vials under nitrogen and contained 2-chlorobenzonitrile (0.0454 mmol, 1 equiv,) 1,1,3,3-tetramethylguanidine (0.0908 mmol, 2 equiv.), arene/heteroarene (1.816 mmol, 40 equiv.), and W(CPh)(depe)$_2$Cl (**1**) chromophore (0.908 μmol, 2 mol%) in 1.5 ml acetonitrile. The reaction mixture was photolyzed at room temperature with white LEDs using our previously described photolysis apparatus. After photolysis the reaction mixture was opened to air and 5 μl of

acetophenone was added as a GC internal standard. The mixture was filtered through an alumina plug and analyzed by GC-MS.

GC-MS Calibrations with Authentic Product. The compounds synthesized as described in this chapter (2',5'-dimethoxy-[1,1'-biphenyl]-2-carbonitrile (**20**), 2-(1-methyl-1H-pyrrol-2-yl)benzonitrile (**4**), 2',4',6'-trimethoxy-[1,1'-biphenyl]-2-carbonitrile (**17**)) were used as authentic product for GC-MS calibrations. [1,1'-biphenyl]-2-carbonitrile (**18**) was purchased and used as received. **18** was also used to calibrate the GC-MS reaction using 2,5-dimethoxybenzene and the result was compared with the calibration using **20**. The calculated yield differed by 2% and **18** was deemed a suitable calibration compound for the products. **18** was used as the calibration for the product of the reaction using mesitylene acceptor instead of 2',4',6'-trimethyl-[1,1'-biphenyl]-2-carbonitrile (**19**), which was not synthesized. This is due to the low preparative scale yield observed for reactions with uphill intermediates, as demonstrated with **20**.

Sample GC-MS Calibration with [1,1'-biphenyl]-2-carbonitrile (18). A stock solution of 54.3 mg **18** was prepared in 10 ml acetonitrile using a volumetric flask. A 1.5 ml aliquot (containing 8.14 mg **18**) was added to a GC vial by syringe and 5 μl (5.15 mg) acetophenone was added. The sample was analyzed by GC-MS and the response factor (K) was calculated using Equation 5.9. The response factor (K) was used to calculate the yield of **18** from the GC-MS scale reaction (Equation 5.10). The response factors determined for the other products are tabulated in Table 5.8.

Compound	Response Factor
2-(1-methyl-1H-pyrrol-2-yl)benzonitrile (**4**)	1.437
[1,1'-biphenyl]-2-carbonitrile (**18**)	0.9704
2',4',6'-trimethoxy-[1,1'-biphenyl]-2-carbonitrile (**17**)	1.336
2',5'-dimethoxy-[1,1'-biphenyl]-2-carbonitrile (**20**)	1.108

Table 5.8. Calculated response factors for GC-MS calibrations with different product molecules.

$$\frac{A_{prod}}{A_{IS}} = K\frac{C_{prod}}{C_{IS}} \qquad \frac{150239456.87}{97949656.21} = K\frac{\frac{8.14\,mg}{1.5\,ml}}{\frac{5.15mg}{1.5\,ml}} \qquad K = 0.9704 \tag{5.9}$$

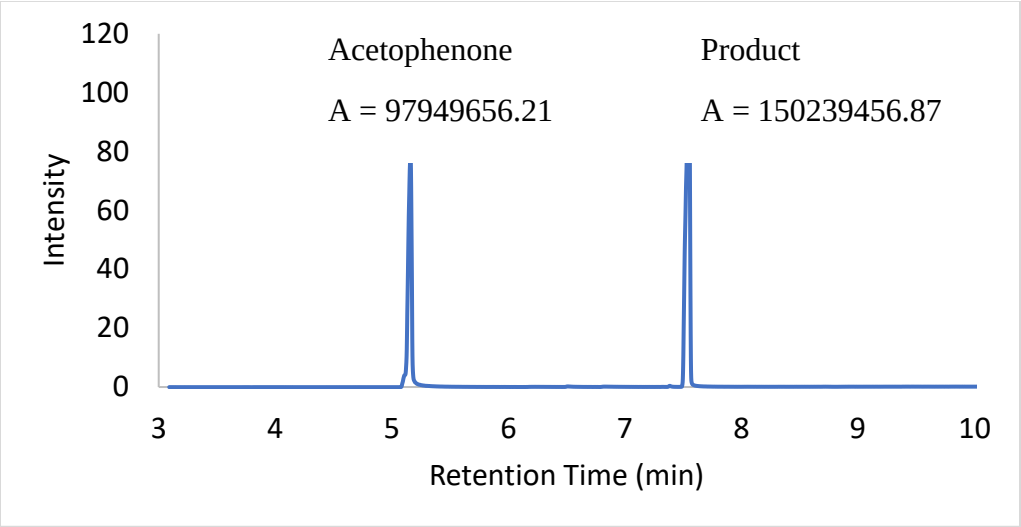

Figure 5.60. GC-MS trace of calibration for [1,1'-biphenyl]-2-carbonitrile (**18**).

$$\frac{A_{prod}}{A_{IS}} = K\frac{C_{prod}}{C_{IS}} \qquad \frac{2708763.38}{38760851.68} = 0.9704\frac{\frac{m_{prod}}{1.5\,ml}}{\frac{5.15mg}{1.5\,ml}} \qquad m_{prod} = 0.371\,mg, 5\%\,yield \tag{5.10}$$

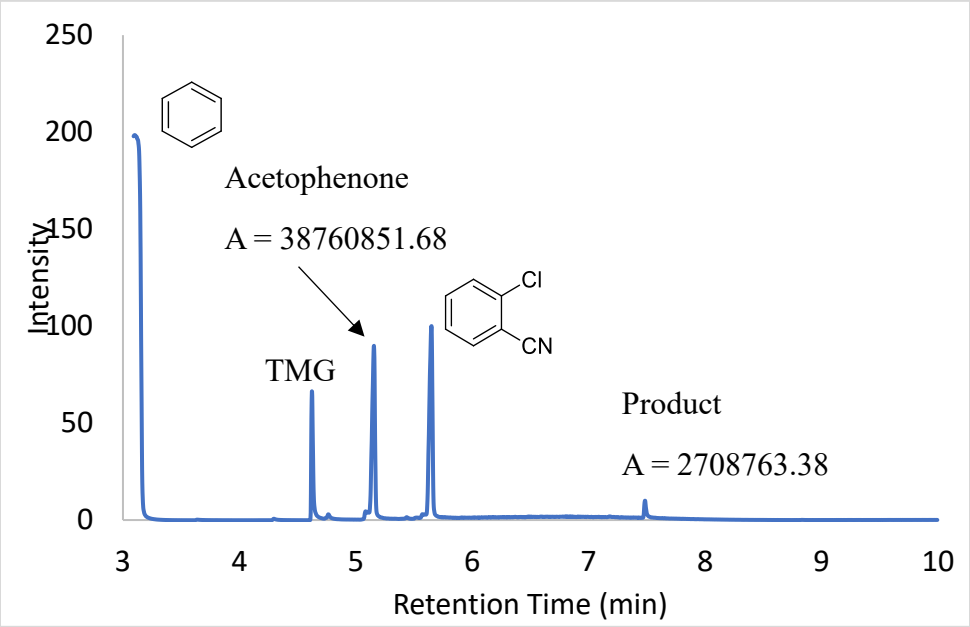

Figure 5.61. GC-MS trace of reaction producing [1,1'-biphenyl]-2-carbonitrile (**18**).

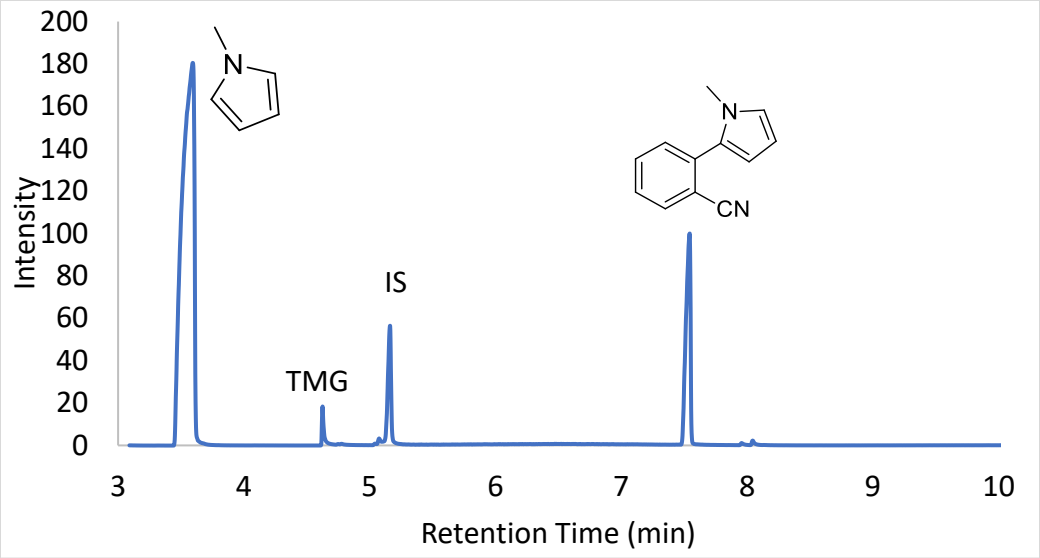

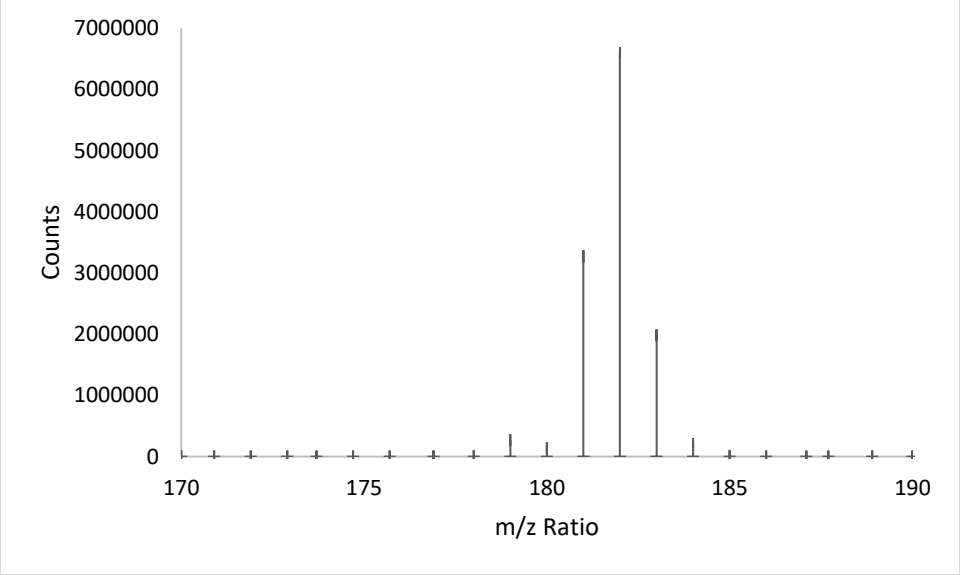

Figure 5.62. a) GC-MS chromatogram and **b)** Mass spectrum at 7.54 min of the reaction producing 2-(1-methyl-1H-pyrrol-2-yl)benzonitrile (**4**).

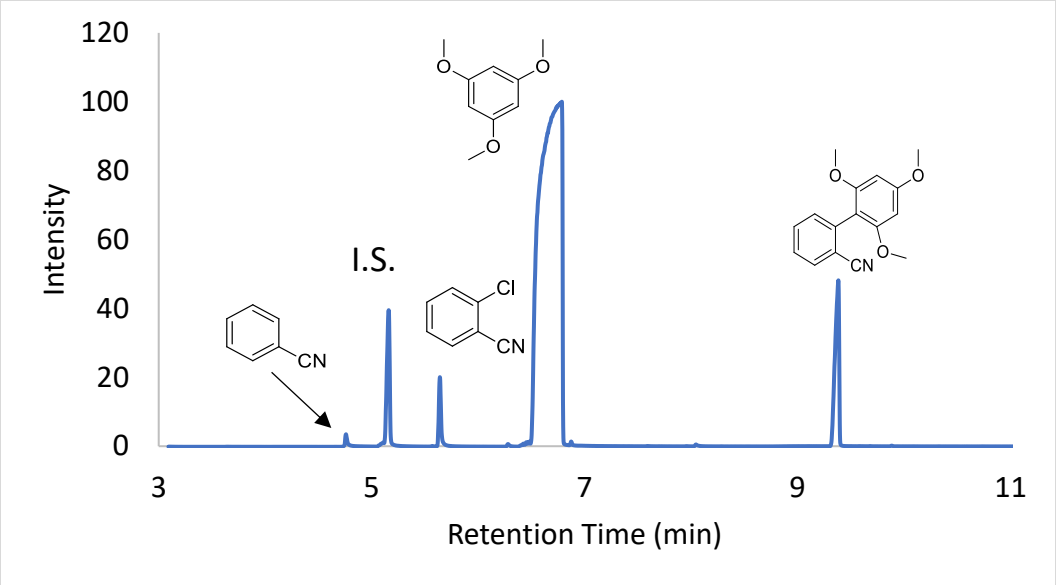

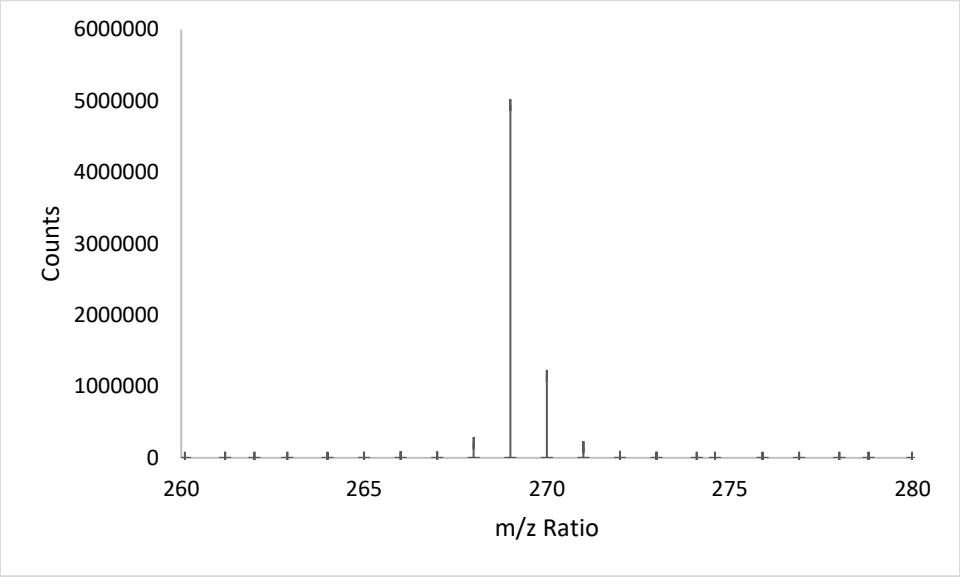

Figure 5.63. a) GC-MS chromatogram and **b)** Mass spectra at 9.38 min of the reaction producing 2',4',6'-trimethoxy-[1,1'-biphenyl]-2-carbonitrile (**17**).

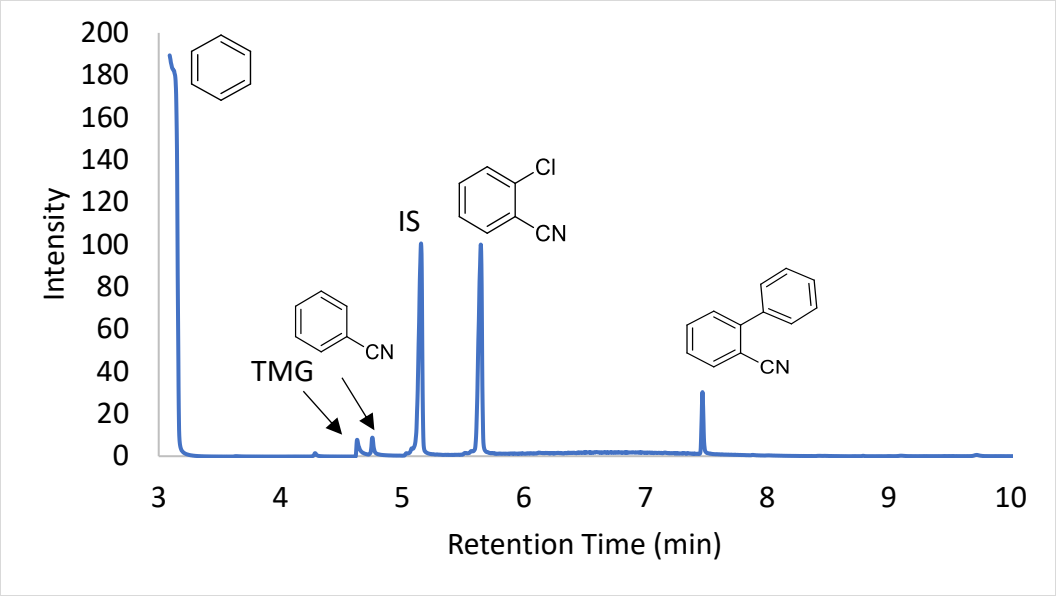

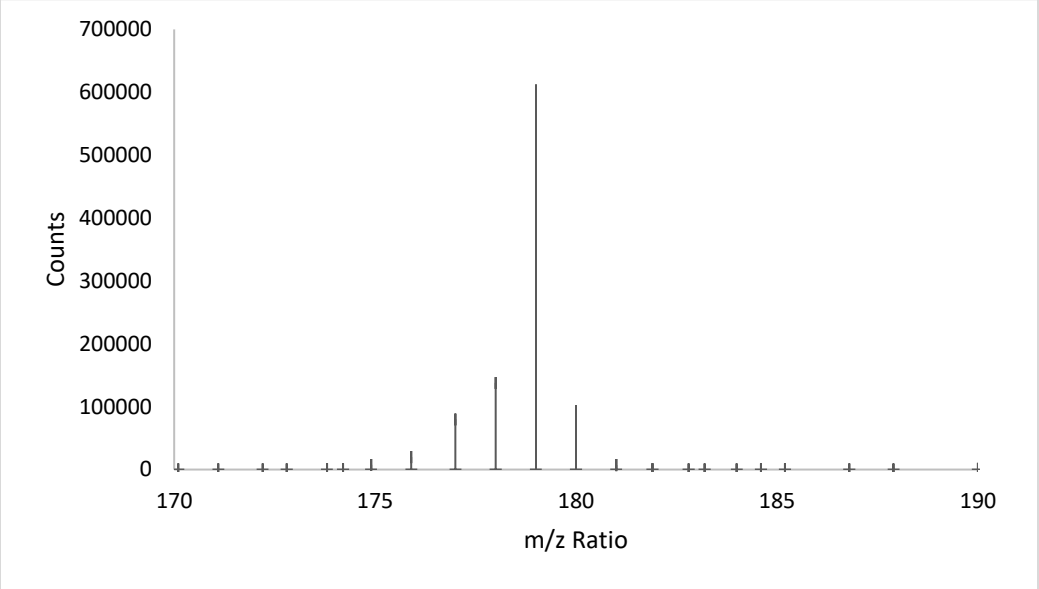

Figure 5.64. a) GC-MS chromatogram and **b)** Mass spectra at 7.47 min of the reaction producing [1,1'-biphenyl]-2-carbonitrile (**18**).

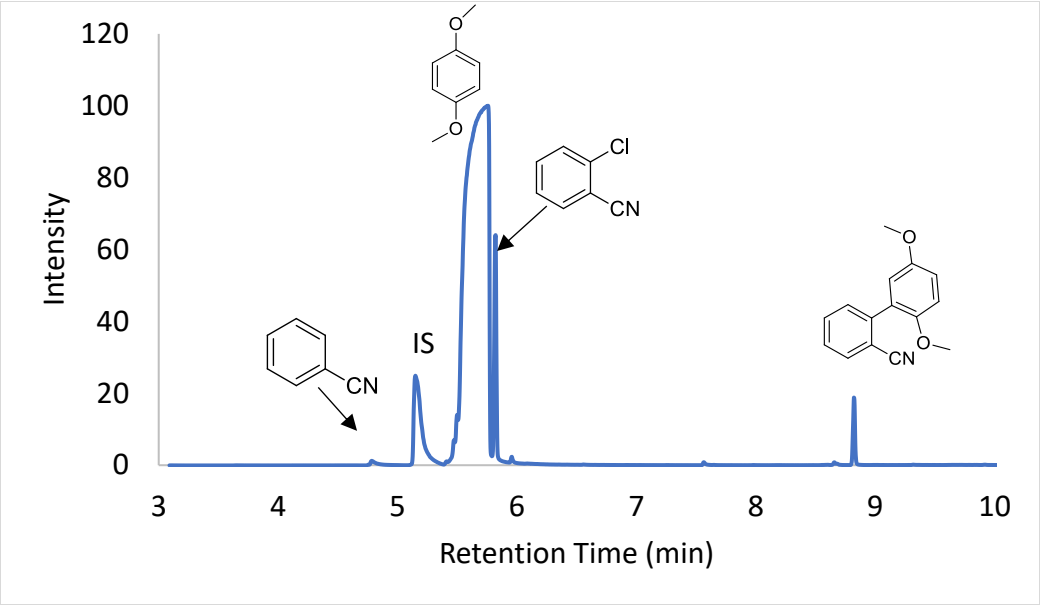

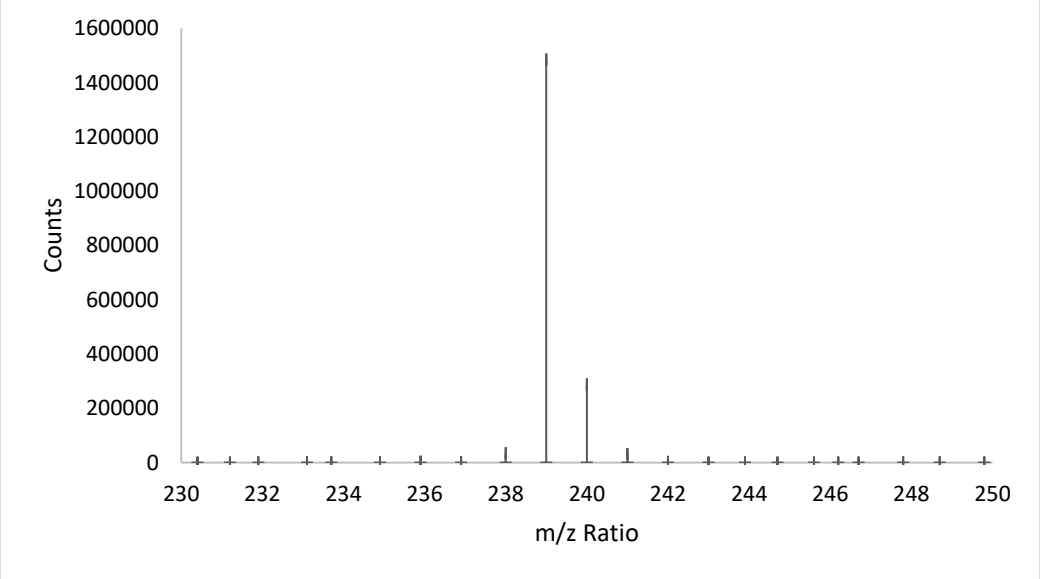

Figure 5.65. a) GC-MS chromatogram and **b)** Mass spectra at 8.83 min of the reaction producing 2',5'-dimethoxy-[1,1'-biphenyl]-2-carbonitrile (**20**).

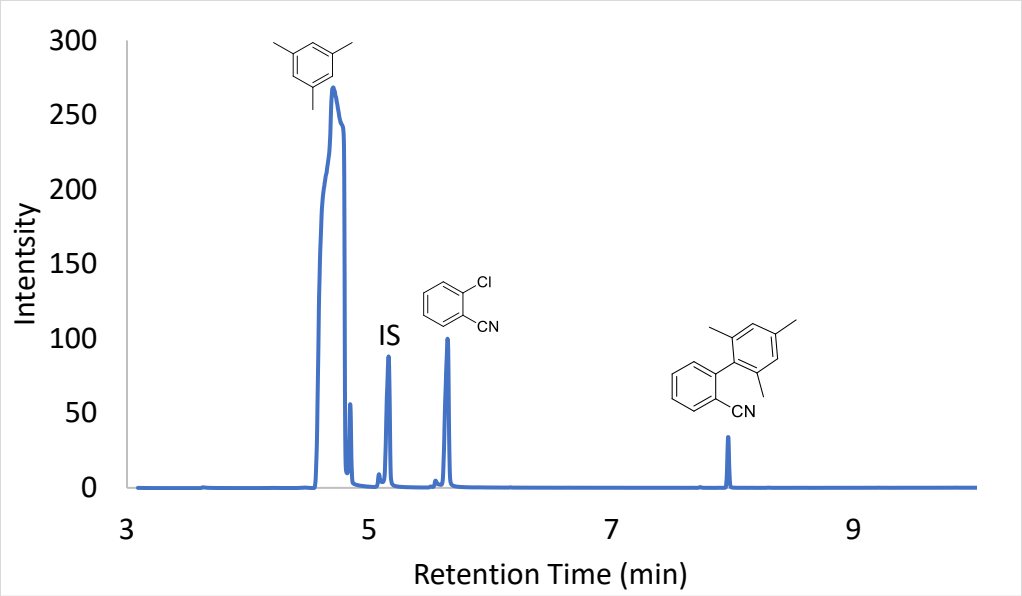

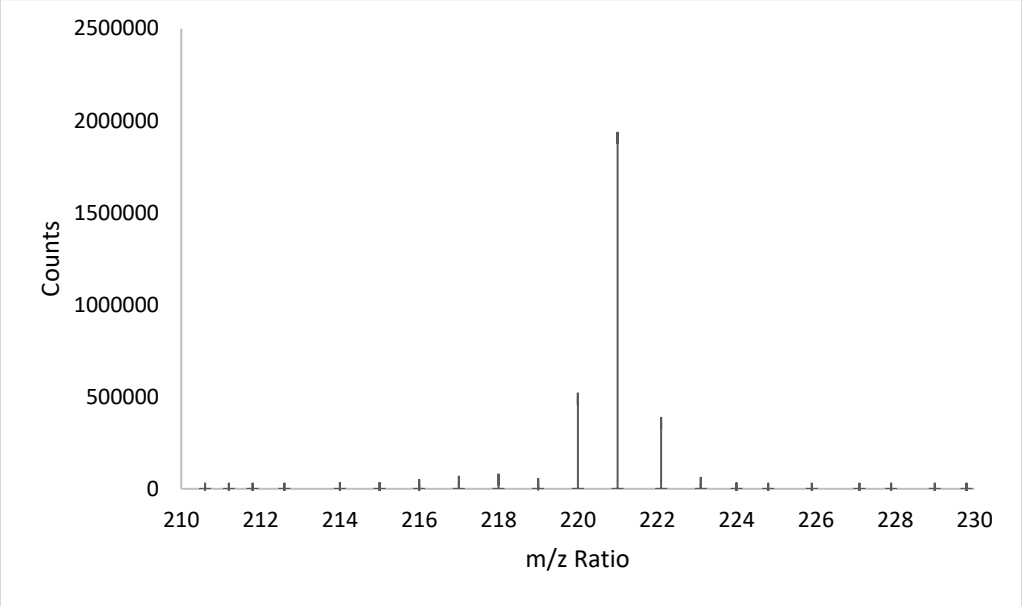

Figure 5.66. a) GC-MS chromatogram and **b)** Mass spectra at 7.96 min of the reaction producing 2',4',6'-trimethyl-[1,1'-biphenyl]-2-carbonitrile (**19**).

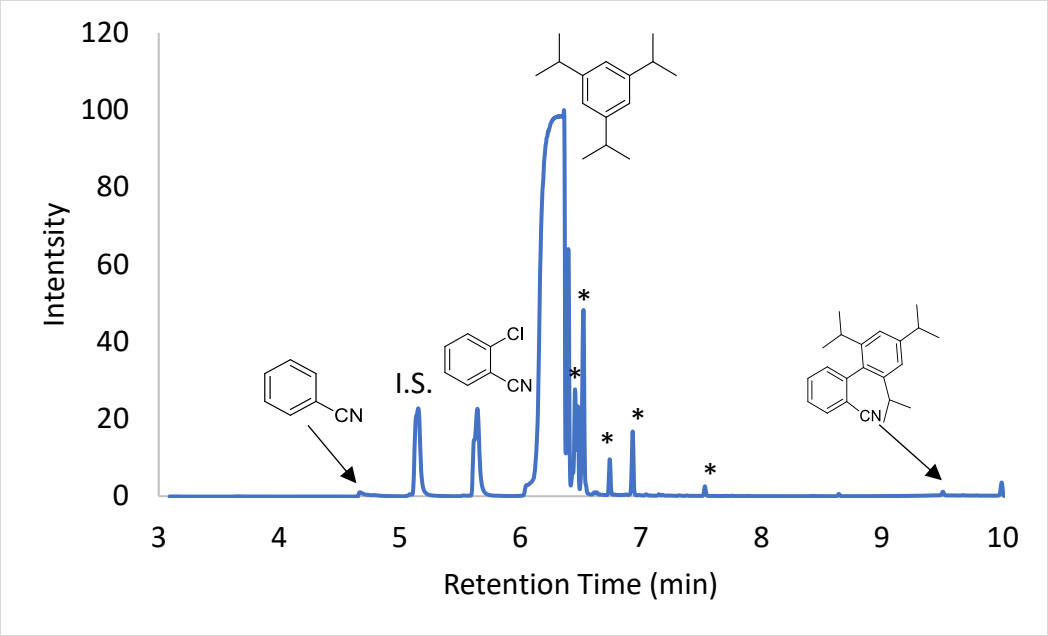

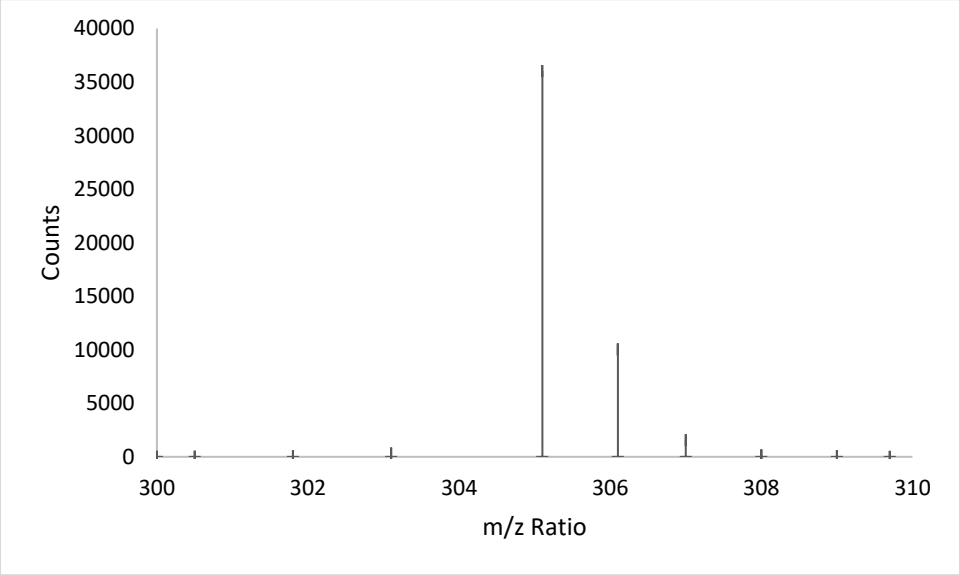

Figure 5.67. a) GC-MS chromatogram and **b)** Mass spectra at 9.48 min of the reaction producing 2',4',6'-triisopropyl-[1,1'-biphenyl]-2-carbonitrile (**21**). * Represents a peak that could not be identified.

Synthesis of 2',4',6'-trimethoxy-[1,1'-biphenyl]-2-carbonitrile (17). To a vial containing a solution of 2-chlorobenzonitrile (0.500 g, 3.63 mmol) in acetonitrile (10 mL) was added 1,1,3,3-tetramethylguanidine (0.841 g, 7.3 mmol, 2 equiv.), W(CPh)(depe)$_2$Cl (0.052 g, 0.0726 mmol, 2 mol%, 7.3 mM solution), and 1,3,5-trimethoxybenzene (6.14 g, 36.5 mmol, 10 equiv.). The vial

was sealed with electrical tape and the solution was photolyzed for 18 hours, resulting in a colour change from pink to brown. The reaction was opened to air, filtered to remove a white solid and acetonitrile was removed by rotary evaporation resulting in a brown oil. The oil was distilled to remove the excess 1,3,5-trimethoxybenzene at 50 ºC at 0.4 torr. The remaining oil was columned through silica using 70:30 hexanes:ethyl acetate resulting in a white solid (0.514 g, 1.91 mmol, 52% yield). ^{1}H NMR (500 MHz, CD_2Cl_2): δ 7.69 (d, J_{HH} = 4 Hz, 1 H, H_A), 7.60 (m, J_{HH} = 6 Hz, 1 H, H_B), 7.39 (m, 2H, H_C and H_D), 6.26 (s, 2H, H_E), 3.87 (s, 3H, H_F), 3.75 (s, 6H, H_G). $^{13}C\{^{1}H\}$0.500 NMR (125.75 MHz, CD_2Cl_2): δ 162.41 (C_M), 158.74 (C_L), 138.31 (C_K), 132.97 (C_C), 132.73 (C_B), 132.24 (C_A), 127.31 (C_D), 119.02 (C_J), 115.16 (C_I), 108.79 (C_H), 91.09 (C_E), 56.11 (C_G), 55.78 (C_F). GC-MS: 269.0 m/z; theor. 269.30 g/mol.

Synthesis of 2-(1-methyl-1H-pyrrol-2-yl)benzonitrile (4). To a vial containing a solution of 2-chlorobenzonitrile (0.500 g, 3.63 mmol) in acetonitrile (10 ml) was added 1,1,3,3-tetramethylguanidine (0.439 g, 3.81 mmol, 1.05 equiv.), $W(CPh)(depe)_2Cl$ (0.052 mg, 0.0726 mmol, 2 mol%, 7.3 mM solution), and N-methylpyrrole (5.89 g, 72.7 mmol, 20 equiv.). The vial was sealed with electrical tape and the solution was photolyzed for 18 hours, resulting in a colour change from pink to brown. The reaction was opened to air, and acetonitrile and N-methylpyrrole were removed by vacuum transfer resulting in a brown oil. The oil was columned through silica using 50:50 hexanes:ethyl acetate resulting in a white solid (0.411 g, 2.42 mmol, 67% yield). ^{1}H NMR (500 MHz, CD_2Cl_2): δ 7.75 (d, J_{HH} = 5 Hz, 1 H, H_A), 7.63 (m, J_{HH} = 8 Hz, 1 H, H_B), 7.43 (m, 2H, H_C and H_D), 6.82 (m, 1H, H_E), 6.37 (dd, $^{3}J_{HH}$ = 4 Hz, $^{4}J_{HH}$ = 1.8 Hz, 1 H, H_F), 6.23 (t, J_{HH} = 3 Hz, 1H, H_G), 3.59 (s, 3H, H_H). $^{13}C\{^{1}H\}$ NMR (125.75 MHz, CD_2Cl_2): δ 137.14 (C_K), 133.83 (C_A), 132.72 (C_B), 131.20 (C_C), 130.34 (C_L), 127.81 (C_D), 125.04 (C_E), 118.97 (C_J), 113.13 (C_I), 111.52 (C_F), 108.36 (C_G), 35.05 (C_H). GC-MS: 182.0 m/z; theor. 182.22 g/mol.

Synthesis of 2',5'-dimethoxy-[1,1'-biphenyl]-2-carbonitrile (20). To a Schlenk flask containing a solution of 2-chlorobenzonitrile (2.00 g, 14.6 mmol) in 40 ml acetonitrile was added 1,1,3,3-tetramethylguanidine (3.36 g, 29.2 mmol, 2 equiv.), W(CPh)(depe)$_2$Cl (0.211 g, 0.293 mmol, 2 mol%, 7.3 mM solution), and 2,5-dimethoxybenzene (20.2 g, 146 mmol, 10 equiv.). The solution was photolyzed for 18 hours, resulting in a colour change from pink to yellow. The reaction was opened to air and acetonitrile was removed by rotary evaporation resulting in a yellow oil. The oil was distilled to remove the excess 2,5-dimethoxybenzene at 80 ºC at 0.85 torr. The remaining brown oil was columned through silica using toluene, resulting in a yellow solid (0.050 g, 0.209 mmol, 1.4% yield). ^{1}H NMR (500 MHz, CD_2Cl_2): δ 7.73 (d, J_{HH} = 8 Hz, 1 H, H_A), 7.64 (m, J_{HH} = 8 Hz), 7.44 (m, 2H, H_C and H_D), 6.97 (m, 2H, H_E, H_F), 6.83 (d, J_{HH} = 2 Hz, 1 H, H_G), 3.79 (s, 1 H, H_H), 3.77 (s, 1 H, H_I). ^{13}C{^{1}H} NMR (125.75 MHz, CD_2Cl_2): δ 135.90 ($C_{N/O}$), 151.01 ($C_{N/O}$), 142.66 (C_M), 133.06 (C_A), 132.79 (C_B), 131.19 (C_C), 128.43 (C_J), 127.90 (C_D), 118.81 (C_L), 117.06 (C_G), 115.07 (C_F), 113.712 (C_K), 112.71 (C_E), 56.28 (C_I), 56.10 (C_H). GC-MS: 239 m/z; theor. 239.27 g/mol.

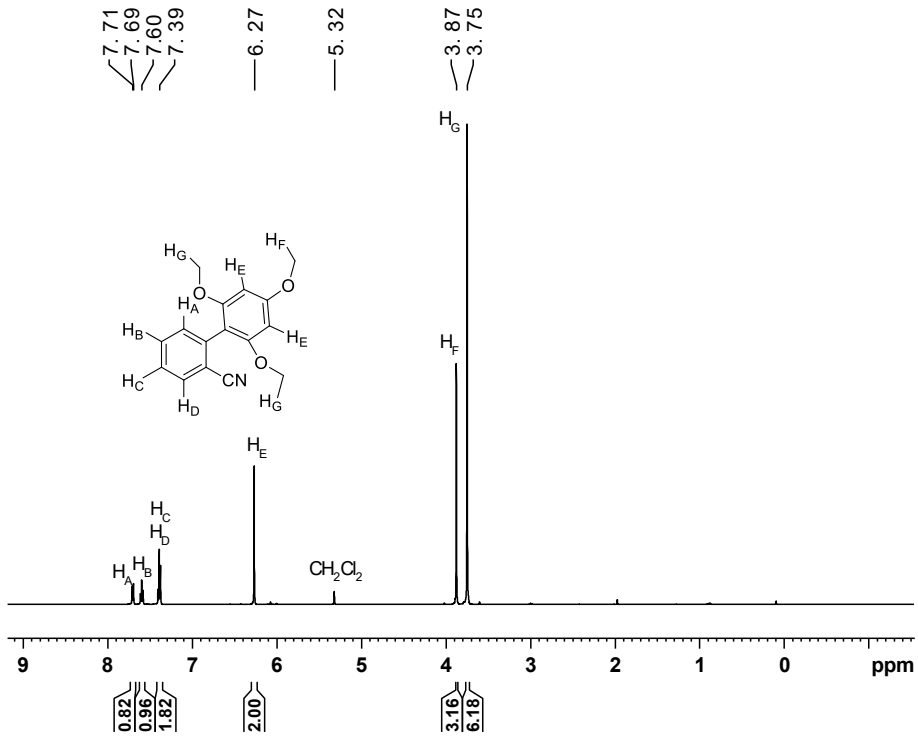

Figure 5.68. ^{1}H NMR spectrum of 2',4',6'-trimethoxy-[1,1'-biphenyl]-2-carbonitrile (**17**) in CD_2Cl_2.

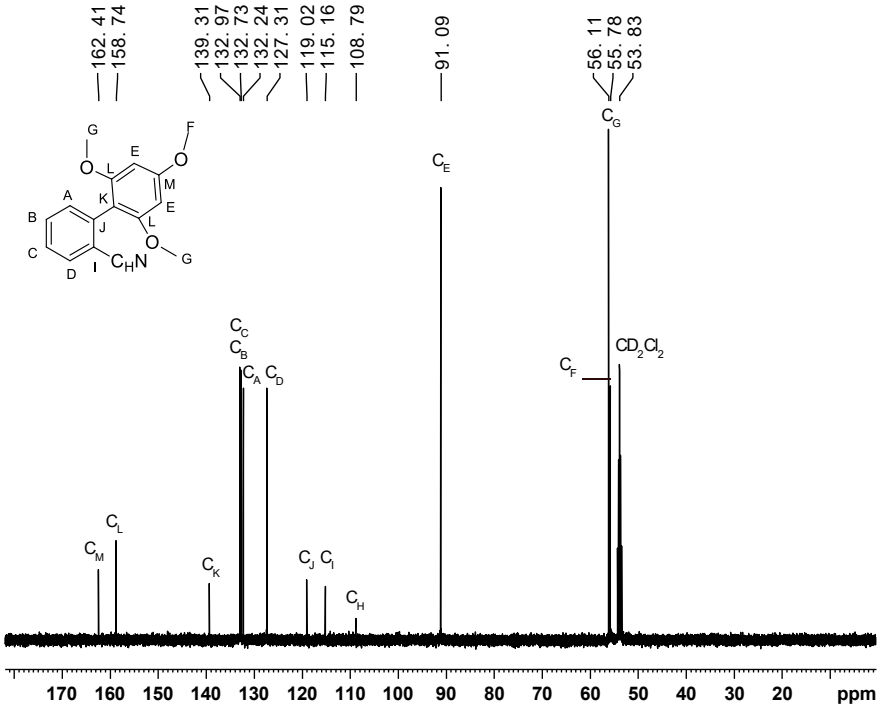

Figure 5.69. $^{13}C\{^{1}H\}$ NMR spectrum of 2',4',6'-trimethoxy-[1,1'-biphenyl]-2-carbonitrile (**17**) in CD_2Cl_2.

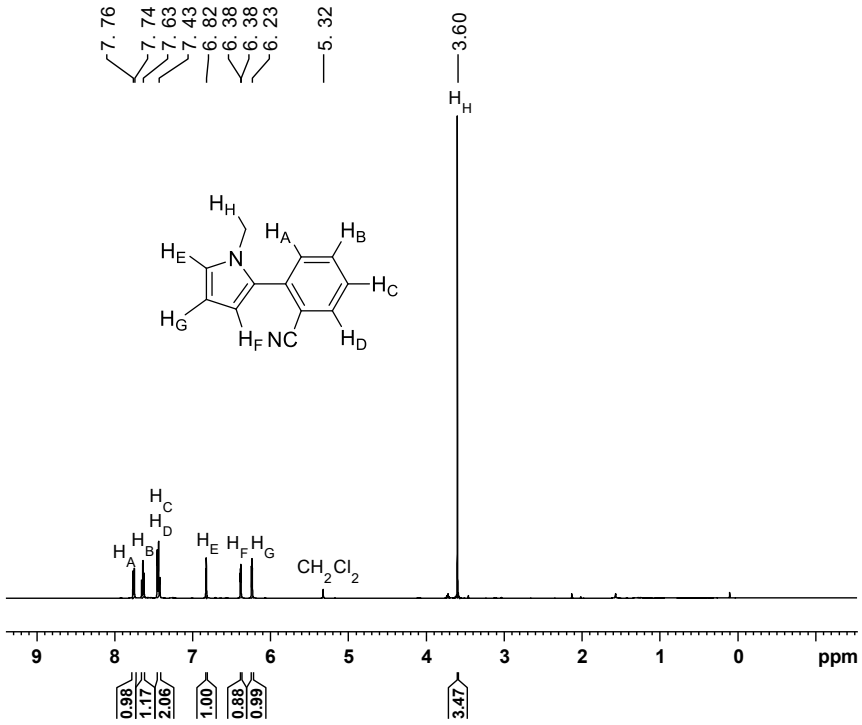

Figure 5.70. ^{1}H NMR spectrum of 2-(1-methyl-1H-pyrrol-2-yl)benzonitrile (**4**) in CD_2Cl_2.

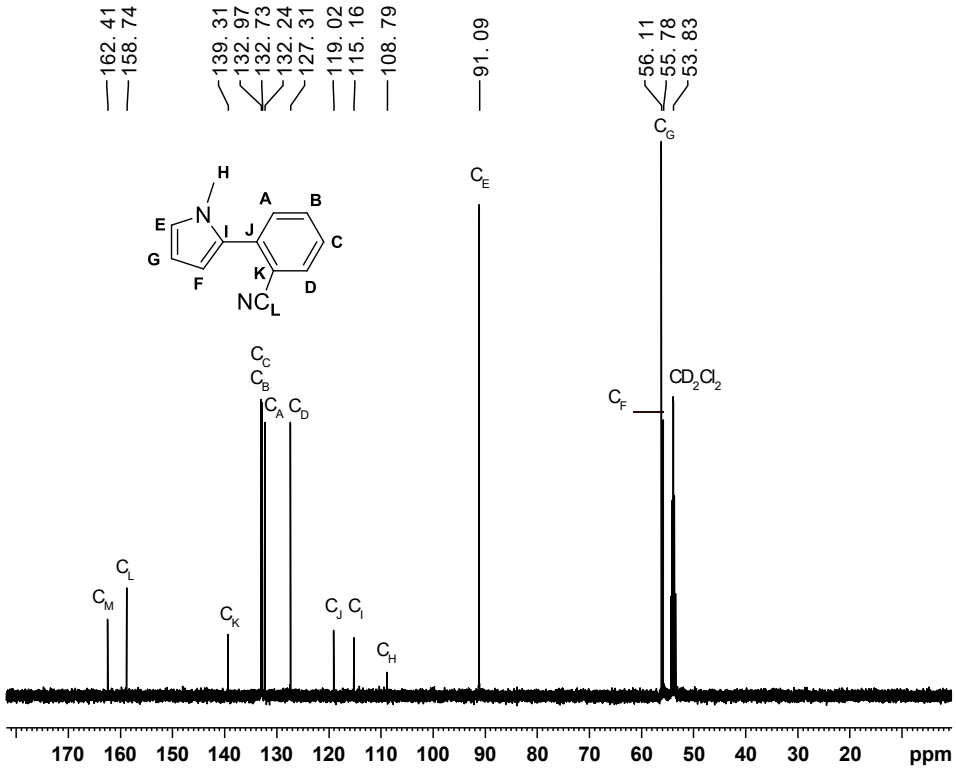

Figure 5.71. ^{13}C{^{1}H} NMR spectrum of 2-(1-methyl-1H-pyrrol-2-yl)benzonitrile (**4**) in CD_2Cl_2.

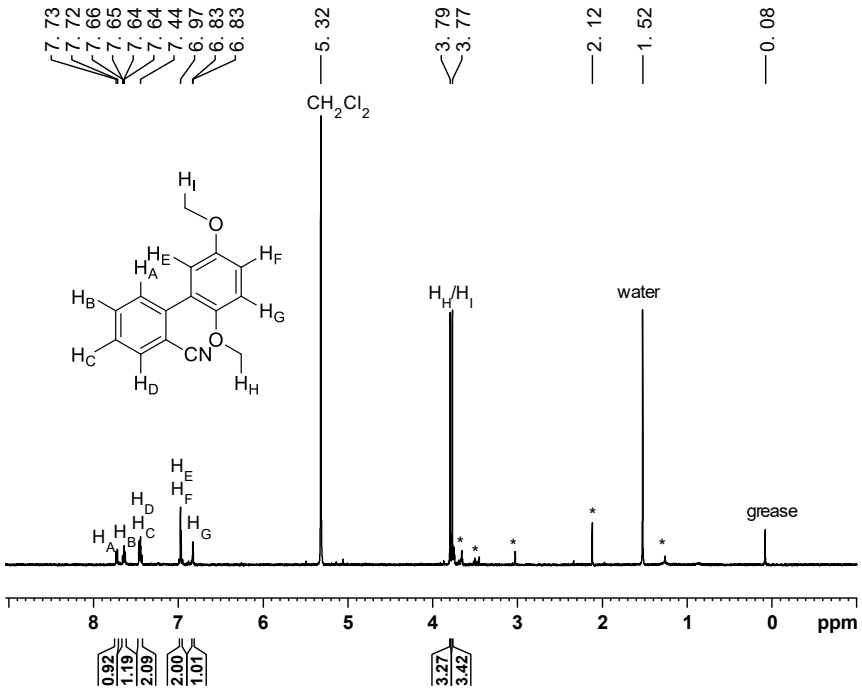

Figure 5.72. ^{1}H NMR spectrum of 2',5'-dimethoxy-[1,1'-biphenyl]-2-carbonitrile (**20**) in CD_2Cl_2. * Represents an impurity that could not be removed.

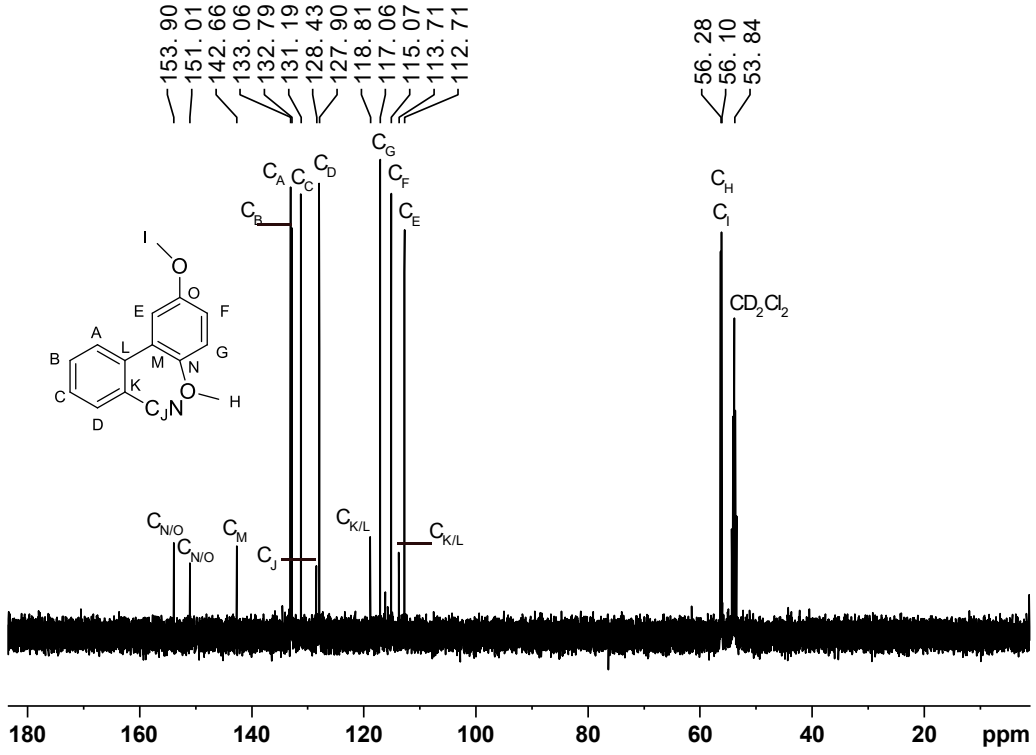

Figure 5.73. ^{13}C{^{1}H} NMR spectrum of 2',5'-dimethoxy-[1,1'-biphenyl]-2-carbonitrile (**20**) in CD_2Cl_2.

5.5. References.

1. Shaw, M. H.; Twilton, J.; MacMillan, D. W. C., Photoredox Catalysis in Organic Chemistry. *J. Org. Chem.* **2016,** *81* (16), 6898-6926.

2. Douglas, J. J.; Sevrin, M. J.; Stephenson, C. R. J., Visible Light Photocatalysis: Applications and New Disconnections in the Synthesis of Pharmaceutical Agents. *Org. Process Res. Dev.* **2016,** *20* (7), 1134-1147.

3. Marzo, L.; Pagire, S. K.; Reiser, O.; König, B., Visible-Light Photocatalysis: Does it make a difference in Organic Synthesis? *Angew. Chem. Int. Ed.* **2018**.

4. Ghosh, I.; Marzo, L.; Das, A.; Shaikh, R.; König, B., Visible Light Mediated Photoredox Catalytic Arylation Reactions. *Acc. Chem. Res.* **2016,** *49* (8), 1566-1577.

5. Uygur, M.; García Mancheño, O., Visible Light-mediated Organophotocatalyzed C–H Bond Functionalization Reactions. *Org. Biomol. Chem.* **2019,** *17* (22), 5475-5489.

6. Wang, C.-S.; Dixneuf, P. H.; Soulé, J.-F., Photoredox Catalysis for Building C–C Bonds from C(sp2)–H Bonds. *Chem. Rev.* **2018,** *118* (16), 7532-7585.

7. Prier, C. K.; Rankic, D. A.; MacMillan, D. W. C., Visible Light Photoredox Catalysis with Transition Metal Complexes: Applications in Organic Synthesis. *Chem. Rev.* **2013,** *113* (7), 5322-5363.

8. Connelly, N. G.; Geiger, W. E., Chemical Redox Agents for Organometallic Chemistry. *Chem. Rev.* **1996,** *96* (2), 877-910.

9. Oger, N.; d'Halluin, M.; Le Grognec, E.; Felpin, F.-X., Using Aryl Diazonium Salts in Palladium-Catalyzed Reactions under Safer Conditions. *Org. Process Res. Dev.* **2014,** *18* (12), 1786-1801.

10. Ghosh, I.; Ghosh, T.; Bardagi, J. I.; König, B., Reduction of Aryl Halides by Consecutive Visible Light-induced Electron Transfer Processes. *Science* **2014,** *346* (6210), 725.

11. Andrieux, C. P.; Blocman, C.; Dumas-Bouchiat, J. M.; Saveant, J. M. Heterogeneous and Homogeneous Electron Transfers to Aromatic Halides. An Electrochemical Redox Catalysis Study in the Halobenzene and Halopyridine Series. *J. Am. Chem. Soc.* **1979,** *101* (13), 3431-3441.

12. Koefoed, L.; Vase, K. H.; Stenlid, J. H.; Brinck, T.; Yoshimura, Y.; Lund, H.; Pedersen, S. U.; Daasbjerg, K., On the Kinetic and Thermodynamic Properties of Aryl Radicals Using Electrochemical and Theoretical Approaches. *ChemElectroChem* **2017,** *4* (12), 3212-3221.

13. Rudshteyn, B.; Vibbert, H. B.; May, R.; Wasserman, E.; Warnke, I.; Hopkins, M. D.; Batista, V. S., Thermodynamic and Structural Factors That Influence the Redox Potentials of Tungsten–Alkylidyne Complexes. *ACS Catal.* **2017,** *7* (9), 6134-6143.

14. Vibbert, H. B. GROUP 6 METAL-OXO AND -ALKYLIDYNE COMPLEXES WITH HIGH REACTIVITY DERIVED FROM π-ANTIBONDING ORBITALS. Ph.D. Thesis, University of Chicago, Chicago, IL, 2018.

15. Qiu, G.; Knowles, R. R., Rate–Driving Force Relationships in the Multisite Proton-Coupled Electron Transfer Activation of Ketones. *J. Am. Chem. Soc.* **2019,** *141* (6), 2721-2730.

16. Morton, C. M.; Zhu, Q.; Ripberger, H.; Troian-Gautier, L.; Toa, Z. S. D.; Knowles, R. R.; Alexanian, E. J., C–H Alkylation via Multisite-Proton-Coupled Electron Transfer of an Aliphatic C–H Bond. *J. Am. Chem. Soc.* **2019,** *141* (33), 13253-13260.

17. Meyer, A. U.; Slanina, T.; Yao, C.-J.; König, B., Metal-Free Perfluoroarylation by Visible Light Photoredox Catalysis. *ACS Catal.* **2016,** *6* (1), 369-375.

18. Chaudhary, S.; Milton, M. D.; Garg, P., A Base- and Metal-free Protocol for the Synthesis of 2-Aryl/heteroaryl Thiazolines. *ChemistrySelect* **2017,** *2* (2), 650-654.

19. Nagib, D. A.; MacMillan, D. W. C., Trifluoromethylation of Arenes and Heteroarenes by Means of Photoredox Catalysis. *Nature* **2011,** *480* (7376), 224-228.

20. Su, Y.; Kuijpers, K. P. L.; König, N.; Shang, M.; Hessel, V.; Noël, T., A Mechanistic Investigation of the Visible-Light Photocatalytic Trifluoromethylation of Heterocycles Using CF3I in Flow. *Chem.: Eur. J.* **2016,** *22* (35), 12295-12300.

21. Beatty, J. W.; Douglas, J. J.; Miller, R.; McAtee, R. C.; Cole, K. P.; Stephenson, C. R. J., Photochemical Perfluoroalkylation with Pyridine N-Oxides: Mechanistic Insights and Performance on a Kilogram Scale. *Chem* **2016,** *1* (3), 456-472.

22. Ju, X.; Liang, Y.; Jia, P.; Li, W.; Yu, W., Synthesis of Oxindoles via Visible Light Photoredox Catalysis. *Org. Biomol. Chem.* **2012,** *10* (3), 498-501.

23. Cheng, J.; Deng, X.; Wang, G.; Li, Y.; Cheng, X.; Li, G., Intermolecular C–H Quaternary Alkylation of Aniline Derivatives Induced by Visible-Light Photoredox Catalysis. *Org. Lett.* **2016,** *18* (18), 4538-4541.

24. Li, G.-X.; Morales-Rivera, C. A.; Wang, Y.; Gao, F.; He, G.; Liu, P.; Chen, G., Photoredox-mediated Minisci C–H Alkylation of N-heteroarenes using Boronic Acids and Hypervalent Iodine. *Chem. Sci.* **2016,** *7* (10), 6407-6412.

25. Fu, W.; Zhu, M.; Zou, G.; Xu, C.; Wang, Z.; Ji, B., Visible-Light-Mediated Radical Aryldifluoroacetylation of Alkynes with Ethyl Bromodifluoroacetate for the Synthesis of 3-Difluoroacetylated Coumarins. *J. Org. Chem.* **2015,** *80* (9), 4766-4770.

26. Xu, P.; Xie, J.; Xue, Q.; Pan, C.; Cheng, Y.; Zhu, C., Visible-Light-Induced Trifluoromethylation of N-Aryl Acrylamides: A Convenient and Effective Method To Synthesize CF3-Containing Oxindoles Bearing a Quaternary Carbon Center. *Chem.: Eur. J.* **2013,** *19* (42), 14039-14042.

27. Zheng, L.; Yang, C.; Xu, Z.; Gao, F.; Xia, W., Difunctionalization of Alkenes via the Visible-Light-Induced Trifluoromethylarylation/1,4-Aryl Shift/Desulfonylation Cascade Reactions. *J. Org. Chem.* **2015,** *80* (11), 5730-5736.

28. Fu, W.; Xu, F.; Fu, Y.; Zhu, M.; Yu, J.; Xu, C.; Zou, D., Synthesis of 3,3-Disubstituted Oxindoles by Visible-Light-Mediated Radical Reactions of Aryl Diazonium Salts with N-Arylacrylamides. *J. Org. Chem.* **2013,** *78* (23), 12202-12206.

29. Bergonzini, G.; Cassani, C.; Lorimer-Olsson, H.; Hörberg, J.; Wallentin, C.-J., Visible-Light-Mediated Photocatalytic Difunctionalization of Olefins by Radical Acylarylation and Tandem Acylation/Semipinacol Rearrangement. *Chem.: Eur. J.* **2016,** *22* (10), 3292-3295.

30. Hansen, C. B. 1. TUNGSTEN PHOTOREDOX CHROMOPHORES CONTAINING AMINEFUNCTIONALIZED DIPHOSPHINE AND N-HETEROCYCLIC CARBENE LIGANDS. 2. THE CHEMISTRY OF LOW-COORDINATE COBALT COMPOUNDS SUPPORTED BY N-HETEROCYCLIC CARBENES AND BULKY AMINES. Ph.D. Dissertation, University of Chicago, Chicago, Illinois, 2017.

31. Morales-Verdejo, C. A.; Newsom, M. I.; Cohen, B. W.; Vibbert, H. B.; Hopkins, M. D., Dihydrogen Activation by a Tungsten–alkylidyne Complex: Toward Photoredox Chromophores that Deliver Renewable Reducing Equivalents. *Chem. Commun.* **2013,** *49* (90), 10566-10568.

32. Holmes, S. J.; Schrock, R. R., A Tungsten T-shaped Methylene Complex and Related Methylidyne Hydride Complexes. *J. Am. Chem. Soc.* **1981,** *103* (15), 4599-4600.

33. Frisch, M. J.; Trucks, G. W.; Schlegel, H. B.; Scuseria, G. E.; Robb, M. A.; Cheeseman, J. R.; Scalmani, G.; Barone, V.; Petersson, G. A.; Nakatsuji, H.; Li, X.; Caricato, M.; Marenich, A. V.; Bloino, J.; Janesko, B. G.; Gomperts, R.; Mennucci, B.; Hratchian, H. P.; Ortiz, J. V.; Izmaylov, A. F.; Sonnenberg, J. L.; Williams; Ding, F.; Lipparini, F.; Egidi, F.; Goings, J.; Peng, B.; Petrone, A.; Henderson, T.; Ranasinghe, D.; Zakrzewski, V. G.; Gao, J.; Rega, N.; Zheng, G.; Liang, W.; Hada, M.; Ehara, M.; Toyota, K.; Fukuda, R.; Hasegawa, J.; Ishida, M.; Nakajima, T.; Honda, Y.; Kitao, O.; Nakai, H.; Vreven, T.; Throssell, K.; Montgomery Jr., J. A.; Peralta, J. E.; Ogliaro, F.; Bearpark, M. J.; Heyd, J. J.; Brothers, E. N.; Kudin, K. N.; Staroverov, V. N.; Keith, T. A.; Kobayashi, R.; Normand, J.; Raghavachari, K.; Rendell, A. P.; Burant, J. C.; Iyengar, S. S.; Tomasi, J.; Cossi, M.; Millam, J. M.; Klene, M.; Adamo, C.; Cammi, R.;

Ochterski, J. W.; Martin, R. L.; Morokuma, K.; Farkas, O.; Foresman, J. B.; Fox, D. J. *Gaussian 16 Rev. C.01*, Gaussian, Inc.: Wallingford, CT, 2016.

34. Waller, M. P.; Braun, H.; Hojdis, N.; Bühl, M., Geometries of Second-Row Transition-Metal Complexes from Density-Functional Theory. *J. Chem. Theory Comput.* **2007,** *3* (6), 2234-2242.

35. Dunning, T. H.; Hay, P. J., Gaussian Basis Sets for Molecular Calculations. In *Methods of Electronic Strucutre Theory.*, Schaefer, H. F., Ed. Springer US: Boston, MA, 1977; pp 1-27.

36. Hay, P. J.; Wadt, W. R., Ab initio Effective Core Potentials for Molecular Calculations. Potentials for the Transition Metal Atoms Sc to Hg. *J. Chem. Phys.* **1985,** *82* (1), 270-283.

37. Warren, J. J.; Tronic, T. A.; Mayer, J. M., Thermochemistry of Proton-Coupled Electron Transfer Reagents and its Implications. *Chem. Rev.* **2010,** *110* (12), 6961-7001.

38. Lee, C.; Yang, W.; Parr, R. G., Development of the Colle-Salvetti correlation-energy formula into a functional of the electron density. *Phys. Rev. B* **1988,** *37* (2), 785-789.

39. Cancès, E.; Mennucci, B.; Tomasi, J., A New Integral Equation Formalism for the Polarizable Continuum Model: Theoretical Background and Applications to Isotropic and Anisotropic Dielectrics. *J. Chem. Phys.* **1997,** *107* (8), 3032-3041.

40. Kaljurand, I.; Kütt, A.; Sooväli, L.; Rodima, T.; Mäemets, V.; Leito, I.; Koppel, I. A., Extension of the Self-Consistent Spectrophotometric Basicity Scale in Acetonitrile to a Full Span of 28 pKa Units: Unification of Different Basicity Scales. *J. Org. Chem.* **2005,** *70* (3), 1019-1028.

41. Morris, R. H., Brønsted–Lowry Acid Strength of Metal Hydride and Dihydrogen Complexes. *Chem. Rev.* **2016,** *116* (15), 8588-8654.

42. Eckert-Maksić, M.; Glasovac, Z.; Trošelj, P.; Kütt, A.; Rodima, T.; Koppel, I.; Koppel, I. A., Basicity of Guanidines with Heteroalkyl Side Chains in Acetonitrile. *Eur. J. Org. Chem.* **2008,** *2008* (30), 5176-5184.

43. Haines, D. E.; O'Hanlon, D. C.; Manna, J.; Jones, M. K.; Shaner, S. E.; Sun, J.; Hopkins, M. D., Oxidation-Potential Tuning of Tungsten–Alkylidyne Complexes over a 2 V Range. *Inorg. Chem.* **2013,** *52* (16), 9650-9658.

44. Pike, S. D.; Thompson, A. L.; Algarra, A. G.; Apperley, D. C.; Macgregor, S. A.; Weller, A. S., Synthesis and Characterization of a Rhodium(I) σ-Alkane Complex in the Solid State. *Science* **2012,** *337* (6102), 1648-1651.

45. Krause, L.; Herbst-Irmer, R.; Stalke, D., An Empirical Correction for the Influence of Low-energy Contamination. *J. Appl. Crystallogr.* **2015,** *48* (6), 1907-1913.

46. Sheldrick, G., A Short History of SHELX. *Acta Cryst. A* **2008,** *64* (1), 112-122.

47. Sheldrick, G., Crystal Structure Refinement with SHELXL. *Acta Cryst. C* **2015,** *71* (1), 3-8.

48. Dolomanov, O. V.; Bourhis, L. J.; Gildea, R. J.; Howard, J. A. K.; Puschmann, H., OLEX2: A Complete Structure Solution, Refinement and Analysis Program. *J. Appl. Crystallogr.* **2009,** *42* (2), 339-341.